USE OF REGOLITH GEOCHEMISTRY TO DELINEATE GOLD MINERALISATION UNDER COVER: A CASE STUDY IN THE LAWRA BELT, NW GHANA

Thesis submitted for the degree of Doctor of Philosophy at the University of Leicester

Emmanuel Arhin

Department of Geology

University of Leicester

March 2013

USE OF REGOLITH GEOCHEMISTRY TO DELINEATE GOLD MINERALISATION UNDER COVER: A CASE STUDY IN THE LAWRA BELT, NW GHANA

Emmanuel Arhin

Abstract

The Birimian rocks of southern Ghana host world-class gold deposits yet no equivalent-sized deposit has been found in the Birimian rocks in northwest Ghana. The reported gold occurrences in the area suggest a favourable environment for concealed mineralisation if the regolith and landscape evolution can be unravelled. A geochemical exploration model based on the evolution of the regolith-landform can help guide the choice of exploration methodology appropriate for the region.

The developed regolith map classifies the landscape into ferruginous (F), relict (R), erosional (E) and depositional (D) domains. Depositional areas cover 72% whereas the remaining 28% represents residual environments. Discrimination, characterisation and identification of regolith materials were carried out by pit and outcrop mapping. Regolith geochemical data provided regolith profile information which helped to distinguish residual regolith from transported types. Binary plots of major and trace element geochemical data were used to determine the compositional variability and different regolith types. Superimposing geochemical data on the regolith map identified residual and transported anomalies, and thus prioritized the weak, subtle and discontinuous anomalies. Gold, Ag and As relations in the regolith were also useful in determining the anomaly type and presence of gold mineralisation. High Au-low Ag with smooth dispersal patterns represents residual anomalies whereas spiky dispersion patterns with high Au-high Ag characterize transported anomalies. The released As into the regolith appears counteracted by the precipitation of Fe-oxyhydroxides, which efficiently scavenge As^{3+} and As^{5+} at neutral pH in the regolith, resulting in the weak As concentrations in the analysed samples. Hence it may not be an appropriate pathfinder element for Au in the study area.

The regolith mapping techniques devised for the study can be used to map complex regolith terrains. The landscape evolution model developed for the area will provide useful insight into the irregular distribution of the regolith and help in designing exploration techniques suitable for the Lawra belt and similar complex regolith terrains of the savannah regions.

Acknowledgements

Funding for this PhD research was made possible by WAXI/AMIRA working on the exploration successes for consortium of Mineral Industries in West Africa. Additional funding also came from the College of Science and Engineering at the University of Leicester and the Government of Ghana through the universities staff development funds via GETFund. Azumah Resources Ltd., an exploration company working in the study area also supported the research by funding the ICP-MS and FA-AAS analyses at a commercial laboratory.

However this thesis would have remained a dream despite the availability of funds, had it not been the advice, support and encouragement of Dr. Gawen Jenkin. For the duration of the PhD he has pushed me, improved me and made me a better researcher and a scientist. I see him as my mentor and wish he extends it to my home University in Ghana to mentor my colleagues.

Prof. Mike Petterson and Dr Dickson Cunningham's passion for the successful outcome of the research cannot be overemphasised. Their unrivalled optimism and enthusiasm in the research kept the thesis to this standard. Without their cooperation with Dr Gawen Jenkin, I might have given up at some point. Please I duly salute you ALL and accept my greatest appreciations.

The following scholars that I consider as my managers; Dr Charles Butt of CSIRO Fellow, Perth, Western Australia, Dr Eric Grunsky of Canadian Geological Survey and Dr Mark Jessell of IRD, France, made available their time, support in a number of ways to get the research to this appreciable end, it gives me utmost pleasure to thank you profusely in my quest of knowledge. Special thanks also go to my friend Prof. Prosper, M. Nude, he has been the captain of my academic life and a motivator. Thanks brother for your encouragement.

The technical officers and analytical staff in the Department of Geology all provided their time and expertise to help me with this project. I am greatly indebted to Nick Marsh, Rob Kelly, Colin Cunningham, Rob Wilson and Cheryl Haidon. A number of faculty members at the Department of Geology have also provided helpful discussion too – thanks to you Mike Norry and Jan Zalasiewicz. There are so many people that

contributed on my way but might not be able to name them all- I say big thank you to all.

It will be unusual if my family is not acknowledged. My wife Comfort Arhin and children kept praying for my success, my Uncle Agyenim Boateng and wife made sure I was secured and safe in the UK and my brother-in-law Kwame Ampofo Borley and family kept reminding me about my mission in the UK. I'd like to thank you All.

Finally, I'd like to thank you my mother-Maame Amma Agyeiwaah. My achievement today is from you and all the great things happening to me today has made possible by you.

Emmanuel Arhin

University of Leicester, March 2013.

Table of Content

Abstract ii

Acknowledgements iii

1.0 Introduction 1

1.1 Problem statement 4
1.2 Background.....6
1.3 Objectives 8
1.4 Thesis Structure 8
Location, Geology, Regolith, Mineralogy and Geochemistry of Gold Deposits in the Birimian Greenstone Belts of Ghana 10

2.0 Introduction 10

2.1 Regolith and climate of Study Area 10
2.1.1 Regolith of study area 10

2.1.2 Climate and rainfall 11

2.2 Location, geological setting and regolith 11
2.2.1 Geology of West African Craton 11

2.2.2 Geology of Ghana 13

2.3 Mineralisation and geology of Kunche-Bekpong and Sabala areas 16
2.3.1 Mineralisation and geology of Kunche-Bekpong 16

2.3.2 Mineralisation and geology of Sabala 19

2.4 Gold mineralisation 19
2.5 Gold mineralisation geochemistry in the Birimian belts of Ghana 20
Literature Review: Gold exploration in NW Ghana and regolith implications for exploration in complex regolith environments 22

3.0 Introduction 22

3.1 Regolith formation, evolution and characterization 22
3.1.1 Regolith 22

3.1.2 Regolith formation and processes 23

3.2 Transfer of elements during weathering 27
3.2.1 Mechanism of element transport from source mineralization. 28

3.3 Factors affecting metal mobility in the regolith 31
3.3.1 Gold in regolith. 34
3.3.2 Geochemistry and mobility of gold.....34
3.3.3 Gold mobility during lateritic deep weathering 35
3.4 Effects of complex regolith on gold exploration.....37
3.5 Arsenic in the regolith 42
3.5.1 Mobility of As in the regolith.....42
3.6 Exploration problems in tropically weathered terrains.....43
3.7 Regolith expressions in gold deposits in complex regolith environments – some case studies.....44
3.7.1 Bounty gold deposit. 45
3.7.2 Cornishman gold deposit.....46
3.7.3 Filon Bleu prospect 47
3.8 Historical Exploration surveys in the Lawra belt, Ghana.....50
3.9 Conclusion.....52
Profile terminology 53
Glossary of Terms.....53
Regolith Research Methods 55
4.0 Introduction 55
4.1 Regolith mapping 55
4.2 Regolith map processing by integration model 58
4.2.1 Landscape or pre-field stage classification 58
4.2.2 Genesis classification 60
4.3 Regolith Stratigraphy.....61
4.4 Regolith geochemistry and profile characterization.....74
4.4.1 Sampling and sample preparation 75
4.4.3 Disaggregation and homogenization.....80
4.5 Analytical Methods.....81
4.6 Quality control and quality assurance (QA/QC) 82
Regolith map making of deeply weathered terrains in the savannah regions of the Birimian Lawra belt of Ghana, West Africa 83

5.0 Introduction 83

5.1 Objective 83

5.2 Data and methods 83
5.2.1 Data 83

5.2.2 Methods 84

5.3 Regolith map making 84

5.3.1 Landscape classification 85

5.3.2 Genesis classification 100

5.4 Discussion 111
5.4.1 The regolith 111

5.4.2 The role of regolith mapping in gold exploration surveys in complex regolith regions. 112

5.5 Conclusion 113
Evolution of Regolith and Landscape in the Lawra Belt, NW Ghana 115

6.0 Introduction 115

6.1 Geomorphology 115
6.1.1 Regolith of the Study Area 116

6.2 Field observations 126
6.2.1 Ferruginous duricrust, relief inversion and landscape evolution of the Lawra belt 128

6.3 Discussion 130
6.4 Landscape evolution model of Lawra belt 135
6.5 Conclusion 137
Geochemical dispersion of gold (Au) and other associated elements in the regolith of the Lawra belt 139

7.0 Introduction 139

7.1 Methods and data analysis 139
7.1.1 Pitting and regolith unit sampling 140

7.1.2 Laboratory analysis of samples using ICP, XRF and FA-AAS 140

7.2 Quality assurance and control (QA/QC) of analysed samples 143
7.3 Results 150
7.3.1 Surface regolith and pit locations.....150
7.3.2 Regolith distribution with depth.....151
7.3.3 Behaviour of selected major and trace elements in the regolith analysed by XRF method.....158
7.3.4 Data analysis 166
7.3.5 Pit by pit interpretation of element mobility in regolith.....177
7.4 Discussion.....184
7.4.1 Major oxides in the regolith 184
7.4.2 Trace elements - high field strength oxides (HFSE) in the regolith.....189
7.4.3 Characterizing and identifying regolith materials using major oxides ..194
7.4.4 Behaviour and relationship between Au and (±Ag or As) in regolith profiles in the study area 194
7.5 Summary and conclusion.....200
Use of regolith geochemistry to delineate gold mineralisation under cover: a case study in the Lawra belt, NW Ghana.....202
8.0 Introduction 202
8.1 Regolith and geochemical gold exploration in areas under cover.....204
8.2 Methods 205
8.2.1 Threshold gold value estimation 206
8.3 Levelling and gridding methods 211
8.3.1 Levelling.....211
8.3.2 Gridding methods.....212
8.4 Results 213
8.5 Gold anomaly delineation in savannah regions: a case study of the Lawra belt 217
8.6 Discussion.....228
8.6.1 Identifying geochemical gold anomalies.....229
8.7 Conclusions 230

Thesis conclusion 232

9.0 Limitations of thesis 232

9.1 Conclusion.....232

9.2 Future outlook.....233
Appendix A: Regolith landform mapping codes 234
Appendix B: Sample preparation protocols for the XRF analysis at the University of Leicester, Geology Department, UK., ICP-MS and ICP-AES techniques……...235
REFERENCES.....238

List of figures

Fig. 1.1 World gold production distributions per producing countries……1

Fig. 1.2 Geology of Ghana and location of the Lawra belt studied ……..3

Fig. 2.1 Climate data of the Lawra belt……11

Fig. 2.2 Simplified geology of the Man Shield .....……...13

Fig. 2.3 Detailed geology of the Lawra belt……16

Fig. 2.4 Gold mineralisation trends in Kunche and drill-hole collars……..18

Fig. 3.1 Typical regolith section across a landscape……..…….23

Fig. 3.2 Typical regolith profiles in savannah and rainforest regions of Ghana……..24

Fig. 3.3 Typical laterite regolith profile ……..25

Fig. 3.4 Schematic of element mobility in savannah regions, showing processes and mechanisms of transport from primary mineralisation into the regolith profile……....30

Fig. 3.5 Processes and migrations of elements from primary mineralisation into the regolith profile……..31

Fig. 3.6 Dispersion halo characteristics of mineralization from primary mineralisation to the regolith……..33

Fig. 3.7 Gold in the top 20-30 m of the regolith section along 35000mN of the Bounty deposit, Australia……...46

Fig. 3.8 Gold dispersion in the regolith at the Cornishman gold deposit along traverse 4912mN……46

Fig. 3.9 Summary of the ore-associated element distribution at the Cornishman gold deposit along traverse 4912mN…….47

Fig. 3.10 Different element distributions in a complex regolith along a traverse CD at Filon Bleu Prospect, Guinea……48

Fig. 4.1 Ghana map showing1: 450000 regolith mapping area shaded grey……56

Fig. 4.2 Lawra belt (grey) and1: 5000 scale regolith mapping areas (shown white)……..57

Fig. 4.3 The 3- step computer based processes in developing regolith terrain map (RTM) in GIS interface……..58

Fig. 4.4 Pit locations at Kunche-Bekpong……...63

Fig. 4.5 Kunche geology……..64

Fig. 4.6 Pit locations at Sabala……65

Fig. 4.7 Sabala regional geology……..66
Fig. 4.8 Examples of horizon development and terminology of deep weathering profiles……67
Fig. 4.9 Graphical pit log sheet used during regolith pit logging and mapping of the regolith profile……..68
Fig. 4.10 Smooth and rounded quartz pebbles and recent terrestrial sediments: evidence of transportation of regolith materials: Environments like these are classified under depositional regime in the FRED classification scheme……....70
Fig. 4.11 Rounded and smooth quartz clasts in laterite: evidence of transportation - this is a clasts-supported transported laterite located near pit SP002 with coordinate 518995E/1143689N……..71
Fig. 4.12 Older laterite embedded in a younger laterite: a suggestion of episodic deposition. The area represents depositional regime……71
Fig. 4.13 Slabby-form laterite demonstrating evidence of episodic deposition: a typical example of transported laterite……..72
Fig. 4.14 Equigranular laterite with a pock-marked surface: This laterite was mapped as residual laterite or duricrust……73
Fig. 4.15 Residual regolith portraying obscured unconformity and angular- to sub-angular quartz clasts: demonstration of relict regolith……74
Fig. 4.16 Sample regolith mapping template for humid tropical regions……76
Fig. 4.17 Sample soil log-sheet……76
Fig. 4.18 A typical vertical panel sample collection at 10 cm intervals of a well-lithified regolith profile. Sample spacing is marked by the nails and white rectangle shows panel sampling dimensions……77
Fig. 4.19 Sample preparation at the field camp. Samples are sieved to <2 mm size fraction……79
Fig. 4.20 Sample splitting stages in the field: a). manual sample homogenization in plastic bag, b) clump disaggregation and oversize removal, c) sample splitting, and, d) library and laboratory samples bagging……..80
Fig. 4.21 Sample preparation flowchart……81

Fig. 5.1 Conceptual SRTM/DEM model used for the landscape classification mapping to delineate residual and transported regolith and also for the extrapolation of semi-residual areas……...87

Fig. 5.2 Residual areas digitally demarcated by gridding topographic AutoCAD elevations from the DEM image assuming points between 100-300 m to be residual……...88

Fig. 5.3 Drape of digitally interpreted residual areas on DEM imagery. This image highlights some problems associated with the use of basic topographic maps in defining residual areas……..90

Fig. 5.4 Edited residual areas derived from a combined map overlay of the AutoCAD elevations contour map and the DEM imagery……91

Fig. 5.5 90 m pixel SRTM-colour digital image of the Lawra belt used to delineate the depositional areas…….92

Fig. 5.6 Depositional areas digitally interpreted from SRTM imagery……..93

Fig. 5.7 Combined map of residual and depositional areas generated during the landscape classification processes……..94

Fig. 5.8 Interpreted regolith-landform terrain map (RTM) produced from landscape classification for the Lawra Birimian belt…….95

Fig. 5.9 **A.** Ortho-rectified and B. processed three band colour composite Landsat imagery of NW Ghana and part of Burkina Faso……....97

Fig. 5.10 Three band gamma-ray ternary image of the study area……100

Fig. 5.11 Ground truth coverage showing regolith sites, accessible tracks and roads of the study area…….101

Fig. 5.12 Plot of regolith mapping units showing the three main coded components of landform unit, regolith material unit and surface modifier……104

Fig. 5.13 Digitized factual genesis classification map produced from ground truth mapping……106

Fig. 5.14 Unusual regolith regimes classified to occur in a wrong place in the landscape from the image processing. For example a relict regime is inferred in an active stream channel, arrowed……107

Fig. 5.15 Map overlays of landscape and genesis classification maps towards the development of final regolith map of Lawra belt……108

Fig. 5.16 Final regolith map developed for the Lawra Birimian Belt…….….109

Fig. 5.17 Spatial regolith-coverage analysis of different regolith-domain estimates from the regolith map……...110

Fig. 5.18 Regolith type land coverage (%) in the Lawra belt…….111
Fig. 6.1 Simplified geological map of the West African Craton……...117
Fig. 6.2 Residual laterite: massive ferruginous duricrust with a pocked-marked surface capping a rounded hill with a flat top……...118
Fig. 6.3 Ferricrete: Fe oxide-cemented colluvial and alluvial sediments including quartz clasts, ferruginous nodules, pisoliths and lithic ferruginous saprolite fragments derived from erosion of residual lateritic regolith……..119
Fig. 6.4 Ferricrete: detrital quartz clasts-supported Fe oxide-cemented colluvial and alluvial sediments that include pisoliths. Smooth and rounded quartz clasts are evidence of distal sediment transport……119
Fig. 6.5 Pisolithic laterite covering hundreds of square metres…….120
Fig. 6.6 Fe oxide-cemented colluvial and alluvial sediments with rounded and sub rounded quartz clasts on top of moderate to high pediment compared to the adjacent landscape……..120
Fig. 6.7 Gradational and soft regolith contact between different layers in a residual regolith profile at Kunche. The interval between the vertical nails is 10 cm……...121
Fig. 6.8 Rock debris overlying saprolite in Kunche area, exposed in an old artisanal mine site…….123
Fig. 6.9 Composite regolith profile in erosional regime: an unconformity marked red and presence of smooth, rounded and sub rounded quartz pebbles are evidence of regolith evolution…….123
Fig. 6.10 Transported overburden overlying ferruginous saprolite with sub-rounded transported lateritic crust embedded in silty sand layer. The profile surface is greyed because of the milky influx water……125
Fig. 6.11 Compound regolith profile near Bekpong River at Kunche-Bekpong depositional regime: unconformity and multiple layers in the fluvial sediments are evidence that the regolith has evolved and still evolving……125
Fig. 6.12 Fluvial deposited sediments at a floodplain of an active stream in the Sabala area……...….126
Fig. 6.13 Depositional regolith materials with a gravel lens between colluvium and saprolite in the Kunche-Bekpong area: landform shows partial

truncation and reworked quartz clasts; a demonstration of proximal transport of sediments……...126

Fig. 6.14 Diagrammatic illustrations of relief inversion in Lawra area: A–D shows the changes during relief inversion in the Lawra study area……130

Fig. 6.15 Summary representation of typical modified land surface changes over long periods of regolith/landform evolution in the study ……132

Fig. 6.16 A). Regolith map of part of the study area. B). Grid profile showing the interrelationship between regolith units and elevation along line AB. AutoCAD elevations extracted from a digital topographic map of northern Ghana used……134

Fig. 6.17 Landscape evolution model of the Lawra belt……..136

Fig. 6.18 The successive planation surfaces of sub-Saharan West Africa……...137

Fig. 7.1 Accuracy and precision of the analytical Au data compared with the CRM data. The blue solid line indicates accuracy of data, red dashed lines indicate precision field around the best-fit line……145

Fig. 7.2 Scatter diagram showing the measure of dispersion around the mean and the per cent standard deviation……147

Fig. 7.3 E-W cross section along L1149550N, pits shows the variations in regolith profiles in Kunche-Bekpong area……153

Fig. 7.4 E-W cross section along L1148600N, pits shows the variations in regolith profiles in Kunche-Bekpong area……154

Fig. 7.5 Schematic regolith cross-section along L1148600N in the Kunche-Bekpong area. Vertical scale exaggerated for clarity……...156

Fig. 7.6 E-W cross sections along L1143100N and L1143500N, pits show the variations in regolith profiles in Sabala area……157

Fig. 7.7 Distribution and geochemical patterns of Au (FA-AAS) and selected major and trace elements analysed (XRF) for pit KP009 in ferruginous regime at Kunche-Bekpong……..160

Fig. 7.8 Distributions of geochemical patterns of Au (FA-AAS) and selected major and trace elements analysed (XRF) for pit KP009 in ferruginous regime at Sabala……161

Fig. 7.9 Distributions and geochemical patterns of Au (FA-AAS) and selected major and trace elements analysed (XRF) for pit KP008 in ferruginous regime at Kunche-Bekpong……..162

Fig. 7.10 Distributions and geochemical patterns of Au (FA-AAS) and selected major and trace elements analysed (XRF) for pit KP003 in ferruginous regime at Kunche-Bekpong……..163

Fig. 7.11 Compositional variability of regolith in terms of metal wt. % of Mg/Al versus K/Al. Rectangles show different classes of regolith materials (after McQueen, 2006).....164

Fig. 7.12A Regolith geochemical data plot showing variations in elements in the regolith profile from upper soils to the saprolite in ferruginous regolith…….……167

Fig. 7.12B Regolith geochemical data plot showing variations in elements in the regolith profile from upper soils to the saprolite in ferruginous regolith…**……..**168

Fig. 7.13A Regolith geochemical data plot showing variations in elements in the regolith profile from upper soils to the saprolite in ferruginous and modified erosional/transported regolith regimes. …….……...169

Fig. 7.13B Regolith geochemical data plot showing variations in elements in the regolith profile from upper soils to the saprolite in ferruginous and modified erosional/transported regolith regimes…….. ……...170

Fig. 7.14 Relationship between As and Ag with Au in the regolith profile. …...173

Fig. 7.15 Relationship between Au, Ag and As along L1149550N in Kunche-Bekpong regolith: plot displays geochemical element patterns in the regolith profiles…..……....174

Fig. 7.16 Relationship between Au, Ag and As along L1148600N in Kunche-Bekpong regolith: plot displays geochemical element patterns in the regolith profiles. High As correlates well with relatively high Au in KP010……..….175

Fig. 7.17 Relationship between Au, Ag and As in Sabala regolith: plot displays geochemical element patterns in the regolith profiles……. 176

Fig. 7.18 Concentrations of selected elements (ppm) except Au (ppb) with depth (cm) in residual laterite at Kunche-Bekpong area……178

Fig. 7.19 Concentrations of selected elements (ppm) except Au (ppb) with depth (cm) in ferruginous regime at Kunche-Bekpong area……..179

Fig. 7.20 Concentrations of selected elements (ppm) except Au (ppb) with depth (cm) at Sabala: A) pits in residual laterites and B) pits in transported laterites……..180

Fig. 7.21 Concentrations of selected elements (ppm) except Au (ppb) with depth (cm) in relict regime at Kunche-Bekpong area..……...182

Fig. 7.22 Concentrations of selected elements (ppm) except Au (ppb) with depth (cm) in semi residual regime at Kunche-Bekpong……...183

Fig. 7.23 Comparison of A). Some major elements and B). Some trace elements in potential source rocks and regolith in some pits in the study area. SB and VB are Birimian sedimentary and volcanic rocks……185

Fig. 7.24 Selected major oxides (%) plots with depth (m) in Kunche-Bekpong and Sabala dugout pits……187

Fig. 7.25 Concentrations of high field strength elements (HFSE) in regolith samples with depth……...192

Fig. 7.26 Concentration ratios of high field strength elements (HFSE) in regolith samples with depth……...193

Fig. 7.27 Concentrations of Au, Ag and As in KP010 to establish the behaviour of these selected elements in the regolith profile… ……196

Fig. 7.28 Relationship between the lower regolith anomalies and mineralisation in Kunche/Bekpong on As/Au plot. Mottled zone, saprolite and sap rock samples are from the current research. ……..199

Fig. 8.1 Grid image map of surface Au geochemistry in the Lawra belt. The high and low Au concentration areas are shown by red and blue colours respectively……...203

Fig. 8.2 Geology and bedrock mineralisation of Kunche-Bekpong area……...204

Fig. 8.3 Gold distribution plot for the ferruginous regime showing a). Frequency-histogram and b) Probability plot for orientation surface geochemical assay results……..208

Fig. 8.4 Gold distribution plots for the relict regime showing a). Frequency-histogram and b) Probability plot for orientation surface geochemical assay results……..209

Fig. 8.5 Gold distribution plots for the erosional regime showing a). Frequency-histogram and b) Probability plot for orientation surface geochemical assay results……..209

Fig. 8.6 Gold distribution plots for the depositional regime showing a). Frequency-histogram and b) Probability plot for orientation surface geochemical assay results…….210

Fig. 8.7 Gold contour map of the Sabala target area……..214

Fig. 8.8 Contour map defining target sizes from different thresholds across the different regolith domains at Kunche-Bekpong……...216

Fig. 8.9 A). Surface Au grid using IDW method in ferruginous regime B). Application of defined threshold for ferruginous regime to define prospective anomalies……...218

Fig. 8.10 A). Surface Au grid using IDW method in relict regime B). Application of defined threshold for relict regime to define prospective anomalies……..220

Fig. 8.11 A). Surface Au grid using IDW method in erosional regime B). Application of defined threshold for erosional regime to define prospective anomalies……...224

Fig. 8.12 A). Surface Au grid using IDW method in depositional regime B). Application of defined threshold for depositional regime to define prospective anomalies……...225

Fig. 8.13 A). Merged surface Au grid of different anomalies in different "FRED" regolith domains B). Definition of anomalies regarding regolith implications on Au mobility in surface regolith……...227

List of tables

Table 3.1 Element mobility during deep weathering under humid conditions……28

Table 3.2 Some geochemical exploration problems and opportunities in deeply weathered terrain……36

Table 3.3 Gold deposits in Australia using geochemistry and regolith studies…..49

Table 3.4 Gold discoveries in West Africa using geochemistry and regolith studies…….....50

Table 4.1 Types and properties of remote sensing data used (WAXI-IRD internal data base)…… ……...58

Table 5.1 Types and resolutions of remote sensing data used in the study…….....84

Table 5.2 Sample record mapping sheet for Genesis classification…….103

Table 5.3 Typical regolith mapping log-sheet used for the Lawra belt genesis classification survey……104

Table 7.1 Analytical limits for data obtained by ICP-MS (ME-MS41) and FA-AAS Au-AA24) analytical protocols……143

Table 7.2 Analytical accuracy and precision of analytical Au and CRM-Au used for the analytical quality of the analysis of Au by FA-AAS technique……...147

Table 7.3 Results of blank samples inserted in batch of samples to monitor analytical contamination……...148

Table 7.4 Relationship between the original and field duplicate results for Au by Fire assay analytical method…….149

Table 7.5 Analytical accuracy and precision of analytical Cu and CRM-Cu used for the analytical quality of the analysis of other elements by ME-MS41 technique……151

Table 7.6 Location of dugout pits in the surface regolith types in Kunche-Bekpong……152

Table 7.7 Location of dugout pits in the surface regolith types in Sabala……143

Table 7.8 Major element (%) and trace element (ppm) XRF data of regolith samples from pits KP003, KP008, KP009 and SP003…….159

Table 7.9 Summary of major element results and averages for different regolith domain units……..165

Table 7.10 Major and trace element contents comparisons in source rocks and the regolith. The granitoids, Birimian sediments and volcanic rocks are averages of two analytical results…….188

Table 7.11 Leach composite sample head assays at the Wa-Lawra gold project (NI-101-43, April 2012 report of Azumah Resources Ltd.) compared with some Au and As results in current study……..198

Table 8.1 Thresholds using mean plus two standard deviation (μ + 2SD), probability plots and experiential method or thresholds estimation incorporating regolith effects on gold mobility……...211.

Introduction and Problem Statement

1.0 Introduction

West Africa, in particular Ghana has produced gold since ancient times (Griffis et al., 2002). In Ghana gold (Au) is among the leading export commodities (Kesse, 1985) and has accounted for as much as 3.5% of the entire world's gold production in 2009 (McKeith et al., 2010). Compared to the other gold producing countries in the world, Ghana's contribution between 1990 and 2009 is low (Fig. 1.1). However 35% of Ghana's gross domestic production (GDP) depends on the gold production. Therefore with decline of gold discoveries over the past two decades (Blain, 2000; Hronsky, 2009; Mckeith et al., 2010) the sustainability of gold industry will be in a balance. This decline may be due in part to the wholesale transfer of conventional geochemical exploration methods developed elsewhere. These conventional exploration methods are best suited to areas with outcrop and generally homogeneous regolith areas. In the Lawra belt of Ghana (Fig. 1.2), which is characterised by complex regolith, reported cases of gold occurrence have been published, but no major gold discovery has been developed into a mine to date (Griffis et al., 2002; Griffis and Agezo, 2000). The conventional exploration methods have proved less successful in detecting mineralisation (Arhin and Nude, 2009) because the implications of the regolith forming the complex overburden to element dispersions are not understood.

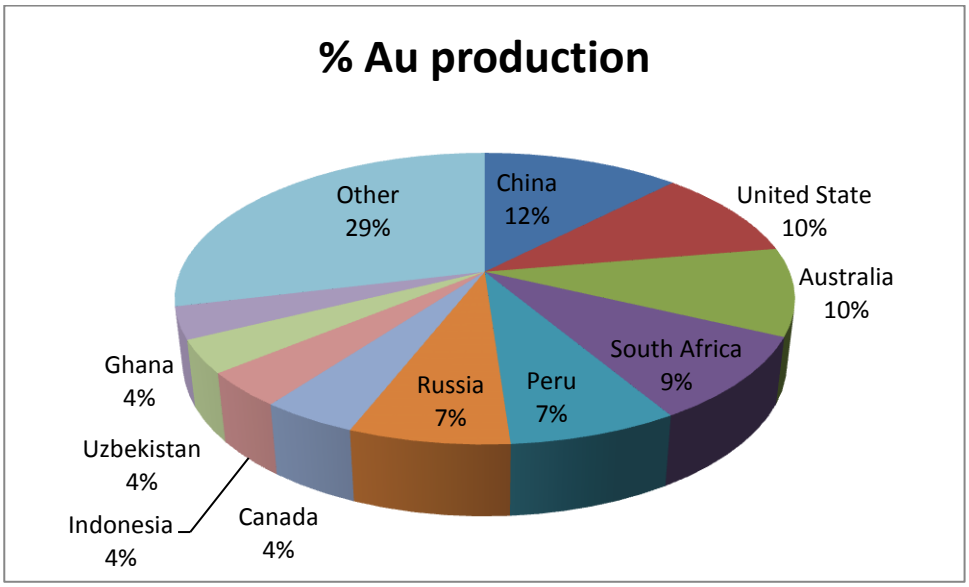

Fig. 1.1 World gold production distributions per producing countries (McKeith et al., 2010)

Elsewhere in the world, especially in Western Australia, regolith materials have increasingly been effectively used within exploration programmes for targeting geochemical anomalies (e.g. McGeogh and Anderson, 1998; Lintern and Sheard, 1999; McQueen et al., 2002) regardless of the regolith complexities. The contrast is that in the Lawra belt within the savannah regions of Ghana, the complex regolith poses problems to successful exploration because little information is available on the characteristics of regolith. However, as indicated by Butt (2004), the easy-to-find mineralisation in less complex regolith environments has been discovered by the conventional exploration approach. The insufficient knowledge of the Lawra belt regolith has led to the disregard of regolith evolution implications on geochemical data interpretation. Therefore to effectively and efficiently delineate mineralisation in the Lawra belt and similar areas in West Africa the surficial geochemical exploration methodology should embrace regolith studies that take into account the regolith evolution and its implication to exploration in complex regolith terrains.

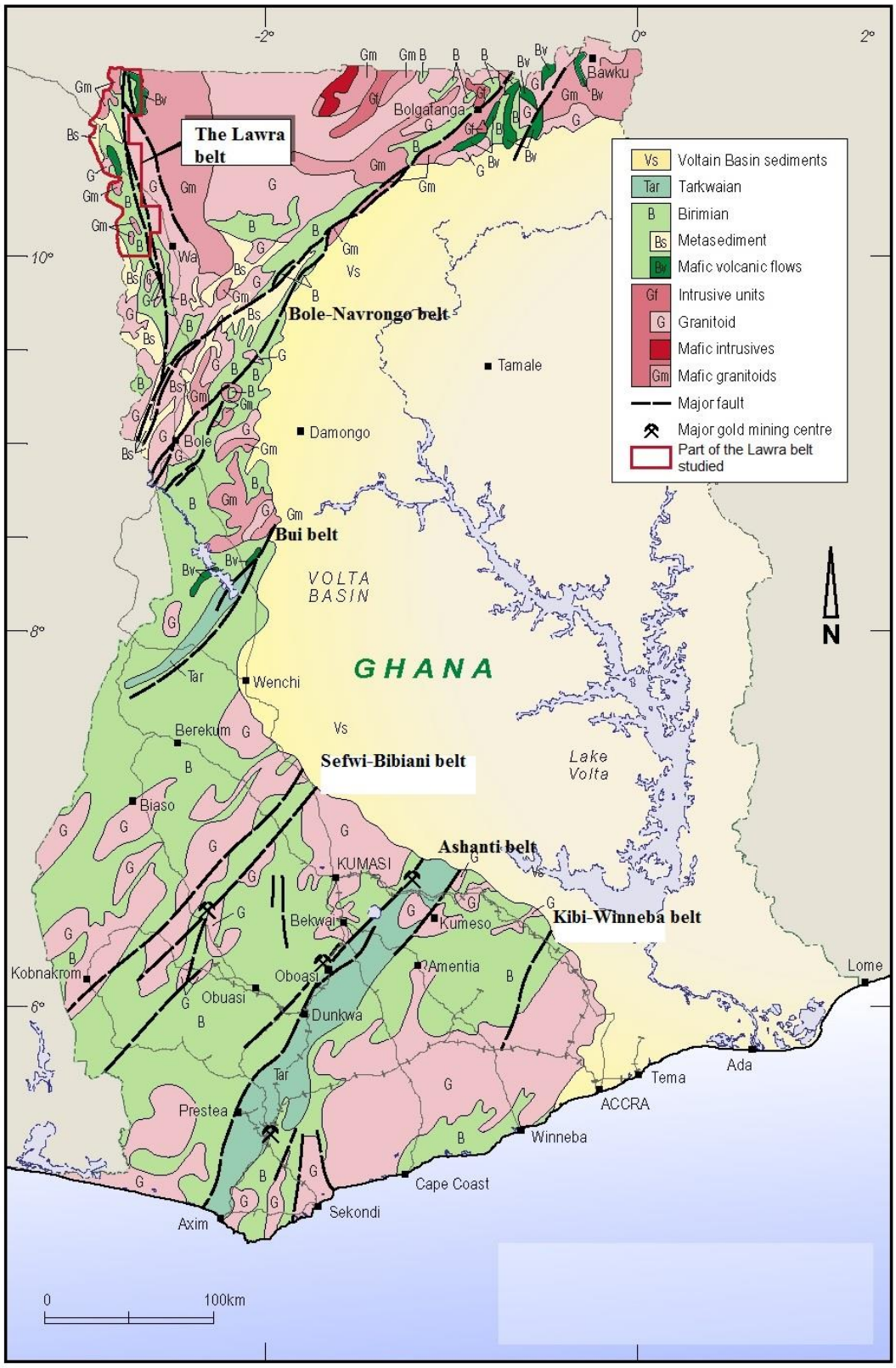

Fig. 1.2 Geology of Ghana and location of the Lawra belt studied (Ghana Geological Survey Map, 2009).

1.1 Problem statement

The surface regolith layers at the Lawra belt are irregularly distributed and have variable compositions. The complexities of the regolith due to the erratic spatial distributions have implications on geochemical exploration. For example gold –poor regolith materials transported and deposited over anomalous areas dilute the underlying anomalies underneath them during surface samples. Erosional surfaces associated with mineralisation shows enhanced anomalies that effect the selection of threshold gold estimates. Griffis et al. (2002) report about exploration methods used by companies that conducted systematic gold exploration indicates their lack of understanding of the regolith environment. The earlier mineral explorers considered the sampled media as confined to one type of regolith material and not to a heterogeneous regolith. However, work by Arhin and Nude (2009) suggests heterogeneous regolith characterises the area. Therefore collecting samples at a fixed depth of up to 40 cm (Griffis et al., 2002) may result in samples being collected from either pre-existing preserved surfaces or newly formed present surfaces consisting of regolith materials of diverse sources. For **e**xample, it is difficult to collect all samples from the upper soil layer without collecting some from other regolith units consisting of laterite, clays and saprolite etc. In addition to this problem the wholesale transfer of successful exploration techniques from homogeneous regolith environment to an environment characterised by heterogeneous regolith may yield results not appropriate for the area. Typical example is the inappropriate selection of threshold gold values, sample media, sample depths and sample spacing. Therefore gold exploration methods that have been successful in discovering gold deposits elsewhere must be reviewed based on the regolith environmental conditions as the complexity of the regolith may influence the geochemical dispersion patterns. The climate, regolith and landscape evolution in the study area are different from southern Ghana where the regolith is homogeneous. The rapid changes in the regolith in the Lawra belt are due to the different processes causing the evolution of the landscape compared to southern Ghana. Therefore, interpreting geochemical data from different regolith materials (consisting of soils, mottled clays, laterite, saprolite etc.) thought to be only from upper soils may generally lead to false and misleading interpretations.

Though Ghana is a major gold producer that has produced over 148 million fine ounces of gold since documentation of gold production started in 1880 (Kesse, 1985; Griffis et

al., 2002) and although the gold occurs in the early Proterozoic Birimian and Tarkwaian rocks that crop out in the south of the country and extend up to the north covering over 45% of the land surface, the bulk of Ghana's gold comes from mines that are located in the tropical rainforest belts of central and south western Ghana (Griffis et al., 2002, Kesse, 1985) with no substantial gold production from the northern part of the country. Though the gold occurrences on the Lawra belt were reported as far back as 1935 (Junner, 1935; Griffis and Agezo, 2000) and since then, many gold exploration companies have sought for gold in the area without success. The lack of success in finding workable gold deposits in this area may be attributed to the wholesale transfer of exploration techniques that have been successful in the tropical rainforest belts of central and south western Ghana to the savannah north without modification (Pobedash, 1965; Roudakov, 1965; Hanssen, 1994) and the lack of understanding the regolith environment. However when similar problems were encountered in Kalgoolrie in Western Australia, (Butt and Zeegers, 1992); in French Guiana (Freyssinet, 1994); at Banankro gold prospect in southern Mali (Butt and Zeegers, 1992; Freyssinet, 1987); in southern India (Santosh and Omana 1991); Siguiri mines and Louro prospect in Guinea (Butt and Zeegers, 1992); Syama and Sadiola mines in Mali (Butt and Zeegers, 1992), they were resolved by classifying and characterizing the regolith and using those factors in designing exploration programmes. A similar approach will yield positive results in northern Ghana.

Regolith-landform mapping is an essential first step, followed by characterization of the regolith materials themselves (Anand and Pain, 2002). It appears the exploration companies that worked in the area did not use regolith-landform maps to interpret the gold geochemical data. In addition there are no exploration models that describe the geochemical pathways and ore-related elements that act as pathfinder elements for gold in a low concentration gold environment (Bradshaw, 1975; Butt and Smith, 1980; Butt and Zeegers, 1992). Bolster (1999) and Butt and Zeegers (1992) accordingly have reported the increasing emphasis on regolith landform mapping, using a combination of remote sensing procedures, followed by field checks to interpret surficial geochemical data. Such regolith landform mapping prior to the execution of the geochemical survey to aid in sample media selections and selection of thresholds are not done. The integration of these maps and their superimposition onto the geochemical maps can deliver inventories of surface materials, interpretable in terms of weathering styles and

geomorphologic processes, but will require field inspection prior to providing definitive exploration guides.

1.2 Background

The presence of transported regolith commonly dilutes and renders unreliable the expression of trace elements including gold from mineralised bedrock or in situ regolith to the surface, especially in semi-arid to arid terrains (Mokhtari et al., 2009). But successful geochemical exploration requires the ability to detect reliable anomalies from complex regolith (Arhin and Nude, 2009). This is of paramount importance in geochemical exploration because evolution of the regolith can alter the anomalous concentrations of gold from the underlying mineralisation. For instance, if the regolith is dominated by transported materials and characterised by barren sediments/rocks, the gold content will decrease in concentration from the mineralised source. The dilution of gold content from the mineralised source can decrease until parts per billion (ppb) level by the transported or ferruginized regolith, which may appreciably exceed the normal background level of the enclosing rocks. As indicated by Butt and Zeegers (1992), the transported sediments dilute the gold concentrations of underlying gold mineralisation along its trail.

However the general protocol of soil survey in the homogeneous regolith environment in southern Ghana is dry, sieve and analyse for gold content (Griffis et al., 2002). Because of the wholesale transfer of technology, this protocol of soil survey is the norm in the heterogeneous regolith environment of northern Ghana. All these affect the gold anomaly detection in lateritized environments in similar fashion to the transported overburden diluting anomalies from the core primary halo. Furthermore, the truncation of the pre-existing surfaces during erosion may also destroy the broad geochemical haloes converting them to narrow geochemical targets that are often treated as spot high anomalies and not followed up. However, challenges posed by complex regolith have been reversed to advantage and have been used to detect mineralisation hidden under cover instead. A typical example of such an area is Australia, where significant gold discoveries were found using regolith maps to guide dispersion mechanisms and also used in suggesting new approaches to sampling techniques (Butt and Zeegers, 1992). The understanding of the regolith in that area, which was captured and represented as a regolith map, has been used to interpret geochemical data over large areas. The regolith

studies in Australia therefore highlighted the significance of having a regolith map as it provided the ability to understand the weathering and geomorphic histories of the blanketing materials and to clearly distinguish transported materials from residual regolith. The identification of rapid changes in the regolith geology, their applications in geochemical surface sampling and the incorporation of evolved regolith factors into the geochemical data interpretation led to many gold discoveries in Australia (Butt and Zeegers, 1992).

However in the savannah regions of Ghana, conventional geochemical exploration expeditions have met with limited success. The conventional geochemical survey is a stepwise method of conducting geochemical surveys where samples are taken first from stream sediments, followed by soils, trenching and drilling in defining anomalous targets. The conventional geochemical survey ignores the regolith complexities and assumes the surface regolith is homogeneous (Arhin and Nude, 2009). As indicated by Arhin and Nude (2009) ferruginous and depositional regolith materials are abundant and widespread in the Lawra Birimian belt of northwest Ghana; they have been unsuccessful as sample media in gold exploration because of a lack of understanding relating to regolith-genesis. It may thus be a worthwhile venture to adopt the Australian strategy for the savannah regions of Ghana. Though earlier explorers made some discoveries, they were not significant enough to merit further exploration and operations were abandoned. However in 2009 a new set of geochemical sampling programmes and re-assessment of the historical data was started by Azumah Resources, an Australian company. The recent Au discoveries by Azumah Resources Ltd., in the Lawra belt were discovered because the company conducted regolith mapping to understand the regolith environment and also used geophysical surveys to support information obtained from surface geochemistry in gold anomaly delineation (Waller et al., 2012). Pit digging, auger and aircore drilling were as well carried out by Azumah Resources in areas of poor exposures for geochemical sampling and bedrock geology mapping. In total 51680 soil samples and 228673 m of auger and aircore drilling were carried out. Their work highlighted the significant role of regolith geology in controlling gold anomalies and showed that geochemical targeting in the Lawra belt was fundamentally compromised without regolith control (Stone, 2009 - Azumah internal report, unpublished). Azumah Resources Limited digitally processed remote sensing data to generate a regolith terrain map (RTM). However, there was no ground

truth mapping to validate the transported regolith and residual areas derived from the processed digital imagery: the regolith terrain map though, was able to reveal more geochemical targets that led to the improvement of the existing gold resources. The review of Au exploration by Azumah Resources confirms the favourable Au prospectivity with a genuine potential for Mineral Resource expansion beyond the latest declared Mineral Resource inventory of 19.7Mt @ 1.6 g/t Au, for 1.0 Moz gold (Measured and Indicated) and 14.8 Mt @ 1.4 g/t Au for 659000 oz gold (Inferred, Waller et al., 2012).

1.3 Objectives

The principal objective of the research is to substantially improve geochemical methods of exploring for gold deposits under cover or obscured by weathering in selected areas within Lawra Birimian belt. The following were carried out:

1. Development of a regolith-landform framework for selected areas in Lawra Birimian belt by conducting regolith-landform mapping and characterising regolith profiles.

2. Investigation of the effect of regolith properties on metal migration.

3. Investigation of geochemical dispersion patterns and processes by a series of case studies.

4. Development of appropriate standard methods of regolith mapping that takes into account weathering and geomorphic histories in the region to control exploration geochemistry and geophysics.

5. Develop protocols for sampling appropriate to different regolith types in order to most efficiently define true anomalies.

1.4 Thesis Structure

The thesis is divided into nine chapters. The introductory ***Chapter one*** describes and discusses the lack of exploration successes in the savannah regions of Ghana. It highlights the probable causes of the exploration failures and outlines thematic areas of research that are deemed significant to substantially improve geochemical methods of exploring for gold deposits under cover or obscured by weathering products. ***Chapter 2*** describes the field area and then gives a brief account of the regional geology as well as

an overview of the regolith environment. The mineralogy and geochemistry of gold deposits in the Birimian greenstone belts of West African Craton and Ghana in particular were also discussed in the chapter. ***Chapter 3*** presents a review and discussions of pertinent literature of related work that has been done in deeply weathered terrains. It explains regolith and the evolution of the regolith structure, details of nomenclature, and formation plus how it impacts on surficial geochemistry. It also highlights areas where successful gold exploration was conducted and achieved success through the use of regolith geochemistry. ***Chapter 4*** outlines the systematic methods applied to achieve the set objective. It details the fieldwork and how the regolith map was developed from terrain to genesis classification stages. The chapter bring out its significance in gold exploration at regolith complex environments. ***Chapter 5*** outlines regolith map making and its role in mineral exploration in areas with complex regolith. ***Chapter 6*** investigates regolith evolution and their implications to gold geochemistry. The general implications of the regolith characterisation to geochemical exploration are discussed also in this chapter. ***Chapter 7*** examines the relationship between Au and other elements using assay results obtained from the ICP-MS and FA-AAS and also examined the behaviour of trace and major elements in the regolith profiles from the XRF dataset. Investigations into the determination of the appropriate pathfinder elements for gold exploration are examined. The impact of weathering, erosion and transportation of the weathered rocks and weathered materials and their relative effects on gold geochemistry is considered in this chapter too. ***Chapter 8*** discusses the use of regolith geochemistry in delineating potential gold deposits under cover in savannah regions of Ghana. The crux of the discussions is based on the individual observations and conclusions drawn from chapters 5-7. In particular about the significance of regolith mapping, regolith characterisation and processes, mineral hosts and pathways as well as the use of pathfinder elements in support for gold exploration surveys in deeply weathered terrain. ***Chapter 9*** draws conclusion for the entire study.

Location, Geology, Regolith, Mineralogy and Geochemistry of Gold Deposits in the Birimian Greenstone Belts of Ghana

2.0 Introduction

This chapter provides a brief account of the regional geology of the West African Craton and the study area, the Lawra belt of NW Ghana. It also gives an overview of the climate and describes the regolith setting in the belt. Detailed description of the mineralogy and geochemistry of gold deposits in the Birimian greenstone belts of West African Craton and more especially of Ghana is also provided in this chapter.

2.1 Regolith and climate of Study Area

2.1.1 Regolith of study area

The regolith of the Lawra belt is characterized by a deep weathering profile, which is preserved and truncated at places, and with widespread lateritization that has a surface veneer of pisoliths and depositional cover of exotic origin. Sheetwash deposits cover low-lying areas and some lateritic slopes. The upland areas are generally marked by scree that decreases in fragment size down-slope and the sheetwash areas are characterized by thin layers of colluvium, which are interspersed with alluvial deposits. The topography of the area is generally low, undulating at some places with isolated hills (Arhin and Nude, 2009). Most of the Lawra belt rises gently between elevations of 100 m and 250 m above mean sea level (Meyerton, 1976). The landscape areas that are characterized by lateritic profiles are capped by hardpans. The hill slopes and high pediments are marked by scree, consisting of small fragments of visibly mineralised and altered rock that decrease in fragment size down-slope. Residual laterite or duricrust that occurs at the topographic highs commonly are formed from in situ weathered materials cemented together by Fe-oxide and clay minerals and thus show equigranular groundmass. The transported regolith or ferricrete is found generally at low pediments, low-lying areas and around drainage catchment areas. Ferricrete or transported laterites are widespread at the high and low pediments and sometimes in stream basins (Nude and Arhin, 2009). They are characterized by rounded and sub-rounded lithic and quartz clasts. Sometimes mature or older laterite is found embedded in an immature or younger laterite with different weathering histories, demonstrating the older laterite to have transported origin. In addition to the regolith types above, certain areas have been overlain by indurated saprolite and usually appear silicified. The erosional areas that expose the saprolite are generally uncommon.

2.1.2 Climate and rainfall

The climatic regime of the Lawra belt is Semi-arid with annual rainfall of about 600-1200 mm (Webber, 1996a). The area shows monomodal rainy season (Fig. 2.1). The monthly totals increase slowly from March and peaks in August after which there is a sharp decrease after October (Kranjac-Bersaljevic et al., 1998). The average monthly rainfall is 986 mm per month. Temperatures are consistently high and averages at 28.6^{o}C. However monthly averages range from 26.4^{o}C at the peak of the rainy season in August to a maximum of 32.1^{o}C in April (Dickson and Benneh, 1995). As it is common for the tropics, diurnal temperature changes exceed monthly variations (Dickson and Benneh, 1995). The total evaporation of 2050 mm (Fig. 2.1) exceeds the annual rainfall more than two folds. These conditions are favourable for lateritization processes to form laterites (Freyssinet et al., 2005, Butt and Zeegers, 1992).

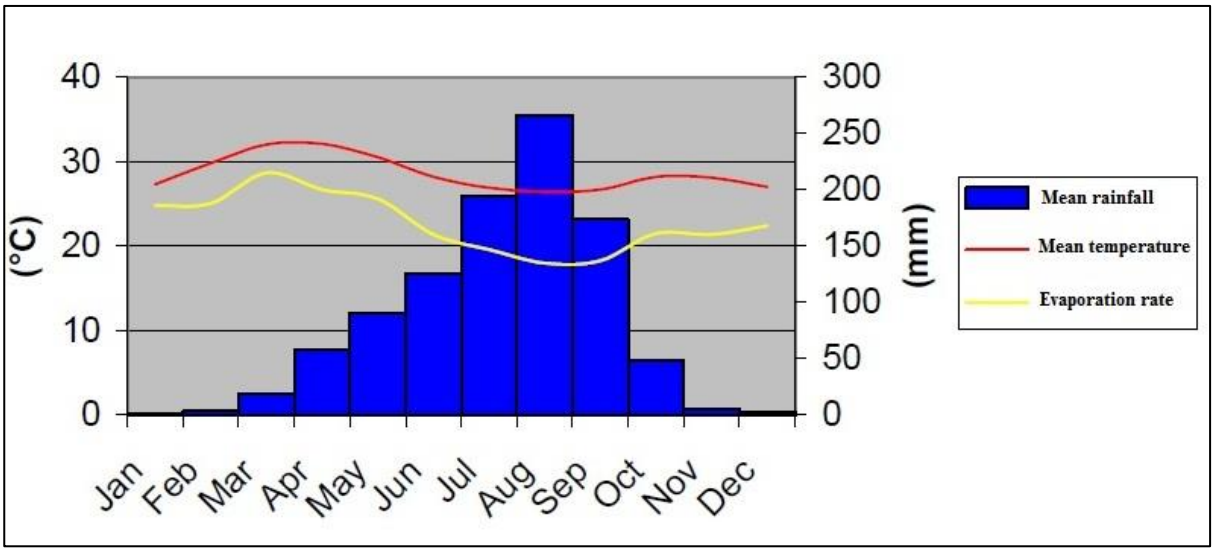

Fig. 2.1 Climate data of the Lawra belt (Data source: Ghana Meteorological Service Department. In: Kranjac-Berisaljevic et al., 1998)

2.2 Location, geological setting and regolith

2.2.1 Geology of West African Craton

The geology of West Africa is divided into a number of discrete geological terrains (Fig. 2.2) as follows:

- the Achaean to Palaeoproterozoic West African Craton;
- the Neoproterozoic "Pan-African" mobile belts;
- the Neoproterozoic to Palaeozoic sedimentary basins; and
- Mesozoic to recent sedimentary cover.

The Lawra belt forms part of the West African Craton which comprises two components: (1) Archean basement, and (2) the surrounding Proterozoic Birimian granite-greenstone area. Both components are exposed in two "Shield" areas: the northern Reguibat Shield (in the north around Mauritania; this is of Achaean age) and the Man Shield (in the south between Ghana and Senegal; this is also of Paleo-Proterozoic age). The two domains are separated by the Taodeni basin of Proterozoic and Palaeozoic age The Archean basement represents the remnant of one or more ancient cratonic nuclei whereas the greenstone belts of the latter represent a series of parallel to sub-parallel ancient island arcs and their associated sedimentary basins (Milési et al., 1991).

The Man shield covers the southernmost third of the Craton. It is divided into two sectors comprising the western portion built up of rocks of Liberian age (3.0-2.5 Ga) and the eastern terrain underlain by Birimian rocks of Palaeoproterozoic age as shown in Fig. 2.2. The Birimian supra-crustal rocks have been folded, metamorphosed and intruded by granitoids.

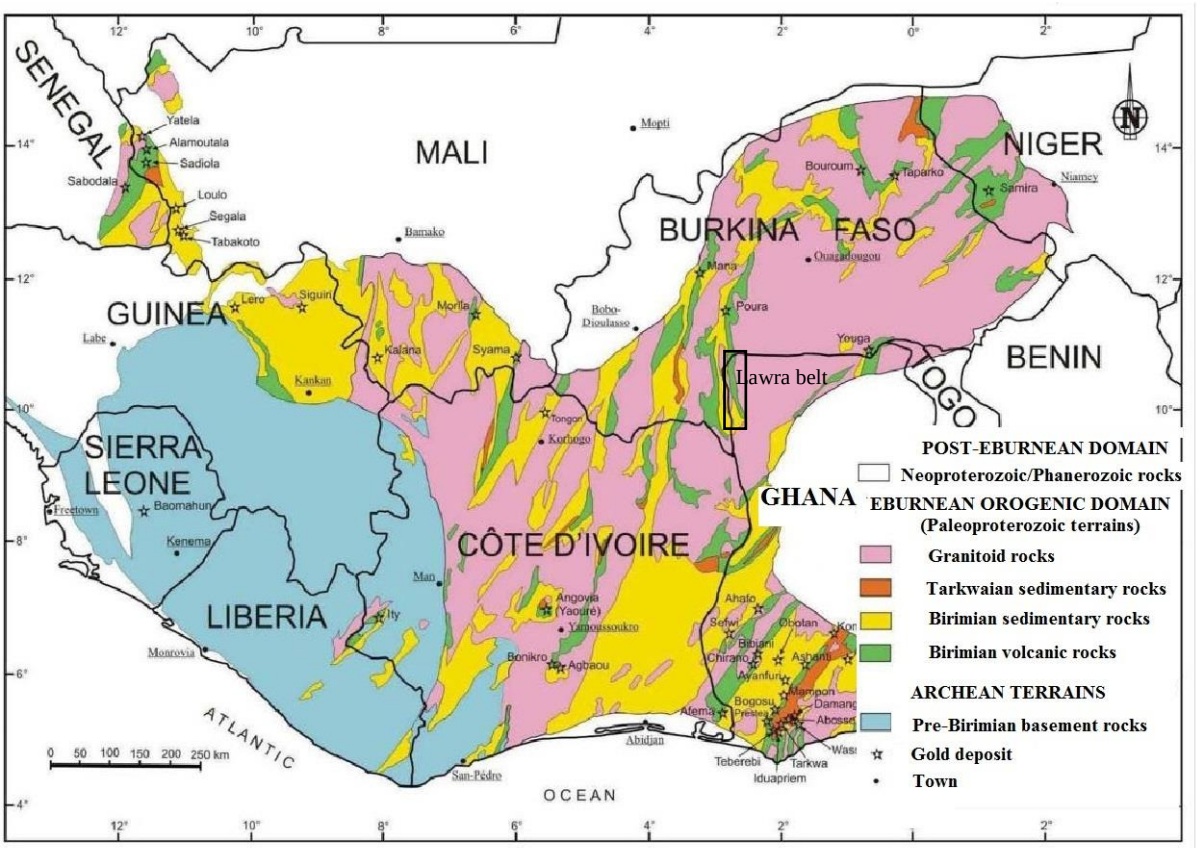

Fig. 2.2 Simplified geology of the Man shield showing narrow arcuate linear volcanic belts and wider sedimentary basins intruded by several generations of granitoids (modified after Debat et al., 2003; Milési et al., 2004). It also shows the location of Lawra belt edged black in rectangle.

2.2.2 Geology of Ghana

The south eastern margin of the Birimian Leo-Man Shield is in southwest Ghana (Milési et al. 1991). The geology of Ghana comprises several linear volcanic "belts" (typically 20-60 kilometres wide), separated by broader sedimentary "basins" (Chapter 1, Fig. 1.2). The Birimian units are intensely folded and faulted, metamorphosed to lower greenschist facies, and cut by linear trends of granitic intrusive. They are locally overlain by less deformed coarse clastic sediments of the Tarkwa Group, which were deposited in discrete basins. In central and eastern Ghana, the Birimian rocks are covered by Neoproterozoic clastic sediments of the Volta Group (Kesse, 1985).

Birimian evolution, possibly accompanying breakup of Achaean cratonic nuclei, commenced around 2350-2300 Ma with plutonic activity and the deposition in

volcano-sedimentary basins, including BIFs (Leube et al., 1990; Taylor et al., 1992; Hirdes et al., 1992). The oldest Birimian rocks in Ghana comprise volcanic and related hypabyssal intrusive with lesser volcanoclastic sediments deposited between 2250-2150 Ma (Hirdes et al., 1992). These include andesitic to basaltic flows and andesitic to dacitic volcanoclastic. Deposition of the older volcanic-dominated Birimian series was followed by a period of greenschist to amphibolite facies metamorphism from about 2150 Ma (Baratoux et al., 2011). Granite emplacement is dated between 2205-2130 Ma in the West African Craton (de Kock et al., 2011, Feybesse at al., 2006, Allibone et al., 2002, Kesse, 1985). However, de Kock et al., (2011) reported the early Eburnean deformational event operating before 2150 Ma in northern Ghana. The first Eburnean phase which took place between about 2200-2130 and 2150-2110 Ma (U-Pb and Pb-Zircon ages on rhyolites and granitoids) is called Eburnean 1 (Allibone et al., 2002). This deformational event corresponds to the major phase of either crustal thickening by nappe stacking (Vidal et al., 2009; Feybesse et al., 2006; Allibone et al., 2002) or 'dome and basin' diapiric uprising and greenstone belt sinking (Lompo, 2009, Vidal et al., 2009).

2.2.2.1 Location and geology of the Lawra Belt

The research area is located in the Lawra Birimian belt in northern Ghana (Kesse, 1985) and the detailed regional geology is shown in Fig. 2.3. The area is 700 km northwest of Accra, the national capital. It is underlain by rocks of the Birimian Super group. The metavolcanic rocks are chiefly metamorphosed lavas and pyroclastic rocks (greenstones) comprising basalts, andesite, rhyolites, dolerites that are intruded at places by gabbros (Leube et al., 1990; Liegeois et al., 1991; Hirdes et al., 1992; Doumbia et al., 1998; Oberthur et al., 1998; Egal et al., 2002; Gasquet et al., 2003; Naba et al., 2004; Feybesse et al., 2006). Nude and Arhin (2009) also observed the north eastern and central parts of the Lawra belt to consist of dark grey to greenish grey, weakly foliated mafic extrusive volcanic rocks, partially assimilated with melanocratic relicts (xenoliths) in close association with granitoids. The metasedimentary units consist of phyllite, sericite-schist and metagreywacke that are locally intruded by felsic and mafic dykes.

Leube et al. (1992) recognised the Birimian rocks of southern Ghana to be intruded by migmatitic bodies and porphyritic granitoids that have generally been classified into

two broad categories. These are hornblende-rich varieties that are closely associated with the metavolcanic rocks and known as the 'Dixcove' or 'belt' type; and mica–rich varieties which tend to border the volcanic belt. The recent work by Baratoux et al., (2011) has confirmed the occurrences of these intrusive bodies in both the sedimentary and the volcanic suites of rocks. The belt granitoids are small discordant to semi-discordant, late or post-tectonic soda-rich hornblende-biotite granites or granodiorites that grade into quartz diorite and hornblende diorite (Hirde et al., 1996). They are generally massive but in shear zones they are strongly foliated. The basin granitoids are large concordant and syntectonic batholitic granitoids commonly banded and foliated. The basin granitoids are two-mica potassic granitoids, containing both biotite and muscovite, with the biotite dominating (Leube et al., 1990). These rocks are generally isoclinally folded, with dips usually greater than 50^{o}. The general foliation in the rocks is N–NNE to S-SSW. Sheared and brecciated quartz veins are extensively developed. Zones of shearing and faulting are locally present in all the rocks but more pronounced in the soft metasedimentary rocks adjacent to intrusive units (Leube et al., 1990). The Birimian and the Tarkwaian rocks were deformed around 2.1 Ga during the Eburnean orogeny (Abouchami et al., 1990; Milési et al., 1991; Taylor et al., 1992). This orogeny was associated with shear-zone mineralisation that is prominent in Ashanti, Sefwi and Lawra Birimian greenstone belts (Kesse, 1985 and Griffis et al., 2002). In addition all rock units show metamorphic mineral assemblages of greenschist facies grade (Beziat et al., 2008)

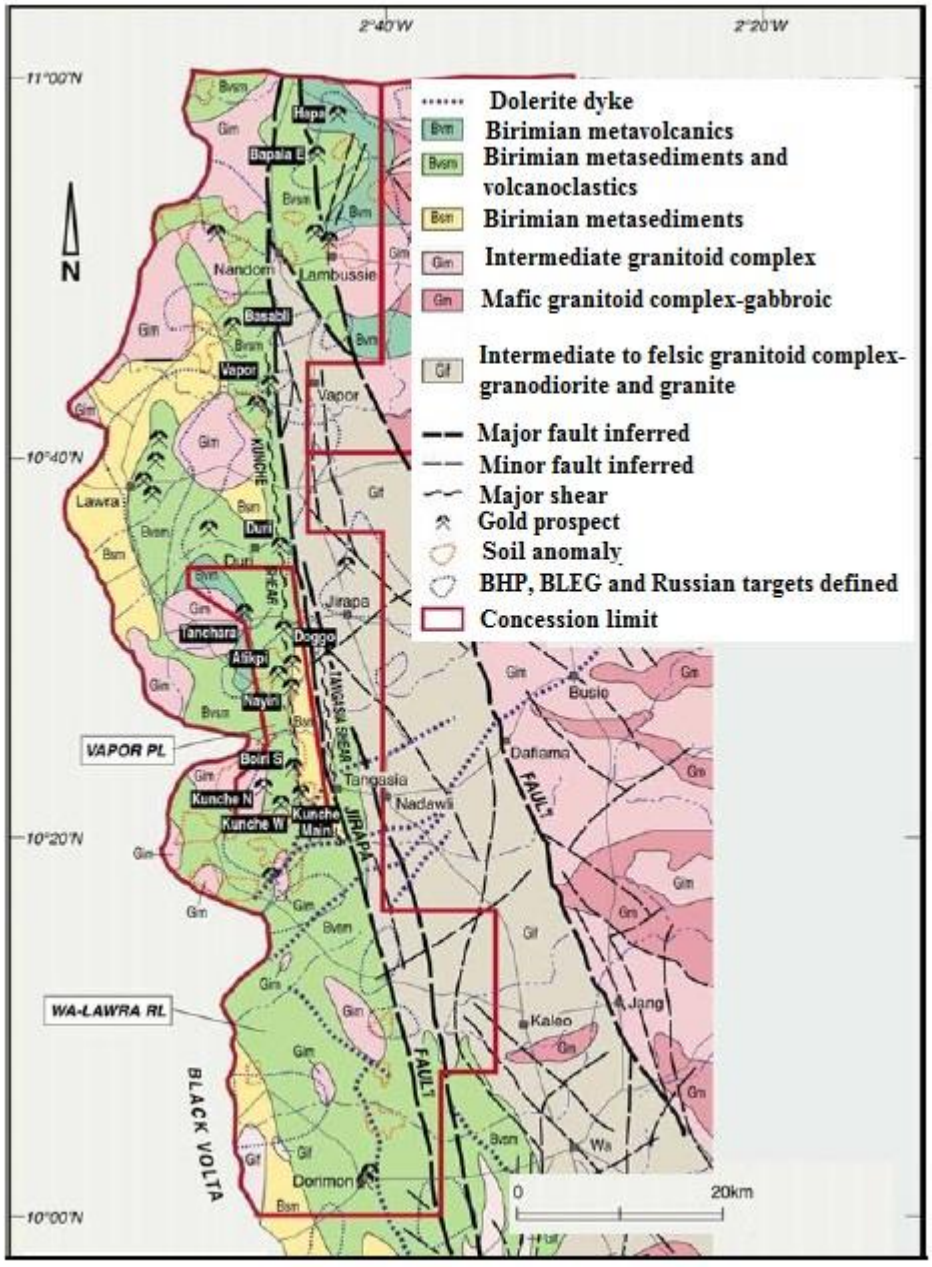

Fig. 2.3 Detailed geology of the Lawra belt (Waller et al., 2012)

2.3 Mineralisation and geology of Kunche-Bekpong and Sabala areas

The mineralisation and geology of Kunche-Bekpong and Sabala areas are presented below.

2.3.1 Mineralisation and geology of Kunche-Bekpong

Mineralisation at Kunche is closely associated with a major approximately N-S to NNW-striking quartz-vein system, characterised by mafic or baked-type vein quartz, with minor sulphide, largely concentrated on vein margins and sediment selvedge (Fig. 2.4). Veining development is mainly in a variety of wackes or in a zone of inter-

banded wackes and phyllite. This zone characterised by veining in the wackes and phyllite varies from irregular and partly replacive, to sharply bounded zones of brittle stockworks is referred to as Kunche shear zone (Waller et al., 2012). Brecciation in the wackes appears to have been achieved largely through shortening and resulted in deformation of the veins without major displacement. The planar through-going shear fabrics appear to overprint the brecciation textures (Waller et al., 2012).

Structurally, the main veins are parallel or sub-parallel to the S1/S2 fabric, typically dipping steeply west, but locally rolling to sub-vertical or steeply east (Griffis et al., 2002). Additionally Waller et al. (2012) recognised the minor veins to occur in different orientations and noted the common occurrence of shallow veins as well as veins sub-parallel to the main vein. This suggests a component of reverse (up-from-west) shear. The wall rocks as well have a strong S1/2 fabric, which may also be composite S3 as a result of D3 shearing. This is locally most intense in sheared phyllitic horizons. Quartz veins are often boudinage in the fabric, but later veins also cut the fabric. Quartz stockworks sometimes in the form of veins generally crosscut the S1/2 fabric. Quartz veins and associated sericite-carbonate alteration crosscut the composite S3 fabric.

In surface outcrop, the southern end of the Kunche-Bekpong comprises some major 1 to 3m thick quartz veins, with smaller parallel veins, within a zone of stockworks veining up to 20 metres wide. Observations in drill cores reported by Waller et al. (2012) show the thickest drill intercepts are comprised of similar wide zones of mineralisation in multiple veins, stockworks, and altered host rocks. In contrast, there is not a single significant quartz vein in the north, but this is an area of strong stockworks veining, with thinner fabric-parallel veining. Brecciation in this area includes hydraulic and reaction-dissolution

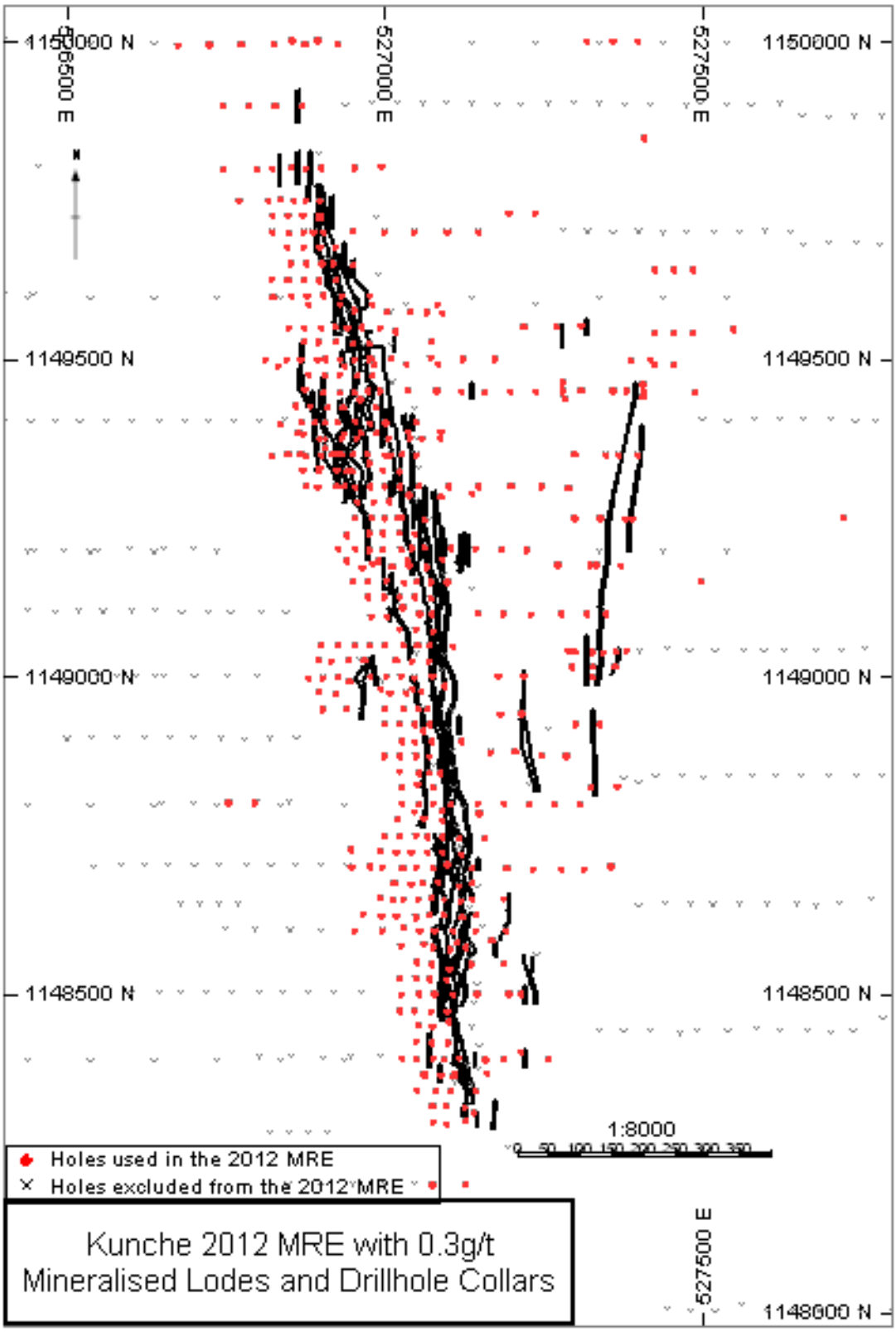

Fig. 2.4 Gold mineralisation trends in Kunche and drill-hole collars (shown red) (Waller et al. 2012)

effects and mosaic breccias include ragged, partly silicified, fragments. Veined

sediments are strongly altered, characterised by incipient irregular silicification at clast margins, with sericite-carbonate-quartz chlorite occurring pervasively and in irregular network veinlets and patches. The latter assemblage can also occur within black quartz veins. Pyrrhotite and arsenopyrites are the dominant sulphides (3-5%) and they occur largely within the altered sediments. Pyrrhotite is typically fine grained, and occurs as either dissemination within the sediments or in veinlets. Arsenopyrites and local pyrite both occur as large rhomboid porphyroblasts, which overprint all fabrics, but do have pressure-shadow overgrowths that indicate syn-mineralization strain.

2.3.2 Mineralisation and geology of Sabala

The Au occurrence in the area reported in the surface geochemical data reported by Ashanti-AGEM Alliance has not seen any detailed geochemical exploration survey. The area is covered by transported laterite and Black Volta sediments. The cover materials masked the outcrop exposures. Waller et al. (2012) have recognised the area to represent lateritized terrace deposits from an older higher-level river channel. As shown in Fig. 2.3 the Sabala area is underlain by Birimian metasediments and volcanoclastic rocks intruded at places by intermediate granitoid complex. However the observations made in the dugout pits and the ground truthing information during the regolith mapping survey confirms Sabala is hosted by similar the same metasedimentary package as Kunche-Bekpong geology. Like Kunche there are associated quartz vein intercalations in the metasedimentary rocks but the veins are white in colour compared to grey or grey-white quartz lenses and stringers in Kunche area. To date there is no known bedrock mineralisation association with the rocks in Sabala apart from the moderate to high Au surface geochemistry identified by Ashanti-AGEM Alliance (Griffis et al. 2002). This anomaly needs to be test-drilled to assess the Au prospectivity of the area.

2.4 Gold mineralisation

The Birimian of the West Africa Craton is an orogenic gold province of global significance, with total gold resources of probably more than 200 Moz (comparable in magnitude to the Yilgarn Craton of Western Australia and the Superior Province of Canada-Franey et al., 2011). The largest deposits in Ghana, at Obuasi and Tarkwa, both have global resources of more than 30 Moz of gold (Griffis et al., 2002; Griffis

and Agezo, 2000).

Gold mineralisation occurs in a variety of styles and settings (Beziat et al., 2008), but the major distinction is between:

(i) a quartz-vein mineralisation style, in which gold is found within deformed quartz veins, principally associated with pyrite or tourmaline, and,

(ii) A disseminated mineralisation style, where gold occurs as disseminated particles dominantly associated with sulphides within the alteration halo of undeformed veins of quartz ± albite ± carbonates.

The undeformed veins in the disseminated mineralisation style normally contain little or no gold. The disseminated mineralisation has lower grades but much higher tonnage, and occurs in highly carbonatized and albitized rocks or pure albitites. The quartz-vein and disseminated mineralisation styles represent variations due to local heterogeneity of the host lithologies, the mineralising fluids and precipitation mechanisms. In the Birimian greenstone belts, albitization and carbonatization have been observed by several authors such as Amedofu, (1999), Allibone et al. (2004) and Beziat et al. (2008) to be common hydrothermal alteration assemblages, as is pyrite and/or arsenopyrite precipitation, which is the dominant control on gold deposition. The quartz-tourmaline veins, where gold is intimately associated with tourmaline, represent an uncommon style of mineralisation. However, timing of gold mineralisation in the Birimian is perceived to be compatible with gold emplacement or deposition during a single regional mineralising event, which occurred at the end of the Eburnean orogenic process (Allibone et al., 2002; Milési et al., 1991). These two mineralisation styles do not exist in isolation. In the Birimian of Ghana the two world-class deposits; AngloGold Ashanti at Obuasi and Newmont Ghana gold at Kenyasi have the two mineralisation styles coexisting. Similar styles of gold mineralisation may occur in the Lawra belt.

2.5 Gold mineralisation geochemistry in the Birimian belts of Ghana

Gold deposits occur as mesothermal auriferous arsenopyrite and quartz vein mineralisation deposits in the Birimian greenstone belts of Ghana (Kesse, 1985; Griffis et al., 2002; Allibone et al., 2004). The mineral assemblage in the Birimian gold deposits is dominated by sulphides, the main minerals including pyrite, arsenopyrite, sphalerite, chalcopyrite and minor galena (Kesse, 1985; Dzigbodi-Adjimah, 1993). The earlier work by Dzigbodi-Adjimah (1991) at Prestea goldfields in the Ashanti belt

showed the metavolcanic rocks contain high amounts of Mn, As, Cr and Sb, whereas the auriferous quartz veins contained high Zn, Pb, Cu, Fe, Sb and Cd, with insignificant amounts in the non-auriferous quartz veins. A similar study on the mineralisation in the Birimian greenstone on that same belt conducted by Amanor and Gyapong (1991) indicated high correlation of Ag, As, Zn, Cu, Pb, Ni, Sb, and Cr with gold.

Literature Review: Gold exploration in NW Ghana and regolith implications for exploration in complex regolith environments

3.0 Introduction

Prolonged weathering, erosion and deposition controlled by geology, topography, climate and vegetation result in changes of landscape and spatial distribution of the regolith materials (Anand and Pain, 2002). These processes, coupled with the savannah climate and sparse vegetation, cover have resulted in a complex regolith architecture that probably accounts for the exploration failures in the study area. However reports by Cohen et al. (2010); Coker (2010); Butt et al. (2000); Freyssinet et al. (2005); Smith, (1996); Butt and Zeegers (1992) indicate discoveries of mineralisation elsewhere in complex regolith environments. Many of the mineral discoveries reported by these authors occurred in Australia with some from West Africa. Therefore to detect mineralisation in the Lawra belt the research adopted the approaches that accounted for the influence of regolith diversities on anomaly concentrations in the surface weathering environment. It therefore reviewed regolith development, the processes and mechanisms that transport elements from primary minerals towards the surface regolith.

3.1 Regolith formation, evolution and characterization

3.1.1 Regolith

Regolith is a word derived from the Greek words, '*rhegos'* meaning blanket or cover and *lithos*-means rock. Literally it means 'rock blanket'. It is used to refer to all weathered Earth surface materials extending between bedrock surface at depth and the land-surface (Ollier and Pain, 1996; Eggleton, 2001; Taylor and Eggleton, 2001; Pain et al., 2001; Fig. 3.1).

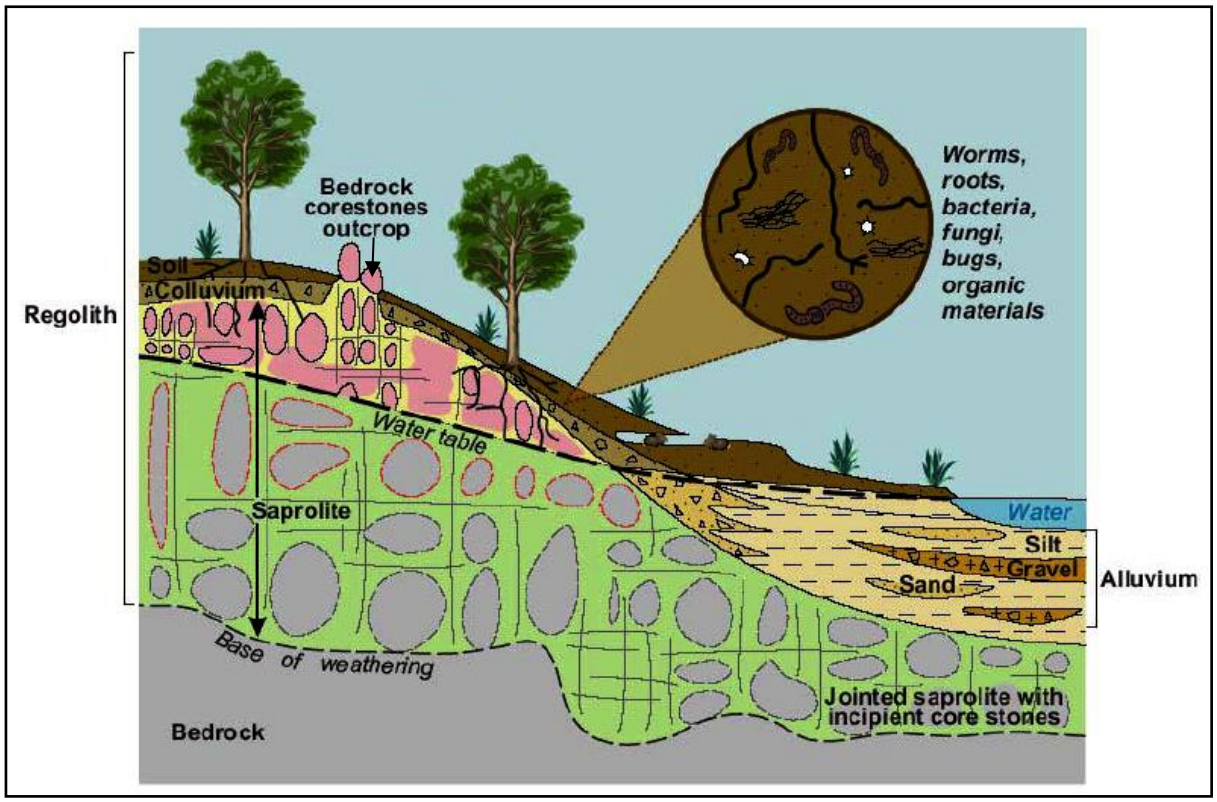

Fig. 3.1 Typical regolith section across a landscape (modified after Roach, 2003). It includes in situ weathered material derived directly from the underlying bedrock, and transported material derived from both bedrock and weathered rocks.

3.1.2 Regolith formation and processes

Bedrock is transformed to erodible regolith through physical, chemical, biological and hydrological processes operating together where rocks, vegetation, atmospheric gases and water interact (White et al., 1996; Anderson et al., 2002; Brantley and White, 2009). The formation of the regolith and the processes that mobilise elements towards the surface of the landscape are discussed below.

3.1.2.1 Formation

The formation of regolith normally propagates downward into bedrock (Taylor and Eggleton, 2001). The balance between rates of erosion and regolith production contribute to both regolith thickness and the overall landscape morphology (Stallard, 1992; Heimsath et al., 1997). The structure of the regolith at any particular location depends on the extent to which chemical weathering transformed the bedrock composition as well as the degree of physical and chemical addition and removal of materials (Scott and Pain, 2008). The sub horizontal layers of the regolith as weathering

progresses downwards in a laterite weathering profile are shown in Figs. 3.2 & 3.3. The nature of the regolith profiles relates to intensities of weathering processes and the prevailing landscape evolution events. The profile formed includes a number of horizons consisting of from bottom to top: sap rock, saprolite, mottled zone, duricrust or ferricrete (Figs. 3.2 and 3.3) for classic laterite profile but the layered sequence may change depending on the regolith and landscape evolution.

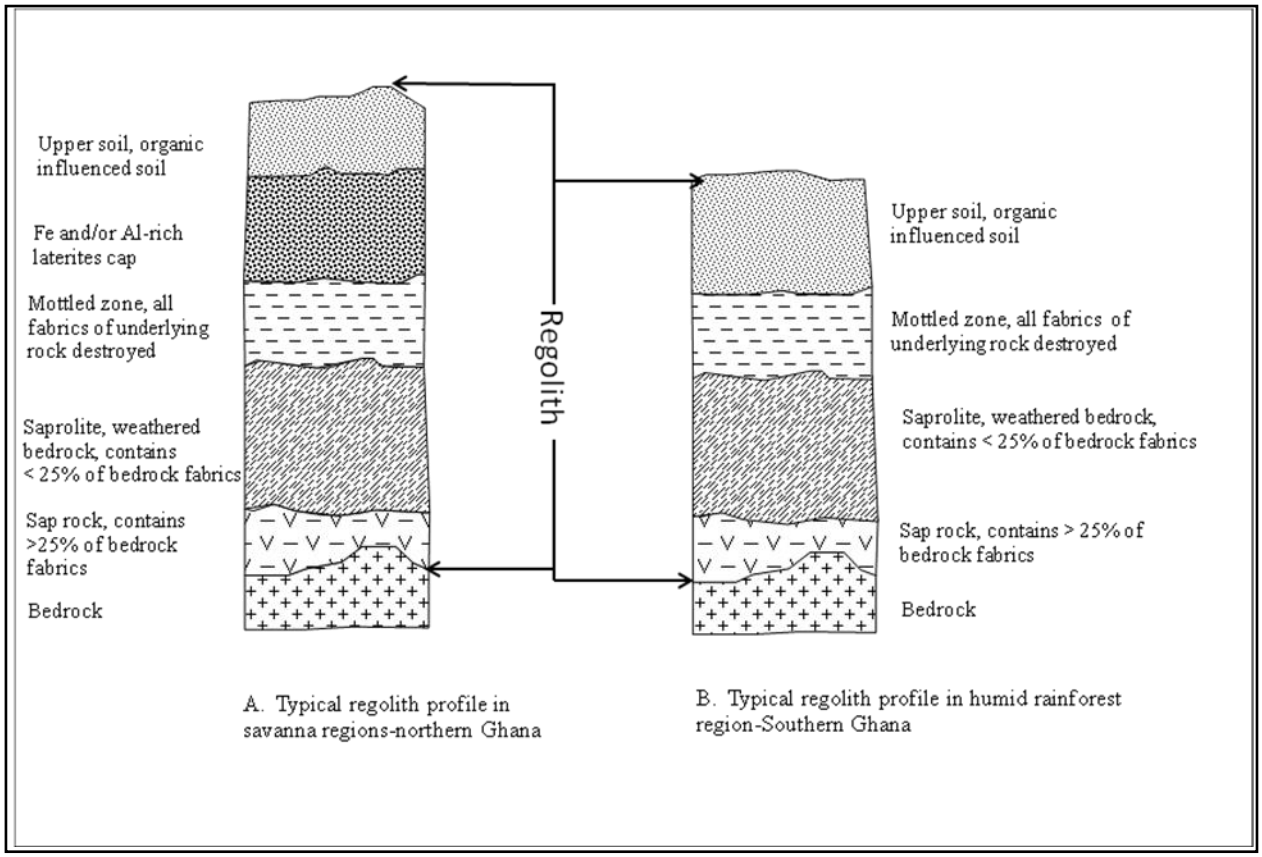

Fig. 3.2 Typical regolith profiles in savannah and rainforest regions of Ghana (Arhin and Nude, 2009).

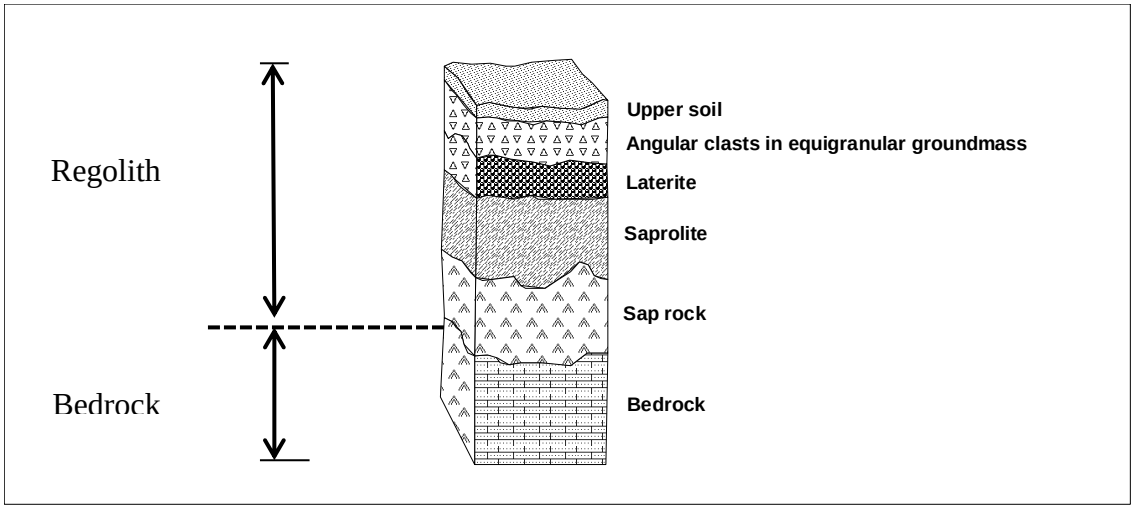

Fig. 3.3 Typical laterite regolith profile (modified from Taylor and Eggleton, 2001).

3.1.2.2 Processes

The landscape of the study area is generally controlled by physical weathering more than chemical weathering because of the long dry seasons (chapter 2, Fig. 2.1). The weathered products from the different weathering mechanisms are irregularly distributed across the landscape during the landscape evolution events. The redistribution of the regolith materials and transformation of the primary minerals to secondary minerals influence the dispersal patterns and pathways of elements. For examples during weathering some of the unstable primary minerals in the weathering environment are transformed and replaced by secondary minerals (Anand and Pain, 2002). The changes that occur can be physical or chemical processes but there are some biological processes too.

The surface processes and the changes in landscape results in the formation of different regolith types. The classification of the different regolith types is based on variations with the typical classic laterite profile (Fig. 3.2). The undisturbed regolith profiles are termed relict and have weathered materials developed in situ from the parent rock whereas the modified regolith may show some variations in the sub horizontal units when compared with the classic laterite profile. The changes in horizons may be cementation of weathered in situ products or cementation of transported sediments by Fe-oxides. This type of profile is termed ferruginous whereas profiles that exhibit truncation of pre-existing preserved surfaces or deposition of new layers over preserved

pre-existing profiles are considered as having erosional and depositional regolith profiles respectively (Arhin and Nude, 2009).

In the residual regolith environments the newly formed layers bear some compositional relationship with the parent rock. The chemical alterations in a residual profile, responsible for the transformation of elements upward migration (Scott and Pain, 2008; Butt et al., 2000) from the bedrock include:

- Leaching of soluble constituents by groundwater, resulting in their relative depletion;

- Precipitation of components such as silica, Fe-oxide and Aluminosilicates as absolute enrichments.

The processes in the regolith preserve relict rock fabrics by pseudomorphing primary minerals and later cement the relict fabrics and other secondary products. The principal secondary minerals constituting the saprolite in the oxidized environments are Fe-Mn oxides, Al-oxides, kaolinite and smectite clays (Butt et al., 2000, Table 3.1).

The ferruginous laterite formed may be in situ or transported; their differences are determined from their mode of formation (Cohen et al., 2010). Laterite formation normally represents the final stage of the lateritic weathering (Butt and Zeegers, 1992). The ferruginized laterite unit in a residual laterite profile, termed duricrust in this study, is mostly formed by Fe-oxide cementation of the weathered parent materials from the underlying rocks. Where these occur they are largely residual (Tardy, 1997) but may well be proximally transported because of the mechanical reworking of weathered products in some residual environments. However, ferricrete similar in surface crust to the duricrust is also formed by Fe-oxide cementation and occurs commonly in depositional environment. Ferricrete is formed usually in paleo-alluvial terraces where terrace sands and gravels are cemented by Fe–oxyhydroxide minerals (Yager et al., 2000) but can occur on hill-slopes and at low-lying areas (Anand, 2001). Laterite formation of duricrust or ferricrete starts during the humid seasons while the cementation and hardening of the weathered materials, colluvium and alluvium by Fe-oxide and clay minerals occur during the dry seasons (Nahon and Tardy, 1992). The primary mineral assemblages in the laterites are almost totally replaced by hematite, goethite, gibbsite and kaolinite in varying proportions, with some quartz and other

resistant minerals. Their chemical composition may differ considerably from that of the underlying bedrock and strong enrichments may be observed for elements such as Fe, Al, Ti, Zr, Cr, V, Mo, As, REE, Th, and W and possibly Au (Butt et al., 2000). Conversely, other elements may be severely leached e.g., Ca, Mg, Zn, Na, Ag, S, Cd, Co, and U (Butt and Zeegers, 1992). The modifications in regolith materials and the compositional changes in the evolving landscape environment pose problems for mineral exploration.

3.2 Transfer of elements during weathering

Summarized in Table 3.1 are the principal effects of deep lateritic weathering on element distributions (Butt et al., 2000). Leaching and retention of a range of elements by mineral transformations (Table 3.1) in the regolith horizons is shown in Fig. 3.4. Hydrologic processes at and below the bedrock/sap rock interface exert a strong control on the extent of element dispersion and material transport. The remnants of most major primary minerals, except quartz, are destroyed in the mottled and ferruginous laterite zones (Butt et al., 2000). The transformation of primary minerals to secondary minerals in the regolith profile involves replacement of more soluble ions by protons (hydrogen ions) and oxidation of some elements. These chemical processes are promoted by the availability of water, gases and biological activity in the regolith. As noted by Roquin et al. (1989), Butt and Smith (1992), Cornell and Schwertmann (1996), Taylor and Eggleton (2001), McQueen and McRae (2004) the relatively immobile elements such as Si, Al and Fe resident in kaolinite, quartz and Fe-oxyhydroxides (such as goethite, hematite, maghemite) and in places gibbsite tend to be retained in the regolith. So the processes result in the association of particular elements in specific minerals or groups of minerals (Scott and Pain, 2008). Thus depending on weathering conditions and the type of regolith formed, particular elements may undergo fractionation during weathering or concentrate in particular regolith components to form regolith-related element associations. To properly interpret geochemical patterns and anomalies in the regolith, it is important to recognize and understand these associations. For example many resistate and immobile elements tend to concentrate with clay and Fe oxides in the ferruginous zones (Mann, 1984). Additionally, host unstable minerals such as sulphides at the weathering front are released and typically persist as secondary sulphides in the regolith profile only if they are preserved within quartz veins or relatively immobile minerals (Table 3.1, Butt et al., 2000).

Table 3.1 Element mobility during deep weathering under humid conditions (after Butt et al., 2000).

Host minerals	Leached elements	Partly retained elements in secondary minerals
Retained in stable minerals (all horizons)	B, Cr, Fe, Hf, K, Nb, REE, Th, Ti, V, W, Zr.	
Released in mottled and ferruginous zones ▪ Aluminosilicates (muscovite, kaolinite) ▪ Fe oxides	K, Rb, Cs Trace elements	Si, Al (kaolinite)
Released in upper saprolite ▪ Aluminosilicates (muscovite) ▪ Ferromagnesians (chlorite, talc, amphibole) ▪ Smectites	Cs, K, Rb Mg, Li Ca, Mg, Na	Si, Al (kaolinite) Fe, Ni, Co, Cr, Ga, Mn, Ni, Ti, V (Fe oxides) Si, Al (Kaolinite)
Released in lower saprolite ▪ Aluminosilicates ▪ Ferromagnesians (pyroxene, olivine, amphiboles, chlorite, biotite)	Ca, Cs, K, Na, Rb Ca, Mg	Si, Al (kaolinite); Ba (barite) Fe, Ni, Co, Cr, Ga, Mn, Ti, V, (Fe and Mn oxides)
Released at weathering front ▪ Sulphides ▪ Carbonates	As, Cd, Co, Cu, Mo, Ni, Zn, S Ca, Mg, Mn, Sr	As, Cu, Ni, Pb, Sb, Zn (Fe oxides)

3.2.1 Mechanism of element transport from source mineralization.

Most minerals formed under igneous and metamorphic conditions are unstable at low temperature and under near-surface hydrous conditions and eventually react to form dissolved components and new mineral precipitates (Scott and Pain, 2008). The mobility of elements from primary minerals depends on the nature of the regolith (i.e. on pre and post–weathering conditions), its depth, and aquifer characteristics (i.e. aquifer grain size and evaporation rates). The past and present landscape evolutional events further influence the element mobilization in the regolith. In the savannah regions (Nahon and Tardy, 1992) the chemical reactions are activated by rise in temperature whereas lateritization processes are accelerated or retarded by changes in climate. Hydromorphic and chemical dispersions facilitate element dispersions in the regolith profiles via groundwater and infiltrated water (Figs. 3.4 & 3.5). Physical

dispersion normally is effective in the surface layers. However, there are areas on the landscape where all three element transporting mechanisms operate together. Each of these element dispersion mechanisms results in different element signatures in the regolith (Fig. 3.5). The nature of dispersion haloes displayed in the regolith relies on flow directions of groundwater, infiltrated water, solution properties, aquifer heterogeneity, adsorption of elements onto specific regolith minerals, elements forming complexes with appropriate ligands as well as inherent geochemical interactions of elements and regolith material types (Anand 2001; Anand et al., 2005). Taylor and Eggleton (2001) also noted gold is transferred upwards in the regolith chemically after forming complexes with different species (e.g. $AuCl_2^-$, Au $(S_2O_3)^{2-}{}_2$. They noted each Au complex has a redox-pH stability range that forms at favourable redox conditions and destabilizes at specific redox.

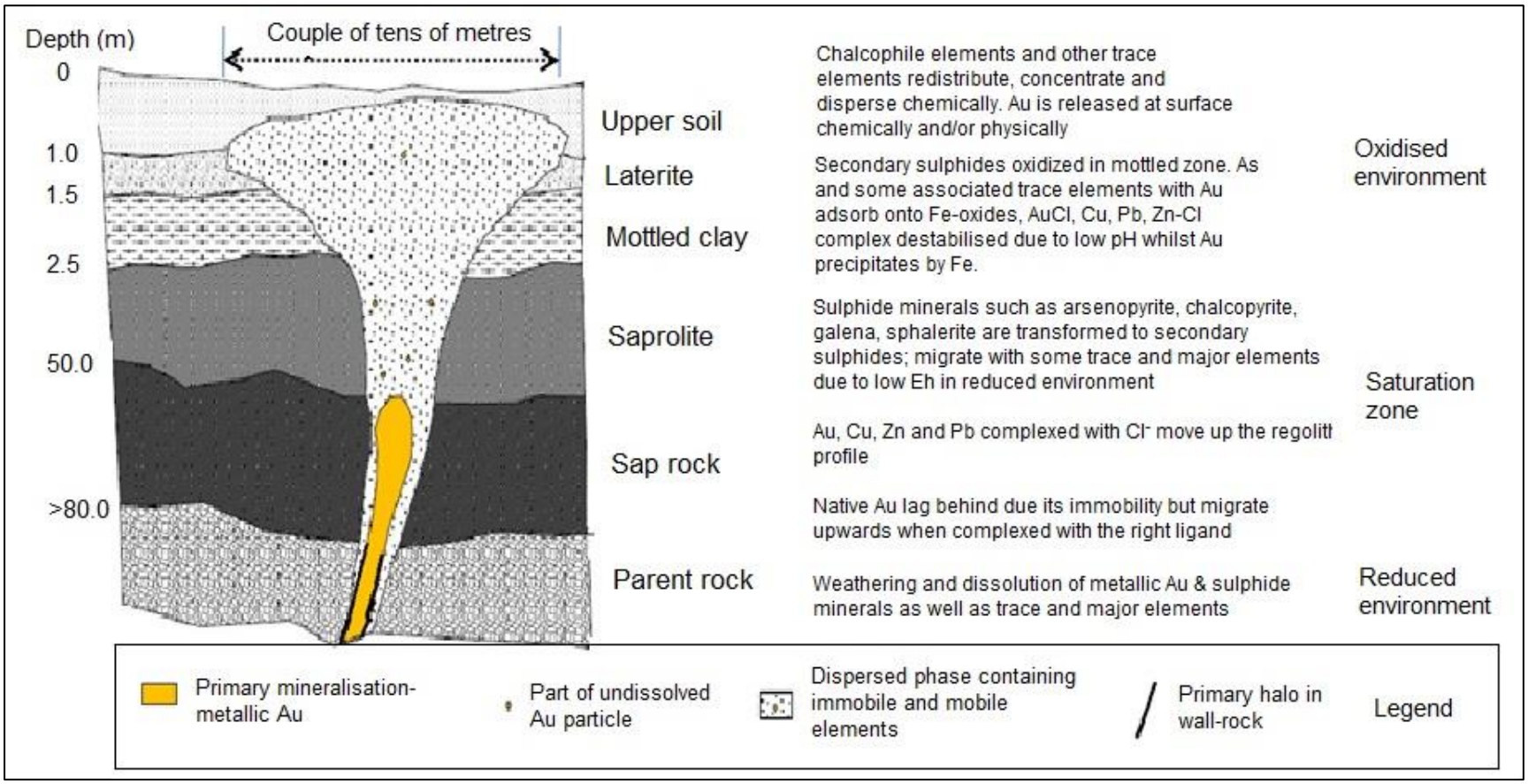

Fig. 3.4 Schematic of element mobility in savannah regions, showing processes and mechanisms of transport from primary mineralisation into the regolith profile (modified after McQueen and McRae (2004); Taylor and Eggleton (2001).

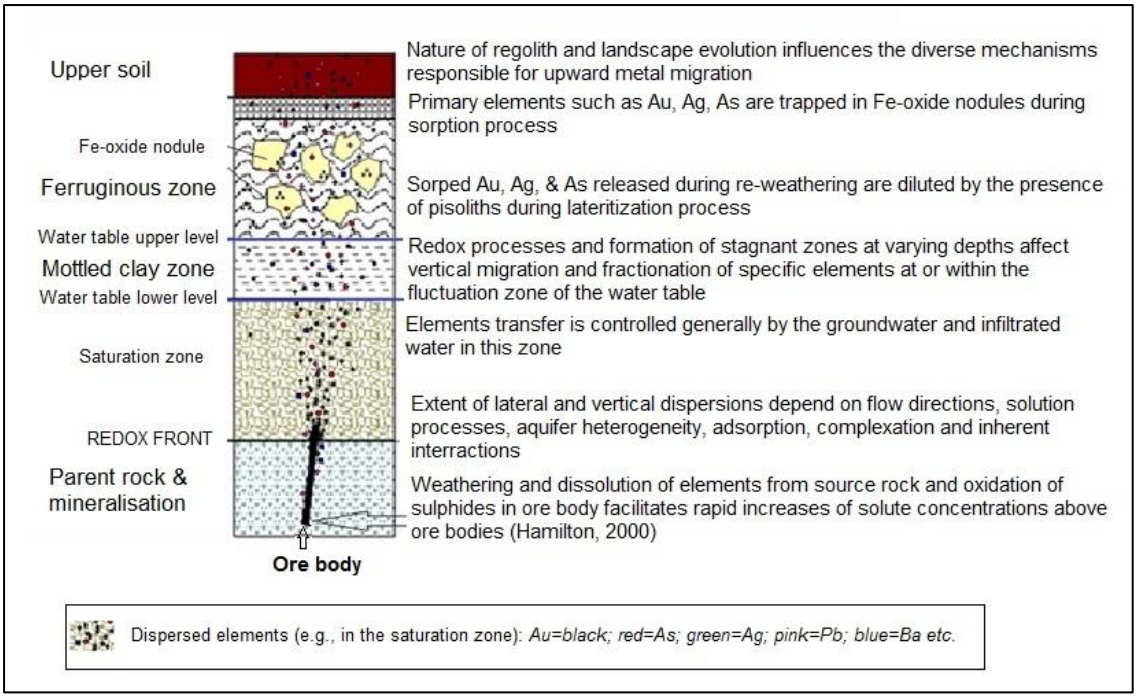

Fig. 3.5 Processes and migrations of elements from primary mineralisation into the regolith profile (modified after Butt et al., 2000)

3.3 Factors affecting metal mobility in the regolith

Mobility of elements in the regolith is controlled by geochemical and surface modifying processes as well as the nature of the regolith (Freyssinet et al., 2005). Considerable leaching occurs in porous regolith whereas element migrations are impeded by impermeable regolith. In the saturation zone, weathering of sulphides in the ore body produces heat. The generated heat from the transformation process increases the groundwater temperatures and facilitates rapid increases of solute concentrations above the ore body. In addition, the alteration of sulphides from reduced state to secondary sulphides such as chalcocite in the oxidised environments at the water table leads to upward and outward migration (Hamilton, 2000). This model of sulphide mineral transformation by exothermic reaction is considered to account for the upward transfer of metals through the saturated cover (Cameron et al., 2004). This type of upward element movement is a common process of element mobility in rainforest environments and uncommon in savannah regions.

Scott and Pain (2008) additionally recognized movements of groundwater and water table fluctuations to have some influence on element mobility in semi-arid and

savannah regions. They believed the exothermic reaction has an influence on the rise and fall of groundwater and the water table. The fluctuation of the water levels in the regolith may partly cause upward element migration during the rainy seasons. During this period the migrated elements are either retained in the regolith or form complexes with other ligands and are sorped into some stable minerals (Butt et al., 2000). However, notwithstanding the contributions of climate mobilizing elements upwards it indirectly also impedes element transfers in some regolith environments. A typical example is the groundwater lowering during the long dry season with one rainy season averaging between 1000 and 1140 mm (Dickson, 1972; Dickson and Benneh, 1988, 1995) in the study area. These conditions support the lateritization process because of the small amount of rainfall in a short time and the high long temperature seasons. Chemical reactions are accelerated by the rise in temperature and cause the cementation of sediments by Fe-oxides and clay minerals in the water fluctuation zones. During the lateritization gold and other elements may be absorbed and adsorbed onto Fe-oxides and Fe-oxyhydroxides and will impact on upward metal transfers to surface (Nahon and Tardy, 1992; Scott and Pain, 2008). Consequently, the transformations of the weathered products to laterites serve as barriers to allow easy element migrations between the underlying parent materials and the surface materials above the newly formed laterites. As indicated in chapter 2 evaporation rates exceed the annual rainfall more than two-folds (Fig. 2.1). This climatic condition favours lateritization process hence the widespread of laterite landforms in the study area. Apart from the chemical and physical element mobilisation processes, plants also take up mineralisation-associated metals that are essential micronutrients (e.g. Zn, Mo, Se) and other ore metals (such as Au, Ni, Cu, Pb) and potentially toxic metals (e.g. As) in significant concentrations (Meharg and Hartley-Whitaker, 2002). The sparse vegetation cover (Dickson and Benneh, 1988; Dickson, 1972) with few sinker-types of trees will contribute insignificantly to this type of element transfer to the surface regolith. However, due to the changes in regolith profile as a result of the evolution of the regolith, anomalous concentrations of elements may differ based on regolith types; a typical example is as shown in Fig. 3.6.

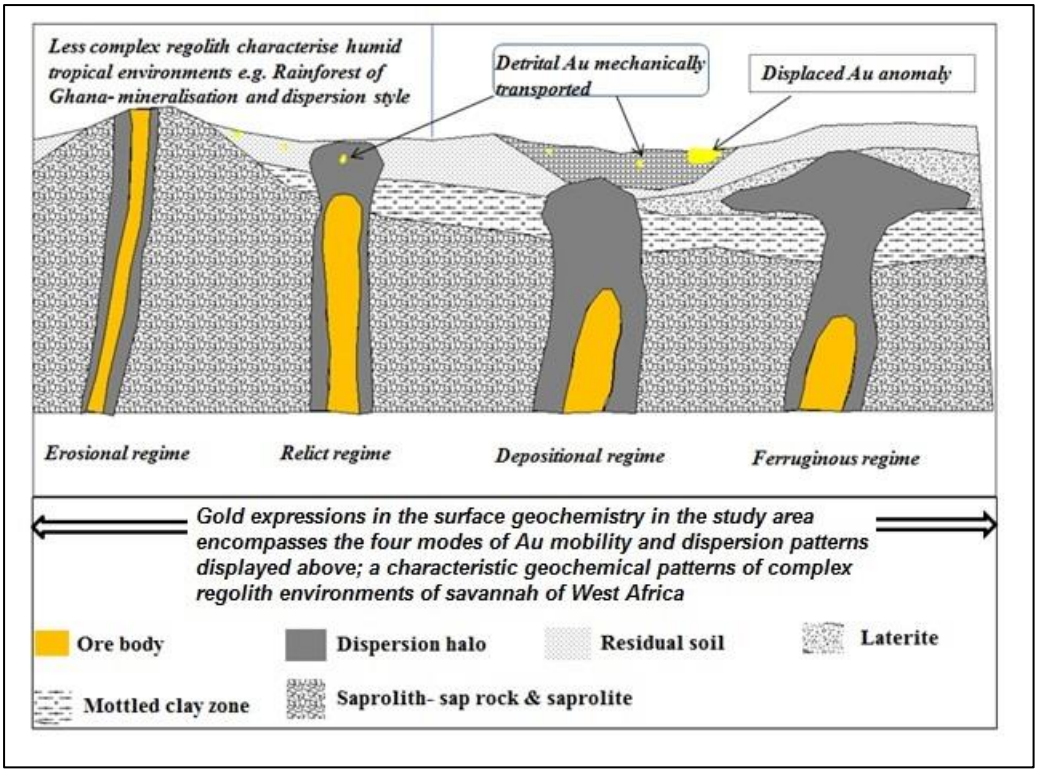

Fig. 3.6 Dispersion halo characteristics of mineralisation from primary mineralisation to the regolith.

There may be many factors due to the changes in the regolith to affect the real expressions of geochemical anomalies in surface regolith. The regolith-landform evolutions will make true and false anomaly distinctions challenging. So in this study the behaviour of major and trace elements mobilisations in the regolith were investigated to facilitate the understanding of the secondary geochemical dispersion mechanisms for successful geochemical gold exploration. The migration of elements in the regolith and determinations of where they reside in the regolith were investigated on the basis that:

a) Au is mobilized, either chemically or physically, in association with chalcophile elements in the Birimian of Ghana.
b) Lateritization forming laterite caps and precipitation of clay minerals filling void spaces during dissolution processes reduces permeability and thus act as barrier to Au migration upwards from its source and
c) Transported sediments from depositional environments dilute or enhance the surficial Au geochemical signatures.

3.3.1 Gold in regolith.

Reports by Griffis et al. (2002), Dzigbodi-Adjimah (1993) and Kesse (1985) show that gold occurrences in early Proterozoic Birimian greenstones in Ghana have associations with sulphide minerals (e.g., arsenopyrite, pyrite, sphalerite, chalcopyrite, pyrrhotite, and galena) in the reduced environment. Similarly Boyle (1979) revealed the relationship of gold with sulphide minerals in their studies on geochemistry of gold. In the Birimian of southern Ghana chalcophile elements such as As, Cu, Pb, Zn etc., are known to be released into the regolith during weathering (Griffis et al., 2002; Dzigbodi-Adjimah, 1993; Bowell et al., 1992 and Kesse, 1985). Investigation into the appropriateness of these elements as pathfinder element for Au exploration surveys as the Birimian belt of the study area is similar to those in southern Ghana (Allibone et al., 2002; Hirdes et al., 1996, 1992; Leube et al., 1992).

Native gold is commonly considered as an immobile element (Scott and Pain, 2008). Nonetheless, Livesidge (1893 a, b) noted the mobility of gold with some complexing agents. He reported experimental results that indicated the possible involvement of organic matter, halide and sulphur complexes in the process. Andrade et al. (1991) have also confirmed the increasing evidence that indicates the mobility of gold in surficial environments. In the surface environment the mobility of Au may be due to both physical and chemical processes. Bowell (1992) observed occasional Au intermixed with Fe-oxides and hydroxides, producing rusty Au. This is particularly common in the top of the saprolite and saprolite-soil interface and is interpreted as the product of the oxidation of Au bearing arsenopyrites in southern Ghana. The arsenopyrites can oxidize completely to goethite. However, due to the rapid change in the pH of the environment over thiosulphate, the complex is unstable and gold is quickly precipitated out and resides in the goethite and specific types of clays (Gee and Anand, 2004). This section in the oxidized environments tends to present probable dissolution, transport and precipitation mechanisms responsible for the distribution of Au in the regolith.

3.3.2 Geochemistry and mobility of gold

Gold geochemistry is complicated because it has three valence states in natural systems e.g., Au (0) in native gold, electrum and colloids Au (I) in waters under reduced conditions and Au (II) in waters under very oxidised, acidic conditions

(McPhail, 2004). In addition to these states, dissolved Au can exist as ions (Au^{+}, Au^{3+}) or as many possible complexes with for example chloride, iodide, sulphide, thiosulphate, cyanide, amine and other organic ligands and chelate (Taylor and Eggleton, 2001). The nature and properties of colloids and other particles and the dissolved Au complexes affect how much Au can be leached, transported and precipitated (Bowell, 1992). These depend directly or indirectly on several geochemical variables, i.e., temperature, pressure, pH, redox, concentrations of elements or compounds that complex with Au (e.g. Cl^{-}, I^{-}, HS^{-}, SO_4^{2+} etc.) and partial pressures of gases (Thornber, 1992). Example each Au complex has a stability constant dependant on pH and concentration of Au and the ligand (Thornber, 1992). The thiosulphate complexes mobilising Au appear common in the reduce environment with the halide complexes especially chloride complexes occurring in the oxidised environment. Thus metallic Au becomes mobile on complexation with halide (CN^{-}, Cl^{-}) in acid-oxidising environments; thiosulphate complexes ($S_2O_3^{2-}$) in alkaline conditions and organic complexes in organic rich environments. In addition to the physical and chemical variables, biota also affects Au geochemistry and mobility.

3.3.3 Gold mobility during lateritic deep weathering

The complex regolith environment presents both challenges and opportunities for mineral exploration (Table 3.2). This is demonstrated for instance in the formation and evolution of deeply weathered lateritic regolith, which results in the mobilization and redistribution of Au, and has considerable significance to the surface signature of mineralization (Butt, 1989; Gray et al., 1992). During lateritization in seasonally humid, warm tropical climates, oxidation at the weathering front deep below the water table produces neutral to acid conditions, with lower pH favoured by felsic rocks and high sulphide contents. Thiosulphate ions, which can complex Au, are formed only by sulphide oxidation in neutral to alkaline conditions, and concentrations of chloride ions and organic matter are very low in the surface environment (Kesse, 1985). Lateral dispersion of Au is evident towards the top of the profile, particularly in the lateritic residuum and mottled horizons (Butt and Zeegers, 1992). This is due to combination of processes i.e., residual concentration, colluvial transport and surface wash of Au grains during land surface reduction and mobility of Au either in solution or as particulates (*e.g.*, colloids or very fine grains of free metal).

Table 3.2 Some geochemical exploration problems and opportunities in deeply weathered terrain (modified after Butt, 2004).

Problems	**Cause**
Difficulty in recognizing parent lithology	Mineralogical, chemical and morphological change
Variable regolith thickness; soils derived from many different parent materials	Different weathering and partial erosion
Spurious secondary enrichment and numerous 'false positive' anomalies	Mobility and re-concentration during weathering, erosion and deposition
Complex geochemical signatures	Superimposition of multiple weathering events
Masking by transported overburden and basin sediments, themselves possibly weathered	Ineffective chemical dispersion during post depositional weathering and diagenesis
Opportunities	**Cause**
Presence of supergene ore deposits	Residual or absolute accumulations, e.g., bauxite, Ni-Co laterite; Au, Nb, P, U deposits; Fe and Mn ores. Industrial minerals
Largely residual regolith as sample medium	Tectonic stability; long exposure; little erosion
Widespread geochemical anomalies in a variety of regolith horizons and materials, e.g., soil, lateritic residuum, lag, pedogenic carbonates	Physical and chemical dispersion over long periods

Some Au may also be contributed directly to the soil in litter after uptake by plants. Reduction of the complexes results in incorporation of fine-grained Au with low Ag contents in Fe oxides, particularly in the lower part of the lateritic residuum and in the mottled zone (Butt, 2004). Such mechanisms normally account for the formation of lateritic Au deposits and Au anomalies, with their mixture of high and low fineness Au, and the presence of ore-grade oxidized mineralisation through the saprolite. Lateral Au dispersion occurs mostly in highly saline environments, especially in palaeochannels, where supergene enrichment may either be in oxidizing or reducing environments, or in the saprolite beneath the channel but may generally be proximal to primary mineralisation in bedrock. Where the profile has been preserved, the

widespread halo in the lateritic residuum is retained, whether at surface or buried (Anand and de Broekert, 2005). Where the regolith has been truncated, leaching of the upper horizons may still have occurred, so the near-surface expression of mineralisation is minimal, although the supergene enrichment is present (Mann, 1984; Scott and Howard, 2001).

3.4 Effects of complex regolith on gold exploration

Butt and Zeegers (1992) noted complex regolith on the landscape makes exploration for gold extremely difficult if the regolith environment is not properly understood. Therefore, to devise an appropriate exploration method that may delineate potential gold within complex regolith requires the understanding of the regolith environment (Anand et al., 2005). Freyssinet (1993) in his studies in Mali contended that a study of regolith in which geology is integrated with geomorphology give better understanding of the gold geochemistry. Such a process may possibly work in savannah regions of northern Ghana. The integrated approach of superimposing the regolith on the geochemistry will give a better understanding as to where samples may be taken in the landscape and what precisely is collected as sample. Taylor and Eggleton (2001) recognised regolith map as a representation of the spatial distribution of regolith units on the landscape. The distributed regolith units were noted by Anand et al. (2001) not always to relate to the underlying parent materials. Report by Arhin and Nude (2009) indicate creation of a regolith map to define the different regolith domains can assist to distinguish residual regolith from transported regolith. Knowledge of the spatial regolith will facilitate separating residual anomalies from false anomalies (Freyssinet, 1994), which may help in detecting mineralisation under cover.

Gold discoveries have been found in similar complex regolith environments in Arid and Semi-arid regions such as Australia, Mali, and Guinea (Butt and Zeegers, 1992). The discovery histories in these areas include the development of regolith maps, which were subsequently superimposed on the geochemical maps during soil geochemical data interpretation. The challenges of data interpretation were eliminated because the developed regolith maps provided information on type of anomalies (Butt and Zeegers, 1992). Bolster (1999) also recommended the use of regolith to improve exploration in complex regolith areas. He however suggested that the regolith maps should be completed early enough in all exploration programmes to greatly reduce the

luck factor in finding potential orebodies under cover. Anand (2001) also proposed the interpretation of any gold response in the surface regolith with respect to the regolith environment to avoid following up non-existing geochemical gold anomalies or false gold anomalies. This implies that the understanding of the regolith terrain may assist in devising exploration methods that can lead in detecting subtle anomalies. It may further help in selecting appropriate sampling media. It is possible that the lack of exploration success in the Lawra belt is because the regolith environment is unknown (Griffis et al., 2002).

Reports on gold exploration in the area show that detailed studies on the effect of regolith on gold exploration were not done (Griffis et al., 2002). However, at Siguiri mines and Louro prospect in Guinea and at Syama and Sadiola mines in Mali exploration successes were achieved (Butt and Zeegers, 1992) because of the detailed studies that were undertaken on the effect of regolith on gold exploration and the consequent applications of regolith factors in soil geochemical assay gold data interpretation. Smith (1996), at Kalgoorlie district in Western Australia demonstrated that when the regolith regimes were understood it was found that the regolith materials that obstructed successful geochemical gold exploration in tropical terrains were used as sampling media. Furthermore, Butt and Zeegers (1992) support regolith mapping and the characterization of the regolith stratigraphy as they were useful at Bottle Creek and Sword Channel mines in Australia to devise exploration methodologies after many unsuccessful exploration programmes. The cover materials either from transported sediments or laterite cap covers dilute or enhance gold concentrations. These depend on the surface modifying processes and the different concentrating mechanisms.

Junner (1935) reported gold occurrences in the Lawra area. Despite this many gold-prospecting companies have explored for gold without success (Griffis et al., 2002). Exploration techniques that were used by the earlier exploration companies were transferred wholly from the successful exploration practices in central and south-western Ghana. Lawra area has savannah climate (chapter 2, Dickson and Benneh, 1988). The landscapes that occur in the savannah climates are typified by widespread laterites and deep weathering profiles (Butt and Zeegers, 1992). Commonly found in the regolith profiles when they are neither truncated nor degraded is the presence of a

thick, hard surficial ferruginous duricrust (Freyssinet, 1993; Zeegers and Lecomte, 1992). However if the upper part of the lateritic profile has been eroded, two main situations may be distinguished (Boulet, 1974; Leprun, 1977; Zeegers and Leprun, 1979), either the:

a. Truncation is rather high in the saprolite and kaolinite inherited from the former weathering profile is the dominant secondary mineral.

b. Truncation is near the base of the pre-existing profile, where rock-forming silicates are present. Weathering of such minerals may result in the formation of smectite.

However, a third situation considering total sum effect may also occur during the mobility of elements in the regolith (i.e., where a lost in one element will result in gain of another element in the regolith). These different situations may merge one into the other over very short distances (Boulet, 1974). These changes in the regolith due to the landscape and regolith evolution and the modifications by lateritization processes require different interpretations of element transfers and different decisions as to the most appropriate exploration procedure. Freyssinet et al. (2005) noted the difficulty in the predictions and behaviour of trace elements in lateritic profiles, especially in complex regolith environments. As the element dispersion processes directly control the formation of the secondary dispersion halo around mineralisation, it has a remarkable influence on the effectiveness of geochemical techniques in such environments (Freyssinet, 1994). Tropical rainforest environment is characterized by high rainfall (1250 mm per year) with alternate wet and dry seasons as well as high temperatures (20-30^{o}) such that chemical weathering occurs at rapid rate (Bowell, 1992). Weathering of the primary ore zone occurs at the saprolite-rock interface and involves the leaching of mobile components from primary mineral assemblages and the formation of stable secondary assemblages. Varying geochemical element dispersion patterns are developed in the regolith from the parent rock and these depend on regolith type and mineralogy. The regolith in the rainforest is generally homogeneous and the Au is released from the ore-bodies by physical disaggregation and chemical dissolution (Bowell, 1992), the latter involving hydroxyl, thiosulphate, cyanide and fulvate complexing. Dissolution and re-precipitation of the Au appears to have taken place largely in situ (Bowell, 1992). Consequently, the Au mineralogy of

the soils is complex with residual and secondary Au grains exhibiting widely different textural and compositional characteristics. The Au mineralogy in regolith soils of southern Ghana appears to be controlled by physico-chemical process active during the lateritic pedogenesis producing residual and supergene enrichment of Au. Much of the secondary Au is intergrown with Fe-oxides and hydroxides (Bowell, 1992). Thus the characteristics of Au and other element dispersions and mechanisms of mobilization in the savannah regions are unknown, and this should be understood if mineralisation hidden under cover is to be unravelled in the present study area.

General element behaviours during weathering in regolith involve a series of chemical and mineralogical changes consisting of a progressive loss of Na^{+}, K^{+}, Ca^{2+}, Mg^{2+} and retention of Si^{4+} (in part), Al^{3+} and $Fe^{3+,}$ as well as the mobilization of minor and trace elements (Fabris et al., 2009; Sheard et al., 2006). The chemical and mineralogical changes expressed in the regolith signify a number of modifications that typically have long and/or complex developmental histories. The changes in surface regolith in the Lawra belt portrayed by irregularly distributed ferruginous laterite capping environments to depositional regimes with patchy erosional surfaces and relict landforms support both chemical and physical changes. The complex distribution of the regolith materials (Arhin and Nude, 2009) presents exploration problems as samples may be collected from different materials. The mixture of different regolith units from dissimilar parent materials may either dilute or enhance geochemical Au signatures in the regolith by geochemical and surface modified processes (Butt et al., 2000). The geochemical anomalies formed in the modified regolith environments may either be residual or transported anomaly and will require distinction (Fig. 3.6) if successful Au exploration is anticipated.

The Au exploration successes in southern Ghana were improved because of the better understanding of the regolith environment by the mineral explorers. In southern Ghana the upper regolith materials usually relate well with the underlying parent rocks and the intact laterite profiles are preserved on higher ranges. These have been interpreted to be an attribute of a deep weathering event in the Palaeocene-Miocene epoch. Areas with distally depositional regolith are found along stream and river channels. Additionally Plio-Quaternary uplift and erosion of the profile has resulted in dissections into saprolite and these normally occur in areas of no vegetation cover. Conversely knowledge of the regolith environment of northern Ghana is less

understood. There is no published report about the evolution of the regolith-landforms in the area. The only published report on regolith is Arhin and Nude (2009) that only described the occurrence of intact laterite profiles occurring in low lying areas and over some previously uplifted regolith profiles. The relationships between genesis and weathering histories of various regolith types and correlations between different regolith units across the landscape are yet to be investigated. It appears the variable regolith types considered to be the same and residual everywhere have consequences for element migrations and dispersions in the regolith profiles.

According to Freyssinet (1993), the differences in regolith and landform modifications in two different climatic zones suggest a wholesale transfer of exploration procedures from one region to another may not work well. This is because of different regolith-landform units formed during weathering and erosional events. The effect of climate on regolith development made Butt and Zeegers (1992) to propose the use of different sampling depths but only effective in geochemical exploration when the regolith architecture is well understood. This again was in agreement to Bolster's (1999) assertion that selections of appropriate sample media, positions and density to depend on the knowledge of the distribution of the regolith materials. As physical, chemical and biological processes cause the regolith and landforms to change so too should the optimal exploration techniques. Geochemical anomaly types are unique and often reflect the characteristics of the regolith regime. Therefore the use of particular exploration techniques that had been successful elsewhere may not necessarily be successful in a new environment especially where there are climatic differences that may impact on the regolith environment. The fundamental problems in complex regolith environments because of the heterogeneity of the regolith materials are the low and high Au assays that are commonly erratically distributed spatially. Areas with erosional landforms have surface samples relating well with underlying mineralisation (Arhin and Nude, 2009). However, in areas of deep colluvial cover that are probably underlain by buried laterite, surface sampling may be fraught with problems such as inadequate collection of samples from the preserved residual surface (Cohen et al., 2010). Gold response obtained in this environment may be false or subtle and may be unrelated to underlying mineralisation (Anand et al., 2001).

It is therefore necessary that the distribution of the regolith materials on the landscape is mapped and characterization of the stratigraphies is established before soil geochemical programmes are undertaken. The selection of appropriate sampling media, sample density and sample depths can be obtained from the regolith maps and the characterizations of the stratigraphies. This chapter therefore reviews the following to help improve the exploration success in the Lawra belt:

a. Regolith formation, evolution, characterization including processes and mechanisms that move regolith and elements in the oxidized environments,

b. Regolith controls on metal transfers,

c. Exploration in deep weathered environments and highlights on the related problems due to the weathering states and

d. Historical and current exploration surveys in the area plus some selected examples of gold exploration surveys in complex regolith environments.

3.5 Arsenic in the regolith

Arsenic is an important pathfinder element for Au and commonly used in mineral exploration because of its generally wider halo around primary mineralisation, which makes easier to detect in geochemical surveys (Yang and Blum, 1999). In primary mineralisation As and Au are commonly associated with arsenopyrites (FeAsS; Boyle, 1999; King, 2002). Arsenic occurs naturally in soils. Under the conditions prevailing at the Earth's surface, inorganic arsenic is progressively released as pentavalent arsenate (As^{5+}) or trivalent arsenite (As^{3+}) species and these form a large variety of minerals (Anthony et al., 2000; Morin and Calas, 2006). However, most arsenate and arsenite minerals are not stable in soils over long period (Morin and Calas, 2006).

3.5.1 Mobility of As in the regolith

Mobility of As in soil is restricted by its adsorption by soil (Korte and Fernando, 1999; Raven et al., 1998). Elkhatib et al. (1984) found that contents of iron oxides and Eh of the soil are the main soil properties controlling arsenite sorption rate by soils. The leaching of As from various soil profiles is inhibited by the presence of hydrated oxides of Fe and Al, clays and organic substances (O'Neill, 1995). From Lin et al. (2008) As has an affinity for oxygen and as such it is always commonly found in oxyanionic forms in solutions. The pH conditions determine the concentrations of

different As species in soils. Example the species $H_2AsO_4^-$ is the most abundant chemical form of As when the soil solution pH is between 3 and 6. The other species $H_2AsO_4^-$ and $HAsO_4^{2-}$ are also present in appreciable concentrations in the soil solution if the pH is between 7 and 8 (Sadiq, 1997).

Oxidation and breakdown of the sulphur minerals by iron- and sulphur oxidising bacteria leads to the mobilisation of As and Au (Garcia-Sanchez and Alvarez-Ayuso, 2003; Papassiopi et al., 2003). In the regolith the speciation of As is controlled by the pH and redox conditions (Smedley and Kinniburgh, 2002; Oremland and Stolz, 2003); where arsenate species (i.e. As (V) as $H_2AsO_4^-$ and $HAsO_4^{2}$) dominate in oxic or oxygen-rich zones and arsenite species (i.e. As (III) as $H_3AsO_3^0$ and $H_2AsO_3^-$ dominate in anoxic or oxygen depletion zones at typical pH conditions between 4 and 8 (Smedley and Kinniburgh, 2002; Oremland and Stolz, 2003). Depending on local conditions, As concentration and partitioning between solid phases and solutions may further modify by changes in pH and redox conditions (Morin and Calas, 2006). For example the concentrations of dissolved arsenate and arsenite are controlled by surface complexation reactions on oxides and hydroxides of Al, Mn and especially Fe (Smedley and Kinniburgh, 2002; Oremland and Stolz, 2003). Reith and McPhail (2007) noted arsenate to adsorbed strongly to Al-, Mn- and Fe-oxides under typical pH conditions and as such unlikely to be mobile whereas arsenite adsorbs less strongly and to fewer minerals and is the more mobile (Smedley and Kinniburgh, 2002; Oremland and Stolz, 2003). Therefore the dissolution of As may be counteracted by the precipitation of Fe-oxyhydroxides, which efficiently scavenge As^{3+} and As^{5+} at neutral pH. The commonly observed increase in solubility of As under reducing conditions is attributed primarily to the reductive dissolution of Fe^{3+}-oxide phases and the subsequent release of adsorbed As.

3.6 Exploration problems in tropically weathered terrains

Geochemical exploration surveys make use of soil and other regolith materials such as upper soil, lag, or saprolite as sample media. However, the evolution of the terrain and the development of the regolith give rise to several problems that hinder effective application of geochemical exploration. Typical exploration problems noticed by Cohen et al. (2010); Coker (2010); Smith (1996); Butt and Zeegers (1992) in tropically weathered terrains that may be common in the study area include:

a. Profound mineralogical, chemical and physical alteration of bedrock and associated mineralisation that makes distinction between even broad lithological classes difficult;
b. Strong leaching of most ore-related elements especially from upper horizons of the regolith, resulting in only subtle surface geochemical signatures of mineralisation;
c. Weak geochemical dispersion haloes generally in laterite environments due to gold grain encrustation during lateritization processes;
d. The development of spurious secondary concentrations of target elements in weathered and barren rocks;
e. Lateral changes in the nature of regolith due to variations in the depth of truncation of earlier pre-existing profiles by the present erosional surface;
f. The presence of a cover of transported overburden from mineralised source rocks deposited on unmineralized rocks to create 'False' anomalies;
g. The presence of a cover of transported overburden from unmineralized source rocks deposited on mineralised rocks to cause anomaly dilution, and the
h. Superimposition, in a single profile of the effects of weathering under different environmental conditions.

As shown by Butt and Zeegers (1992); Smith (1996); Cohen et al. (2010) and Coker (2010), effective geochemical exploration surveys can only be achieved by the recognition of these problems and the processes that influence element concentrations in the regolith so that selection of techniques of sampling and data interpretation appropriate to detect hidden mineralisation can be applied. This requires a review of historical exploration surveys in complex regolith environments including the study area to understand the implications of regolith on gold exploration.

3.7 Regolith expressions in gold deposits in complex regolith environments –some case studies.

The regolith expressions of gold in surficial regolith materials are best interpreted using knowledge of regolith studies and the understanding of element behaviour in deeply weathered environment. Typical case studies that showcase the complexities of element distributions and concentrations in the regolith and how they were overcome using regolith geochemistry are given below for the Bounty and Cornishman gold deposits in Australia and Filon Bleu prospect in Guinea.

Climate of gold deposits found in complex regolith in Australia used in the case studies for the current research has a tropical savannah climate, characterised by wet and dry seasons. These areas have variable rainfall compared to a distinct rainy season in the Lawra belt. Common among the Australian case study areas to the Lawra belt is the high temperatures and the sparse vegetation covers. Landforms in the Australian case study areas compares well with the Lawra belt i.e., all have undulating landforms with occasional topographic highs. At Bounty gold deposit the drainage systems are poorly developed and have an annual rainfall of about 450 mm and potential annual evaporation of 1200 mm. Similar to Lawra belt the drainage systems are poorly developed but the annual rainfall and potential evaporation rates (Fig. 2.1) appear higher case study areas in Australia. However, the regolith, where complete, the profile has an upper ferruginous horizon (Fe-rich clays and lateritic residuum), underlain by mottled clays, bleach saprolite and unweathered rock (Lintern et al., 1990) to be similar to the regolith environment of the Lawra belt (Arhin and Nude, 2009. The similar environmental and climate conditions make it appropriate to devise exploration techniques applied at Bounty and Cornishman gold deposit for the study. A summary of gold deposits discovered using this approach in Australia and parts of West Africa are shown in Tables 3.3 and 3.4.

3.7.1 Bounty gold deposit.

Smith (1987) recognized gold dispersion at the Bounty gold deposit to be controlled by both hydromorphic and mechanical dispersion. The surface residual anomaly caused by the hydromorphic dispersion increased the gold magnitudes towards the main mineralized body and decays away from it (Fig. 3.7; Lintern et al., 1990). However, the reverse was the case for the displaced anomaly controlled by the mechanical dispersion. The displaced anomaly (Fig. 3.7) was high close to ore grade at surface but was unrelated to any underlying mineralisation. These types of displaced anomalies are often followed because of the high assay expressions in surface samples. This is a classic example of ‘false’ anomaly that is only noticeable if the regolith environment is understood.

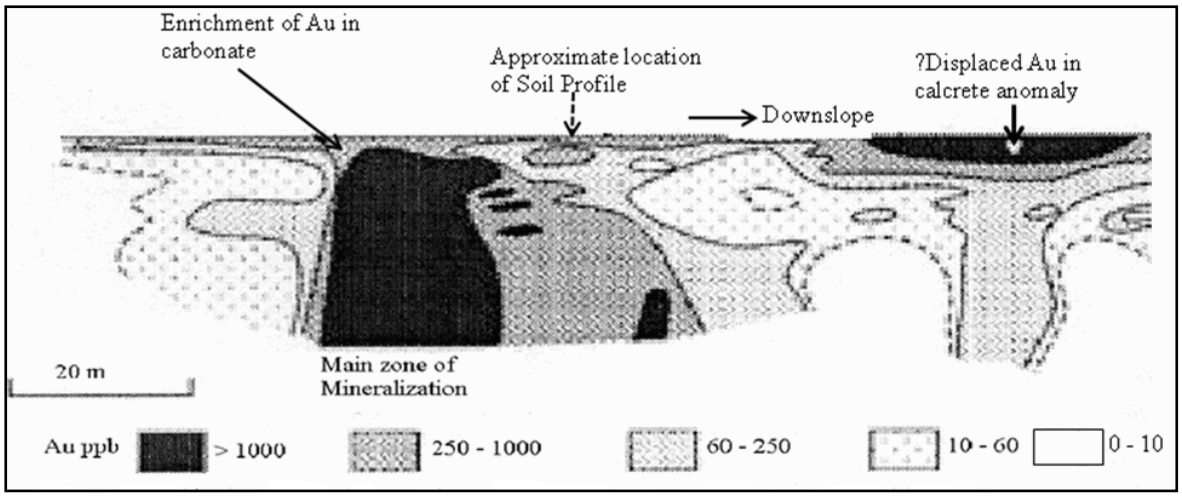

Fig. 3.7 Gold in the top 20 - 30 m of the regolith section along 35000mN of the Bounty deposit, Australia (after Smith, 1987).

3.7.2 Cornishman gold deposit

Also at Cornishman gold deposit Markwell (1993) found gold around the mineralised body not to be significantly dispersed by supergene processes and hence, does not represent a large exploration target (Fig. 3.8). The surface Au expression at surface may be an attribute of transported regolith overlying mineralisation. As it is the common practice in the exploration companies high Au assays are normally followed up (Griffis et al., 2002).

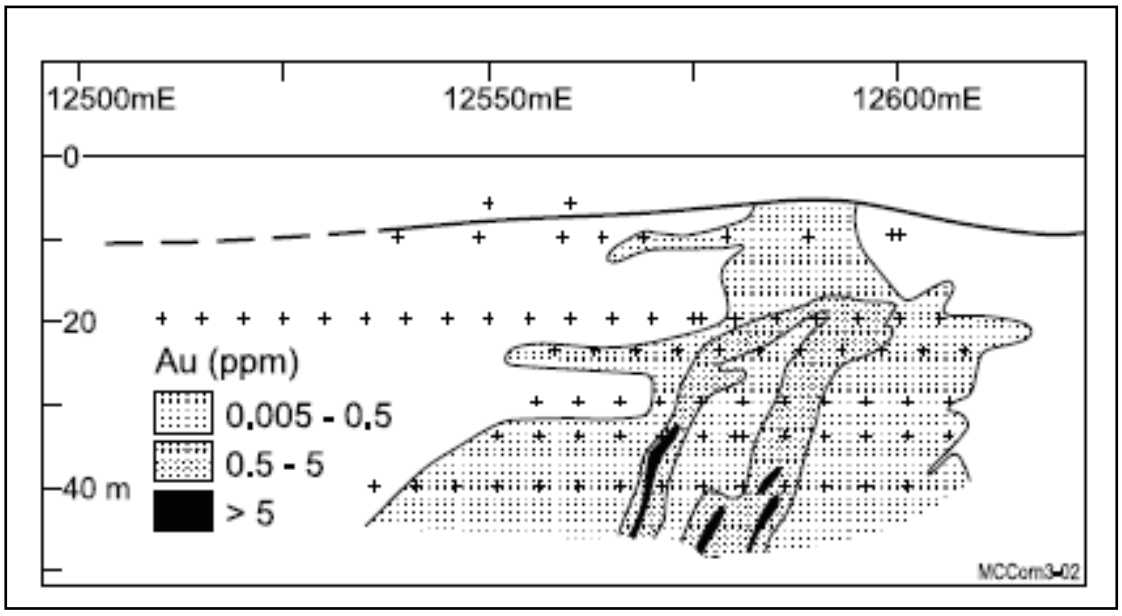

Fig. 3.8 Gold dispersion in the regolith at the Cornishman gold deposit along traverse 4912mN (after Markwell, 1993).

The weak geochemical Au expressions in the surface regolith often lead to the abandonment of exploration survey if the regolith environment is not understood. The surface regolith due to the regolith evolutions can be relict representing residual weathered materials, depositional consisting of transported sediments of diverse origin, ferruginous-where the transported and in situ weathered products have been transformed by Fe-oxides and clay minerals and erosional where the pre-existing preserved surfaces have been truncated. All these regolith types have different influence on geochemical anomalies (Cohen et al., 2010). In some of the regolith domains anomalies may be enhanced or diluted or assay results may be subtle (Butt and Zeegers, 1992). Arhin and Nude's (2009) work in the belt show the occurrences of these regolith types. The low Au expressions in the surface regolith at Cornishman Gold resulted in the use pathfinder elements for the determination of the concealed gold deposit because of their understanding of the regolith environment. As indicated by Markwell, (2005) and shown in Fig. 3.9 the pathfinder elements were useful to detect mineralisation under cover.

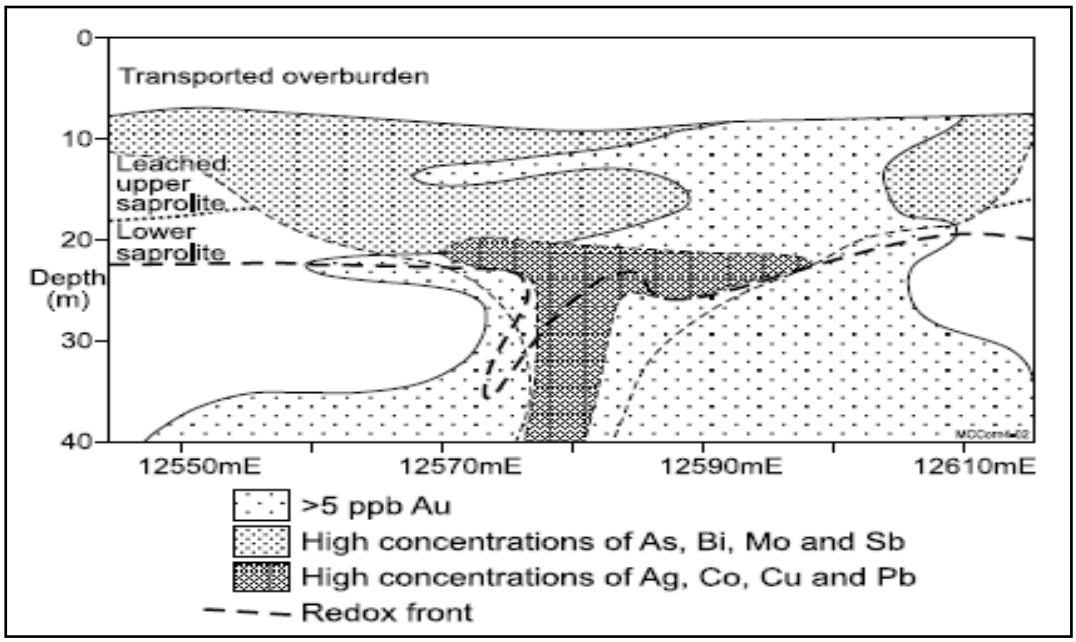

Fig. 3.9 Summary of the ore-associated element distribution at the Cornishman gold deposit along traverse 4912mN (after Markwell, 1993).

3.7.3 Filon Bleu prospect

Figure 3.10 shows a gold geochemical response in a small vein type gold occurrence (BRGM, unpublished internal report) in a Precambrian volcano-sedimentary rocks setting.

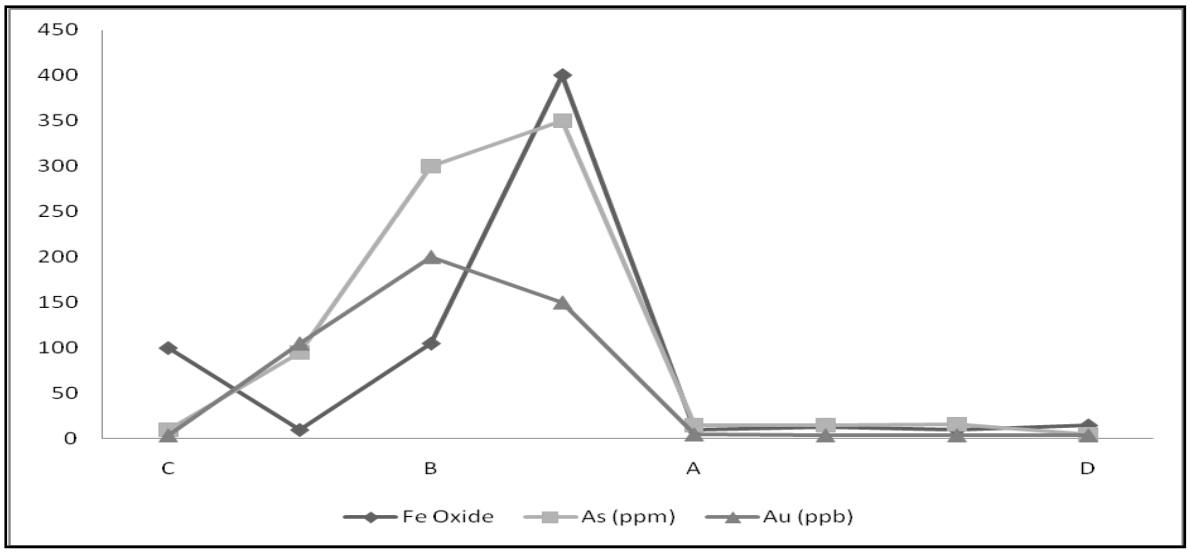

Fig. 3.10 Different element distributions in a complex regolith along a traverse CD at Filon Bleu Prospect, Guinea (modified after Butt and Zeegers, 1992).

Section B to A represent pre-existing lateritic profiles and is dissected with sub outcropping saprolite developed over basic volcanics. C to B is an outcropping cuirasse and A to D is cuirasse covered by mostly residual silty soil of about 0.5 to 1 m thick with some degradation of the cuirasse at some places. Soil geochemistry samples were taken at about 30 cm depth and also from cuirasse outcrops. The soil samples were sieved and fine (<125 µm) size fractions recovered for analysis of 34 elements by ICP after alkaline fusion and Au by AAS after aqua regia-HF digestion. The hard cuirasse samples were crushed and pulverized before analysis. The Fe_2O_3, As, and Au contents along the traverse showed specific geochemical dispersion characteristics according to the different weathering situations. As shown in Fig. 3.10, high gold were obtained at the truncated environment with diminishing Au dispersion halo in areas where cuirasse is covered by residual soils. Also As appeared to be less influenced by the type of weathering profile present but had highest values at outcropping cuirasse environments. The use of Fe-rich phases consisting of nodules and pisoliths as preferential sample medium for the determination of arsenic (As), and Au in geochemical exploration irrespective of the weathering profiles is vital (Butt and Zeegers, 1992). Similar conclusions were reached by Mazzucchelli and James (1966) and Smith et al. (1987) in Australia.

Table 3.3 Gold deposits in Australia using geochemistry and regolith studies (Butt et al., 2005).

Deposits	**Resource x 10^6 Oz**	**Upper Regolith**	**Sample Type**	**Impact[(1)]**
Yilgarn Star	1.6	Clay (2-5 m)	Soil	**Definitive**
Bronzewing	3.1	Transported (2-50 m)	Buried laterite	**Primary**
Mt. McClure	0.9+	Shallow Residual	Soil	**Primary**
Nimary	0.7+	Shallow Residual	Lateritic lag	**Primary**
Jundee	1.3	Shallow Residual	Lag	**Primary**
Callie	1.1	Aeolian sand (5 m)	Bedrock	**Primary**
Redback/Dogbolter	0.6	Aeolian sand/laterite	Soil/laterite	**Primary**
Chalice	0.5	Thin transported	Soil	**Primary**
Sunrise	1.25	Transported	Soil	**Definitive**
Cadia	8.3	Transported	Auger/soil	**Definitive**
Rustler's Roost	1.3	Shallow Residual	Drainage	**Incidental**
Mckinnons	0.1	Residual	Drainage/soil	**Primary**
Tick Hill	0.4	Residual	Drainage/soil	**Primary**
Kanowna Belle	4.0	Residual/transported (2-5 m)	Soil	**Definitive**
Marymia	1.0	Shallow Residual	Soil	**Ancillary/Definitive**
Plutonic	**7.2**	Shallow Residual	Lateritic lag/soil	**Primary**

The explanation of the impact classifications is as follows:

Primary: *leading technique in exploration programme that located ore.*

Definitive: *ore may not have been found, first indication but critical techniques in discovering ore nearby.*

Ancillary: *geochemistry supported data from other techniques in discovery process.*

Incidental: *discovery independent of geochemistry, but available data show geochemistry would have been effective if other techniques had not been used.*

Table 3.4 Gold discoveries in West Africa using geochemistry and regolith studies (modified after Butt and Zeegers, 1992).

Prospects	Work Done	Exploration Problem(s)	Regolith Characteristics	Impact or Results
Diouga (Burkina Faso)	Studied regolith mineralogy, multi element survey (Ambrosi, 1984)	Scattered Au occurrences (BRGM unpublished report)	Transported/laterite caps	Upgraded Au occurrences (Butt and Zeegers, 1992)
Filon Bleu Au (Guinea)	Multi element survey detected arsenic as best pathfinder element (Lecomte and Zeegers, 1992)	Weak geochemical soil signatures	Complex regolith	Found a deposit
In Mali	P, V, Cr, As, Nb, Mo were used as pathfinder elements	Subdued geochemical gold expression in soils	Complex regolith	Discovered potential mineralization (Butt and Zeegers, 1992)

3.8 Historical Exploration surveys in the Lawra belt, Ghana

First mining activities in the study area date back to the 1920's and 1930's when the Gold Coast geological survey recorded several gold occurrences while mapping in the area. These earlier mining activities (illicit artisanal mining) were undertaken by the local people, which are locally known as 'galamsey' (Griffis et al., 2002; Kesse 1985). The locals panned for gold in streams and scavenged for gold after heavy rains from heaps of sheetwash deposits and behind rock bars in gullies and valleys in some towns and villages. The galamsey and the gold occurrences in northern Ghana were first reported in 1935 by Junner.

Formal gold exploration survey started in this area in 1960 after collaborative Russian-sponsored geological mapping and prospecting between Ghana Geological Survey and their Soviet counterpart identified and confirmed the gold occurrences reported by Junner (Griffis and Agezo, 2000; Pobedash, 1965). In this geochemical survey, Ghana and Soviet Geological Surveys employed traditional geochemical survey techniques that included stream sediment sampling, soil sampling, trenching and lithological sampling. This exploration survey did not lead to any gold discovery

and exploration stopped until 1990. In the early 1990's BHP-Minerals undertook a regional stream sediment survey using the bulk leach extractable gold (BLEG) technique in order to cover the entire Lawra belt, an area spanning *ca.* 6000 km^2. A sample density of 10 km^2 was used (Griffis et al., 2002). The BLEG survey identified several anomalous targets that included Dorimon, Duri, Basabli, Kunche, Yagha, Lawra north gold occurrences etc., but were not followed up by soil geochemical survey due to company's policy. There was a complete cessation of gold exploration work in the area until 1996.

In 1996 Ashanti-AGEM Alliance acquired the 150 km by 40 km land cover of the Lawra belt for reconnaissance gold exploration. This was the period of the 3rd gold boom in Ghana for their quest to discover a 'superfine' out of the BHP-Minerals identified BLEG targets. Ashanti-AGEM Alliance introduced a new exploration technique called 'multimedia' geochemical survey, which included sampling stream sediments, termite mounds, laterite lags, rock chips and soil samples concurrently. The soil sampling grids were set out on an initial 1000 m x 100 m grid after which the significant gold anomalies, defined by 100 ppb gold threshold value, were infilled to 200 m x 100 m and then to 100 m x 50 m grids (Griffis et al., 2002). This was done regardless of the regolith types. The other multimedia samples were collected 100 m away from both sides of the soil gridline. Also any stream that crossed the soil line had its active sediments sampled and sieved to <125 µm for gold analysis. Well over 45000 soil samples were collected in this survey. This geochemical soil survey by Ashanti-AGEM Alliance is considered the most extensive surficial geochemical survey in the belt by a single company (Carter, 1997). The gold results from this survey were mixed; many of them were weak, and subtle, together with some isolated highs and generally speckled geochemical patterns along with discontinuous Au anomalies. The integration of the gold expressions in the different multimedia samples detected some anomalies, but the defined anomalies were not as large as the anomalies commonly defined in similar surface samples in southern Ghana (where there are active mines and no regolith complexities). Nonetheless eight geochemical targets were defined from the combined interpretation of the multimedia survey and the extensive soil survey. Two of the targets were test drilled. One was a reconfirmation of the BHP BLEG target (Duri) and the other a newly anomalous target defined by the multimedia (Kunche) but it was only the Kunche anomaly that

returned about 240 koz of gold resource; the other at Duri had an insignificant intersection of <1 g/t over 2 m (Carter, 1997; Griffis et al., 2002). The disappointing drill results of only 240 koz of gold from Kunche and no significant discovery hole at Duri in a greenstone belt whose gold occurrence was reported in 1935 led to the discontinuation of further exploration survey by the group in the belt. They however, farmed-out the entire license area to SEMAFO Ghana who also abandoned the project after obtaining insignificant gold results from trenching at the time of a poor gold price in the world market (Bailie and Arhin, 2000). It is apparent to notice that the earlier explorers failed to incorporate the implications of regolith on gold exploration and never tried to establish the relationships between the various regolith types and their correlations with the subtle and spot-high anomalies. The exploration companies that worked in the area were consistent in the application of the traditional geochemical methods used in less complex regolith environment in southern Ghana to a complex regolith terrain of NW Ghana.

Currently Azumah Resources Ltd. is exploring the area. Their report indicates a discovery of 1.1 Moz Au in the entire study area (Azumah Resources Internal report, 2011). This discovery possibly constitutes about 1.0 % of gold endowment in the area comparing the size of area where the discoveries are coming from to the entire size of the Lawra belt. On the basis of the total prospective area explored versus the total area of the Lawra greenstone belt, the other 99% is probably under cover and needs to be unravelled. Therefore the key to discover the hidden mineral potential under cover requires reviewing exploration successes in similar environments across the world. It has been noted by several authors (e.g. Butt and Zeegers, 1992; Smith, 1996; Bolster, 1999, Cohen et al., 2010; Coker, 2010) that regolith affects surface geochemical expressions. It is also known that the presence of the regolith has great significance in providing both problems to and opportunities for, exploration (Butt and Zeegers, 1992). Therefore the understanding of the regolith environment is important in detecting mineralisation under cover.

3.9 Conclusion

The Lawra Birimian belt is within a deeply weathered terrain characterized by complex regolith. The modifications of the regolith due to weathering, erosion, transportation and deposition enhance or dilute Au signatures in the regolith and thus

have serious implications for gold geochemical exploration surveys. Mineralisation can be displaced or concealed, diluted or enhanced. Identifying the real anomaly needs the understanding of the regolith to be able to detect mineralisation undercover. In conclusion a regolith map must be created for the study area, investigation of trace and major element behaviour in the regolith profile must be carried out, and the integration of the regolith map and the Au assay data is essential to delineate anomalous geochemical targets.

Profile terminology

There is no universally agreed system for the terminology of deeply weathered regolith, whether for whole profiles, individual horizons or for many distinctive secondary structures, despite being a subject of discussions for many years (Butt and Zeegers, 1992). This has resulted in a controversy among different authors about the use of some regolith terms. Accordingly, comparisons of like situations in widely separated regions are greatly hindered by the inadequacy of existing terminology and lack of consensus in its use. In the context of current research, applications of the principal terms used in Butt and Zeegers (1992) are used and are given in the *glossary of terms* below.

Glossary of Terms

***Alluvium*:** a general term for clay, silt sand and gravel deposited as sorted or semi-sorted sediment during comparatively recent geological time on a bend or flood plain of a river or stream.

***Cuirasse*:** is a French term, meaning iron crust. It is a highly indurated horizon of the ferruginous zone of a lateritic regolith with a massive pisolithic, nodular or vesicular fabric. In general use cuirasse refer to those hardpans whose origin of formation is not known; they can either be residual or transported.

Cutan: is a modification of the texture, structure or fabric of a soil material at a natural surface due to the concentration of particular constituents.

Duricrust: indurated materials at or just below the surface. The material may be ferruginous, aluminous, siliceous or calcareous calcrete or a combination of these. It is also referred to as 'residual laterite'.

Ferricrete: a conglomerate of surficial sands and gravels cemented into a hard mass by iron oxide derived from the oxidation of percolating solutions of iron 'salt' or more

generally indurated materials formed by in situ cementation or replacement or both of pre-existing regolith by Fe-oxides and oxyhydroxides precipitated from soil water or groundwater. This is also referred to as 'transported laterites'.

Hardpan: a subsurface indurated horizon or hard subsoil or clay.

Lag: a veneer or pavement of fragments of diverse origins or compositions on the land surface. This is commonly applied to highly ferruginous concretions. Fragments may be faceted, rounded or varnished.

Laterite: a highly weathered material, depleted in alkalis and alkaline earths, composed primarily of secondary oxides and oxyhydroxides of Fe (goethite, hematite, maghemite) and hydroxides of aluminium (e.g. gibbsite).

Mottled zone: a horizon, generally, within the regolith profile characterized by localized spots, blotches and streaks of Fe oxides and oxyhydroxides that with further mobilization and concentration become organized into secondary structures.

Pisoliths: a spherical or ellipsoidal concretionary or accretionary body resembling a *pea* in shape and limited in size to bodies of over 2 mm diameter.

Sap rock: a compact, slightly weathered rock with low porosity and contains >25% of the preserved rock fabric or <20% of weatherable minerals altered.

Saprolite: a weathered bedrock which contains <25% of the preserved rock fabric or weathered bedrock in which fine fabrics, originally expressed by the arrangement of the primary mineral constituents of the rock are retained and have > 20% of weatherable minerals altered.

Soil: The upper part of the regolith that supports plant life.

Transported overburden: Refers to materials of exotic or redistributed origin such as alluvium, colluvium, sheetwash, evaporitic sediment, aeolian clay, piedmont fan deposits and glacial debris that blanket fresh or bedrock. It may be friable, or partly or wholly consolidated, cemented by Fe oxide, silica, carbonate, gypsum or clay.

Regolith Research Methods

4.0 Introduction

Repeated weathering, erosion and deposition greatly influence the expression of mineralisation in the regolith. They determine the mechanisms of Au dispersion and complicate the distinction between residual and transported regolith which thereby makes anomaly delineation difficult. The consequence of the regolith modifications is the numerous Au exploration failures. Therefore it is better to understand the regolith to help identify Au mineralisation in the area. In developing better knowledge of the regolith the study followed the approach recommended by Pain and Kilgour (2004), Eggleton and Taylor (2001) and Butt et al. (2000), namely to develop maps that show spatial variations in regolith materials that may influence element dispersion. Consequently, this research adopted the following procedures:

a. Regolith maps were developed from field information and remote sensing imageries;
b. Characterization of regolith profiles and
c. A geochemical survey was conducted that accounts for the effects of the regolith on Au dispersion.

4.1 Regolith mapping

The regolith maps created were: 1). 1:450000 scale for the entire Lawra belt (Fig. 4.1 and 4.2). The locations of Kunche-Bekpong and Sabala designated for the prospect scale regolith mapping are shown in Fig. 4.2. Each regolith/landform unit recorded was grouped as regolith mapping units and was classified based on similarities amongst mapping units in terms of the nature of pedology, topography and geological features (Arhin and Nude, 2009). These regolith-landform attributes were defined by three main descriptors; regolith material descriptor in upper case letters, landform descriptor in lower case letters and a numerical induration modifier. These three variables allowed each regolith unit to be given a unique code.

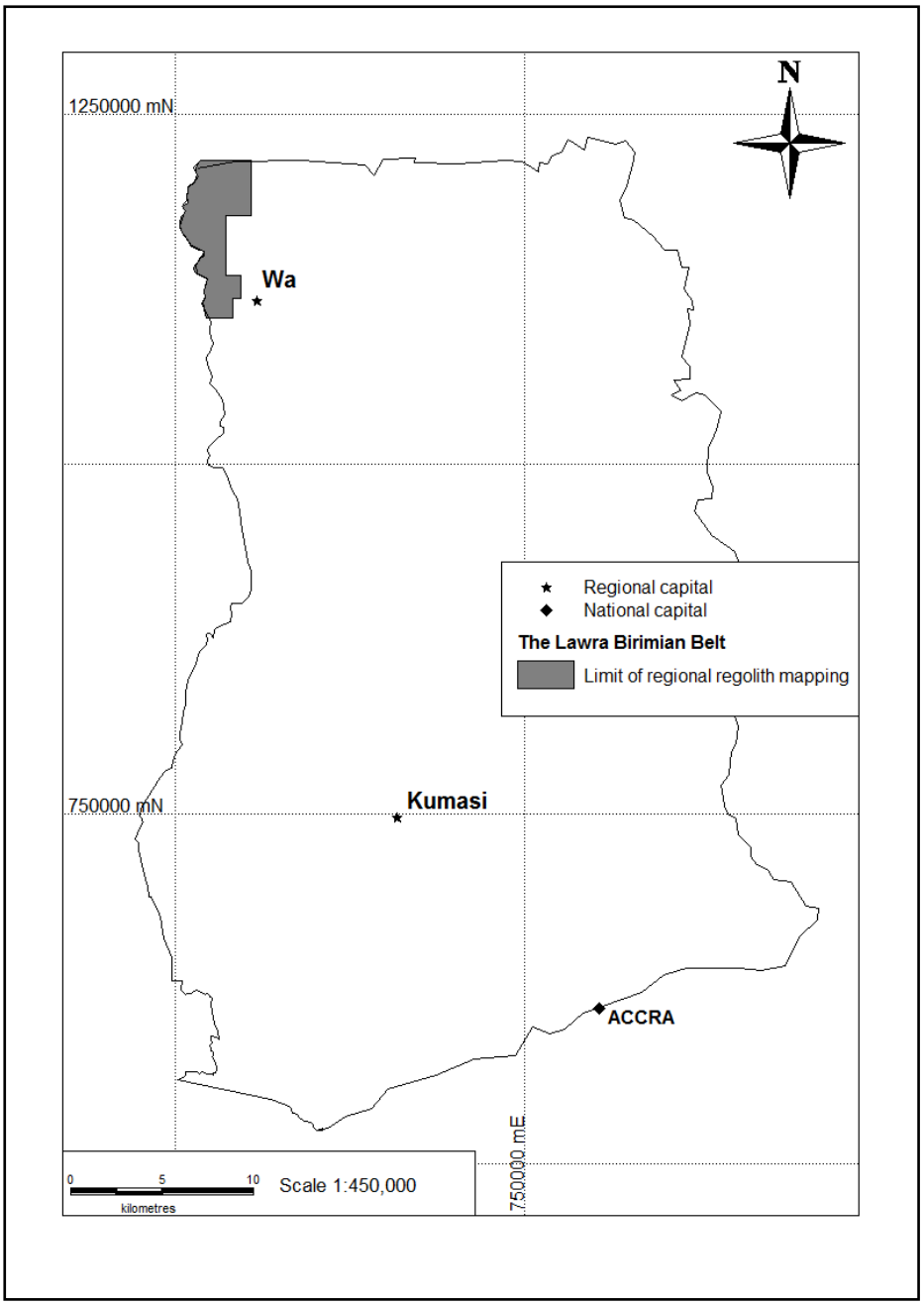

Fig. 4.1 An outline of Ghana map showing the Lawra belt area (shaded grey) to be mapped for spatial distributions of the regolith materials

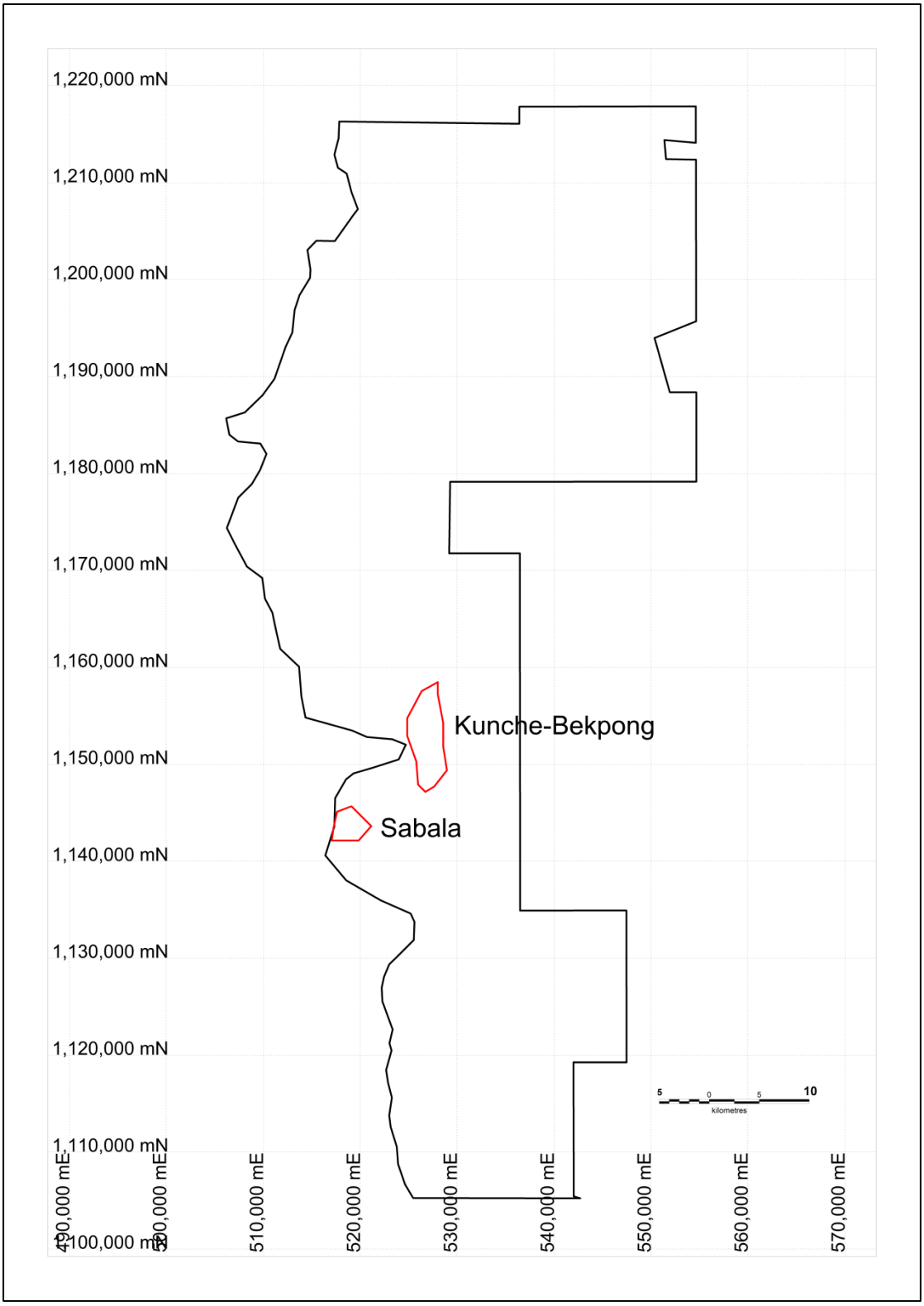

Fig. 4.2 Outline of the Lawra belt and the selected areas for the prospect scale regolith mapping shaded red.

4.2 Regolith map processing by integration model

Regolith map processing involves a model that integrates extractions from remote sensing and field ground truth mapped data. MapInfo-Discover GIS was used to combine the derived regolith information from the landscape and genesis classification schemes. The GIS map developments in this thesis used mercator projection, WGS 84 map datum and Universal Transverse Mercator (UTM) coordinate system. The superimposition of the derived patterns displayed in the same map projection was processed further in the GIS environment to classify the terrain first into residual and transported regolith. The regolith map for the study was obtained following a three-step process of the integration model (Fig. 4.3).

STEP 1 STEP 2 STEP 3

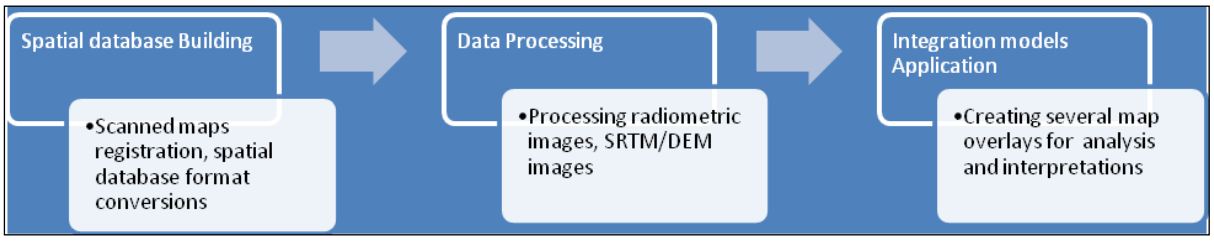

Fig. 4.3 The 3- step computer based processes in developing regolith terrain map (RTM) in GIS interface.

The regolith mapping development has two parts: landscape and genesis classification that are used to develop a factual map after which an interpretive map is developed. The map development is based on a genetic model from which a sampling strategy and geochemical data interpretation maps can be derived.

4.2.1 Landscape or pre-field stage classification

This comprised the identification of land surfaces types through remote sensing analysis. Table 4.1 shows data used, their properties and spatial resolutions.

Table 4.1 Types and properties of remote sensing data used (WAXI-IRD internal data base)

Data type	Band No.	Spectra range (μm)	Ground resolution (m)	Bits
Landsat	1	0.45-0.52		Best 8 of 9
	2	0.53-0.61		
	3	0.63-0.69		
	4	0.78-0.90		
	5	1.55-1.75		
	6	10.4-12.5		
Radiometric			1:100000	
SRTM/DEM			90 m pixels	

The classification of the terrain using the remote sensing data relied on well-established spatial, genetic and environmental correlation techniques between landforms and regolith as suggested by Laffan and Lees (2003). Each dataset was used to add a different component of information to the final regolith map. For example, radiometric data were employed for their ability to reveal information on the surface materials when differentiation between regolith materials was inconclusive with other imagery. Digital Elevation Models (DEM) and Shuttle Radar Topography Mission (SRTM) were useful for adding landform and geomorphic information to the mapped regolith units. It also enabled areas of low topographic relief and rises to be differentiated. Landsat and Radiometric imagery overlays at the same scale were also helpful as they discriminate inferred boundaries by highlighting different components of the regolith. Using MapInfo-Discover software the above listed data were registered to the same map grid, projection and datum. They were then processed, integrated, displayed and visualized to classify the landscape into residual and transported regolith based on the assumption that landforms are surrogate to regolith (Craig, 2001, Craig et al., 1997a, b; 1998, Chan, 1988).

All the remote sensing data available for the regolith mapping studies were digitally processed. The SRTM images were used specifically to map geomorphic features like relief and drainage systems. Radiometric data were used to distinguish the residual and transported environments whereas Landsat was used to discriminate between residual and transported laterites. Detailed interpretations of SRTM and Radiometric

image processing used in development of the regolith terrain map (RTMAP) for the study area is presented in chapter 5.

Conversely Landsat data were processed further by principal component analysis (PCA) in order to observe the subtle variations in the surface regolith. PCA allowed most of the information within all the bands (represented by the variance) to be compressed into a much smaller number of bands with little loss of information (Gibson and Power, 2000). This reduced the dimensionality of the data and made it easier to interpret than the original data (Jensen, 1996). PCA transformation has high variance in data of which each succeeding component has the highest discrepancy possible under the constraint that it is orthogonal to the preceding components (Jensen, 1996). In principle the first PCA band contains the largest percentage of data variance than the second PCA data. The last PCA bands commonly are noisy because they contain very little variance, much of which is due to noise in the original spectral data. PCA bands normally produced more multihued colour-composite images than spectral colour composite images because the data are uncorrelated (Richards, 1999). PCA applied to combined images results in high spatial resolution and produce wide range of colours that make the different regolith units easily discernible.

4.2.2 Genesis classification

This is a follow up survey after the image processing has been completed. Its objective is to validate the correctness of the interpretations of the processed images by ground truth survey. In this research two field seasons of fieldwork each lasting for about two (2) months were carried out. The first fieldwork consisted of transects of the accessible tracks and roads to gain overview of the area and the regional setting of the regolith. During this period pits were dug at selected areas, records were kept for the visited sites and samples were collected from different regolith horizons. Detailed regolith mapping and follow up sample collection at areas that were unclear or interesting were undertaken during the second fieldwork.

The mapping scheme used was adopted and modified from the Hocking et al. (2007), Anand et al., (2001) and Pain et al. (1991, 2001) acronym ‘RED’ classification which groups the regolith-landform into relict (R), erosional (E) and depositional (D) regimes, by addition of the ferruginous areas as a separate regime to give the FRED

classification. The relict regime refers to where the full laterite profile is preserved, whereas the erosional regime refers to areas where the original profile has been partially or wholly eroded. This could be to lower saprolite or even bedrock. Both relict and erosional regimes are residual. The ferruginous regime included in the FRED classification refers to a mapping term where it is difficult to decide whether a hardened ferruginous unit is residual (i.e., a lateritic duricrust and hence part of the Relict regime) or transported (i.e., a ferricrete and hence part of the Depositional regime). The FRED classification scheme forms the basis of the interpretational regolith map developed for the study area.

The field studies gathered information about various regolith types and landform attributes. The coordinates of this information were collected with global position system (GPS) receiver along grid lines, road cuts, footpaths and trails. Additionally soil texture, sphericity of quartz pebbles, litho-relics, indurations, type of cementing matrix, texture of other weathered materials, grain composition, sand grain mineralogy, nature of topography and geological features were recorded. The mapping units with the same characteristics and weathering histories were grouped together and did not require the application of any specific model of landscape evolution. The categorization of the mapping units to a single-similar classifying unit is referred to as classification unit. The classification units for the different regolith regimes, shown as regolith polygons, were shown distinctively on the interpretive map. This map was created by drawing lines through the observational points picked and registered by GPS. These points were thematically transferred on a base-map in a GIS environment after which the points with similar themes were digitized to form the regolith polygons. Different shades of colours were used for different regolith-landform regimes.

4.3 Regolith Stratigraphy

Validation of the merged regolith map from landscape and genesis classification was enhanced by exposing and characterizing the regolith stratigraphy. Sixty pits distributed across the different regolith regimes (Figs. 4.4 & 4.5) were excavated and compared with the typical laterite profile modified from Taylor and Eggleton (2001, Fig. 4.5). The regional geological settings for the regolith mapped areas are also

shown in Figs. 4.5 and 4.7 respectively. Different sub-horizon zones defined in all the excavated pits based on the

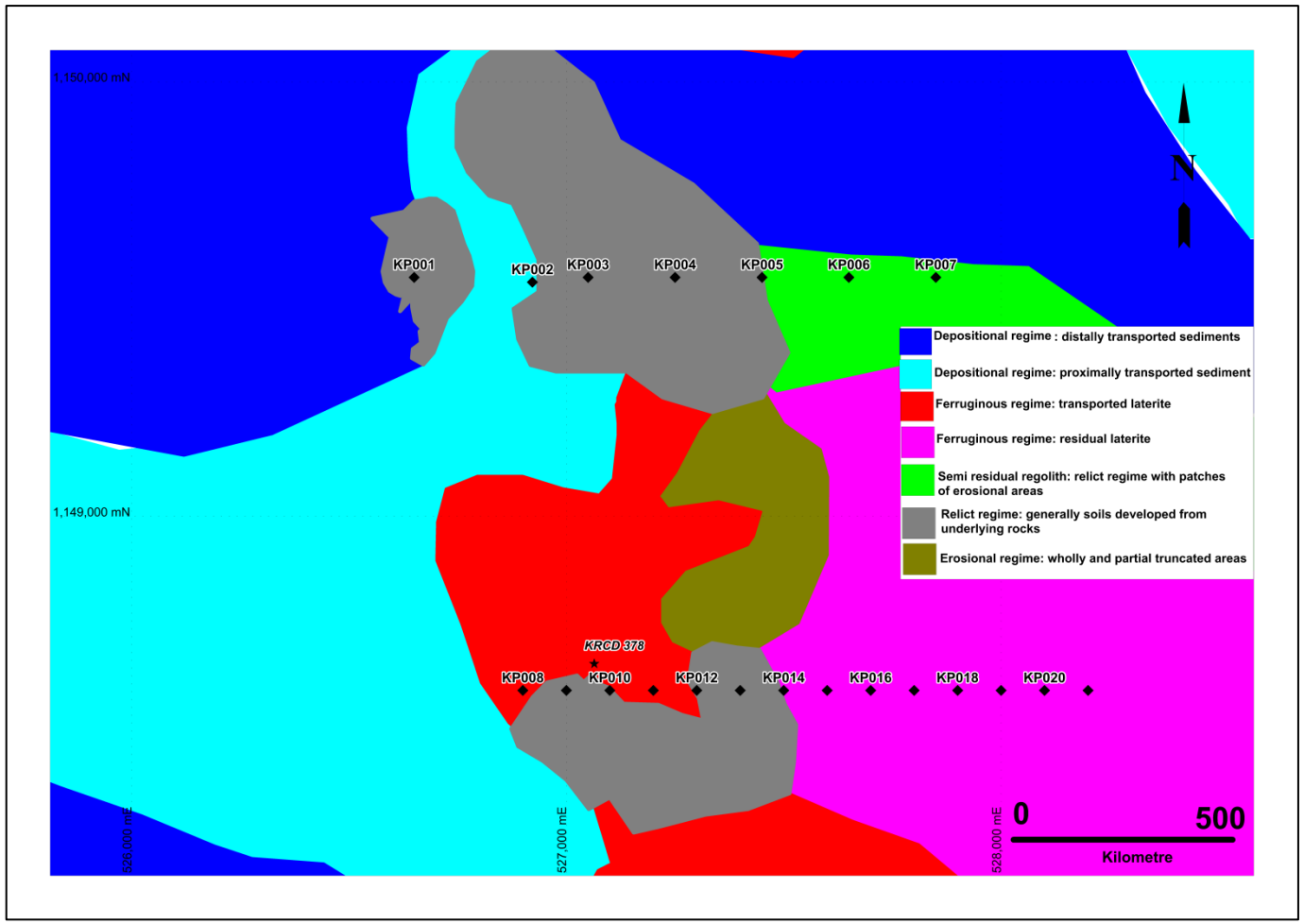

Fig. 4.4 Pit locations at Kunche-Bekpong target area on the prospect scale regolith map

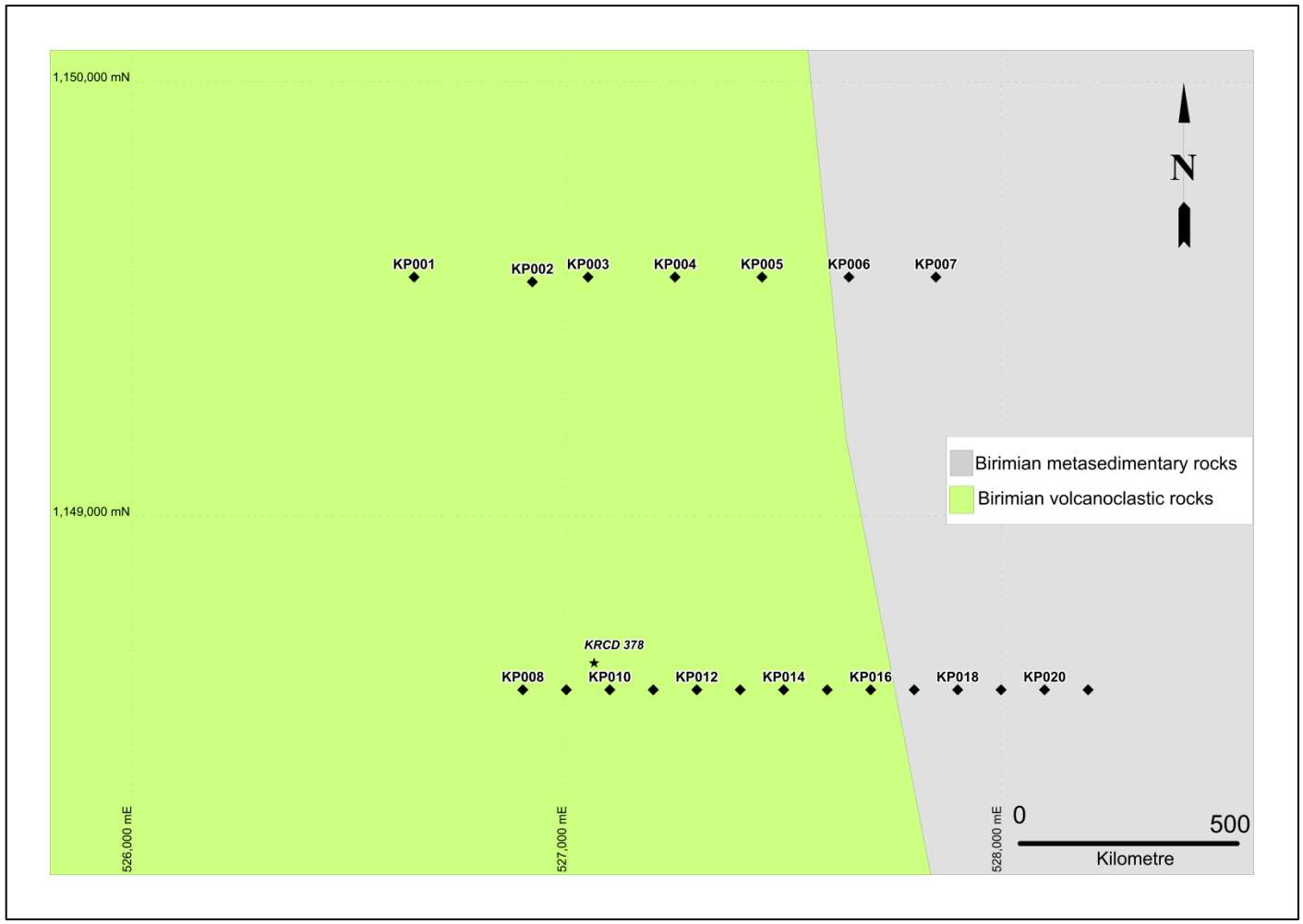

Fig. 4.5 Kunche geology

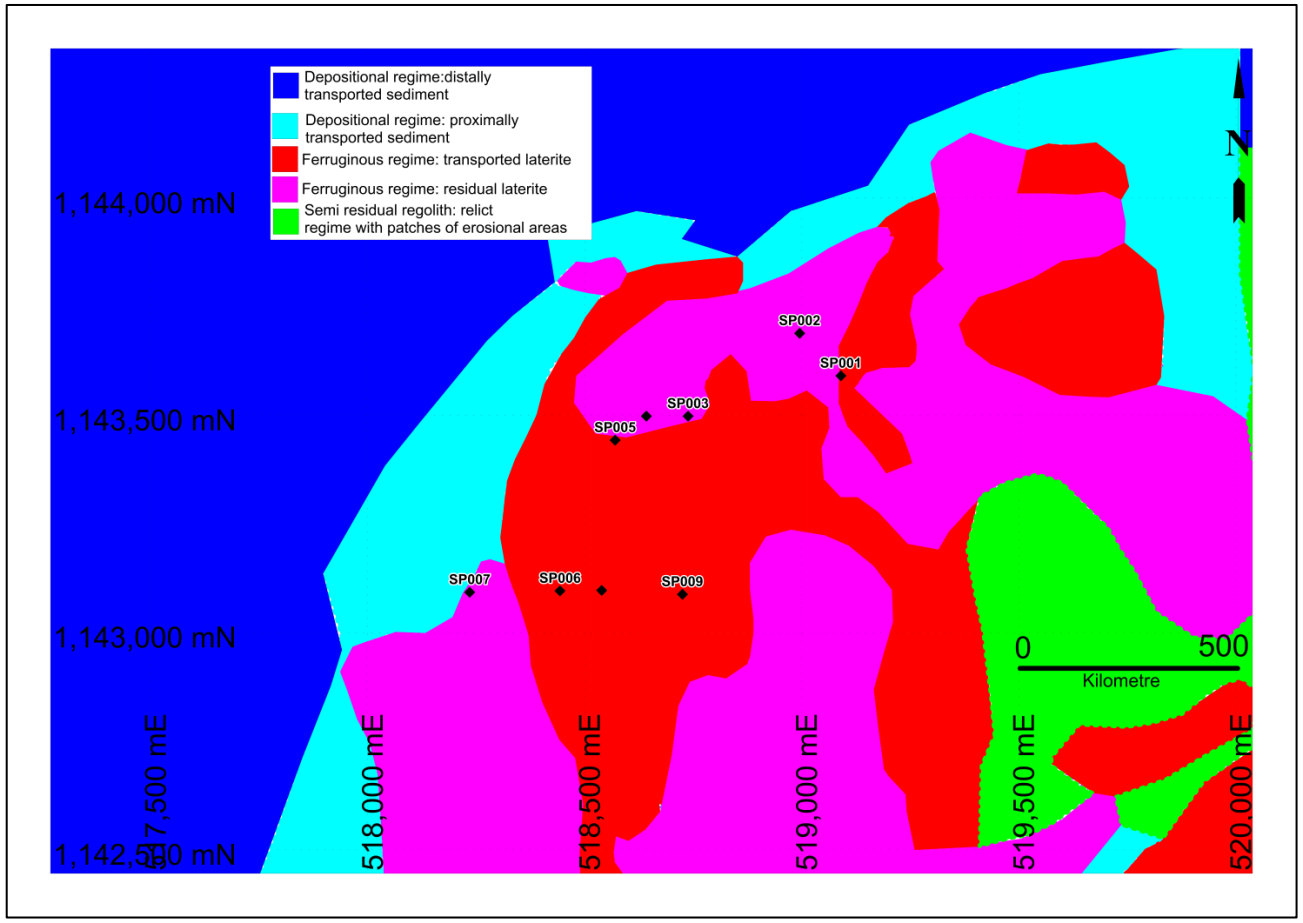

Fig. 4.6 Pit locations at Sabala target area on the prospect scale regolith map

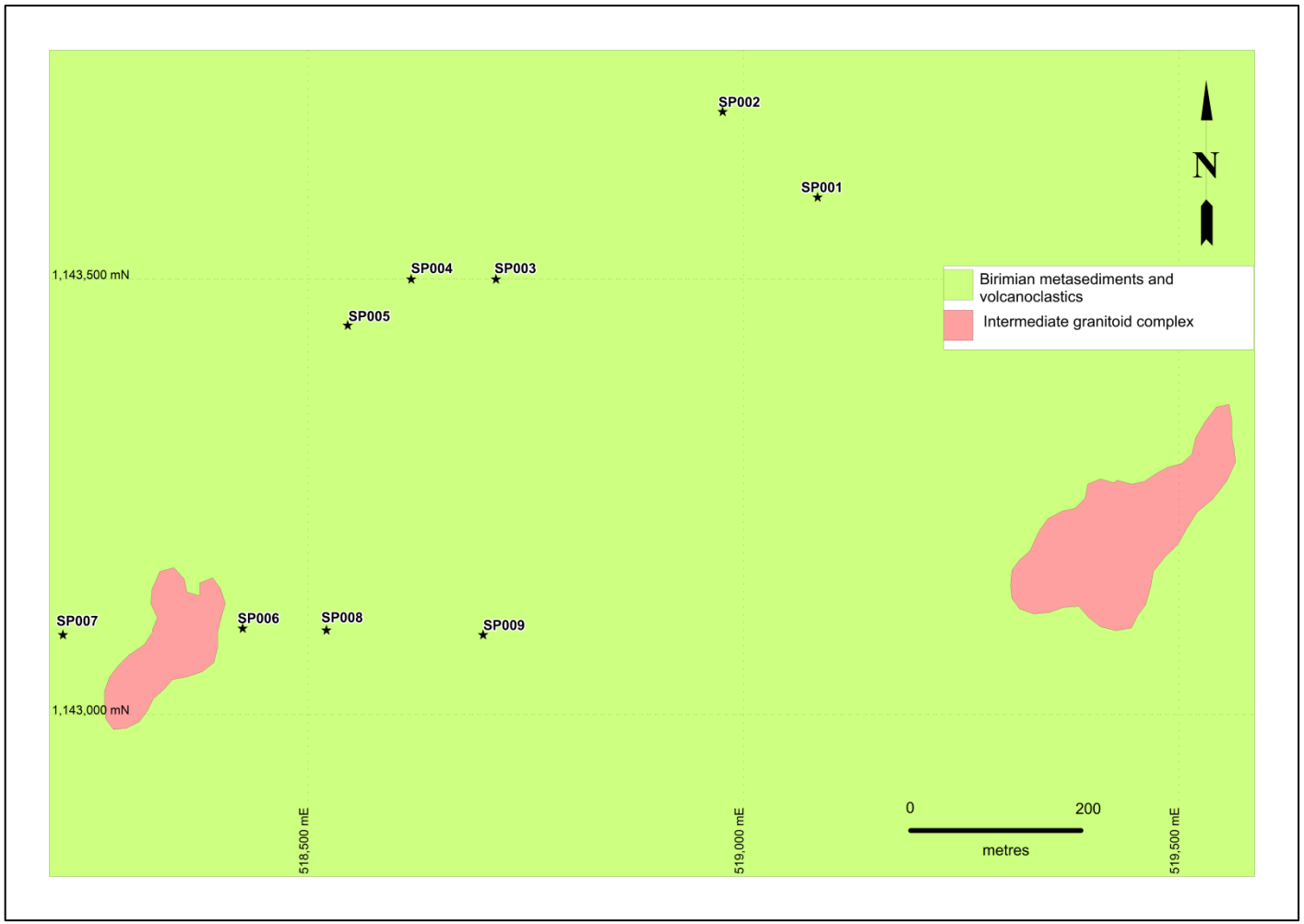

Fig. 4.7 Sabala regional geology

physical and chemical characteristics were logged. Zones marked by erosional unconformities, extent of depositional sediments and zones of lateritization that showed indurations and occurrence of secondary overprints such as ferruginous, silicification or calcareous cementation were mapped. Notes were also taken of the degree of sphericity of lithic and quartz clasts, deformation of grains, nature of contact exhibited by different regolith horizons and degree of consolidation of soil. Visual sand grain morphological studies using a set of sieves from 2 mm to 8 mm screen sizes and hand lens were carried out. The assessments of this information were used to characterize the regolith profiles. Typical regolith horizon arrangements in different regolith regimes and pit datasheet used for the regolith characterization are presented in Figs. 4.8 & 4.9

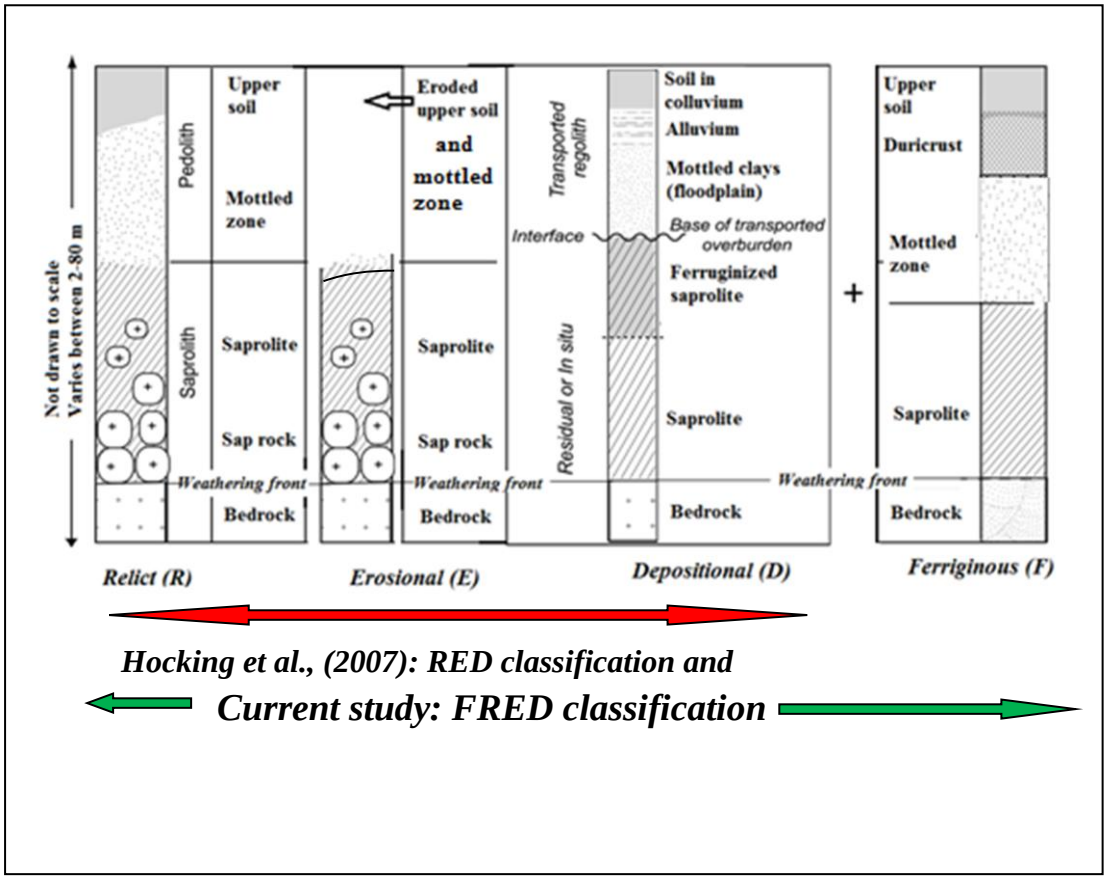

Fig. 4.8 Examples of horizon development and terminology of deep weathering profiles (modified from Taylor and Eggleton, 2001).

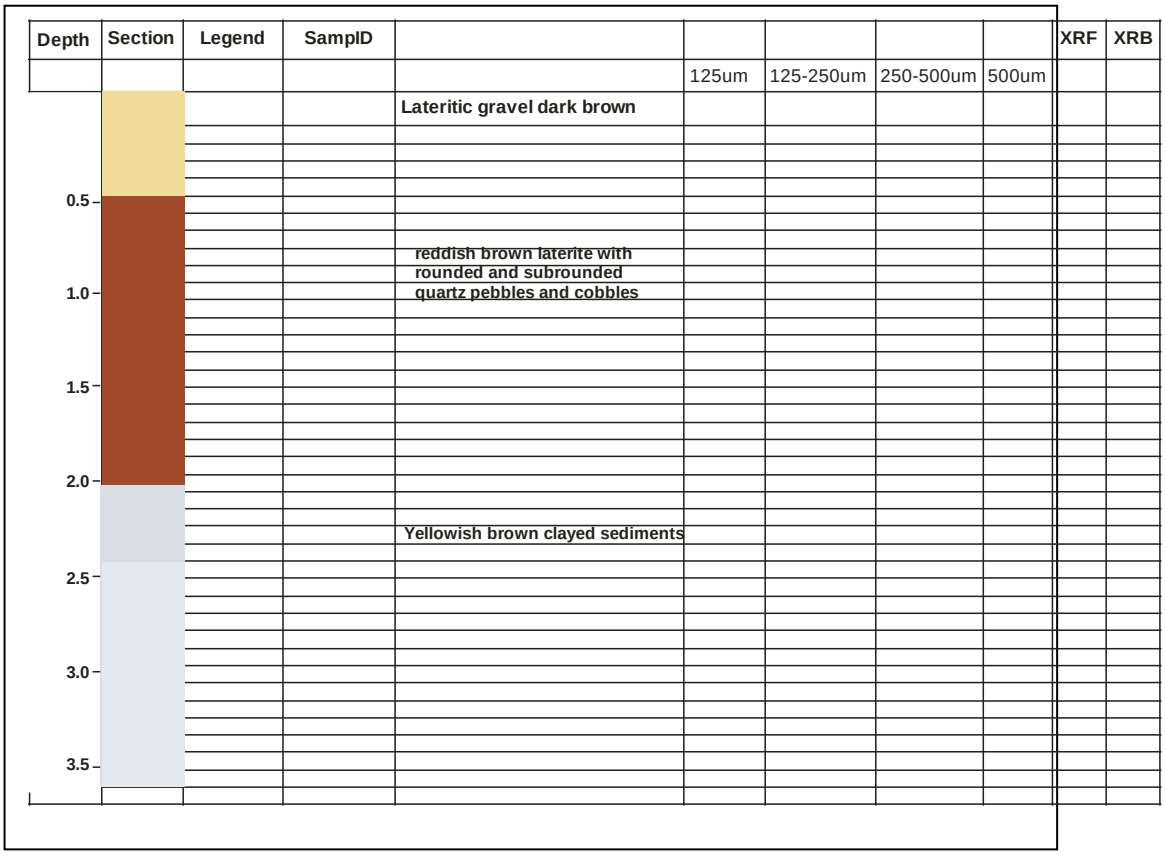

Fig. 4.9 Graphical pit log sheet used during regolith pit logging and mapping of the regolith profile.

In the field the regolith profiles were characterized by interpreting the logged data (Fig. 4.9). Additionally semi-quantitative data that supported the regolith characterization was carried out. This method involved mineralogical and geochemical studies on regolith materials at different classified regolith regimes. This method was used successfully by Pain et al. (2000) to characterize regolith. So to increase the authenticity of the characterized regolith profiles each regolith layer in selected dugout pits were sampled for major and trace elements studies whereas the sieved samples were visually studied in the field for changes in grain morphology.

The contrasting regolith features seen in the pits and other exposures mapped to establish the genesis and histories of various regolith types and their correlations between various regoliths across the landscape are also presented in Figs. 4.10 – 4.15. The characterization of the regolith in the field depended mostly on the evidence of relict features left after the regolith-landform evolution events. For example, a regolith unit that contains rounded sand grains or fragments like those shown in Fig. 4.8 suggests alluvial regolith material transport across the landscape. The rough edges

of the angular sand grains and angular lithic fragment are disintegrated and transformed during the transporting processes to rounded sand grains. Furthermore in laterite cap environments the presence of older laterite embedded in a younger or newly formed laterite demonstrates a depositional environment (Fig. 4.11). Similarly, layered laterites denote different episodic times of sedimentation, compaction and lateritization and therefore represent depositional environments with occasional modified indurations of surface crust where they occur (Fig. 4.12). Also regolith profiles that exhibit an obscured unconformity and have predominant angular and sub-angular quartz clasts in the surface regolith (Fig. 4.13) represent relict environments. Similarly, laterites with equigranular groundmass (Fig. 4.14) are considered as duricrust or residual laterite and normally occur in the relict regime. The horizons that have predominantly euhedral grains with original crystal shapes with gradational horizons from one horizon to another suggest proximity to source. These environments have characteristics of a relict regime (Fig. 4.15).

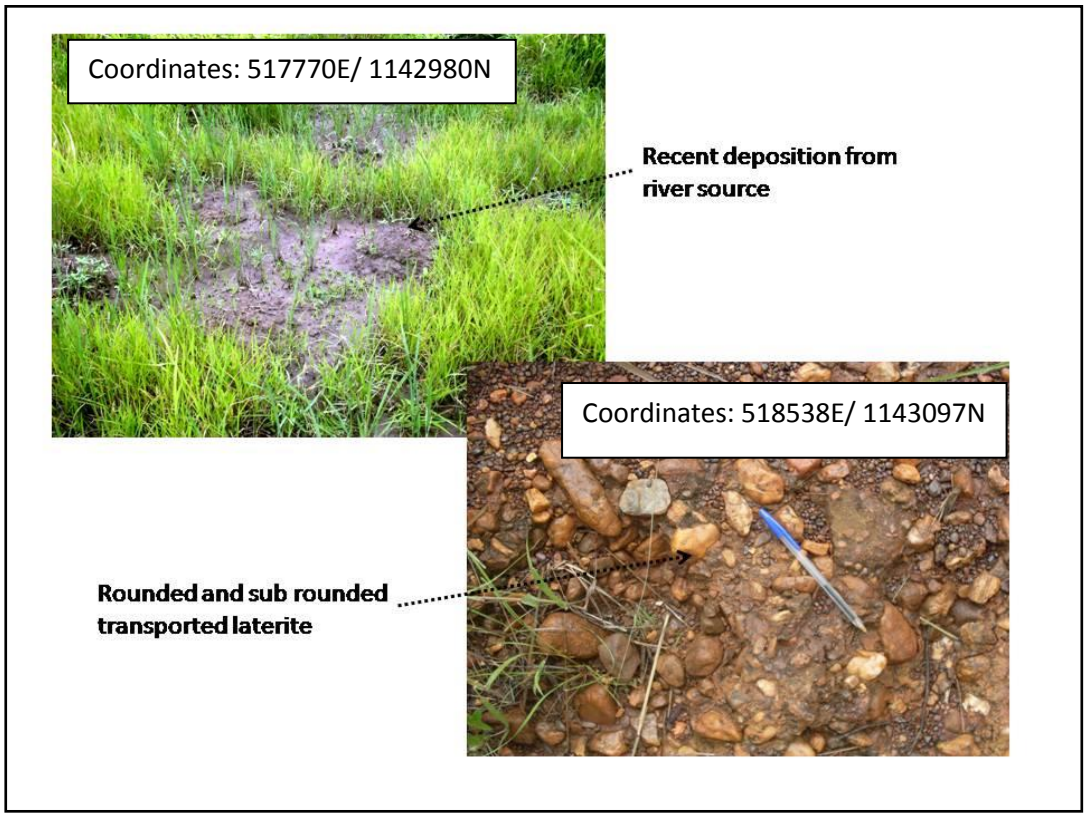

Fig. 4.10 Smooth and rounded quartz pebbles and recent terrestrial sediments: evidence of transportation of regolith materials: Environments like these are classified under depositional regime in the FRED classification scheme.

Fig. 4.11 Rounded and smooth quartz clasts in laterite: evidence of transportation - this is a clast-supported transported laterite located near pit SP002 with coordinate 518995E/1143689N.

Fig. 4.12 Older laterite embedded in a younger laterite: a suggestion of episodic deposition. The area represents depositional regime (GPS coordinate: 519500E/1144200N).

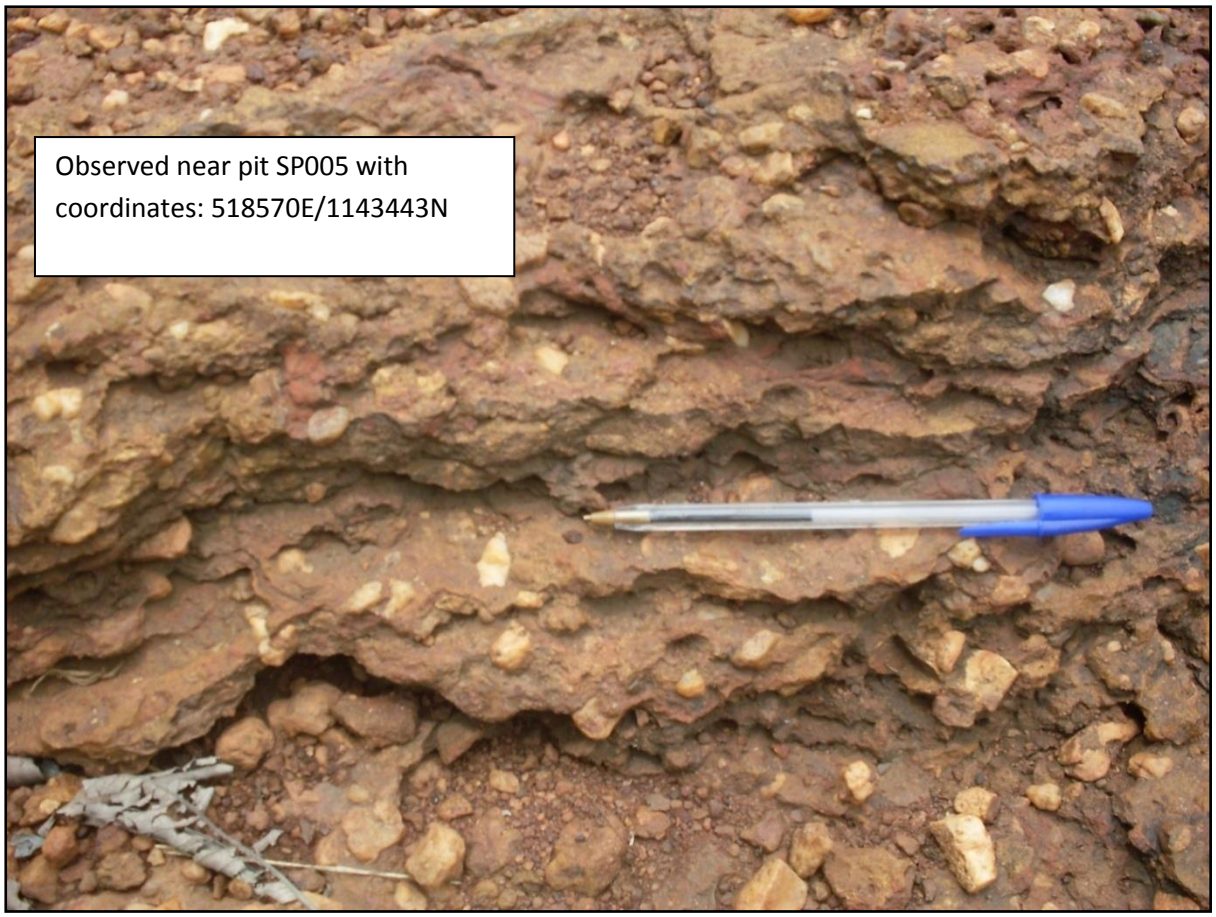

Fig. 4.13 Slabby-form laterite demonstrating evidence of episodic deposition: a typical example of transported laterite.

The residual laterites are characterized by equigranular groundmasses that usually form matrix materials (Fig. 4.14). Differentiation between the residual and transported laterites was based on the nature of the groundmass, the shape of the included fragments as well as the layering characteristics.

Fig. 4.14 Equigranular laterite with a pock-marked surface: This laterite was mapped as residual laterite or duricrust.

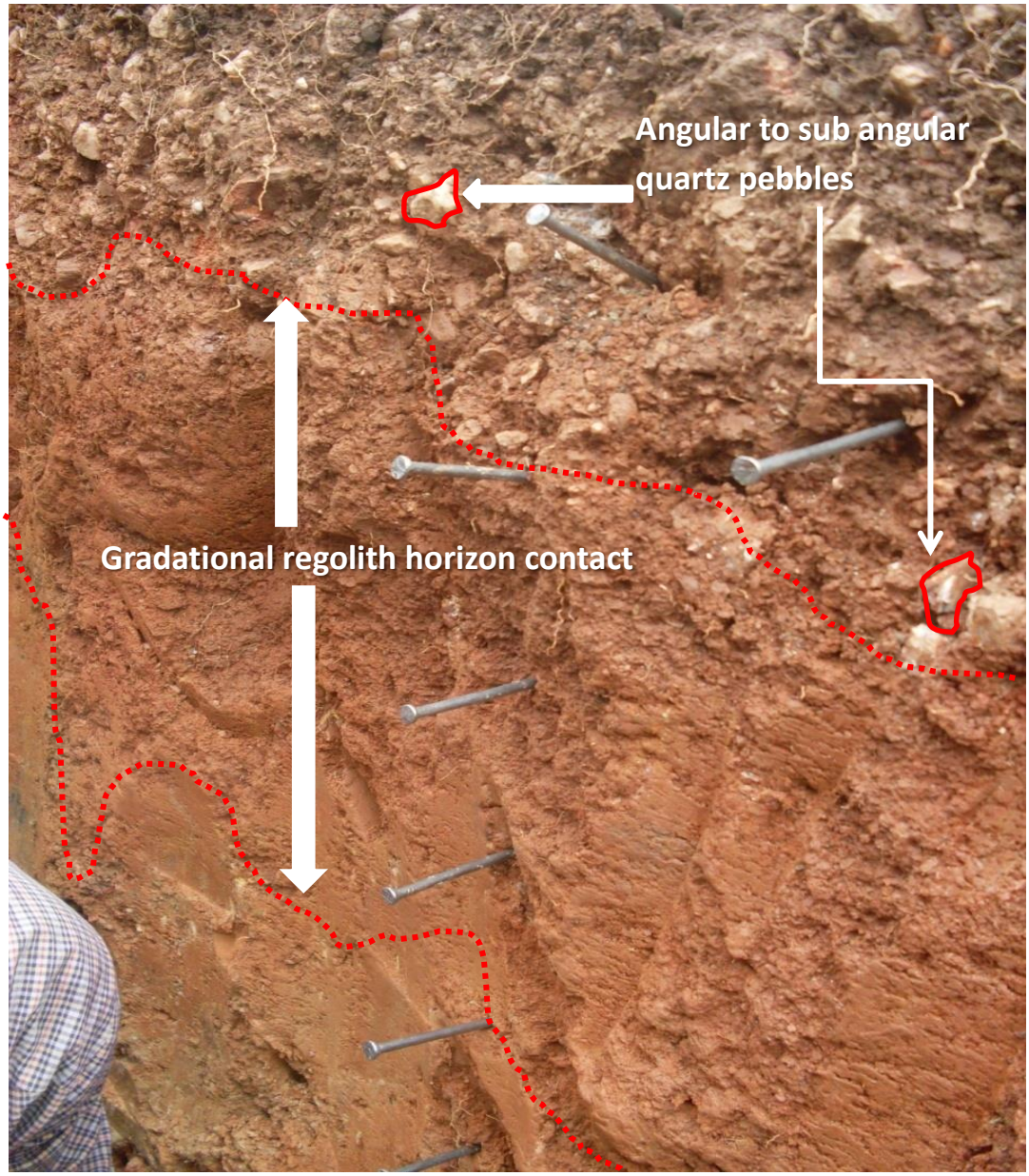

Fig. 4.15 Residual regolith portraying obscured unconformity and angular- to sub-angular quartz clasts: demonstration of relict regolith.

4.4 Regolith geochemistry and profile characterization

As explained in section 3.3, the regolith is a product of rock weathering. Regolith formed in place normally has similar mineralogy and composition (i.e. similar assemblage of resistant minerals and ratios of immobile elements) to the parent rock whereas transported regolith has variable mineralogy and composition compared to the underlying bedrocks. During the weathering of mineral deposits trace elements are displaced from their original host minerals, are dispersed and subsequently occur in newly formed secondary minerals in the regolith (Anand et al., 2010, Gleuher et al.,

2008). Metals released during host mineral weathering are inherited in the secondary minerals such as the Fe-oxides and clay minerals. The geochemical interactions of these secondary minerals with weathering fluids have the potential to adsorb and absorb Au and other trace elements in their lattice. This may create an anomaly in a specific mineral phase (e.g. in Burkina Faso – Bamba et al., 2002, and Syama mine in Guinea – Bowell et al., 1996). The concentration and distribution of the trace elements forming anomalies in the regolith depends on the element mobility pathways, porosity of the regolith unit and the environmental conditions.

Apart from direct mapping in the field, characterization of regolith profiles can be carried out by comparing its mineralogical and geochemical composition with that of the underlying bedrock. This is because primary mineral relicts retained in the regolith profile can be determined by appropriate analytical methods. The interpretation of the analysed geochemical data can be used to establish the relationships between the adjacent horizons. This information is useful to determine complete preservation or modification of regolith profile. This implies sampling and analysing the regolith for trace and major elements can be used to delimit the subtle changes in the regolith profile.

4.4.1 Sampling and sample preparation

To investigate geochemical variations and dispersions to aid characterization of the regolith, samples were taken from 60 vertical regolith profiles in pits set out to cover the full range of regolith regimes at Kunche-Bekpong and Sabala (Fig. 4.6 & 4.8). The pits were firstly logged to provide information about the changes in regolith horizons. Log sheets shown in figures 4.9, 4.16-4.17 were simultaneously used for sampling and characterization of regolith profiles.

Waypoint	Landscape location		Landform	Regolith material	Sphericity	Mapping unit	Surface crust	Geomorphic changes	Remark(s)
	UTM-E	UTM-N							

Fig. 4.16 Sample regolith mapping template for humid tropical regions

Waypoint	Landscape location		Sample type	Depth (m)	Soil type	Colour	Texture	Lithic fragment %	Quartz fragment %	Comments
	UTM-E	UTM-N								

Fig. 4.17 Sample soil log-sheet

4.4.1.1 Sampling

Before sampling the pit walls were marked by nails at 10 cm sample interval (Figs. 4.15 and 4.18). Zones encountered typically included from the bottom upwards: saprolite, mottled zones, duricrust, ferricrete, upper soils that could either be preserved pre-existing or present surfaces. These were sampled using a panel sampling method. The panel samples are planar samples made up of multiple chips collected from a north face of the regolith profile with dimensions of 2 x 0.1 m (Fig. 4.18). The samples were taken upwards from the bottom of the pit to the top of the regolith profile. Samples collected in the survey were placed on an aluminium sample tray and were split into three portions after sieving to 4 mm size fraction in the field.

Fig. 4.18 A typical vertical panel sample collection at 10 cm intervals of a well-lithified regolith profile. Sample spacing is marked by the nails and white rectangle shows panel sampling dimensions.

4.4.1.2 Sample Preparation

The sample preparation was carried out in two stages: field-based and laboratory-based stages. The field-based sample preparations comprised the processing of the "bulk raw samples" to <2 mm size fractions whereas the laboratory-based sample processes dealt with further reduction of the field samples from <2 mm size fraction to <125 μm size fraction. These samples were placed on a food-grade tray, sun dried in the free atmosphere, disaggregated and homogenized for particle size screening (Fig. 4.19).

The coarse lithic and quartz fragments ≥8 cm were removed and discarded from the bulk sample materials in the sample tray before sieving. Two sample tickets bearing the same numbers were placed accordingly into an already labelled sample bag and onto a sample tray for the samples. The sample numbering followed the sequence of sampling and were not controlled by which pit was dug first. Visual inspections of the samples were conducted at this stage to remove oversize lithic and quartz clasts. The remaining samples left in the sample tray were then sieved through a 4 mm sieve (Fig. 4.19). The field sieved samples were then poured into a designated labelled sample bag for further sample preparations at the field camp into <2 mm size fraction.

Precautions were taken throughout the sample collection and sample preparations. Example care were taken to avoid contamination e.g. from jewellery and organic carbon bearing materials; against inclusion of any foreign rock material and dust; and avoidance of cross contamination from other samples. As a preventative measure equipment and surfaces were carefully cleaned between uses with clean water.

Fig. 4.19 Sample preparation at the field camp. Samples are sieved to <2 mm size fraction.

4.4.3 Disaggregation and homogenization

The dried samples were sieved further through a 2 mm plastic sieve to remove coarse particles. Any clay clumps or soil aggregates that failed to pass through the sieve were gently disaggregated using a porcelain pestle and mortar. The sieved samples were thoroughly mixed after disaggregation. They were then passed through a riffle splitter (Fig. 4.20).

Fig. 4.20 Sample splitting stages in the field: a). manual sample homogenization in plastic bag, b) clump disaggregation and oversize removal, c) sample splitting, and, d) library and laboratory samples bagging.

The sample preparation steps used are presented as a flowchart in Fig. 4.21. The carefully homogenized samples were divided into three portions: one portion was sent for gold and multi-element analysis at a commercial laboratory, the second portion were to be processed further for XRF, XRD and SEM analysis at the University of Leicester, Geology laboratory and the third portion was kept as an archive sample.

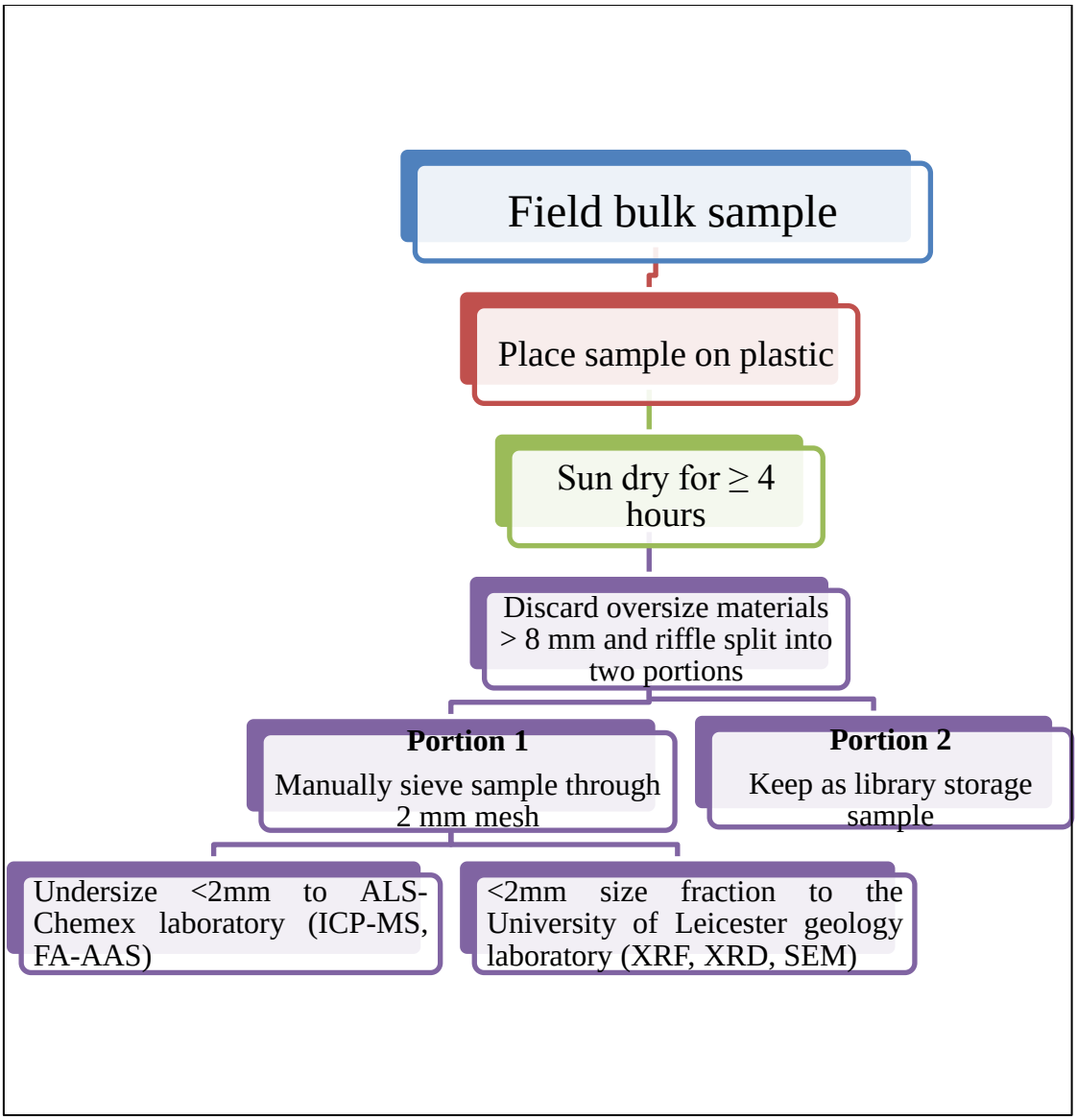

Fig. 4.21 Sample preparation flowchart

4.5 Analytical Methods

The analytical methods used for the multi-elements was inductively coupled plasma mass spectrometry (ICP-MS), Fire assay with atomic absorption spectrometry finish (FA-AAS) for gold (Au), X-ray fluorescence (XRF) for major and trace elements, X-ray diffraction (XRD) measures the regolith mineralogy and Scanning Electron Microscopy (SEM) techniques was used for grain morphological studies. The multi-element and Au ICP-MS analysis use analytical code ME-MS41 and FA-AAS respectively at ALS-Chemex laboratory. Detailed methods descriptions are presented in subsequent chapters 6, 7 and 8.

4.6 Quality control and quality assurance (QA/QC)

The quality of the analytical data starts from the controls established during the sample collection and preparation stages. In this research contamination risk was minimized by making sure that field assistants removed any hand jewellery and avoid skin contact with sample material or with those parts of equipment that were in contact with sample. Where contact was unavoidable, powder-free, disposable latex gloves were worn and washed in water for every new sample to be prepared. Also labelling of containers and sample bags were done on the outside to avoid contaminating the samples. Cross-contamination was curtailed through thorough clean-ups if equipment were to be re-used. For instance, sieves were cleaned with brushes, water and dried up with silky cloths. Also dust coats were washed daily after work before being re-used the following day. In addition, mislabelling risk was eliminated by always having a sample label e.g. field calico bag with its sample tag accompanying the sample throughout the process of sample preparation. Lastly, segregation risk was reduced by avoiding pouring or tipping or scooping raw sample material in order to split it. The complete analysis programme of the QA/QC used a range of standard quality assurance (QA) samples from field duplicates, certified referenced samples from GEOSTATS and blank samples from an unmineralized geological province in Ghana to control the analytical quality and of the survey.

Regolith map making of deeply weathered terrains in the savannah regions of the Birimian Lawra belt of Ghana, West Africa

5.0 Introduction

A regolith map is a representation of the spatial association of regolith units on the landscape. A regolith map developed for exploration purposes will normally categorize regolith materials into regimes based on regolith evolution and weathering histories to depict the relationships between parent and surface materials. Well-developed regolith maps can guide surface geochemical anomaly interpretations. In complex regolith terrains, residual anomalies can be distinguished from transported anomalies by matching the regolith map with surface geochemical data. Similarly, mechanisms that transport regolith materials and influence element dispersal patterns during repeated weathering, erosion and deposition events can be determined. Accordingly, this chapter introduces mapping techniques for generating regolith maps and highlights the role of regolith mapping for gold exploration in complex regolith terrains.

5.1 Objective

The objective is to create a regolith map of the Lawra area to:

- Distinguish residual and transported regolith material to provide an improved understanding of the genesis and history of various regolith types;
- Use the generated regolith maps to interpret surficial gold geochemical data and support correlations between Au anomalies and the various regolith units across the landscape, and
- Assess and define new economic mineral potential under the complex regolith covers (Chan, 1989).

5.2 Data and methods

5.2.1 Data

Data used in generating the regolith maps were:

- Remotely sensed datasets comprising radiometric, Landsat and SRTM/DEM data acquired from the WAXI-IRD Office.
- Drill cores, RC chips and historical surface geochemical data collected from Azumah Resources Ltd., and

- Ground truth mapping of the regolith mapping units.

5.2.2 Methods

Mapping the regolith requires considerable in-house study prior to fieldwork followed by substantial field verification of the initial image analysis and data collection. In this study, the following research approach was followed:

- Landscape classification involves remote sensing image and map interpretation. Landform unit (chapter 4, section 4.3.1) boundaries derived from the images were compiled onto a map. Two copies of 1:50000 map sheets were made; one of the maps was kept at the office for digitizing any required base map data and for general reference purposes. The second map was taken into the field and used for mapping, data collection and image verification. Regolith landform unit (RLU) boundaries derived from satellite image analysis were later transferred onto the field map before going into the field. This copy was amended as necessary in the light of field results.
- Genesis classification is the field verification of observations obtained from the images and maps. Field checks were made of the relationships between different regolith landform characteristics, geology, and regolith and soil types that cannot be directly observed on the images.
- Regolith characterization was carried out where gross regolith profile characteristics existed, including evidence of secondary induration, truncation and any material cover that may have been deposited over time.
- All data obtained in the pre-fieldwork and fieldwork stages were integrated, interpolated and manipulated using MapInfo-Discover GIS software to create a unified regolith map.

5.3 Regolith map making

Regolith maps are the most common method of representing and visualising regolith information. They provide the user with a representation of the spatial association of regolith units from which relevant information is extracted for geochemical gold exploration. In this study the regolith mapping was undertaken in two distinct stages: a pre-fieldwork stage and a fieldwork stage. The pre-fieldwork stage was known as the 'Landscape classification' whereas the fieldwork stage was designated as 'Genesis classification'. The landscape classification classifies the terrain into residual, semi

residual and depositional regimes through the use of remote sensing imagery interpretation whereas the genesis classification uses the 'FRED' classification scheme (where F represents the ferruginous regime; R the relict areas, E the erosional environments and D the depositional areas) to distinguish the regolith mapping units during the ground truth field mapping into four regolith classes. The concept of mapping the regolith for exploration purposes originated from Australia and the common known classification scheme is 'RED' (Anand et al., 2001) where R is relict; E is erosional and D represents depositional regime. The RED classification is good but the encrustation of detrital gold grains by Fe-oxides and clay minerals during lateritization (Butt and Zeegers, 1992) and the weak but broader lateral dispersions observed in laterite (Butt et al., 2000; Anand et al., 1993) have necessitated the use of the 'FRED' classification for this study. The widespread laterite coverage have been noticed by Butt and Bristow, (2012), Arhin and Nude, (2009) and Bamba et al. (2002) in savannah regions of West Africa including this study and may influence Au expressions in surface samples.

5.3.1 Landscape classification

The pre-fieldwork stage comprised the identification of land surface types through remote sensing analysis. Table 5.1 shows the data used, their properties and spatial resolutions.

Table 5.1 Types and resolutions of remote sensing data used in the study

Data type	Band No.	Spectra range (µm)	Ground resolution (m)	Bits
Landsat	1	0.45-0.52	30	Best 8 of 9
	2	0.53-0.61		
	3	0.63-0.69		
	4	0.78-0.90		
	5	1.55-1.75		
	6	10.4-12.5		
	5	2.145-2.185		
	6	2.185-2.225		
Radiometric			50	
SRTM/DEM		90 m pixels		

The classification of the terrain relied on well-established spatial, genetic and environmental correlation techniques between landforms and regolith as suggested by Laffan and Lees (2003). Each dataset was used to add a different component of information to the final regolith map. For example radiometric data were utilized for their ability to reveal information on the surface materials when differentiation was inconclusive with other imagery. Digital elevation models (DEM) were useful for adding landform and geomorphic information to the mapped regolith units, enabling areas of different topographic relief to be differentiated. Landsat and radiometric imagery overlays at the same scale were helpful as they discriminate inferred boundaries by highlighting different components of the regolith. Using MapInfo software in a GIS environment the above listed data were registered to the same map grid, the same map projection and the map datum. They were then processed, integrated, displayed and visualized to classify the landscape into residual and transported regolith. This was based on the assumption that regolith resides in landforms and that landforms are surrogate to regolith (Craig 2001, Craig et al., 1998; Chan 1988).

5.3.1.1 SRTM/DEM

The first step of the landscape classification was the distinction of the residual and transported regolith using the SRTM/DEM model, and to a lesser extent the geological information of the area. The definition of the residual and transported regolith classes were achieved by processing the SRTM/DEM imagery on the assumption that highlands, ridges, rolling hills and high pediment terrains are characterised by residual regolith; the hill slopes and base of hills are covered by semi residual regolith materials and the stream catchment areas are overlain by transported regolith materials and are depositional in nature (Fig. 5.1).

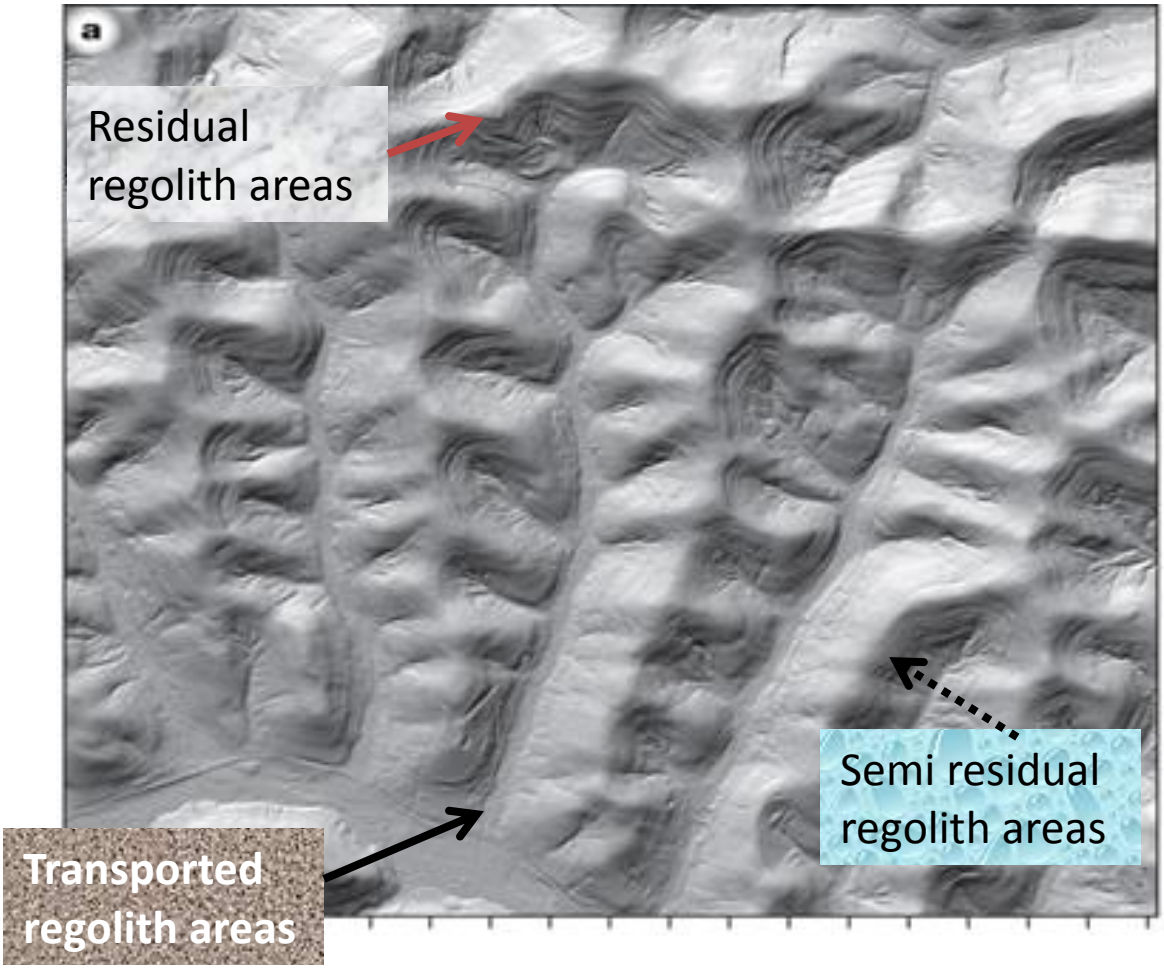

Fig. 5.1 Conceptual SRTM/DEM model used for the landscape classification mapping to delineate residual and transported regolith and also for the extrapolation of semi-residual areas.

The residual areas were classified from the DEM images by selecting minimum elevations between 100 m and 300 m as slope thresholds to define the residual terrains (Fig. 5.2). The slope thresholds selections were based on the topographical variations which show the eastern side of the Lawra belt is characterised by elevations of ≥300 m and the western low-lying areas marked by the Black Volta and Bekpong rivers to have elevations of <100 m. However the selected slope thresholds of 100-300 m elevation were fraught with difficulties because some of the hilltops were fairly flat which resulted in conflicting regolith regimes. However, the combined manipulations of the contoured topographic elevations on the digital elevation model (DEM) imagery supported by additional information from the radiometric and Landsat images aided in defining more reliable residual areas (Fig. 5.3). With some map editing the true representations of the residual areas were demarcated that avoided residual areas being

defined within rivers (Fig. 5.4). The depositional environments were also defined by digitizing the catchment areas of rivers and streams from the SRTM image.

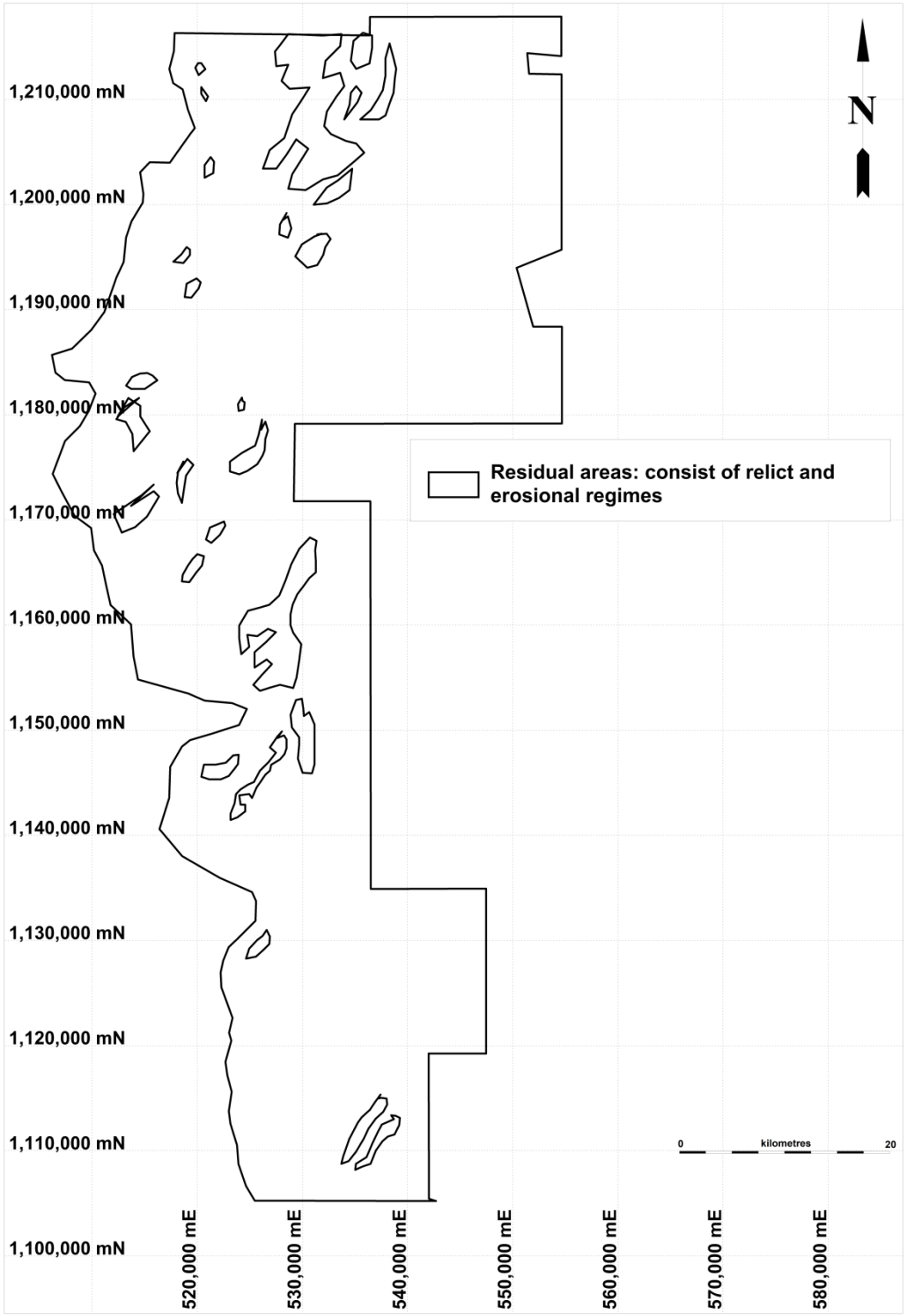

Fig. 5.2 Residual areas digitally demarcated by gridding topographic AutoCAD elevations from the DEM image assuming points between 100-300 m to be residual.

The depositional areas were defined by interpreting the colour SRTM (Shuttle Radar Topography Mission). Areas shown purplish blue in Figure 5.5 were mapped as having distal sediments because of their distances to the active drainage system while the bluish areas were delineated as proximal transport sediments. The classified catchment areas were screened-digitized on the computer and were saved as a separate map layer (Fig. 5.6) in MapInfo format. These layers were draped onto the interpreted residual layer (Fig. 5.7) to obtain the preliminary regolith terrain map (RTM) for the study area. Additionally complementary information reflecting the mineralogy and geochemistry of surface materials to a depth of 30 cm was derived from the analysis of airborne gamma-ray radiometric image, whilst the subtle changes in the regolith in unsure areas were obtained from Landsat images. A map layer was constructed of this information and was draped onto the combined map derived from superimposing residual and depositional areas. A final RTM map was then developed after merging the three map layers that provided information on residual, erosional and depositional areas (Fig. 5.8). These approaches serve as the principal steps for mapping regolith and classifying the landscapes into regolith regimes at the pre-fieldwork stage. To address the numerous uncertainties as to the types of regolith from the landscape classification necessitated the complementary information from the genesis classification for authentication purposes. The genesis classification utilizes the information obtained in the landscape classification to probe the unsure areas whilst observing and mapping the regolith units in the field through outcrops, boulders and making observations in pits.

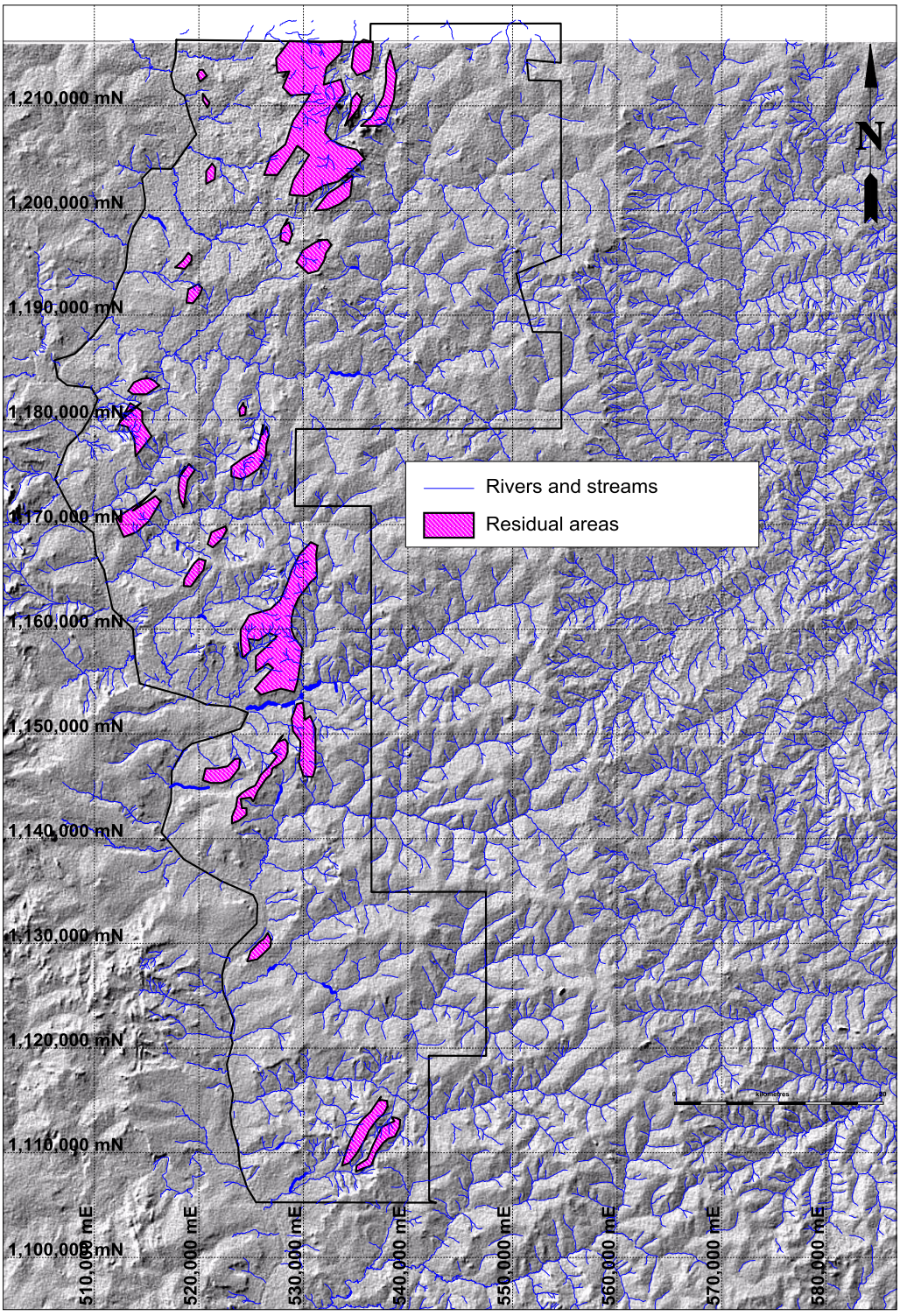

Fig. 5.3 Drape of digitally interpreted residual areas on DEM imagery. This image highlights some problems associated with the use of basic topographic maps in defining residual areas. (Note**:** some residual areas appeared to fall into active stream and river channels)

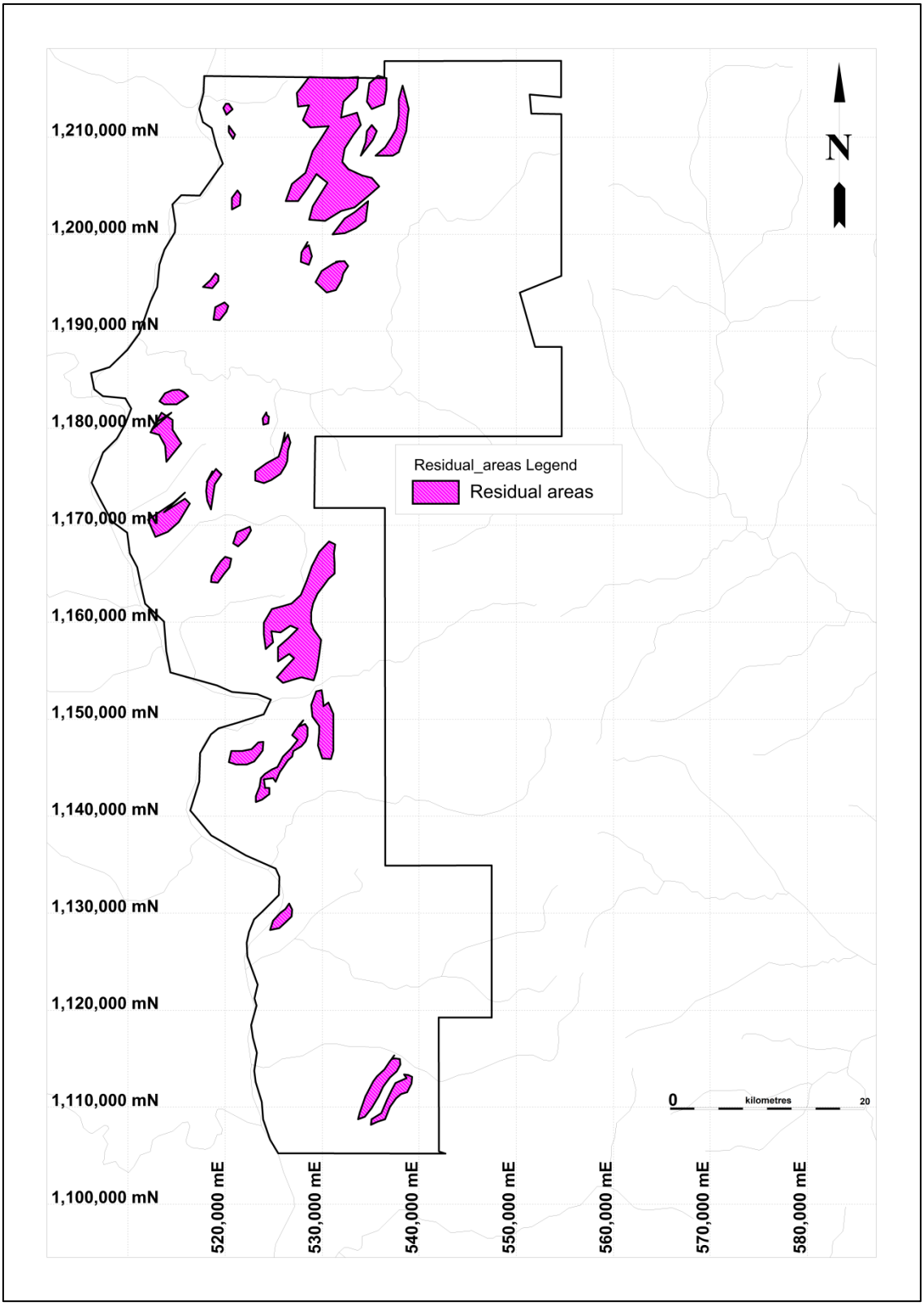

Fig. 5.4 Edited residual areas derived from a combined map overlay of the AutoCAD elevations contour map and the DEM imagery

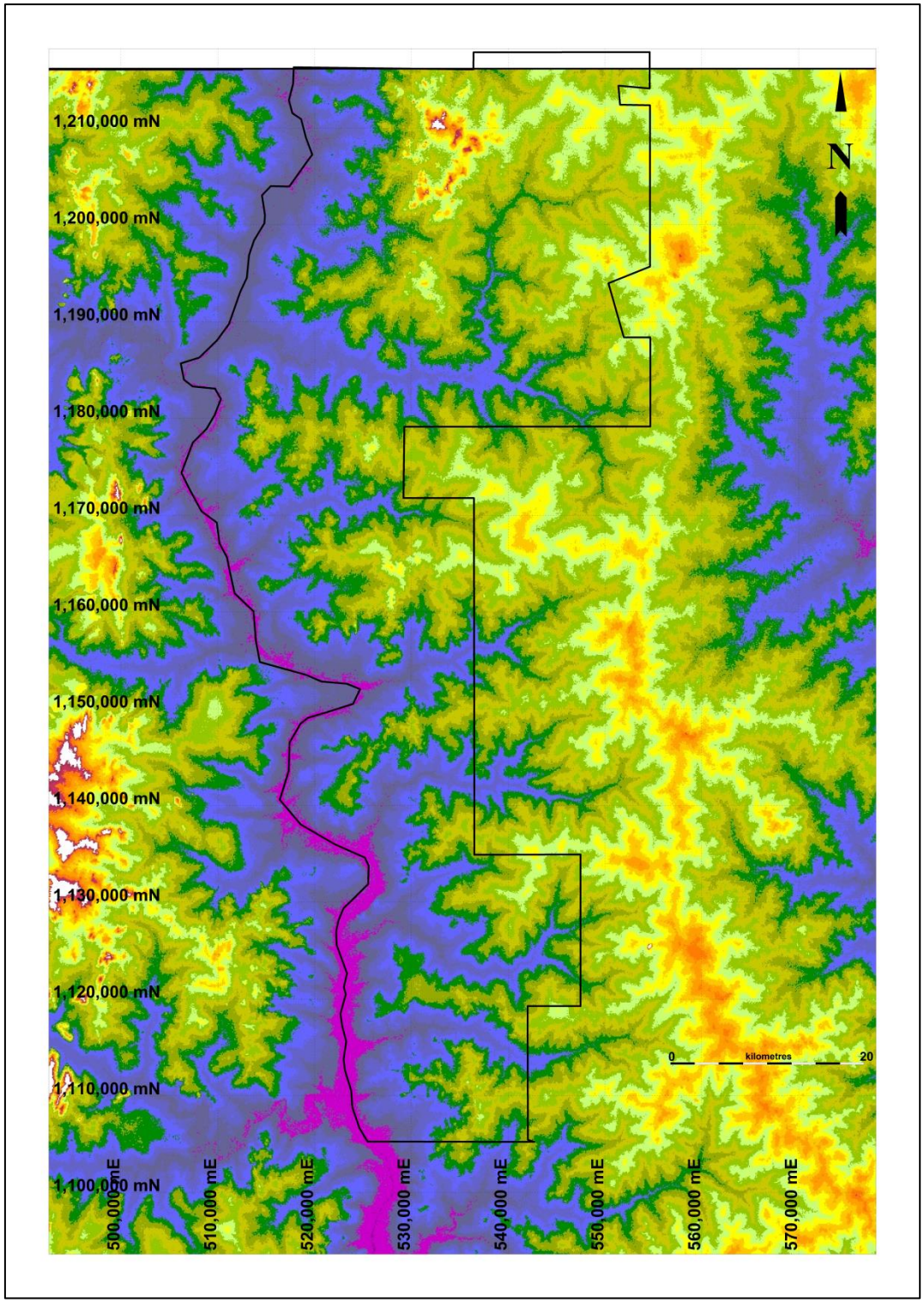

Fig. 5.5 90 m pixel SRTM-colour digital image of the Lawra belt used to delineate the depositional areas.

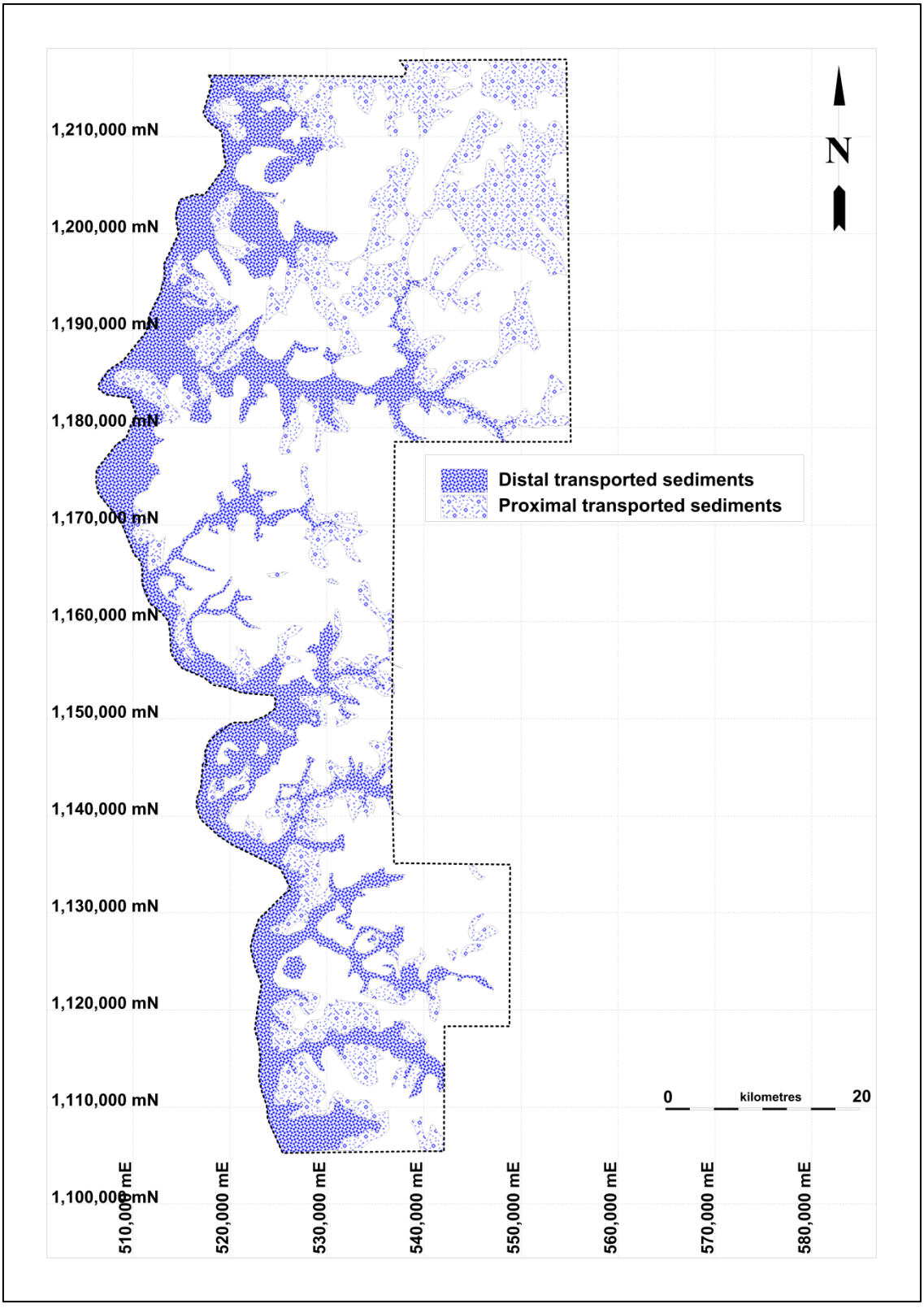

Fig. 5.6 Depositional areas digitally interpreted from SRTM imagery

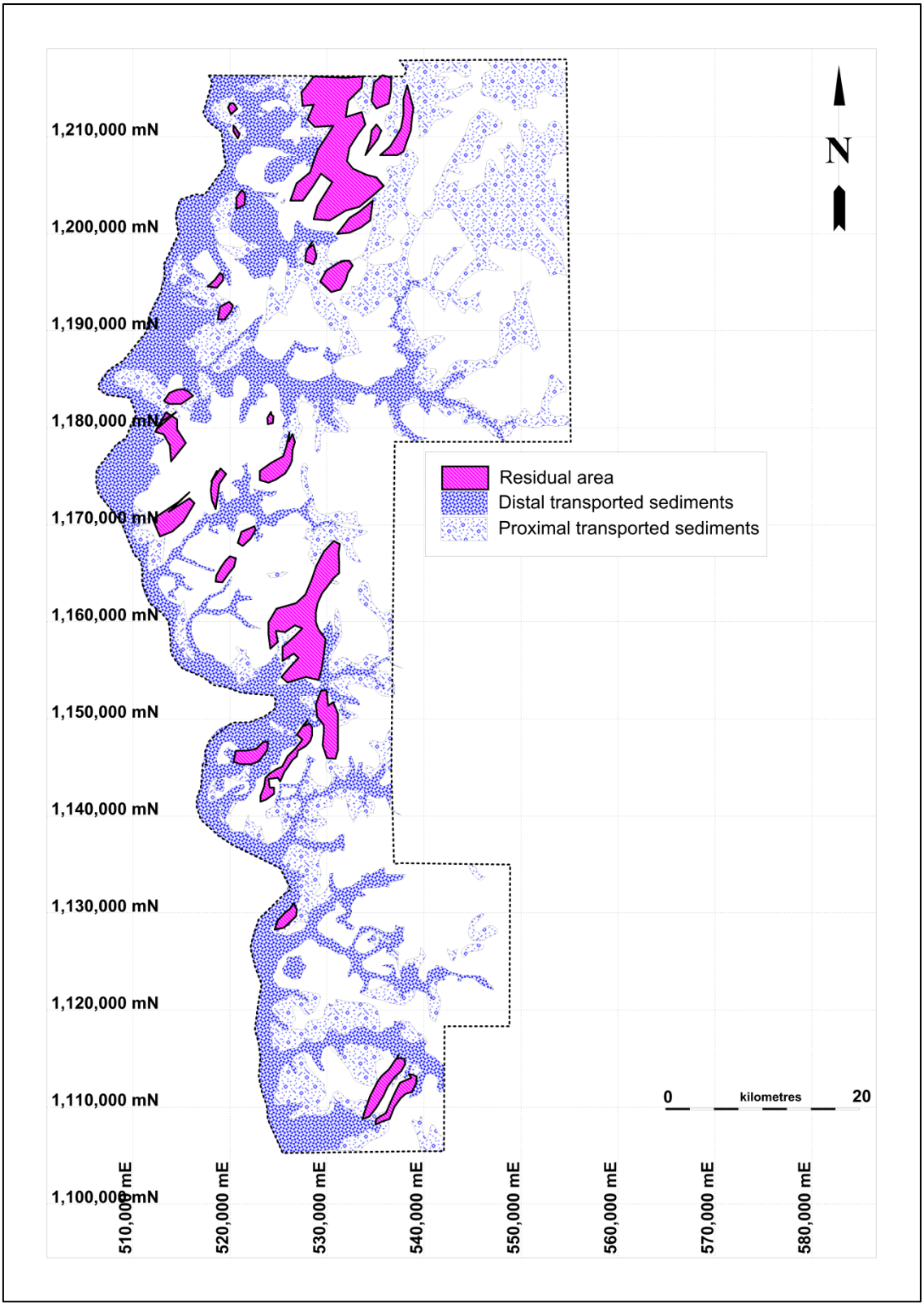

Fig. 5.7 Combined map of residual and depositional areas generated during the landscape classification processes.

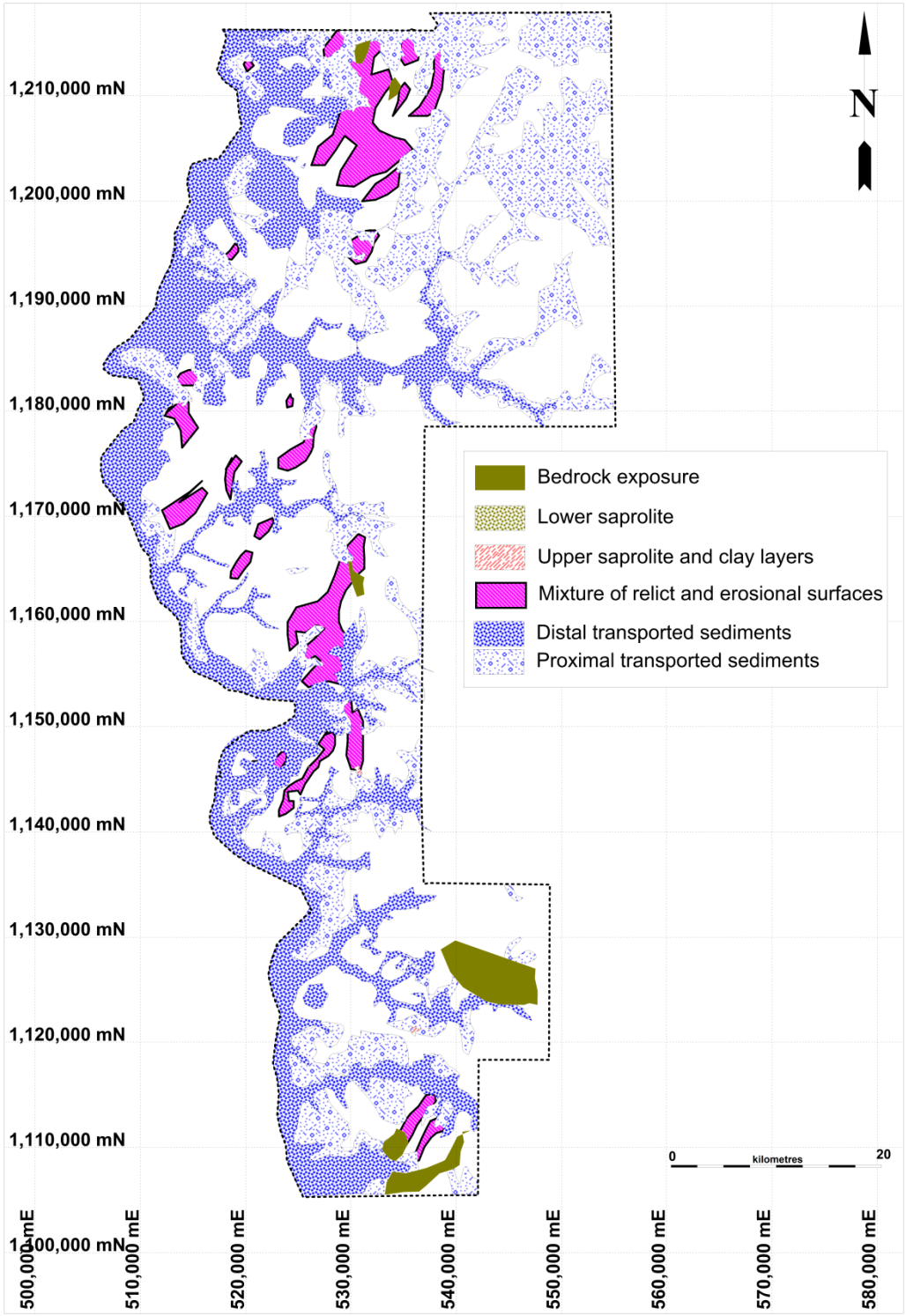

Fig. 5.8 Interpreted regolith-landform terrain map (RTM) produced from landscape classification for the Lawra Birimian belt.

5.3.1.2 Landsat imagery

The difficulty to clearly identify the boundaries of the different regolith regimes because of the regional scale of the mapping programme necessitated the adoption of Wilford et al. (2001) mapping method. The method suggests that spectrally homogeneous areas within Landsat TM imagery correspond to regolith-landform units and can be used appropriately for the description and mapping of the regolith landform units (RLUs). In this research, six (6) broad-bands with 30 m resolution (Table 5.1) cover the visible to shortwave infrared (SWIR) were processed to detect diagnostic absorptions and reflections of common materials and minerals in the wavelength regions of the broad Landsat bands (Fig. 5.9 B). This feature was used through the selection of a 'three-band colour composites (TCC) during the principal component analysis (PCA) in a GIS environment, using ENVI 4.7 software. The three-band colour composite used bands 3-2-1 and RGB to produce images with similar tones to the ortho-rectified image (Fig. 5.9 A). TM bands 1 to 4 are useful in Landsat image processing to detect spectral response of vegetation and Fe minerals including hematite and goethite (Wilford, 1992). As the differentiation of residual and transported laterites is sometimes difficult from field observations, manipulations of these bands using different combinations were used to detect the subtle changes in them. Example false colour composite images used to separate different weathering materials by Wilford et al., 1997) was applied to the Landsat data of the study area. Some of the ratio combinations used includes:

- 3/1 and 5/4 for mapping ferruginous saprolite and lags;
- 5/7 for identifying residual and transported clays; and
- 4/2 separating ferruginous units from non-ferruginous regolith.

The PCA of the stacked TCC datasets were useful for feature recognition (Fig. 5.9 A) as well as differentiation and classification of polygons mapped as shown in Fig. 5.9 B. Further integration of the false colour images with gamma-ray spectrometry data which were later draped over DEM enhanced the terrain visualisation for the classifications of the residual and transported laterites (Fig. 5.9 B).

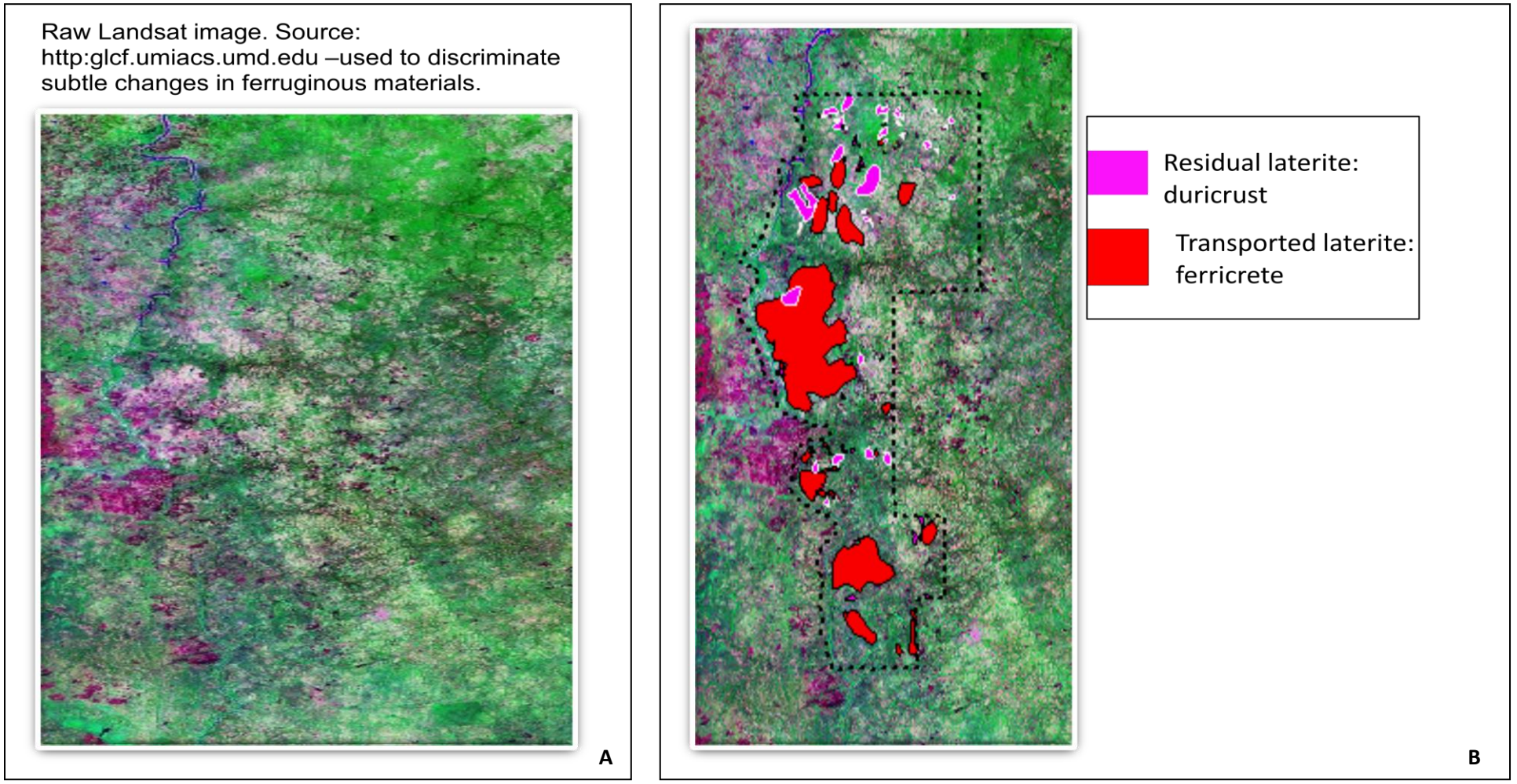

Fig. 5.9 **A.** Ortho-rectified and B. processed three band colour composite Landsat imagery of NW Ghana and part of Burkina Faso

5.3.1.3 Gamma-ray spectrometry-Radiometric

The radiometric data measures the natural radiation from Potassium (K), Thorium (eTh) and Uranium (eU) in the upper 30 cm of the Earth's surface (i.e. from rocks and weathered materials-Fig. 5.10). Raw K, Th and U datasets are generated by summing the count rates within the established (IAEA, 2003) energy windows of ^{40}K (%), ^{208}Tl (eTh) and ^{214}Bi (eU) elements. Potassium abundance is measured directly as gamma-rays are emitted when ^{40}K decays to argon. However, uranium and thorium equivalents in parts per million are measured indirectly (Wilford, 1992) from gamma rays of daughter products of thorium and uranium. Hence the abundance of parent elements is inferred, and is referred to as eTh and eU. From Dickson and Scott (1997) the measured gamma radiations have a relationship to the primary mineralogy and geochemistry of bedrock materials. Emissions of gamma-rays from the Earth's surface largely reflect its geochemistry and mineralogy; however regolith formation typically alters the concentration of this radionuclide's from the primary bedrock source. These suggest that weathered bedrock exposures releases and redistributes radioelements and that their subsequent distribution enables the interpretation of some of the geochemical properties of the regolith materials such as K, Th and U contents. However K, Th and U behave quite differently from one another during bedrock weathering and pedogenesis (Wilford et al., 1992). As a rule, K concentration decreases with increasing weathering (Wilford, 1992). This is because K is highly soluble under most weathering environments and is rapidly leached from a regolith profile whereas Th and U tend to increase in concentration due to their affinity with iron oxides and clays (Dickson and Scott, 1997). These measurements are displayed as pseudocoloured images or combined as false colour composites with K in red, Th in green and U in blue. The white and black hues in the gamma-ray radiometric image are the high and low abundances respectively of all three of the radioelements. The gamma- ray images were expressed as % for K and ppm for Th and U.

So in determining the different regolith domain types, the three radioelements K, Th and U were plotted separately using different polygon symbols to delineate low, moderate and elevated concentrations of the radio-nuclides (Fig. 5.10). The three plotted layers were stacked together (Fig. 5.10) to form a ternary radiometric map to discriminate areas where:

a. All three radioelements intersect and were high.
b. Intersection of three low radioelements
c. Intersection of two elevated radioelements.
d. Intersections of two low radioelements.
e. Isolated high areas of individual radioelements
f. Isolated low areas of individual radioelements etc.

The ternary radiometric image (Fig. 5.10) was used to refine the regolith boundaries. The description of the regolith units were done based on the general rule that K concentration decreases with increasing weathering (Butt and Zeegers, 1992, Wilford et al., 1992,). The rule indicates elevated K abundance areas are associated with slightly weathered saprolite and outcrops. The field regolith mapping identified most of the areas shown on the images to have high K content to have relations with granite outcrops. Conversely, low K concentration areas were associated with colluvial and sheetwash transported materials. Thorium-rich areas are characterised by shallow outcrop or areas overlain by colluvial materials dispersed down slope of exposed basement rock (Wilford et al., 1992). The third rule was that U-rich areas have relationship with depositional environments. In addition to these rules Dickson et al. (1996) and Wilford et al. (1997) recognized the processes of Th and U to scavenge Fe-oxides and clays also has relations to elevated eTh and eU in gamma ray spectrometry. These areas were associated with ferruginous materials. Ollier and Pain (1996) further argued for deeply weathered residual plateaus surfaces covered by ferruginous pisolithic regolith materials to have high Th signatures. Using these analogues; areas on the radiometric image that showed high Th and shown green on the image were delineated as semi residual regolith regimes. K-rich environments shown red were mapped as residual. The distinction of the regolith in K-rich areas could either be relict or erosional regime. The distinctions of residual regolith from laterites through the use of radiometric were generally impossible from the image interpretations. The actual types of the regolith environment for these areas were elucidated from the ground truth surveys. The third radioelement U is characterised by shades of blue on the image and represents depositional regolith regime. Furthermore areas with lower counts of the three radioelements were defined in the landscape classification scheme as undifferentiated regolith and are shown black on the imagery.

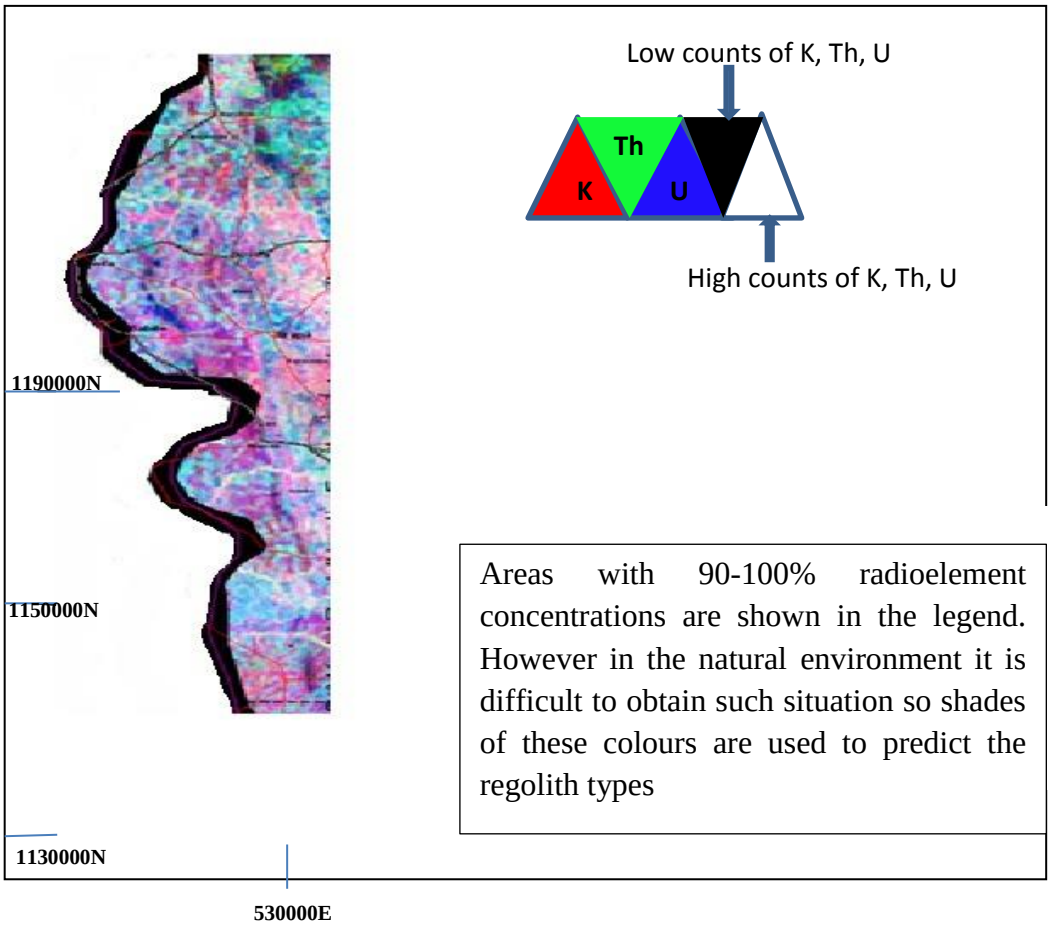

Fig. 5.10 Three band gamma-ray ternary image of the study area.

5.3.2 Genesis classification

Two field seasons of fieldwork, each lasting for about two months, were conducted to validate and ground truth the interpretation of the remote sensing imagery. The first field season (Phase I) fieldwork followed the preliminary image interpretations and consisted of transects of the accessible tracks and roads to gain an overview of the area and the regional setting of the regolith (Fig. 5.11). Pits were dug at selected areas, records were kept of the visited sites and samples were collected from different regolith horizons from the dugout pits. Detailed regolith mapping and follow-up sample collections at areas that remained unclear in terms of regolith characteristics and areas of interest were undertaken during the second field season (Phase II). Details of the work done during the field seasons are presented below. The validation of the 'FRED' classification in the area was enhanced by characterising the regolith stratigraphy through pitting, as that provided more information on the regolith and geomorphic histories of the area.

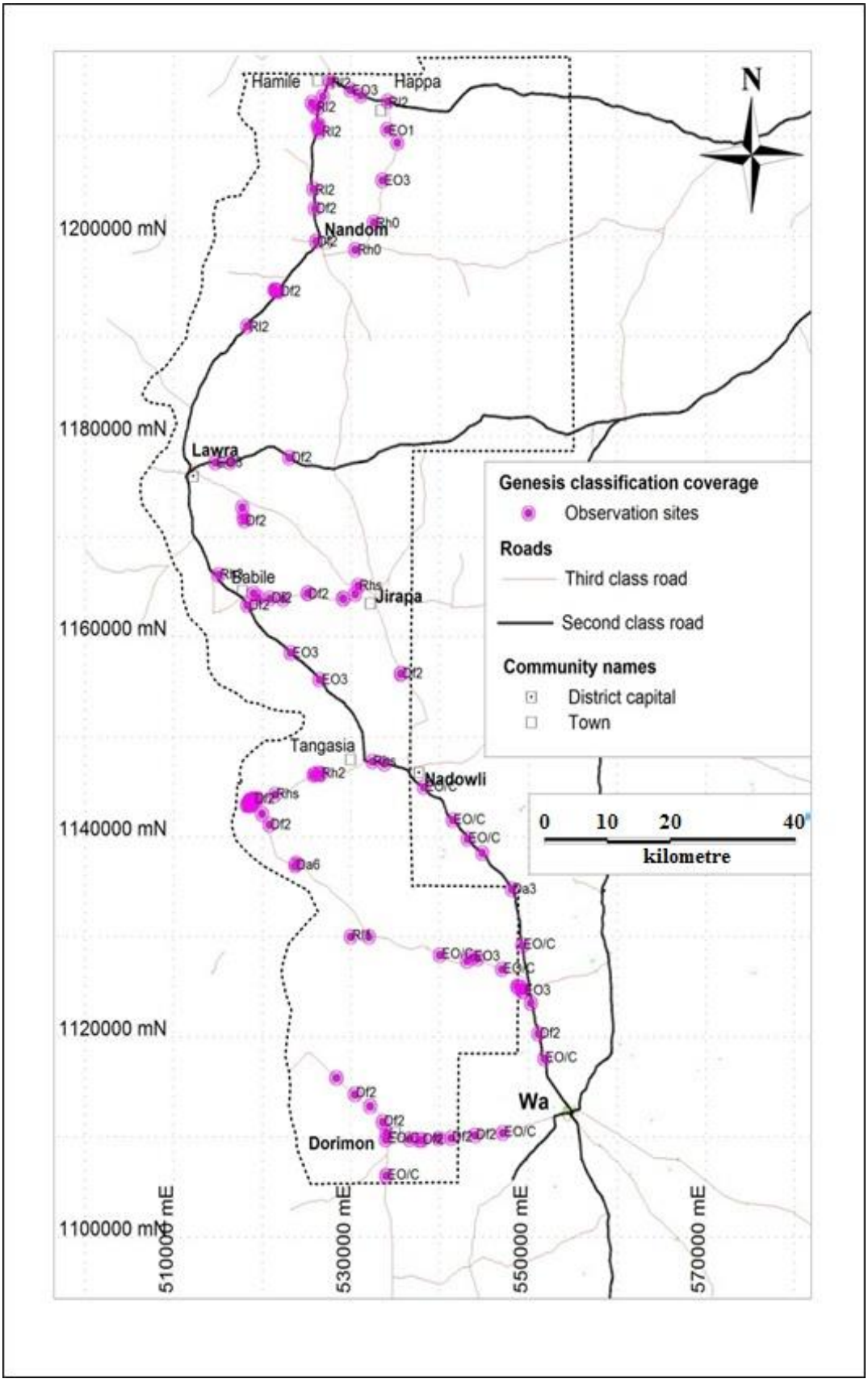

Fig. 5.11 Ground truth coverage showing regolith sites, accessible tracks and roads of the study area.

5.3.2.1 Regolith characterization

The authentication of the provisional regolith map was established by characterising the regolith stratigraphy of the regolith regimes identified. This was done by excavating 54 pits, primarily to eliminate uncertainties about the origin of the regolith profiles in the landscape through time. The locations of the pits are presented in Figs. 4.4 and 4.5 in chapter 4. Details of the pit profile logging information are presented in chapter 4, sections 4.4 and 4.5.1.

5.3.2.2 Regolith ground truth-mapping

The regolith materials mapped in the field were referred to as mapping units and represent surficial areas of similar landform and regolith characteristics that can be identified at the scale that the mapping was performed (Pain et al., 1991). These units described in the regolith-landform mapping were typical associations of materials and areas of similar attributes and do not necessarily represent 'pure' or 'uniform' regolith materials and landforms. The 'purity' of regolith-landform units is scale-dependant and varies with map size (Wilford et al., 2001). During the field mapping campaign, each regolith mapping unit was defined using three main components or descriptors. These were shown on the ground truth regolith maps as *map symbols* and were depicted as alphanumeric codes (Fig. 5.12 and Table 5.2) in the FRED classification system. The first two letters were capitalized and indicate the code for the landform units. The second two letters were lower case and indicate the regolith materials whilst a numerical subscript acts as a modifier to distinguish small but important variations between similar regolith landform units. Table 5.2 represents the recorded sheet format used in capturing the field information. The regolith codes are in Appendix A.

Table 5.2 Sample record mapping sheet for Genesis classification

Landform unit/symbol	**Regolith material**	**Surface modifier**	**Regime**
Hillcrest	Duricrust	Fe-oxide	Ferruginous
HC	dc	1	HCdc1

Since landform is surrogate to regolith the following mapping guide was employed at each field site mapped. These were to:

- Examine the features of interest and decide what sort of landform the area denotes, for example, whether the area is characterised by hills, valleys, rough plain, gullies, erosional rises, alluvial plains, relict deposits etc.

- Decide what material the feature is made of (i.e., quartz, clay-rich rock, sand, gravel, polymictic sediments, cracking clays, saprolite etc.).

Determine whether there are any surficial indurations or binding to form duricrust or ferricrete. During the ground truth-mapping visits were made to selected field sites marked on the regolith terrain map. Observations of the exposed regolith-landform units along cut grid lines, road cuts, footpaths and trails whilst visiting these locations are recorded and plotted to show the spatial distributions of the regolith-landform units (Fig. 5.11 and Fig. 5.12). Throughout the genesis classification mapping the mappable units with the same characteristics and similar weathering histories were grouped as a single classifying unit. This was done by symbolizing the different regolith units with different colours and patterns (Fig. 5.13). Nonetheless, there were some limitations during the polygonization of the mapping units to create the classification units or the regolith regimes. Whilst the geological map records solid lithology and defines stratigraphy, regolith maps record the real regolith–landform units and their definition depends to some extent on the scale of the map. For instance for a geological map, once the stratigraphic boundaries of a geological unit are defined, anything that falls within these boundaries become, automatically, part of that unit. However, the same is not true for a regolith map, because regolith mapping units have impurities that relate to the way landscape materials are set. A typical example is the presence of small areas of residual regolith in a depositional environment, or alluvium in mapping units that are dominated by saprolite (Fig. 5.14). The misrepresentations of the landscape classification from the image processing method were resolved by integrating gamma-ray and Landsat images and digital elevation models. Example residual areas conflicting with depositional regime were identified when large-scale river catchments occupy high topographic terrains during the Landsat and DEM imagery integration processes. Similarly K concentrations were used as a gauge of degree of surface weathering; enriched K environment represented residual areas. The final resolutions of these conflicts were carried out by merging the two maps 'Landscape and Genesis classification maps' (Fig. 5.15). The final informed regolith map for the study area was then developed and is shown in Fig. 5.16.

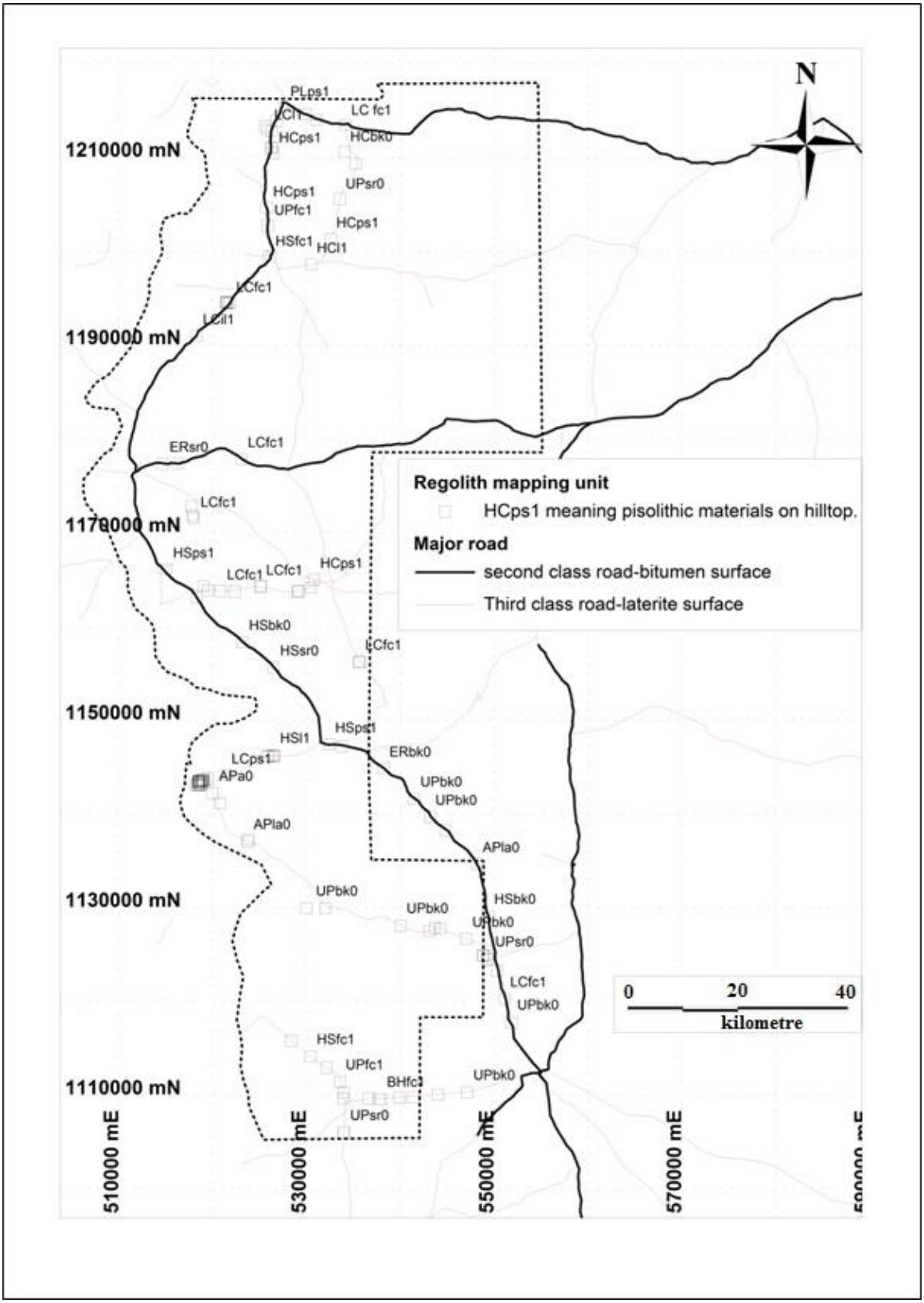

Fig. 5.12 Plot of regolith mapping units showing the three main coded components of landform unit, regolith material unit and surface modifier.

Table 5.3 Typical regolith mapping log-sheet used for the Lawra belt genesis classification survey.

Way Point	UTM-E	UTM-N	Landform	Regolith Material	Surface crust	Mapping unit	Plotting mapping unit	Geomorphic changes
RM001	518299	1190989	LC	il	1	Rl2	LCil1	l3
RM002	521829	1194459	LC	fc	1	Df2	LCfc1	
RM003	521659	1194509	LC	fc	1	Df2	LCfc1	
RM004	521517	1194478	LC	fc	1	Df2	LCfc1	
RM005	521453	1194566	ER	s	0	Rs	ERs0	
RM006	521401	1194595	UP	ps	1	Rl2	UPps1	
RM007	526083	1199443	HS	fc	1	Df2	HSfc1	
RM008	525901	1202728	UP	fc	1	Df2	UPfc1	
RM009	525761	1204659	HC	ps	1	Rl2	HCps1	
RM010	526465	1210434	HC	ps	1	Rl2	HCps1	
RM011	526222	1211003	BS	bk	0	Eo2	BSbk0	
RM012	526574	1211097	HS	ps	1	Rl2	HSps1	
RM013	525888	1212923	LC	l	1	Rl2	LCl1	
RM014	525573	1213297	LC	l	1	Rl2	LCl1	
RM015	526280	1212808	OW	i	1	Da3	OWi1	

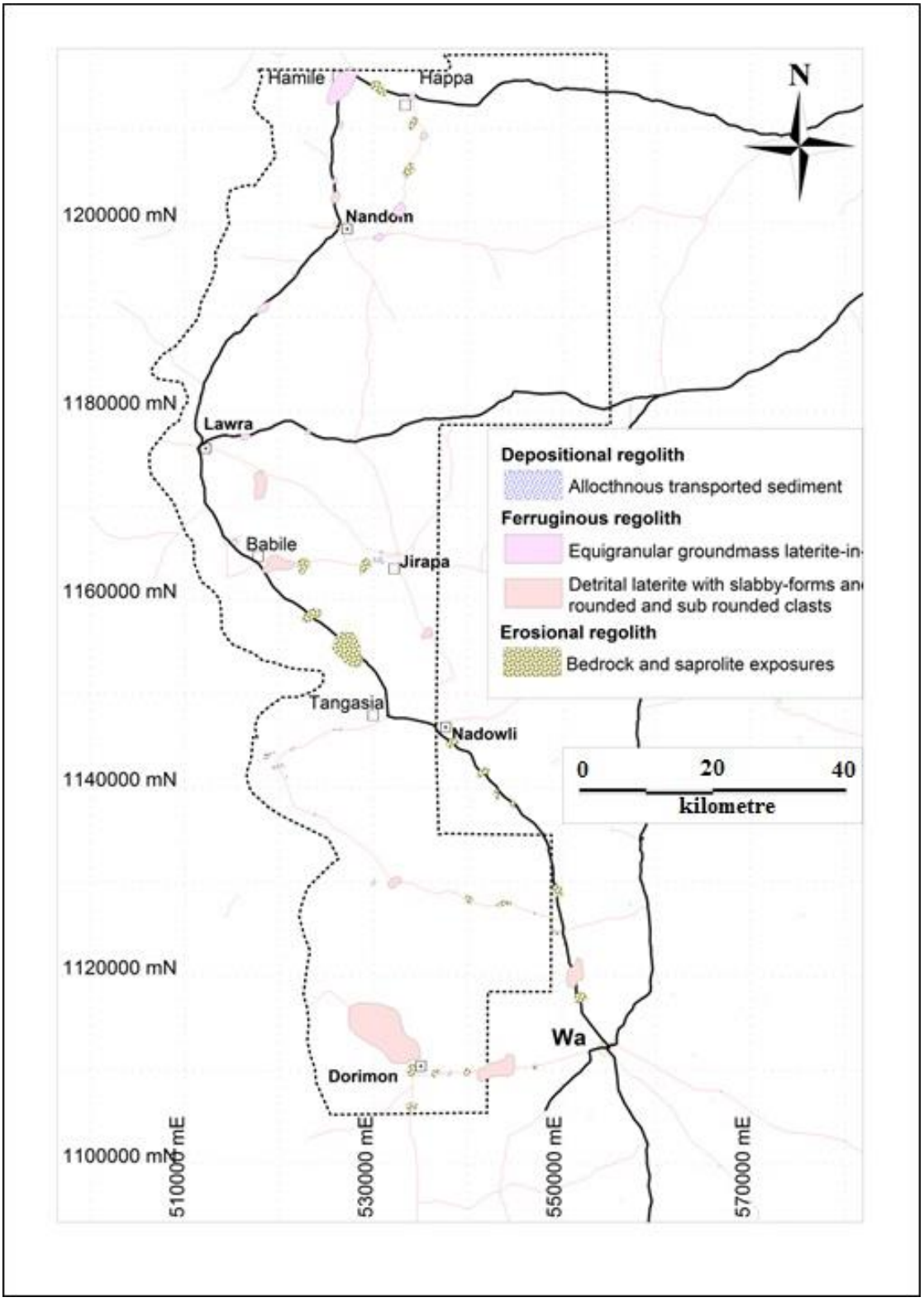

Fig. 5.13 Digitized factual genesis classification map produced from ground truth mapping.

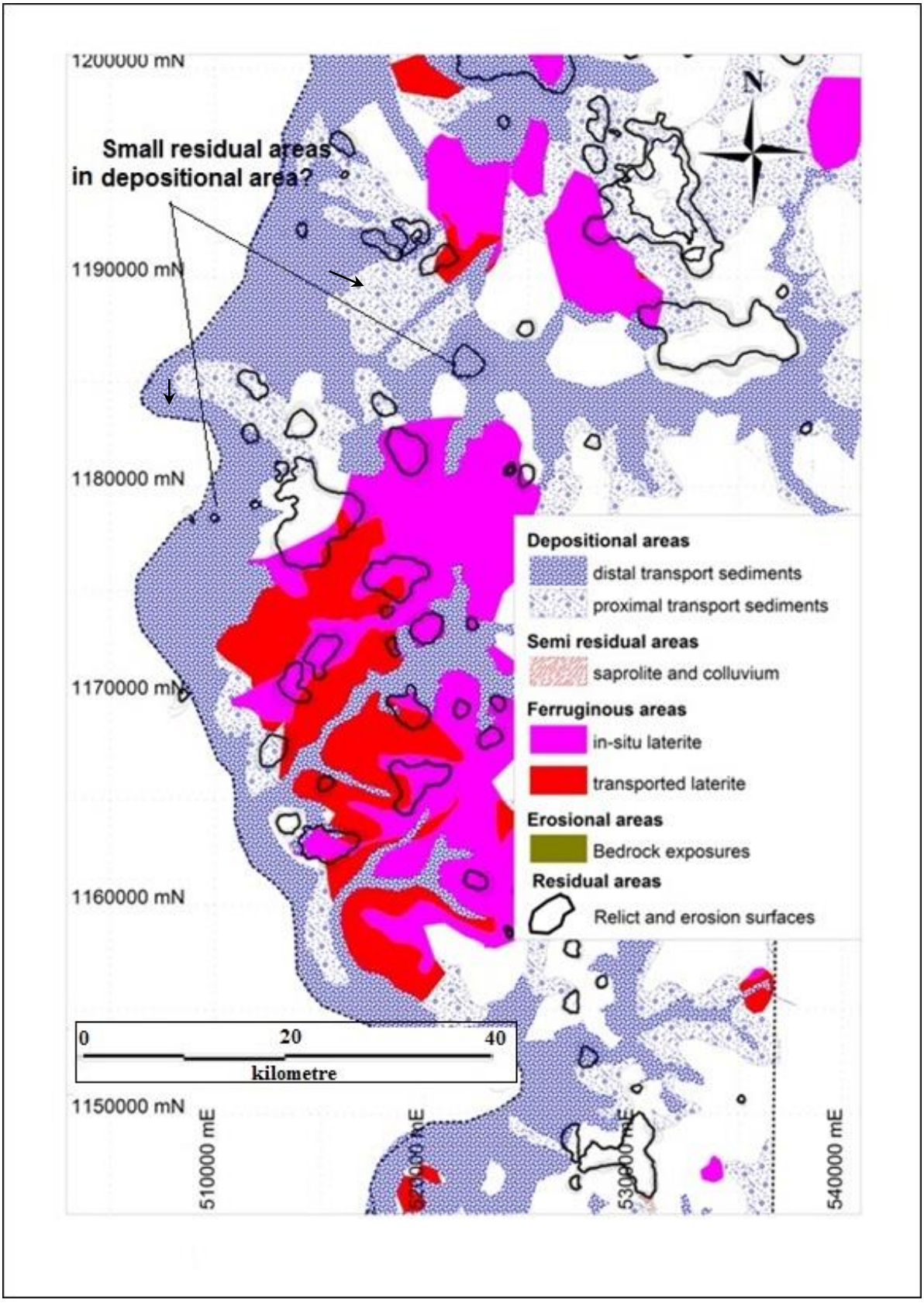

Fig. 5.14 Unusual regolith regimes classified to occur in a wrong place in the landscape from the image processing. For example a relict regime is inferred in an active stream channel, arrowed.

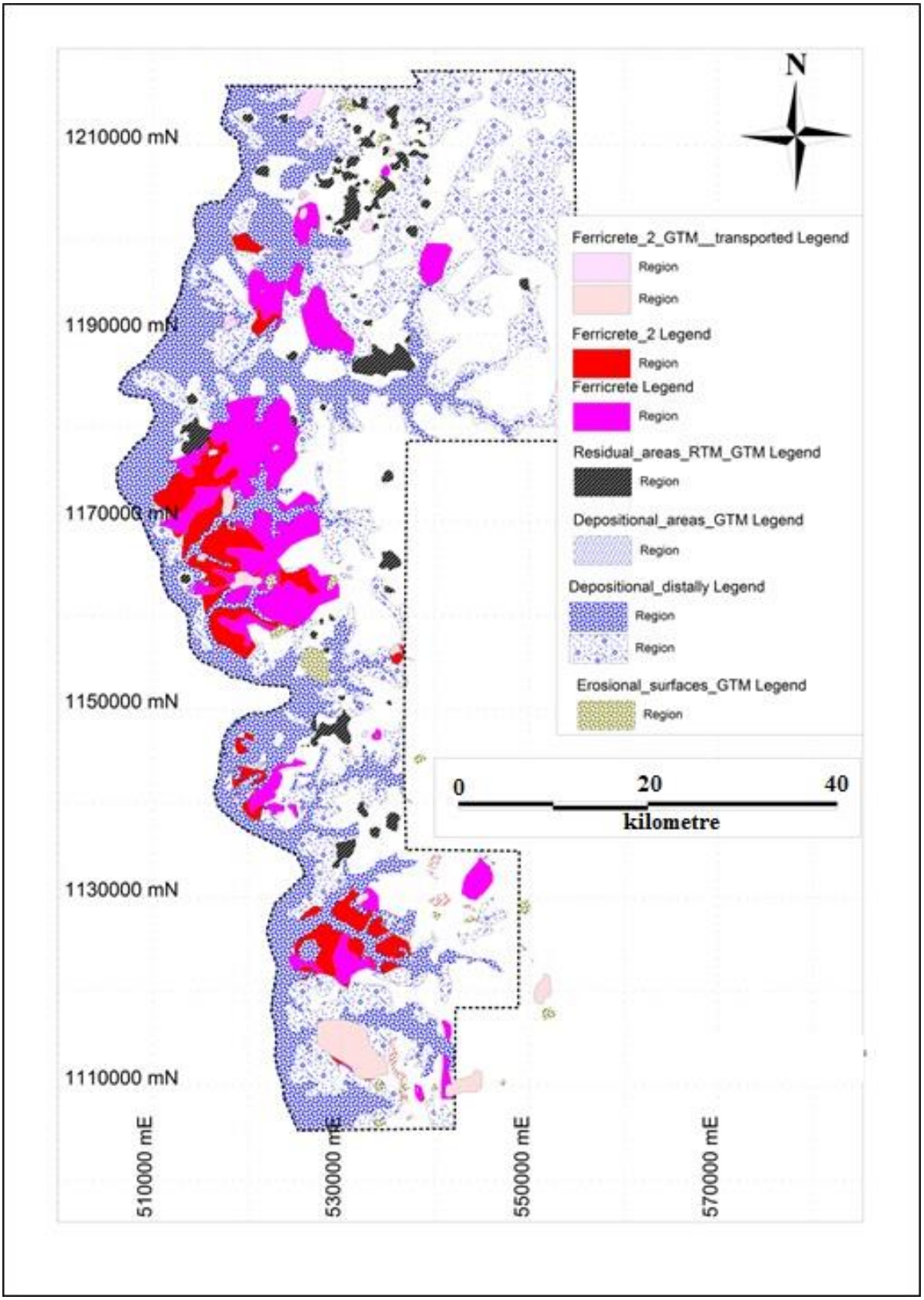

Fig. 5.15 Map overlays of landscape and genesis classification maps towards the development of final regolith map of Lawra belt.

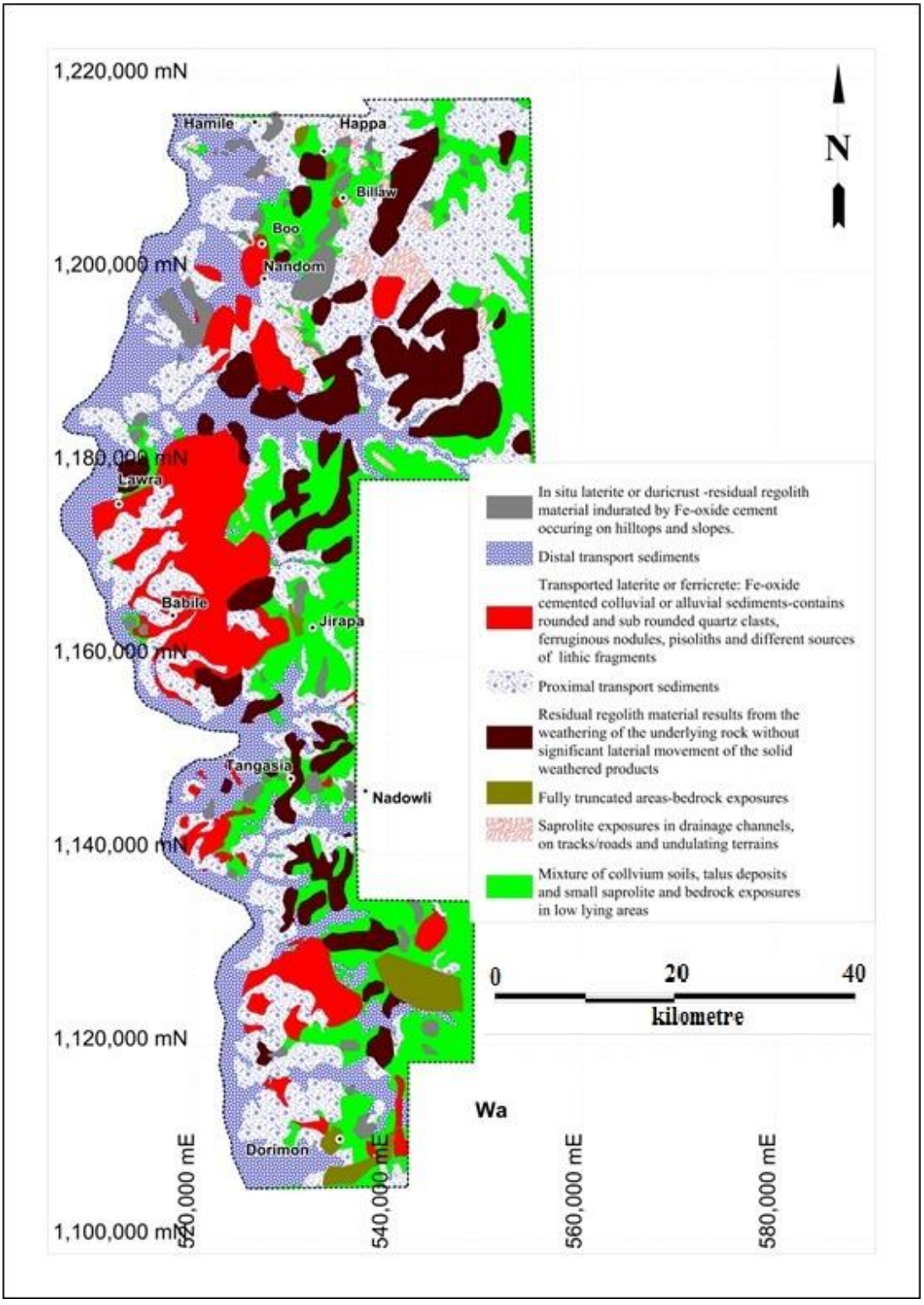

Fig. 5.16 Final regolith map developed for the Lawra Birimian Belt.

The total spatial area coverage of the different regolith domains is calculated from the final regolith map (Fig. 5.16) using MapInfo-Discover software. The respective aerial extents are shown in Fig. 5.17. The derived total coverage of the regolith regimes manipulated from the regolith map (Fig. 5.16) is of benefit to mineral resource companies for planning of exploration programmes as well as interpreting geochemical results. The spatial regolith coverage analysis (Figs. 5.17 and 5.18) of the regolith map (Fig. 5.16) reveals that most of the Lawra Birimian belt is covered by transported sediments (72 %) with patchy residual environments making up the remainder (28%).

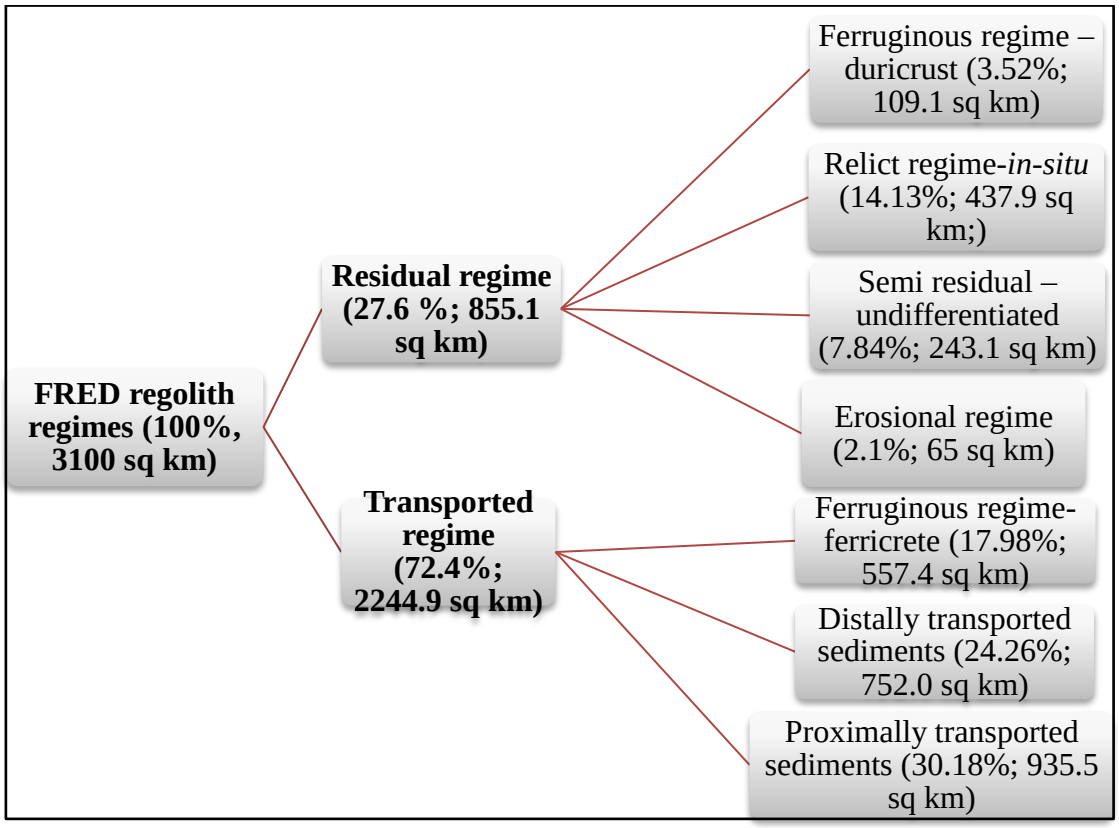

Fig. 5.17 Spatial regolith-coverage analysis of different regolith-domain estimates from the regolith map.

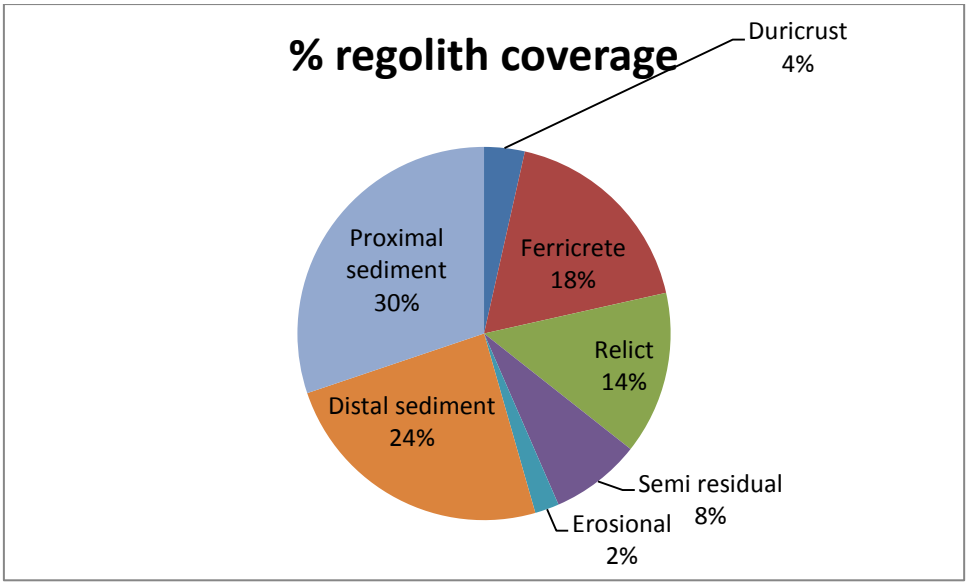

Fig. 5.18 Regolith type land coverage (%) in the Lawra belt

5.4 Discussion

The implications of regolith and its role on geochemical exploration are presented below.

5.4.1 The regolith

The suggestion by Butt and Zeegers (1992), Anand et al. (2001) and Cohen et al. (2010) that landscape is a mosaic of different regolith-landform units is supported by the current research and shown in Fig. 5.16. The rapid changes that occur in the landscape over time during weathering, erosion, transportation, deposition and lateritization as geomorphology and climate changes have implications for geochemical gold exploration. The changes can enhance local re-distribution of surface regolith materials that may cause surface geochemical expressions to be misleading. Whilst enhancements of geochemical signatures are expressed in the regolith elsewhere due to the nature of the source material, it may be diluted at another locality. If the source material is related to mineralisation then an enhanced geochemical response may be recorded and vice versa. Therefore the understanding of the regolith may contribute considerably to the way surficial geochemical data are interpreted. These sorts of regolith heterogeneity and the uneven distributions and characterisation of the regolith materials on the landscape affect geochemical dispersions. Mixed geochemical patterns of high, weak, subtle and discontinuous signals result. Interpretation cannot be effective if the regolith environment is not understood. It is apparent that the low-lying

topography and sparse vegetation cover of the Lawra belt may account for the relatively easy sediment transport (Dickson, 1972) in the area. The implication is that the transported overburden that blankets the present surface may itself have been weathered after deposition, and its superimposition in a single profile shields the underlying mineralisation from detection. Butt et al. (2000) argued that the rapid changes in the regolith geology after weathering, erosion, transportation and deposition influence the surface geochemical expressions obtained from such surface materials. They indicated that whilst some of the geochemical anomalies may be residual; others may be transported. In each of these regolith materials the dispersion mechanisms or metal transfers may vary because of differences in the mineralogy, pH and Eh of the regolith environments. Therefore, for successful exploration in complex regolith environments such as the Lawra belt, the distinction between residual and transported regolith has to be made in order to define reliable geochemical anomalies. Reports by Butt and Zeegers (1992); Smith (1996); Bolster (1999); Cohen et al. (2010) and Coker (2010) suggest that each of these regolith-landform associations has associated unique geochemical expressions.

5.4.2 The role of regolith mapping in gold exploration surveys in complex regolith regions.

Understanding the regolith environment is of great importance to interpret appropriately the geochemical results from areas under cover. Fig. 5.16 displays the different classes of regolith materials on the landscape. From this map (Fig. 5.16) discrimination of residual regolith from transported areas can be done during surface geochemical interpretation. This suggests that a well-developed regolith map can help to reduce false-anomaly follow ups. The reported subtle, low and high Au assays by Griffis et al. (2002) are explained by the large coverage of transported and laterite covers shown in Fig. 5.16. As indicated by Anand et al. (2001) transported regolith can dilute and enhance Au expressions in the surface regolith samples. Typical of this kind of regolith is the 72% depositional regolith mapped in the study area. This type of regolith can commonly yield large, subtle, discontinuous and isolated high anomalies more often than the underlying mineralisation itself (Scott and Pain, 2008). It is therefore possible to have potential anomalies go undetected because of the misinterpretation of Au assays due to the lack of understanding of the regolith environment. As noted by Freyssinet et al. (2005) laterites can dilute Au assays through

Au-grain encrustations during lateritization processes or Au anomalies can be diluted by Au-poor sediments in depositional environments. Similarly transported Au-rich sediments can result in enhanced Au anomalies in surface samples and may not relate to underlying mineralisation. This type of anomaly is shown commonly as displaced anomaly in surface regolith during detrital dispersion mechanism. However, the characteristics of this type of anomaly can be understood from information derived from the regolith map and will assist in differentiating real and false anomalies. The integration of geochemical data, plot and regolith map can help in the proper interpretation of surface geochemical Au signatures in different regolith regimes. This approach if applied can aid in prioritizing the defined anomalies since different regolith materials may have different effects on gold mobility in the oxidised environments. The compositional variability of the surface regolith as shown in the study suggests the inappropriateness of using a single threshold value for the various regolith regimes. It perceives high Au assay areas in a particular regolith domain may overshadow Au anomalies in low Au concentration regolith areas. It thus proposes the use of different threshold values for different regolith domain to provide them equal weights of identifying mineralisation as the different threshold estimates for the various regolith domains account for the effects of regolith on the element dispersions and concentrations. Moreover the knowledge of the rapid and irregular distributions of the regolith materials can guide in selecting appropriate sample media and also provide an insight to the choice of practical sample spacing.

5.5 Conclusion

The regolith of the Lawra belt has formed continuously over the years, evolved and continues to evolve under the present climate. This has resulted in a complex regolith formation. The mapping of the regolith with the FRED classification scheme identified 72% of the landscape to be covered by transported regolith that comprise transported laterites and recent deposits of distal and proximal sediments. The remaining 28% consist of relict, semi residual, erosional and ferruginous in-situ regolith. It was recognised during the study that landscape classification alone was unable to identify some regolith features from the image processing stage. Therefore for the development of regolith maps aimed to detect mineralisation under cover require field inspection of the regolith situation to confirm and update the landscape classification findings. It

therefore concludes the following to be carried out for Au exploration geochemical survey purposes:

i. Landscape classification of the regolith be done at a scale of 1:50000 and be used as a base map for the field regolith mapping.
ii. Genesis classification is carried out after the landscape classifications of the landscape.
iii. Characterisation of the regolith profile should be done by digging pits, observing and logging other field regolith exposures.
iv. Modification of regolith boundaries should be carried out immediately and should be done in the field. This should be done on the base map because all the regolith information and especially the landscape are available with you in the field. So as a recommendation any decision about locations of boundaries and inclusion or exclusion of areas in various units must be done in the field and preferably as soon as possible following the observation.

In conclusion the applications of the regolith mapping techniques used in this research will help resolve the difficulties of selecting sample media and spacing. Additionally the integration of regolith map and surface geochemical maps or images can highlight unreliable anomalies that hitherto may be followed up because a displaced anomaly may be considered as real. Therefore to better meet the exploration objective of discovering new world-class orebodies or potential anomalies that are hidden under cover; application of regolith map during surficial data interpretation is vitally important.

Evolution of Regolith and Landscape in the Lawra Belt, NW Ghana

6.0 Introduction

Distinguishing between transported and residual anomalies requires an understanding of the structure of the regolith and its distributions in the surface environment. Regolith mapping of the Kunche area by Arhin and Nude (2009) observed that some hills are capped by duricrust, whereas extensive areas are covered by transported sediments with patchy erosional surface in places. These surfaces mapped at Kunche may relate to a particular age, climatic episode or period of epeirogenic uplift. The irregular modifications of regolith-landform reported by Arhin and Nude (2009) and that reported by Bamba et al. (2002) at Poura (Burkina Faso) located north of the study area all describe occurrences of relief inversions. The materials making up the relief inversion surfaces were thought originally to have been developed in place by virtue of their locations in topographic high areas. Evidence of rounded detrital clasts and lithic fragments of diverse origin are found in high levels in the relief inversion areas (Butt and Bristow, 2012). It is therefore essential to investigate the landscape changes caused by repeated weathering, differential erosion, deposition, and lateritization processes in the Lawra belt to develop a landscape evolution model that can be used to assist in geochemical exploration surveys.

6.1 Geomorphology

The study area is dominated by the flood plains of the Black Volta, which marks the western border of the Lawra belt, and the Bekpong River, which drains west to the Black Volta (chapter 5; Fig. 5.17). Extensive areas with elevations of ≤100 m above sea level typify the west side, with only minor relief provided by a few 200 m to ≥350 m high ridges that characterize the eastern part. The relief controls the degree of preservation of the regolith profile. For example the ridges have the summits covered by indurated weathered products and quartz veins. Also many of the isolated hills are protected by ferruginous duricrust of which some are residual laterite and others are ferricrete (ferruginous sediment).

The topographies of Kunche-Bekpong and Sabala target areas consist of low-lying and rolling-hill landscapes and moderate pediments with a few isolated hills. The elevations of the isolated hills range generally from >100 m to 350 m above sea level. The eastern part of Kunche has elevations about 100-200 m but the western part has low

topographies of about ≤100 m similar to the <100 m landscape in Bekpong area. The Sabala area consists of undulating uplands and erosional scarps. Most parts of the low lying and undulating plains have patches of transported laterite cover formed by Fe-oxide-cementing colluvial or/and alluvial sediments that include quartz clasts, ferruginous nodules and lithic fragments (mainly collapsed saprolite) derived from the erosion of residual lateritic regolith.

6.1.3 Regolith of the Study Area

The entire West African Craton (including the Lawra belt-Fig. 6.1) has been subjected to deep tropical weathering with the formation of residual and transported regolith profiles (Anand, 2001). Through mapping the area it is apparent that the regolith formed from the weathering of the underlying bedrocks is quite complex. Variations in regolith porosities, chaotic grain size distributions, inconsistent compositional changes and disordered spatial distributions of the surface regolith materials are common. These physical alterations in the regolith depend on the relative rates of surface modification caused by weathering, fluctuations of the water table, repeated cycles of erosion and deposition, geological controls, bioturbation and some chemical processes (Taylor and Eggleton, 2001). These processes are dynamic and can move regolith materials in any direction. The different regolith domains identified and classified after mapping the study area are explained below.

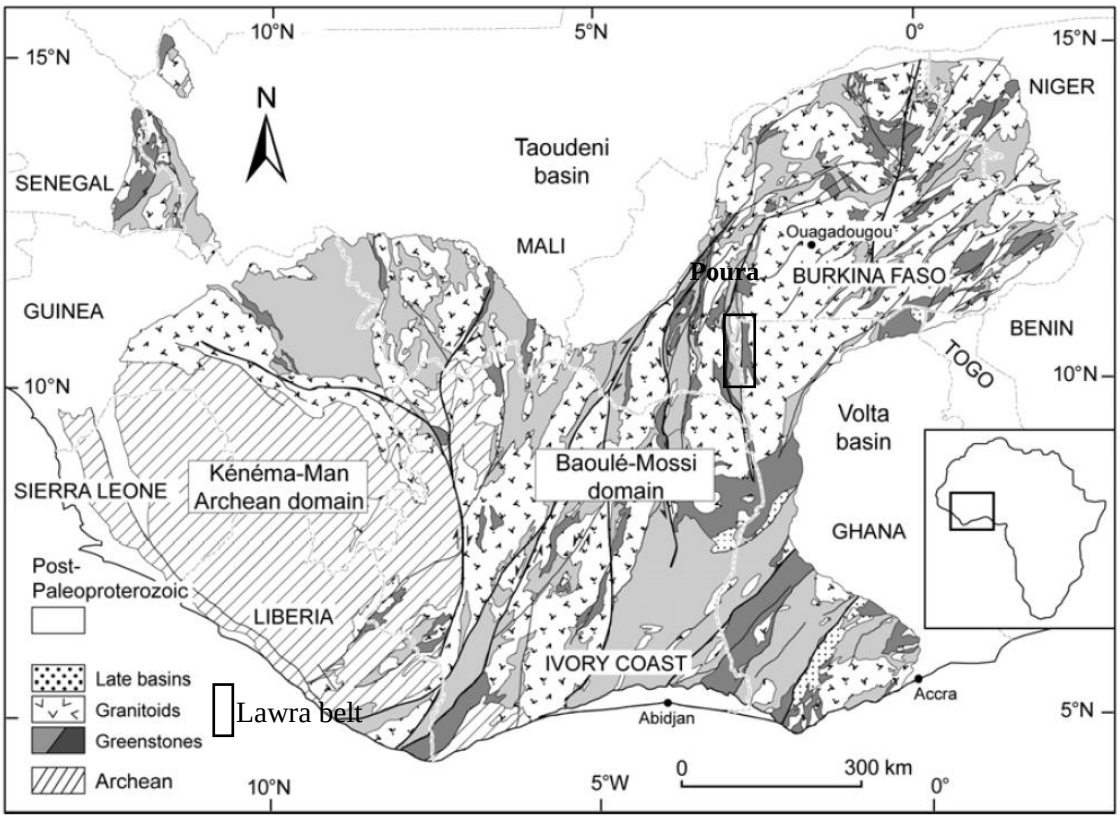

Fig. 6.1 Simplified geological map of the West African Craton (modified after BRGM SIGAfrique - Milési et al., 2004); Paleoproterozoic greenstones are divided into: light grey-intermediate to acid volcanoclastic and volcano-sediments, dark grey-mafic to intermediate lavas and volcanic products.

6.1.3.1 Landforms of ferruginous regolith

These landforms consist of both ferruginous duricrust and ferricrete. The ferruginous duricrust normally occurs as escarpment-bounded mesas that preserve the complete lateritic regolith developed by in situ weathering of underlying bedrock. The occurrences are widespread but form only 3.5% of the landscape as plateau remnants left following erosion (Fig. 6.2) or are found as duricrust caps on isolated hilltops. Although they form isolated rounded hills but are not always the highest part of the landscape compared to the adjacent topography. The hills commonly have a convex form, capped with ferruginous duricrust, with saprolite exposed on the flanks. The soil and lag materials developed on the laterite caps consist of pisoliths, clay-nodules, litho-relics and Fe-oxide coated mapping units. The nodules are normally equigranular and the lithorelics have similar internal fabrics, indicating derivation from the same bedrock. In pits, the nodules can be seen developing from mottles in ferruginous

saprolite. The thickness of duricrust caps range between 1.5 to 2 m. Commonly found over the duricrust hills are thin veneer of lateritic lag or gravelly soil covers.

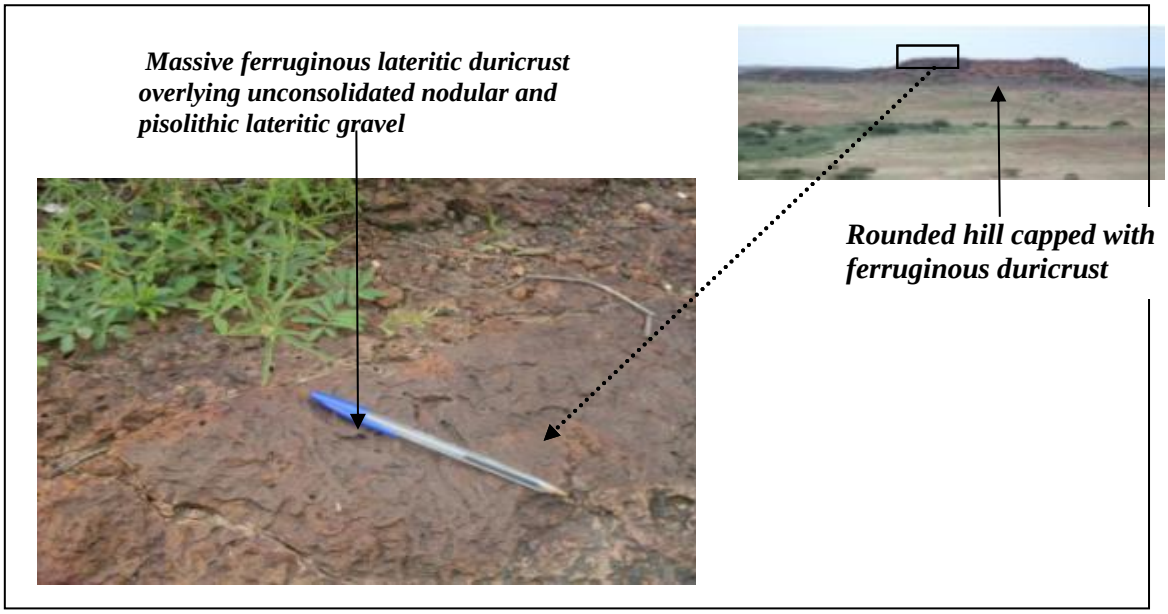

Fig. 6.2 Residual laterite: massive ferruginous duricrust with a pocked-marked surface capping a rounded hill with a flat top.

The ferricrete, or transported laterite as it is termed in this study, covers about 18% of the landscape (chapter 5, section 5.3.2.1, Fig. 5.16). It occurs on hilltops, moderate pediments, on slopes and at the low-lying areas (Figs. 6.3 – 6.6). Ferricrete is formed by the cementation of intensely indurated distal colluvium and alluvium (Figs. 6.3 and 6.4). This regolith-landform type forms complex landscapes that could influence geochemical data interpretation. Some of the ferricrete shows some geomorphological characteristics typical of a ferruginous duricrust with which it can be confused. The hardpans formed in these environments consist of exotic transported materials of variable compositions that exhibit evidence of transportation rather than residual lateritic duricrust. However like the ferruginous duricrust, some ferricrete also is formed in high topographic areas and overlies saprolite (Fig. 6.6).

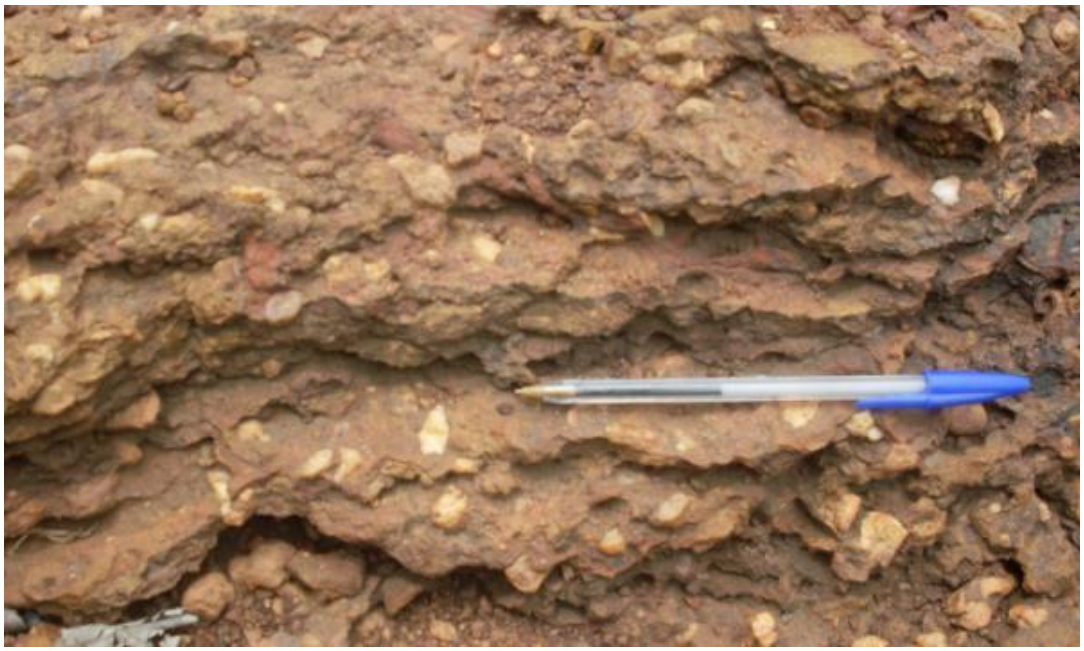

Fig. 6.3 Ferricrete: Fe oxide-cemented colluvial and alluvial sediments including quartz clasts, ferruginous nodules, pisoliths and lithic ferruginous saprolite fragments derived from erosion of residual lateritic regolith.

Fig. 6.4 Ferricrete: detrital quartz clasts-supported Fe oxide-cemented colluvial and alluvial sediments that include pisoliths. Smooth and rounded quartz clasts are evidence of distal sediment transport.

Fig. 6.5 Pisolithic laterite covering hundreds of square metres.

Fig. 6.6 Fe oxide-cemented colluvial and alluvial sediments with rounded and sub rounded quartz clasts on top of moderate to high pediment compared to the adjacent landscape. This is a typical case of overturned topography or relief inversion.

6.1.3.2 Landforms of relict regolith

The relict regimes in the study area have cumulative profiles developed directly from the weathering of the parent rocks. The relict fabrics of the parent materials are preserved in the regolith units overlying the saprolite. The lithorelics and other rock fragments disintegrated from the parent rock during physical weathering processes tend to be angular or sub angular in shape. The contact between the residual regolith profile and the bedrock is a gradational and often diffuse boundary. Examination of the relict regolith profile from top to bottom shows sub-horizontal zones to form from the weathering and geochemical differentiation of the underlying parent materials. As indicated by Butt and Zeegers (1992) the regolith profile in a lateritic residual regolith should have the following horizons (from the base): sap rock, saprolite, mottled zone, ferruginous and/or aluminous duricrust, and/or gravels, and soil. The pit dug in a relict regime (Fig. 6.7) has all the horizons indicated by Butt and Zeegers.

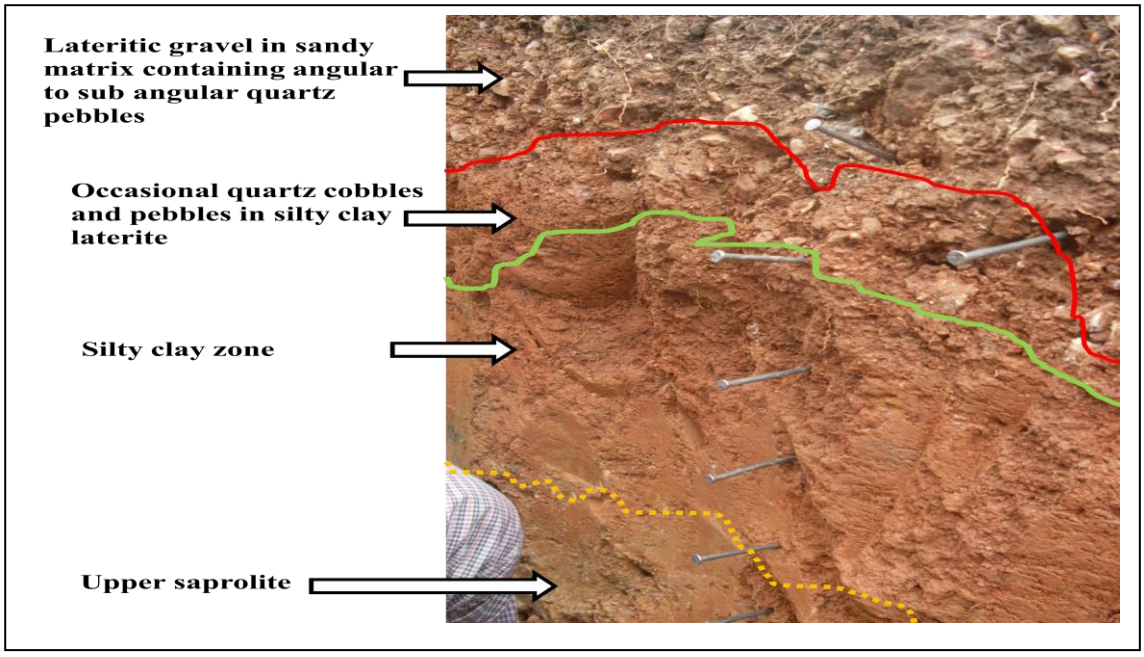

Fig. 6.7 Gradational and soft regolith contact between different layers in a residual regolith profile at Kunche. The interval between the vertical nails is 10 cm.

6.1.3.3 Landforms of semi residual regolith

The semi residual regolith generally has uniform size nodules, a mixture of sub-angular, sub-rounded and rounded lithic units with dissimilar internal fabrics. The sub angular lithic clasts commonly predominates the other shapes. The boundaries between adjacent horizons in the profile are usually gradational and sometimes obscured,

making it difficult to distinguish it from relict regolith In contrast to relict and erosional regolith this regolith unit is derived from rocks different from its immediate underlying rock.

6.1.3.4 Landforms of erosional regolith

The surface characteristic of the erosional regime consists of outcropping saprolite or, more commonly, residual soils derived from saprolite. This unit covers only 2% of the area and is conventionally regarded (e.g., Zeegers and Lecomte, 1992) as consisting of areas where a pre-existing lateritic regolith has been partially eroded, so that the lateritic duricrust, mottled clay zone and varied amounts of saprolite are absent. It may also include areas in which the profile never fully developed (Butt and Bristow, 2012). This landform has a composite profile at some places and shows overprinting and mixing between weathering profiles from the parent rock and proximally transported lithic units. Thin layers of soils on top of eroded surfaces are common in this landform. However there are some isolated areas where saprolite is seen overlain by lateritic lag and/or transported sediments (Fig. 6.8). The ferruginous fragments in these lag materials consist of collapsed ferruginous saprolite, rather than pisoliths and nodules. Although this regolith/landform type only occupies 2% of the entire study area it forms complex regolith (Fig. 6.9) that could influence geochemical data interpretation. At surface the regolith shows some geomorphological characteristics typical of a depositional landform whereas a few centimetres below the surface regolith is erosional surface.

Fig. 6.8 Rock debris overlying saprolite in Kunche area, exposed in an old artisanal mine site.

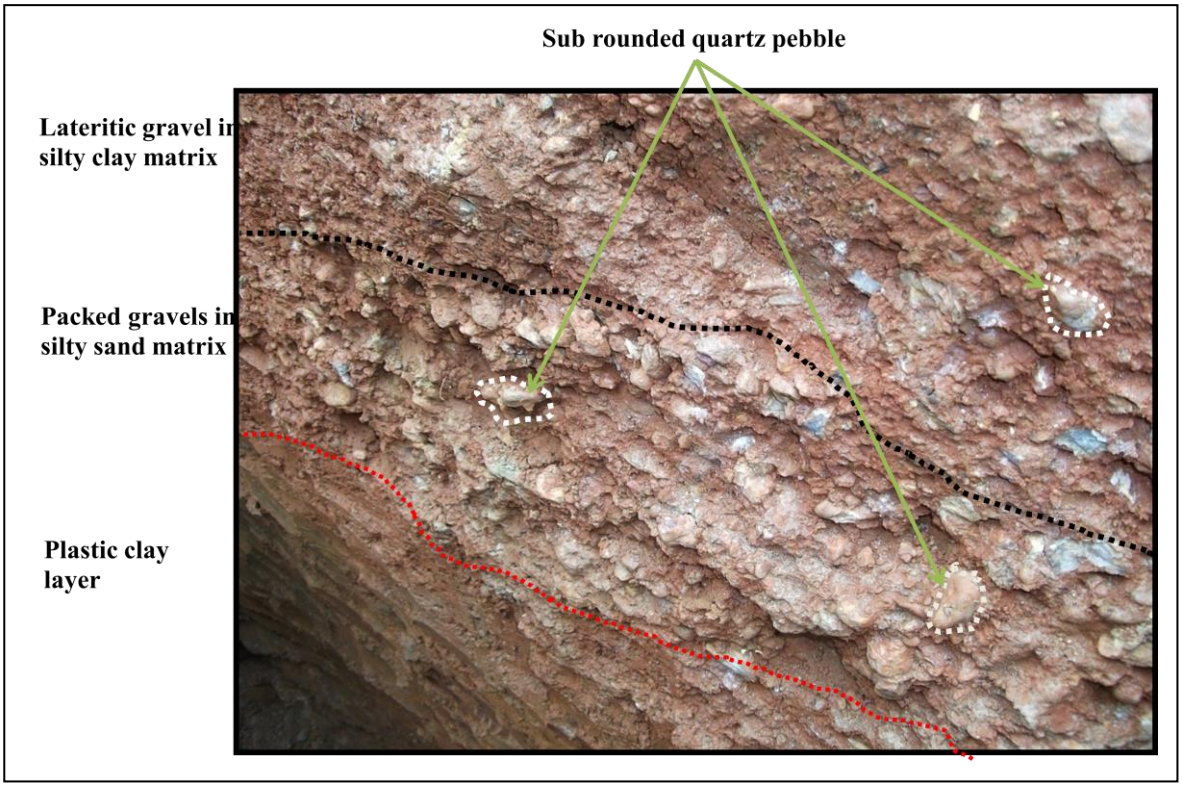

Fig. 6.9 Composite regolith profile in erosional regime: an unconformity marked red and presence of smooth, rounded and sub rounded quartz pebbles are evidence of regolith evolution.

Fig. 6.9 is a typical example of semi residual regolith or erosional regolith with proximal transported overburden. Fresh Bedrock areas were considered as part of the erosional landform. But the occurrence of this is rare, occupying about 2% of the area, most commonly forming strike ridges, prominent rounded or dome-like inselbergs and localized exposures on erosional plains and in streams and rivers.

6.1.3.5 Landforms of depositional regolith

Depositional regime is characterized by compound profiles. The profiles are formed by sedimentation and weathering processes. These processes control the modifications of the upper regolith and are episodic. Characterising this landform areas are fluvial sediments and gravel colluvium some of which were transported recently. The transported sediments vary in composition and sedimentation at places. In some areas there are products of lateritization in between recent and paleo-sediments while in some areas polymictic colluvium overlie pre-existing preserved surface. The transported sediments at the surface regolith seemingly may appear to be the same everywhere however concealed beneath them the regolith profiles have different regolith architectures as:

1. Older profiles that consist of fresh transported sediments, immature indurated laterite and clay-rich sediments (Fig. 6.10) confined to palaeochannels. These layers contain alluvial and colluvium of varying provenance, different composition and diverse age.
2. Areas where laterite is covered by fluvial sediments (Fig. 6.11).
3. Areas where pre-existing preserved surfaces is covered by recently transported sheet wash deposits (Fig. 6.12)
4. Areas where saprolite is overlain by a mixture of gravel colluvium and rock debris (Fig. 6.13).

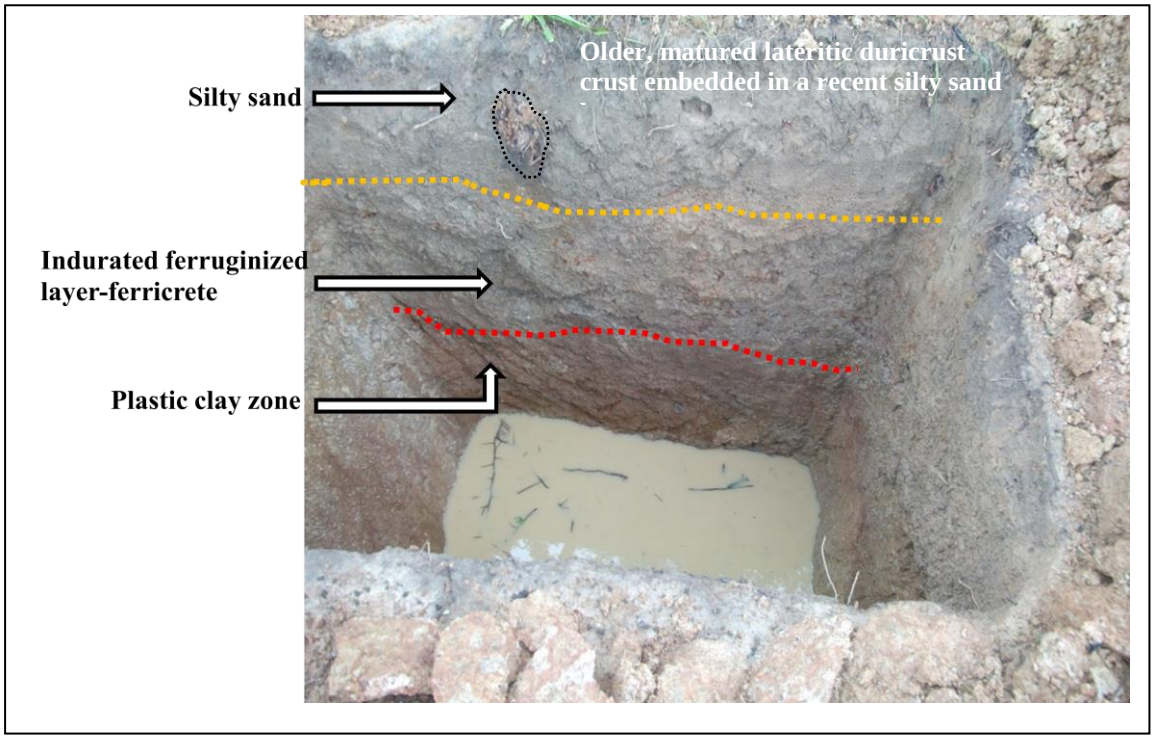

Fig. 6.10 Transported overburden overlying ferruginous saprolite with sub-rounded transported lateritic crust embedded in silty sand layer. The profile surface is greyed because of the milky influx water.

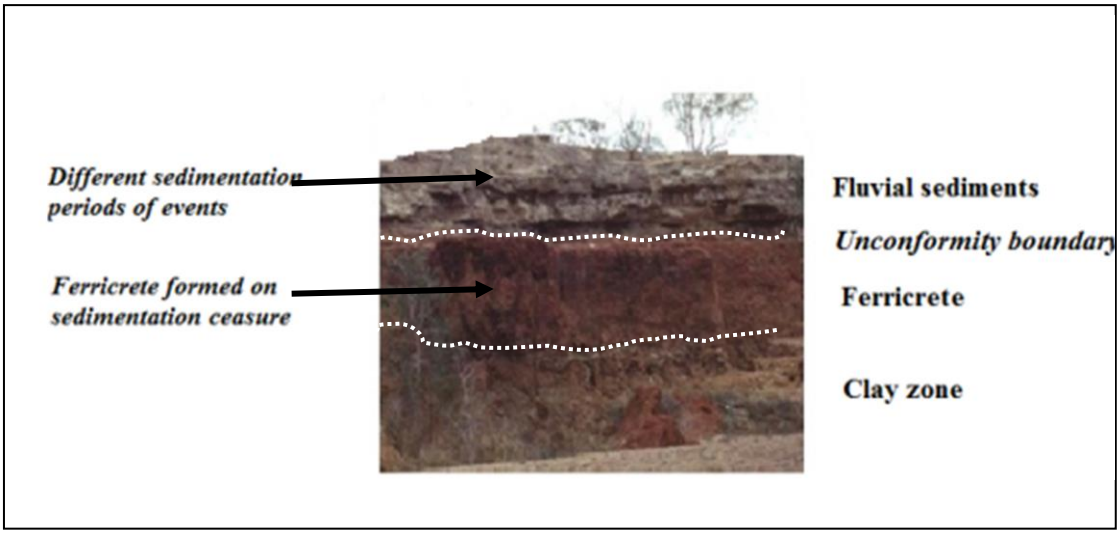

Fig. 6.11 Compound regolith profile near Bekpong River at Kunche-Bekpong depositional regime: unconformity and multiple layers in the fluvial sediments are evidence that the regolith has evolved and still evolving.

Fig. 6.12 Fluvial deposited sediments at a floodplain of an active stream in the Sabala area.

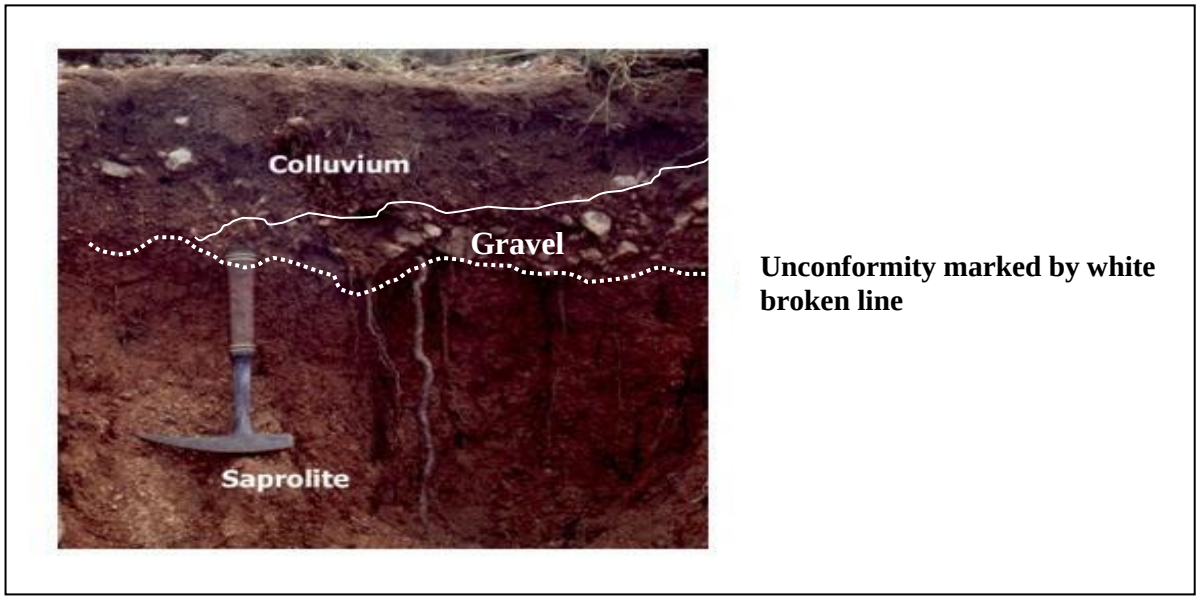

Fig. 6.13 Depositional regolith materials with a gravel lens between colluvium and saprolite in the Kunche-Bekpong area: landform shows partial truncation and reworked quartz clasts; a demonstration of proximal transport of sediments.

6.2 Field observations

Vast areas of the study are covered by depositional regolith interspersed with patchy ferruginous and erosional surfaces (Fig. 5.16). The depositional regolith consists of

distal sediments, commonly Black Volta and Bekpong River deposits, with some proximal colluvial and alluvial sediments transported by streams and sheetwash deposits after flash floods. The flood plains of the drainage systems and other low-lying areas are characterized by depositional regolith. The depositional areas have thicker overburden thickness than it is at the outcrop areas. On the lower slopes, gravel merges with sandy silt and is inter-layered with sand. Lateritic duricrust appears to be missing in the depositional environment but ferricrete is observed buried under loose transported sand in some localities (Arhin and Nude, 2009). Excavations in the open-wash terrains showed pockets of goethite-rich laterite ('bog-iron') probably formed by chemical and biochemical precipitation of hydromorphically transported Fe. Outcrops of fresh rocks are rare especially in the western part of the study area but there are granitic outcrops at the eastern part, in streams and also at the dissected slope areas.

Hilltops and plateaus capped by ferruginous duricrust were mapped in the study area (Fig. 6.3). Similar high level plateaus and hills capped by ferruginous duricrust have been observed by other authors: Bowell et al. (1996) in southern Ghana; Butt and Bristow (2012) in Mali and several locations in Burkina Faso. Ferruginous capping hills and ridges are common in the north-eastern part of the study area especially near Billaw and Happa (Fig. 5.16). The profiles of the exposed sections of the duricrust capped–hills take the forms of the crest of the hills; some exhibit convex contacts whereas others show concave or flat table contact between the ferruginous duricrust and the underlying saprolite.

There is high-level ferricrete at least 2-3 m thick (Fig. 6.5) capping high pediment that contains rounded and sub-rounded pebbles with occasional cobbles in Sabala area. In addition, at Nandom, Boo and Hamile, also in the Lawra belt, ferricrete over 3 m thick occurs on higher-level plateaus of about 20-50 m elevation (Fig. 5.16). The ferricrete is generally strongly indurated on the higher levels and has pisoliths with preserved cutans developed in cavities, suggesting they have been re-weathered. The lower units beneath all have characteristically tubular voids imparting considerable porosity. In profile the boundaries between the ferricrete and the underlying saprolite either have concave or sharp horizontal contacts. Similar high-level ferricrete, with a much thicker ferruginous horizon, made up of cobble unit in contact with saprolite; cap a mesa at Gaoua in Burkina Faso (Butt and Bristow, 2012). Elsewhere in West Africa Boeglin

and Mazaltarim (1989), Boeglin (1990) and Tardy (1997) found laterite outcrops whose surface crust contains detrital quartz cobbles and pebbles of pisolithic duricrust similar to ferricrete mapped in the current study and shown in Figs. 6.4 & 6.5. These ferruginous duricrust and ferricrete are later eroded, contributing to the sediments on hill slopes and in the valley floor. The steeper upland areas with an average elevation of 250-300 m have thin cover of soil and lithic fragments with bedrock generally close to surface. Blocks of ferruginous duricrust released by erosion degrade to ferruginous gravels on the lower slopes. However in the valley floors and low-lying terrains underlain by laterites are lateritic lag rubbles and pisolithic surface cover. Ferricrete dominated areas distinctly have polymictic surface lag and can be a useful guide to distinguish ferricrete from lateritic residuum. There are widespread areas of local relief inversion (Fig. 6.6). This occurs when low areas of the landscape become filled with transported sediment that hardens into material that is more resistant to erosion than the material that surrounds it. Detailed description of the relief inversion in the study area is presented in section 6.2.1. The widespread occurrences of ferricrete in West Africa have been documented in remote sensing imagery interpretation by Butt and Bristow (2012).

6.2.1 Ferruginous duricrust, relief inversion and landscape evolution of the Lawra belt

In the Lawra area, ferruginous duricrust and ferricrete are formed by climatic and other environmental changes. The original lateritic regolith weathers and erodes. The eroded weathered materials and sediments are then cemented by Fe-oxides and clay minerals after which they are hardened as the climate changes from the short rainy season to a long dry season (Dickson, 1972). The cemented in situ weathered materials after hardening, referred to as ferruginous duricrust, become resistant to erosion. The surrounding materials around the newly formed ferruginous duricrust become susceptible to erosion. The differences in hardness of the ferruginous duricrust and the surrounding regolith unit therefore enhance differential erosion. The progressive erosion of the surrounding regolith units' results in the ferruginous duricrust capped hills.

Conversely the eroded ferruginous duricrust and the initial lateritic regolith materials are transported down slope during which time some fill the upland valleys and drainage

channels whilst some are transported to the low lying areas. The upper part of the infill materials in the valleys and drainage channels hardens through precipitation of iron cements and clay minerals to form thick ferricrete as the climate changes (Anand and Pain, 2002). Cemented debris of the transported alluvium and colluvium in valleys and cementation of the upper part of the ferruginous relict materials in the fluctuation zones of the water table levels cause ferricrete and duricrust to harden during the dry phases. Subsequent reversion to seasonally wetter conditions causes renewed leaching and dissolution. As the hardened duricrust and ferricrete protects the underlying saprolite the result is the lowering of the flanking landscape and the eventual emergence of the former low-lying ferricrete as a topographic high. The landscape evolution processes illustrating relief inversion is presented in Fig. 6.14 (A-D). Pisoliths released from repeated erosion of the older ferricrete persist on slopes and accumulate in drainage channels following a change to drier conditions (Fig. 6.14 C). Accumulations in the drainage channels and valleys are re-cemented again to form secondary ferricrete at a lower level in the landscape (Fig. 6.14 D). Erosion continues progressively even after the formation of the secondary ferricrete in the drainage channels. Beside the newly formed secondary ferricrete is alluvial incision that removes part of the flanking un-cemented materials, leaving the secondary ferricrete standing as a ribbon-like mesa following the original drainage course.

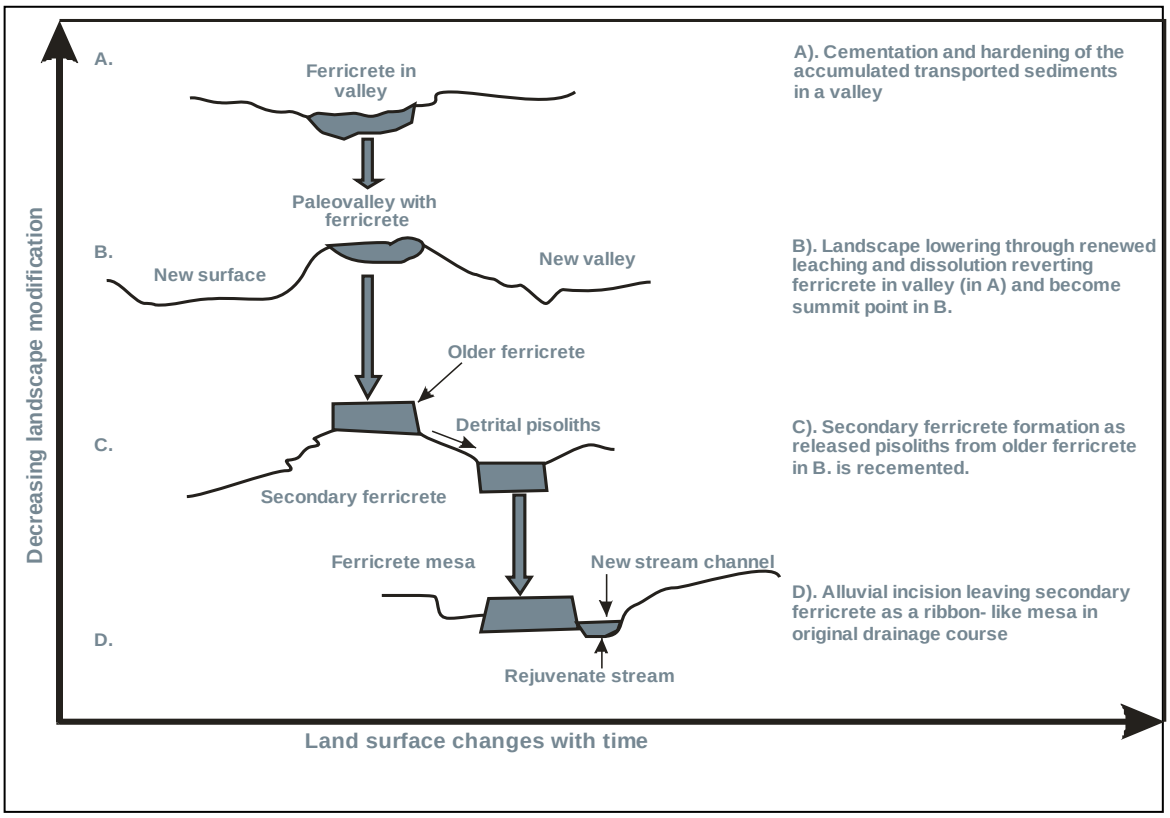

Fig. 6.14 Diagrammatic illustrations of relief inversion in Lawra area: A–D shows the changes during relief inversion in the Lawra study area.

6.3 Discussion

The extensive distal and proximal sediment transport coupled with the contrasting genetic relationships of lateritic duricrust and ferricrete with the underlying saprolite complicates the delineation of gold geochemical anomalies. The irregular distributions of the regolith materials pose challenges to exploration for bedrock mineralisation because of their ability to dilute and enhance geochemical anomalies. This is exacerbated when differences between the ferruginous duricrust and ferricrete are unknown. Residual gold is enriched in the residual lateritic duricrust in southern Ghana (Bowell et al., 1996) and elsewhere in West Africa (Freyssinet, 1993). Gold is sometimes concentrated in lateritic residuum overlying mineralized bedrock and saprolite to form a mineable resource (Butt, 1989; Freyssinet et al., 2005). Understanding that the lateritic residuum has formed in place has led to its use as an appropriate exploration sample media in Australia (Smith and Anand, 1992; Smith et al., 1992). However, whilst superficially similar, ferricrete has no relationship to

residual gold concentration (Anand, 2001; Bamba et al., 2002) and hence is would be a misleading sample media.

Observations of the ferruginous duricrust in the study area and similar types observed by other authors in southern Ghana, Burkina Faso, Mali and Guinea demonstrate that most of the ferruginous duricrust on the plateaus and the low lying areas is dominantly ferricrete, formed by Fe-oxide cementation of colluvial and alluvial sediments. Residual lateritic duricrust occurs only in small areas and normally caps isolated hills and mesas. It commonly formed on topographic highs; examples are the residual lateritic duricrust blanketing the volcanic outcrop hills between Lambussie-Billaw and Happa. However, residual lateritic duricrust occurs also at intermediate and lower levels in some places. Butt and Bristow's (2012) work in Burkina Faso revealed a similar pattern.

The presence of ferricrete at higher elevations (Fig. 6.14 B) suggests considerable relief inversion during the evolution of the landscape. The layered polymictic detrital clasts laterite (Fig. 6.4), smooth rounded to sub-rounded quartz clasts (Fig. 6.5), and older and strong indurated laterite cemented together with much younger laterite (Fig. 4.10) thus indicate they were derived in part from a widespread lateritic duricrust and recent terrestrial sediments. The series of repeated weathering, erosion and deposition as well as the landscape evolutions explained in section 6.2.1 in the study area results in the different landforms and planation surfaces (Fig. 6.15). Within the toposequence in the study area, the early residual ferruginous duricrust forms a near continuous layer at the hillcrests and the upper slopes.

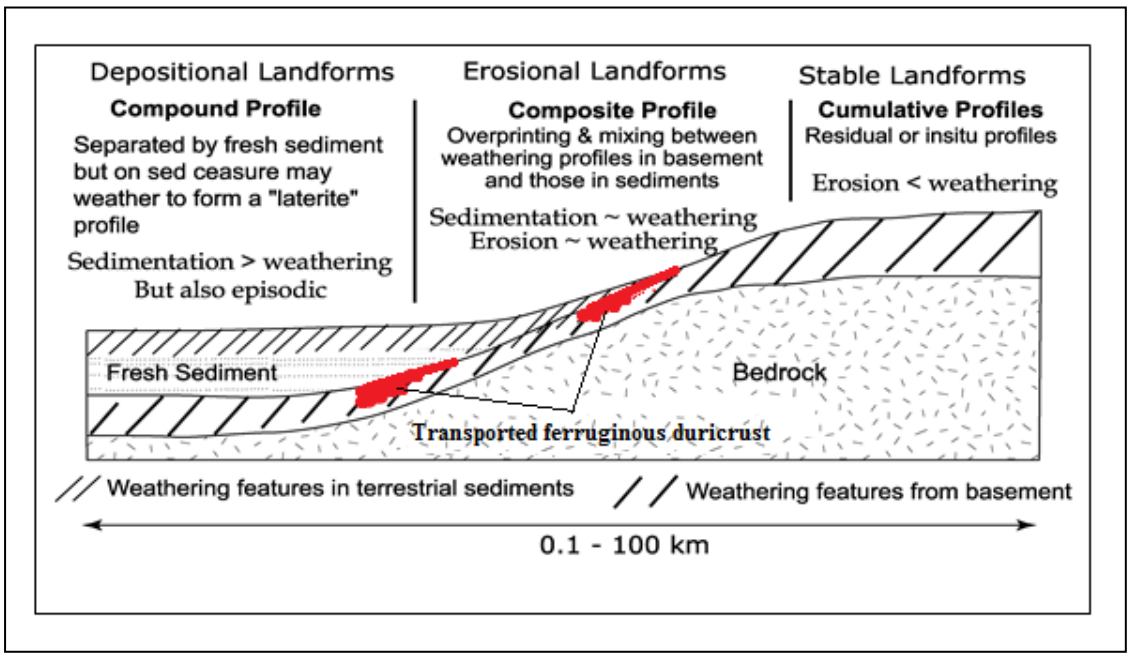

Fig. 6.15 Summary representation of typical modified land surface changes over long periods of regolith/landform evolution in the study area (modified after Taylor and Eggleton, 2001).

The repeated weathering and erosion degrades the original duricrust. Blocks of duricrust released by headwater erosion degrade to ferruginous gravel on the lower slopes alongside the colluvium and the alluvium of valley floors (Fig. 6.16 A). The upper parts of the newly formed surfaces subsequently become indurated to form lateritic duricrust in response to the drying of the of the upper profile due to lowering of the water-table induced by tectonic uplift or to a change to a more arid climate or both. Differential erosion induced by changes in climate removes the less resistant surroundings near the newly formed indurated laterite that occur at lower levels to the original duricrust. The differential erosion events subsequently exposed saprolite and in places fresh rock (Fig. 6.16 B). The incomplete removal of the pisolithic pebbles, nodules, weathered and fresh lithic fragments and quartz clasts result in the deposition of coarse proximal and distal colluvium across the landscape which leads to the formation of ferricrete shown Figs. 6.3-6.6 and Fig. 4.10. The re-weathered products are again eroded and transported to the low-lying areas during flash floods and by the drainage systems. The eroded materials of diverse source fill the valleys, gullies and cover the partly and wholly truncated low-lying areas. This generally buries the

previously exposed bedrock, saprolite and remnants of some residual duricrust. The deposition of the distal and proximal colluvium and alluvium exhibits either broad concave or fairly flat surfaces characteristic of Fig. 6.14 C. Lateritization of the transported sediments characterized by the development of mottles, nodules and pisoliths suggests a period of increased humidity following deposition. A change from humid to dry climates results in the induration of the cemented transported sediments by Fe-oxide and clay minerals to form younger ferricrete The repeated weathering episodes coupled with the subsequent differential erosion enhanced by changes in climate and environmental conditions will continually cause the regolith and the landscape to evolve. Therefore if the objective of exploring in areas under cover is an improved gold exploration survey that results in discovering hidden mineralization, then regolith and landscape evolution need more attention and they should be properly understood.

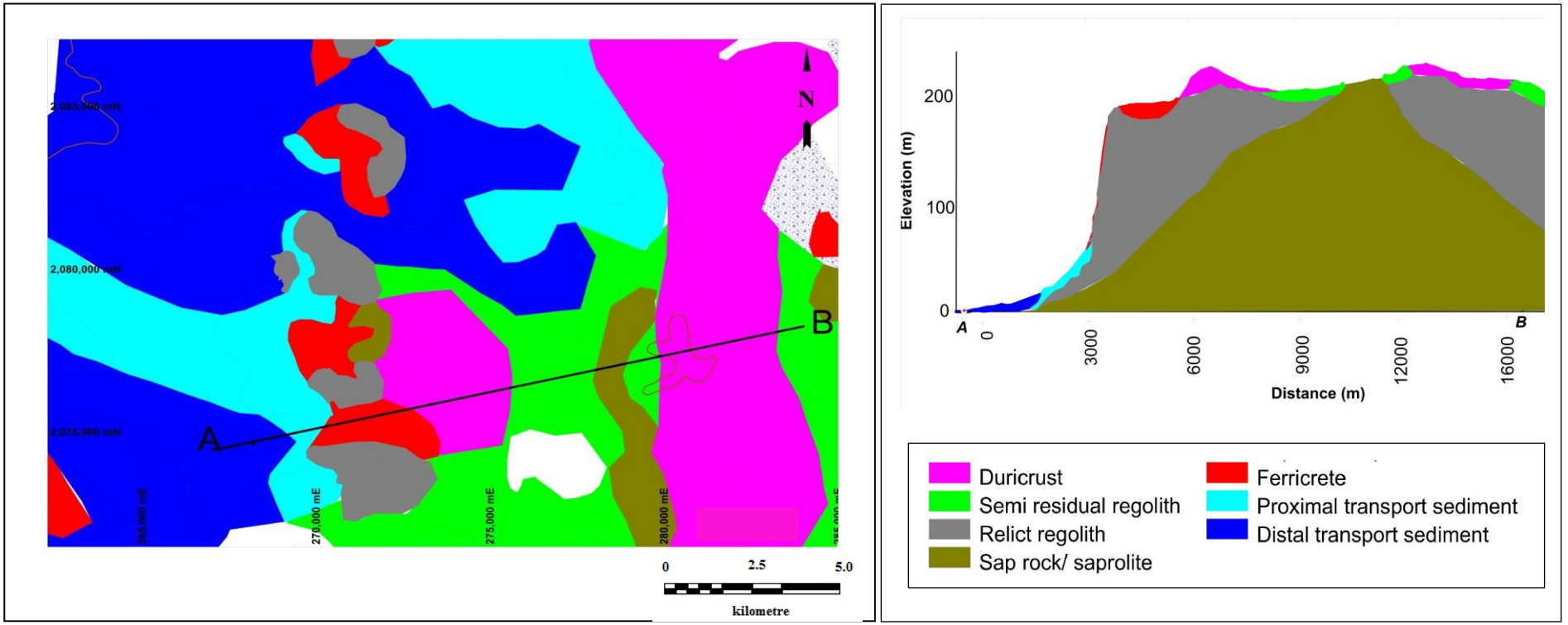

Fig. 6.16 A). Regolith map of part of the study area. B). Grid profile showing the interrelationship between regolith units and elevation along line AB. AutoCAD elevations extracted from a digital topographic map of northern Ghana used.

6.4 Landscape evolution model of Lawra belt

The field observations and the interrelationship between regolith units and elevation along line AB (Fig. 6.16) shows some transported laterites (not formed from direct chemical weathering of the underlying rocks) occupy topographic high areas. Therefore, to help the planning of geochemical exploration, the changing terrain over time has been reconstructed to develop a landscape evolution model (Fig. 6.17). The model development was based on the findings obtained in the study and is consistent with other authors such as Butt and Bristow (2012), Bamba et al. (2002) Bolster (1999) in the West African sub region. This model was based on headwater erosion of the initial lateritic regolith (Fig. 6.17 A) and the formation of ferricrete (Fig. 6.17 B), followed by relief inversion (Fig. 6.17 C) and formation of isolated duricrust-cap hills (Fig. 6.17 D) as remnants of ferruginous duricrust following weathering and erosion.

The landscapes of sub-Saharan West Africa were observed and defined by Michel (1973) to comprise a succession of surfaces at different elevations and ages, from the Labé surface at 1400-850 m near Fouta Djallon, Guinea, to the lowest pediment associated with alluvial plains in the valleys of the present major rivers (Fig. 6.18). The last four surfaces are consistent with field observations seen and mapped during the regolith/landform mapping. However, the highest planation surfaces; Labé, Dongol Sigon and African surfaces, were not observed and have either been completely eroded or did not exist in the region. The ages ascribed to the surfaces from the African surface to Bas glacis in a recent dating of landform surfaces in northern Burkina by Beauvais et al. (2008) are; Eocene (59-45 Ma), Oligocene (34-29 Ma), Late Oligocene-Early Miocene (24-18 Ma) and Middle Miocene-Late Miocene (12-7 Ma) respectively. This implies that regolith surfaces of the Lawra belt relative age falls between Oligocene-Late Miocene to present, as the landscape is still actively evolving.

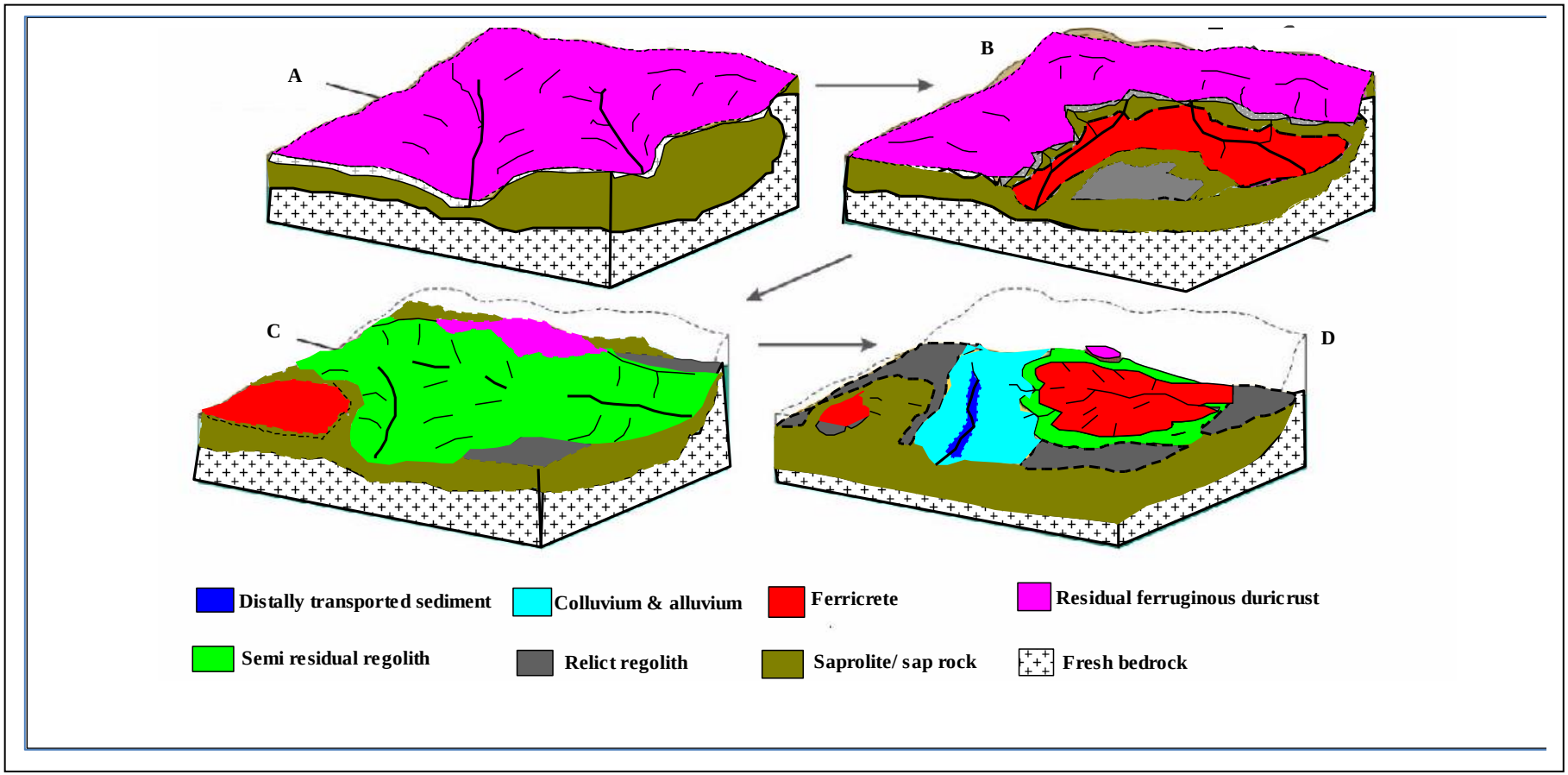

Fig. 6.17 Landscape evolution model of the Lawra belt.

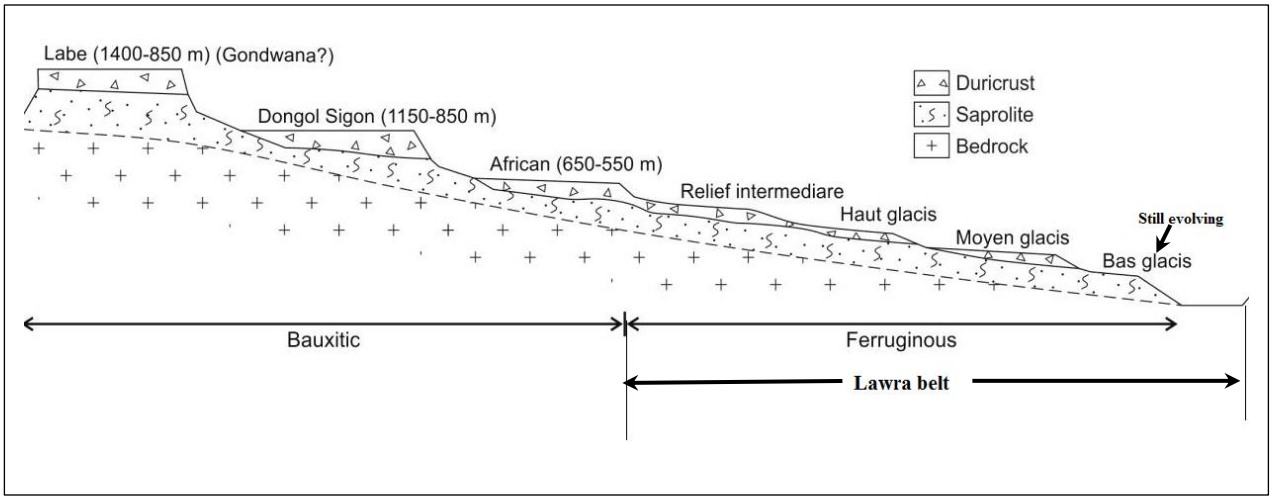

Fig. 6.18 The successive planation surfaces of sub-Saharan West Africa (Burke and Gunnell, 2008; Michel, 1973)

6.5 Conclusion

Field observations have revealed the widespread and the irregular spatial distributions of ferricrete (i.e. ferruginous and indurated colluvial/alluvial regolith sediments) covering about 18% of the study area. The ferricrete occupies some of the hilltops, hill slopes, and plateau tops as well as low-lying plains. The ferricrete thickness ranges between 1->2 m on hill tops and about 2- 4 m on plateaus. Those that occupy the low-lying areas have thinner thickness and are often buried under proximal or distal transported sediments. The plateaus were earlier considered as remnant of the residual land surface following erosion hence the ferruginous laterite capping them were thought to be residual. However, the regolith mapping in the study area observed the presence of ferricrete forming the summit regolith material on some plateaus. This suggests that these surfaces are depositional with erosional debris cemented by later lateritization events. Contrastingly, the partly eroded plateau landforms in the present-climate capped by ferricrete are similar in surface crust to the duricrust capped hills formed over a residual lateritic regolith because Fe-oxide cement is used in the formation of both regolith units. The only difference between them is in situ weathered materials are cemented by Fe-oxides and clay minerals in the case of duricrust whereas transported sediments form the major regolith units in ferricrete. Their recognition and spatial distribution is significant for the understanding of regolith/landform evolution

of the area. Additionally their distinction is essential for the development of geochemical exploration models in complex regolith environments such as the Lawra Belt.

The study also found residual lateritic landforms to be uncommon. These findings show that:

1. Erosion products are not entirely removed from the landscape. This means that repeated weathering events can affect both the transported and the exposed residual material;
2. There are also relief inversions in some areas, which suggest unconformable land surface evolution;
3. Large areas of the landscape (~72%) are covered by distal and proximal sediments of diverse origin. Evidence of sediment transport is shown in the shapes of the lithic and quartz clasts in the depositional regolith, and,
4. The superficial similarities amongst the upper regolith materials overlying the compound, composite and cumulative regolith profiles require pit excavations for regolith characterization and geochemical survey purposes.

The occurrence of ferricrete landforms in adjacent countries, noted by field observation and inferred from satellite imagery, demonstrates that relief inversion is a very widespread phenomenon. Since their source material can either be local or far, distinguishing them from residual duricrust before their use as sample media is important. It is concluded that the regolith of the Lawra belt falls in age between Oligocene-Late Miocene and the present, as the landscape is still actively evolving. Careful characterization of the regolith, including dating if possible, will be essential to differentiate the duricrust from the ferricrete. The study therefore suggests the incorporation of its findings in the exploration search methodology to address the implications of regolith evolution on Au geochemical exploration.

Geochemical dispersion of gold (Au) and other associated elements in the regolith of the Lawra belt

7.0 Introduction

Over 50% of the study area is covered by transported regolith made up of distal and proximal sediments (chapter 5). The mode of formation of the regolith thus varies across the area and could lead to hidden Au anomalies going undetected if an Au only approach of geochemical analysis is used. Careful examination of the mapped regolith in the study area reveals some anomalies are masked by the complex regolith. Therefore to detect the hidden anomalies in the complex regolith through discriminating residual anomalies from transported anomalies the following were carried out:

a) Pits were dug down to the saprolite to expose the regolith profiles for logging and sampling.
b) The use of regolith geochemistry to validate and support field regolith logging was investigated. This could help discriminate between regolith units, in particular for novices in regolith mapping.
c) Surface and geochemical processes that control element migration in complex regolith were investigated to understand which anomalies are real and require a follow up survey.
d) Sieved fractions were analysed for 51 elements to establish the pathfinder elements for exploration for Au in this environment.

7.1 Methods and data analysis

To define mineralisation in the area three methods were used to gather and analyse data, establish the associated elements suitable for Au exploration and determine pathfinder elements from associated elements:

1. Pit digging and regolith unit sampling;
2. Laboratory analysis of field samples using ICP-MS, XRF and Fire assay (FA-AAS);
3. Examination of behaviour of Au, major and trace element distributions in the regolith profile.

7.1.1 Pitting and regolith unit sampling

Pits were dug in regolith regimes mapped and classified as ferruginous, relict and depositional, as well as modified erosional regimes (chapter 5; section 5.6). Sampling method details can be found in chapter 4; section 4.3.2.

7.1.1.1 Precautions taken during the panel sampling

Precautions taken at all regolith regimes to avoid cross contaminations were:

a. Samplers were not allowed to wear jewellery (e.g. gold rings),
b. Sieves were cleaned ultrasonically at the end of a day's work at the field camp. In between sampling the sieves were cleaned with a nylon bristle paintbrush. The brushing of the sieve was done from underside only with a gentle circular motion. The collecting bowls and pans were cleaned with pieces of cloth.
c. Metal-free scoops and nylon sieve-mesh housed in plastic frames were used to avoid metal contamination.
d. The top 10 cm of humus soil and rootlets were removed at all sample locations.

To standardize the sample weight before sieving in the field the raw moist field sample weight was measured to 5 kg using a digital weighing scale. The field samples were dried in the sun and later reduced to 2 kg by sieving out and discarding the coarser material in excess of 2 mm. The <2 mm portion was bagged, labelled and sent to the field camp where they were sieved further to <125 µm. The prepared samples for ICP-MS and FA-AAS were transported to ALS-Chemex laboratory (the samples were collected in Ghana and sent to South Africa for analyses) and those for XRF to the University of Leicester Geology Department for chemical analysis. All the field data were recorded on field sheets (Fig. 4.5 & 4.6).

7.1.2 Laboratory analysis of samples using ICP, XRF and FA-AAS

The <125 µm sieved samples were divided into three 100 g portions for ICP, XRF and FA-AAS analytical techniques. The ICP and FA-AAS analysis were performed on the <125 µm fractions whereas a 50 ml subsamples were further ground to a finer powder for the preparation of pressed pellets and fusion beads for XRF analysis. Detailed method descriptions are presented in Appendix B.

7.1.2.1 ICP analytical method

The inductively coupled plasma (ICP) method employed ALS-Chemex sample analysis protocol ME-MS41 that uses both atomic emission spectrometry (ICP-AES) and mass spectrometry (ICP-MS) techniques. The combined methods used in this analytical protocol consist of near-total and partial extraction methods. Detail methods descriptions of the ICP-MS and ICP-AES are in Appendix B. The near-total technique uses ICP-AES method and characterises the base metals such as Ag, Cd, Co, Cu, Mo, Ni, Pb, Sc and Zn whereas elements most appropriate for aqua regia leach like As, Bi, Hg, Sb, Se, and Te were characterised in the samples by the ICP-MS method. (Unpublished ALS-Group analytical protocols: Galway-Ireland; www.alsglobal.com). The data reported from aqua regia leach represent only the leachable portion of the particular analyte; this implies that recovery percentages for many analyte from more resistive major elements can be very low.

In this method samples are digested with aqua regia in a graphite heating block and left to cool. The resulting solution is diluted with deionized water and subsequently subjected to ICP-AES analysis. Results of the initial analysis are reviewed for high concentrations of bismuth (Bi), mercury (Hg), molybdenum (Mo), silver (Ag) and tungsten (W). ICP-MS analysis then commences for the remaining suite of elements. The analytical results are corrected later for inter-element spectral inferences. Table 7.1 shows the lower and upper limits of selected elements used, with the complete package of the 51 elements analysed by this method also shown in Appendix C.

Table 7.1 Analytical limits for data obtained by ICP-MS (ME-MS41) and FA-AAS (Au-AA24) analytical protocols

Element	Symbol	Unit	ME-MS41		FA-AAS	
			Lower limit	Upper limit	Lower limit	Upper limit
Silver	Ag	ppm	0.01	100	x	x
Arsenic	As	ppm	0.01	10000	x	x
Aluminium	Al	%	0.01	25	x	x
Gold	Au	ppm	0.2	25	0.005	10
Copper	Cu	ppm	0.2	10000	x	x
Iron	Fe	%	0.01	50	x	x
Lead	Pb	ppm	0.02	10000	x	x
Sulphur	S	%	0.01	10	x	x
Zinc	Zn	ppm	2	500	x	x
Magnesium	Mg	%	0.01	25	x	x
Manganese	Mn	%	5	50	x	x
Calcium	Ca	%	0.01	25	x	x
Sodium	Na	%	0.01	10	x	x
Phosphorus	P	%	10	10000	x	x
Iron	Fe	%	0.01	50	x	x
Titanium	Ti	%	0.005	10	x	x

Not analysed by FA-AAS = x

7.1.2.2 Fire assay with atomic absorption spectrometry finish (FA-AAS)

A 50 g portion of the <125 µm size fraction of the original sample was mixed with lead oxide (litharge) and other fluxes such as sodium carbonate, borax, silica and potassium nitrate. The resultant sample and flux mixture were fused in a furnace at about 1150^{o}C. The fusion reduces the litharge to molten lead and silica to a borosilicate slag. Precious metals in the sample, for example Au and Ag, were collected by the molten lead droplets. The lead and slag were separated after cooling. The bead was digested in 0.5 ml dilute

nitric acid in the microwave oven. This was followed by an addition of 0.5 ml concentrated hydrochloric acid. The bead was further digested in a microwave at a lower power setting. The digested solution was then cooled, diluted to a total volume of 4 ml with de-mineralised water, and analysed by atomic absorption spectroscopy against matrix-matched standards.

7.2 Quality assurance and control (QA/QC) of analysed samples

The objective of performing QA/QC analysis on the quality control samples is to evaluate the quality of the data. This is vital in geochemical exploration because the confidence required in drawing conclusions from the exploration data depends on the outcome of the QA/QC analysis. In this study the quality control (QC) samples used to estimate accuracy, precision and sources of sampling and laboratory analytical errors for Au were certified reference materials (CRM), field duplicates and blank samples. Due to the limited funds available for the study, QA/QC analysis was performed only for copper (Cu) instead of assessing the analytical errors for all the multielements analysed. The choice of conducting QA/QC on Cu was because of the close proximity of Cu-Au deposit of Volta Resources Gaoua project located about 40 km WNW of Azumah's Kunche deposit.

The following procedures were carried out in evaluating the quality of the data:

- Scatter plots to evaluate the relationship between the certified values for the reference material denoted by X and the corresponding analysed value of same standards at the ALS laboratory by Y
- Regression based error calculations using Williams (1986) formulae for accuracy and precision on the analytical data were also calculated. Williams (1986) formulae are presented below as equation 7.1 and 7.2.

$$Accuracy = \left(\frac{\overline{Y}}{\overline{X}} - 1 \right) * 100\% \qquad \text{Equation 7.1}$$

$$Precision_{individual} = \frac{Y - \left(\left(\frac{\overline{Y}}{\overline{X}} \right) * X \right)}{X} * 100\% \qquad \text{Equation 7.2}$$

Williams (1986)

X (or Au $_{CRM}$) and Y (or Au $_{analytical}$) are the certified and analysed values for all individual samples considered in the dataset. $\overline{X}$ and $\overline{Y}$ are the averages of the certified and analysed values respectively and Precision $_{individual}$ equals the percentage precision of one CRM analysis.

The best line of fit for Williams' equation by principle has to pass through the origin and conforms to Y = X for perfectly accurate data (i.e., poor accuracy is shown by deviation of ideal y = x line). However, precision of analytical data depends on the scatter around the mean (i.e., larger the scatter of the data the poorer the precision). Fig. 7.1 representing the QA/QC results for the Au standard samples in this research conformed to the equation Y = 1.024 X. Table 7.5 also shows the relationship between Cu $_{CRM}$ versus the analysed Cu $_{CRM}$ results.

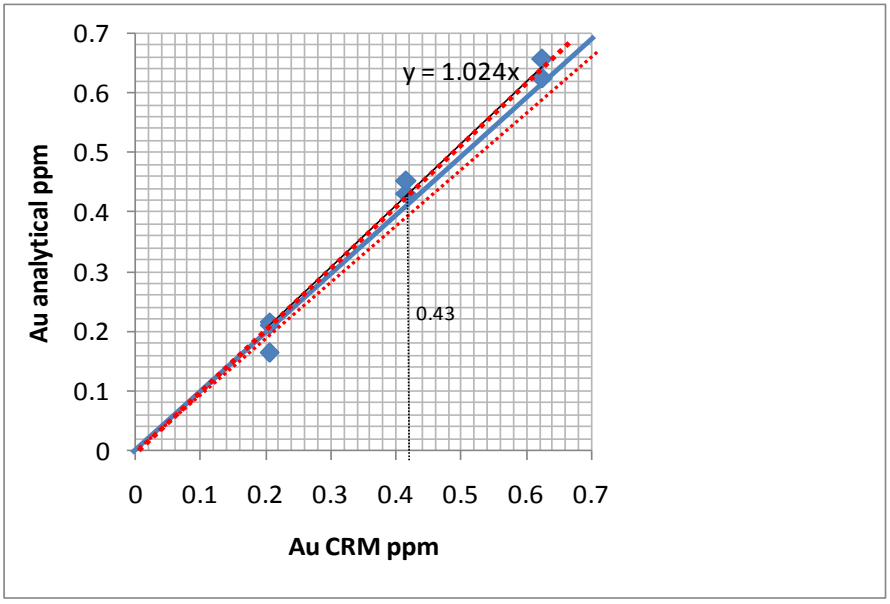

Fig. 7.1 Accuracy and precision of the analytical Au data compared with the CRM data. The blue solid line indicates accuracy of data, red dashed lines indicate precision field around the best-fit line.

Table 7.2 Analytical accuracy and precision of analytical Au and CRM-Au used for the analytical quality of the analysis of Au by FA-AAS technique.

Sample ID	**Au $_{CRM}$**	**Au $_{analytical}$**	**Au $_{analytical}$/Au $_{CRM}$**	**%Precision$_{(individual)}$**
813315	0.205	0.164	0.800	-22.4
813431	0.205	0.217	1.059	3.5
813449	0.416	0.433	1.041	1.7
813569	0.625	0.626	1.002	-2.2
813689	0.416	0.452	1.051	2.7
813259	0.625	0.657	1.051	2.7
814315	0.205	0.212	1.034	1.0
Total	**2.697**	**2.761**		**9.3:*Standard deviation of the 7 samples***

Interpretation of Fig. 7.1 and Table 7.2 show the accuracy and precision of the analytical data as +2.4% and ±9.3%.

Table 7.3 Results of blank samples inserted in batch of samples to monitor analytical contamination

Sample ID	Gold (ppm)
813710	**<0.005**
814090	**0.008**
814151	**<0.005**

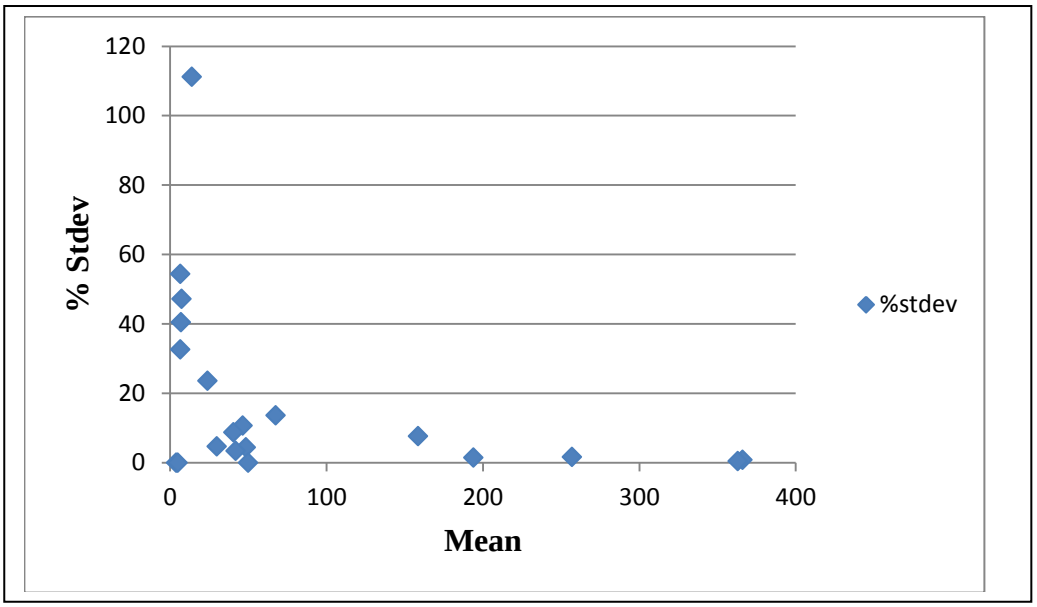

Fig. 7.2 Scatter diagram showing the measure of dispersion around the mean and the per cent standard deviation.

Table 7.4 Relationship between the original and field duplicate results for Au by Fire assay analytical method.

Sample ID	Orig. Au(X) ppb	Dup. Au (Y) ppb	Range (X-Y)	Mean (μi)	Stdev.	% Stdev
813354	4	4	0	4	0.0	0.0
813401	47	50	3	48.5	2.1	4.3
813434	61	74	13	67.5	9.2	13.6
813462	50	43	7	46.5	5.0	10.6
813473	196	192	4	194	2.8	1.5
813488	43	38	5	40.5	3.5	8.7
813566	43	41	2	42	1.4	3.4
813596	364	368	4	366	2.8	0.8
813649	10	5	5	7.5	3.5	47.1
813710	150	167	17	158.5	12.0	7.6
813735	364	362	2	363	1.4	0.4
814086	5	5	0	5	0.0	0.0
814146	31	29	2	30	1.4	4.7
814206	28	20	8	24	2.7	23.6
814231	260	254	6	257	4.2	1.7
814270	9	5	4	7	2.8	40.4
814311	4	9	5	6.5	3.5	54.4
814364	8	5	3	6.5	2.1	32.6
814625	50	50	0	50	0.0	0.0
814675	25	3	22	14	15.6	111.1
814700	22	100	78	61	55.2	90.4
814750	8	5	3	6.5	2.1	32.6
Average					**6**	**22**

Also from Table 7.4 and Fig. 7.2 two of the field duplicates collected with sample numbers 814700 and 814675 have high standard deviations of 55.2 and 15.6 ppb. However the typical average standard deviation of the analytical data is 6 ppb (Table 7.4). The removal of the two high standard deviation samples (814675 and 814700) reduces the typical average standard deviation from 6 ppb to 3 ppb (i.e. 50% error margins). Similarly the removal of the two samples with high per cent standard deviations of 111.1 and 90.4 with sample standard deviations of 15.6 and 55.2 ppb reduced the typical averages of standard

and per cent standard deviations to 3 ppb and 14% respectively. The two high standard deviated samples represent only 9% of the entire samples analysed and contributes about 50% errors in the data analysis. The errors in these samples may either be from the fieldwork or the laboratory analysis. However the examination of the sample logged information these samples indicate they are collected from a depositional environment of Kunche-Bekpong. The disparities in assay results between the original and the corresponding duplicate samples could be due to the compositional diversities of the regolith in depositional environments hence the large non-reproducibility of assay results. Since the two samples have a typical standard deviation of 35 ppb and represent only 9% of the total samples analysed the analytical results received from the laboratory could be accepted because the errors may be more field bound rather than it being errors from the laboratory analysis.

For the blanks, two samples recorded Au values below detection of <0.005 ppm and one assayed 0.008 ppm Au. The 0.008 ppm Au assayed in the third blank sample is far below the estimated background of 0.05 ppm traditionally used for Au exploration in the area (Griffis et al., 2002). It is possible that the failed blank sample is due to poor source of material, which was collected from a stream flowing over Au-poor Kumasi granite (Kesse, 1985), rather than it being indicative of a contamination problem. The results obtained from all the controlled samples (CRM standards, field duplicates and blanks) suggest good sampling and analytical precision and give confidence in the analytical data given the usual difficulties associated with Au and its nugget effect problems (Grunsky, 2010).

The relative per cent difference or error of the analysed Cu_{CRM} compared to the certified reference material GBM 904-1 obtained from GEOSTATS-Australia shown in Table 7.5 is 0.57% and average standard deviation of 0.29 from the 12 certified reference standards inserted in the batch of samples. This shows an insignificant error in the analysed Cu compared to the certified reference materials analysed by ALS-Chemex. Considering an average per cent error of <1% and an average standard deviation of 0.29 therefore makes the analytical data for all the other elements suitable for use in anomaly delineation for the current study.

Table 7.5 Analytical accuracy and precision of analytical Cu and CRM-Cu used for the analytical quality of the analysis of other elements by ME-MS41 technique.

ID No.	Orig Cu CRM-ppm (Xi)	Analysed Cu CRM – ppm (Xm)	Xm/Xi	Precision individual	% Precision	Difference (Xm-Xi)	Relative % Difference
593	162.00	161.00	0.99	0.00	-0.05	1.00	0.62
595	162.00	163.00	1.01	1.01	100.62	-1.00	-0.62
597	162.00	160.80	0.99	0.99	99.26	1.20	0.74
602	162.00	160.00	0.99	0.99	98.77	2.00	2.24
605	162.00	161.50	1.00	1.00	99.69	0.50	0.31
608	162.00	161.00	0.99	0.99	99.38	1.00	0.62
611	162.00	160.00	0.99	0.99	98.77	2.00	1.23
614	162.00	161.00	0.99	0.99	99.38	1.00	0.62
617	162.00	159.50	0.98	0.98	98.46	2.50	1.54
620	162.00	163.00	1.01	1.01	100.62	-1.00	-0.62
623	162.00	162.20	1.00	1.00	100.12	-1.00	-0.12
626	162.00	160	0.99	0.99	98.77	2.00	1.23
	Av.=162	**Av.=161**		**Stdev=0.29**	**28.73**	**Ave.=0.92**	**Ave.=0.57**

Average Xm/Xi = $\bar{Y}$ = 0.99

7.3 Results

Results of the major oxides and trace elements obtained in the regolith profiles are presented as follows:

a. Surface regolith and pit spatial locations.
b. Behaviour of selected major and trace elements in the regolith
c. Distribution of regolith units with depth
d. Regolith geochemistry and impact of different regolith horizons on element mobility
e. Pit by pit interpretation of element mobility in regolith

7.3.1 Surface regolith and pit locations

Regolith maps were created from ground truth mapping and remote sensing data interpretations (Chapter 4, Figs. 4.4 and 4.5. The pits were excavated at relict, semi residual, relict/residual laterite contact and ferruginous regimes. Elevation differences of the landscape were measured from a levelled horizontal baseline setup with a nylon rope. This was necessary because of the low-lying topography that characterized most of the

pitting areas. Tables 7.6-7.7 show the regolith regime types and pit locations with pit identification numbers.

Table 7.6 Location of dugout pits in the surface regolith types in Kunche-Bekpong

Regolith type	Pit location identification numbers
Ferruginous regime - transported laterite	KP008, KP009 and KP010
Ferruginous regime – residual laterite	KP015, KP016, KP017, KP018, KP019, KP020 and KP021
Relict regime	KP001, KP003, KP004, KP011 and KP012
Semi residual regolith	KP006 and KP007
Relict/residual laterite	KP004

Table 7.7 Location of dugout pits in the surface regolith types in Sabala

Regolith type	Pit location identification numbers
Ferruginous regime – transported laterite	SP001, SP005, SP006 and SP008
Ferruginous regime – residual laterite	SP002, SP003, SP004 and SP007

7.3.2 Regolith distribution with depth

The relationship between surface regolith materials and subsurface regolith units vary with different environments. In depositional environments the surface regolith is different from the underlying substrate, whilst direct relationships between surface regolith and the underlying regolith occur in relict and erosional areas. Pits were therefore dug to ascertain the relationship between surface regolith and the subsurface regolith units and the thicknesses of the regolith horizons. Regolith profiles of pits dug at Kunche-Bekpong are presented in Figs. 7.3-7.4. A generalized schematic cross section along L1148600N that demonstrates differences between the surface and subsurface regolith is presented in Fig. 7.5) whereas Sabala pit profiles are shown in Fig. 7.6.

The saprolite and sap rocks identified in the dugout pits in Kunche-Bekpong and at Sabala consist of phyllite, tuffaceous phyllite, tuff and some schistose rock units (Figs, 2.3, 4.5 and 4.7). KP006, KP007, KP018 and KP020 are underlain by phyllite whereas the remaining pits occur in metavolcanic and volcano-sedimentary rock units. KP009 and

KP010 have about 25% of lithic fragments tuffaceous phyllite in the saprolite. The saprolite formed from the metasedimentary units contains generally angular quartz clasts some of which are smoky whilst some are milky white in colour. However most of the pits were dug up to the upper saprolite which exhibit complete destruction of the parent fabric of the underlying rock. This makes the identification of the actual underlying rock name difficult to distinguish. For that reason the use of saprolite and sap rock were used in this thesis to represent the lower portions of the sub regolith units.

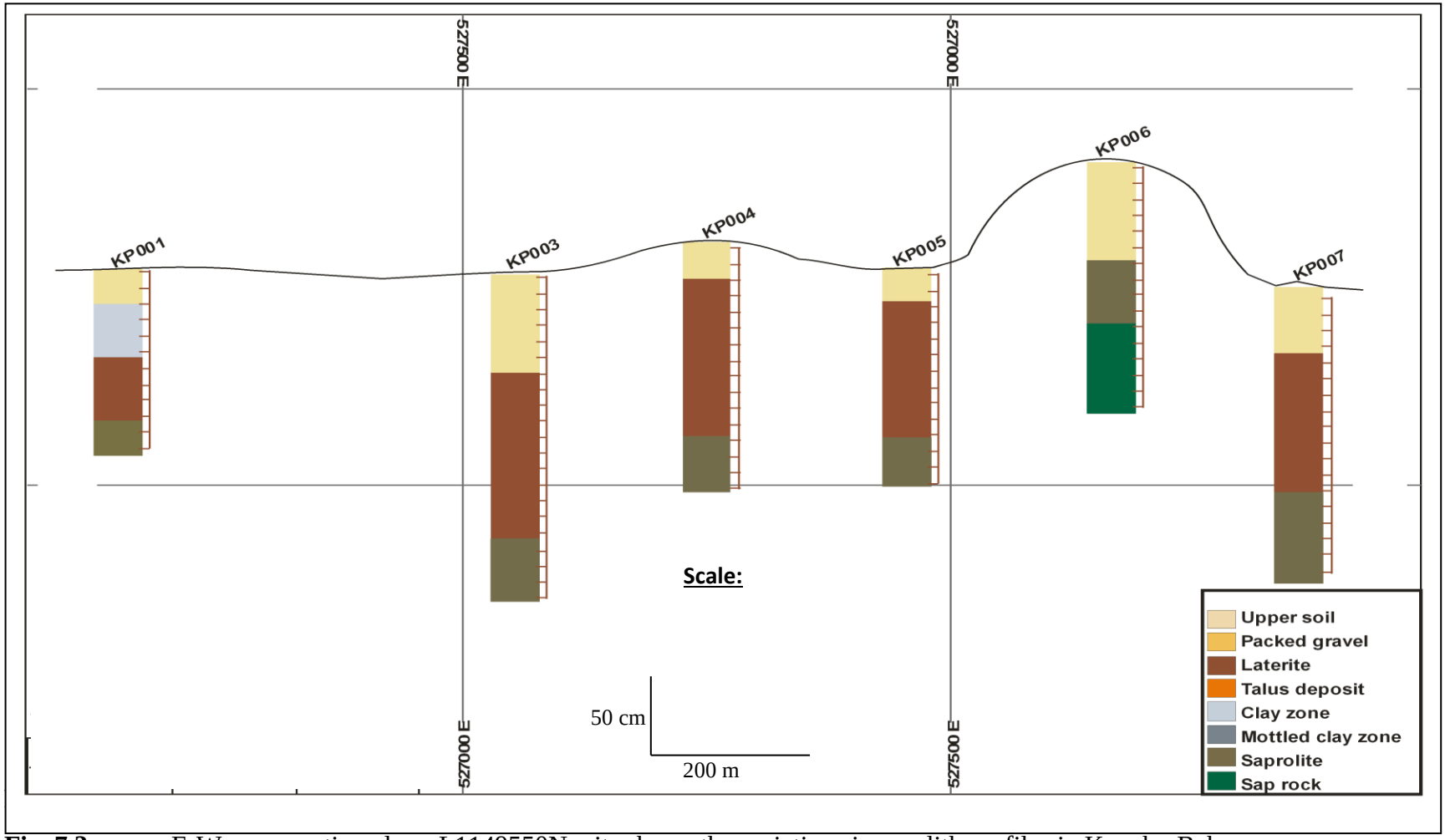

Fig. 7.3 E-W cross section along L1149550N, pits shows the variations in regolith profiles in Kunche-Bekpong area.

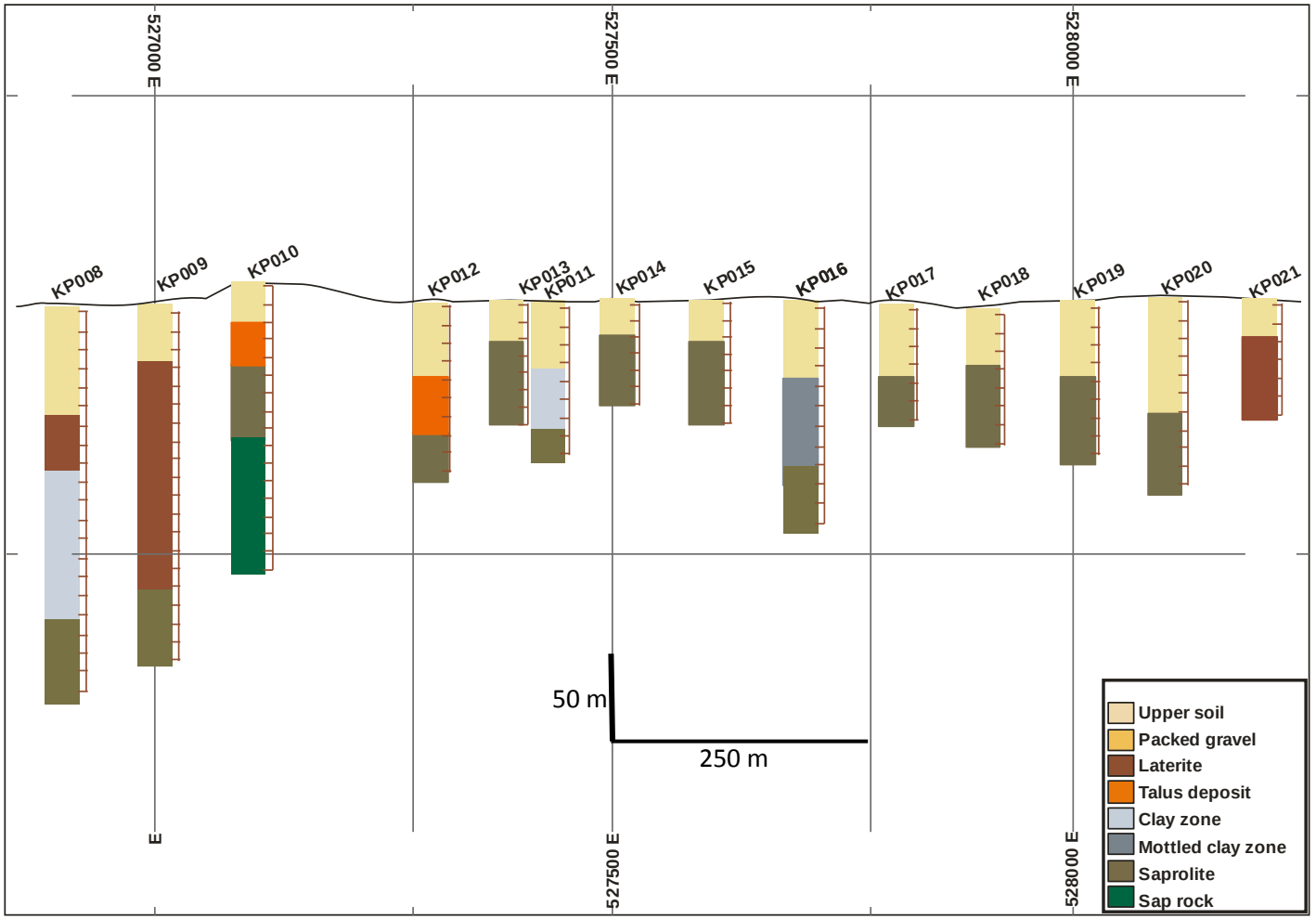

Fig. 7.4 E-W cross line along L1148600N shows the variations in regolith profiles in Kunche-Bekpong area.

The surface regolith materials (Fig. 7.3) have silt and loamy soil covers. With no pit excavations to expose the differences in profiles the classification of the regolith regime could be puzzling. The regolith profiles exposed in the pits show the relationships between surface regolith and the underlying regolith vary. For example at KP001 the surface regolith directly relates to the underlying regolith and thus shows relics of the underlying parent materials preserved in the surface regolith. However in KP003-KP005 the upper part of the regolith has been eroded and been replaced by lateritized scree. Laterites formed in these environments may be transported, but the degree of transportation from their source may not be far. Surface regolith in these areas bears no relationship to the underlying regolith.

Examinations of the regolith suggest repeated weathering, erosion, deposition and lateritization modify the regolith material (chapter 6). In this local environment pits KP001 and KP006 were dug through partial and wholly eroded terrains whereas KP003, KP005 and KP007 were dug in a ferruginous regime. KP004 occurs in a semi-residual regime. The mapping data from KP005 and KP007 shows evidence of transportation. From the landscape architecture it is likely that there was down-slope movement of erosional materials from KP006 to KP005 and KP007. Erosional transport of regolith materials from KP004 probably added some sediment to the upper regolith materials in KP003. The validation of the regolith in these areas was possible because the areas were opened up for regolith stratigraphy studies via pit digging.

Pits KP013-KP020 was characterized by erosional landscapes and the upper soils overlie either the clay zone or saprolite. KP018, KP009 and KP021 represent the ferruginous regolith environment and have laterites over clay zone and saprolite. KP008 may be a residual laterite because it has similar residual laterite profile shown in Fig. 4.5. However in KP009 the laterite overlies saprolite, an indication of pre-existing preserved surface truncation by mechanisms that modify landscape during regolith evolution. This implies that the materials forming the laterite in this area were not developed directly from the underlying parent rock but rather were transported from a different source. The laterite in KP009 therefore can be considered as transported laterite or ferricrete. It is appropriate to

suggest that laterite in KP009 came from KP010 via mechanical transport of regolith material. Also in KP010 and KP012 there is a talus deposit on top of the saprolite. The talus deposits have relic features like the underlying rock. Therefore, because of the similarities in composition between the talus and the underlying rocks, the area represents a residual environment.

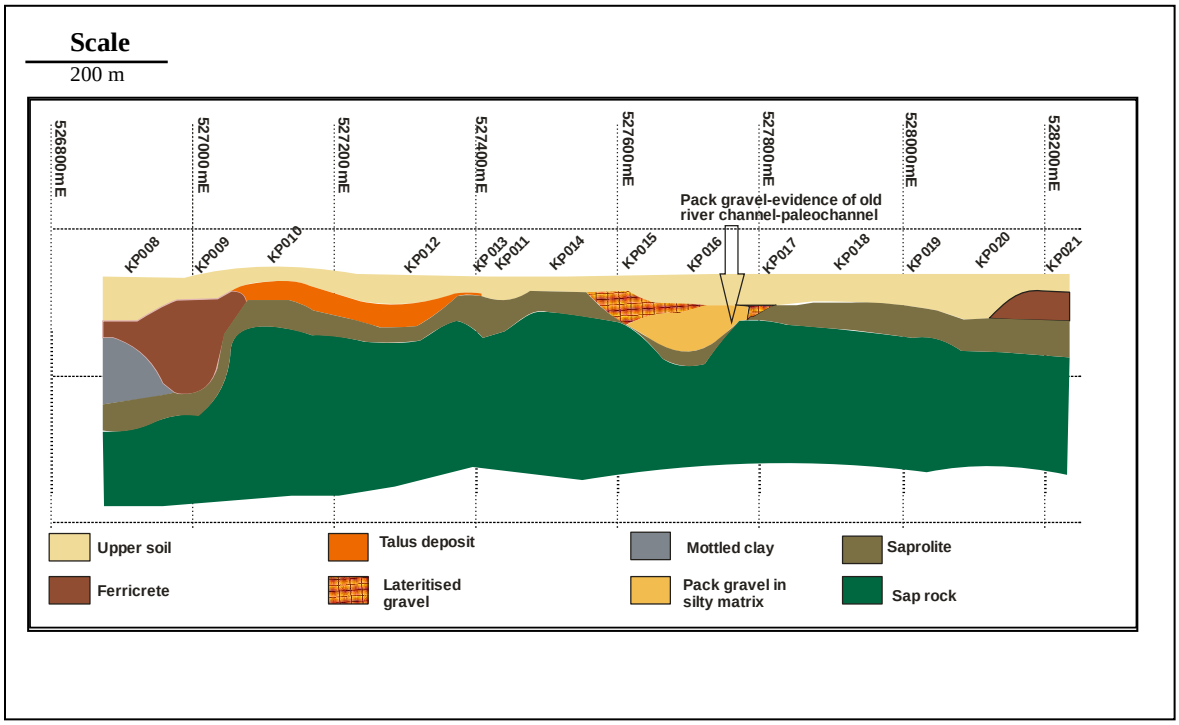

Fig. 7.5 Schematic regolith cross-section along L1148600N in the Kunche-Bekpong area. Vertical scale exaggerated for clarity.

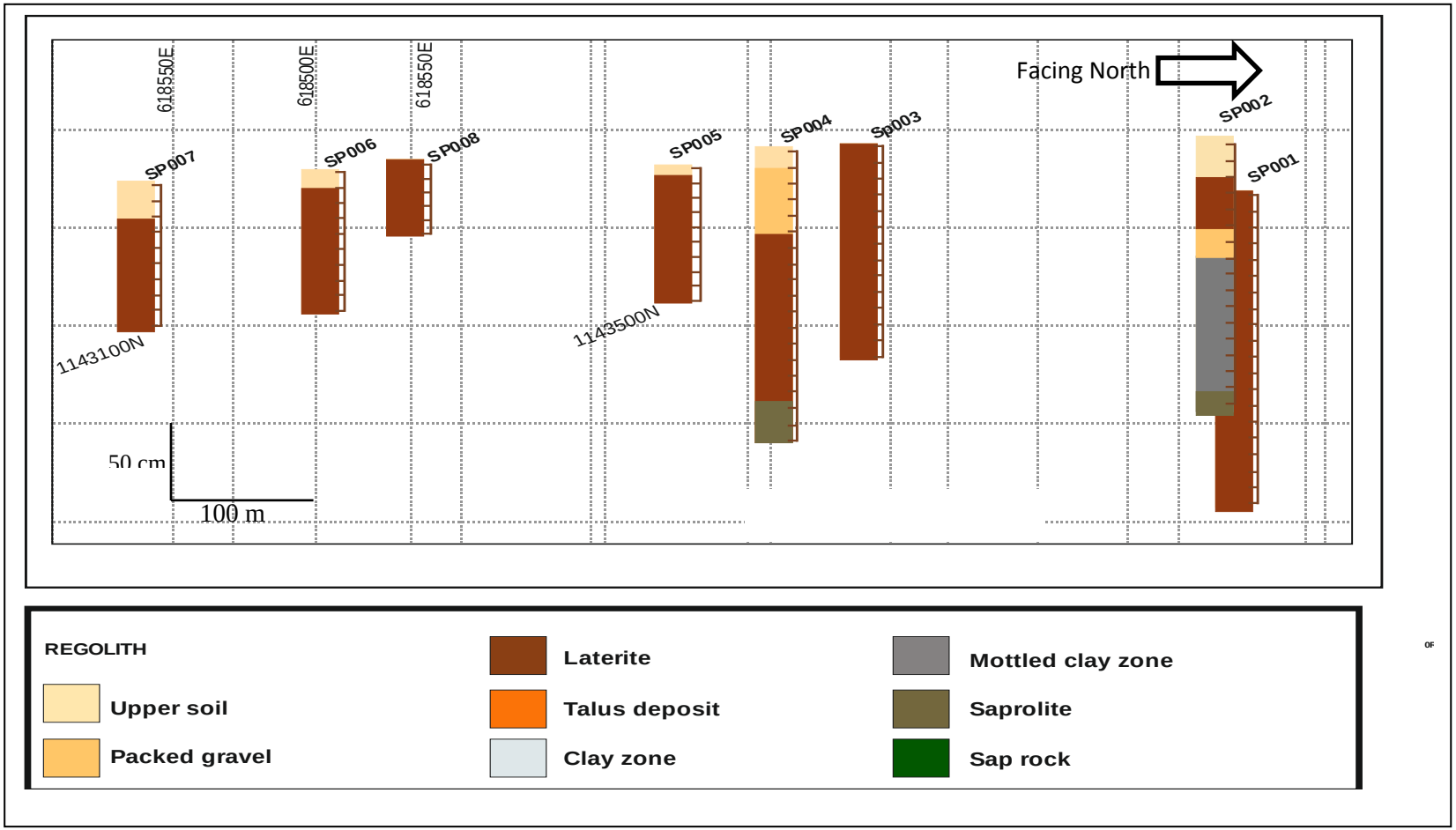

Fig. 7.6 E-W cross sections along L1143100N and L1143500N, pits show the variations in regolith profiles in Sabala area.

The spatial distribution of the regolith materials and the matching of exposed regolith profiles by pit digging to the classic laterite profile in Sabala also revealed some dissimilarity between surface regolith and the underlying regolith. Some areas have pisolithic and silty soils as upper regolith materials (Fig. 7.6). Beneath these regolith layers were thick layers of pack gravel of varying composition and porosities representing relic deposits of palaeochannels. The differences in regolith stratigraphy were seen in SP004 and SP002 where the immature pack gravels are inverted in the profile. In SP004 the pack gravel overlies laterite whereas in SP002 the pack gravel is beneath the laterite and on top of the mottled clay. Examination of pit SP004 places the environment in the composite regolith profile where the pre-existing surface has been wholly eroded and replaced by pack gravel consisting of smooth, rounded and sub-angular quartz pebbles. The lower portion of the transported sediment has been lateritized and on top of that is a layer of immature pack gravels. In contrast SP002 represents a partial truncated surface also covered by similar immature pack gravels with a recently developed layered laterite.

7.3.3 Behaviour of selected major and trace elements in the regolith analysed by XRF method

Regolith materials sieved to <125 μm were analysed by XRF method. The results obtained only reflect a component of the bulk regolith materials because the sieving process discarded the coarser fractions. Differences in the major and selected trace elements indicate variations in regolith materials. The analyses of major oxides and trace elements for regolith samples in KP003, KP008, KP009 and SP003 to determine residual regolith as well as to assess the compositional variations of the regolith materials were listed in Table 7.8. The behaviours of elements from surface regolith down to the saprolite are shown in Figs. 7.7-7.10. The compositional variability of the regolith materials was also determined by Mg/Al versus K/Al and is presented in Fig. 7.11. Table 7.9 shows averages of major element for different regolith domain units analysed by XRF technique.

Table 7.8 Major element (%) and trace element (ppm) XRF data of regolith samples from pits KP003, KP008, KP009 and SP003

Regolith	Gravel	Ferricrete	Saprolite	Gravel	Ferricrete	Clay	Pisolithic soil	Ferricrete	Saprolite	Gravel	Ferricrete	Indurated sediment	
Depth (m)	**0.8**	**1.5**	**2.0**	**0.7**	**1.1**	**1.5**	**0.4**	**1.5**	**2.4**	**0.5**	**0.8**	**1.5**	**Detection limit**
Sample	**813510**	**813512**	**813513**	**813531**	**813532**	**813533**	**813536**	**813537**	**813538**	**814072**	**814073**	**814074**	
Pit No.		**KP003**			**KP008**			**KP009**			**SP003**		
Major oxides													
SiO2	65.55	60.20	58.52	71.55	62.81	59.40	71.15	61.25	54.81	75.31	49.24	50.75	0.01
TiO2	0.92	0.96	0.87	0.86	0.87	0.73	0.84	0.87	0.97	0.92	0.80	0.93	0.01
Al2O3	17.96	21.49	22.35	14.30	19.06	20.10	14.26	20.34	26.12	8.27	21.37	26.19	0.01
Fe2O3	6.22	6.80	7.98	4.65	6.96	7.57	3.96	7.64	7.19	8.61	18.22	11.13	0.01
MnO	0.14	0.09	0.07	0.02	1.03	0.05	0.04	0.03	0.02	0.06	0.03	0.02	0.01
MgO	0.41	0.48	0.70	0.64	0.81	2.12	0.45	0.48	0.41	0.19	0.18	0.16	0.01
CaO	0.03	0.01	0.03	0.03	0.02	0.14	0.19	0.00	0.00	0.09	0.00	0.00	0.01
Na2O	0.05	0.05	0.06	0.10	0.06	0.04	0.05	0.03	0.02	0.06	0.00	0.00	0.01
K2O	1.72	2.20	2.21	1.74	2.01	2.39	1.63	1.93	1.88	0.43	0.20	0.18	0.01
P2O5	0.04	0.02	0.03	0.03	0.02	0.01	0.06	0.04	0.05	0.09	0.12	0.10	0.01
SO3	0.01	0.01	0.01	0.01	0.01	0.01	0.02	0.00	0.01	0.01	0.01	0.00	x
Ti (%)	0.55	0.58	0.52	0.52	0.52	0.44	0.50	0.52	0.58	0.55	0.48	0.56	
Mg/Al	0.03	0.03	0.04	0.05	0.05	0.12	0.04	0.03	0.02	0.03	0.01	0.01	
K/Al	0.15	0.16	0.15	0.19	0.17	0.19	0.18	0.15	0.11	0.08	0.01	0.01	
SiO2/ Al2O3	3.65	2.80	2.62	5.00	3.30	2.96	4.99	3.01	2.10	9.11	2.30	1.94	
LOI	6.67	7.16	7.38	6.03	7.16	7.37	7.21	7.29	8.96	5.54	9.01	10.39	
Total	99.71	99.46	100.21	99.96	99.83	99.93	99.87	99.90	100.39	99.57	99.18	99.85	
Trace element													
Nb	11.50	11.80	10.10	9.60	10.50	7.20	9.00	10.40	8.10	14.10	15.70	18.40	2
Zr	314.9	252.8	217.9	411.1	337.2	186.2	370.5	325.0	298.1	691.1	466.3	395.5	2
Th	5.10	4.90	5.30	5.00	5.80	4.20	4.70	5.90	4.80	7.20	10.70	10.80	1
U	1.90	1.70	2.00	2.10	2.20	1.40	2.10	2.20	1.60	2.70	3.80	2.80	0.2
Sc	19.80	23.30	23.70	14.80	18.60	18.90	13.80	17.00	20.40	22.80	6.90	17.80	1
Y	23.60	21.90	25.10	21.30	22.40	26.10	19.00	20.70	22.90	18.30	13.00	12.80	1
Ti/Zr	0.00	0.00	0.00	0.00	0.00	0.00	0.00	0.00	0.00	0.00	0.00	0.00	
Nb/Zr	0.04	0.05	0.05	0.02	0.03	0.04	0.02	0.03	0.03	0.02	0.03	0.05	
Nb/Y	0.49	0.54	0.40	0.45	0.47	0.28	0.47	0.50	0.35	0.77	1.21	1.44	
Nb/Ti	20.9	20.5	19.4	18.6	20.1	16.5	17.9	19.9	13.9	25.6	32.7	33.0	
Zr/Y	13.34	11.54	8.68	19.30	15.05	7.13	19.50	15.70	13.02	37.77	35.87	30.90	

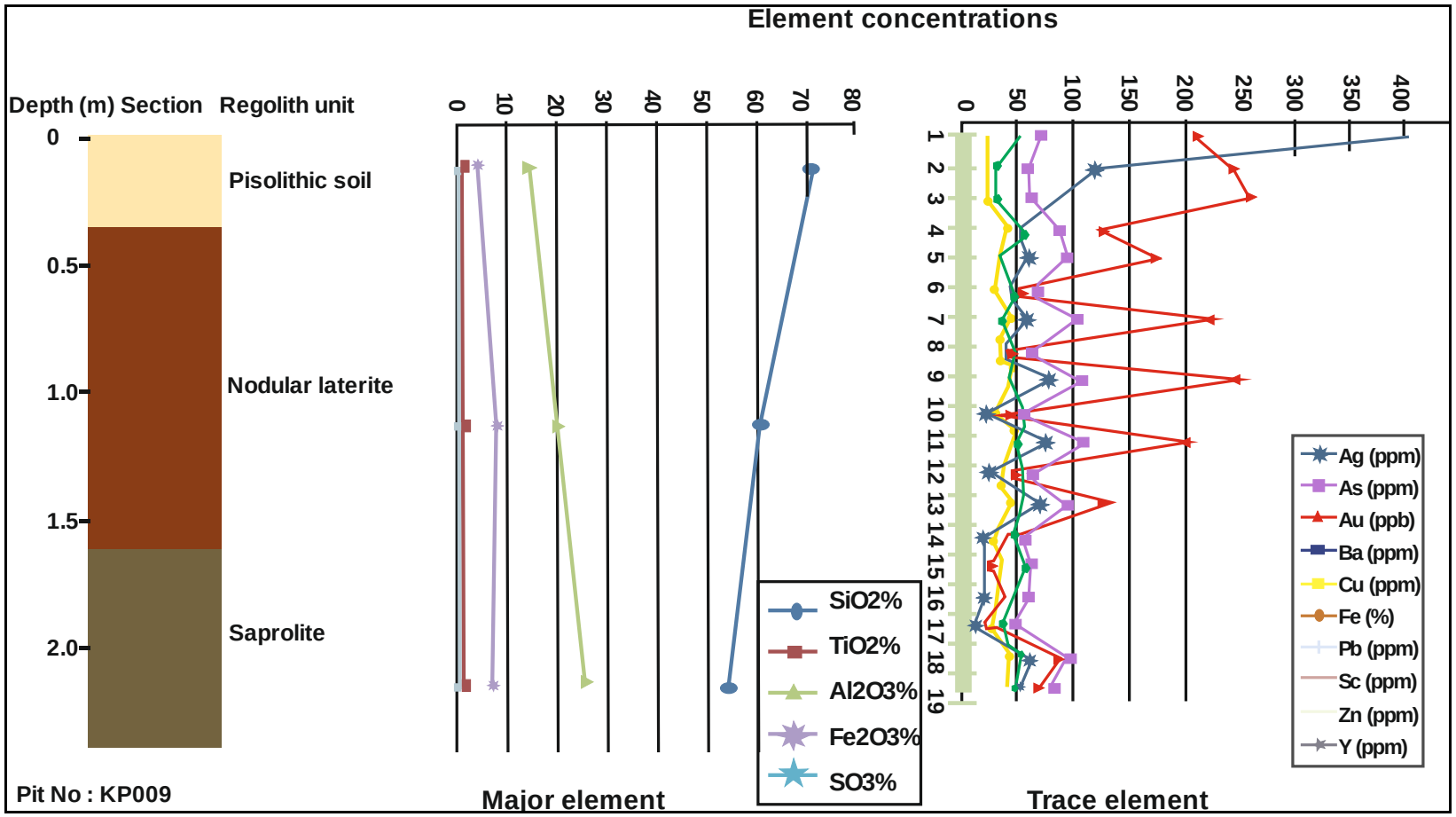

Fig. 7.7 Distribution and geochemical patterns of Au (FA-AAS) and selected major and trace elements analysed (XRF) for pit KP009 in ferruginous regime at Kunche-Bekpong.

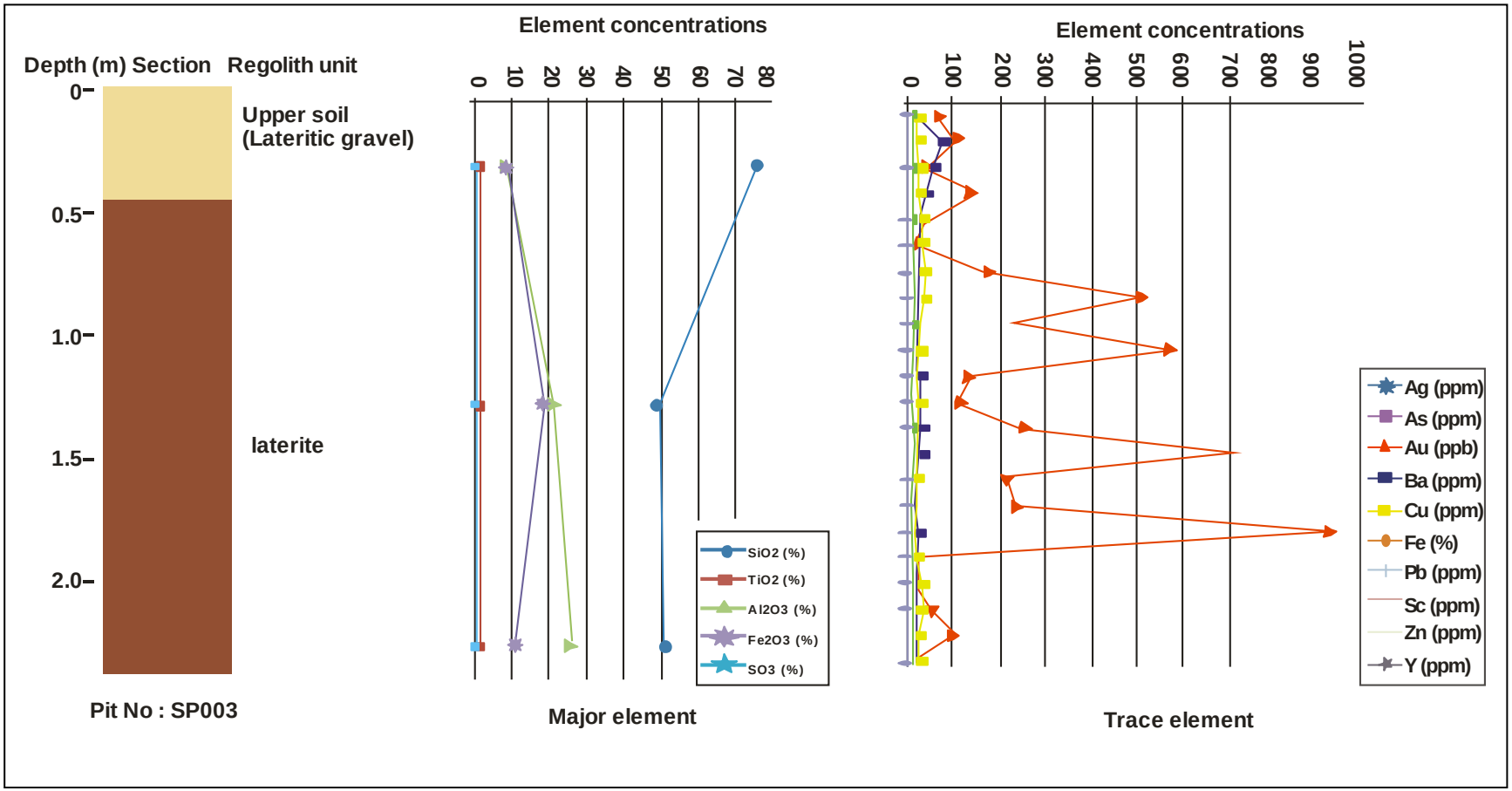

Fig. 7.8 Distributions of geochemical patterns of Au (FA-AAS) and selected major and trace elements analysed (XRF) for pit KP009 in ferruginous regime at Sabala.

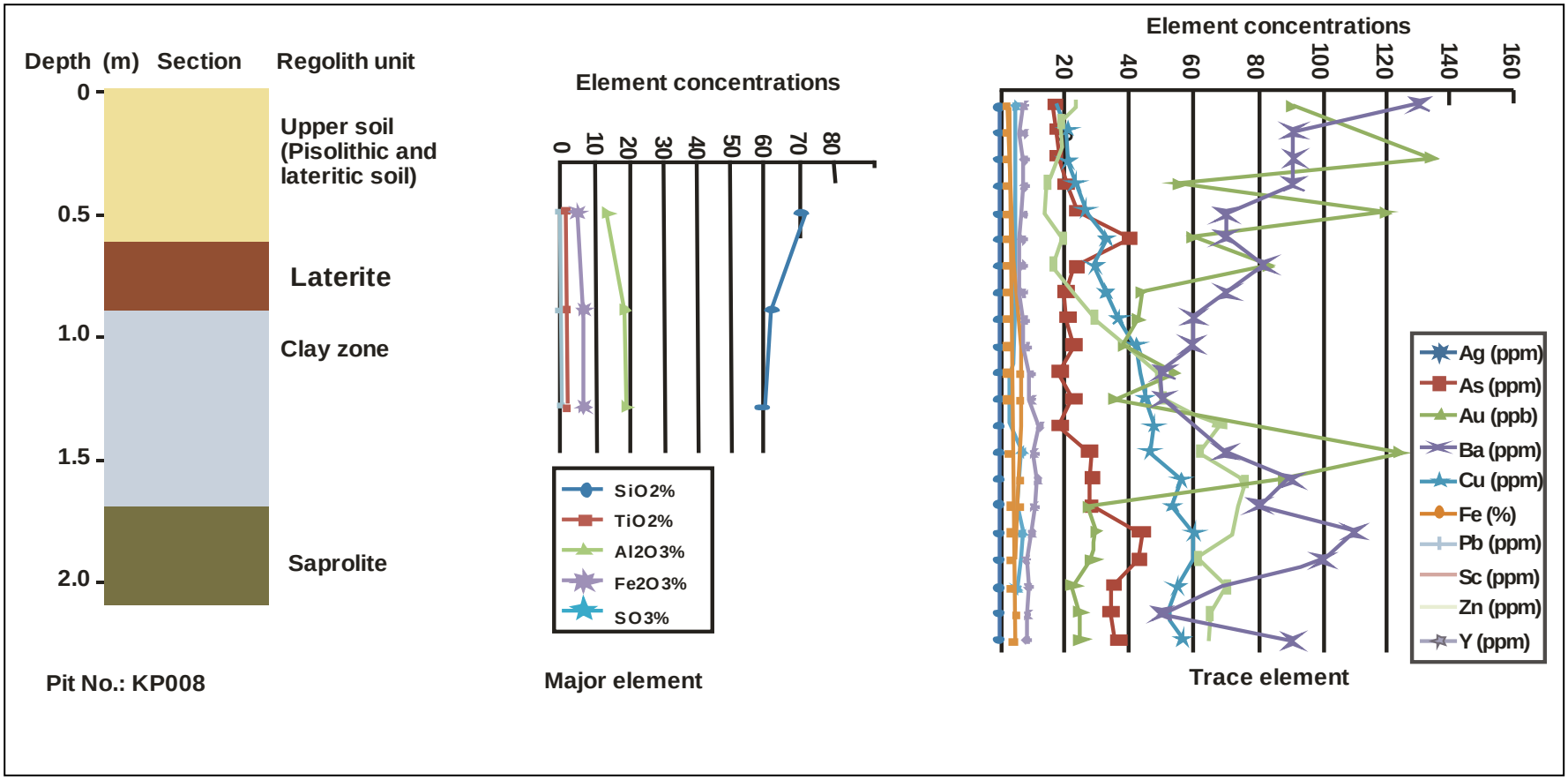

Fig. 7.9 Distributions and geochemical patterns of Au (FA-AAS) and selected major and trace elements analysed (XRF) for pit KP008 in ferruginous regime at Kunche-Bekpong.

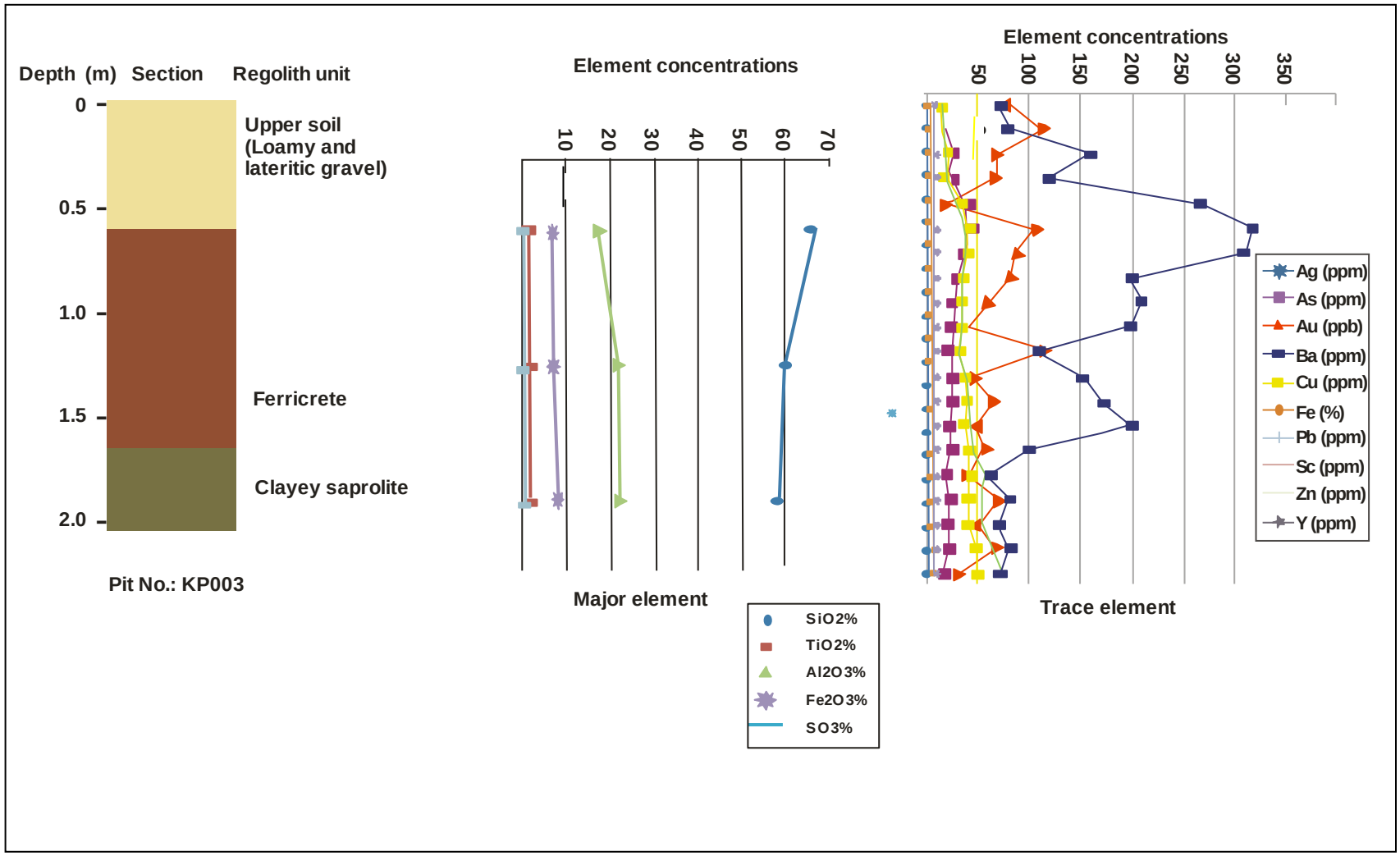

Fig. 7.10 Distributions and geochemical patterns of Au (FA-AAS) and selected major and trace elements analysed (XRF) for pit KP003 in ferruginous regime at Kunche-Bekpong.

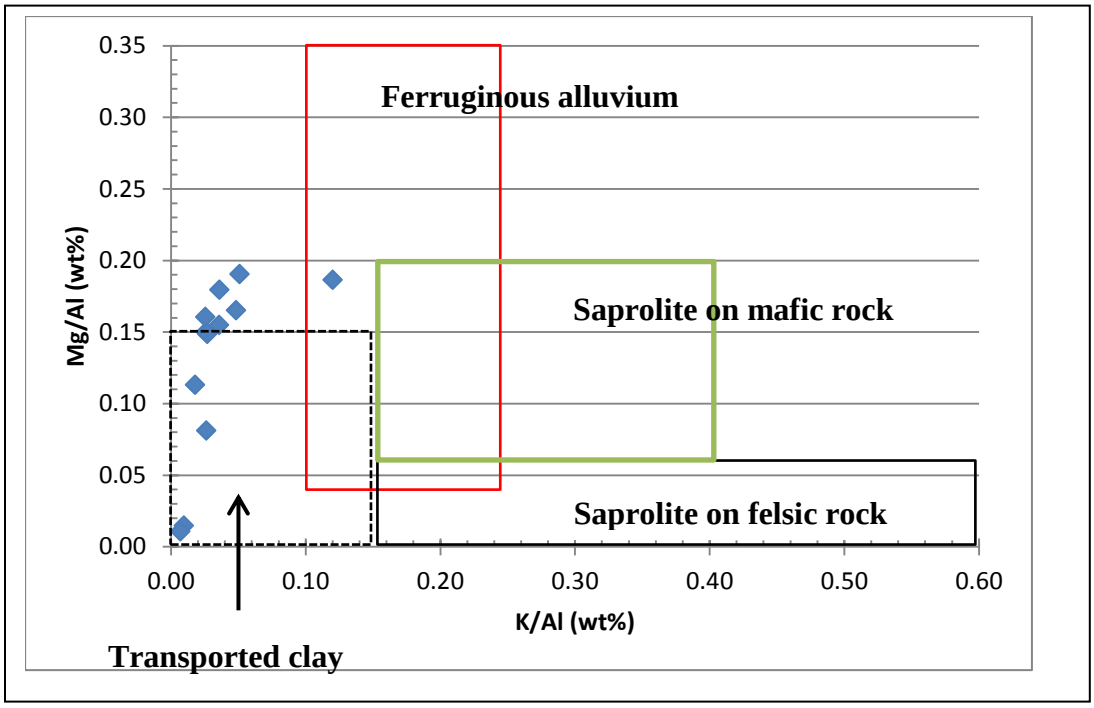

Fig. 7.11 Compositional variability of regolith in terms of metal wt. % of Mg/Al versus K/Al. Rectangles show different classes of regolith materials (after McQueen, 2006).

Table 7.9 Summary of major element results and averages for different regolith domain units

SampID	Regolith	Depth (m)	SiO_2	TiO_2	Al_2O_3	Fe_2O_3	MnO	MgO	CaO	Na_2O	K_2O	P_2O_5	SO_3	LOI	Total
813510	Lateritic gravel	0.5-0.7	65.6	0.9	18	6	0.1	0.4	0.0	0.1	1.7	0.0	0.0	7	99.7
813531		0.5-0.8	71.6	0.9	14	5	0.0	0.6	0.1	0.1	1.7	0.0	0.0	6	100.0
814072		0.0-0.4	75.3	0.9	8	9	0.1	0.2	0.1	0.1	0.4	0.1	0.0	5	100.0
Average			**70.8**	**0.9**	**13**	**6**	**0.1**	**0.4**	**0.1**	**0.1**	**1.3**	**0.1**	**0.0**	**6**	
813512	Ferricrete	1.2-1.7	60.2	1.0	21	7	0.1	0.5	0.0	0.1	2.2	0.0	0.0	7	99.5
813532		0.7-1.0	62.8	0.9	19.	7	0.0	0.8	0.0	0.1	2.0	0.0	0.0	7	100.0
813537		0.3-1.6	61.3	0.9	20.	8	0.0	0.5	0.0	0.0	1.9	0.0.	0.0	7	100.0
814073		0.4-0.8	49.2	0.8	23	18	0.0	0.2	0.0	0.0	0.2	0.1	0.0	9	99.2
814074		0.8-3.3	50.8	0.9	26	11	0.0	0.2	0.0	0.0	0.2	0.1	0.0	10	100.0
Average			**56.9**	**0.9**	**22**	**10**	**0.0**	**0.4**	**0.0**	**0.0**	**1.3**	**0.1**	**0.0**	**8**	
813513	Saprolite	1.7-2.0	58.5	0.9	22	8	0.1	0.7	0.0	0.1	2.3	0.0	0.0	7	100.0
813538		1.6-2.4	54.8	1.0	26	7	0.0	0.4	0.0	0.0	1.9	0.1	0.0	9	100.0
Average			**56.5**	**0.9**	**24**	**8**	**0.0**	**0.6**	**0.0**	**0.0**	**2.0**	**0.0**	**0.0**	**8**	100.0
813533	Clay zone	1.0-1.3	59.4	0.7	20	8	0.1	2.1	0.1	0.0	2.4	0.0	0.0	**7**	100.0
813536	Pisolithic soil	0.0-0.3	71.2	0.8	14	4	0.0	0.4	0.2	0.1	1.6	0.1		**7**	

7.3.4 Data analysis

Reports of many Au discoveries in complex regolith of Australia (Anand, 2001; Anand et al., 1993; Butt and Zeegers, 1992) indicate good associations of Au and chalcophile elements. These associations have helped in detecting hidden Au anomalies in areas under cover. In the Birimian of southern Ghana, Au exploration is conducted through the application of pathfinder elements (Griffis et al., 2002; Dzigbodi-Adjimah, 1993 and Kesse, 1985). Adopting a similar technique to determine the associated elements to define pathfinder elements for Au exploration in the Birimian of northern Ghana may be useful in the identification of the concealed mineralisation. The regolith geochemical data was used to determine the behaviour of major and trace elements in regolith profiles. Also the identification of sample compositional variability was applied to the geochemical data to distinguish the different anomaly types.

7.3.4.1 Regolith geochemistry in the determination of different regolith horizons

Regolith geochemistry data obtained from the excavated pits in the different regolith domains provided some regolith profile information that might be used to map the regolith horizon contacts. Contrasts in Fe/S ratio values plotted with depth approximately relate to the limits of the different regolith horizons. Some of the plots of Fe/S ratios from the surface regolith to the saprolite in the study areas are shown in Figs. 7.12 (A, B) and 7.13 (A, B).

A.

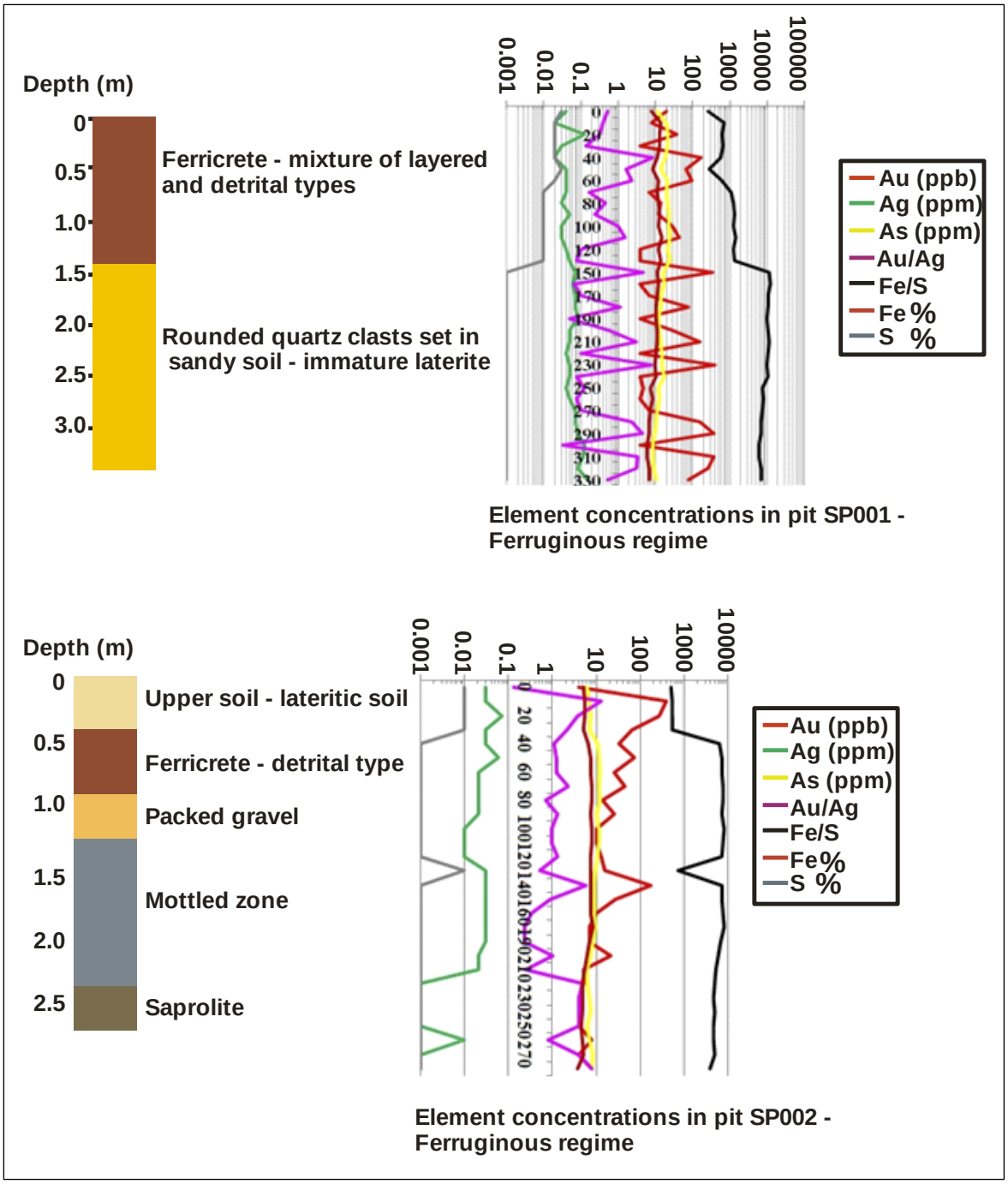

Fig. 7.12 (A, B) Regolith geochemical data plot showing variations in elements in the regolith profile from upper soils to the saprolite in ferruginous regolith. B is on the next page.

B.

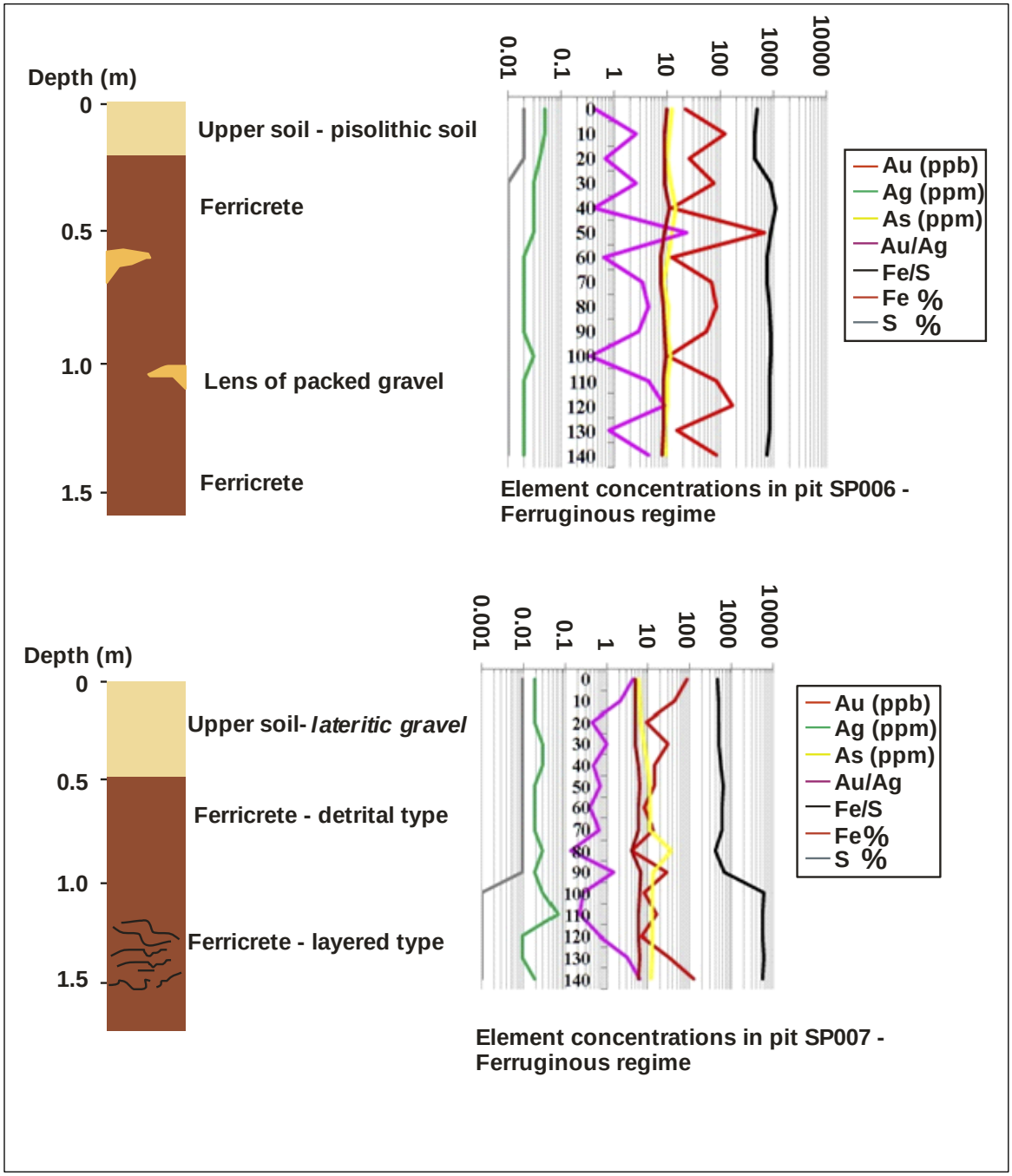
Depth (m)
0
0.5
1.0
1.5
Upper soil - pisolithic soil
Ferricrete
Lens of packed gravel
Ferricrete
0.01
0.1
1
10
100
1000
10000
Au (ppb)
Ag (ppm)
As (ppm)
Au/Ag
Fe/S
Fe %
S %
Element concentrations in pit SP006 - Ferruginous regime
Depth (m)
0
0.5
1.0
1.5
Upper soil- lateritic gravel
Ferricrete - detrital type
Ferricrete - layered type
0.001
0.01
0.1
1
10
100
1000
10000
Au (ppb)
Ag (ppm)
As (ppm)
Au/Ag
Fe/S
Fe%
S %
Element concentrations in pit SP007 - Ferruginous regime

A.

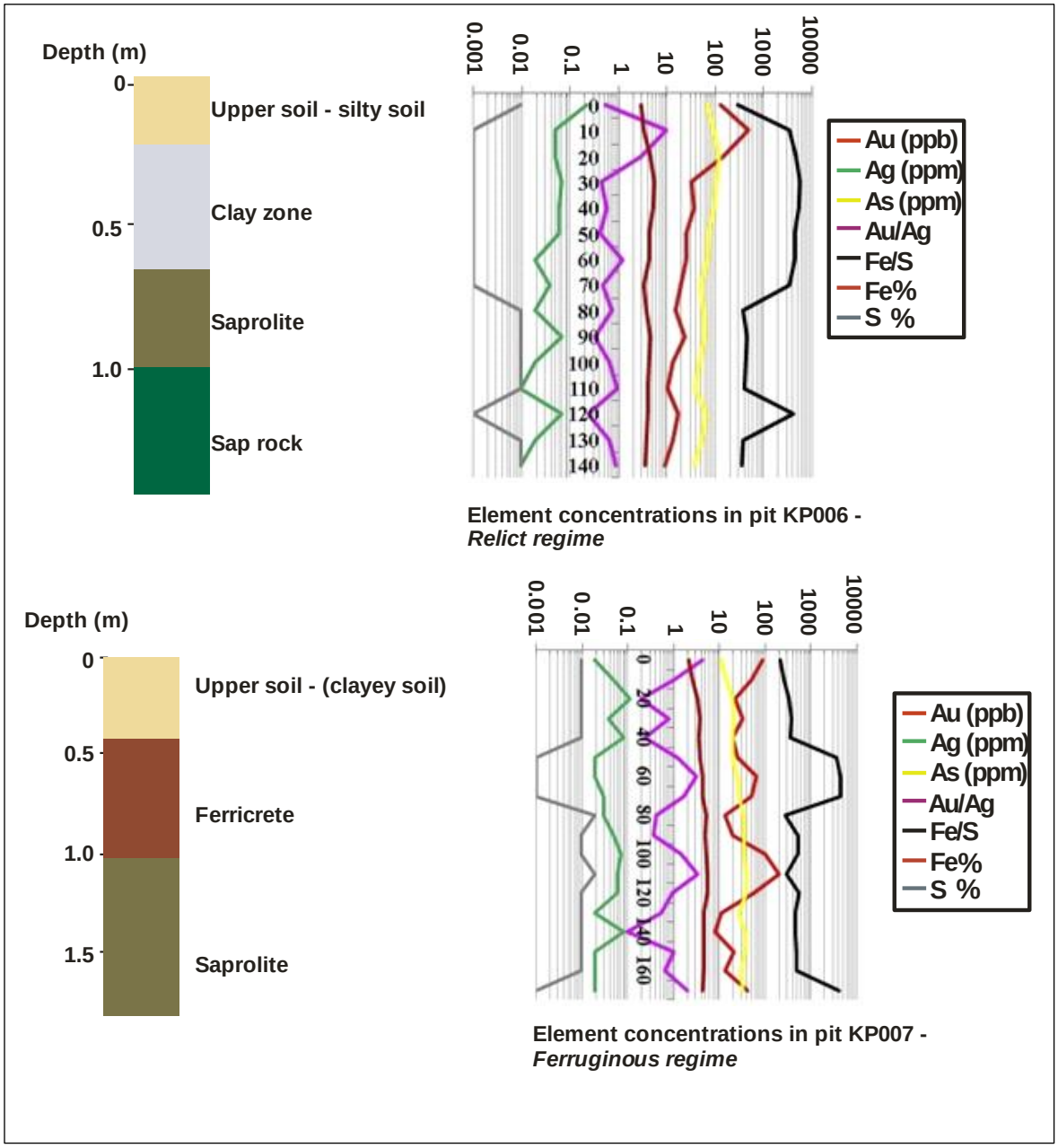

Fig. 7.13 (A, B) Regolith geochemical data plot showing variations in elements in the regolith profile from upper soils to the saprolite in ferruginous and modified erosional/transported regolith regimes. B is on the next page

B.

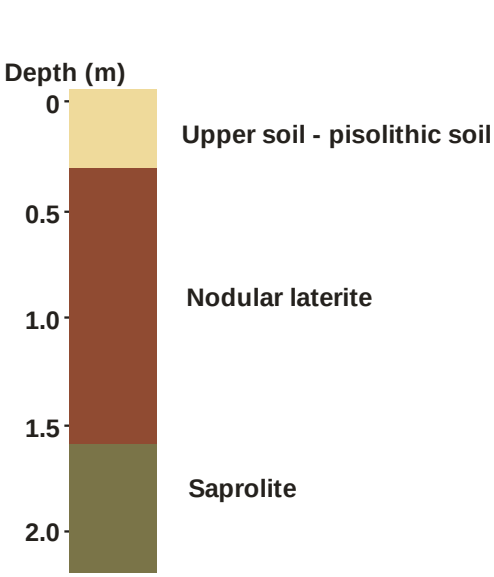

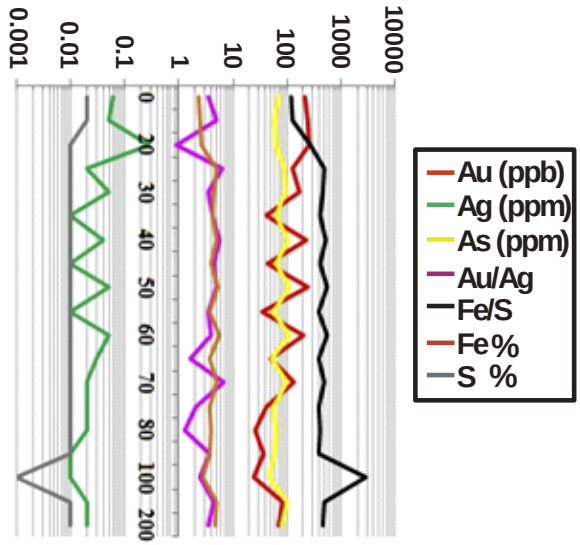

Element concentrations in pit KP009 - *Ferruginous regime*

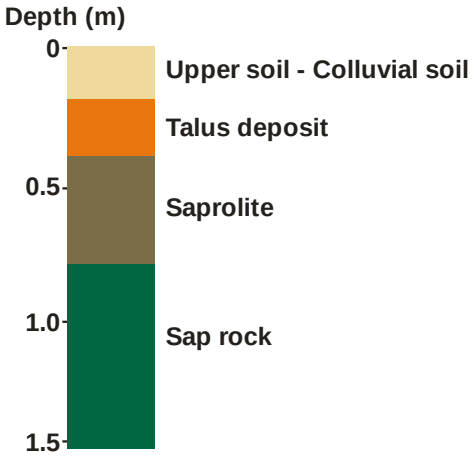

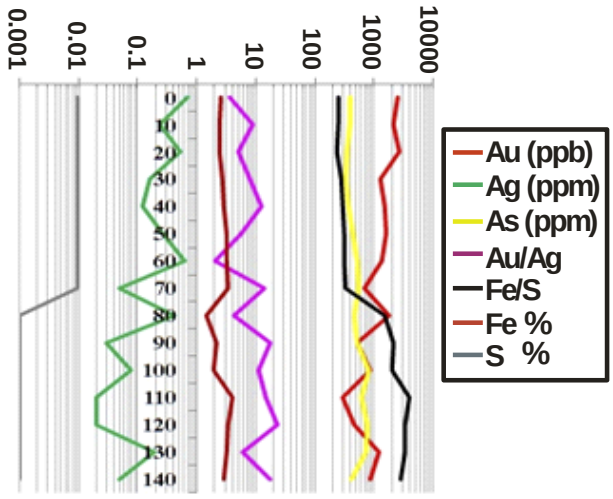

Element concentrations in pit KP010 - *Modified erosional regime*

7.3.4.2 Au, Ag and As distribution through the regolith

In the regolith there is a poor correlation of Ag with Au and no correlation of As with Au. The Au-Ag correlation seems to be controlled by the Au content. The high Au areas with assays >1 ppm show relatively good correlation between Au and Ag but the two elements appear uncorrelated at low concentration Au areas below 1 ppm Au. Arsenic on the other hand shows no correlation with Au. The relationship between As and Ag with Au is illustrated in Fig. 7.14 where the overall geochemical data collected in the study have been plotted. The poor correlations of As or Ag with Au may be due to the different processes dispersing and concentrating elements, scavenging the elements during lateritization and diluting or enhancing elements during intermixing of transported sediments from diverse sources with in situ regolith materials. As presented in chapter 3, section 3.5.1; the weak concentration of As in the surface regolith samples are due to the precipitation of Fe-oxyhydroxides which scavenge As^{3+} and As^{5+} at natural pH. However there is relative higher As concentrations in bedrock samples analysed by Azumah Resources Ltd. (Waller et al., 2012). The commonly observed increase in solubility of As under reducing conditions can be attributed primarily to the reductive dissolution of Fe^{3+}-oxide phases and the subsequent release of adsorbed As (Smedley and Kinniburgh, 2002; Oremland and Stolz, 2003). This implies the use of arsenic, as a pathfinder element for Au anomaly delineation in the surface regolith may be inappropriate in regolith environments characterised by widespread laterite cover.

Additionally, the relationship of these elements in terms of residual concentration can be influenced by the repeated weathering, differential erosion, re-deposition of eroded sediments and the different geochemical processes acting on them. As noted by Scott and Pain (2008) elements can be mobile or immobile depending on the environmental conditions. In the study of Zeegers and Lecomte (1992) of exploration in areas of low to moderate relief in the savannah regions, they noted strong leaching of trace elements particularly Cu, Zn, Cd and Ag in the regolith whilst some trace elements are retained or relatively concentrated in Fe-rich zones. Arsenic was identified to be among the retained elements in Fe-rich zones in the regolith. Au generally is considered immobile but is dispersed in the regolith after forming a complex or is transported as detrital grains by the

surface processes. These three elements behave differently in different weathering regimes (Scott and Pain, 2008) so to understand their relationship their behaviour in the different pits along a transect lines were examined (Figs 7.15–7.17).

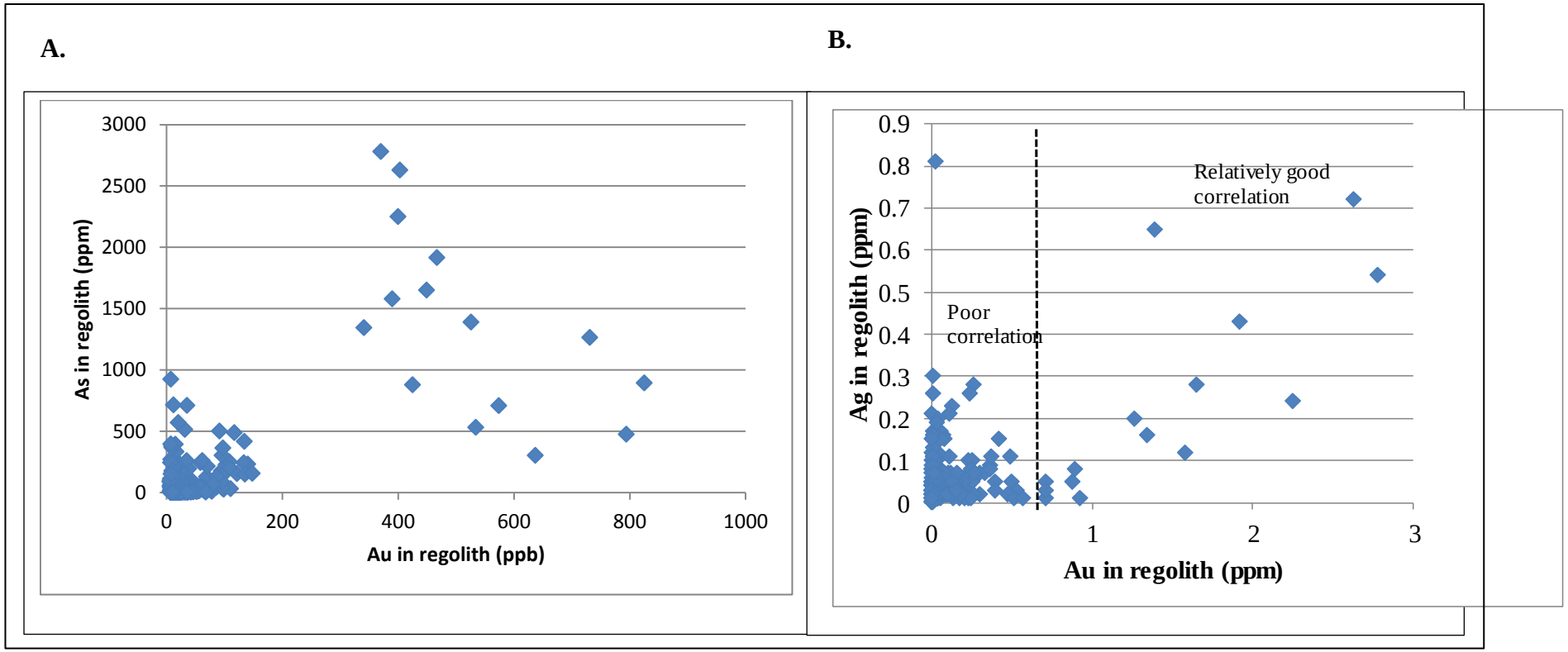

Fig. 7.14 Relationship between As and Ag with Au in the regolith profile. These plots disregard the regolith domain type.

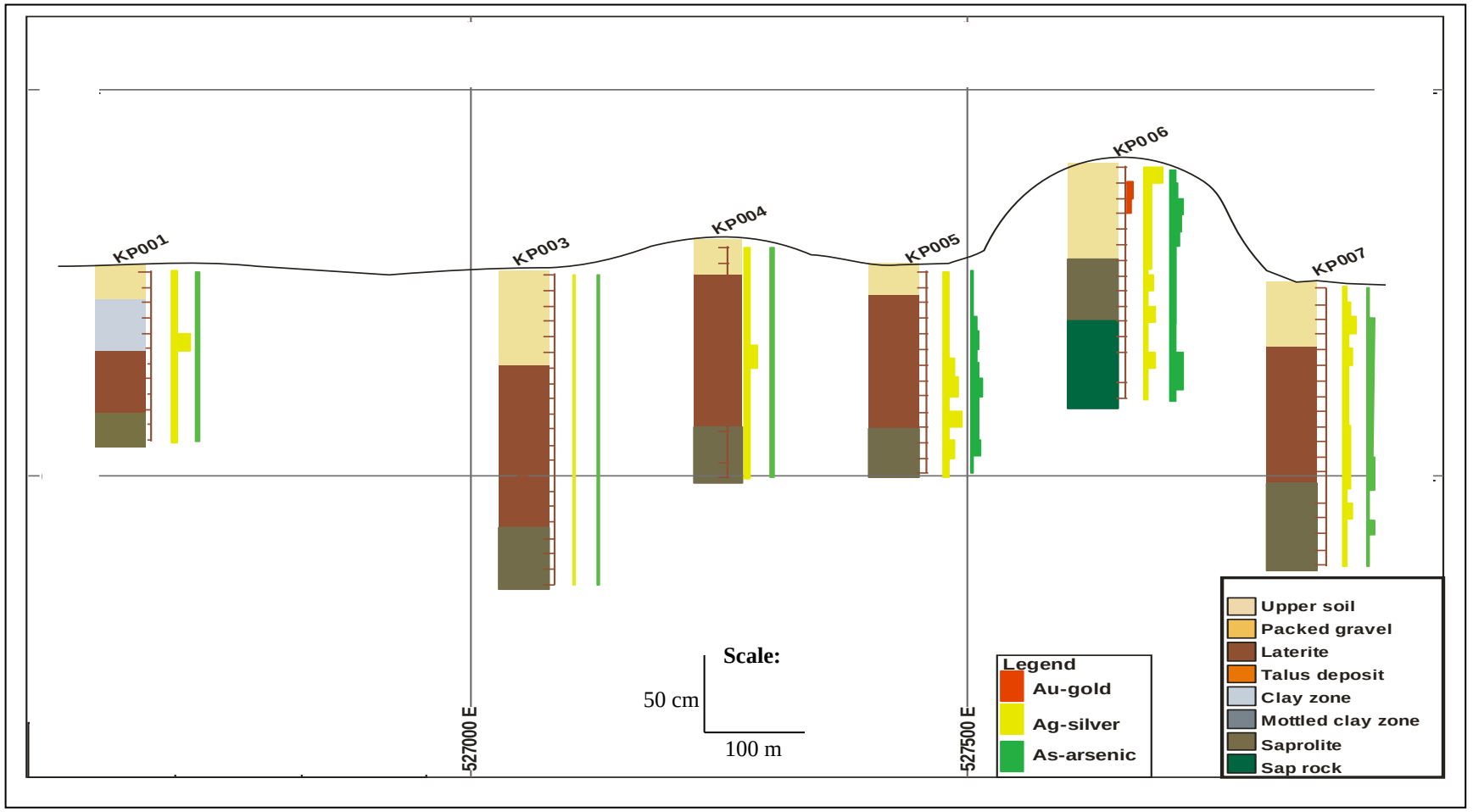

Fig. 7.15 Relationship between Au, Ag and As along L1149550N in Kunche-Bekpong regolith: plot displays geochemical element patterns in the regolith profiles.

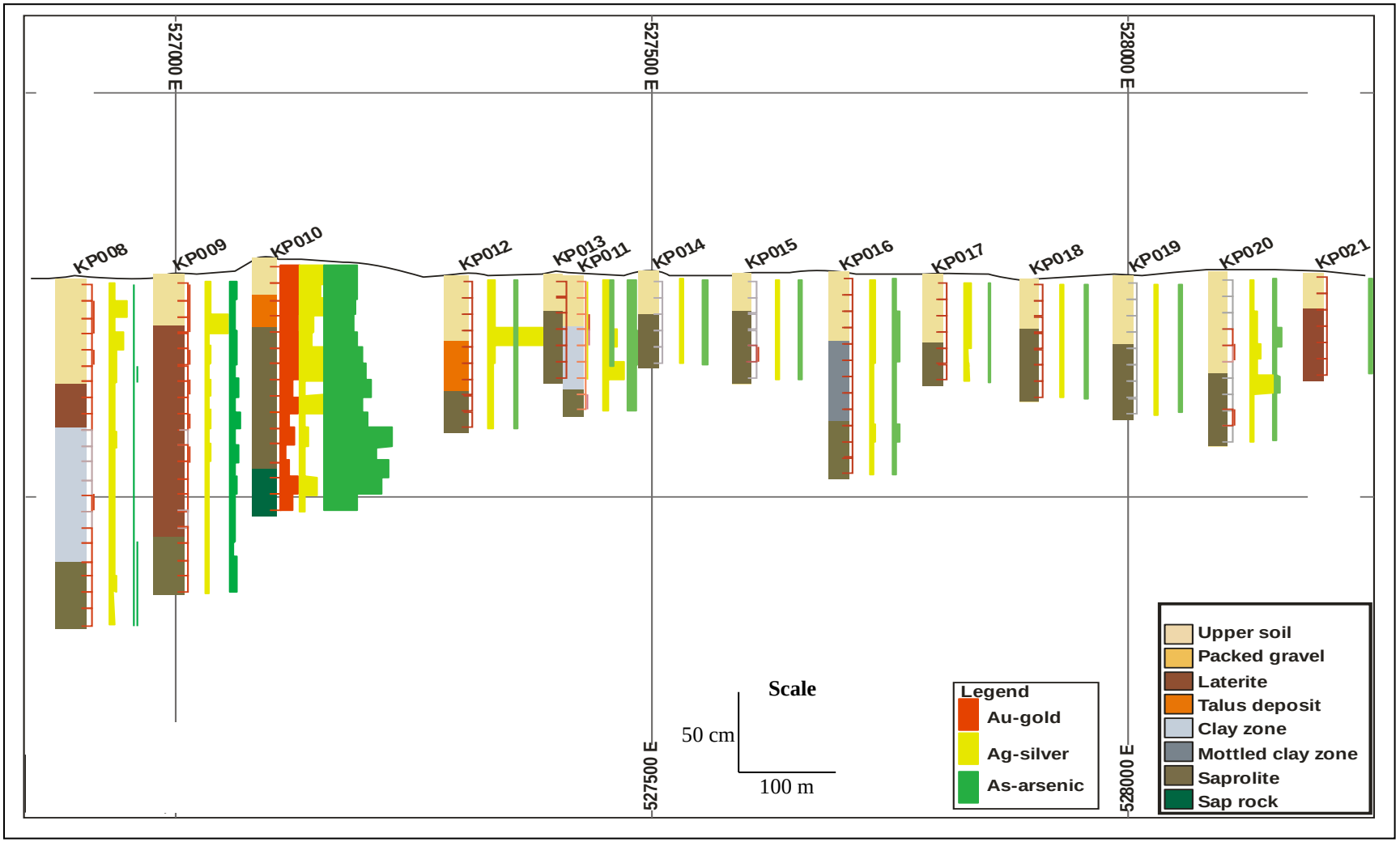

Fig. 7.16 Relationship between Au, Ag and As along L1148600N in Kunche-Bekpong regolith: plot displays geochemical element patterns in the regolith profiles. High As correlates well with relatively high Au in KP010.

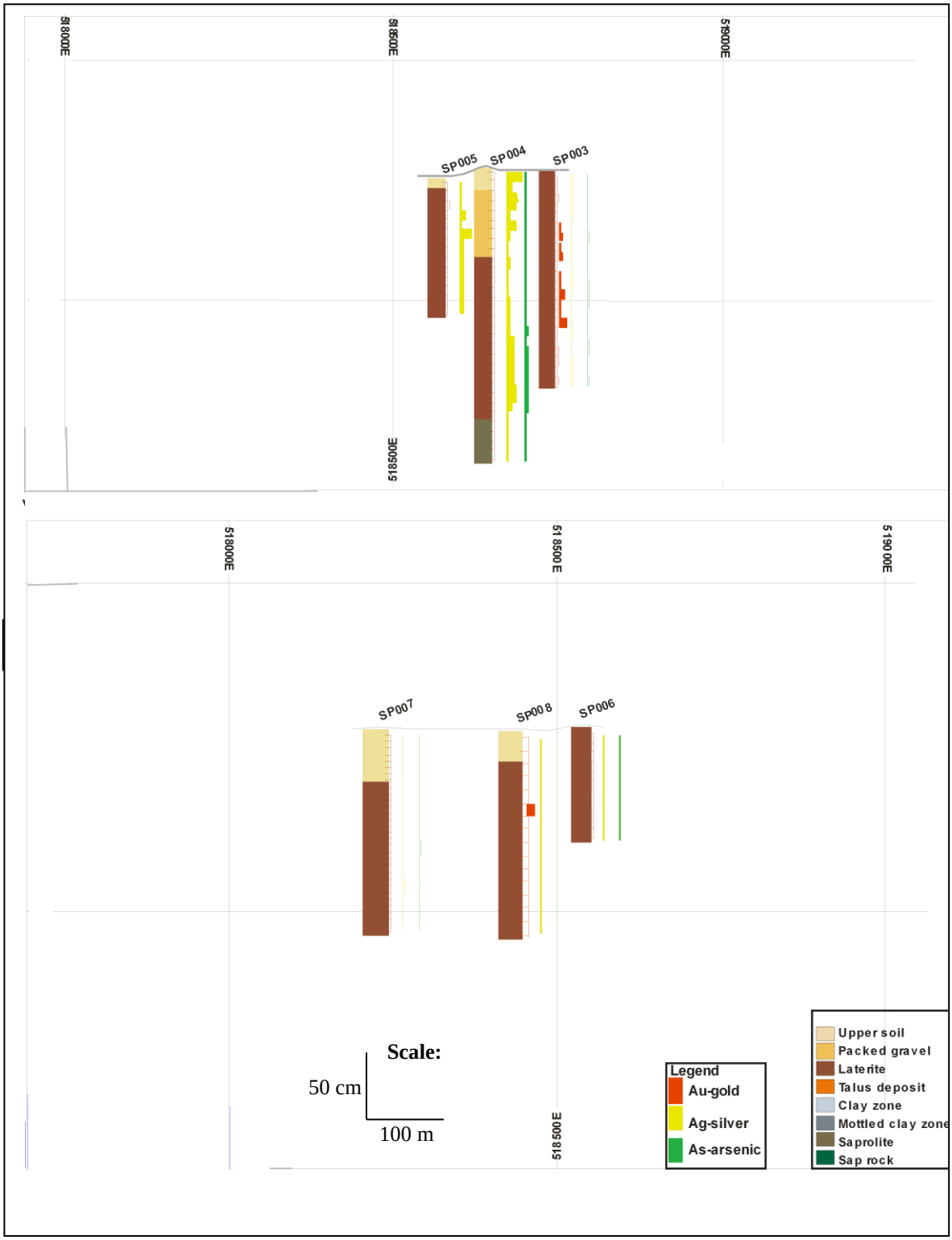

Fig. 7.17 Relationship between Au, Ag and As in Sabala regolith: plot displays geochemical element patterns in the regolith profiles.

7.3.5 Pit by pit interpretation of element mobility in regolith

Mobility of elements in the regolith at Kunche-Bekpong and Sabala are presented with considerations to the following:

- Spatial variability of selected elements (Au, As, Ag, Cu, Pb, Zn, Ba etc.) in different regolith domains,
- Processes and transport mechanisms of selected elements from the underlying mineralised body to the ground surface.

Plots of the selected elements down the regolith profiles are shown in Figs. 7.17–7.21. Element concentrations on the charts show maximum assays and bottom of each chart is zero.

7.3.5.1 Ferruginous regime

The ferruginous regime consists of residual laterite (duricrust) and transported laterite (ferricrete). Pits dug at areas characterized by residual laterite include KP015 – KP021, SP002 – SP004 and SP007 and those excavated at transported laterite environments include KP008 - KP009 and SP001, SP005, SP006 and SP008. Some of the Au and other element dispersions in the pits in this regime–type are presented in Figs. 7.18–7.20.

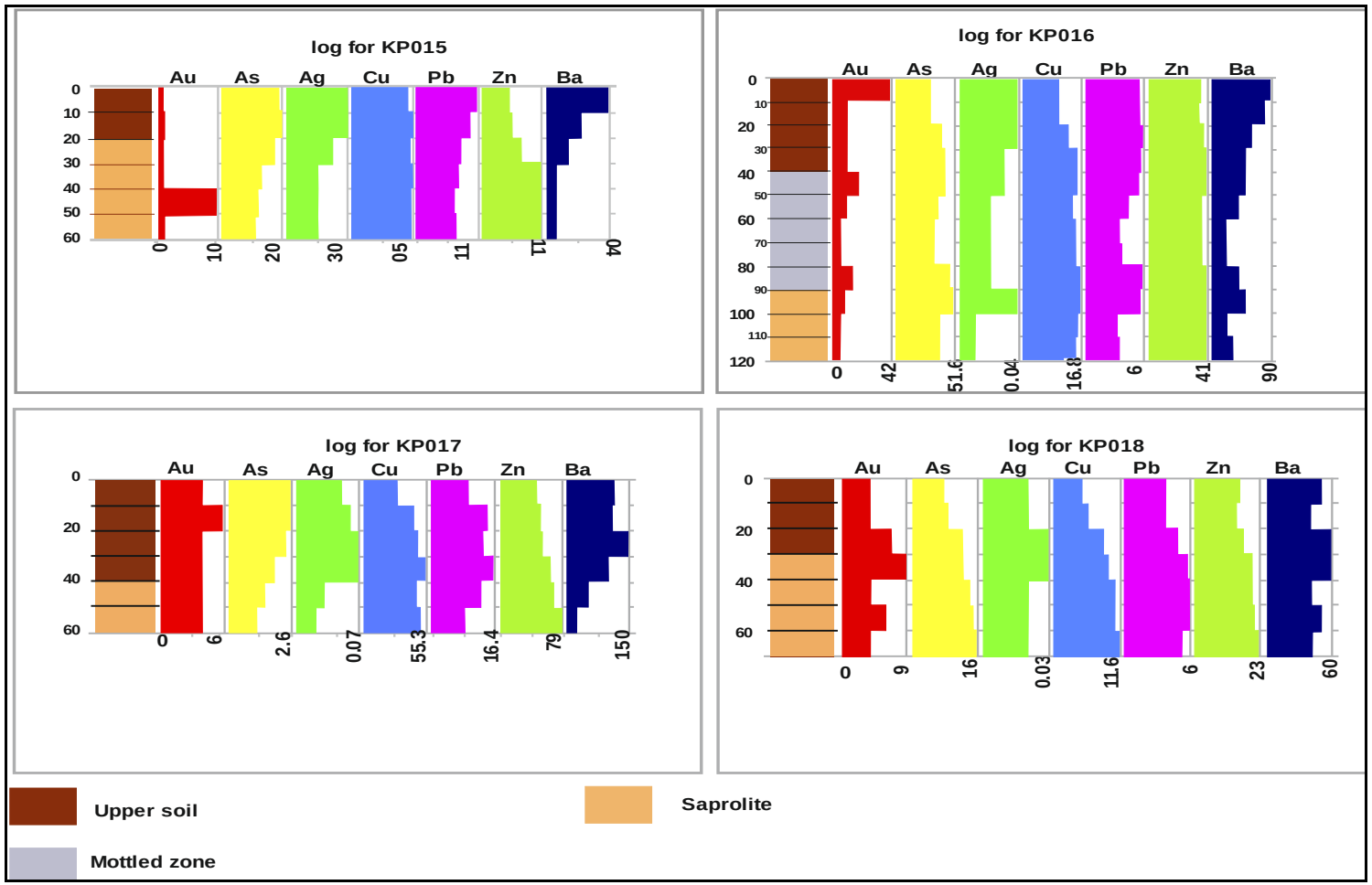

Fig. 7.18 Concentrations of selected elements (ppm) except Au (ppb) with depth (cm) in residual laterite at Kunche-Bekpong area.

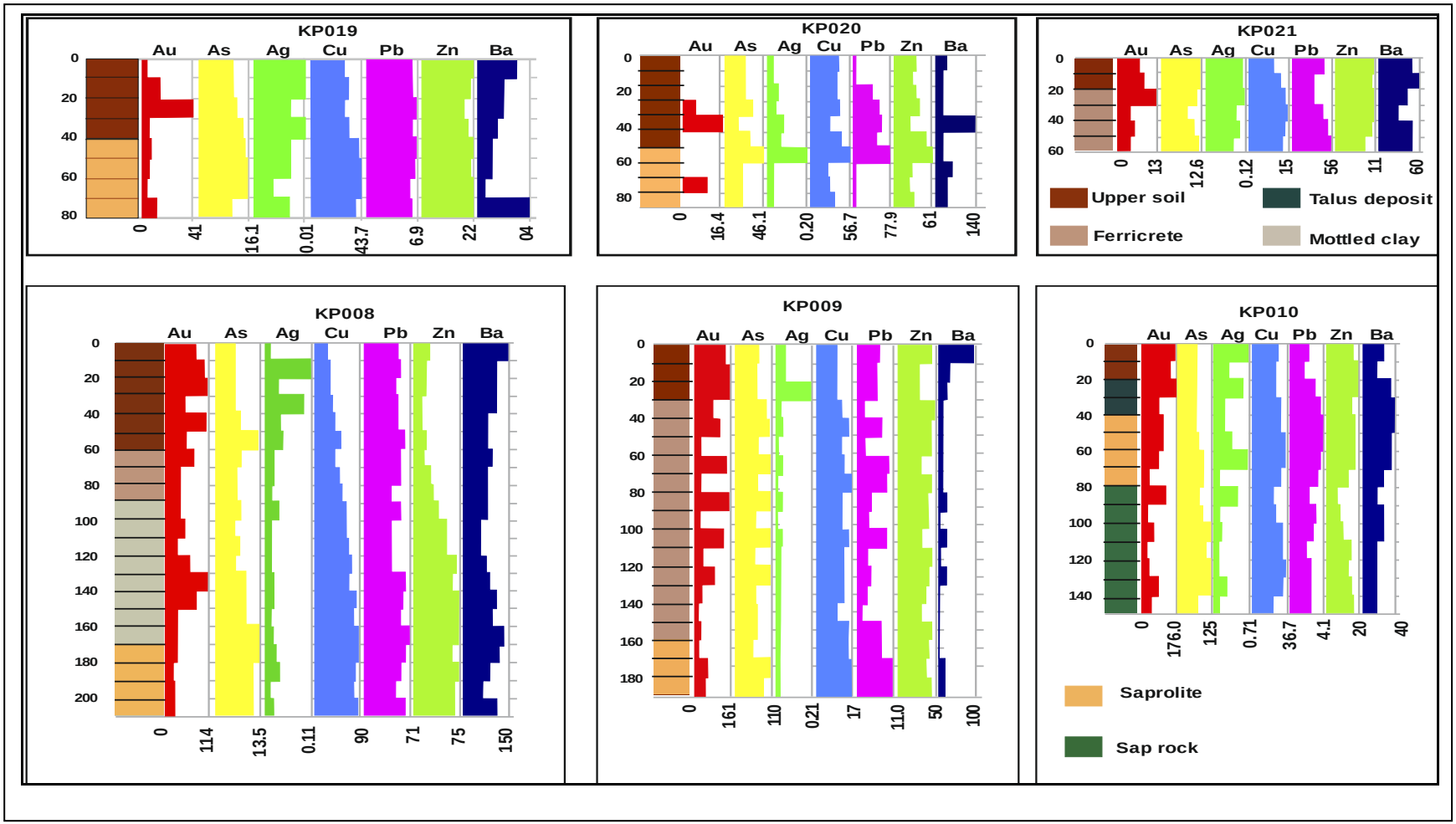

Fig. 7.19 Concentrations of selected elements (ppm) except Au (ppb) with depth (cm) in ferruginous regime at Kunche-Bekpong area.

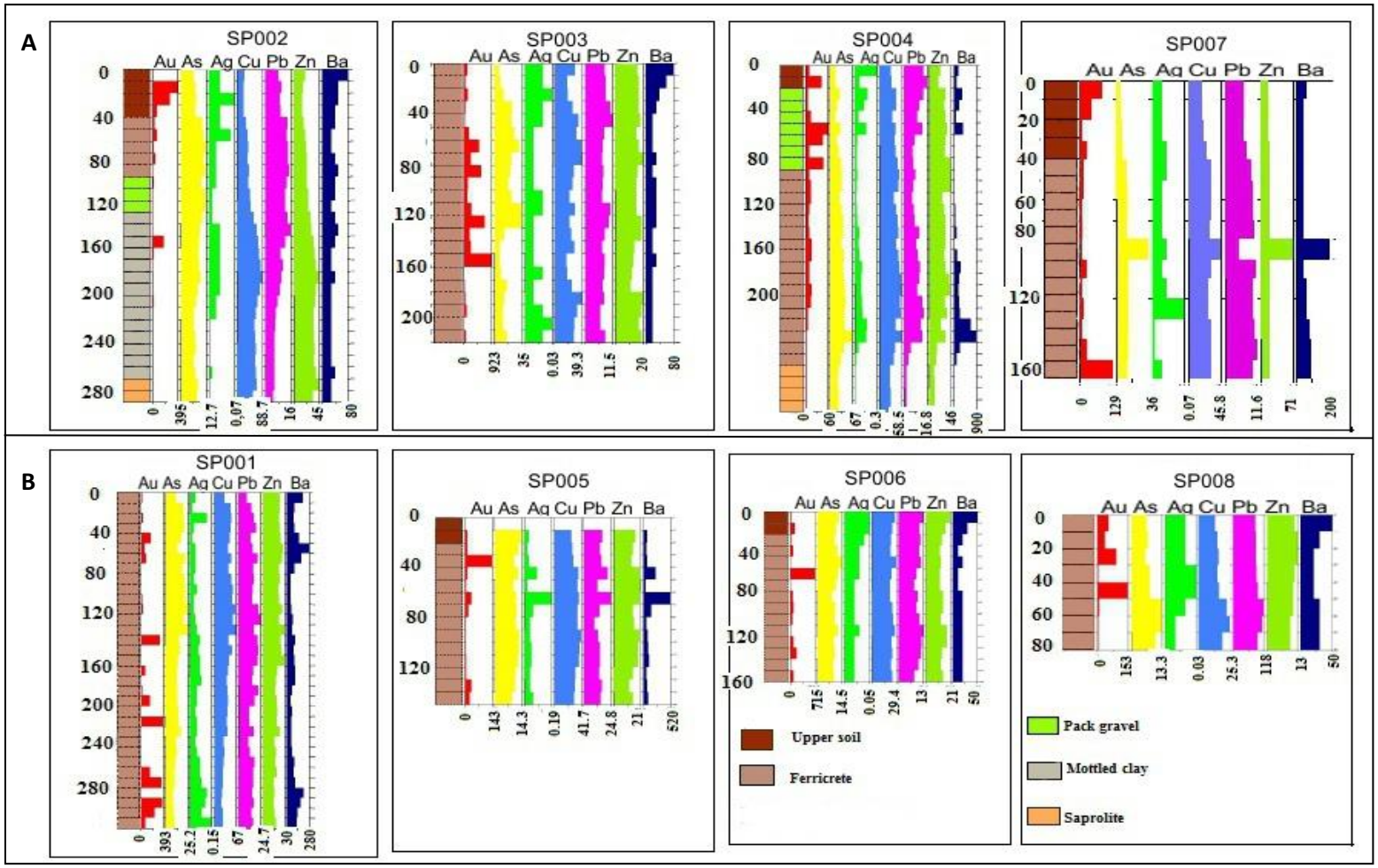

Fig. 7.20 Concentrations of selected elements (ppm) except Au (ppb) with depth (cm) at Sabala: A) pits in residual laterites and B) pits in transported laterites.

7.3.5.2 Relict regime

This regime is made up of in situ and moderately transported surface regolith materials developed as a result of weathering of the underlying parent rocks. Generally the surface regolith are in place but there are some locations where evidence of sub angular rock fragments and quartz clasts formed the top regolith layer. Where the rock fragments have similar internal fabrics like the underlying bedrock they were considered to have been derived from the underlying bedrock and considered as part of the same regime (section 6.1.3.2) but with some proximal transport. Degree of transportation of these regolith units were ascertained to be part of the relict regime by examining the amount of relict fabric of the parent material preserved in the surface regolith as well as the shapes of the rock fragments (Section 6.1.3.2). Concentrations of selected elements assay results obtained in this regime are shown in Fig. 7.21.

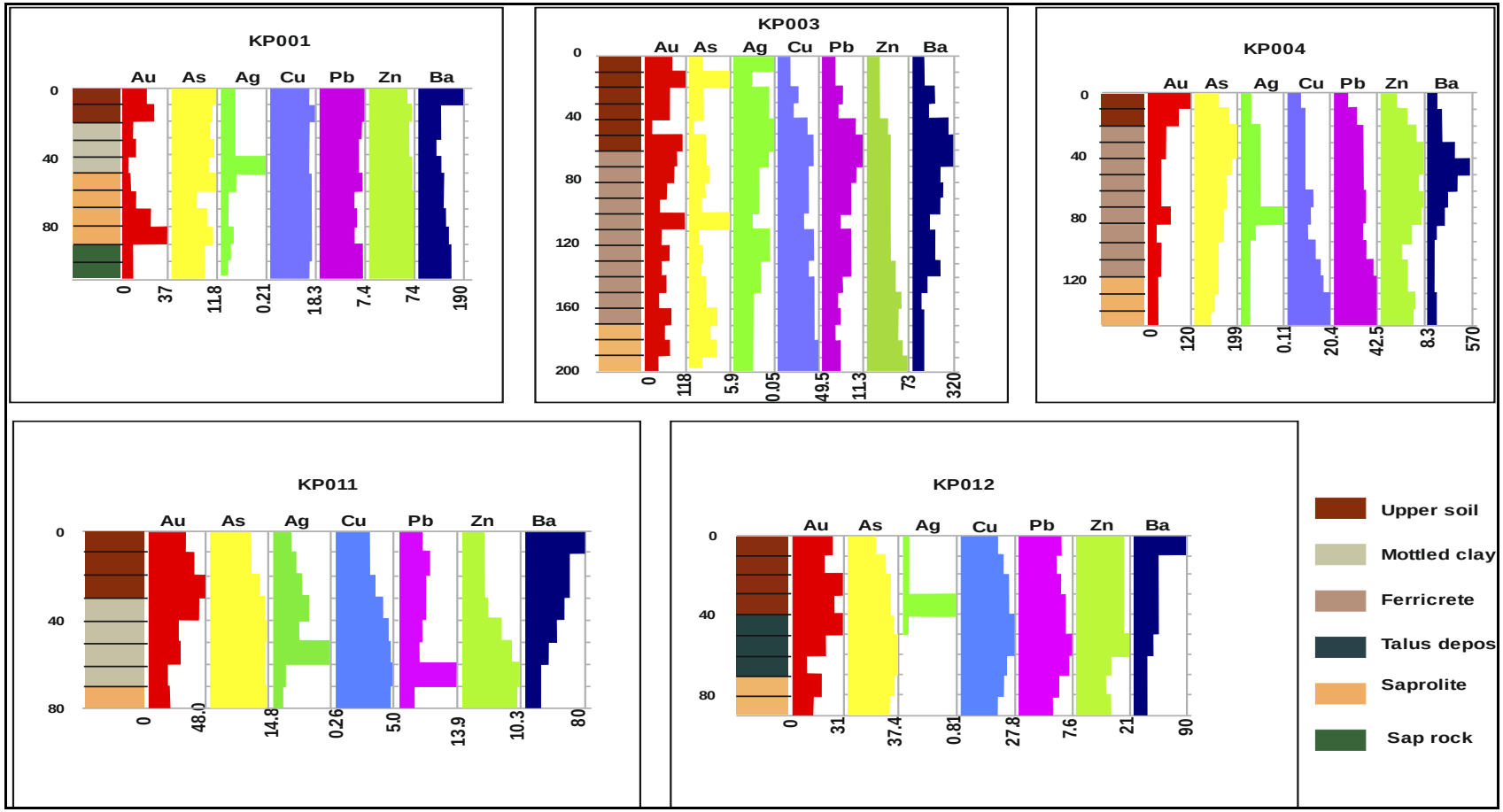

Fig. 7.21 Concentrations of selected elements (ppm) except Au (ppb) with depth (cm) in relict regime at Kunche-Bekpong area.

7.3.5.3 Semi-residual regolith

Semi residual regolith is an area in the landscape that has a variety of regolith materials that resemble relict and erosional regolith with a thin veneer of silty and loamy soils as top surface regolith materials. Characterizing this area to either relict or erosional in the field is difficult especially for beginners in regolith mapping. Diagnostic features characterizing this regime are the dominance of sub angular and sub-rounded fragments in somewhat unevenly distributed regolith. Therefore geochemical patterns of elements portrayed in this regime may show some displaced anomalies and will require understanding of element transport mechanisms to ascertain the anomaly-type. Fig. 7.22 shows the patterns of elements in this regime at Kunche-Bekpong.

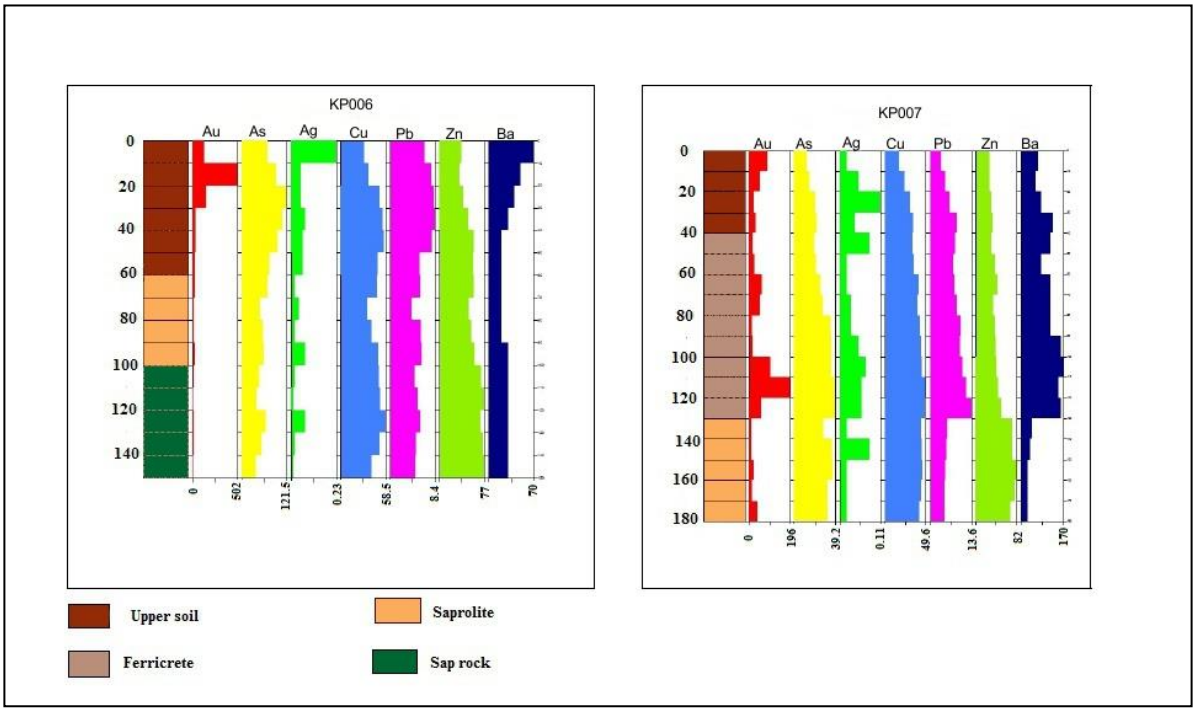

Fig. 7.22 Concentrations of selected elements (ppm) except Au (ppb) with depth (cm) in semi residual regime at Kunche-Bekpong.

7.4 Discussion

7.4.1 Major oxides in the regolith

Comparisons of the compositions of the regolith to potential source rocks e.g. to granites from the Birimian rocks of southern Ghana and schist of metasedimentary rocks in south Cameroon were compared. Figure 7.23 compares the potential source rocks major and trace elements content (Nyarko et al., 2012) with major and trace element behaviours in the regolith. These were carried out to help define origin of the residual regolith. The underlying rocks in the sampled areas generally are granites and metasedimentary rocks (Arhin and Nude, 2009; Griffis et al., 2002). From Table 7.8, the weight per cent (wt. %) contents of MnO, MgO, CaO, Na_2O, K_2O and P_2O_5 in the 12 regolith samples analysed were within the range of 0.02-1.03; 0.16-2.12; 0-0.19; 0-0.1; 0.18-2.39; and 0.02-0.12 respectively. The contents of MnO, MgO, CaO, Na_2O + K_2O and P_2O_5 in similar granitic rocks in the Birimian of southern Ghana measured 0.02-0.05; 0.05-0.99; 1.16-3.68; 6.20-8.74 and 0.01-0.21 (Nyarko et al., 2012). This showed small wt. % gains of MnO of 0.98 and 1.13 wt. % in MgO and some loss of 0.09 wt. % in P_2O_5 but much larger loss of 3.5 wt. % in CaO between the regolith and granite. Similarly Kamgang Kabeyene Beyala et al. (2009) report values of MnO (0.02-0.08); P_2O_5 (0.03-0.13); CaO (0-0.06); and Na_2O in a lateritic profile over chlorite schist, similar to some rock types in the metasedimentary suite of rocks in the study area. The comparison of the oxide contents obtained in the research samples also showed a gain of 0.95 wt. % MnO, 0.13 wt. % of CaO but with low 0.01 losses in P_2O_5. These are within the range obtained in the lateritic profile reported by Kamgang Kabeyene Beyala and company. However McQueen et al. (2004) and McQueen and Munro (2003) noted the chemical changes in residual regolith to involve progressive loss of Na^+, K^+, Ca^{2+}, Mg^{2+} and retention of Si^{4+}, Al^{3+} and Fe^{3+}, which is consistent with the chemical changes observed in the regolith. The small gains in MnO and MgO in the regolith may be due probably to element fractionation by combined mechanical and chemical processes during the past and present landscape evolutional events (Scott and Pain, 2008). As shown in Figs. 7.7-7.10, SiO_2 and Al_2O_3 showed contrasting element-content trends in the upper and lower regolith. Relationship between SiO_2 and Al_2O_3 in the regolith profiles with depth have been re-plotted and shown in Fig. 7.24. The variations between SiO_2 and Al_2O_3 in all the four pits (KP003, KP008, KP009 and SP003) have

A.

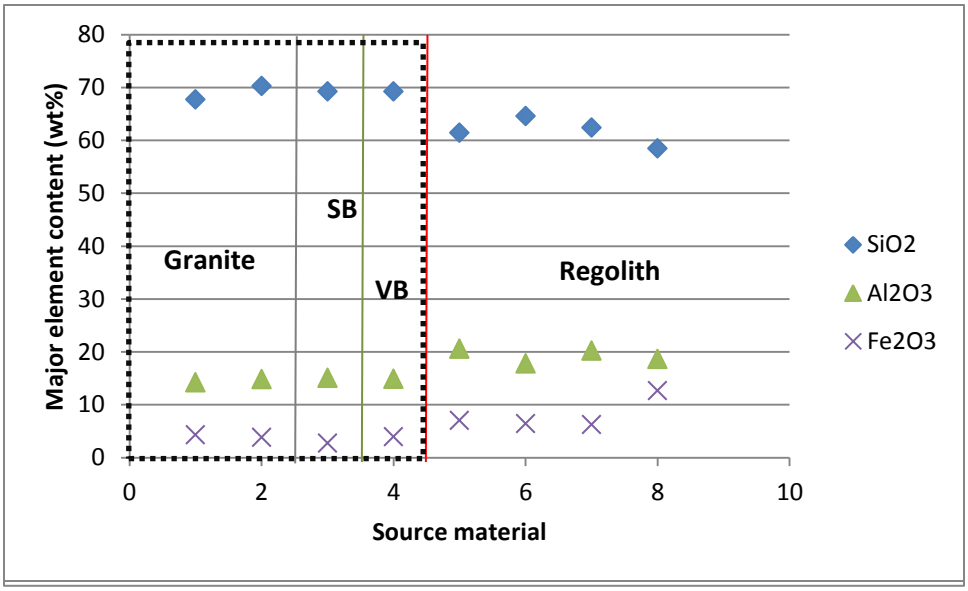

B.

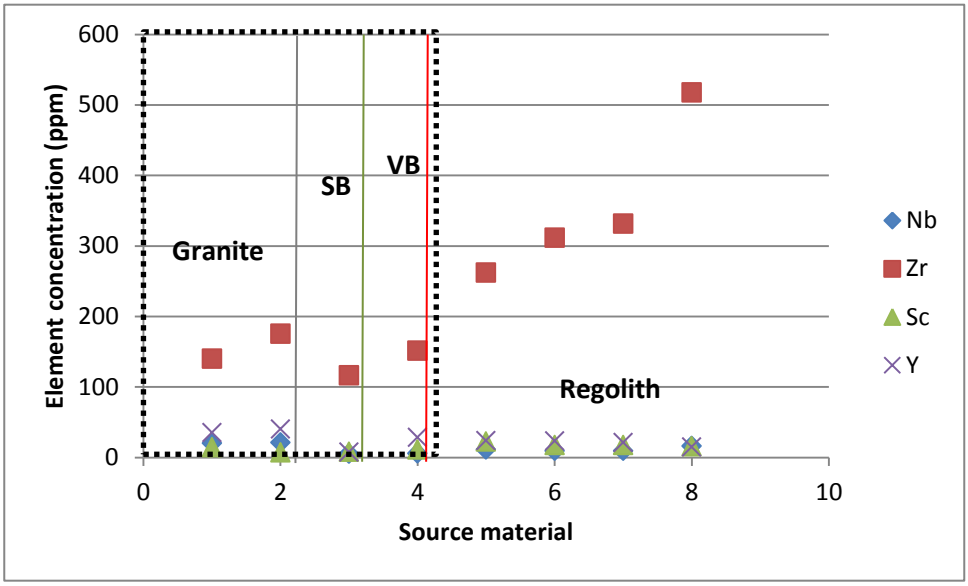

Fig. 7.23 Comparison of A). Some major elements and B). Some trace elements in potential source rocks and regolith in some pits in the study area. SB and VB are Birimian sedimentary and volcanic rocks.

relatively good correlations from the lower regolith to the upper regolith materials. Aluminium is considered as one of the least mobile of the major elements during weathering (Butt et al., 2000) because of the very low solubility of Al_2O_3 between pH 5 and 8. In normal in situ weathering Al_2O_3 remains constants whilst SiO_2 show some decrease when Fe_2O_3 show significant increase with MgO exhibiting some significant decrease. CaO and Na_2O show complete removals with some decrease in K_2O. However from Fig. 7.23 there is some increase in SiO_2 with a corresponding decrease in Al_2O_3. These changes in major oxide contents in the regolith may be as a result of mechanically reworked regolith materials that undergo a range of transformations enriching SiO_2 and depleting Al_2O_3 with time and changing environmental conditions. SiO_2 in KP003, KP008 and KP009 increased gently upwards. However in SP003 there is much higher enrichment of SiO_2 in the upper regolith. The sharp deviation in SiO_2 between the upper and the lower regolith in SP003 may probably be due to a high proportion of resistate vein quartz-rich material that have been deflated during profile collapse under gravity. The changes in the elements trajectories from the parent materials to the surface environments could also be due to dilutions from influx transported materials (Gong et al., 2010). The presence of these quartz-rich materials can dilute the concentration of other elements (Figs. 7.7-7.10) or the other oxides have been removed to solution due to their susceptibility to weathering (Scott and Pain, 2008).

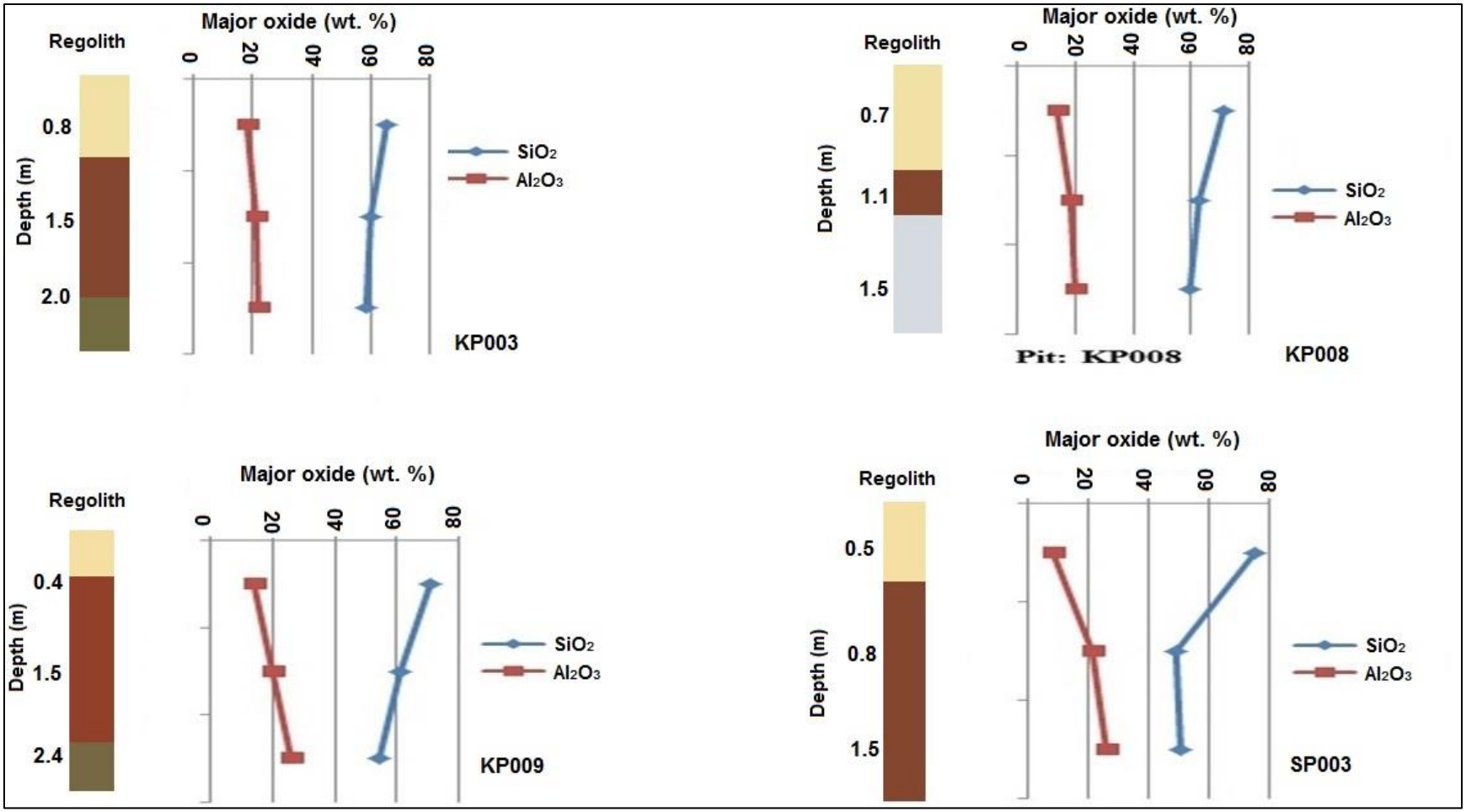

Fig. 7.24 Selected major oxides (%) plots with depth (m) in Kunche-Bekpong and Sabala dugout pits.

Table 7.10 Major and trace element contents comparisons in source rocks and the regolith. The granitoids, Birimian sediments and volcanic rocks are averages of two analytical results.

Source	**Turekian & Wedepohl (1961)**		**Leube et al. (1990)**		**This research**			
Sample	**Granitoid-1**	**Granitoid-2**	**Birimian sedimentary rocks**	**Birimian volcanic rocks**	**KP003-Regolith**	**KP008-Regolith**	**KP009-Regolith**	**SP003-Regolith**
Major oxide (wt. %)	**Ayamfuri**	**Obuasi**			**Kunche**			**Sabala**
SiO_2	67.72	70.23	69.24	69.24	61.42	64.59	62.4	58.43
Ti O_2	0.41	0.24	0.32	0.36	0.92	0.82	0.89	0.88
Al_2O_3	14.24	14.8	15.05	14.86	20.6	17.82	20.24	18.61
Fe_2O_3	4.31	3.84	2.73	3.95	7.00	6.39	6.26	12.65
MnO	0.03	0.03	0.04	0.07	0.10	0.37	0.03	0.04
MgO	0.95	0.54	0.97	1.33	0.53	1.19	0.45	0.18
CaO	2.3	1.64	2.19	3.24	0.02	0.06	0.06	0.03
Na_2O	4.46	2.91	4.37	4.53	0.05	0.07	0.03	0.02
K_2O	2.09	3.42	2.58	2.13	2.04	2.04	1.81	0.27
Trace element (ppm)								
Nb	20	21	4.8	5.3	11.13	9.1	9.17	16.07
Zr	140	175	116	151	261.87	311.5	331.2	517.63
Sc	14	7	7.6	11	22.27	17.43	17.07	15.5
Y	35	40	7.4	28	23.53	23.27	20.87	14.7

As presented in Table 7.9 there is more SiO_2 in the surface regolith layers than they occur in subsurface layers like ferricrete and saprolite. Of all the twelve samples analysed for the major element studies, SiO_2 content of 71 wt.% are associated with the lateritic gravels and pisolithic soils whereas 56 wt.% are in ferricrete and saprolite. However, when an average of the total SiO_2 content in the regolith was compared to the contents in the source rocks a fractional depletion was found (Fig. 7.23). Equally there are isolated instances where high concentrations of SiO_2 were measured in the surface layers. Environments with high SiO_2 content in surface regolith layers may be due to the deflated resistate vein quartz-rich materials. Conversely Al_2O_3 appears not to change from saprolite through ferricrete to lateritic gravel (Fig. 7.23 A) but there is still an increase in Al_2O_3 and decrease in SiO_2 when the total contents in the regolith profiles are compared with the source rocks. This thus contradicts the behaviour of the major elements as they are mobilized in the profiles. As portrayed in Figs. (7.23 and 7.24) mobility of elements in complex regolith terrains should be considered with the understanding of the different regolith domains as regolith modifying and geochemical processes varies in different regolith layers. In normal residual weathering environment some SiO_2 can undergo progressive loss in the surface regolith whereas Al_2O_3 remain immobile (Scott and Pain, 2008). This explains the fractional depletion of total SiO_2 in the regolith profiles to the source rocks but landscape evolution processes can also contribute to the compositional variations of the surface layers (e.g., Fig. 7.23). Determination of regolith types can be noticed geochemically by observing the dispersal patterns e.g., the spiky geochemical patterns may represent transported regolith whereas the fairly smooth element dispersal patterns will be for in situ regolith.

7.4.2 Trace elements - high field strength oxides (HFSE) in the regolith

The difficulty in identifying parent rock types from regolith materials appear to be a problem in areas under cover because of the profound mineralogical and chemical changes related to different processes and mechanisms involved in the landscape evolutions. Therefore the identification of residual regolith from transported regolith in this study was carried out by investigating the relationship of some least mobile elements (Zr, Nb, Ti etc.) in the regolith profile with depth (Fig.7.25). As shown in Fig. 7.25 there are positive correlations between Zr samples collected from the upper regolith in KP003, KP008, KP009 and SP003 pits. However, the Zr relative enrichment upwards especially in the

surface regolith compared to other regolith elements may be an attribute of incremental accumulations from mechanically transported sediments of Zr-bearing grains introduced in the weathering environment. Comparison of Zr contents in source rocks and regolith confirms Zr-bearing grain enrichment from the source rocks to the overlying regolith materials. Zr content of > 500 ppm was measured in regolith samples compared to < 200 ppm assays in the source rocks (Table 7.10). The variations in Zr contents in KP003, KP008 and KP009 appear gentler in relations to the source rocks but a bigger Zr content was recorded in samples in the upper part of SP003. The fractional enrichment of Zr may be accumulations of Zr grains from transported matter from a different source. Hence SP003 regolith may be transported whereas the other pits may either be relict or semi residual in character. The increased content of Zr is in agreement with the observation of Tate et al. (2007) that aeolian materials in regolith may have high Zr relative to the in situ material.

Similarly, the element concentration ratio plots (Fig. 7.26) show fractional enrichment of Zr between the lower regolith horizons to the upper regolith in all regolith regimes. Apart from the enrichment of Zr, there is a marginal Ti enrichment also in the relict regolith (e.g., KP003). It may be that the Ti is hosted in anatase a common residual Ti-bearing mineral common in the regolith (Butt and Zeegers, 1992). Scott and Radford (2007) indicated the persistence of Ti in weathering environment once it is altered from Ti-bearing silicates or alteration of ilmenite and rutile in the regolith. Since Ti, Nb and Zr can coexist in the same system and are all classified as resistate elements, plot of their ratios are useful to determine the nature of the regolith (McQueen, 2004).

The correlation of Nb/Ti and Zr/Y ratios in KP003 is different from the ratios in KP008 and KP009. Pit KP003 exhibit relict regolith characteristics because Nb/Ti and Zr/Y ratios appear to increase steadily in element concentrations upwards with a subtle change at 1.5 m depth. The ratios of the covariant element pairs deviate from their lines of dispersion. The deviations of the covariant element pairs from the lower parts of the regolith to the upper regolith (Fig. 7.26) are probable evidence of additions of different source materials into the regolith profiles. So in this study, discrimination of residual from transported

regolith depended on the extents of deviation of the covariant pairs of elements from the source rocks to the surface regolith layers. The deviation between the element dispersal trends from the lower regolith to the upper regolith is greater in SP003 compared to the other elemental trends in the other pits. This implies more transported matter additions to the surface regolith in SP003, hence classified as transported regolith. Also high Zr content was noted in surface regolith than in the lower regolith in SP003. Contrastingly there were no changes in Zr contents in the other pits in the entire profiles between the lower and the upper regolith materials. This implies that the other pits occur in residual environments.

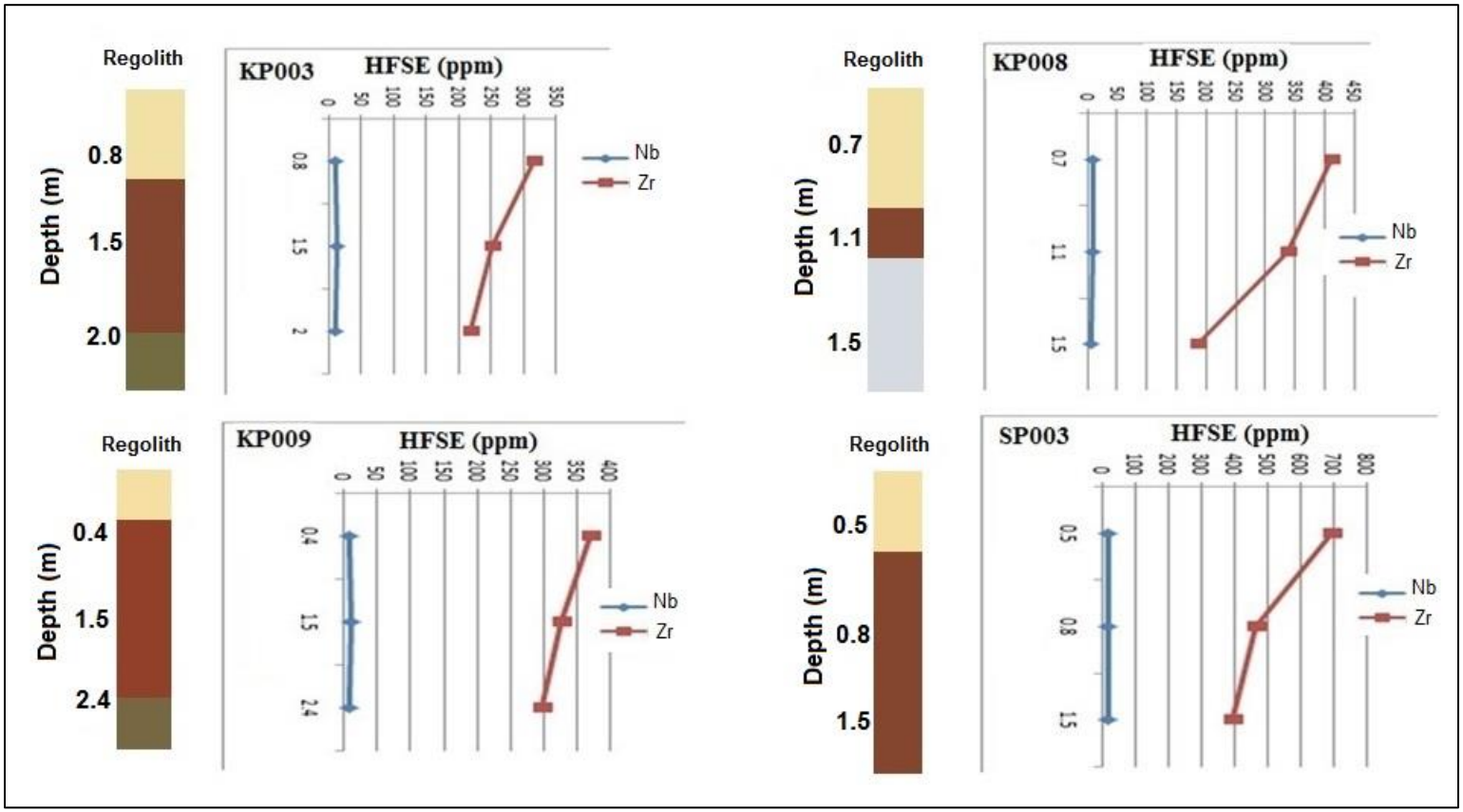

Fig. 7.25 Concentrations of high field strength elements (HFSE) in regolith samples with depth

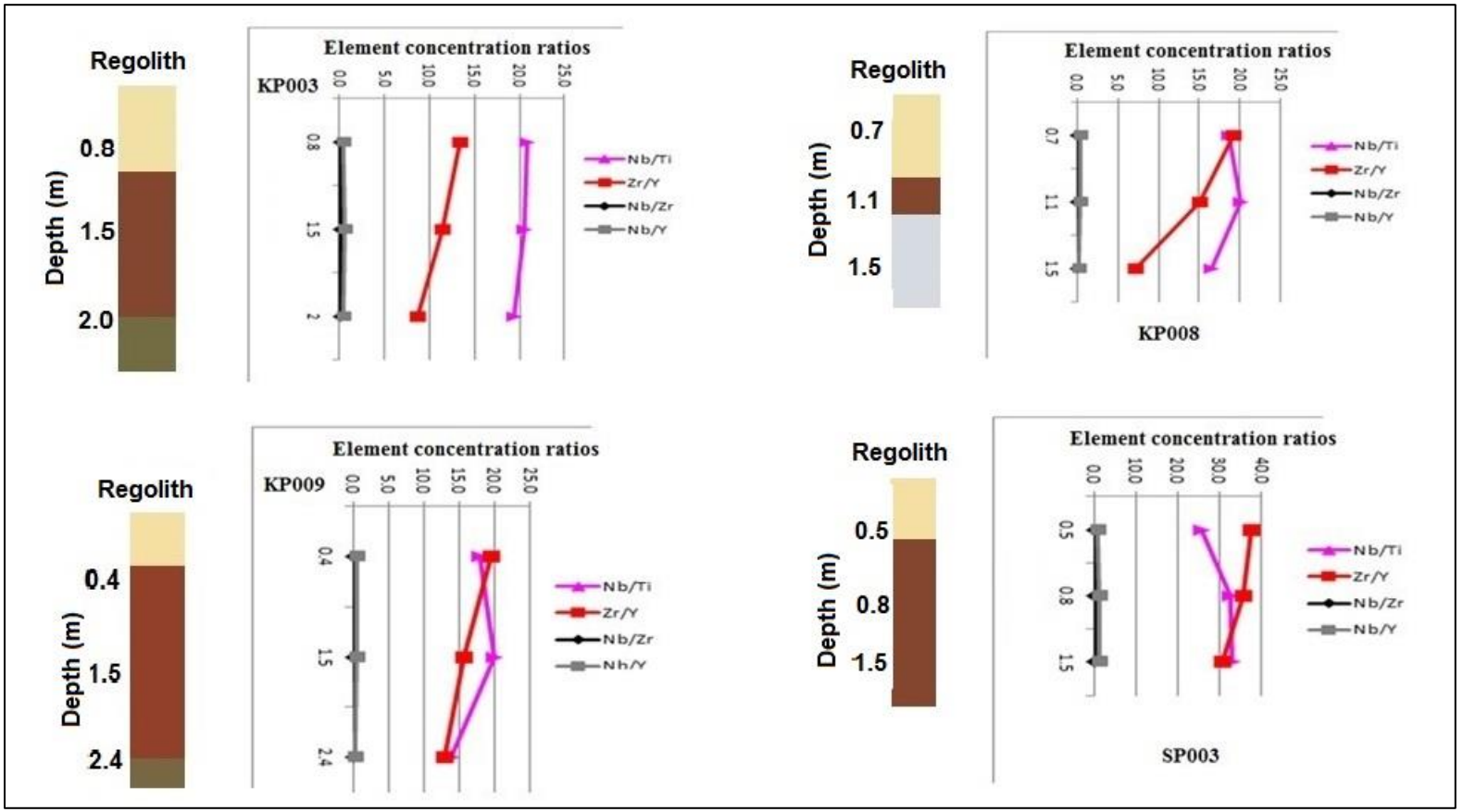

Fig. 7.26 Concentration ratios of high field strength elements (HFSE) in regolith samples with depth

7.4.3 Characterizing and identifying regolith materials using major oxides

Mg/Al versus K/Al plot (Fig. 7.11) showed five samples classified as transported clays, a sample as ferruginous alluvium and others occurring between transported clays and ferruginous alluvium. The samples that fall outside the defined regions may be relict or semi residual regolith because of their high Mg contents. According to Butt et al. (2000) and as presented in Table 3.1 Mg is released at the weathering front because of its susceptibility to weathering which makes it unstable in oxidized environment. Its presence in the regolith portrays some relict unit of the parent rock and shows less regolith and landscape modifications. The source of these samples may have limited sorting of regolith mapping units and low levels of post-depositional weathering. Plots like 7.11 is useful in surface geochemical data interpretations because the surface geochemical Au assays are either enhanced if the sample is from Au-rich saprolite or diluted if samples were collected from either Au-poor transported clay or ferruginous alluvium. Relict and semi residual regolith materials normally relate to underlying mineralization. This approach is useful during the orientation surveys as they guide in selecting sample media even before the creation of regolith map. Also novices in regolith mapping can use this technique to classify regolith domains where regolith mapping units cannot be defined clearly or unsure. In addition to the use of Mg/Al and K/Al plots Fe/S ratios might also be used by novice in regolith mapping to determine changes in regolith horizons e.g., to mark out limits of ferruginous laterite zones in profiles (Figs. 7.12–7.13).

7.4.4 Behaviour and relationship between Au and (±Ag or As) in regolith profiles in the study area

The Au and other element results indicate some relationships between Au and Ag in determining the anomaly type and Au and As linkage in the saprolite as a pathfinder element. The Au, Ag and As relationships seem to be subdued in clay zones, enhance generally in surface layers and ferricrete/saprolite interface and erratic in the nodular laterite and ferricrete zones (Figs. 7.12 & 7.13). However, these forms of element dispersion characteristics in regolith profiles have been identified by Freyssinet et al., (1989 a, b), Lecomte and Zeegers (1992), Zeegers and Lecomte (1992) to be due in part to mobility either in solution or as particulate free metal. The evolution of the regolith by different weathering mechanisms coupled with multiple geochemical processes that act on the primary minerals through the profile can affect the dispersions processes.

Results in pit KP010 is used to illustrate the relationship between Au and the two elements (Ag and As). This is shown in Fig. 7.27. The dispersal patterns of these elements are spiky from surface to 1.4 m depth whereas from 1.4 m to the bottom of pit the data vary more smoothly. Despite the erratic assay results shown above the sap rock, there is a fractional enrichment of Ag in the regolith profile. This enrichment suggests the mobility of Ag in the regolith environment irrespective of the weathering environment and the state of the landscape evolution. Conversely Au showed some enrichment in the sap rock and fractional depletion in the clayey saprolite and then enrichment towards the top of the profile. The > 1000 ppb Au anomalies in the upper regolith materials and the sap rock (Fig. 7.27) may be due to:

- Residual concentration, colluvial transport and surface wash of Au grains during landscape evolution and
- Au mobility either in solution or as particulates (e.g., colloids or very fine grains of free metal) in the regolith profile.

The source of anomaly in the upper regolith is contributed by all these geochemical and surface processes hence resulting in the spiky geochemical patterns. However the increase in Au concentrations towards the surface may suggest introduction of materials from a different source that may or may not bear relationship to the underlying rock and mineralization (Gong et al., 2011). It appears the chemical and detrital dispersion of Au high up in the regolith profile due to the past and present landscape evolutional events have contributed to the high Au assay results in the upper oxidized zone similar to the lower oxidized environment (sap rock) This area was mapped to have a transported regolith overlying erosional surface (chapter 6; Fig. 6.9) with some locally transported materials that retained significant amount of lithic fragment and quartz clasts overlying the saprolite. Perhaps the transported materials are Au-rich and through the mechanical dispersion increased the concentrations in the surface regolith. Areas with similar profiles may enhance or dilute anomalies depending on the source of transported sediments that may overlie the eroded surfaces. So characterizing and identifying regolith materials during the exploration survey is essential.

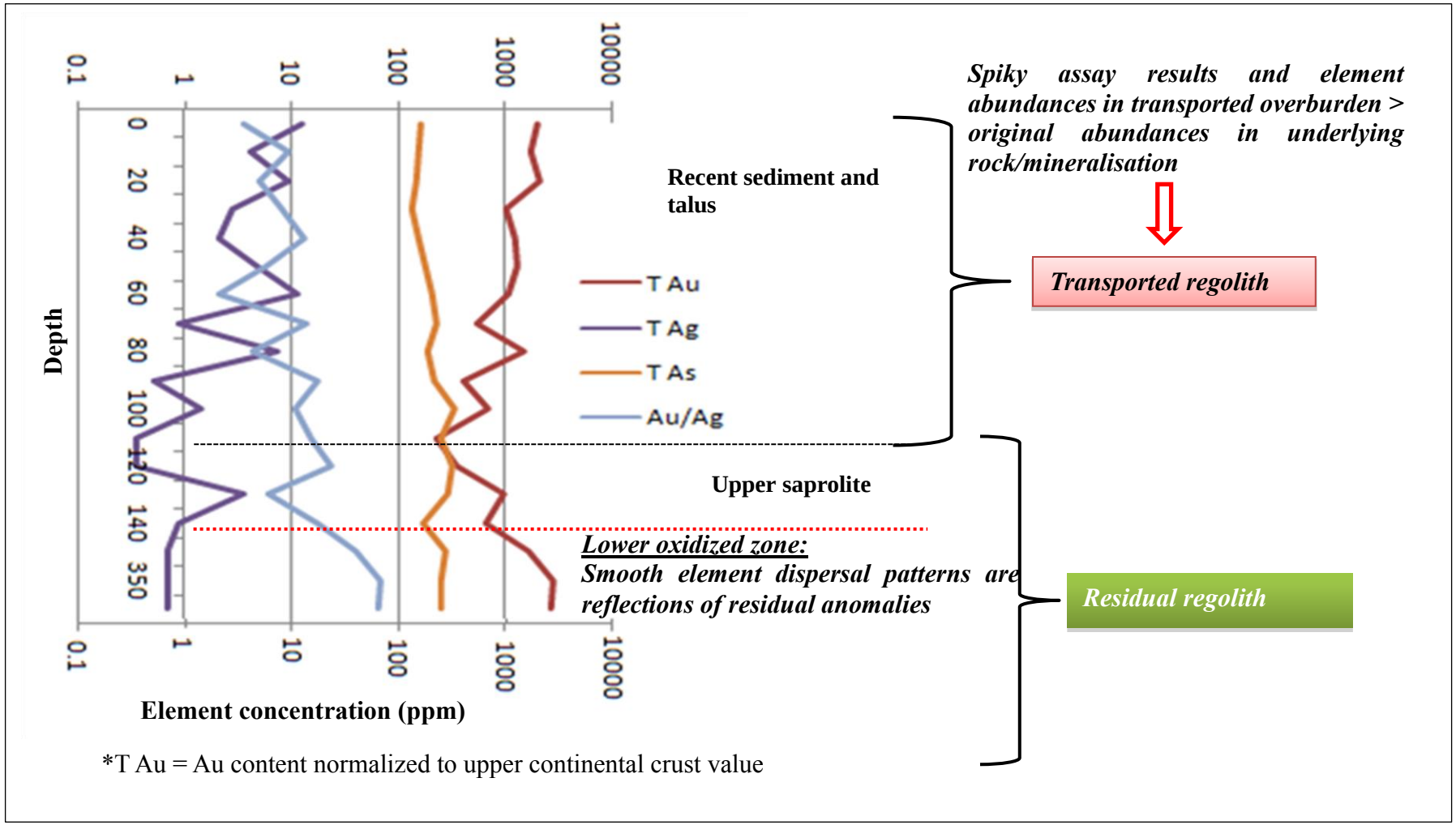

Fig. 7.27 Concentrations of Au, Ag and As in KP010 to establish the behaviour of these selected elements in the regolith profile

As seen in Fig. 7.27 high Au correlates with low Ag in the residual regolith and also indicates fairly smooth geochemical patterns. There also appear to be depletion of Au relative to Ag towards the surface from 1.4 m depth perhaps due to selective leaching. However the Au-Ag relationship in the area marked as transported regolith appears erratic because of the varying sources of the regolith materials. Samples that retained some amount of the parent material with mineralisation still exhibited high Au-low Ag relation whereas the reworked, redistributed and re-concentrated transported materials either show low Au-low Ag or high Au-high Ag correlations. The different mechanisms of element dispersions and the implications of the erosional transport from far and near in the surface regolith results in the spiky Au-Ag dispersion patterns. Au and Ag however behave quite differently at different levels in the regolith profile and this is shown in Fig. 7.27. Comparison of Ag contents and Au/Ag ratios shows Ag depletion in the lower oxidized zone from 1.4 m depth to the sap rock whereas the zone just above it (1.2–1.4 m) shows enrichment. This implies that underlying mineralisation in complex regolith environments may not always relate to the surface anomalies unless the regolith controls such as implications of regolith types on element dispersions and concentrations have been applied.

7.4.4.1 Au – As relationship in the regolith

The relationship between Au and As appear weak and subtle as illustrated in the different regolith domain profile results presented in Figs. 7.15-7.22. The non-correlation between the two elements may be due to the irregular spatial distribution of the regolith materials caused by the landscape evolution, scavenging effect of As by Fe-oxyhydroxides in the oxidised regions and/or either Au or As or both are unrelated to the underlying bedrock and mineralisation. Assuming these are the case then an appropriate pathfinder element for geochemical Au exploration can be obtained from the lower oxidized zone characterized by saprolite and sap rock formed directly from the underlying bedrocks. The complexities of the regolith (Chapter 5, Fig. 5.16 & 5.18) suggest As cannot be used as pathfinder element for Au anomaly definition during surface geochemical surveys due to the extensive coverage of laterite and transported depositional regolith coverage. The highest Au assay results recorded in KP010 are not in the lower oxidized zone but the most

smoothened geochemical patterns for Au, Ag and As seems to relate to the bottom part of this zone (Figs. 7.16 and 7.22). There is some correlation between Au and As in this zone. Similarly the ratio of Au/As in the saprolite samples seem to have good correlation with Kunche Oxide, Bekpong Oxide/Transition and Bekpong Primary composite samples (Table 7.11; Waller et al., 2012)-Azumah report). The oxide defined by Azumah Resources is considered in this research as part of the ore that has been a subject to supergene weathering and therefore is starting the evolution of the bedrock towards becoming part of the regolith. As seen in Table 7.11, it appears either As is enriched, or Au is diluted. Apparently from Fig.7.28 there is no correlation between Au and As in Kunche-Bekpong regolith and hence could not be used as a pathfinder to explore for Au in the study area.

Table 7.11 Leach composite sample head assays at the Wa-Lawra gold project (NI-101-43, April 2012 report of Azumah Resources Ltd.) compared with some Au and As results in current study.

Sample type	**Au1 (ppm)**	**Au2 (ppm)**	**Au3 (ppm)**	**As1 (ppm)**	**As2 (ppm)**	**Au ave.**	**As ave.**
*KP010 Mottled zone	0.48	x	x	794	x	0.475	794
*KP010 Saprolite	1.27	x	x	731	x	1.265	731
*KP010 Sap rock	0.89	x	x	425	x	0.878	425
Kunche Oxide	1.60	1.68	1.63	700	690	1.637	695
Kunche Transition	2.78	2.99	2.56	640	636	2.777	638
Kunche Primary	2.92	2.53	2.32	639	633	2.590	636
Bekpong Oxide/Transition	1.80	2.17	2.44	913	908	2.137	910
Bekpong Primary	1.99	1.71	1.71	933	1010	1.803	971

** - Samples from current research*

x - Sample not taken

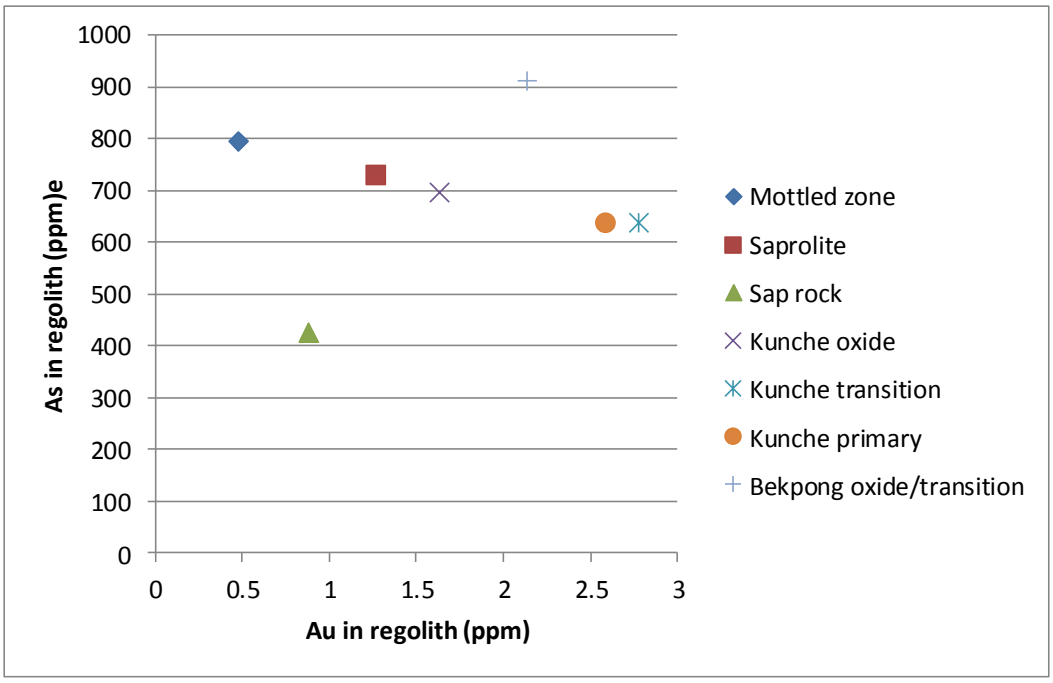

Fig. 7.28 Au-As relationship in Kunche-Bekpong area. Mottled zone, saprolite and sap rock samples are from the current research and the other data from Azumah Resources Ltd (Waller et al., 2012).

7.5 Summary and conclusion

The average SiO_2 content show enrichment in all the potential source rocks to the regolith total SiO_2 content put together for the four pits used in the study. However, an increase in SiO_2 content was noticed in the surface layers of the profiles with near constant SiO_2 in the subsurface regolith units. The increase in the surface layers have been attributed to addition of SiO_2-rich regolith materials especially from deflated resistate quartz veins by mechanical and chemical processes during the past and present landscape evolution events. Al_2O_3, the least mobile oxide in the oxidized zone, shows a fractional overall enrichment in the regolith profile when compared with the source rocks contents. In the pits Al_2O_3 content tends to decrease upwards whereas SiO_2 increases upwards. The contrast between the total major oxide contents in the regolith profile to the source rocks may be an increase of Fe and Al due to the lateritization processes that enrich the concentration of these elements, by removing other more soluble constituents.

The residual accumulation of Zr from the parent source increases steadily upwards. The upward steadily lines of dispersion is reflected in the covariant element pairs of Zr/Y and Nb/Ti. Deviations in the lines of dispersion occur when other source materials are added into the profile. The additions from other sources results either in the increase or decrease of the covariant element pairs. In this study significant increase in Zr showing positive dispersion line pattern was noted between the lower regolith and the surface materials at SP003 compared to KP003, KP008 and KP009. SP003 therefore is classified as part of the transported regolith whereas the others are mapped as relict or semi residual regolith.

The compositional variability of the regolith materials can be useful in characterising and identifying regolith materials by plotting Mg/Al versus K/Al. Plot of these shows the behaviour of the two mobilised elements with a relatively immobile major oxide in the regolith profile. Samples taken from transported clay and ferruginous alluvium areas in this study plotted in the demarcated region specified by McQueen (2006) to be occupied by samples from those environments. The other samples occupied a region with much higher Mg content indicating an area with less modification and contain soluble element in the weathering environment. Samples with greater Mg/Al ratios may either be relict or semi

residual and can be validated in the field. The application of this method is more useful during an orientation survey stage as it provides information on sample media selection for the systematic exploration survey.

There are some weak correlations between Au and Ag and between Au and As in the regolith profile. However, the correlations seem to weaken in the upper regolith because of the modification of the regolith profiles by repeated weathering, erosion, deposition and lateritization. The different weathering mechanisms and geochemical processes in the different regolith layers allow some elements to behave differently. Au and Ag behaved differently in different levels (i.e., in lower and upper oxide zones) of KP010. This implies that geochemical data interpretation in complex regolith environments should be carried out by including regolith controls such as the effect of regolith types on element mobilization mechanisms in the evolved regolith environments.

Au-As correlation is weak and mixed in the surface regolith materials. This may be due to the irregular regolith distribution during the landscape evolution as well as the scavenging of As by Fe-oxyhydroxides in the oxidised environment. The overall correlation of Au and As in Kunche-Bekpong area is poor and so its application as pathfinder element in the complex regolith of Lawra belt is inappropriate.

In conclusion exploration for Au in the study area cannot use As to look for Au in the low concentration terrain. However, major and trace element contents in the regolith can be used to discriminate residual anomalies from transported ones as well as to establish the compositional variations of the regolith materials.

Use of regolith geochemistry to delineate gold mineralisation under cover: a case study in the Lawra belt, NW Ghana

8.0 Introduction

The grid image (Fig. 8.1) of the historical soil Au geochemistry obtained from Azumah Resources Ltd., suggests the study area contains gold mineralisation. However, Griffis et al. (2002) indicate marked discrepancies at the grass root exploration stages, where many high soil Au assay areas returned insignificant and generally weaker Au assays from sub-surface regolith sampling (Ashanti-AGEM Alliance internal report-Carter, 1997-unpublished). The recent exploration survey by Azumah Resources Ltd., has also indicated the bedrock mineralisation of the study area have an association with metasedimentary rocks (Figs. 2.3 & 8.2) intruded by granites. The metasedimentary rocks are intercalated with sheared "smoky" quartz veins and quartz veinlets. Close examination of the many exploration failures during the current study suggests that not all the high assays have associations with underlying mineralisation. It is likely that the evolution of the regolith, as discussed in chapter 6, affects the dispersion and concentration of elements in the regolith environment. Therefore, as noted in chapters 5 to 7, the delineation of prospective anomalies from surface soil Au geochemical data needs the application of regolith geochemistry to distinguish residual anomalies from the transported or false anomalies.

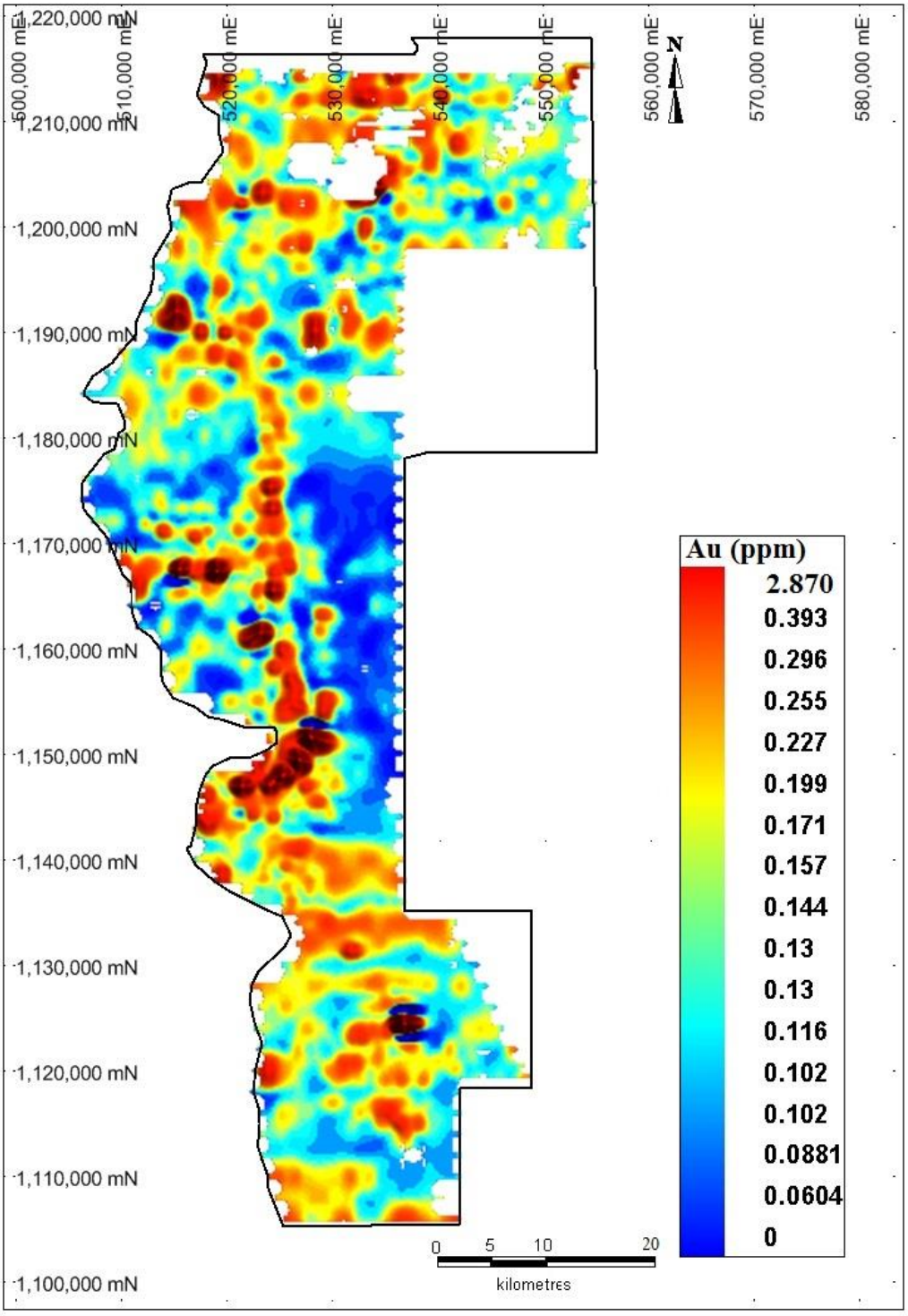

Fig. 8.1 Grid image map of surface Au geochemistry in the Lawra belt. The high and low Au concentration areas are shown by red and blue colours respectively.

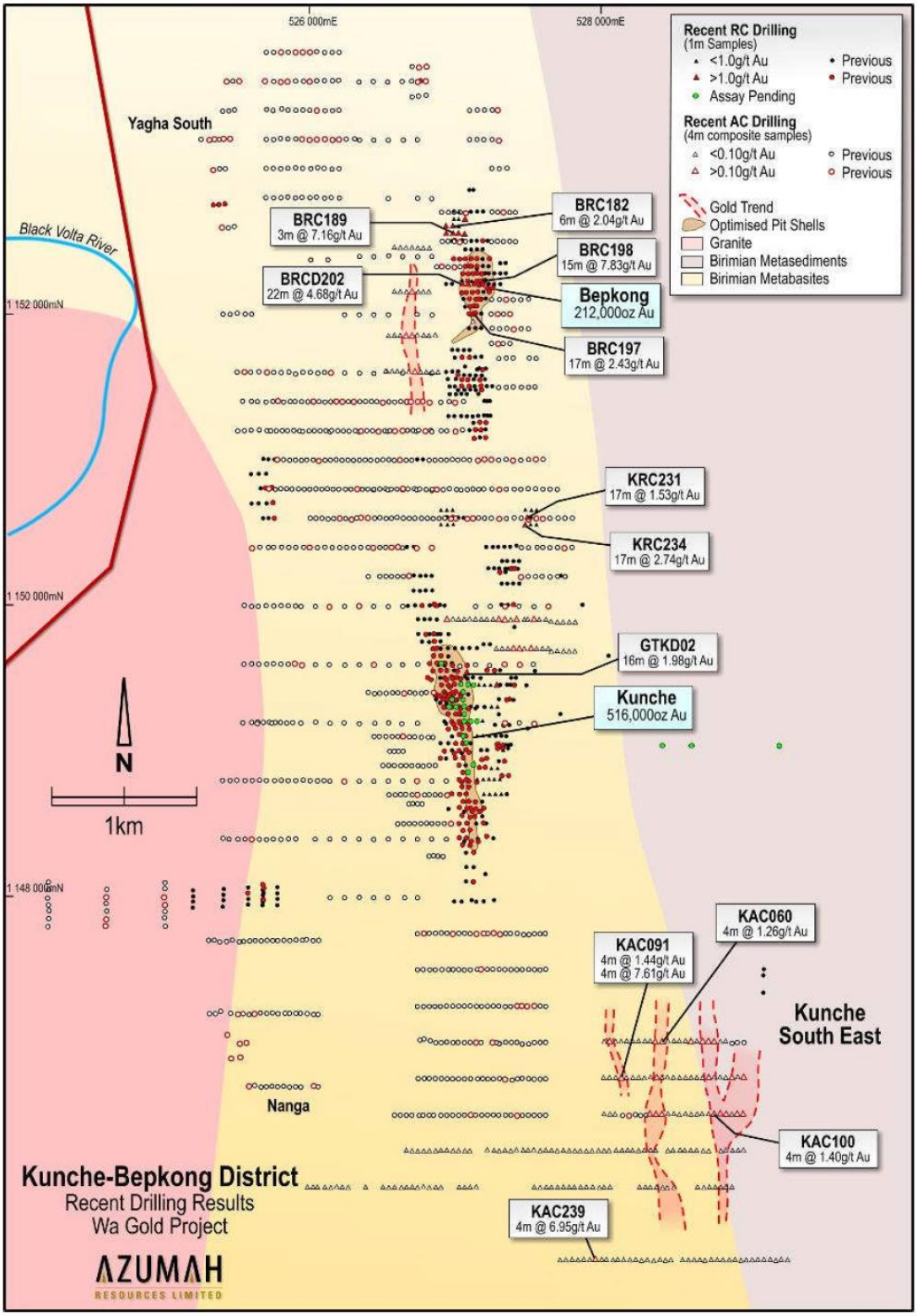

Fig. 8.2 Geology and bedrock mineralisation of Kunche-Bekpong area

8.1 Regolith and geochemical gold exploration in areas under cover

Geochemical Au exploration surveys commonly have two major objectives to discover new Au deposits. These are:

1. To locate abnormal concentrations of target elements (e.g. Au in the current study) or pathfinder elements (such as Ag, As, Pb, Zn, etc.) and
2. To identify the host mineralized rocks.

The irregular distribution of regolith material influences element dispersion, so the surface geochemical data interpretation phase in this research included regolith controls on element mobility for anomaly delineation. Different threshold gold values were calculated separately for ferruginous (F), relict (R), erosional (E) and depositional (D) regimes. Individual maps were created to show a unified picture of the surface gold geochemistry patterns from which significant gold anomalies were defined and integrated to represent the entire area. This concept of using different threshold Au values that account for regolith-landform controls on anomaly delineation from surface geochemical data follows suggestions by Arhin and Nude (2009), Bolster (2007, 1999), Anand et al. (2001), Butt and Zeegers, (1992) that argued that no single threshold Au value is appropriate in delineating prospective Au anomalies without missing prospective targets.

8.2 Methods

To improve upon exploration successes in the area two sets of data were used. These were:

1. Different geochemical datasets arising from different geochemical surveys. The datasets were categorised as historical surface soil geochemical datasets (from Ashanti-AGEM Alliance and Azumah Resources soil surveys) and current regolith sample data (from the present research). Different normalised gridded image maps (normalisation carried out using threshold Au values calculated from the historical and current orientation survey data) were used to create a unified picture of the surface geochemistry across the different regolith regimes.
2. Local small-scaled regolith maps of Kunche-Bekpong and Sabala were superimposed on the geochemical maps to establish the relationship between

regolith types and mineral deposits, and the distribution of various regolith types with economic potential.

Using this approach the Au dispersion-patterns in the different regolith domains were assessed separately using the statistical q-q plot method. The result of the natural breaks in Au dispersion using the q-q plot was constrained with respect to the characteristics of the different regolith environment (FRED). Geochemical plots in the GIS interface using thematic and contour maps were created for the Sabala and Kunche-Bekpong targets to demonstrate the anomaly patterns using the defined threshold Au values. This was done because visualisation of the geochemical data in a picture-form is most effective at evaluating a geochemical anomaly as the human eye is more adept at recognising patterns from pictures than from tables of numbers (Grunsky, 2010).

8.2.1 Threshold gold value estimation

Statistical methods have been widely applied to interpret geochemical data sets to define anomalies. The threshold estimations calculated from the statistical procedures apply the concept that the threshold Au values mark the outer (lower and upper) limits of normal variation for a particular population of geochemical data and that the values within the thresholds are referred to as background and those above or below are known as anomalies. These methods that use statistical or mathematical models are subject to random and systematic errors (Sinclair, 1991). In this study anomaly delineation was obtained by identifying an appropriate threshold. This was done by taking into account the effects of regolith on the data. As a result of the complexity of regolith (chapter 6), three methods of threshold classifications were applied after separating the data into the different regolith regimes:

1. The Hawkes and Webb (1962) mean + 2SD.
2. The Stanley and Sinclair (1989a) experiential model, and,
3. The Stanley and Sinclair (1989a) model-based subjective threshold estimation model.

In the past, the mean + 2SD method of threshold estimation was used to statistically define an anomaly in a single population of normal distributed data (Hawkes and Webb, 1962).

This method works well for normally distributed data. Unfortunately, the geochemical data in the Lawra belt is generally heterogeneous and negatively skewed to the low concentration Au assays, probably because of the dilution of the regolith materials sampled by Au-poor transported sediments. However, despite the non-normality of the data, the orientation survey data were sub grouped into the "FRED" regolith regime types for the individual calculations of mean (μ) and standard deviation (SD).

The second method used was the experiential method. This method places emphasis on the absolute abundances of the data in a highly subjective way. It thus evaluates the data from histogram plots to determine the distribution patterns in the data. It then estimates the threshold by comparing the most recurring assays to an assay of known mineralisation in a similar regolith regime. The overlap between the frequently assay data with the average assay of a known anomaly that previously defined mineralisation is selected as the threshold value. An example is given in Fig. 8.7 where a 50 ppb Au assay defined broader and more continuous anomalies than 100 ppb. The 100 ppb is the threshold estimate from a statistical threshold estimate model. It follows from experience that a smaller threshold of <50 ppb will define larger and continuous anomaly size than the 50 ppb. The same technique was used for the other regolith regimes. The application of this method however is inadequate in complex regolith environments if the geochemical data are not sorted into the different regolith regimes.

The last method used was the model-based subjective threshold estimation. This method uses a probability q-q plot for a set of selected geochemical values. It works principally on the concept that background and anomalous data form separate, potentially identifiable populations arising from different causes and characterized by different statistical parameters (Sinclair, 1991). The threshold estimates were obtained using the generally abundant background data which defined the background populations and then recognized the anomalous samples by their departure from the first break in the data. As seen in chapter 6 regolith evolutions may contribute to the development of several different populations in the data obtained from the regolith profiles. The populations may relate to background and anomalous zones. In this research the first population defined by the first

break in the data is considered as background data whereas those above represent the anomalous areas. Each of the different population sets has relations to mineralisation or to the underlying geology (Grunsky, 2010). In this method the break-point between the first two populations sets were selected as the threshold value for the different regolith regimes. The histogram and probability plots of the orientation survey data sorted into regolith types are presented in Figs 8.3–8.6. Table 8.1 compares the threshold estimates for the three different methods.

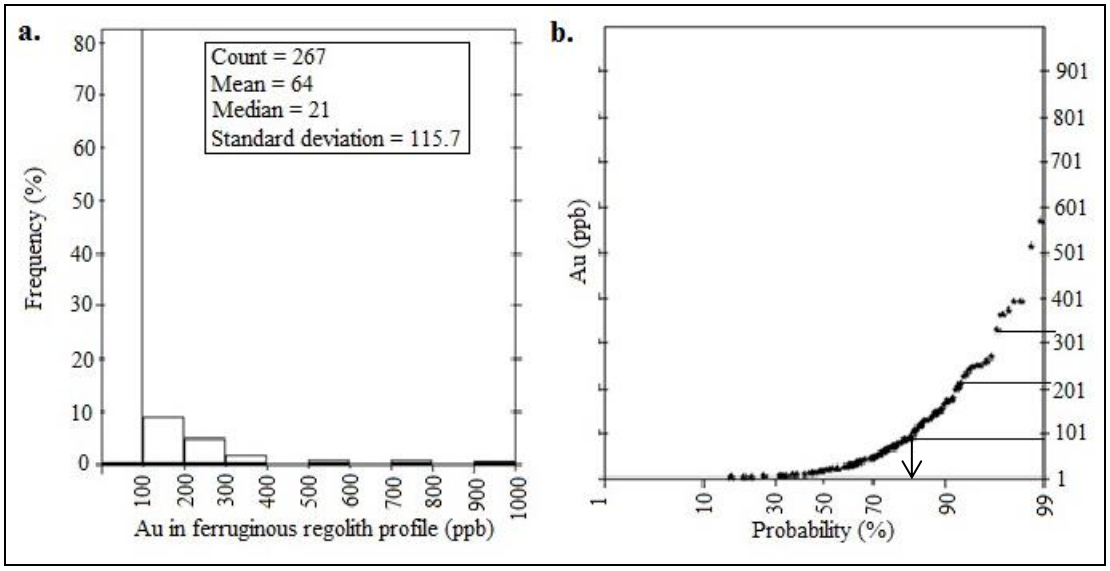

Fig. 8.3 Gold distribution plot for the ferruginous regime showing a). Frequency-histogram and b) Probability plot for orientation surface geochemical assay results.

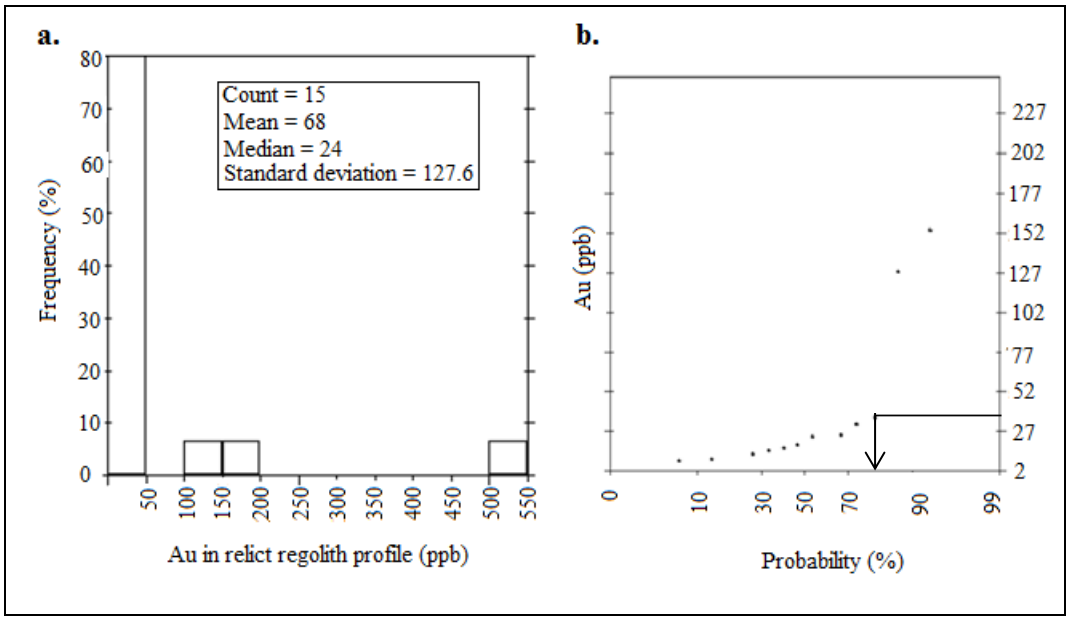

Fig. 8.4 Gold distribution plots for the relict regime showing a). Frequency-histogram and b) Probability plot for orientation surface geochemical assay results.

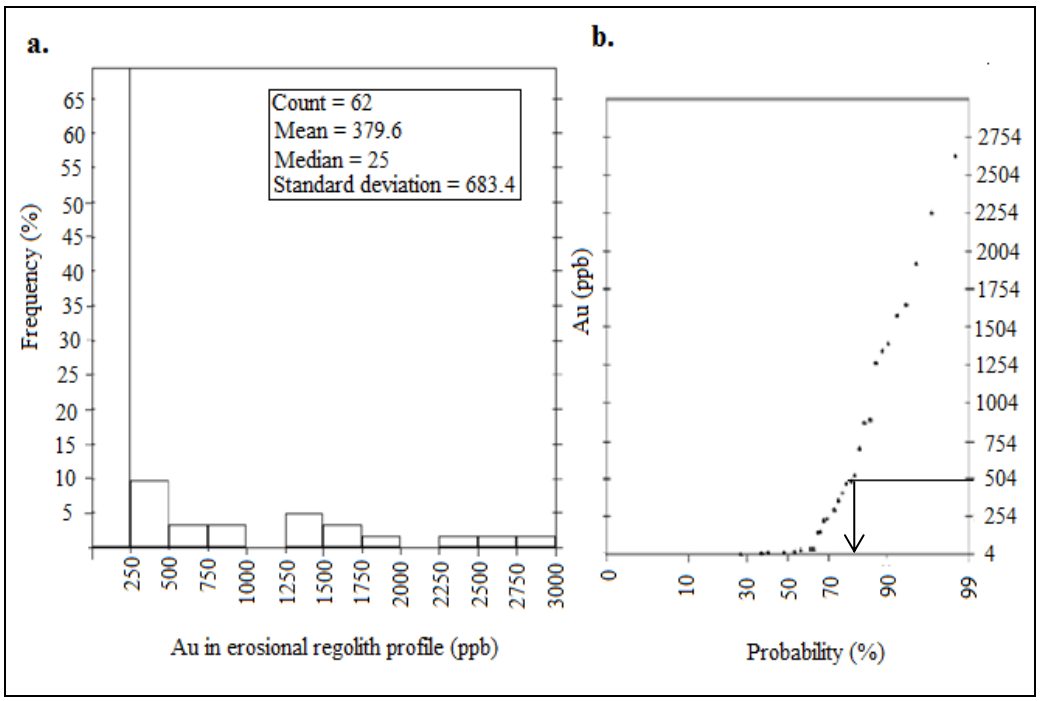

Fig. 8.5 Gold distribution plots for the erosional regime showing a). Frequency-histogram and b) Probability plot for orientation surface geochemical assay results.

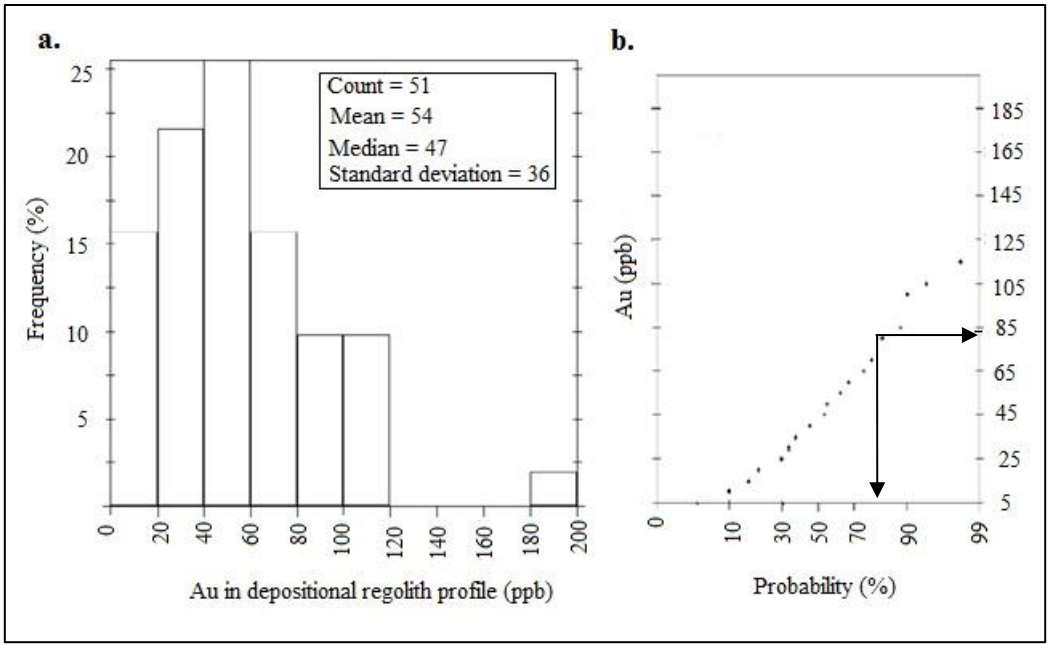

Fig. 8.6 Gold distribution plots for the depositional regime showing a). Frequency-histogram and b) Probability plot for orientation surface geochemical assay results.

As shown in Figs. 8.3–8.6, there is more than one population of data in the surface geochemical data set. Each regolith regime contains multiple populations, each with their own threshold value that relates to the underlying mineralisation or geology. This may be as a result of modification of the weathered materials through groundwater interaction and electrochemical mobility (diffusion) enhanced by different source materials. The outcome of the statistical data analysis using the probability plots resulted in a 101 ppb threshold value for ferruginous, 40 ppb for relict, 504 ppb for erosional and 84 ppb for depositional regimes. It is worth noting that these threshold values defined by the probability plots ignored the implications of regolith on Au migration in the oxidised environment. The statistically defined threshold values for ferruginous and depositional regimes may not be able to delineate the subtle and weak anomalies without regolith controls, as the processes controlling element mobility may dilute or enhance Au concentration in the regolith profile. For example in ferruginous regimes Au grains may be coated by Fe-oxyhydroxides and clay minerals reducing its concentration (Figs. 7.9-7.11). Similarly transported sediments may dilute Au concentrations in the depositional regime. All these modification processes in the regolith could obscure the true Au concentration in depositional

environments (Fig. 7.15). Threshold Au values lower than those defined for ferruginous and depositional regimes may be appropriate, based on the regolith affecting element mobilisation in the surface environment. The experiential threshold estimates or application of regolith constraint in estimating Au threshold values is user-defined, subjective and partly based on local knowledge of Au mobility in the regolith was also used. Table 8.1 summarises the threshold gold values in the study area.

Table 8.1 Thresholds using mean plus two standard deviation (μ + 2SD), probability plots and experiential method or thresholds estimation incorporating regolith effects on gold mobility *(Au unit is ppb). Depositional values generally low because of sample dilution by barren transported sediments and easy leaching due to high permeability.*

Regolith regime	Mean (μ)	Standard deviation (SD)	μ + 2SD	μ + SD	Probability q-q plot	Experiential estimate
Ferruginous	64	116	295	180	100	40
Relict	68	128	323	196	40	50
Erosional	380	683	1746	1063	504	100
Depositional	36	36	126	90	84	40

8.3 Levelling and gridding methods

8.3.1 Levelling

The available geochemical data for anomaly delineation in the Lawra belt comprise several different surveys, carried out at different times, collected from different sample media and analysed using different laboratories with different analytical techniques. Levelling the different exploration survey data to minimise mismatches between populations so as to present a composite picture suitable for regional exploration with respect to the regolith environments was necessary for the study, but difficult in practice. The challenge of levelling the different exploration survey data was due to the problem of matching statistics across the various surveys as few of the survey areas overlap and in reality none of the sample sites coincide.

So in order to use the available geochemical data to delineate prospective geochemical targets using sufficient consistent sample size for neighbouring surveys, the historical geochemical data was interpolated onto a regular grid to allow the application of any of the gridding image methods. Gridded points of the historical data were used to generate the anomaly maps of the Lawra belt.

8.3.2 Gridding methods

Gridded data are the result of converting scattered individual geochemical data points into a regular grid of interpolated values ("gridding"). The surface soil geochemical data after gridding is easier to analyse and display than the original scattered points. There are five main gridding methods:

1. Inverse distant weighting (Kuijpers, 2004)
2. Minimum curvature (Carranza, 2009)
3. Triangulation (Watson, 1992)
4. Kriging (Goodchild et al., 1996)
5. Density method (Carranza, 2009)

However, in this research it was the inverse distant weighting (IDW) method that was used to create an image for the surface historical geochemical data. This method uses exact and smooth surfaces and shows the gradational changes of the assay values by its distance from the sample point or grid node being interpolated. As indicated in chapter 3, the historical geochemical data in the study area is a combined data from different exploration surveys carried out in different times by different companies. The difficulty in setting up survey grids to coincide with earlier survey grids perhaps is the cause of the fairly randomly distributed data points in the historical data. Despite the unevenly grid patterns in some localities, the IDW gridding method was able to create perfect grid images because of its ability to grid both evenly and fairly randomly uniform distributed input points across an area to be gridded. Its flexibility and reliability made it most appropriate as a method of choice for the study area. In this method each grid cell value in an output surface is calculated using a weighted average of all values surrounding it that lie within a specified search distance. The weighting values assigned to each point within a search ellipse are determined by its distance from the grid node being interpolated. The principle of IDW

interpolation reflects Waldo Tobler's first law in geography which states that "*Everything is related to everything but near things are more related than distant things"* (Tobler, 1970). This means that points which are close to an output pixel will obtain large weights and that points which are farther way from an output pixel will obtain small weights. This method is suitable for surface geochemical data where a degree of smoothing is beneficial in deciding on anomalies.

8.4 Results

For the purpose of comparing anomalous zones using the threshold Au values, the regional surface geochemical data for the selected areas, Sabala and Kunche-Bekpong were contoured. Figure 8.7 represents the gold dispersion patterns in soil survey in the Sabala area. According to Griffis et al. (2002) this area is considered unmineralized and has not seen any follow-up work after the initial regional survey carried out in the late 1990's by the Ashanti Exploration Company.

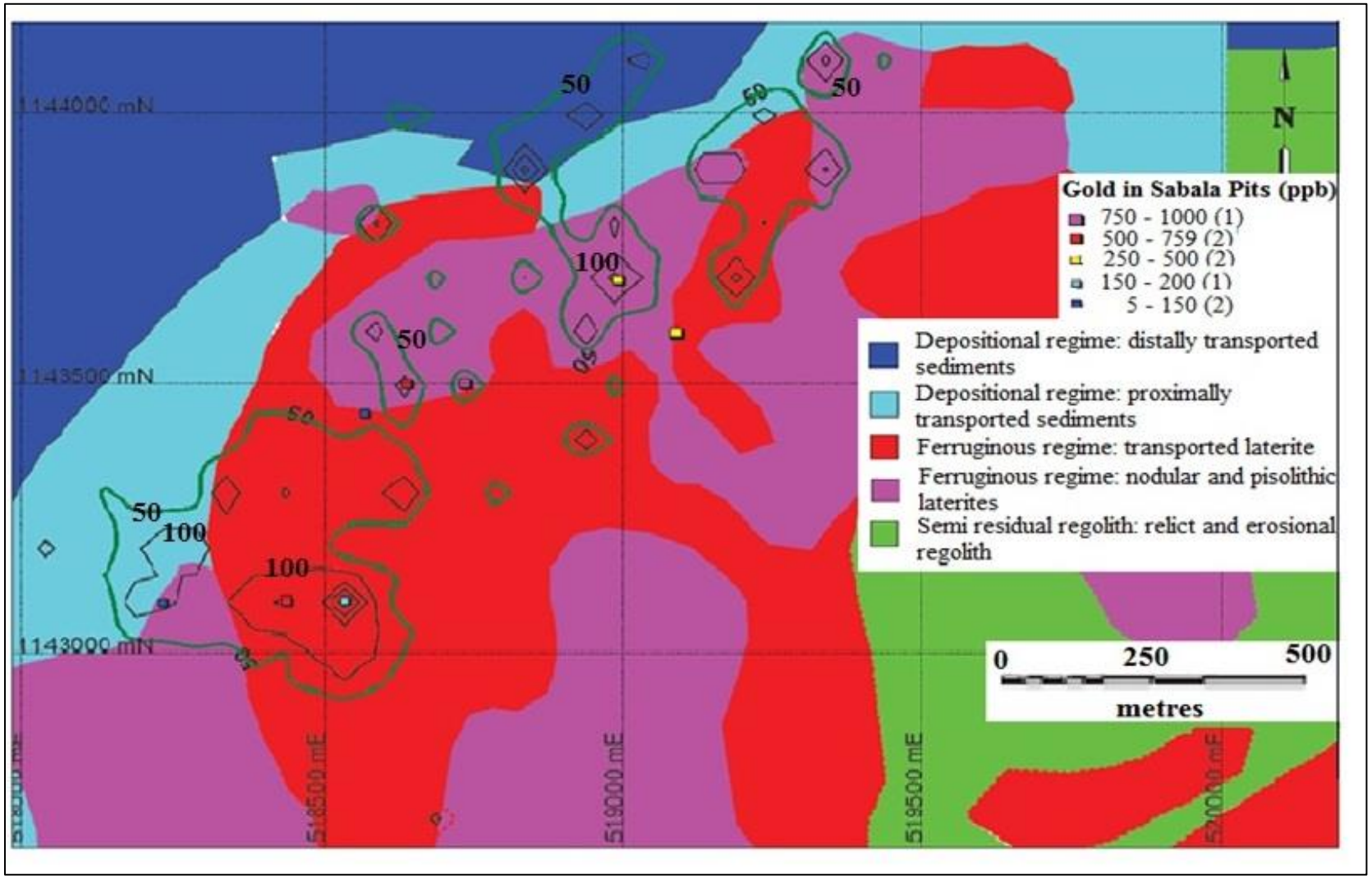

Fig. 8.7 Gold contour map of the Sabala target area.

Fig. 8.8 shows gold dispersion patterns of soils over Kunche-Bekpong regolith map. The complexity of the regolith (chapter 6) complicates geochemical data interpretation especially in areas characterized by laterite and transported sediment cover. This is demonstrated in Figs. 8.7 and 8.8. The probability plot threshold Au estimates seems lower for the different regolith regimes compared to Hawke and Webb (1962) threshold estimate approach for the same regolith domains. However the experiential threshold estimate approach with much lower thresholds can be useful in detecting hidden anomalies. The experiential method incorporates the regolith constraints on element dispersion and concentrations in anomaly definition processes. For example, in Fig. 8.7 the 100 ppb threshold defined for ferruginous regime by the probability plot method defined small anomalies of aerial extents which may not merit follow up surveys. Conversely, the 50 ppb experiential threshold was able to define much bigger anomalies with significant continuity compared to the 100 ppb threshold value. Similarly anomaly definitions set up to prioritize high assay threshold areas (e.g., like those defined by model-based subjective method) may overlook potential low concentration Au anomalies (Fig. 8.8). The Au deposit discovered by Azumah Resources Limited extends across residual, lateritic residuum and laterite cap areas as well as depositional environments (Waller et al., 2012). This suggests it is inappropriate to use a single threshold gold value for Au exploration in complex regolith terrains.

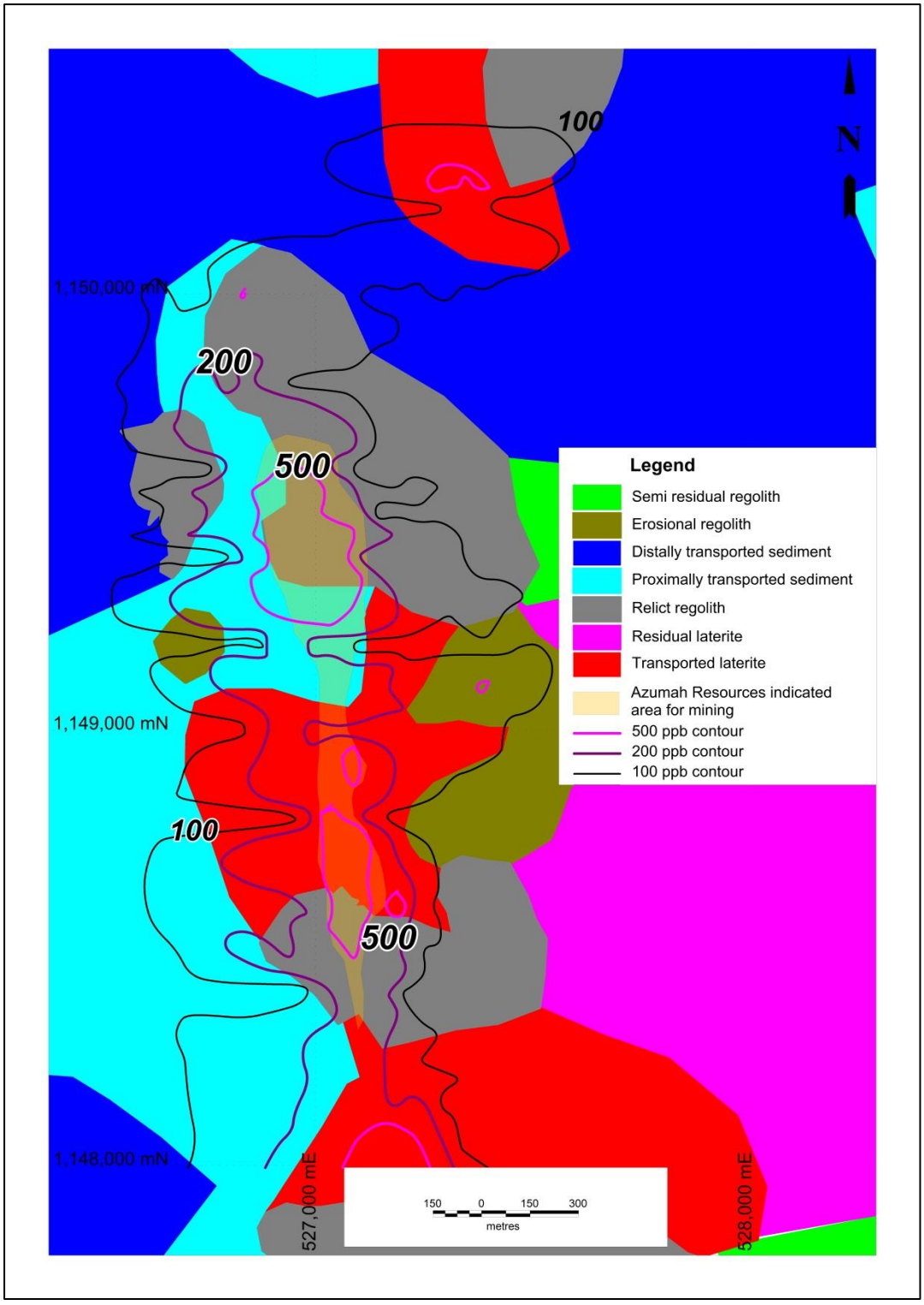

Fig. 8.8 Contour map defining target sizes from different thresholds across the different regolith domains at Kunche-Bekpong.

8.5 Gold anomaly delineation in savannah regions: a case study of the Lawra belt

In this study the prospective anomalous geochemical targets were defined by first assessing the nature of anomalies in different regolith domains. Regolith gold anomalies were interpreted with respect to regolith type. The Au-rich and Au-poor regolith materials irregularly distributed on the surface layers of the landscape normally affect the real gold signatures especially in complex regolith environments. Gold results from the regolith surface samples representing the different regolith classes are shown in Figs. 8.9-8.113. The anomaly maps show point gridded maps> A. with no application of threshold based on regolith type and B. anomaly patterns based on thresholds defined for the regolith types. The thresholds were defined from the orientation survey results.

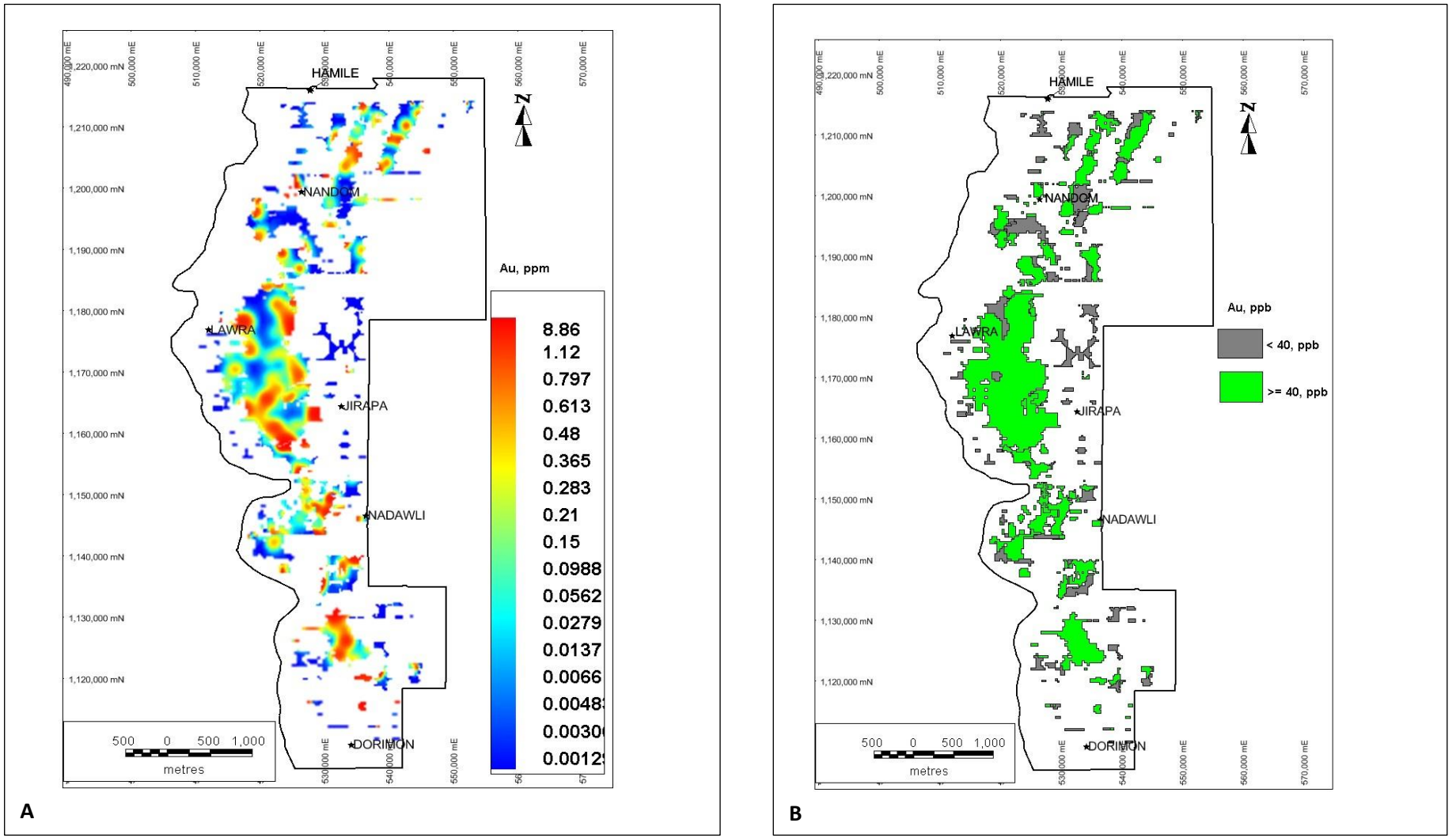

Fig. 8.9 A). Surface Au grid using IDW method in ferruginous regime B). Application of defined threshold for ferruginous regime to define prospective anomalies.

Laterites generally make up the ferruginous regime. About 22% of the study area is covered by laterite (chapter 5, Fig. 5.18). The laterite from the regolith map, as shown in Fig. 5.17, constitutes both residual and transported laterites (Fig. 5.18). The transported laterite covers about 18% of the ferruginous regime with 4% making up the residual laterite. The Fe oxide cemented colluvial or alluvial sediments that form the transported laterite or ferricrete (chapter 6) have quite different origins hence cannot be used as sample media. As seen in Fig. 8.9 A patchy, subtle and isolated anomalous areas are portrayed which could be due to the encrustation of fine detrital gold during the lateritization process and probably the masking effect from the transported laterites originating from barren lateritized source in the regime. However, broader and continuous anomaly definitions are seen in Fig. 8.9 B, which may be useful to test for hidden anomalies at the early stages of the exploration. The sample preparation methods (chapter 4) used in the area sieve the samples to 2 mm and perform Fire assay (chapter 7) on <125 μm size fractions. The encrusted detrital Au grains may be sieved out during the preparation process resulting in only a fraction of Au content in the areas sample being analysed. The other cause of low concentration Au assays in the hardened ferruginized units probably may be due in part to the improper analytical technique applications, especially the commonly used partial analysis by exploration companies instead of total analysis.

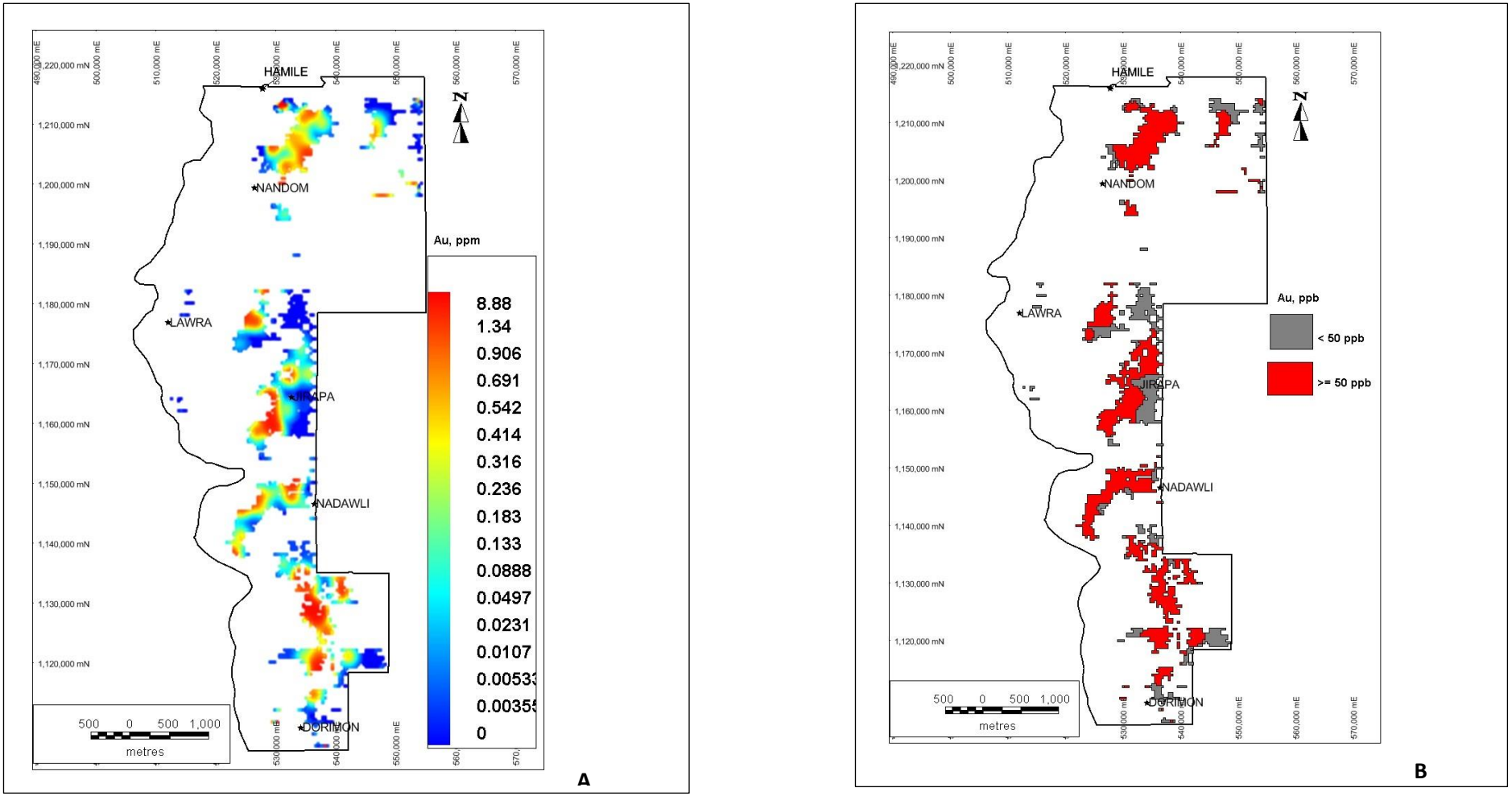

Fig. 8.10 A). Surface Au grid using IDW method in relict regime B). Application of defined threshold for relict regime to define prospective anomalies.

The relict regime covers about 22% of the entire study area (chapter 5, section 5.3.2.2, Fig. 5.17). The high Au areas >500 ppb in this regolith regime appear patchy and small in size (Fig. 8.10 A). These types of anomalies based on size alone may not merit further exploration when compared to anomalies in southern Ghana where the search methodology was transferred from. The anomalies in the relict areas seem to exhibit spot-high-discontinuous anomalies that reflect the patchy occurrence of the relict regimes or could be due to the secondary modification of the surface layer by lateritization to produce duricrust. The developed duricrust in relict environments can get Au grains to be coated by Fe-oxide and clay minerals during the lateritization processes and may as well serve as a barrier between the underlying mineralisation and the thin veneer of soil overlying the duricrust which is sampled during surface geochemical survey. However to define continuous anomalies in the area the understanding of the regolith will be essential to guide the selection of an appropriate threshold. As identified in the study threshold defined by the probabilty plot (40 ppb) or experiential method (50 ppb) may be necessary to detect anomalies in the relict regime instead of high threshold. Fig. 8.10 B thus shows continous anomalous size and may merit follow up surveys than the spot-high anomalies shown in Fig. 8.10 A.

The erosional regime mapped during the study shows only 2% coverage of the Lawra belt (Fig. 5.17). The spot-high Au areas in the erosional regime are not contigous (Fig. 8.11). The speckled Au geochemical patterns of this regime is probably due to the dominance of the flood plain of the Black Volta River covering most low-lying areas to the west. The immediate east of the Lawra belt is a north-south-trending ridge of moderate elevation between 350-450 m (Dickson, 1972). The interpreted Au results appraised from the historical surface geochemical data are mostly along the moderate elevation ridge trend (Fig. 8.11). Apart from this regional gradient the entire Lawra belt is relatively flat country with minor relief provided by a few low-lying ridges (some due to quartz veins and silicification) and isolated hills (many protected by a laterite cap). Transported sediments from Black Volta, other streams and sheetwash deposits probably dilute Au assays along their trails resulting in gaps of low or no significant Au assays inbetween the spot-high anomalies seen in the Au geochemical grid image (Fig. 8.11 A). Similar anomalous patterns were defined using the defined threshold value. This may be due to the limited exposed surfaces in the study area. However the anomalous patterns using threshold value will vary if most areas of the Lawra belt is characterised by erosional regolith because of the different regolith units and geochemical dispersion processes characterising the erosional environments. The limited

exposed erosional surfaces mapped (chapter 5) suggests most part of the Lawra belt is under depositional landforms (Figs. 5.17 & 5.18). The likelihood of streams/rivers and sheetwash deposits covering the pre-existing preserved and erosional surfaces can not be over estimated and that the diversity of regolith should be incorporated in the exploration search methodologies if hidden Au anomalies are to be delineated. For instance as seen in Fig. 8.11 spot-high anomalies defining vaguely a northwest trending anomaly needs not be treated spurious but should be followed up.

The depositional environments (Fig. 8.12, Fig. 5.18) covers about 54% of the Lawra belt and consist of 24% distal sediment and 30% proximal sediments (chapter 5, section 5.3.2.2, Fig. 5.17). Gold assay results from the transported sediments represent transported anomalies from diverse sources. The variable gold distributions that showed several single spot-high anomalies (Fig. 8.12 A) surrounded by background assays is due to the evolution of the regolith that transforms the original homogeneous regolith to complex heterogeneous regolith. The causes of these anomaly patterns may be due to chemical and mechanical fractionation of elements during weathering (Scott and Pain, 2008) resulting in detrital dispersion in the surface regolith. The distribution of Au by this process will be erratic depending on the water velocities and nature of transported sediments (chapter 3). The ionic diffusion may contribute very little to the Au anomaly patterns formed because the Au anomaly generation takes place in water saturated zones. Rainfall is low and occurs in a short single rainy season (Dickson, 1972) hence water saturated zones are generally uncommon. Another Au anomaly generation is formed by capillary process, which contribute also to Au geochemical patterns shown in Fig. 8.12). However this process may be counteracted in porous sands by the seasonal influx from rainfall but could be greater, albeit slower in clays where the grain size is smaller and the inflitration is less. Lastly bioturbation by burrowing termites is powerful mechanism to bring Au and other regolith particles from depth to the surface. Arhin and Nude (2010) attribute the generation of many of Au anomalies in the depositional environment in the study area to this process.

Considering the different mechanisms mobilizing and concentrating Au in the regolith it will be difficult to distinguish which anomaly in this area is related or close to the underlying mineralisation. The geochemical anomaly patterns shown when the unique threshold defined for depositional regime showed broader size and relatively contigous anomaly patterns (Fig. 8.12 B). The anomalies coincident with controls on known mineralisation in the study area that persist for a longer distance should be subjected to auger or rotary airblast (RAB) drilling

for concealed mineralisation. The differences in anaomly patterens in FRED regimes require the prediction of reliable Au anomalies to undertake studies to aid in the understanding of mechanisms that are responsible for dispersing ore and pathfinder indicator elements through transported cover. The combined anomalies defined from the different regolith domains is shown in Fig. 813.

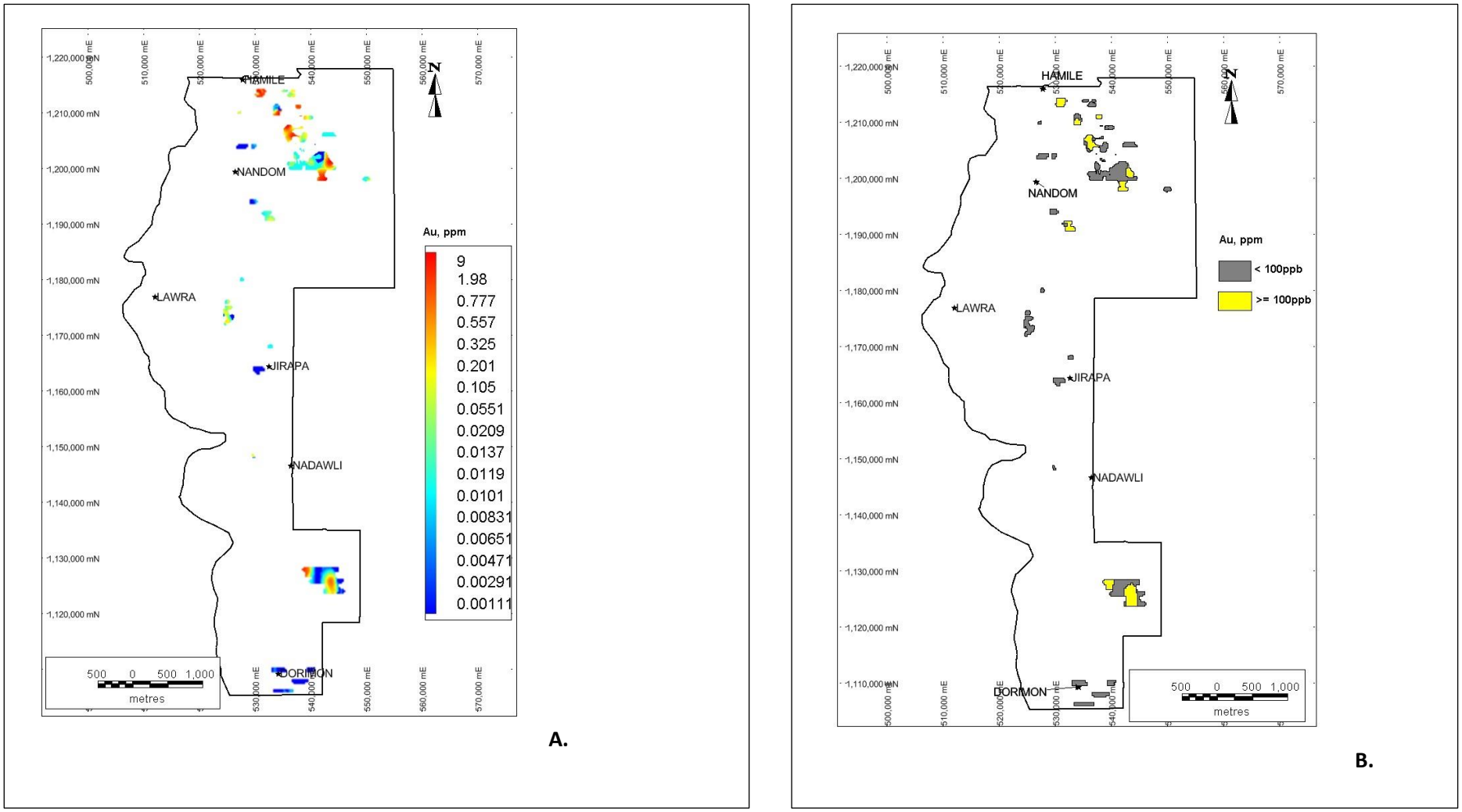

Fig. 8.11 A). Surface Au grid using IDW method in erosional regime B). Application of defined threshold for erosional regime to define prospective anomalies.

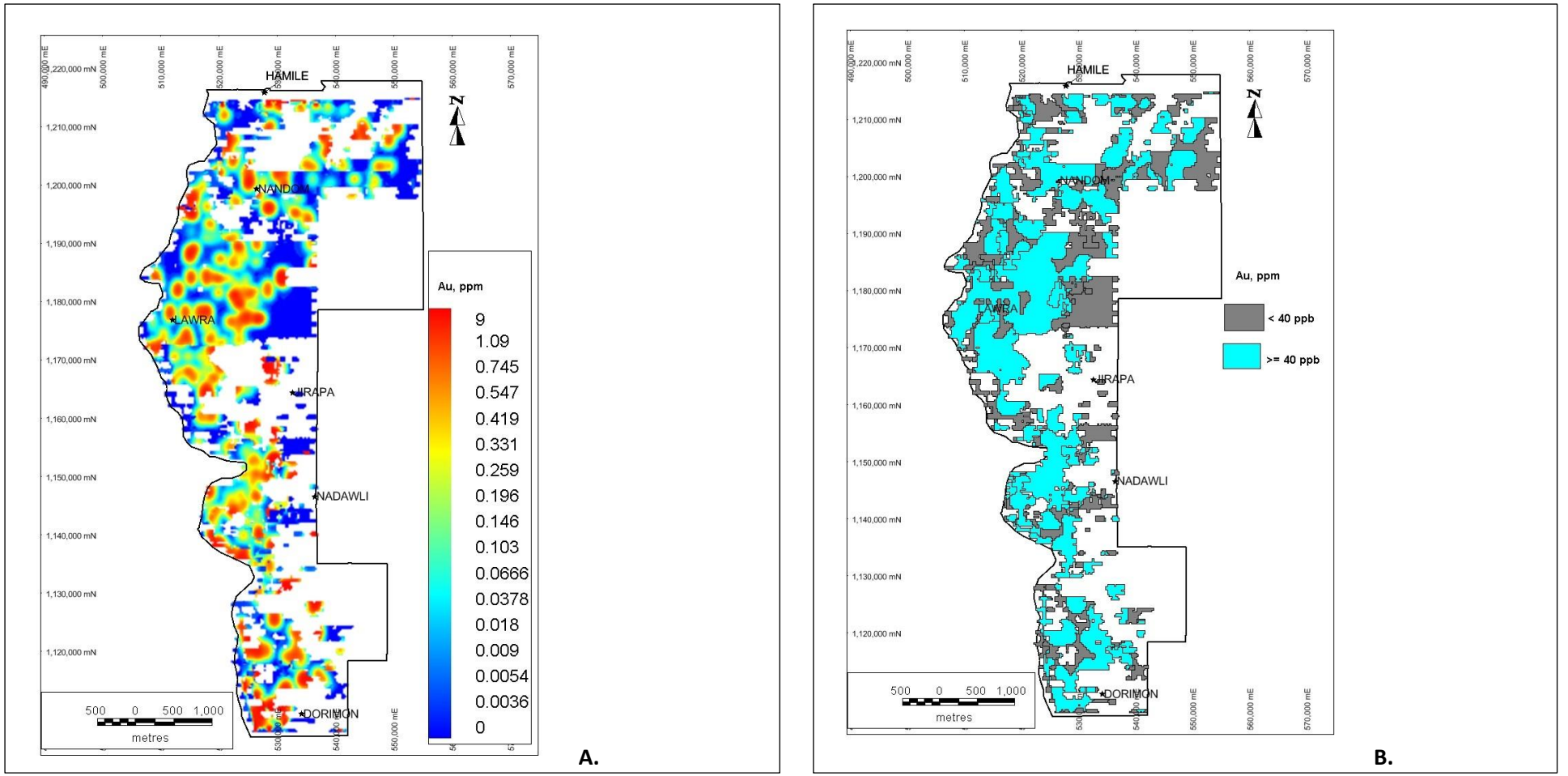

Fig. 8.12 A). Surface Au grid using IDW method in depositional regime B). Application of defined threshold for depositional regime to define prospective anomalies.

The anomalies in the different regolith were manipulated, integrated using the same map datum and projection in GIS interface to create a combined map that showed the prospective areas in the Lawra belt (Fig. 8.13). The minimum assay limits that defined the anomalies in the deferrent regolith regimes were smoothed and integrated during the manipulation of the surface geochemical data. The map layers defining anomalies and non-anomalous areas for the different regolith regimes after the manipulation were merged using the same projection and map datum. The method of merging the anomalies defined in the different regolith regimes gave each anomaly equal chance of hosting mineralisation irrespective of the individual gold values recorded in the individual samples. Prioritization of potential anomalies then became easier in this sense as the implications of the regolith had already been factored into the anomaly status. The prospective anomalous areas are shown in different colours to depict anomalies defined by different thresholds derived for the regolith domains (Fig. 8.13 B).

Anomalies defined from the surface Au geochemistry in Fig. 8.13 A show several discontinous anomalies many of which are unrelated to bedrock mineralisation, e.g. Duri and Basabli anomalies (Waller et al. 2012). These were identified during recent RC drilling programme to define additional orebodies (Franey, 2013-Personal communication). The known mineralisation areas Kunche and Bekpong seem to have weaker surface Au geochemistry (Fig. 8.13 A) compared to anomalies defined in Duri and Basabli when regolith constraints were not considered. Follow up exploration surveys normally in less complex regolith terrain may conduct follow up surveys in the "red" areas shown in Fig. 8.13 A since Au in soils are higher compared to the blue areas. However in areas under cover such as the study area (Fig. 5.16), some of the anomalies may be residual whilst others may be transported. The mechanisms that transport Au from the bedrock source may be acted upon by both physical and chemical dispersions. These processes may enhance and dilute surface Au geochemistry and thus make anomaly delineation challenging if regolith environment is unknown. True anomaly delineation may be detected by interpreting surface geochemical data with respect to the regolith type. Demonstration of that method of detecting anomalies under cover is shown in Fig. 8.13 B. Broader and continuous anomalies are defined by the different threshold Au values estimated for the various regolith regimes. Anomaly prioritization for follow up surveys can be decided on with ease based on regolith type, size and continuity of the anomaly.

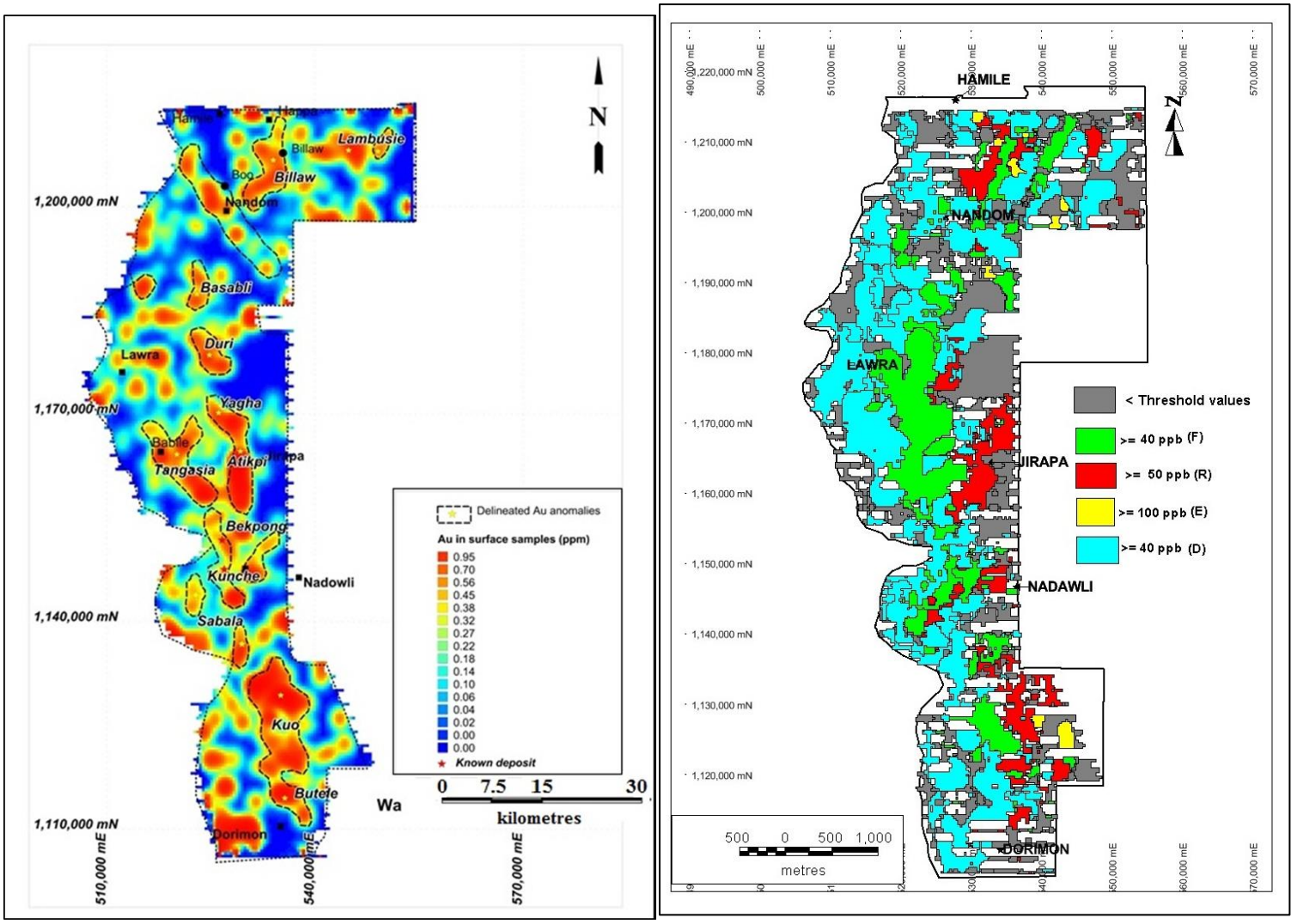

Fig. 8.13 A). Merged surface Au grid of different anomalies in different "FRED" regolith domains B). Definition of anomalies regarding regolith implications on Au mobility in surface regolith.

8.6 Discussion

Figs. 8.3–8.6 and Table 8.1 show that selecting background and threshold values of Au, regardless of the media type, can be difficult, because of its "nugget-like" behaviour and its non-normality. Hence the assumption of normality of data suggested by Hawkes and Webb, (1962) is violated by the geochemical datasets obtained for the study area. Therefore the use of any type of parametric or even non-parametric method that estimates background and threshold values for Au in any automatic way may have challenges in detecting true and reliable anomalies without follow-up surveys of some 'false' anomalies. However in this research the q-q plots threshold alone was not able to describe the distribution of the data because of the regolith evolution.

In this study, a careful examination of the q-q plots or normal probability plots showed where "breaks" occur. These breaks generally separate out the various background contributions as well as those values associated with mineralization. In the case of the ferruginous regolith profile (Fig. 8.3), there are natural breaks at ~ 101, 200, 300 and 400 ppb. Thus, there are potentially 4 populations that may reflect values that are associated with various parent materials and/or mineralisation. In the case of the relict regolith (Fig. 8.4), there is a break at ~40 ppb, but there are too few samples to make any meaningful estimate beyond this. This was expected because most of the Lawra belt is overlain by transported regolith (Fig. 5.16) and only 22% of the area is characterized by a relict regime (Figs. 5.17 & 5.18). For the erosional regolith (Fig. 8.5), there are natural groupings at ~ 504 and 1004 ppb. The depositional regolith (Fig. 8.6) shows a fairly continuous, almost "normal" distribution. There is a possible break at ~45 and 65 ppb, however, the 65 ppb appears very high considering dilution from distant transported sediments that may be unrelated to mineralisation.

Conversely the evaluation of the orientation survey data shows not too much difference between the average assays of ferruginous and relict regimes (Figs. 8.3 & 8.4). However there is a vast difference between the averages of erosional regime (Fig. 8.5) and the other regimes. This suggests that the use of single threshold value for anomaly delineation in complex regolith environment may not be able to detect mineralisation in all regolith regimes. Threshold Au values estimated by model-based subjective statistical approach alone cannot detect anomalies in ferruginous and depositional areas as indicated in Table 8.1. However, the Au deposit discovered by Azumah Resources Ltd. in the study area extends

across relict, erosional, ferruginous and depositional areas (Fig. 8.8). It therefore appears that the combined use of probability q-q plot and experiential estimate approach in anomaly delineation is appropriate to define anomalous areas in areas under cover.

8.6.1 Identifying geochemical gold anomalies

The global geochemical plot where regolith constraint was not considered in anomaly delineation as shown in Fig. 8.1 has maximum Au assay of 2.87 ppm. Threshold Au values used in exploration in southern Ghana is normally ≥0.2 ppm. It is likely that the same threshold has been used by companies that worked here because there is report of wholesale transfer of exploration methodology from southern Ghana to northern Ghana (Arhin and Nude, 2009; Griffis et al., 2002). If this is done then anomalies in ferruginous and depositional areas may be overlooked. Besides, the high Au assays shown in Fig. 8.1 occur in a much bigger area mapped to be overlain by both relict and erosional regolith. This implies some of the high areas have been influenced by the regolith. The anomaly types need to be distinguished if mineralisation is to be discovered because many of the high assays may be unrelated to mineralisation. Independent classifications of anomalies in the various regolith regimes appear to address the problem of following false anomalies. The principle in this approach is given anomalies in each regolith regime equal chance of hosting mineralisation and it thus works by incorporating the implications of regolith on element dispersions and concentrations. The anomalies defined by estimated thresholds for the FRED regimes can detect mineralisation. The traditional use of single high threshold values often results in under exploration generally in areas under cover because of the usual low Au expressions. As seen in the study anomalies in ferruginous, relict and depositional regimes will be overshadowed by the high threshold usually set for anomaly delineations where regolith constraints are not considered. However the approach of defining anomalies independently in the different regolith regimes before merging the individual anomalies together as one in the study showed the prospectivity of Au mineralisation (Fig. 8.13 B) compared to the global plot in Fig. 8.1.

The challenge of prioritizing the prospective anomaly for follow up survey is also reduced because of the understanding of the regolith environment. Anomalies that fall into less modified regolith from the parent material and showed continuous and consistent high anomalies are followed up first. In this case anomalies in erosional and relict regimes are the first priorities if associated with high assays and big aerial coverage. Similarly anomalies in

ferruginous and depositional regimes with comparable anomalies are also given the same attention. As indicated by Cohen et al. (2010) Au anomalies can be detected in all forms of regolith environments. As seen in the study the average Au assays obtained in the orientation survey samples were 64 ppb for ferruginous, 68 ppb for relict, 379.6 ppb for erosional and 54 ppb for depositional regimes. The averages showed the erosional regime to have high Au assays with low Au assay in the depositional regime (Figs. 8.3–8.6). It does not imply that Au anomaly cannot be found in the low concentration areas but if the regolith environment is not understood the concealed anomalies in the low concentration environments occurring mostly in depositional and ferruginous laterite areas may go undetected. The Au deposit discovered in the study area by Azumah Resources Ltd. has mineralisation occurring in the four regolith domains (Fig. 8.8). Earlier companies that worked in the area interpreted the geochemical data without considering the implications of the regolith and thus found the area to be less prospective. In this study equal weights of importance were assigned to anomalies in the different regolith types and were prioritised based on their relationship to the parent mineralisation for follow up survey by integrating the regolith map to the geochemical plots. With this approach many more prospective anomalies have been delineated (Fig. 8.13 B) that requires follow up investigations with the objective of discovering more Au deposits.

8.7 Conclusions

The study therefore concludes that surface geochemical data should be considered separately with respect to different regolith regimes. The importance of interpreting surface geochemical data separately for all regolith domains is that high Au assays do not imply mineralisation. High Au assays can be displaced through detrital dispersion. Similarly potential mineralisation can be masked by transported Au-poor sediments. All these are products of regolith-landform evolution processes. So to really define realistic anomalies that relate to mineralisation, equal weights of importance should be accorded to anomalies defined by the different thresholds estimates for the different regimes. Therefore for threshold estimations in complex regolith environments, no single threshold value should be used as it often overlooks the subtle anomalies at low concentration Au areas. So as noticed in the study, the experiential method of estimating threshold should be applied on geochemical data from the different regolith regimes separately for the threshold estimates. This approach is useful for grass root exploration and the probability plot approach can be used to estimate thresholds for follow up surveys. Threshold values of 40 ppb for ferruginous, 50 ppb for relict, 100 ppb for erosional and 40 ppb for depositional regimes are proposed for Au exploration in the Lawra

belt. All these thresholds if applied with better understanding of the regolith environment can lead to the discoveries of the hidden deposits. Discrepancies may only occur in the anomaly expressions whilst some anomalies are robust with high assays others will be subtle. The considerations of the regolith effects on element mobility and concentrations and the use of different threshold values for the various regimes helped to delineate more anomalous Au targets of interest (Fig. 8.13) similar to the anomalies that defined Kunche and Bekpong deposits. In addition the prioritization of the defined anomalies for follow up survey can be done by integrating the regolith map and the geochemical datasets. It is concluded that the proper interpretation of regolith geochemical data and the understanding of the regolith environment are useful to delineate Au mineralisation in areas under cover.

Thesis conclusion

9.0 Limitations of thesis

The results obtained for the scanning electron microscopy (SEM) and XRD studies to obtain the grain morphologies and clay content types of the regolith samples were performed on sieved regolith materials so the SEM and XRD techniques were unable to provide the true information of the regolith which could have been useful in determining the shapes of the regolith materials used in determining the origin and mineralogy of regolith. Additionally, the study had to infer the bedrock mineralisation from work done by Azumah Resources Ltd instead of collecting samples from bedrock to ascertain the mineralisation in the current study. This limitation made it difficult to establish the relationship between Au and other elements especially with As in the bedrock and the overlying regolith. Finally the limited funding made it difficult to insert more certified reference materials for the multielements to check the analytical qualities of the data. Despite these limitations, the following conclusions were established from the study.

9.1 Conclusion

True anomaly follow-ups are a prerequisite for all successful exploration surveys. This requires discriminating transported regolith from residual types. The conclusions drawn in the research suggest the following should be carried out for the successful delineation of hidden anomalies in complex regolith terrains.

- Regolith studies at the beginning of exploration to include regolith mapping and characterisation. The regolith mapping should be consistent with the methods used in this research.
- Classification of the regolith domains should use "FRED" classification scheme.
- Pit digging to expose the concealed regolith profiles should follow immediately the "Genesis classification" of regolith mapping units.
- Fe/S ratios can be used by novices in regolith mapping to speculate the regolith horizon boundaries but actual limits of the horizons can be logged in the pits.
- Assessment of the regolith evolution to establish evidence of landscape modification should be carried out alongside the regolith mapping.
- The relationship between Au and Ag is useful in determining mechanisms of element mobility in the regolith. High Au-low Ag relates to a residual anomaly whereas high Au-high Ag represents transported anomalies. Use this relationship to reduce following many "false" anomalies
- Threshold Au values should be calculated for different regolith-types. Calculated thresholds should be used to normalize the geochemical data separately so that equal

weight of importance can be applied to the different geochemical data with respect to the regolith-types

- Contour maps from regolith-type based on threshold Au values and density grid image plots from normalized geochemical data can be used to prioritize prospective anomalies for follow-up surveys

The establishment of an appropriate sampling preparation protocol for laterite samples considering implications of lateritization as it encrusts the fine grain gold is vital. These should form the basis of any laterite geochemistry research in the near future. Additionally evaluation of the data should include multi-element analysis as some of the elements may have relationship to Au mineralisation and can be used as pathfinder element for Au exploration. Robust gold anomalies in the study area are rare because of the extensive depositional regolith that dilutes geochemical anomalies. Therefore through the identification of pathfinder elements in the multi element data possibly may lead to the delineation of Au anomalies concealed by the complex regolith.

9.2 Future outlook

This research aimed at helping exploration geologists to delineate mineralisation under cover in complex regolith terrains. It has been able to outline steps in developing regolith maps; highlighted the role of regolith in exploration and showed the importance of geochemical dispersion of Au and other associated elements in the regolith. However, it was not able to establish a model for distinguishing between transported laterite from residual laterite. Using residual laterite as a sample media in areas under cover is essential.

Appendix A: Regolith landform mapping codes

LANDFORM		**REGOLITH UNIT**		**SURFACE CRUST**		**COLOUR**	
Erosional rise	**ER**	***Unit***	***code***	None	**0**	Red	**R**
Smooth slope	**SS**	Clay-rich bedrock (undifferentiated)	**c**	Iron	**1**	Green	**G**
Dissected slope	**DS**	Non-cracking clay bedrock	**k**	Carbonate	**2**	Blue	**B**
Open wash	**OW**	Cracking clay bedrock	**s**	Sulphate	**3**	Yellow	**Y**
Unconfined stream	**CH**	Quartz rich bedrock	**q**	Halite	**4**	Brown	**Bn**
Smooth plain	**EP**	Silty sediment	**l**	Bauxitic	**5**	Ochre	**O**
Rough plain	**DP**	Sandy sediment	**a**			Olive green	**OG**
Erosional stream terrace	**ET**	Gravel	**g**	**GEOMORPHIC FEATURES**		***Modifier***	
Alluvial plain	**AP**	Boulders	**b**			Light	**l**
Talus deposit	**TA**	Silt+ sand	**la**	Structural landform	**L1**	Dark	**d**
Colluvial fan	**FC**	Silt+ gravel	**lg**	Weathering landform	**L2**		
Aeolian plain	**WP**	Silt+ boulder	**lb**	Erosional landform	**L3**	**BOUNDARY TYPE**	
Hill top	**HT**	Sand+ boulders	**ab**	Depositional landform	**L4**	Sharp	**sh**
Hill slope	**HS**	Sand+ clay	**ac**			Gradational	**gr**
Base of hill	**BH**	Polymictic sediment	**pm**	**HORIZON TYPE**		Diffuse	**df**
Laterite	**LC**	Laterite lag	**ll**	Upper soil	**us**	Undifferentiated	**ud**
		Pisolithic soil	**ps**	Laterite cap	**lh**		
		Duricrust	**dc**	Mottled zone	**mc**		
		Ferricrete	**fc**	Pallid zone	**pz**		
		Mottled clay	**mz**	Saprolite	**sp**		
		Saprolite	**sr**	Bedrock	**bh**		
		Indurated laterite	**il**				

Appendix B: Sample preparation protocols for the XRF analysis at the University of Leicester, Geology Department, UK.

I. Pressed pellets preparation for XRF analysis

Seven (7) g of the milled powder was placed into a small plastic beaker and then weighed using a beam balance. Eight-ten drops of Moviol 88 solution binding agent was added to the 7 g weighed powder; just enough to bind the powder together in small lumps. The binding agent was used only for mechanical stability. However, the amount of binder required to stabilize the pellets depends on the rock type and the abundance of clay minerals. This usually varies from about 8-12 drops for basic rocks to 15-20 drops for very low-density acidic rocks. In this study the materials analysed were regolith materials that consist of weathered materials from both basic and acidic rocks. So 10 drops of the binding agent was used. The mixture of the powder and the binding agent was then placed in a die (cylindrical hollow metal of about 2 cm in diameter). The surface of the die was smoothed, and the top of the die as well as the plunger were then placed inside an automatic hydraulic press. The press of the complete die was set on a 50 ton ram pressure. The die was removed when it was no longer under pressure. The pressed die was inverted after removal and replaced on the small manual press with the aluminium ring in place of the bottom section, where the pellet was pushed out of the barrel section of the die. The hydraulic press was also used occasionally to remove the clay-rich pellets.

The removed pellets were placed on a rack to dry for a minimum of 3 - 4 hours. As a quality assurance precaution, all the equipment used was thoroughly cleaned between samples, and after use, with damp tissue and then thoroughly dried with dry tissue, to avoid contamination. The dried pellets were labelled and the pellet numbers written in pencil on the side, in preparation for XRF analysis.

II. Fusion beads preparation for XRF analysis

The fusion beads were prepared by measuring about 4 to 5 grams of the sample powder into a 10 ml glass vial. The vials were labelled using a felt tip marker pen with sample number. The measured sample powders were dried overnight in a drying oven at 110^{o}C to remove low-temperature absorbed volatiles. The dried sample powders were then stored in desiccators. To avoid sample loss through spillage and cross contamination, plastic snap tops were put on the vials.

The cooled samples were measured again to determine the weight loss during ignition (LOI). This was performed in fused Al_2O_3 (ALSINT) ceramic crucibles. The weight of the crucible (W1) and the combined weights of the crucible plus sample before (W2) and after ignition (W3) were recorded. The ignitions were performed in a muffle furnace at 950^{o}C for between 60 to 90 minutes. The ignited samples were allowed to cool to a room temperature in desiccators before reweighing. The reweighed ignited powders were then transferred to a clean 10 ml glass vials with plastic snap tops for storage again in desiccators. This was done prior to fusion beads preparation. The percentage weight loss (LOI) was subsequently determined using the following formula:

LOI = 100*(W2 - W3)/ (W2 - W1)

ICP-MS

ICP-MS is an acronym for Inductively Coupled Plasma-Mass Spectrometry. It is a fast, accurate and extremely sensitive multielements analytical technique. It is used for the determination of trace elements in a variety of liquid and solid sample materials. In a typical ICP-MS application the samples are placed in solution by acid digestion. The solution is sprayed into flowing argon and passed into a torch which is inductively heated to approximately 10000^{o} C. At this temperature, the gas and almost everything in it is atomized and ionized forming plasma which provides a rich source of both excited and ionized atoms. The chemical analysis is based on the principles of vaporisation, dissociation and ionization of chemical elements when introduced into the hot plasma. The positive ions in the plasma are focused down a quadruple mass spectrometer. These ions are separated according to their mass/charge ratios by a high resolution magnetic sector mass analyser. The signals of element concentrations detected are counted using fast digital electronics. This method has low detection limits for most multielements analysis of solids, solutions and slurries to part per trillion (ppt) levels in a variety of matrices samples.

ICP-AES

The ICP-AES is composed of two parts: the ICP and the optical spectrometer. This analytical technique is a well-established and cost effective technique for multielements analysis. Samples (in solution) are introduced as an aerosol into a plasma at temperatures in the order of 6000-10000^{o} C. In this analytical method, the aqueous sample is pumped and atomized with argon gas into the hot plasma. This process effectively converts the elements present to

gaseous atoms, which are elevated to excited states. As the atoms “relax” to a lower excited or “ground” state they emit light radiations at characteristic wavelengths of its elements. A mirror reflects the light through the entrance slit of the spectrometer onto a grating that separates the element wavelengths onto a photo multiplier tube. A computer converts the electronic signal from the photomultiplier tubes into concentrations. The intensity of the emission is indicative of concentration of the element within the sample. The ICP-AES is best suited for elements in low weight per cent to parts per million concentrations range and has particular advantages over ICP-MS for some elements such as Na, K, Ca, and S.

REFERENCES

Abouchami, W., Boher, M., Michard, A., and Albarede, F., 1990, A major 2.1 Ga event of mafic magmatism in West Africa: an early stage of crustal accretion. J. Geophys. Res. 95 (B11), 17605–17629.

Agyei Duodu, J., Loh, G. K., Boamah, K. O., Baba, M., Hirdes, W., Toloczki, M., and Davis, D. W., 2009, Geological map of Ghana 1:1,000,000; Geological Survey of Ghana, Map 1:1 M.

Allibone, A., Hayden, P., Cameron, G., and Duku, F., 2004, Palaeoproterozoic gold deposits hosted by Albite and Carbonate-altered Tonalite in the Chirano District, Ghana, West Africa. Economic Geology, vol. 99, no. 3; p. 479-497; DOI: 10.2113/99.3.479.

Allibone, A., Teasdale, J., Cameron, G., Etherridge, M., Uttley, P., Soboh, A., Appiah-Kubi, J., Adanu, A., Arthur, R., Mamphey, J., Odoom, B., Zuta, J., Tsikata, A., Pataye, F., Fameyeh, S., and Lamb, E., 2002, Timing and structural controls on gold mineralisation at the Bogoso gold mine, Ghana, West Africa. Economic Geology, vol. 97, p. 949-969.

Amanor, J. A. and Gyapong, W. A., 1991, 'The geology of Ashanti Goldfields. In: G. O. Kesse (Editor), Proceedings of International Conference on the Geology of Ghana (1988), p. C1 – C18.

Ambrosi, J. P., 1984, Pétrologieet Géochemied'une sequence de Profils Latêritiques Cuirassés Ferrugineux de la Rêgion de Diouga, Burkina Faso: unpublished Ph.D. thesis, University of Poitiers, 223 p.

Amedofu, S.K., 1995, Gold in Ghana. Pangea 23, p. 5–14.

Anand, R. R and Pain, M. 2002, Regolith geology of the Yilgarn Craton, Western Australia: implications for exploration, Australian Journal of Earth Science, vol. 49, p. 3-163.

Anand, R. R. 2001, Evolution, classification and use of ferruginous regolith materials in gold exploration, Yilgarn Craton, Western Australia: Geochemistry: Exploration, Environment, Analysis, vol. 1, p. 221-236.

Anand, R. R., and de Broekert, P., 2005, Regolith-landscape evolution across Australia: Thematic Volume CRC LEME Perth, 354 p.

Anand, R. R., and Pain, M., 2002, Regolith geology of the Yilgarn Craton and its implications to exploration: One paper thematic issue of the Australian Journal of Earth Sciences, vol. 49, p. 3-164.

Anand, R. R., Wildman, J.E., Varga, Z. S. and Phang, C., 2001, Regolith evolution and geochemical dispersion in transported and residual regolith– Bronzewing gold deposit: Geochemistry: Exploration, Environment, Analysis, vol. 1 (12), p. 256–276.

Anand, R. R., Churchward, H. M., Smith, R. E., Smith, K., Gozzard, J. R., Craig, M. A. and Munday, T. J., 1993**,** Classification and Atlas of Regolith Landform Units – Exploration Perspectives for the Yilgarn Craton. CSIRO/AMIRA Project P240A, CSIRO Division of Exploration Geoscience, Restricted Report 440R (Re-issued as Open File Report **2**, CRC LEME, Perth, 1998).

Anderson, S. P., Dietrich, W. E., and Brimhall, G. H., 2002, Weathering profiles, mass-balance analysis, and rates of solution loss: linkages between weathering and erosion in a small, steep catchment. Geological Society of America, Bulletin, vol. 114, p. 1143-1158.

Andrade, W. O., Machesky, M. L. and Rose, A. W., 1991, Gold distribution and mobility in surficial environment, Carajas region, Brazil: Journal of Geochemical explor., vol. 40 (1-3), p. 95-114.

Arhin E., and Nude P. M., 2009, Significance of regolith mapping and its implication for gold exploration in northern Ghana: a case study at Tinga and Kunche. Geochemistry: Exploration, Environment, Analysis, vol. 9, p. 63-69.

Arhin E., and Nude P. M. 2010, Use of termiteria in surficial geochemical surveys: evidence for < 125 μm size fractions as the appropriate media for gold exploration in northern Ghana: Geochemistry: Exploration, Environment and Analysis, vol. 10, p. 401-406.

Azumah Resources press release December, 2010, Multiple new zones discovered at Wa gold Project: http//www.azumahresources.com.au/press releases.

Azumah Resources press release June, 2011, Numerous promising targets now being drilled as part of wider exploration push at 1.2 M Oz Wa project: http//www.azumahresources.com.au/press releases.

Bailie, N., and Arhin, E., 2000, Terminal report on geology and mineralization of Tinga-Wa projects, SEMAFO Gh. Prepared for Ghana Minerals Commission (unpublished technical report).

Bamba, O., Parisot, J. C., Grandin, G., and Beauvais, A. 2002, Ferricrete genesis and supergene gold behaviour in Burkina Faso, West Africa: Geochemistry: Exploration, Environment, Analysis, vol.2, p.3-13.

Baratoux, L., Matelka, V., Naba, S., Jessell, M. W., Grégoire, M., and Ganne, J., 2011, Juvenile Palaeoproterozoic crust evolution during the Eburnean orogeny (~2.2-2.0 Ga), Western Burkina Faso. Precambrian Research, vol. 191, p. 18-45.

Beauvais, A., Ruffet, G., Henocoque, O., and Colin, F. 2008, Chemical and physical erosion rhythms of the West African Cenozoic morphogenesis: the ^{39}Ar-^{40}Ar dating of supergene K-Mn oxides. Journal of Geophysical Research 113, doi: 10.1029/2008JF000996.

Béziat, D., Dubois, M., Débat, P., Nikiéma, S., Salvi, S. and Tollon, F., 2008, Gold metallogeny in the Birimian Craton of Burkina Faso. Journal of African Earth Sciences, vol.50, p. 215-233.

Blain, C., 2000, Fifty-year trends in minerals discovery-commodity and ore-type targets: Exploration and Mining Geology, vol. 9, p. 1-11.

Boeglin, J. L. 1990, Évolutions minéralogique et géochimique des cuirasses ferrugineuses de la région de Gaoua. (Burkina Faso). PhD Thesis, Institut de Géologie, Université Louis Pasteur, Strasbourg. 188 p (unpublished).

Boeglin, J. L., and Mazaltarim, D. 1989, Géochimie, degrés d'évolution et lithodépendence des cuirasses ferrugineuses de la région de Gaoua au Burkina Faso. Sciences Geologiques (Bulletin) 42, 27- 44.

Bolster, S. 2007, Regolith mapping, landscape evolution and geochemical

applications. Exploration 07: International Conference on Mineral Exploration, Workshop 2, p. 19-21.

Bolster, S. J. S. 1999, Regolith mapping: is it really necessary? In: Ho, S. E., Geffress, G., and Davies, B. (Eds) Exploration geochemistry for the new millennium. Bulletin 30, Australian Institute of Geoscientists, Perth, p. 125-135.

Boulet, R., 1974, *Toposéquences des sols Tropicaux en Haute Volta. Equilibre et Déséquilibre Pédobioclimatique.* Memoire, 85, ORSTOM, Paris, 272 p. (In French).

Bowell, R. J., 1992, Supergene gold mineralogy at Ashanti, Ghana: Implications for the supergene behaviour of gold. Mineralogical Magazine, vol. 56, p. 545 – 560.

Bowell, R. J., Afreh, E. O., Laffoley, N. D'A., Hassen, E., Abe, S., Yao, R. K., and Pohl, D. 1996, Geochemical exploration for gold in tropical soils-four contrasting case studies from West Africa: Trans. Inst. Min. Metall., sect. B, 105, B12 – B33.

Bowell, R. J., Foster, R. P., and Gize, A. P., 1993, The mobility of gold in the tropical forest soils. Economic Geology, vol. 88, p. 999-1016.

Boyle, R. W., 1979, The geochemistry of gold and its deposits: Geological Survey of Canada, Bulletin 280: p. 1–254.

Bradshaw, P. M. D. (Compiler and Editor), 1975**,** Conceptual models in exploration geochemistry-The Canadian Cordillera and Canadian Shield. Journal of Geochemical Exploration, vol. 4, issue 1, 213 p.

Brantley, S. L., and White, A. F., 2009, Approaches to modelling weathered regolith, chapter 12. In: Oelkers E. H., and Schott, J. (Eds), Thermodynamics and kinetics of water-rock interactions: Reviews in Mineralogy and Geochemistry, vol. 70, p. 435-484.

Burke, K., and Gunnell, Y. 2008, The African erosion surface: continental-scale synthesis of geomorphology, tectonics and environmental change over the past 180 million years. Memoir 201, Geological Society of America, Boulder, U.S.A, 66 P.

Butt, C. R. M., 2004, Understanding the regolith in tropical and subtropical terrains: the key to exploration under cover. In: J. Muhling, R. Goldfarb, N. Vielreicher, F. Bierlein,

E. Stumpfl, D.I. Groves and S. Kenworthy (Editors). SEG 2004: Predictive Mineral discovery under cover. *Extended Abstracts.* Publication 33, Centre for Global Metallogeny, University of Western Australia, p. 74-78.

Butt, C. R. M., 2001, Dispersion of gold and associated elements in the lateritic regolith, Mystery Zone, Mt Percy, Kalgoorlie, Western Australia. Geochemistry: Exploration, Environment, Analysis, vol. 1, p. 291 – 306.

Butt, C. R. M., 1989, Genesis of supergene gold deposits in the lateritic regolith of the Yilgarn Block, Western Australia. In: Keays, R. R., Ramsay, W. R. H., and Groves D. I (Eds), The Geology of Gold Deposits: The Perspective in 1988. Economic Geology Monograph 8, p. 460-470.

Butt, C. R. M., and Bristow, A. P., 2012, Relief inversion in the geomorphological evolution of sub-Saharan West Africa: Geomorphology 2012, doi: 10.1016/j.geomorp.2012.11.024.

Butt, C. R. M., and Smith, R. E., 1992, Characteristic of the weathering profile. In: C. R. M. Butt and H. Zeegers, (Eds), chapter III.3: Semi-arid and arid terrains. Regolith Exploration Geochemistry in Tropical and Subtropical Terrains, Elsevier, Amsterdam, p. 299-304.

Butt, C. R. M., and Zeegers, H. 1992, Regolith Exploration in Tropical and Subtropical Terrains: Handbook of Exploration Geochemistry 4. Elsevier, Amsterdam, 607 p.

Butt, C. R. M., and Smith, R. E., 1980, (compilers and editors), Conceptual models in exploration geochemistry in Australia, Elsevier Scientific Publishers, Amsterdam, The Netherlands, 275 p.

Butt, C. R. M., Lintern, M. J. and Anand, R. R. 2000, Evolution of regolith and landscapes in deeply weathered terrain–implications for geochemical exploration: Ore Geology Reviews, vol. 16, p. 167–183.

Butt, C.R.M., Robertson, I.D.M., Scott, K.M. and Cornelius, M., 2005, Regolith expression of Australian ore systems, 347 p.

Cameron, E. M., Leybourne, M. I., Hall, G. E. M., and McClenaghan, M. B., 2004, Finding deeply buried deposits using geochemistry: Geochemistry: Exploration, Environment, Analysis, vol. 4, p. 7-32.

Carter, P., 1997, Wa reconnaissance terminal report. Prepared for the Mineral Commission, Ghana: unpublished internal report for Ashanti-AGEM Alliance.

Chan, R. A., 1988, Regolith terrain mapping for mineral exploration in Western Australia. Zeitschrift fur Geomorphologie Supp. Bnd, vol. 68, p. 205–221.

Chan, R. A., 1989, Regolith terrain mapping – a geomorphic base for mineral exploration. The Australian Institute of Mining and Metallurgy, vol. 294(2), p. 25–28.

Cohen, D. R., Kelley, D. L., Anand, R. and Coker, W. B., 2010, Major advances in Exploration geochemistry, 1998-2007: Geochemistry: Exploration, Environment, Analysis, vol. 10, p. 3-16.

Coker, W. B., 2010, Future research directions in exploration geochemistry: Geochemistry: Exploration, Environment, Analysis, vol. 10, p. 75-80.

Cornell, R. M., and Schwertmann, U., 1996, *The iron oxides.* VCH Publishers, New York.

Craig, M. A., 2001, Regolith mapping for geochemical exploration in the Yilgarn Craton, Western Australia: Geochemistry: Exploration, Environment, Analysis, vol. 1, p. 383 – 390.

Craig, M. A., 1997 a, Wiluna Thematic Regolith Landform Map (showing granite and greenstone saprolite associations): Australian Geological Survey Organisation, 1:250000 Regolith landforms Map.

Craig, M. A., 1997 b, Regolith maps and their exploration significance. *In*: Cassidy, K. F., Whitaker, A. J. & Liu, S. F., and (Eds) Kalgoorlie ’97: An International Conference on Crustal Evolution, Metallogeny and Exploration of the Yilgarn Craton – An update, extended abstracts: Australian Geological Survey Organisation Record 1997/41.

Craig. M. A., Rogers, L. and Churchward, H. M. 1998, Kurnalpi Regolith Landforms.

Australian Geological Survey Organisation, 1:250 000, Regolith Landforms Map.

Débat, P., Nikiema, S., Mercier, A., Lompo, M., Beziat, D., Bourges, F., Roddaz, M., Salvi, S., Tollon, F., and Wenmenga, U., 2003, A new metamorphic constraint for the Eburnean orogeny from Paleo Proterozoic formations of the Man shield (Aribinda and Tampelga countries, Burkina Faso). Precambrian Res., vol. 123 (1), p. 47–65.

De Kock, G. S., Armstrong, R. A., Siegfried, H. P., and Thomas, E., 2011, Geochronology of the Birimian Super group of the West African Craton in the Wa-Bole region of west-central Ghana: implications for the stratigraphic framework. Journal of African Earth Sciences, vol. 59, p. 1-40, doi: 10.1016/j.afrearsci.2010.08.001, p. 291-294.

Dickson, K. B., 1972, A historical geography of Ghana. Journal of Asian and African Studies, Centre for Global Metallogeny, vol. 7, p. 253-255.

Dickson, B.L. and Scott, K.M. 1997, Interpretation of aerial gamma-ray surveys adding the geochemical factors: AGSO Journal of Australian Geology & Geophysics, vol. 17(2), p. 187-200.

Dickson, B. L., Frazer, S. J. and Knisey-Henderson, A., 1996, Interpreting aerial gamma-ray surveys utilizing geomorphological and weathering models. Journal of Geochemical Exploration vol. 57, p. 75-88.

Dickson, K. B., and Benneh, G. A., 1995, A New Geography of Ghana. 3rd Revised Edition. Longman.

Dickson, K. B., and Benneh, G. A., 1988, A New Geography of Ghana. Longman 87 p.

Doumbia, S., Pouclet, A., Kouamelan, A., Peucat, J.J., Vidal, M., and Delor, C., 1998, Petrogenesis of juvenile-type Birimian (Palaeoproterozoic) granitoids in Central Cote-d'Ivoire, West Africa: Geochemistry and Geochronology. Precambrian Res., vol. 87 (1/2), p. 33–63.

Dzigbodi-Adjimah, K. 1993, Geology and geochemical patterns of the Birimian gold deposits, West Africa: Journal of Geochemical Exploration, vol. 47 (1-3), p. 305-320.

Dzigbodi-Adjimah, K., 1991, 'On the genesis of the Birimian Gold Deposits of Ghana'. In: G. O. Kesse (Ed), Proceedings of International Conference on the Geology of Ghana (1988), p. F1 – F9.

Egal, E., Thieblemont, D., Lahondere, D., Guerrot, C., Costea, C.A., Iliescu, D., Delor, C.,Goujou, J.C., Lafon, J.M., and Tegyey, M., 2002, Late Eburnean granitization and tectonics along the western and north-western margin of the Archean Kenema-Man domain (Guinea, West African Craton). Precambrian Res., vol. 117 (1/2), p. 57–84.

Eggleton, R. A., 2001, (compiler) Regolith Terminology: Cooperative Research Centre for Landscape Evolution and Mineral Exploration, Perth/Canberra, 375p.

Eggleton, R. A., and Taylor, G., 2001, Regolith geology and geomorphology: Chichester, Wiley & Sons, 516 p.

Fabris, A. J., Keeling, J. L., and Fidler, R. W., 2009, Surface geochemical expression of bedrock beneath thick sediment cover: Curnamona Province, South Australia. Geochemistry: Exploration, Environment, Analysis, vol. 39 (3), p. 237-246.

Feybesse, J. L., Billa, M., Guerrot, C., Duguey, E., Lescuyer, J.-L., Milési, J. P., and Bouchot, V. 2006. The paleo Proterozoic Ghanaian province: geodynamic model and ore controls, including regional stress modelling. Precambrian Res., vol. 149 (3/4), p. 149–196.

Freyssinet, P., 1994, Gold mass balance in lateritic profiles from savannah and rain forest zones: Catena, vol. 21, p. 59 – 172.

Freyssinet, P. 1993, Gold dispersion related to ferricrete pedogenesis in South Mali: application to geochemical exploration. Croquet de la Recherché Meniere, 510, 25-40.

Freyssinet, P., Butt, C. R. M., Morris, R. C., and Piantone, P., 2005, Ore-forming processes related to lateritic weathering. In: Hedenquist, J. W., Thomson, J. F. H., Goldfarb, R. J., Richards, J. P. (Eds), Economic Geology 100th Anniversary Volume. Economic Geology Publishing Company, New Haven, Connecticut, p. 681-722.

Freyssinet, P., Lecomte, P., and Edimo, A., 1989 b, Dispersion of gold and base

metals in the Mbourguéné lateritic profile, East Cameroun: Journal of Geochemical Exploration, vol. 32, p. 99 – 116.

Freyssinet, P., Zeegers, H., and Tardy, Y., 1989 a, Morphology and geochemistry of gold grains in lateritic profiles from South Mali: Journal of Geochemical Exploration, vol. 32, p. 99 – 116.

Freyssinet, P., Zeegers, H. and Tardy, Y., 1987, Neoformation d'or dan les cuirasses latéritique: dissolution, migration, précipitation. C. R. Acad. Sci., Paris, vol. 305, p. 867 – 874. (In French).

Gasquet, D., Barbey, P., Adou, M., and Paquette, J. L., 2003, Structure, Sr–Nd isotope geochemistry and zircon U–Pb geochronology of the granitoids of the Dabakala area (Cote d'Ivoire): evidence for a 2.3 Ga crustal growth event in the Palaeoproterozoic of West Africa? Precambrian Res., vol. 127 (4), p. 329–354.

Gee, R. D., and Anand, R. R., 2004, Advances in Regolith Research- A CRC LEME perspective: *In Pacrim 2004,* Adelaide, SA, 19-22 September, 2004, p. 29-44.

Gibbson, P. J., and Power, C. H., 2000, Introductory remote sensing: digital image processing and applications: Routledge, ISBN 0 415 189616, 249 P.

Gleuher, M. L., Anand, R. R., Eggleton, R. A., and Radford, N., 2008, Mineral hosts for gold and trace metals in regolith at Boddington gold deposit and Scuddles massive copper-zinc sulphide deposit, Western Australia: an LA-ICP-MS study. Geochemistry: Exploration, Environment, Analysis, vol. 8, p. 157-172.

Gong, Q., Deng, J., Yang, L., Zhang, J., Wang, Q., and Zhang, G., 2011, Behaviour of major and trace elements during weathering of sericite-quartz schist: Journal of Asian Earth Sciences, vol. 42, p. 1 – 13.

Gong, Q., Zhang, G., Zhang, J., Jiang, B., and Ma, N., 2010, Behaviour of REE fractionation during weathering of dolomite regolith profile in Southwest China. Acta Geologica Sinica 84, 1447 – 1469.

Gray, D. J., Butt, C. R. M., and Lawrance, L. M., 1992, In: C.R.M. Butt and H. Zeegers (Editors), Regolith Exploration geochemistry in tropical and sub-tropical terrain. Handbook of exploration geochemistry, Elsevier, Amsterdam vol. 4, p. 461-482.

Griffis, J., Barning, K., Agezo, F. L., and Akosa, F., 2002, Gold deposits of Ghana, prepared on behalf of Ghana Mineral Commission, Accra, Ghana, 432 p.

Griffis, R. J., and Agezo, F. L., 2000, "Mineral occurrences and exploration potential of northern Ghana", Minerals Commission Report, Accra.

Grunsky, E. C. 2010, The interpretation of geochemical survey data: Geochemistry: Exploration, Environment, Analysis, vol. 10, p. 27-74.

Hamilton, S. M. 2000, Spontaneous potentials and electrochemical cells. *In:* Hale, M (Ed), Geochemical remote sensing of the subsurface, Elsevier, Amsterdam, vol. 7, p. 3-16.

Hanssen, E., 1994, Wa – Lawra Belt Regional Stream Sediment Survey. Unpublished, internal report (B.H.P., Accra Office).

Hawke, H. E., and Webb, J. S., 1962, Geochemistry in mineral exploration: Geochimica et Cosmochimica Acta, vol. 27, issue 6, p. 715-716.

Heimsath, A. M., Dietrich, W. E., Nishiizumi, K., and Finkel, R. C., 1997, The soil production function and landscape equilibrium. Nature 388, p. 358-361.

Hocking, R. M., Langford, R. L., Thorne, A. m., et al., 2007, A classification system for regolith in Western Australia (March 2007 update) *Western Australia Geological Survey Record*, **2007/8,** 19 p.

Hirdes, W., Davis, D. W., Ludtke, G., and Konan, G., 1996, Two generations of Birimian (Paleo Proterozoic) volcanic belts in north-eastern Cote d'Ivoire (West Africa): consequences for the 'Birimian controversy'. Precambrian Res., vol. 80 (3/4), p. 173–191.

Hirdes, W., Davis, D. W., and Eisenlohr, B. N., 1992, Reassessment of Proterozoic granitoid ages in Ghana on the basis of U/Pb zircon and monazite dating. Precambrian Research, vol. 56, p. 83-99.

Hirdes, W., Konan, K. G., N'Da, D., Okou, A., Sea, P., Zamble, Z. B., and Davis, D. W., 2007, Geology of the northern portion of the Oboisso area, Côte d'ivoire. Sheets 4A, 4B, 4B BIS, 4. Direction de la Géologie, Abidjan, Côte d'ivoire and Bundesanstalt für Geowissen schaften und Rohstoffe, Hanover.

Hronsky, J. M. A., 2009, The exploration search space concept: Key to a successful exploration strategy: University of Western Australia and Curtin University of Technology, Centre for Exploration Targeting Quarterly News, no. 8.

International Atomic Energy Agency, 2003, Guidelines for radioelement mapping using gamma ray spectrometry data: Technical Report 1363, 173 p.

Jessen, J. R., 1996, Introductory digital image processing: a remote sensing perspective: Prentice-Hall, Upper Saddle River, N. J., 318 p.

Junner, N. R., 1935, Gold in the Gold Coast. Ghana Geological Survey, Bulletin No 47.

Kamgang Kabeyene Beyala, V., Onana, V. L., Priso, E. N. E., Parisot, J., C., and Ekodeck, G. E., 2009, Behaviour of REE and mass balance calculations in a lateritic profile over chlorite schist in South Cameroun, Chemie der Erde vol. 69, p. 61 – 73.

Kesse, G. O. 1985, The mineral and rock resources of Ghana: A. A. Balkema Press, Rotterdam, Netherlands, 610 p.

Kranjac-Berisaljevic, G., Bayorbor, T. B., Abdulai, A. S., and Obeng, F., 1998, Rethinking natural resources degradation in Semi-arid Sub-Saharan Africa: the case of Semi-arid Ghana. Revised January 1999. (http://www.odi.org.uk/rpeg/soil-_degradation/ghlit.pdf.

Laffan, S. W. and Lees, B. G., 2003, Predicting regolith properties using environmental correlation: a comparison of spatially global and spatially local approaches, Geoderma 120, p. 241-258.

Lakin, H. W., Curtin, G. C and Hubert, A. E., 1974, Geochemistry of gold in weathering cycle: Bulletin No. 1330. United States Geological Survey, 80 p.

Lecomte, P., and Zeegers, H., 1992, Exploration in areas of low to moderate relief. Humid tropical terrains (rainforest). Chap III. 2: in C. R. M., Butt and Zeegers, (Eds),

Handbook of Exploration geochemistry: Regolith exploration geochemistry in tropical and subtropical terrains, Elsevier Science Publ., 4, 57 – 76.

Leprun, J. C., 1977, *Géochimie de la surface et forms du relief, IV la degradation des cuirasses ferrugineuses, etude et importance du phenoméne pédologique en Afrique de l'Ouest.* Sciences Geologiques, Bulletin, vol. 30, p.265-273 (In French).

Leube, A, Hirdes, W., Mauer, R., and Kesse, G. O., 1990**,** The early Proterozoic Birimian Super group of Ghana and some aspects of its associated gold. Precambrian Research, vol. 46(1-2), p. 139-165.

Liegeois, J.P., Claessens, W., Camara, D., and Klerk, J., 1991, Short-lived Eburnean orogeny in Southern Mali. Geology, tectonics, U–Pb and Rb–Sr geochronology. Precambrian Res., vol. 50 (1/2), p. 111–136.

Lintern, M. J., and Sheard, M. J. 1999, Regolith geochemistry and stratigraphy of the Challenger gold deposit. MESA journal vol. 14, p. 9-14.

Lintern, M. J., and Scott, K. M., 1990, The distribution of gold and other elements in soils and vegetation at Panglo, Western Australia, CSIRO, Report No. 129R, 50p.

Listova, L. P., Vainshtein, A. Z., and Ryabinina, A. A., 1968, Dissolution of gold in media forming during oxidation of some sulphides: Chem. Abstr., vol. 68, p. 88967h.

Liversidge, A., 1893 a, On the origin of gold nuggets: Journal and Proceedings of the Royal Society of New South Wales, vol. 27, p. 303-343.

Liversidge, A., 1893 b, On the crystallization of gold in hexagonal forms. Journal and Proceedings of the Royal Society of New South Wales, vol. 27, p. 343-347.

Lompo, M., 2009, A model of subsidence of an oceanic plateau magmatic rocks in the Man-Leo Shield of the West African Craton Geodynamic evolution of the 2.25-2.0 Ga Palaeoproterozoic. In: Reddy, S. M., Mazumder, R., Evans, D.A.D., Collins, A. S., (Eds), Palaeoproterozoic Supercontinents and Global Evolution, p. 231-254.

Mann, A. W., 1984, Redistribution of gold in the oxidized zone of some Western Australian deposits. In: Gold Mining, Metallurgy and Geology. Proceedings of the

Regional Conference on Mining and Metallurgy, Perth and Kalgoolrie, October 1984. Australasian Institute of Mining and Metallurgy, Melbourne, p. 1-12.

Markwell, T. S., 2005, Cornishman gold deposit, Southern Cross mining district, Western. Australia. In: C.R.M Butt, I.D.M. Robertson, K.M. Scott and M. Cornelius, Regolith expression of Australian ore systems; p. 242-244.

Markwell, T. S., 1993, Gold mobility within the supergene environment in the amphibolites-grade lode-gold Cornishman Deposit: Western Australia, unpublished Honours Thesis, University of Western Australia, 67 p.

Mazzucchelli, R. H., and James, C. H., 1966, Arsenic as a guide to gold mineralization in laterite-covered areas of Western Australia: Trans. Inst. Min. Metall., Sect. B. Appl. Earth Sci., vol. 75, p. 286-294.

McGeough, M., and Anderson, J. A., 1998, Discovery of White Dam Au-Cu mineralization, AGSO record 1998/25: 69-71.

McKeith, T. D., Schodde, R. C. and Baltis, E. J., 2010, Gold discovery trends. SEG Newsletter, number 81, p. 1-20.

McQueen, K. G., 2006, Unravelling the regolith with geochemistry. In *Regolith 2006 – Consolidation and Dispersion of ideas.* (Eds R. W., Fitzpatrick and P. Shand) p. 230 – 235. CRC LEME, Perth.

McQueen, K. G., 2004, The nature, origin and exploration significance of the regolith, Girilambone-Cobar region. In: McQueen, K. G., and Scott, K. M. (Eds), *Exploration Field Workshop Cobar Region 2004 Proceedings,* CRC LEME, Perth, p. 51-56.

McQueen, K. G., and McRae, A., 2004, New ways to explore through the regolith in western New South Wales. In: *Pacrim 2004 congress, Proceedings,* p. 232-238. The Australian Institute of Mining and Metallurgy, Melbourne.

McQueen, K. G., and Munro, D. C., 2003, Weathering-controlled fractionation of ore and pathfinder elements at Cobar, NSW. In: Roach, I. C. (Ed), *Advances in Regolith,* CRC LEME, Canberra, p. 296-300.

McQueen, K. G., Pillans, B. J. and Smith, M. I., 2002, Constraining the weathering history of the Cobar region, western NSW, *in* Press, V.P., ed., Geosciences 2002: Expanding Horizons. Abstracts of the 16th Australian Geological Convention: Adelaide Convention Centre, Adelaide, SA, Australia, Geological Society of Australia, p. 426.

Meharg and Hartley-Whitaker, 2002, Arsenic uptake and metabolism in arsenic resistant and non-resistant plant species: New Phytologist, vol. 154, p. 29-43.

Meyerton, E. T., 1976, Ghana study NRG/247. A metallogenic map of north-western Ghana. Minerals Department, ESSO Eastern Inc, Canada, p. 109.

Michel, P., 1973, Les bassins des fleuves Sénégal et Gambie. Etude gémorphologique. Memoire ORSTOM 63, 732 p.

Milési, J. P., Feybesse, J. L., Ledru, P., Dommanget, A., Ouedraogo, M. F., Marcoux, E., Prost, A., Vinchon, C., Sylvain, J. P., Johan, V., Tegyey, M., Calvez, J. Y., and Lagny, P., 1989, *West African gold deposits.* Chronique de la recherché minière, BRGM Report No. 497, 3-98.

Milési, J. P., Feybesse, J. L., Pinna, P., Deschamps, Y., Kampunzu, H., Muhongo, S., Lescuyer, J. L., Le Goff, E., Delor, C., Billa, M., Ralay, F., and Heinry, C., 2004. Geological map of Africa 1:10 000 000, SIGAfrique project, 20th conference of African Geology, BRGM, Orleans, France, 2-7 June, http://www.sigafrique.net.

Milési, J. P., Ledru, P., Ankrah, P., Johan, V., Marcoux E., and Vinchon Ch., 1991, The metallogenic relationship between Birimian and Tarkwaian gold deposits in Ghana. Mineralium Deposita, vol. 26(3), p. 228-238.

Mokhtari, A. R., Cohen, D. R. and Gatehouse, S. G., 2009, Geochemical effects of deeply buried Cu-Au mineralization on transported regolith in an arid terrain. Geochemistry: Exploration, Environment, Analysis, vol. 9, p. 227-236.

Naba, S., Lompo, M., Debat, P., Bouchez, J. L., and Beziat, D., 2004, Structure and emplacement model for late-orogenic Paleo Proterozoic granitoids: the Tenkodogo-Yamba elongate pluton (Eastern Burkina Faso). J. Afr. Earth Sci., vol. 38 (1), p. 41–57.

Nahon, D., and Tardy, Y., 1992, The ferruginous laterites. In: Butt, C. R. M., and Zeegers, H., 1992 (Eds), Regolith Exploration in Tropical and Subtropical Terrains: Handbook of Exploration Geochemistry, Elsevier, Amsterdam, vol. 4, p. 41 – 55.

Ntiamoah-Agyarkwa, 1979, Relationship between gold and manganese mineralization in the Birimian of Ghana, West Africa. Geological Magazine, Cambridge University Press, vol. 116, p. 345-352.

Nude P. M., and Arhin E., 2009, Overbank sediments as appropriate geochemical sample media in regional stream sediment surveys for gold exploration in savannah regions of northern Ghana, Journal of Geochemical Exploration, vol. 103, p. 50-56.

Nyarko, E. S., Asiedu, D. K., Osea, S., Dampare, S., Zakaria, N., Hanson, J., Osei, J., Enti-Brown, S., and Tulasi, D., 2012, Geochemical characteristics of the basin-type granitoids in the Winneba area of Ghana: The Proceedings of the International Academy of Ecology and Environmental Sciences, www.iaees.org

Oberthuer, T., Vetter, U., Davis, D. W., and Amanor, J.A., 1998. Age constraints on gold mineralisation and Paleo Proterozoic crustal evolution in the Ashanti belt of southern Ghana. Precambrian Res., vol. 89 (3/4), p. 129–143.

Ollier, C. D., 1977, Terrain classification: methods, applications and principles. In: Hails, J. R. (ed.): Applied Geomorphology, p. 277–316.

Ollier, C. D., and Pain, C. F., 1996, Regolith, Soils and Landforms: Chichester: Wiley, 316 p.

Ollier, C., and Pain, C., 1995, Regolith, soils and landforms, Wiley and sons: Chichester, p. 256-273.

Pain, C. F., Chan, R., Craig, M., Hazel, M., Kamprad, J., and Wilford, J., 1991, RTMAP BMR regolith database field handbook-*BMR Record 1991/29.*

Pain, C. F., Craig, M. A., Gibson, D. L. and Wilford, J. R., 2001, "Regolith-landform Mapping: an Australian approach" In: Bobrowsky, P. T. (Editor*),* Geoenvironmental mapping, method, theory and practice. A. A. Balkema, Swets and Zeitlinger Publishers, the Netherlands: p. 29-56.

Pain, C., and Kilgour, P., 2004, Regolith mapping- A discussion *in* Roach I.C., (Ed.),Advances in regolith, CRC LEME 2003, p. 309-313.

Pain, C., Chan, R., Craig, M., Gibson, D., Kilgour, P. and Wilford, J., 2001, RTMAP Database Field Book and Users Guide: CRCLEME, Perth, Report **138**.

Pain, C., Chan, R., Craig, M., Hazell, M., Kampard, J., and Wilford, J., 1991, RTMAP BMR Regolith Database Field Handbook: Bureau of Mineral Resources, Geology and Geophysics Australia, Record **1991/29**.

Pain, C.F., Craig, M.A., Gibson, L., and Wilford, J.R., 2001, Regolith-landform mapping: an Australian approach, *in* Bobrosky, P.T., ed., Geoenvironmental mapping, method, theory and practice: A.A. Balkema, Swets and Zeitlinger Publishers, the Netherlands, p. 29-56.

Pobedash, I. D., 1965, Report on the geology and minerals of the South-western part of the Wa field sheet, Archive report/ Ghana Geological Survey Department, no. 51. Publisher: Minerals Commission/GTZ publication project, 1991. *Translation by Joachim Y. Dugbley.*

Pobedash, I. D., 1965, Report on the geology and minerals of the South-western part of the Wa field sheet, Archive report/ Ghana Geological Survey Department, no. 51. Publisher: Minerals Commission/GTZ publication project, 1991. *Translation by Joachim, Y. Dugbley.*

Richards, J. A., 1999, Remote sensing digital image analysis: Springer-Verlag, Berlin, 240 p, Spectral Angle Mapper.

Roach, I., 2003, Advances in Regolith Proceedings of the CRCLEME Regional Regolith Symposia 2003, Adelaide, ISBN 0731552210, Australia, 446 p.

Roquin, C., Dandjinou, T., Freyssinet, P., and Pion, J. C., 1989, The correlation between geochemical data and SPOT satellite imagery of lateritic terrain in southern Mali. In: S. E. Jenness (Editor), Geochemical Exploration 1987. Journal of Geochemical Exploration, vol. 32, p. 149-168.

Roudakov, V. M., 1965, Report on the Geology and Minerals of the North-western Part of the Wa Field Sheet. Archive Report No. 50, 145 p. Ghana Geological Survey Department.

Santosh, M. and Omana, P. K., 1991, Very high purity gold from lateritic Weathering profiles of Nilambur, Southern India. Geology, p. 746 – 749.

Scott, K. M., and Howard, R. W., 2001, Hydrothermal alteration and geochemical dispersion in the regolith at Panglo, Eastern Goldfields, Western Australia: Geochemistry: Exploration, Environment, Analysis, vol. 1, issue 4, p. 312-322.

Scott, K. M., and Pain, C. F., 2008, Regolith Science, ISBN 978 1 4020 8859 9, Springer CSIRO Publishing, Australia, 472 P.

Scott, K. M., and Radford, N. W., 2007, Rutile compositions at the Big Bell Au deposit as a guide for exploration. Geochemistry: Exploration, Environment, Analysis, vol. 7, no. 4, p. 353-361.

Sheard, M. J., Lintern, M. J., Prescott, J. R., and Huntley, D. J., 2006, Great Victoria Desert: new dates for South Australia's oldest desert dune system. MESA journal (Quarterly Earth resources journal of primary industries and resources South Australia), vol. 42, p. 15-26.

Sinclair, A. J., 1991, A fundamental approach to threshold estimation in exploration geochemistry: probability plots revisited. Journal of Geochemical Exploration, vol. 41, p. 1-22.

Smith, A. D., and Hunt, R. J., 1985, Solubilisation of gold by Chromo bacterium violaceum: J. Chem. Technol. Biotechnol., vol. 35B, p. 110-116.

Smith, B. H., 1987, Dispersion of gold in soils. In: Meaningful sampling in gold exploration Bulletin 7. Australian Institute of Geoscientists, Sydney, p. 55-82.

Smith, R. E., 1996, Regolith research in support of mineral exploration in Australia. Journal of Geochemical Exploration, vol. 57, p. 159-173.

Smith, R. E., Anand, R. R., Churchward, H. M., Robertson, I. D. M., Grunsky, E. C.,

Gray, D. J., Wildman, J. E., and Perdrix, J. L., 1992, Laterite geochemistry for detecting concealed mineral deposits, Yilgarn Craton, Western Australia. CSIRO Australia Division of Exploration Geoscience, Perth. Restricted Report 236R. Re-issued as CRC LEME Open File Report 50, 1998, CRC LEME Perth, 170 p. www.crcleme.org.au/Pubs/OFRSindex.html.

Smith, R. E., and Anand, R. R., 1992, Mt Gibson Au deposit, Western Australia. In: Butt, C. R. M., Zeegers, H. (Eds). Regolith exploration geochemistry in tropical and subtropical terrains. Handbook of Exploration Geochemistry 4. Elsevier, Amsterdam, pp. 313-318.

Smith, R. E., Perdrix, J. L., and Davis, J. M., 1987, Dispersion into pisolithic laterite from the Greenbushes, mineralized Sn-Ta pegmatite system, Western Australia. In: R.G. Garnett (Editor), Geochemical Exploration 1985. Part 2. J. Geochem. Explor. vol. 28, p. 251-265.

Smith, R.E., 1996, Regolith research in support of mineral exploration in Australia: Journal of Geochemical Exploration, vol. 57, p. 159-173.

Stallard, R. F., 1992, Tectonic processes, continental freeboard and the rate controlling step for continental denudation. In Global Biogeochemical Cycles, Butcher, S. S., Charlson, R. J., Orians, G. H., Wolfe, G. V., (eds), p. 93-121.

Stanley, C. R., and Sinclair, A. J., 1989 a, Comparison of probability plots and the gap statistics in the selection of thresholds for exploration geochemistry data. Journal of Geochemical Exploration, vol. 32, p. 355-357.

Stone, S., 2009, Azumah strengthens dominant position in NW Ghana with new gold acquisition. *Media press release.* P. 1-6, ACN 112 320 251.

Tardy, Y. 1997, Petrology of laterites and tropical soils. A. A. Balkema, Rotterdam, 408 p.

Tate S. E., Greene, R. S. B., Scott, K. M., and McQueen, K. G., 2007, Recognition and characterization of the aeolian component in soils in the Girlambone region, north western New South Wales, Australia, *Catena* 69, p. 122 – 133.

Taylor, G., and Eggleton, R. A., 2001, Regolith geology and geomorphology: John Wiley & Sons, 248 p.

Taylor, P. N., Moorbath, S., Leube, A., and Hirdes, W., 1992, Early Proterozoic crustal evolution in the Birimian of Ghana: constraints from geochronology and isotope geochemistry. Precambrian Res., vol. 56, p. 97–111.

Tobler, W. R., 1970, A computer model simulation of urban growth in the Detroit region. Economic Geography, vol. 42, issue 2, p. 234– 40.

Turekian, K. K., and Wedepohl, K. H., 1961, Distribution of the elements in some major units of the Earth's Crust: Geol. Soc. Amer. Bull., 72, p. 175 -192.

Vidal, M., Gumiaux, Cagnard, F., Pouchet, A., Ouattara, G., and Pichon, M., 2009, Evolution of Palaeoproterozoic "weak type" orogeny of West African Craton (Ivory Coast). Tectonophysics, vol. 477, p. 145-159.

Waller, C., Franey, N., Hodgson, S., and Widenbar, L., 2012, NI-43-101 Technical Report for Azumah Resources LTD., Wa Gold Project, Ghana, 114 p.

Watkins K. P., Fleming B. S., Carrello F., Witt W. K., and Ringrose, C. R., 1997, The Cornishman gold deposit – a brown field's discovery in the Southern Cross Greenstone Belt, Western Australia. Case histories of discovery of New Generation gold mine '97 Conference Proceedings, Australian Mineral Foundation, Adelaide, South Australia, p. 16.1-16.10.

Webber, P., 1996 a, News from the village: agrarian change in Ghana. Geography Review, vol. 9, issue 3, p. 25-30.

White, A. F., and Brantley, S. L. (Eds.), 1995, Chemical weathering rates of silicate minerals. Reviews in Mineralogy, vol. 31, Mineralogical Society of America.

White, A. F., Blum, A. E., Schulz, M. S., Bullen, T. D., Harden, J. W., and Peterson, M. L., 1996, Chemical weathering rates of a soil chronosequence on granitic alluvium, I, Quantification of mineralogical and surface area changes and calculation of primary silicate reaction rates. Geochimica et Cosmochimica ACTA, vol. 60, p. 2533-2550.

Wilford, J. R., 1992, Regolith mapping using integrated Landsat TM imagery and high resolution gamma-ray spectrometric imagery-Cape York Peninsula: Bureau of Mineral Resources Record 1992/78: 35 pp.

Wilford, J. R., Bierwirth, P. N. and Craig, M. A., 1997, Application of airborne gamma-ray spectrometry in soil/regolith mapping and applied geomorphology: AGSO Journal of Australian Geology & Geophysics, vol.17 (2), p. 201-216.

Wilford, J. R., Bierwirth, P. N., and Craig, M. A., 1997, Application of airborne gamma-ray spectrometry in soil/regolith mapping and applied geomorphology: AGSO Journal of Australian Geology and Geophysics 17(2), p. 201 – 216.

Wilford, J. R., Dent, D. L., Dowling, T. and Braaten, R., 2001, Rapid mapping of soils and salt stores using airborne radiometric and digital elevation models: AGSO research newsletter, 33-40.

Williams, A., 2006, Measurement uncertainty: the key to the use of recovery factors, CITAC, p. 30-37.

Yager, D. B., Church, S. E., Verplanck, P. L., Wirt, L., 2003, Ferricrete, manganocrete and bog iron occurrences with selected sedge bogs and active iron bogs and springs in the upper Animas River watershed, San Juan County, Colorado, US Geol. Surv. Miscellaneous Field Studies Map MF-2406.

Zeegers, H., and Lecomte 1992, Seasonally humid tropical terrains (savannahs). In: Govett (Editor), Regolith exploration geochemistry in tropical and sub-tropical terrains, Elsevier, Amsterdam, vol. 4, p. 203-240.

Zeegers, H., and Leprun, J. C., 1979, Evolution des concepts en altérogie tropicale et consequences potentielles pour les prospecions géochimiques en Afrique occidentale Soudano-Sahélienne. *Bull. Bur. Rech. Geol. Miners,* vol. 2, p. 229-239. (In French).

Appendix C:Pits, Au and other elements in the regolith of the Lawra area analysed by ICP and FA-AAS Techniques

Sample ID	Pit ID	UTM-E	UTM-N	From (m)	To (m)	Ag ppm	Al ppm	As ppm	Au ppb	Au ppm	B ppm	Ba ppm	Be ppm	Bi ppm	Ca %	Cd ppm	Ce ppm	Co ppm	Cr ppm	Cs ppm	Cu ppm	Fe %	Ga ppm	Ge ppm	Hf ppm	Hg ppm	In ppm	K %	La ppm	Li ppm	Mg ppm	Mn ppm	Mo ppm	Na ppm	Nb ppm	Ni ppm
813351	KP001	526650	1149550	**0**	**10**	0.05	2.68	9.9	25	<0.2	<10	80	0.74	0.09	0.31	0.02	44.3	22.4	120	1.83	48.3	4.46	9.61	0.15	0.18	0.01	0.013	0.25	40.7	16.5	1.08	249	0.25	<0.01	0.2	68.3
813352	KP001	526650	1149550	10	20	0.04	2.58	9.4	8	<0.2	<10	80	0.7	0.08	0.25	0.02	42.3	19.4	134	2.25	40.6	4.22	8.61	0.13	0.15	<0.01	0.012	0.32	26.8	14.9	0.99	233	0.17	<0.01	0.18	60.6
813353	KP001	526650	1149550	20	30	0.04	2.42	10.3	10	<0.2	<10	70	0.75	0.07	0.22	0.01	45.6	22	142	2.07	39.8	3.88	8.36	0.13	0.16	0.01	0.011	0.33	29.1	15.8	0.98	252	0.16	<0.01	0.16	63
813354	KP001	526650	1149550	30	40	0.21	2.43	9.7	<5	<0.2	<10	80	0.71	0.07	0.23	0.02	50.8	24	140	2.1	40.7	3.88	8.05	0.13	0.14	<0.01	0.011	0.33	29.4	15.2	1.06	297	0.13	<0.01	0.12	63.9
813355	KP001	526650	1149550	40	50	0.06	2.31	10.6	6	<0.2	<10	90	0.74	0.07	0.24	0.01	48.7	24.6	139	2.12	42.2	3.76	7.6	0.13	0.13	0.01	0.01	0.33	30.9	14.9	1.09	323	0.15	<0.01	0.12	66.5
813356	KP001	526650	1149550	50	60	0.03	2.44	6.3	10	<0.2	<10	90	0.7	0.07	0.24	0.02	50.1	25.2	124	2.12	42.6	3.76	8.11	0.14	0.14	<0.01	0.01	0.34	29.5	15.2	1.22	345	0.11	<0.01	0.1	72.9
813357	KP001	526650	1149550	60	70	0.03	2.42	8.8	22	<0.2	<10	100	0.82	0.07	0.24	0.02	42.1	27.2	117	2.57	43.6	3.86	7.87	0.15	0.14	<0.01	0.01	0.35	29.4	16.2	1.22	379	0.08	<0.01	0.11	73.3
813358	KP001	526650	1149550	70	80	0.04	2.33	9.7	37	<0.2	<10	110	0.79	0.06	0.24	0.01	35.5	22.9	107	2.06	41.9	3.75	6.51	0.2	0.12	0.01	0.018	0.34	32.2	13.4	1.17	320	0.08	<0.01	0.11	69.1
813359	KP001	526650	1149550	80	90	0.03	2.3	8.1	10	<0.2	<10	120	0.83	0.06	0.26	0.01	58.6	24.1	100	2.18	43.2	3.54	6.99	0.2	0.11	0.01	0.02	0.33	39.2	14.2	1.19	361	0.08	0.01	0.09	77.2
813360	KP001	526650	1149550	90	100	0.02	2.33	8.1	8	<0.2	<10	120	0.85	0.07	0.25	0.03	57.6	25.5	109	2.04	40.9	3.54	7	0.18	0.11	0.01	0.015	0.32	37.9	13.9	1.24	342	0.17	0.01	0.05	75.4
813361	KP001	526650	1149550	100	110	0.05	2.53	11.8	19	<0.2	<10	190	0.78	0.07	0.35	0.02	46	21.9	125	1.51	41.5	4.1	8.41	0.15	0.18	0.02	0.021	0.26	32.4	13.9	0.92	279	0.41	<0.01	0.25	65.5
813386	KP003	527050	1149550	**0**	**10**	0.05	0.62	10.9	83	<0.2	<10	70	0.25	0.06	0.1	0.01	16.45	7.1	24	0.29	11.1	1.28	2.99	0.09	0.04	0.01	0.011	0.04	10.7	4.2	0.06	254	0.28	<0.01	0.2	14.2
813387	KP003	527050	1149550	10	20	0.02	0.69	11.9	116	<0.2	<10	80	0.3	0.07	0.07	<0.01	18.05	7.4	25	0.34	12.4	1.46	3.48	0.1	0.02	<0.01	0.015	0.04	11.5	4.4	0.05	215	0.35	<0.01	0.2	15.2
813388	KP003	527050	1149550	20	30	0.04	1.04	21.8	69	<0.2	<10	160	0.41	0.09	0.07	0.01	35.9	26.6	45	0.47	20.9	2.5	5.18	0.1	0.02	0.02	0.017	0.05	13.2	8.2	0.06	703	0.72	<0.01	0.18	27.9
813389	KP003	527050	1149550	30	40	0.04	1.05	18.9	68	<0.2	<10	120	0.38	0.09	0.07	0.01	24.9	15.8	38	0.45	18	2.19	4.94	0.09	0.03	0.01	0.018	0.05	13.2	7.4	0.06	391	0.51	<0.01	0.17	22.4
813391	KP003	527050	1149550	40	50	0.05	1.52	39.7	18	<0.2	<10	270	0.62	0.11	0.06	0.01	70.2	67.6	85	0.55	33.7	4.79	7.61	0.08	0.03	0.01	0.025	0.06	11.7	14.8	0.06	1640	1.47	<0.01	0.18	62.9
813392	KP003	527050	1149550	50	60	0.05	1.78	41.8	107	<0.2	<10	320	0.72	0.12	0.05	0.02	119	104.5	85	0.63	41.6	5.76	9.2	0.1	0.05	0.01	0.032	0.07	11.7	24	0.06	2510	1.66	<0.01	0.2	101
813393	KP003	527050	1149550	60	70	0.04	1.68	38.7	89	<0.2	<10	310	0.76	0.12	0.05	0.02	125	99.9	73	0.61	40.7	5.53	8.69	0.09	0.07	0.02	0.027	0.06	12.4	23.4	0.05	2420	1.35	0.01	0.19	97.3
813394	KP003	527050	1149550	70	80	0.03	1.55	30.2	81	<0.2	<10	200	0.59	0.12	0.05	0.01	94	63.6	58	0.59	34.7	4.75	7.78	0.09	0.08	<0.01	0.028	0.06	11.4	19.1	0.05	1560	0.96	<0.01	0.18	83.6
813395	KP003	527050	1149550	80	90	0.03	1.35	26.2	59	<0.2	<10	210	0.53	0.11	0.04	0.01	96.1	60.9	46	0.59	33.1	4.08	7.29	0.09	0.1	0.02	0.026	0.06	12.4	19.6	0.05	1500	0.77	<0.01	0.15	81.9
813396	KP003	527050	1149550	90	100	0.03	1.33	25.6	42	<0.2	<10	200	0.54	0.12	0.04	0.01	101	53.7	45	0.58	34.6	3.9	7.61	0.09	0.1	0.01	0.028	0.06	13	17.6	0.06	1240	0.7	<0.01	0.14	71.9
813397	KP003	527050	1149550	100	110	0.02	1.31	22.5	118	<0.2	<10	110	0.48	0.12	0.05	0.01	41.4	20.9	41	0.59	31.1	3.59	7.2	0.1	0.13	0.01	0.023	0.06	13.7	10.2	0.07	487	0.49	<0.01	0.15	35.9
813398	KP003	527050	1149550	110	120	0.04	1.37	24.6	45	<0.2	<10	150	0.54	0.12	0.05	0.01	78.5	42.9	47	0.61	38.5	4.09	7.79	0.1	0.11	0.01	0.026	0.06	14.6	13	0.07	1060	0.6	<0.01	0.13	50.2
813399	KP003	527050	1149550	120	130	0.04	1.4	24.4	66	<0.2	<10	170	0.51	0.12	0.05	0.01	75	37.3	50	0.6	40.2	4.2	7.58	0.08	0.13	0.01	0.025	0.06	14.3	10.9	0.07	877	0.64	<0.01	0.13	42.7
813401	KP003	527050	1149550	130	140	0.03	1.42	20.8	47	<0.2	<10	200	0.47	0.13	0.06	0.01	71	42.8	48	0.55	36.4	4.27	7.02	0.09	0.11	0.01	0.026	0.06	15.1	11.1	0.09	1140	0.56	0.01	0.12	43.1
813402	KP003	527050	1149550	140	150	0.03	1.47	23	59	<0.2	<10	100	0.51	0.12	0.06	0.01	38.9	24.6	52	0.56	41.9	4.5	7.8	0.09	0.12	0.01	0.023	0.05	16.4	10.5	0.1	610	0.53	<0.01	0.1	45.5
813403	KP003	527050	1149550	150	160	0.02	1.45	17.4	39	<0.2	<10	60	0.47	0.1	0.07	0.01	17.15	16.9	57	0.45	42.2	5.18	7.82	0.1	0.07	0.01	0.021	0.04	16.2	10.7	0.16	423	0.36	<0.01	0.07	43.8
813404	KP003	527050	1149550	160	170	0.02	1.49	21.9	72	<0.2	<10	80	0.52	0.11	0.06	0.01	30.5	18.8	57	0.52	40.6	4.88	7.73	0.1	0.13	0.01	0.025	0.05	15.8	9.9	0.12	492	0.48	<0.01	0.09	44.4
813405	KP003	527050	1149550	170	180	0.02	1.45	19.6	55	<0.2	<10	70	0.48	0.11	0.07	0.01	21	15.8	56	0.52	41.8	4.67	7.65	0.11	0.1	0.01	0.022	0.04	18	11.3	0.16	409	0.44	<0.01	0.09	43.7
813406	KP003	527050	1149550	180	190	0.02	1.55	20.3	69	<0.2	<10	80	0.57	0.11	0.07	0.02	30.2	24.1	68	0.45	48.3	5.28	8.47	0.11	0.09	<0.01	0.025	0.04	17.6	12.3	0.19	605	0.43	<0.01	0.06	53.6
813407	KP003	527050	1149550	190	200	0.02	1.55	14.5	32	<0.2	<10	70	0.49	0.09	0.08	0.01	29.6	30	66	0.36	49.5	5.15	8.77	0.1	0.06	<0.01	0.022	0.03	19.5	17.4	0.3	734	0.31	<0.01	<0.05	63.3
813408	KP004	527250	1149550	**0**	**10**	0.02	0.71	9.7	120	<0.2	<10	110	0.23	0.06	0.08	0.01	19.25	8.3	28	0.28	12.5	1.53	3.31	0.08	0.03	<0.01	0.01	0.03	11.5	4.3	0.06	218	0.22	<0.01	0.18	15.1
813410	KP004	527250	1149550	10	20	0.02	1.06	15.4	81	<0.2	<10	170	0.37	0.08	0.07	0.01	33.2	23.1	40	0.46	19.5	2.38	5.05	0.1	0.03	<0.01	0.016	0.04	15.3	7.1	0.07	595	0.47	<0.01	0.2	25.9
813411	KP004	527250	1149550	20	30	0.04	1.42	19.9	42	<0.2	<10	180	0.49	0.1	0.06	0.01	47.9	36.6	51	0.59	26.8	3.39	6.96	0.09	0.03	<0.01	0.025	0.05	13.6	10.3	0.06	812	0.66	<0.01	0.19	38.8
813412	KP004	527250	1149550	30	40	0.04	1.47	19	45	<0.2	<10	360	0.56	0.1	0.05	0.02	64.3	58.8	50	0.6	26.8	3.64	7.07	0.09	0.04	0.01	0.026	0.05	14.3	11.2	0.05	1840	0.63	<0.01	0.15	50.3
813413	KP004	527250	1149550	40	50	0.04	1.31	16.5	33	<0.2	<10	570	0.51	0.09	0.04	0.02	78.2	84.6	48	0.52	25.6	3.61	6.33	0.08	0.05	<0.01	0.021	0.05	16.4	10.1	0.05	3060	0.6	0.01	0.11	54.3
813414	KP004	527250	1149550	50	60	0.04	1.16	13.6	31	<0.2	<10	370	0.49	0.09	0.04	0.02	77.3	65.6	50	0.49	26.2	3.57	5.99	0.09	0.06	<0.01	0.021	0.05	16.7	10.7	0.05	1970	0.49	<0.01	0.13	51.2
813415	KP004	527250	1149550	60	70	0.04	1.18	13.8	23	<0.2	<10	250	0.52	0.09	0.04	0.02	85.3	57.2	49	0.53	29.4	3.88	6.77	0.13	0.07	<0.01	0.024	0.05	19	11.9	0.06	1380	0.5	<0.01	0.1	56.9
813416	KP004	527250	1149550	70	80	0.11	1.08	12.6	56	<0.2	<10	200	0.52	0.09	0.04	0.01	73.7	47.6	43	0.55	27.5	3.5	6.31	0.14	0.09	0.01	0.023	0.04	17.8	10.3	0.06	1180	0.49	0.01	0.14	51.9
813417	KP004	527250	1149550	80	90	0.03	1.19	12.1	19	<0.2	<10	120	0.46	0.09	0.04	0.01	46.9	30.2	44	0.56	26.4	3.56	6.48	0.12	0.11	0.01	0.023	0.04	16.5	8.9	0.08	699	0.33	0.01	0.11	40.4
813418	KP004	527250	1149550	90	100	0.02	1.27	10.8	20	<0.2	<10	90	0.45	0.09	0.05	0.01	36.8	30.3	49	0.58	28.6	3.48	7.2	0.13	0.14	0.01	0.024	0.05	20.2	9.4	0.1	599	0.35	0.01	0.11	40.5
813419	KP004	527250	1149550	100	110	0.02	1.28	10.7	28	<0.2	<10	70	0.47	0.09	0.06	0.01	24.9	22.8	52	0.57	29.6	3.59	7.25	0.15	0.1	0.01	0.022	0.04	20.1	9.6	0.14	456	0.28	0.01	0.1	40.7
813420	KP004	527250	1149550	110	120	0.02	1.55	10.5	28	<0.2	<10	80	0.51	0.1	0.07	0.01	36.2	30.9	62	0.55	37.5	4.12	8.51	0.15	0.1	0.01	0.026	0.04	23.7	14.9	0.26	665	0.33	0.01	0.07	58.5
813421	KP004	527250	1149550	120	130	0.02	1.68	9.9	20	<0.2	<10	80	0.55	0.09	0.07	0.01	38.1	30.3	71	0.49	40.1	4.42	8.66	0.16	0.1	0.01	0.026	0.04	25.4	18.9	0.38	656	0.34	0.01	0.06	71.1
813422	KP004	527250	1149550	130	140	0.02	2.01	8.1	24	<0.2	<10	120	0.57	0.11	0.09	0.02	49.6	37.3	78	0.43	41.6	4.93	9.36	0.19	0.11	<0.01	0.03	0.03	30.9	21.2	0.69	955	0.25	0.01	<0.05	93.8
813423	KP004	527250	1149550	140	150	0.02	2.15	6.9	18	<0.2	<10	90	0.5	0.09	0.1	0.02	43.4	31.6	83	0.38	42.5	5.17	9.17	0.15	0.12	<0.01	0.027	0.03	30.8	20.3	0.83	792	0.21	0.01	<0.05	99.1
813429	KP005	527450	1149550	**0**	**10**	0.03	1.06	17.6	41	<0.2	<10	90	0.32	0.07	0.19	0.01	23.1	7.4	52	0.32	18.5	2.22	4.06	0.11	0.06	0.01	0.01	0.05	13.8	6.5	0.22	230	0.28	0.01	0.15	23.8
813430	KP005	527450	1149550	10	20	0.03	1.29	20.4	85	<0.2	<10	90	0.36	0.07	0.17	<0.01	25.6	8	58	0.37	22.6	2.61	5.03	0.13	0.06	0.01	0.013	0.04	16.1	8	0.23	199	0.31	0.01	0.14	26.8
813432	KP005	527450	1149550	20	30	0.04	1.51	24	29	<0.2	<10	100	0.42	0.08	0.15	0.01	28.3	10.4	63	0.46	25	3.02	5.86	0.12	0.05	<0.01	0.013	0.04	16.8	9.4	0.22	266	0.4	0.01	0.12	29.5
813433	KP005	527450	1149550	30	40	0.05	1.84	31.8	37	<0.2	<10	90	0.47	0.09	0.14	0.01	31.2	11.2	78	0.52	31.1	3.69	7.47	0.12	0.06	<0.01	0.016	0.05	17	12.2	0.23	174	0.71	0.01	0.11	37.1
813434	KP005	527450	1149550	40	50	0.05	1.82	62.3	61	<0.2	<10	160	0.51	0.11	0.26	0.02	56.1	30	88	0.57	33.4	4.5	7.87	0.11	0.05	<0.01	0.021	0.05	13.2	15.9	0.15	823	1.7	0.01	0.09	59.8
813435	KP005	527450	1149550	50	60	0.04	1.81	57.4	45	<0.2	<10	150	0.48	0.15	0.09	0.02	56.2	28.9	71	0.65	33.5	3.85	7.81	0.11	0.06	<0.01	0.019	0.06	17.8	15.9	0.15	740	0.62	<0.01	0.11	62
813436	KP005	527450	1149550	60	70	0.11	1.78	85.4	109	0.6	<10	90	0.47	0.17	0.08	0.02	36.8	23.7	78	0.55	37.5	4.37	8.02	0.12	0.09	0.01	0.017	0.05	18.4	13.7	0.2	485	0.42	<0.01	0.09	68.7
813437	KP005	527450	1149550	70	80	0.16	1.98	92.4	73	0.6	<10	60	0.48	0.17	0.1	0.01	27.1	15.4	83	0.5	40.6	4.79	8.28	0.13	0.09	<0.01	0.017	0.04	23.2	13.4	0.31	276	0.38	<0.01	0.09	61.7
813438	KP005	527450	1149550	80	90	0.04	1.96	78.5	29	<0.2	<10	60	0.43	0.14	0.12	0.02	42.7	18.1	86	0.36	40.8	4.83	7.88	0.15	0.1	<0.01	0.013	0.03	31	16.4	0.61	455	0.29	<0.01	0.06	82.6
813440	KP005	527450	1149550	90	100	0.2	1.91	86.3	44	0.5	<10	60	0.42	0.17	0.13	0.01	44.8	20.4	74	0.39	41.2	4.32	7.63	0.15	0.11	<0.01	0.015	0.04	30.9	16.4	0.61	406	0.28	<0.01	0.06	70.4
813441	KP005	527450	1149550	100	110	0.05	1.98	73.6	26	<0.2	<10	60	0.36	0.16	0.16	0.02	49.9	23.3	62	0.3	44.8	4.38	7.55	0.16	0.14	<0.01	0.014	0.03	35.6	18.3	0.93	481	0.23	<0.01	<0.05	74.9
813442	KP005	527450	1149550	110	120	0.12	2.14	98.9	27	<0.2	<10	50	0.35	0.18	0.19	0.02	40.9	26	85	0.31	51.5	4.58	7.5	0.14	0.11	<0.01	0.01	0.03	28.8	20.6	1.02	462	0.32	<0.01	<0.05	80.6
813443	KP005	527450	1149550	120	130	0.03	2.11	78.1	9	<0.2	<10	50	0.29	0.13	0.19	0.02	37.5	15.3	53	0.21	38.7	4.49	7.9	0.16	0.12	<0.01	0.011	0.02	32.3	18.3	1.2	318	0.19	<0.01	<0.05	59.8
813444	KP006	527650	1149550	**0**	**10**	0.23	1.33	69	128	0.7	<10	70	0.3	0.15	0.21	0.04	37	13.9	67	0.4	31.1	2.96	5.05	0.11	0.08	0.01	0.012	0.06	18.7	7.8	0.31	300	0.52	<0.01	0.21	34.6
813445	KP006	527650	1149550	10	20	0.05	1.49	91.5	502	<0.2	<10	50	0.34	0.19	0.14	0.03	36	14.4	81	0.52	36.8	3.41	5.56	0.11	0.06	<0.01	0.014	0.05	17	8.9	0.28	339	0.68	<0.01	0.18	38
813446	KP006	527650	1149550	20	30	0.05	2.09	121.5	154	<0.2	<10	40	0.41	0.24	0.11	0.05	29.7	14.5	105	0.62	50.7	4.73	7.7	0.1	0.06	<0.01	0.019	0.05	14.9	10.7	0.31	132	0.86	<0.01	0.21	50.1
813447	KP006	527650	1149550	30	40	0.07	2.54	110.5	32	<0.2	<10	30	0.41	0.24	0.1	0.04	30.7	18.8	106	0.6	55	5.53	8.6	0.11	0.07	<0.01	0.02	0.04	15.3	13.6	0.41	111	0.82	<0.01	0.18	58.8
813448	KP006	527650	1149550	40	50	0.06	2.45	96.7	36	<0.2	<10	20	0.32	0.21	0.1	0.03	33.4	20.7	99	0.51	56.7	5.35	8.21	0.12	0.08	<0.01	0.015	0.03	17.7	15.8	0.58	102	0.6	<0.01	0.11	62.6
813451	KP006	527650	1149550	50	60	0.06	2.05	74.9	25	<0.2	<10	20	0.25	0.17	0.09	0.03	40.4	17	91	0.5	48.3	4.27	6.4	0.13	0.08	0.01	0.013	0.02	22.2	14.6	0.6	65	0.42	<0.01	0.06	53.4
813452	KP006	527650	1149550	60	70	0.02	2.03	68.8	25	<0.2	<10	20	0.2	0.15	0.1	0.02	42.9	13.4	96	0.5	47	4.41	6.42	0.18	0.1	0.01	0.009	0.02	24.1	13.4	0.66	62	0.35	<0.01	<0.05	51.2
813453	KP006	527650	1149550	70	80	0.04	1.63	49.5	19	<0.2	<10	20	0.16	0.11	0.1	0.01	42.3	10.2	80	0.45	35	3.46	4.86	0.18	0.07	0.01	0.007	0.02	23.7	10.5	0.64	52	0.25	<0.01	<0.05	41
813454	KP006	527650	1149550	80	90	0.02	1.78	56.2	15	<0.2	<10	20	0.18	0.14	0.11	0.02	41.9	13	95	0.45	41	3.91	5.77	0.19	0.08	<0.01	0.011	0.02	24.3	11.4	0.7	72	0.29	<0.01	<0.05	46.2
813455	KP006	527650	1149550	90	100	0.07	2.07	58.8	24	<0.2	<10	30	0.23	0.16	0.12	0.02	39.1	13.2	115	0.44	49.2	4.57	6.44	0.19	0.08	<0.01	0.015	0.02	22.8	11.8	0.81	86	0.29	<0.01	<0.05	56
813456	KP006	527650	1149550	100	110	0.02	2.1	46.7	13	<0.2	<10	30	0.2	0.11	0.13	0.02	42.7	14.3	120	0.42	50.2	4.26	6.78	0.19	0.09	<0.01	0.012	0.02	24.1	14.6	0.98	88	0.21	<0.01	<0.05	64.5
813457	KP006	527650	1149550	110	120	0.01	2.14	39.4	10	<0.2	<10	30	0.18	0.1	0.14	0.02	52.2	17.3	111	0.41	51.5	4.04	6.67	0.22	0.07	<0.01	0.008	0.02	24.7	15.8	1.1	114	0.18	<0.01	<0.05	71.9
813458	KP006	527650	1149550	120	130	0.07	1.96	64.9	17	<0.2	<10	30	0.24	0.14	0.13	0.03	43.3	14	107	0.49	58.5	4.17	6.43	0.2	0.09	<0.01	0.011	0.02	23	14.6	0.96	86	0.36	<0.01	<0.05	66.8
813459	KP006	527650	1149550	130	140	0.02	1.98	53.5	13	<0.2	<10	30	0.22	0.11	0.13	0.03	39.8	13.6	93	0.48	50.8	3.89	5.94	0.19	0.08	0.01	0.01	0.02	19.8	14.1	0.98	91	0.25	<0.01	<0.05	68.2

Appendix C:Pits, Au and other elements in the regolith of the Lawra area analysed by ICP and FA-AAS Techniques

Sample ID	Pit ID	UTM-E	UTM-N	From (m)	To (m)	Ag ppm	Al ppm	As ppm	Au ppb	Au ppm	B ppm	Ba ppm	Be ppm	Bi ppm	Ca %	Cd ppm	Ce ppm	Co ppm	Cr ppm	Cs ppm	Cu ppm	Fe %	Ga ppm	Ge ppm	Hf ppm	Hg ppm	In ppm	K %	La ppm	Li ppm	Mg ppm	Mn ppm	Mo ppm	Na ppm	Nb ppm	Ni ppm
813460	KP006	527650	1149550	140	150	0.01	1.91	36.6	9	<0.2	<10	30	0.17	0.08	0.13	0.02	38.9	15.6	107	0.38	40.9	3.6	5.32	0.19	0.07	0.01	0.009	0.01	20.2	13.7	1.04	116	0.15	<0.01	<0.05	66.1
813461	KP007	527850	1149550	**0**	**10**	0.02	0.95	11.2	86	<0.2	<10	70	0.32	0.06	0.17	0.01	26.2	7.1	45	0.3	16.8	2.13	3.88	0.16	0.06	0.01	0.01	0.04	13.8	4.7	0.2	282	0.26	<0.01	0.19	19.9
813462	KP007	527850	1149550	10	20	0.05	1.3	14.8	50	<0.2	<10	60	0.37	0.08	0.13	0.01	30.3	9.1	49	0.4	23.6	2.55	5.56	0.06	0.05	0.01	0.014	0.04	16.6	6.5	0.2	237	0.34	<0.01	0.22	24.8
813463	KP007	527850	1149550	20	30	0.11	1.61	19.4	22	<0.2	<10	80	0.46	0.09	0.11	0.01	37.9	15.6	58	0.51	30.3	3.28	6.93	0.07	0.05	0.01	0.02	0.04	19.5	7	0.2	381	0.48	0.01	0.23	30.2
813464	KP007	527850	1149550	30	40	0.04	1.84	21.3	32	<0.2	<10	130	0.52	0.11	0.11	0.02	54	25.4	60	0.58	34.4	3.86	7.75	0.08	0.05	0.01	0.022	0.05	21.1	7.4	0.18	798	0.51	0.01	0.21	34.5
813465	KP007	527850	1149550	40	50	0.08	1.65	19.2	19	<0.2	<10	120	0.67	0.11	0.1	0.02	54.8	25	53	0.6	33	3.54	7.45	0.06	0.06	0.01	0.022	0.05	22.7	8.7	0.15	671	0.54	0.01	0.2	34.6
813466	KP007	527850	1149550	50	60	0.02	1.52	20.3	25	<0.2	<10	80	0.52	0.1	0.11	0.01	43.4	19.7	52	0.55	35.4	3.74	7	0.12	0.07	0.01	0.017	0.04	23.2	7.2	0.18	474	0.42	0.01	0.14	34.8
813467	KP007	527850	1149550	60	70	0.02	1.53	25.2	62	<0.2	<10	120	0.56	0.11	0.11	0.01	48.4	28.6	60	0.52	41	4.48	7.02	0.13	0.08	0.01	0.019	0.04	22.5	6.6	0.17	731	0.52	0.01	0.14	38
813468	KP007	527850	1149550	70	80	0.03	1.47	27.3	49	<0.2	<10	120	0.57	0.11	0.08	0.01	50.4	34.5	59	0.54	39.7	4.53	7.12	0.12	0.08	0.02	0.019	0.04	19.5	5.8	0.13	727	0.65	<0.01	0.19	35.5
813469	KP007	527850	1149550	80	90	0.03	1.53	34.3	13	<0.2	<10	120	0.66	0.13	0.09	0.01	53.5	35.2	70	0.54	42.9	5.37	7.04	<0.05	0.1	0.15	0.021	0.04	21.1	5.2	0.14	746	0.75	<0.01	0.16	38.5
813470	KP007	527850	1149550	90	100	0.05	1.49	35.3	19	<0.2	<10	160	0.76	0.12	0.1	0.02	63	44.7	65	0.55	43.8	5.16	7.3	<0.05	0.11	0.15	0.023	0.04	23	5.9	0.16	1000	0.78	<0.01	0.13	42.5
813472	KP007	527850	1149550	100	110	0.07	1.6	35	101	<0.2	<10	170	0.64	0.13	0.09	0.01	72.7	48.8	70	0.54	44.8	5.34	7.37	<0.05	0.1	0.16	0.022	0.04	21.5	6.1	0.19	1090	0.86	<0.01	0.14	45.4
813473	KP007	527850	1149550	110	120	0.06	1.7	38.3	196	0.4	<10	150	0.76	0.13	0.11	0.01	67.3	48.6	75	0.59	49.6	5.73	7.95	<0.05	0.15	0.14	0.024	0.05	19.6	6.6	0.2	974	0.8	<0.01	0.13	49.2
813474	KP007	527850	1149550	120	130	0.06	1.79	39.2	57	<0.2	<10	160	0.71	0.13	0.13	0.02	73.7	55	76	0.54	48	5.63	7.98	<0.05	0.15	0.12	0.026	0.04	19.9	7.4	0.29	1140	0.74	<0.01	0.09	53.8
813475	KP007	527850	1149550	130	140	0.02	2.21	27.6	11	<0.2	<10	50	0.29	0.08	0.22	<0.01	47	25.4	77	0.29	43.9	4.63	7.45	<0.05	0.08	0.09	0.014	0.02	25.1	11.8	0.88	435	0.28	<0.01	<0.05	63.8
813476	KP007	527850	1149550	140	150	0.08	2.12	35.8	8	<0.2	<10	40	0.34	0.08	0.23	0.01	44.5	21.9	75	0.26	44.4	4.69	7.39	<0.05	0.08	0.07	0.013	0.02	26.1	12.3	0.9	362	0.25	<0.01	<0.05	66.2
813477	KP007	527850	1149550	150	160	0.02	2.26	36.7	20	<0.2	<10	30	0.29	0.08	0.27	0.01	51.5	22.6	76	0.18	45.5	4.85	7.51	<0.05	0.06	0.07	0.011	0.01	29.5	13.5	1.04	370	0.2	<0.01	<0.05	70.9
813478	KP007	527850	1149550	160	170	0.02	2.21	31.3	13	<0.2	<10	30	0.31	0.08	0.25	0.01	40.4	16.5	76	0.22	43.6	4.74	7	<0.05	0.07	0.07	0.013	0.01	24.6	12.6	0.98	269	0.2	<0.01	<0.05	68.2
813479	KP007	527850	1149550	170	180	0.02	2.02	31.8	40	<0.2	<10	30	0.27	0.08	0.21	0.01	36.2	16.6	74	0.26	41.6	4.34	6.38	<0.05	0.07	0.06	0.012	0.02	20.2	11	0.87	270	0.19	<0.01	<0.05	58.7
813480	KP008	526900	1148600	**0**	**10**	0.02	0.93	16.7	90	<0.2	<10	130	0.46	0.08	0.22	0.03	27.3	9.8	51	0.59	16.6	2.07	3.97	<0.05	0.06	0.09	0.015	0.07	13.5	4.1	0.15	354	0.35	<0.01	0.27	24.4
813481	KP008	526900	1148600	10	20	0.21	0.99	17.8	113	<0.2	<10	90	0.44	0.09	0.08	0.02	29.4	10.6	56	0.73	19.9	2.14	4.41	<0.05	0.03	0.08	0.016	0.06	12.9	4.8	0.14	186	0.66	<0.01	0.22	27.5
813482	KP008	526900	1148600	20	30	0.05	1.14	18.2	134	<0.2	<10	90	0.46	0.09	0.06	0.02	26.6	11.2	56	0.79	21	2.42	4.83	<0.05	0.03	0.06	0.014	0.05	11.7	5.5	0.14	161	0.45	<0.01	0.18	28.9
813483	KP008	526900	1148600	30	40	0.17	1.15	20.1	56	<0.2	<10	90	0.54	0.11	0.04	0.01	34.5	16.2	54	0.85	23.5	2.73	5.57	<0.05	0.02	0.04	0.017	0.05	12	6.1	0.11	232	0.58	<0.01	0.19	34.2
813484	KP008	526900	1148600	40	50	0.07	1.23	23.6	120	<0.2	<10	70	0.63	0.14	0.04	0.02	34.4	13.9	54	0.91	26.5	3.19	6.55	<0.05	0.03	0.05	0.02	0.05	12	5.8	0.09	142	0.54	<0.01	0.23	35.2
813485	KP008	526900	1148600	50	60	0.08	1.27	39.7	60	<0.2	<10	70	0.62	0.11	0.1	0.01	43.1	17.7	91	0.86	33	4.07	6.72	<0.05	0.03	0.06	0.023	0.06	11.4	6.4	0.12	209	1.3	<0.01	0.2	42.4
813486	KP008	526900	1148600	60	70	0.04	1.3	23.2	83	<0.2	<10	80	0.59	0.11	0.04	0.01	32.5	15	56	1.04	28.6	3.32	6.62	<0.05	0.04	0.04	0.024	0.06	10.6	6.8	0.1	217	0.53	<0.01	0.19	40.1
813487	KP008	526900	1148600	70	80	0.04	1.4	19.8	44	<0.2	<10	70	0.46	0.1	0.04	0.01	31.9	13.8	53	1.04	32.2	3.02	7.16	0.12	0.04	0.01	0.023	0.06	10.5	8.6	0.14	212	0.43	<0.01	0.16	38.7
813488	KP008	526900	1148600	80	90	0.03	1.66	20.3	43	<0.2	<10	60	0.48	0.1	0.06	0.01	17.7	8	60	1.12	36.3	3.32	7.87	0.13	0.05	0.01	0.024	0.06	11.2	8.5	0.21	110	0.38	0.01	0.14	42.5
813490	KP008	526900	1148600	90	100	0.06	1.93	22.8	39	<0.2	<10	60	0.52	0.1	0.07	0.01	33.1	15.2	69	1.03	41.4	3.96	8.74	0.13	0.06	0.01	0.025	0.06	13	8.8	0.31	250	0.38	0.01	0.12	52.8
813491	KP008	526900	1148600	100	110	0.03	2.08	18.2	54	<0.2	<10	50	0.49	0.11	0.11	0.01	28.9	14.3	75	0.92	43	3.83	8.23	0.15	0.06	0.01	0.02	0.05	18.1	10.2	0.55	254	0.27	0.01	0.08	61.1
813492	KP008	526900	1148600	110	120	0.03	2.02	21.9	36	<0.2	<10	50	0.46	0.1	0.1	0.02	35.3	15.1	74	1.1	44.6	3.7	8.46	0.15	0.06	0.01	0.022	0.06	18	10.2	0.52	282	0.31	0.01	0.08	58.6
813493	KP008	526900	1148600	120	130	0.03	2.34	18.1	70	<0.2	<10	60	0.46	0.09	0.14	0.03	38.6	15.9	88	0.94	47.9	4.26	8.48	0.16	0.06	0.01	0.019	0.04	25.2	12.1	0.83	315	0.24	0.01	0.06	67.6
813495	KP008	526900	1148600	130	140	0.04	2.18	27.2	124	<0.2	<10	70	0.45	0.1	0.19	0.02	64	20.5	98	0.87	45.8	4.34	8.43	0.17	0.06	<0.01	0.02	0.05	23.4	11.8	0.79	534	1.55	0.01	0.05	66.5
813496	KP008	526900	1148600	140	150	0.04	2.43	28.3	88	<0.2	<10	90	0.47	0.09	0.3	0.04	90	30.5	95	0.76	55.9	4.69	8.6	0.19	0.07	<0.01	0.018	0.05	27.2	12.9	1.06	697	1.2	0.01	0.05	78.4
813497	KP008	526900	1148600	150	160	0.03	2.38	27.9	28	<0.2	<10	80	0.42	0.1	0.24	0.05	62.5	23.9	99	0.76	53.1	4.58	8.07	0.18	0.07	0.01	0.017	0.05	26.9	12.8	1.07	548	1.23	0.02	<0.05	71.9
813498	KP008	526900	1148600	160	170	0.04	2.39	43.5	30	<0.2	<10	110	0.49	0.13	0.21	0.05	90.8	37.8	92	0.8	59.8	4.61	8.14	0.16	0.06	<0.01	0.018	0.05	24.6	13.8	1.03	754	0.67	0.02	0.05	78
813499	KP008	526900	1148600	170	180	0.05	2.18	43	28	<0.2	<10	100	0.49	0.16	0.17	0.05	70.9	30.5	87	0.88	59.6	4.48	8.21	0.17	0.08	0.01	0.019	0.06	19.5	12	0.84	633	1.01	0.02	0.05	68.7
813500	KP008	526900	1148600	180	190	0.06	2.22	34.8	22	<0.2	<10	70	0.43	0.12	0.2	0.05	62.9	26.7	100	0.8	54.5	4.51	7.12	0.18	0.06	0.01	0.015	0.05	23.8	11.7	1.03	550	1.32	0.01	<0.05	66
813551	KP008	526900	1148600	190	200	0.02	1.94	34.3	25	<0.2	<10	50	0.63	0.09	0.11	0.06	50.4	19.2	96	1.7	52	5.17	8.35	0.18	0.12	<0.01	0.023	0.06	19.1	9	0.66	397	0.24	0.01	0.06	62.5
813552	KP008	526900	1148600	200	210	0.04	2.07	36.1	25	<0.2	<10	90	0.59	0.09	0.14	0.04	58.6	21.5	97	1.35	56.6	4.99	8.14	0.17	0.09	<0.01	0.023	0.07	19.2	10.5	0.75	528	0.65	0.01	0.05	62.5
813553	KP009	527000	1148600	**0**	**10**	0.06	1.29	70.4	214	<0.2	<10	400	0.5	0.14	0.77	0.07	36.9	11	51	0.88	25	2.36	5.35	0.14	0.1	0.02	0.018	0.14	17.6	5.9	0.21	395	0.44	<0.01	0.37	28.6
813554	KP009	527000	1148600	10	20	0.05	0.91	58.4	246	<0.2	<10	120	0.41	0.11	0.15	0.03	33.9	11.3	51	0.8	24.9	2.53	5.34	0.13	0.04	0.02	0.018	0.08	12.6	4.2	0.1	236	0.53	<0.01	0.28	24.6
813556	KP009	527000	1148600	20	30	0.28	0.92	61.7	261	0.7	<10	90	0.41	0.11	0.11	0.02	35.2	12.1	57	0.86	25.8	2.66	5.48	0.14	0.04	0.03	0.02	0.08	13.3	4.3	0.09	230	0.56	<0.01	0.26	24.9
813557	KP009	527000	1148600	30	40	0.05	1.25	94.8	175	<0.2	<10	60	0.53	0.14	0.04	0.02	39.4	23	86	0.94	35.4	4.51	7.43	0.15	0.05	0.02	0.027	0.07	11.6	6.2	0.07	256	0.84	<0.01	0.33	36.2
813558	KP009	527000	1148600	40	50	0.04	1.42	103	228	<0.2	<10	60	0.54	0.14	0.05	0.02	36.6	18.1	97	0.93	40.7	5.02	9.05	0.16	0.07	0.01	0.031	0.07	12.8	5.8	0.07	215	0.97	<0.01	0.36	40.9
813559	KP009	527000	1148600	50	60	0.05	1.49	108.5	252	0.2	<10	80	0.54	0.14	0.05	0.02	48.1	29	108	0.94	44.3	5.32	9.35	0.16	0.08	0.02	0.032	0.07	13.9	6.2	0.06	300	0.97	<0.01	0.33	43.4
813560	KP009	527000	1148600	60	70	0.05	1.48	109.5	201	<0.2	<10	80	0.66	0.14	0.05	0.02	57	35.2	116	1.01	47.4	5.56	9.19	0.17	0.08	0.01	0.032	0.07	17.8	6	0.05	291	0.82	<0.01	0.31	50.2
813562	KP009	527000	1148600	70	80	0.02	1.17	95.6	134	<0.2	<10	70	0.56	0.12	0.04	0.02	44.5	24.5	144	0.81	42.5	4.98	8.96	0.17	0.12	0.01	0.029	0.05	15.6	4.1	0.04	236	0.59	0.01	0.26	54.5
813563	KP009	527000	1148600	80	90	0.02	1.05	95.8	88	<0.2	<10	60	0.55	0.12	0.03	0.02	33.5	15.4	171	0.72	41.9	4.93	8.82	0.16	0.12	0.01	0.028	0.04	14	3.5	0.03	150	0.48	<0.01	0.18	52.2
813564	KP009	527000	1148600	90	100	0.02	0.92	87.3	130	<0.2	<10	50	0.52	0.13	0.04	0.02	37.8	15.8	189	0.62	40.8	4.83	8.03	0.16	0.17	0.01	0.027	0.03	15	2.7	0.03	158	0.44	<0.01	0.18	53.1
813565	KP009	527000	1148600	100	110	0.02	0.85	80.8	71	<0.2	<10	50	0.43	0.11	0.03	0.01	32.9	12.5	168	0.58	38.7	4.62	8.04	0.16	0.17	0.01	0.026	0.03	13.7	2.4	0.03	133	0.42	<0.01	0.19	44.6
813566	KP009	527000	1148600	110	120	0.01	0.66	62.9	43	<0.2	<10	40	0.37	0.08	0.03	0.01	25.6	7.7	179	0.46	32.3	4.11	7.14	0.14	0.21	0.01	0.021	0.03	11.1	1.8	0.02	80	0.25	<0.01	0.13	40.9
813567	KP009	527000	1148600	120	130	0.01	0.61	61.4	45	<0.2	<10	30	0.37	0.07	0.02	0.01	23.4	6.4	171	0.44	32.6	4.01	7.11	0.15	0.25	0.01	0.02	0.03	11.3	1.8	0.02	55	0.22	<0.01	0.11	41.4
813568	KP009	527000	1148600	130	140	0.01	0.41	55.1	36	<0.2	<10	20	0.34	0.05	0.02	0.02	22.3	5	197	0.2	31.1	3.73	6.28	0.14	0.35	<0.01	0.015	0.02	10.5	0.7	0.02	46	0.11	<0.01	0.09	63.4
813570	KP009	527000	1148600	140	150	0.03	0.45	54.2	51	<0.2	<10	20	0.33	0.05	0.02	0.02	21	4.3	186	0.24	31.4	3.82	6.41	0.15	0.3	<0.01	0.014	0.02	10.2	0.8	0.01	35	0.13	<0.01	0.09	51.4
813571	KP009	527000	1148600	150	160	0.02	0.48	54.9	43	<0.2	<10	20	0.32	0.06	0.02	0.02	21.8	4.7	184	0.26	31.1	3.78	6.44	0.14	0.24	<0.01	0.017	0.02	9.5	1	0.02	56	0.17	<0.01	0.07	39.9
813572	KP009	527000	1148600	160	170	0.02	0.47	62.3	26	<0.2	<10	20	0.37	0.11	0.02	0.02	22.1	6.4	218	0.23	34.7	3.99	6.32	0.15	0.3	<0.01	0.02	0.02	9.4	0.8	0.02	65	0.13	<0.01	0.08	52.7
813573	KP009	527000	1148600	170	180	0.01	0.49	58.7	37	<0.2	<10	20	0.37	0.08	0.02	0.02	25.9	5.2	188	0.32	32.8	3.82	6.37	0.16	0.26	0.01	0.02	0.02	11	1.2	0.02	43	0.16	<0.01	0.08	43.4
813574	KP009	527000	1148600	180	190	0.01	0.31	47.8	25	<0.2	<10	10	0.35	0.05	0.02	0.02	20.1	3.9	145	0.17	25.6	2.85	4.23	0.09	0.25	0.1	0.013	0.02	7.4	0.6	0.02	27	0.09	<0.01	0.05	44.7
813579	KP010	527100	1148600	**0**	**10**	0.72	0.59	403	2630	4.1	<10	30	0.28	0.2	0.02	0.02	12.85	2.2	50	0.3	26.3	2.62	4.5	0.09	0.03	0.15	0.018	0.04	5.1	1.9	0.02	24	1	<0.01	0.14	7.1
813580	KP010	527100	1148600	10	20	0.24	0.47	400	2250	1.5	<10	20	0.25	0.17	0.02	0.05	10.15	2.1	50	0.25	23.6	2.52	4.19	0.09	0.07	0.19	0.017	0.03	4.4	1.4	0.01	20	0.9	<0.01	0.1	5.4
813581	KP010	527100	1148600	20	30	0.54	0.88	370	2780	2.7	<10	40	0.34	0.19	0.03	0.02	18.5	2.8	53	0.47	24.2	2.42	4.84	<0.05	0.02	0.03	0.02	0.05	7.3	3.1	0.02	32	0.93	<0.01	0.2	9
813583	KP010	527100	1148600	30	40	0.16	1.44	341	1345	0.8	<10	50	0.48	0.19	0.02	0.01	26.5	4	61	0.71	28	2.81	6.91	<0.05	0.02	0.04	0.025	0.06	9.7	5.6	0.03	35	0.95	<0.01	0.35	14.7
813584	KP010	527100	1148600	40	50	0.12	1.49	390	1580	0.8	<10	50	0.43	0.2	0.02	0.01	26	4.1	67	0.68	28.7	2.98	6.81	<0.05	0.02	0.04	0.026	0.06	9.4	5.6	0.03	36	0.94	<0.01	0.31	14.9
813585	KP010	527100	1148600	50	60	0.28	1.6	449	1650	1.3	<10	40	0.45	0.22	0.01	0.01	34.4	4.9	70	0.74	33	3.21	7.83	<0.05	0.07	0.06	0.028	0.06	11.7	5.7	0.03	36	1.02	<0.01	0.33	16.5
813586	KP010	527100	1148600	60	70	0.65	1.33	526	1390	3	<10	40	0.39	0.22	0.01	0.01	33.4	4.3	67	0.62	32.3	3.16	7.32	0.05	0.08	0.05	0.029	0.05	11.7	4.3	0.02	29	1.08	<0.01	0.27	13.9
813587	KP010	527100	1148600	70	80	0.05	0.99	574	708	0.6	<10	30	0.28	0.16	0.01	0.01	26.4	3	75	0.41	30.8	3.39	7.09	<0.05	0.1	0.03	0.023	0.04	10.5	2.7	0.01	18	0.78	<0.01	0.16	10.2
813588	KP010	527100	1148600	80	90	0.43	0.4	467	1915	2.6	<10	20	0.14	0.31	<0.01	0.01	19.75	1	32	0.24	20.8	1.52	2.63	<0.05	0.13	0.02	0.013	0.03	9.2	1.2	<0.01	5	1.19	<0.01	<0.05	3.1
813589	KP010	527100	1148600	90	100	0.03	0.48	534	531	0.5	<10	30	0.16	0.1	0.01	0.01	36.6	1.4	68	0.2	22.1	2.22	4.8	0.05	0.12	0.01	0.019	0.02	17.3	1.2	0.01	8	0.57	<0.01	0.05	4.8
813590	KP010	527100	1148600	100	110	0.08	0.34	825	894	0.9	<10	30	0.24	0.22	<0.01	0.02	29	1.1	47	0.15	32.4	2.03	3.38	0.05	0.14	0.01	0.022	0.02	12.1	0.6	<0.01	5	0.58	<0.01	<0.05	3.9
813591	KP010	527100	1148600	110	120	0.02	0.48	637	304	0.2	<10	20	0.27	0.05	<0.01	0.01	15.35	1.6	105	0.13	33.4	4.03	7.36	<0.05	0.15	0.02	0.028	0.02	6.6	0.8	<0.01	10	0.38	<0.01	<0.05	5.6
813592	KP010	527100	1148600	120	130	0.02	0.43	794	475	0.5	<10	20	0.32	0.16	<0.01	0.02	17.45	1.5	80	0.15	35.7	3.37	5.76	<0.05	0.14	0.01	0.025	0.02	7.1	0.8	<0.01	8	0.95	<0.01	<0.05	5.2
813593	KP010	527100	1148600	130	140	0.2	0.4	731	1265	1.5	<10	20	0.28	0.21	<0.01	0.01	15.15	1.5	76	0.15	32.3	3.31	5.53	<0.05	0.14	0.01	0.023	0.02	5.9	0.8	<0.01	9	0.98	<0.01	<0.05	5.1

Appendix C:Pits, Au and other elements in the regolith of the Lawra area analysed by ICP and FA-AAS Techniques

Sample ID	Pit ID	UTM-E	UTM-N	From (m)	To (m)	Ag ppm	Al ppm	As ppm	Au ppb	Au ppm	B ppm	Ba ppm	Be ppm	Bi ppm	Ca %	Cd ppm	Ce ppm	Co ppm	Cr ppm	Cs ppm	Cu ppm	Fe %	Ga ppm	Ge ppm	Hf ppm	Hg ppm	In ppm	K %	La ppm	Li ppm	Mg ppm	Mn ppm	Mo ppm	Na ppm	Nb ppm	Ni ppm
813594	KP010	527100	1148600	140	150	0.05	0.35	425	878	0.6	<10	20	0.21	0.18	<0.01	0.02	26.8	1.4	73	0.1	20.8	2.88	5.82	<0.05	0.13	0.01	0.022	0.02	11.6	0.5	<0.01	9	0.51	<0.01	<0.05	5
813595	KP011	527200	1148600	**0**	**10**	0.07	1.03	96.2	304	<0.2	<10	80	0.49	0.13	0.09	0.02	38.9	11.6	67	0.53	27	3.04	6.08	<0.05	0.05	0.02	0.017	0.07	12.7	3.7	0.05	292	1.36	<0.01	0.34	41.8
813596	KP011	527200	1148600	10	20	0.09	1	97.3	364	0.2	<10	60	0.49	0.13	0.02	0.02	35.6	9.9	58	0.52	26.6	2.94	6.14	<0.05	0.07	0.01	0.016	0.05	10.4	3.7	0.03	145	0.6	<0.01	0.29	33.7
813597	KP011	527200	1148600	20	30	0.11	1.31	117	488	0.3	<10	60	0.54	0.15	0.01	0.01	38.7	10.7	66	0.62	32.5	3.65	7.5	<0.05	0.08	0.01	0.02	0.06	11.4	4.8	0.02	132	0.69	<0.01	0.29	40.2
813598	KP011	527200	1148600	30	40	0.15	1.37	134.5	417	<0.2	<10	50	0.62	0.16	0.01	0.01	41	14.2	69	0.68	38.8	4.02	8.81	0.05	0.09	0.01	0.023	0.05	12.7	5.5	0.02	175	0.8	<0.01	0.3	49.1
813599	KP011	527200	1148600	40	50	0.1	1.33	140.5	233	0.3	<10	40	0.53	0.15	0.01	0.02	33.5	10.8	80	0.59	43.9	4.83	9.13	0.05	0.1	0.01	0.019	0.05	12	4.5	0.02	146	0.65	<0.01	0.22	61.9
813600	KP011	527200	1148600	50	60	0.26	1.07	133.5	242	1.2	<10	30	0.43	0.15	0.01	0.02	28	8.7	87	0.49	45.1	4.79	8.12	0.05	0.14	0.02	0.018	0.04	11.4	3.4	0.01	113	0.56	<0.01	0.18	66.7
813601	KP011	527200	1148600	60	70	0.04	0.73	135.5	149	<0.2	<10	20	0.48	0.11	<0.01	0.03	22.8	7.9	93	0.31	50	4.76	7.06	<0.05	0.16	0.01	0.013	0.03	9.6	2.2	0.01	114	0.42	<0.01	0.12	79.2
813603	KP011	527200	1148600	70	80	0.03	0.62	148	156	<0.2	<10	20	0.41	0.1	<0.01	0.03	23.5	8.8	75	0.28	48.1	4.35	6.46	<0.05	0.17	0.01	0.013	0.03	9.6	2	0.01	117	0.38	<0.01	0.1	76
813610	KP012	527300	1148600	**0**	**10**	0.03	0.71	18.3	23	<0.2	<10	90	0.36	0.08	0.1	0.02	45.5	8	45	0.38	17.1	2.2	4.16	0.05	0.04	0.02	0.012	0.04	17.9	1.5	0.04	294	0.5	<0.01	0.31	18.8
813611	KP012	527300	1148600	10	20	0.03	0.76	23.2	18	<0.2	<10	40	0.34	0.1	0.01	<0.01	40.5	6.4	50	0.39	20.3	2.85	4.48	<0.05	0.05	0.01	0.017	0.03	14	1.5	0.01	51	0.5	<0.01	0.29	18.9
813612	KP012	527300	1148600	20	30	0.03	0.87	29.2	31	<0.2	<10	40	0.32	0.1	0.01	<0.01	41.9	6.9	57	0.42	23.4	3.48	4.97	<0.05	0.08	0.01	0.015	0.03	13.1	1.7	0.01	54	0.51	<0.01	0.33	21.9
813613	KP012	527300	1148600	30	40	0.81	0.86	29.1	25	<0.2	<10	40	0.36	0.11	0.01	<0.01	48.1	7.6	56	0.42	24	3.41	5.31	0.05	0.07	0.01	0.018	0.03	14.6	1.7	0.01	58	0.49	<0.01	0.31	23.7
813614	KP012	527300	1148600	40	50	0.04	0.93	31.1	31	<0.2	<10	40	0.35	0.11	0.02	<0.01	53.6	8.7	54	0.47	26.4	3.41	6	0.05	0.09	0.01	0.021	0.03	18.3	2	0.01	67	0.56	<0.01	0.33	25.3
813615	KP012	527300	1148600	50	60	0.02	0.85	37.4	19	<0.2	<10	30	0.44	0.13	0.03	<0.01	58.2	9.5	51	0.43	27.8	3.84	5.67	0.05	0.12	0.01	0.02	0.03	17.1	1.7	0.01	93	0.52	<0.01	0.35	25
813616	KP012	527300	1148600	60	70	0.02	0.54	33.7	8	<0.2	<10	20	0.26	0.15	0.07	<0.01	33.1	6.6	40	0.27	22.2	3.23	4.28	0.07	0.14	0.01	0.015	0.02	11.2	1.1	0.01	66	0.44	<0.01	0.45	15.4
813617	KP012	527300	1148600	70	80	0.02	0.47	31.8	16	<0.2	<10	20	0.25	0.11	0.03	<0.01	34.3	5.9	35	0.23	20.6	2.88	3.44	0.08	0.16	0.01	0.013	0.01	10.1	1	0.01	52	0.4	<0.01	0.43	13.9
813618	KP012	527300	1148600	80	90	0.01	0.4	29.2	12	<0.2	<10	20	0.19	0.09	0.03	<0.01	23.2	4.2	38	0.13	16.9	3.31	2.47	0.07	0.13	0.01	0.01	0.01	6.3	0.5	0.01	44	0.29	<0.01	0.36	11.9
813626	KP013	527400	1148600	**0**	**10**	0.04	0.83	15.6	20	<0.2	<10	70	0.46	0.1	0.13	0.02	46.9	20.7	54	0.36	40.3	3.56	6.14	0.13	0.06	0.02	0.017	0.04	15.9	2	0.04	310	0.78	<0.01	0.32	32.4
813627	KP013	527400	1148600	10	20	0.04	0.85	16.5	7	<0.2	<10	40	0.42	0.1	0.02	0.02	47	14.8	57	0.32	49.3	4.31	6.76	0.13	0.07	0.02	0.016	0.03	12.7	1.7	0.02	94	0.67	<0.01	0.24	38.2
813628	KP013	527400	1148600	20	30	0.04	0.85	16.2	5	<0.2	<10	30	0.41	0.1	0.01	0.02	39.5	13.4	59	0.32	53.1	4.58	7.19	0.13	0.09	0.02	0.018	0.03	12.9	1.6	0.01	77	0.66	<0.01	0.23	43.2
813629	KP013	527400	1148600	30	40	0.03	0.74	21.2	<5	<0.2	<10	20	0.42	0.14	0.01	0.03	28.2	16.4	66	0.2	64.5	5.86	7.92	0.14	0.11	0.01	0.021	0.02	11.3	0.9	0.01	105	0.63	<0.01	0.19	61.6
813630	KP013	527400	1148600	40	50	0.03	0.72	20.9	<5	<0.2	<10	20	0.38	0.11	0.01	0.02	34	20.9	64	0.2	61.7	5.63	8.18	0.14	0.12	0.01	0.02	0.02	12.5	1	0.01	127	0.6	<0.01	0.19	56.7
813631	KP013	527400	1148600	50	60	0.04	0.75	21.5	<5	<0.2	<10	20	0.46	0.13	0.01	0.02	35.3	19.5	64	0.21	65.8	5.66	8.13	0.14	0.13	0.01	0.019	0.02	13.3	1.1	0.01	138	0.59	<0.01	0.18	55.4
813647	KP014	527500	1148600	**0**	**10**	0.05	1.4	27.4	38	<0.2	<10	70	0.57	0.1	0.07	0.02	69.4	22.5	65	0.44	46.7	4.17	6.62	0.13	0.07	0.03	0.019	0.04	14.7	5.9	0.22	601	0.65	<0.01	0.27	52.6
813648	KP014	527500	1148600	10	20	0.05	1.79	28.8	27	<0.2	<10	50	0.58	0.11	0.04	0.01	55.3	20.7	71	0.52	54.7	4.8	7.97	0.14	0.08	0.02	0.02	0.03	15.8	7.3	0.24	428	0.68	<0.01	0.24	60.8
813649	KP014	527500	1148600	20	30	0.04	2.21	25.7	10	<0.2	<10	30	0.48	0.12	0.04	0.01	45.2	18.7	73	0.51	60.4	5.38	9.15	0.14	0.1	0.02	0.022	0.03	18.4	9.1	0.38	319	0.56	<0.01	0.19	70.6
813651	KP014	527500	1148600	30	40	0.03	2.17	20.5	7	<0.2	<10	30	0.42	0.11	0.04	<0.01	42.7	17	70	0.45	58.5	5.01	8.73	0.17	0.11	0.02	0.021	0.03	21.8	9.9	0.51	283	0.44	<0.01	0.14	71
813652	KP014	527500	1148600	40	50	0.03	2.22	17.6	6	<0.2	<10	30	0.35	0.1	0.05	0.01	41.1	17.6	71	0.41	60.5	4.89	8.8	0.17	0.11	0.01	0.019	0.02	24.9	10.8	0.63	276	0.34	<0.01	0.11	73.8
813668	KP015	527600	1148600	**0**	**10**	0.04	0.92	21.5	<5	<0.2	<10	90	0.47	0.1	0.12	0.03	39.5	14.5	68	0.32	45.7	4.17	6.26	0.13	0.06	0.02	0.016	0.05	13.4	2	0.05	341	0.63	<0.01	0.35	46.2
813670	KP015	527600	1148600	10	20	0.04	1.02	22.8	5	<0.2	<10	50	0.41	0.11	0.01	0.02	37.7	18.4	74	0.32	49.5	4.91	7.14	0.13	0.07	0.02	0.018	0.04	11.3	3.2	0.02	241	0.56	<0.01	0.3	51.4
813671	KP015	527600	1148600	20	30	0.03	0.91	19.7	<5	<0.2	<10	30	0.34	0.12	<0.01	0.02	27.9	11.9	71	0.25	47.7	5.16	7.1	0.12	0.09	0.02	0.017	0.03	8.7	1.8	0.01	159	0.45	<0.01	0.22	54.6
813672	KP015	527600	1148600	30	40	0.02	0.54	14.6	<5	<0.2	<10	10	0.26	0.21	<0.01	0.02	12.8	11.5	61	0.08	49.2	5.5	6.93	0.11	0.17	0.01	0.015	0.01	5.1	0.5	<0.01	185	0.21	<0.01	0.12	72.1
813673	KP015	527600	1148600	40	50	0.02	0.53	13.5	38	<0.2	<10	10	0.26	0.14	<0.01	0.02	13.45	11.4	62	0.08	48.6	5.43	6.88	0.12	0.17	0.01	0.014	0.01	5.1	0.6	<0.01	184	0.21	<0.01	0.13	73.8
813674	KP015	527600	1148600	50	60	0.02	0.49	12.1	<5	<0.2	<10	10	0.27	0.13	<0.01	0.02	14.35	11.5	60	0.07	48	5.31	6.79	0.13	0.19	0.01	0.014	0.01	5.1	0.6	<0.01	197	0.19	<0.01	0.13	73.7
813687	KP016	527700	1148600	**0**	**10**	0.04	0.73	27.6	42	<0.2	<10	90	0.46	0.08	0.09	0.02	32.6	22.1	65	0.36	33	3.35	5	0.12	0.05	0.02	0.012	0.04	17.4	2.4	0.07	554	0.43	<0.01	0.24	36.9
813688	KP016	527700	1148600	10	20	0.04	0.8	28.1	9	<0.2	<10	80	0.41	0.09	0.08	0.02	37	25.9	65	0.39	33.5	3.53	4.92	0.11	0.05	0.02	0.011	0.04	17.5	2.6	0.07	533	0.41	<0.01	0.23	35.1
813690	KP016	527700	1148600	20	30	0.04	1.06	37.5	8	<0.2	<10	60	0.49	0.12	0.04	0.01	38.6	25.2	68	0.5	43.8	4.43	6.65	0.14	0.08	0.01	0.016	0.04	20.5	3	0.06	362	0.5	<0.01	0.22	43.8
813691	KP016	527700	1148600	30	40	0.03	1.09	41.3	8	<0.2	<10	50	0.5	0.11	0.03	0.01	30.2	19.7	67	0.49	51	5.07	7.04	0.15	0.1	0.01	0.016	0.04	17.8	3	0.05	307	0.47	<0.01	0.21	47.1
813692	KP016	527700	1148600	40	50	0.03	0.98	41.5	17	<0.2	<10	50	0.43	0.11	0.02	0.01	28.7	18.8	65	0.45	52.1	5.06	6.9	0.14	0.11	0.01	0.015	0.03	16	2.8	0.04	318	0.44	<0.01	0.18	46.3
813693	KP016	527700	1148600	50	60	0.02	0.81	35	8	<0.2	<10	40	0.39	0.1	0.02	0.01	23.6	13.6	60	0.39	48.4	4.72	6.11	0.13	0.12	0.01	0.013	0.03	16.2	2.1	0.03	190	0.29	<0.01	0.16	41.2
813694	KP016	527700	1148600	60	70	0.02	0.6	32.2	<5	<0.2	<10	20	0.32	0.09	0.01	0.01	20.7	10.5	56	0.3	50.7	4.55	5.36	0.13	0.14	0.01	0.011	0.02	15	1.4	0.03	155	0.18	<0.01	0.12	38.1
813695	KP016	527700	1148600	70	80	0.02	0.55	30.8	<5	<0.2	<10	20	0.35	0.08	0.01	0.01	21.3	12.8	60	0.28	50.3	4.74	5.13	0.12	0.15	0.01	0.011	0.02	15.2	1.3	0.02	195	0.14	<0.01	0.11	37.4
813696	KP016	527700	1148600	80	90	0.02	0.49	45.6	13	<0.2	<10	40	0.36	0.13	0.01	0.02	22	15.8	56	0.31	54.7	4.86	5.17	0.11	0.19	0.01	0.01	0.03	12.2	1	0.02	303	0.34	<0.01	0.12	56.4
813697	KP016	527700	1148600	90	100	0.04	0.4	51.6	7	<0.2	<10	50	0.48	0.13	<0.01	0.04	29.8	20.4	51	0.24	56.8	4.68	4.96	0.16	0.24	0.01	0.011	0.02	12.1	0.7	0.02	414	0.33	<0.01	0.13	61.8
813698	KP016	527700	1148600	100	110	0.01	0.4	36.5	<5	<0.2	<10	20	0.41	0.12	<0.01	0.01	18.9	10.7	59	0.24	53.3	4.71	4.78	0.14	0.19	0.01	0.01	0.02	12.6	0.7	0.02	163	0.18	<0.01	0.09	48.9
813699	KP016	527700	1148600	110	120	0.01	0.37	37.6	<5	<0.2	<10	30	0.42	0.13	<0.01	0.02	19.75	12.6	55	0.24	52.2	4.54	4.54	0.14	0.18	0.01	0.01	0.02	12.7	0.7	0.02	200	0.19	<0.01	0.09	51.4
813706	SP001	519090	1143591	**0**	**10**	0.04	1.56	11.7	21	<0.2	<10	210	1	0.08	0.43	0.03	75.2	13.3	90	0.59	31.9	7.77	7.99	0.15	0.12	0.03	0.042	0.05	17.8	2.5	0.08	491	2.06	<0.01	1.46	13.7
813707	SP001	519090	1143591	10	20	0.02	1.94	20.6	8	<0.2	<10	100	1.23	0.14	0.18	0.02	82.9	11.9	147	0.39	51.7	13.7	9.58	0.15	0.19	0.03	0.061	0.03	14.8	1.5	0.04	332	3.19	<0.01	1.54	12.9
813708	SP001	519090	1143591	20	30	0.12	1.63	21.1	39	4.8	<10	90	1.17	0.13	0.17	0.01	106	8.9	138	0.34	52.8	12.4	9.48	0.14	0.19	0.02	0.056	0.03	13.4	1.2	0.04	319	3.16	<0.01	1.45	12.7
813709	SP001	519090	1143591	30	40	0.03	1.79	22.2	<5	<0.2	<10	100	1.21	0.16	0.18	0.01	115	8.9	134	0.36	50.9	13.05	9.9	0.14	0.2	0.03	0.062	0.03	13.1	1.3	0.04	349	3.39	<0.01	1.54	13.3
813710	SP001	519090	1143591	40	50	0.02	1.59	18.6	167	<0.2	<10	150	1.06	0.14	0.33	0.02	97.9	8.4	119	0.42	48.9	11.05	8.75	0.15	0.16	0.03	0.054	0.03	14.8	1.5	0.06	368	2.8	<0.01	1.63	13.1
813711	SP001	519090	1143591	50	60	0.04	1.64	14.1	66	<0.2	<10	280	0.99	0.08	0.64	0.04	120.5	8.2	89	0.63	43.2	8.61	8.62	0.15	0.15	0.04	0.047	0.05	18.3	2.2	0.1	518	2.5	<0.01	1.62	14.5
813712	SP001	519090	1143591	60	70	0.04	1.72	22.5	93	<0.2	<10	180	1.16	0.14	0.36	0.03	163.5	8.4	120	0.43	54.7	12.25	10.1	0.15	0.15	0.03	0.059	0.03	15.6	1.5	0.06	465	3.04	<0.01	1.62	13.7
813713	SP001	519090	1143591	70	80	0.04	1.6	19.7	7	<0.2	<10	100	0.99	0.09	0.23	0.02	128.5	7.5	114	0.36	44.4	11.2	9.91	0.15	0.17	0.02	0.054	0.02	13.9	1.2	0.03	350	2.56	<0.01	1.2	12.7
813714	SP001	519090	1143591	80	90	0.03	1.59	22.3	14	<0.2	<10	50	1.13	0.08	0.12	0.01	168.5	7.9	112	0.3	53.3	12.3	10.15	0.16	0.29	0.01	0.062	0.01	12	0.9	0.02	281	2.69	<0.01	0.76	14.6
813715	SP001	519090	1143591	90	100	0.05	1.63	23	12	<0.2	<10	50	1.21	0.08	0.1	0.01	125	7.5	114	0.28	57.1	13	9.85	0.13	0.28	0.01	0.053	0.01	11.3	0.9	0.02	247	2.82	<0.01	0.65	14.3
813716	SP001	519090	1143591	100	110	0.03	1.6	22.9	29	<0.2	<10	50	1.26	0.08	0.09	0.01	158.5	7.6	107	0.28	55.7	12.35	9.74	0.13	0.29	0.02	0.062	0.01	11.8	0.8	0.01	252	2.64	<0.01	0.56	13
813717	SP001	519090	1143591	110	120	0.03	1.67	24.9	45	<0.2	<10	60	1.48	0.07	0.08	0.01	215	8.8	132	0.27	63.7	14.65	10.35	0.15	0.3	0.02	0.061	0.01	11	0.7	0.01	328	3.25	<0.01	0.68	14
813718	SP001	519090	1143591	120	130	0.04	1.59	21.4	<5	<0.2	<10	80	1.31	0.07	0.08	0.01	286	7.8	118	0.31	58.4	12.35	9.92	0.16	0.3	0.02	0.062	0.01	12.9	0.9	0.01	409	2.94	<0.01	0.6	12.6
813720	SP001	519090	1143591	130	140	0.05	1.58	25.2	<5	<0.2	<10	70	1.49	0.06	0.07	0.01	220	9.8	119	0.27	67	13.7	9.49	0.15	0.28	0.02	0.054	0.01	11.2	0.8	0.01	361	2.71	<0.01	0.51	16.6
813721	SP001	519090	1143591	140	150	0.07	1.39	16.4	333	<0.2	<10	110	0.73	0.12	0.07	0.01	232	10.9	117	0.3	45.8	11.35	9.01	0.14	0.27	0.01	0.058	0.01	11.2	0.8	0.01	526	2.79	<0.01	0.46	10.1
813722	SP001	519090	1143591	150	160	0.06	1.33	17.1	<5	<0.2	<10	90	0.84	0.14	0.07	0.01	273	11.7	108	0.25	55.4	12.3	8.42	0.15	0.27	0.01	0.061	0.01	11.5	0.7	0.01	461	2.59	<0.01	0.41	13.6
813723	SP001	519090	1143591	160	170	0.07	1.28	14.7	7	<0.2	<10	100	0.76	0.17	0.08	0.01	219	20.8	105	0.3	48	10.9	8.29	0.14	0.23	0.01	0.06	0.01	11.4	1.5	0.01	522	2.4	<0.01	0.48	12.2
813724	SP001	519090	1143591	170	180	0.07	1.39	13.8	79	<0.2	<10	110	0.72	0.09	0.07	0.01	155.5	28.1	91	0.34	43.1	10.3	9.14	0.13	0.28	0.01	0.06	0.01	11.9	2	0.01	580	2.61	<0.01	0.46	11.5
813725	SP001	519090	1143591	180	190	0.08	1.44	12.7	<5	<0.2	<10	110	0.65	0.08	0.07	0.01	115.5	25.4	84	0.37	38.8	10.15	8.58	0.14	0.3	0.01	0.06	0.01	12.2	1.9	0.01	558	2.48	<0.01	0.44	9.8
813726	SP001	519090	1143591	190	200	0.05	1.45	13.5	28	<0.2	<10	70	0.69	0.08	0.06	<0.01	195.5	6	88	0.3	40.1	11	9.49	0.14	0.29	<0.01	0.072	0.01	12.5	0.6	0.01	385	2.92	<0.01	0.5	7.5
813727	SP001	519090	1143591	200	210	0.05	1.42	14.1	155	<0.2	<10	50	0.7	0.08	0.05	0.01	158.5	10.3	87	0.29	42.9	11.35	9.28	0.14	0.26	0.01	0.073	0.01	12.6	0.8	0.01	327	2.5	<0.01	0.42	9.2
813728	SP001	519090	1143591	210	220	0.04	1.38	15.3	<5	<0.2	<10	70	0.93	0.08	0.04	<0.01	124	19.3	111	0.32	40.5	10.35	9.98	0.17	0.22	0.01	0.058	0.01	12.3	1.5	0.02	384	1.97	<0.01	0.38	13.9
813729	SP001	519090	1143591	220	230	0.05	1.37	15.3	393	<0.2	<10	60	0.9	0.08	0.04	0.01	124.5	20.7	106	0.32	38.4	9.96	10.05	0.18	0.24	0.01	0.059	0.01	14.7	1.6	0.01	344	1.82	<0.01	0.33	12.8
813730	SP001	519090	1143591	230	240	0.05	1.39	17.6	<5	<0.2	<10	60	1.13	0.09	0.03	0.01	173	16.9	104	0.3	40.5	10.45	9.75	0.18	0.25	0.02	0.058	0.01	13.3	1.2	0.01	336	1.76	<0.01	0.28	15
813731	SP001	519090	1143591	240	250	0.04	1.37	12.1	5	<0.2	<10	60	0.79	0.08	0.02	0.01	134	20.4	79	0.36	30.6	7.59	8.83	0.18	0.3	0.01	0.045	0.01	14.8	1.6	0.01	326	1.39	<0.01	0.24	10.8
813732	SP001	519090	1143591	250	260	0.05	1.36	13	<5	<0.2	<10	70	0.82	0.08	0.02	0.01	152.5	19.6	83	0.33	31.3	8.27	8.58	0.18	0.23	0.01	0.052	0.01	13.2	1.6	0.01	370	1.56	<0.01	0.29	11.3

Appendix C:Pits, Au and other elements in the regolith of the Lawra area analysed by ICP and FA-AAS Techniques

Sample ID	Pit ID	UTM-E	UTM-N	From (m)	To (m)	Ag ppm	Al ppm	As ppm	Au ppb	Au ppm	B ppm	Ba ppm	Be ppm	Bi ppm	Ca %	Cd ppm	Ce ppm	Co ppm	Cr ppm	Cs ppm	Cu ppm	Fe %	Ga ppm	Ge ppm	Hf ppm	Hg ppm	In ppm	K %	La ppm	Li ppm	Mg ppm	Mn ppm	Mo ppm	Na ppm	Nb ppm	Ni ppm
813733	SP001	519090	1143591	260	270	0.07	1.32	11.6	7	<0.2	<10	100	0.72	0.09	0.01	0.01	178	26.3	84	0.33	29.4	7.69	8.45	0.17	0.23	0.02	0.047	0.01	13	1.8	0.01	507	1.46	<0.01	0.25	11
813734	SP001	519090	1143591	270	280	0.07	1.3	10.7	158	<0.2	<10	90	0.57	0.09	0.02	0.01	153.5	20.8	75	0.34	28.3	7.05	7.74	0.1	0.25	0.02	0.045	0.01	13.6	1.9	0.01	463	1.37	<0.01	0.24	10.4
813735	SP001	519090	1143591	280	290	0.08	1.06	10.1	364	<0.2	<10	110	0.56	0.07	0.01	0.01	122.5	25.7	80	0.3	26.8	6.98	6.96	0.09	0.22	0.01	0.043	0.01	10.4	2.1	0.01	566	1.5	<0.01	0.31	9.8
813736	SP001	519090	1143591	290	300	0.12	1.24	8.8	<5	<0.2	<10	220	0.59	0.09	0.01	0.01	124	50.4	77	0.42	24.7	6.19	6.94	0.08	0.28	0.02	0.038	0.01	13.4	4.2	0.01	1010	1.4	<0.01	0.22	11.8
813737	SP001	519090	1143591	300	310	0.11	1.1	8.6	375	<0.2	<10	170	0.5	0.08	0.01	0.01	111	42.5	78	0.34	23.1	6.08	6.56	0.09	0.25	0.01	0.037	0.01	11.1	3.6	0.01	834	1.35	<0.01	0.22	10.5
813738	SP001	519090	1143591	310	320	0.08	1.21	9.4	249	<0.2	<10	140	0.58	0.09	0.01	0.01	120	35.5	80	0.35	26.6	6.75	7.07	0.08	0.26	0.01	0.041	0.01	12.2	3.1	0.01	684	1.42	<0.01	0.23	10.8
813739	SP001	519090	1143591	320	330	0.15	1.18	10.5	80	<0.2	<10	130	0.55	0.09	0.01	0.01	110	33.8	90	0.37	26.9	6.93	8.11	0.1	0.26	0.01	0.05	0.01	13.1	2.7	0.01	638	1.47	<0.01	0.23	12
813740	SP002	518995	1143689	**0**	**10**	0.03	0.81	6.6	<5	<0.2	<10	80	0.55	0.11	0.12	0.02	42.9	10	108	0.87	25.5	5.1	5.63	0.07	0.08	0.02	0.029	0.05	13.1	1.8	0.07	438	0.93	<0.01	0.79	15.3
813741	SP002	518995	1143689	10	20	0.03	0.92	7.3	395	<0.2	<10	50	0.5	0.1	0.05	0.01	50.8	14.6	117	0.81	21.9	5.56	6.61	0.07	0.05	0.02	0.037	0.04	11.5	1.7	0.04	518	1.13	<0.01	0.84	12.2
813742	SP002	518995	1143689	20	30	0.07	1.01	7.5	271	5.3	<10	50	0.56	0.1	0.04	0.01	53.4	16.7	109	0.99	23.7	5.5	7.33	0.06	0.04	0.02	0.037	0.04	10.6	2.1	0.04	383	1.17	<0.01	0.82	13.7
813743	SP002	518995	1143689	30	40	0.03	1.12	7.3	67	<0.2	<10	40	0.52	0.12	0.04	0.01	63.4	16.6	93	1.18	23.7	5.35	7.62	0.06	0.06	0.02	0.038	0.04	10.4	2.5	0.04	308	1.05	<0.01	0.72	14
813744	SP002	518995	1143689	40	50	0.03	1.75	10.9	33	<0.2	<10	40	0.58	0.15	0.05	0.01	80	23.3	87	1.49	30.7	6.52	11.25	0.08	0.18	0.02	0.054	0.05	11	3.8	0.04	419	1.45	<0.01	0.6	20
813745	SP002	518995	1143689	50	60	0.06	2.2	11.7	75	<0.2	<10	30	0.67	0.2	0.05	<0.01	81.5	13.9	87	1.77	34.3	7.28	13.15	0.08	0.32	0.01	0.056	0.06	15.6	5	0.05	312	1.56	<0.01	0.34	23.4
813746	SP002	518995	1143689	60	70	0.02	2.3	12.7	25	<0.2	<10	30	0.69	0.19	0.04	0.01	103	11.9	95	1.88	37.5	7.65	14.2	0.1	0.37	0.01	0.064	0.06	18.5	5.1	0.05	336	1.58	<0.01	0.25	23.8
813747	SP002	518995	1143689	70	80	0.02	2.11	11.6	45	<0.2	<10	40	0.72	0.18	0.04	0.01	90.8	11.4	104	1.9	36.7	7.82	12.5	0.09	0.42	0.01	0.059	0.06	19.7	4.8	0.05	407	1.44	<0.01	0.24	22.2
813748	SP002	518995	1143689	80	90	0.02	2.16	12.4	14	<0.2	<10	50	0.71	0.21	0.04	0.01	90.4	12.9	100	1.9	41.4	7.87	13.9	0.1	0.41	0.01	0.06	0.06	20.5	4.8	0.05	480	1.52	<0.01	0.23	23.9
813749	SP002	518995	1143689	90	100	0.02	2.02	10.5	26	<0.2	<10	40	0.71	0.18	0.03	<0.01	69.7	10.4	86	2.11	38.4	7.37	12.15	0.09	0.4	0.01	0.055	0.06	21.1	4.8	0.05	450	1.23	<0.01	0.23	21.5
814079	SP005	518570	1143443	**0**	**10**	0.03	1.59	14.3	13	<0.2	<10	70	0.53	0.11	0.05	0.01	78.9	48.4	96	0.48	27.1	9.43	9.98	0.1	0.06	0.02	0.051	0.03	10.3	2.1	0.03	993	1.97	<0.01	0.94	10.9
814080	SP005	518570	1143443	10	20	0.02	1.8	12.8	13	<0.2	<10	60	0.44	0.13	0.05	0.01	76.5	22.3	76	0.54	28	9.98	11.65	0.1	0.21	0.03	0.061	0.02	8.7	1.5	0.02	695	1.7	<0.01	0.56	9.1
814081	SP005	518570	1143443	20	30	0.03	1.72	10.5	143	<0.2	<10	70	0.46	0.13	0.06	0.01	113	10	77	0.55	29.8	9.12	12.4	0.1	0.32	0.02	0.064	0.02	9.8	1.4	0.02	495	1.57	<0.01	0.34	9.2
814082	SP005	518570	1143443	30	40	0.09	1.7	12.4	13	<0.2	<10	230	0.57	0.12	0.08	0.01	174	11.6	88	0.49	37.8	13.65	13.1	0.14	0.45	0.03	0.064	0.01	10.6	1.1	0.02	1420	1.96	<0.01	0.34	9.3
814083	SP005	518570	1143443	40	50	0.02	1.84	10	8	<0.2	<10	40	0.65	0.17	0.03	<0.01	65.3	9.5	78	1.96	36.4	6.64	11.5	0.09	0.36	0.01	0.051	0.06	18.8	4.5	0.05	409	1.15	<0.01	0.23	20.4
814084	SP005	518570	1143443	50	60	0.19	1.54	11.4	35	<0.2	<10	520	0.48	0.1	0.07	0.03	194	17	74	0.44	38.1	12.3	11.7	0.1	0.44	0.03	0.053	0.01	9.5	0.9	0.02	2950	2	0.01	0.26	8.7
814085	SP005	518570	1143443	60	70	0.06	1.71	11.8	18	<0.2	<10	150	0.42	0.11	0.07	0.01	84.2	11.7	67	0.61	36.1	9.68	12.4	0.09	0.49	0.02	0.062	0.02	10.9	1.2	0.02	907	2.07	0.01	0.31	9
814086	SP005	518570	1143443	70	80	0.04	1.65	11.3	5	<0.2	<10	60	0.39	0.11	0.08	<0.01	72.5	6.7	74	0.57	36.3	8.38	12.5	0.09	0.55	0.02	0.06	0.01	11.6	1	0.02	413	1.94	0.01	0.27	9.7
814087	SP005	518570	1143443	80	90	0.04	1.64	12.9	5	<0.2	<10	80	0.43	0.11	0.07	0.01	89.3	7.5	110	0.47	41.7	10.15	12.85	0.1	0.49	0.02	0.069	0.01	12	0.8	0.02	569	2.13	0.01	0.28	10.2
814088	SP005	518570	1143443	90	100	0.05	1.63	12.9	<5	<0.2	<10	90	0.37	0.13	0.08	0.01	83.8	8	96	0.61	38.7	9.24	13.8	0.09	0.54	0.03	0.07	0.02	12.8	1.2	0.02	674	2.02	0.01	0.28	10
814089	SP005	518570	1143443	100	110	0.05	1.63	12.4	8	<0.2	<10	110	0.41	0.12	0.08	0.01	87.2	8.3	95	0.57	38.4	9.26	13.35	0.09	0.53	0.03	0.07	0.02	12.4	1.1	0.02	752	2.08	0.01	0.3	10.2
814090	SP005	518570	1143443	110	120	0.04	1.74	11.2	6	<0.2	<10	60	0.36	0.12	0.08	0.01	85.4	6.7	60	0.7	32.8	7.56	13.1	0.08	0.56	0.03	0.061	0.02	14.1	1.3	0.03	425	1.83	0.01	0.24	8.8
814091	SP005	518570	1143443	120	130	0.04	1.7	10.8	35	<0.2	<10	70	0.39	0.14	0.08	<0.01	90.6	7.7	58	0.77	32.1	7.36	14.35	0.08	0.64	0.03	0.066	0.02	14.7	1.8	0.03	490	2.11	0.01	0.27	8.7
814092	SP005	518443	1143443	**0**	**10**	0.06	1.5	9.3	25	<0.2	<10	90	0.33	0.11	0.08	0.01	90.9	7.2	74	0.47	31.1	7.35	11.95	0.09	0.52	0.02	0.058	0.01	13.5	1	0.03	537	1.74	0.01	0.22	8.9
814110	SP006	518443	1143096	10	20	0.05	1.66	12.7	23	<0.2	<10	50	0.45	0.13	0.09	0.01	57.6	7.7	157	0.53	27.9	9.9	10.7	0.11	0.12	0.03	0.061	0.03	10.1	1.7	0.04	326	2.35	0.01	1.19	13.8
814111	SP006	518443	1143096	20	30	0.05	1.89	11.1	130	<0.2	<10	30	0.44	0.12	0.03	0.01	38.6	6.3	129	0.68	24.8	9.12	11.15	0.1	0.16	0.02	0.059	0.03	10	1.9	0.03	145	2.2	0.01	1.2	11.7
814112	SP006	518443	1143096	30	40	0.04	1.95	10.4	28	<0.2	<10	20	0.44	0.12	0.02	0.01	45.6	5.6	102	0.71	23.3	8.89	11.15	0.11	0.19	0.02	0.057	0.03	10.8	2.1	0.02	116	2.11	0.01	1.25	10.4
814113	SP006	518443	1143096	40	50	0.03	1.87	11.8	81	<0.2	<10	10	0.32	0.11	0.01	<0.01	71.3	6.8	85	0.42	23	9.04	10.1	0.1	0.28	0.02	0.049	0.02	10.5	1.2	0.01	156	1.81	0.01	0.68	9.5
814114	SP006	518443	1143096	50	60	0.03	1.98	14.5	13	<0.2	<10	20	0.37	0.11	0.01	<0.01	59.2	5.1	97	0.45	29.4	11.4	11.85	0.13	0.43	0.02	0.063	0.01	11.7	1.1	0.01	151	2.38	0.01	0.5	9.1
814115	SP006	518443	1143096	60	70	0.03	1.62	12.2	715	<0.2	<10	10	0.29	0.12	0.01	0.01	55.7	4	88	0.35	23.6	8.99	10.45	0.11	0.42	0.02	0.06	0.01	10.9	0.8	0.01	106	1.84	0.01	0.38	7.5
814116	SP006	518443	1143096	70	80	0.02	1.53	10.9	13	<0.2	<10	10	0.24	0.1	0.01	0.01	51.5	3.8	79	0.3	22.1	7.72	9.04	0.11	0.38	0.02	0.05	0.01	11.1	0.8	0.01	104	1.56	0.01	0.33	6.9
814117	SP006	518443	1143096	80	90	0.02	1.49	8.7	70	<0.2	<10	20	0.28	0.11	0.01	0.01	100	4.6	84	0.3	22.1	7.63	8.38	0.1	0.39	0.01	0.049	0.01	11.4	0.8	0.01	123	1.61	0.01	0.28	7.7
814118	SP006	518443	1143096	90	100	0.02	1.73	10.6	89	<0.2	<10	20	0.3	0.1	0.01	0.01	74.2	4.3	87	0.35	24.7	8.46	9.63	0.12	0.4	0.01	0.052	0.01	12.6	0.9	0.01	117	1.68	0.01	0.29	7.8
814120	SP006	518443	1143096	100	110	0.02	1.77	10.4	58	<0.2	<10	20	0.29	0.09	0.01	0.01	72.3	3.9	91	0.36	25.6	9.08	10.5	0.12	0.38	0.01	0.057	0.01	13.4	0.9	0.01	120	1.78	0.01	0.26	7
814121	SP006	518443	1143096	110	120	0.03	1.52	12	11	<0.2	<10	20	0.35	0.1	0.01	0.01	115.5	4.9	100	0.3	28.1	9.35	9.98	0.13	0.41	0.01	0.054	0.01	13.3	0.7	0.01	150	1.65	0.01	0.24	8.1
814122	SP006	518443	1143096	120	130	0.02	1.62	9.9	90	<0.2	<10	20	0.31	0.09	0.01	<0.01	95.6	4.1	82	0.31	23.9	8.65	9.16	0.12	0.4	0.02	0.049	0.01	13.8	0.8	0.01	130	1.52	0.01	0.24	7.3
814123	SP006	518443	1143096	130	140	0.02	1.7	10.4	181	<0.2	<10	20	0.26	0.1	0.01	<0.01	83.2	4	87	0.34	24.7	8.48	9.51	0.1	0.41	0.01	0.051	0.01	12.9	0.8	0.01	123	1.66	0.01	0.26	8
814124	SP006	518443	1143096	140	150	0.02	1.86	9.3	16	<0.2	<10	20	0.3	0.1	0.02	<0.01	63.2	3.9	85	0.46	23.4	8.56	9.91	0.11	0.39	0.01	0.051	0.01	12.7	1.2	0.01	116	1.83	0.01	0.3	7.7
814125	SP006	518443	1143096	150	160	0.02	1.48	9.8	90	<0.2	<10	20	0.28	0.08	<0.01	0.01	55	4.5	83	0.31	24.8	7.95	7.99	0.11	0.34	0.01	0.044	0.01	11.1	0.7	<0.01	122	1.51	0.01	0.3	7.8
814143	SP007	518235	1143093	**0**	**10**	0.02	0.8	6.1	88	<0.2	<10	60	0.41	0.1	0.08	0.01	30.4	12.1	109	0.49	17.8	4.7	5.71	0.09	0.05	0.01	0.03	0.04	12.2	1.9	0.04	391	0.84	<0.01	0.58	13.9
814144	SP007	518235	1143093	10	20	0.02	0.97	6.6	44	<0.2	<10	50	0.49	0.1	0.05	0.02	39.5	18.1	104	0.66	20.7	4.84	6.38	0.1	0.06	0.01	0.031	0.04	13	2.5	0.04	412	0.97	0.01	0.59	16.3
814145	SP007	518235	1143093	20	30	0.02	1.12	7	9	<0.2	<10	50	0.5	0.11	0.04	0.01	49.2	15.6	100	0.78	21.8	4.9	7.28	0.1	0.1	0.01	0.033	0.04	12.6	2.9	0.04	293	0.97	0.01	0.57	17
814146	SP007	518235	1143093	30	40	0.03	1.42	8.1	31	<0.2	<10	50	0.57	0.12	0.05	0.01	43.5	15.7	83	0.99	26.1	5	8.87	0.1	0.13	0.01	0.039	0.05	14.8	3.8	0.04	277	1.12	0.01	0.58	20.8
814147	SP007	518235	1143093	40	50	0.03	1.78	10.2	14	<0.2	<10	50	0.63	0.14	0.04	0.01	54.4	19.5	87	1.18	30	5.7	10.65	0.11	0.21	0.01	0.045	0.06	17.1	4.7	0.04	356	1.33	0.01	0.5	24.9
814148	SP007	518235	1143093	50	60	0.02	1.82	11.5	14	<0.2	<10	50	0.59	0.14	0.04	0.01	66.5	22.2	89	1.16	30.9	6.09	11	0.12	0.26	0.01	0.048	0.06	18.7	4.6	0.04	467	1.42	0.01	0.38	25.3
814149	SP007	518235	1143093	60	70	0.02	1.9	11.5	8	<0.2	<10	50	0.65	0.15	0.04	0.01	77.3	21.8	79	1.23	30.3	6.02	11.05	0.12	0.28	0.01	0.048	0.06	22.2	4.9	0.04	480	1.39	0.01	0.33	25
814150	SP007	518235	1143093	70	80	0.02	1.81	11.3	13	<0.2	<10	50	0.67	0.14	0.04	0.01	78.7	21.9	75	1.18	29.9	5.93	10.95	0.12	0.3	0.01	0.046	0.06	22	4.9	0.04	494	1.38	0.01	0.32	24.5
814151	SP007	518235	1143093	80	90	0.03	2.41	36	<5	<0.2	<10	200	0.64	0.07	0.61	0.03	33.9	25.8	171	2.46	45.8	4.02	9.02	0.21	0.21	<0.01	0.021	0.47	15.2	32.2	1.27	739	0.48	0.03	0.05	77.1
814152	SP007	518235	1143093	90	100	0.02	1.87	13.3	29	<0.2	<10	50	0.68	0.14	0.04	0.01	75.7	24.3	81	1.18	32.3	6.62	11.7	0.13	0.38	0.01	0.049	0.06	24.8	4.6	0.05	535	1.56	0.01	0.33	26.5
814153	SP007	518235	1143093	100	110	0.03	1.85	12.9	8	<0.2	<10	60	0.76	0.12	0.04	0.01	79.3	28.1	81	1.12	28.9	6.11	11.8	0.12	0.36	0.02	0.05	0.06	26.9	4.5	0.05	614	1.35	<0.01	0.32	24.1
814154	SP007	518235	1143093	110	120	0.07	1.75	12.4	16	<0.2	<10	60	0.73	0.12	0.05	0.01	77.2	30.3	74	1.13	29	5.82	11.1	0.13	0.38	0.02	0.045	0.06	27.8	4.6	0.05	662	1.25	<0.01	0.31	23.4
814155	SP007	518235	1143093	120	130	0.01	1.82	12.6	7	<0.2	<10	80	0.83	0.13	0.05	0.01	82.2	30.6	71	1.2	30.8	5.96	11.85	0.14	0.41	0.01	0.051	0.06	31.4	5	0.05	770	1.26	<0.01	0.28	25.5
814156	SP007	518235	1143093	130	140	0.01	1.77	12.6	32	<0.2	<10	100	0.79	0.13	0.05	0.01	80.1	37.4	79	1.14	31.8	6.17	11.25	0.14	0.39	0.01	0.044	0.06	33	5.1	0.05	1020	1.28	<0.01	0.26	25.9
814157	SP007	518235	1143093	140	150	0.02	1.66	11.7	129	<0.2	<10	90	0.78	0.12	0.05	0.01	71.8	30.9	70	1.06	31.7	5.94	10.65	0.15	0.37	0.01	0.046	0.06	33.4	4.7	0.05	855	1.11	<0.01	0.26	25.2
814171	SP008	518539	1143097	**0**	**10**	0.02	1.49	6.3	56	<0.2	<10	50	0.42	0.09	0.09	0.01	34.6	4.5	96	0.58	13	5.37	8.25	0.09	0.1	0.02	0.036	0.03	10.8	2.1	0.05	281	1.35	<0.01	0.87	7.5
814172	SP008	518539	1143097	10	20	0.02	1.93	7.3	38	<0.2	<10	30	0.48	0.1	0.02	0.01	34.3	4.6	126	0.74	15.3	6.09	10.55	0.1	0.15	0.02	0.048	0.03	10.6	2.8	0.03	150	1.6	<0.01	0.96	8.9
814173	SP008	518539	1143097	20	30	0.02	2.55	5.9	95	<0.2	<10	20	0.51	0.11	0.01	0.01	45.5	4.9	90	1.04	16.3	5.55	13.45	0.1	0.19	0.02	0.051	0.04	15.1	4.2	0.04	95	1.62	<0.01	1.09	11.9
814174	SP008	518539	1143097	30	40	0.03	2.52	7.9	5	<0.2	<10	20	0.55	0.11	0.01	0.01	40.9	4.6	93	0.98	15.5	6.87	12.75	0.09	0.19	0.01	0.05	0.03	13.1	3.6	0.03	86	1.81	<0.01	1.11	10.7
814175	SP008	518539	1143097	40	50	0.03	2.54	7.9	153	<0.2	<10	20	0.54	0.11	0.01	0.01	39.5	4.9	91	0.94	16.6	7.8	12.15	0.1	0.24	0.02	0.049	0.03	12.7	3.4	0.03	101	1.88	<0.01	1.1	10.2
814176	SP008	518539	1143097	50	60	0.02	2.55	13.1	7	<0.2	<10	30	0.56	0.1	0.01	<0.01	35.9	4.4	101	0.66	22.7	12.5	13.1	0.1	0.43	0.01	0.067	0.02	12.1	2	0.02	133	2.65	<0.01	0.91	8.3
814177	SP008	518539	1143097	60	70	0.01	2.24	13.3	<5	<0.2	<10	30	0.47	0.1	0.02	<0.01	39.1	3.5	87	0.58	25.3	11.95	14.1	0.11	0.61	0.01	0.073	0.02	12.5	1.3	0.01	138	2.72	<0.01	0.61	6.8
814178	SP008	518539	1143097	70	80	0.01	2.01	10.6	<5	<0.2	<10	30	0.3	0.1	0.02	<0.01	44.6	2.7	65	0.49	18.9	9.95	11.9	0.1	0.56	0.01	0.061	0.01	11.8	1	0.01	156	1.95	<0.01	0.38	5.2
814201	SP002	518995	1143689	**0**	**10**	0.01	2.19	12.2	10	<0.2	<10	40	0.82	0.15	0.03	0.01	75.6	10.4	95	1.95	44.5	8.17	12.85	0.13	0.47	0.01	0.051	0.07	21.5	4.3	0.06	426	1.4	<0.01	0.26	24.4
814202	SP002	518995	1143689	10	20	0.01	2.09	12.1	10	<0.2	<10	30	0.91	0.14	0.03	<0.01	77.4	9.4	102	1.99	48.9	8.16	12.8	0.13	0.47	<0.01	0.052	0.07	23	4	0.06	401	1.27	<0.01	0.23	24.3
814203	SP002	518995	1143689	20	30	0.01	1.89	11	13	<0.2	<10	40	0.86	0.15	0.02	<0.01	90.4	10.8	90	2.39	57.6	7.51	12.65	0.12	0.5	0.01	0.049	0.07	23.9	4.2	0.06	505	1.11	<0.01	0.22	26.1
814204	SP002	518995	1143689	30	40	0.03	1.52	9.7	16	<0.2	<10	50	0.84	0.17	0.06	0.01	108	11.8	117	2.25	67.2	7.4	10.8	0.18	0.51	0.02	0.046	0.06	21.5	3.5	0.07	574	1.09	<0.01	0.35	26.3

Appendix C:Pits, Au and other elements in the regolith of the Lawra area analysed by ICP and FA-AAS Techniques

Sample ID	Pit ID	UTM-E	UTM-N	From (m)	To (m)	Ag ppm	Al ppm	As ppm	Au ppb	Au ppm	B ppm	Ba ppm	Be ppm	Bi ppm	Ca %	Cd ppm	Ce ppm	Co ppm	Cr ppm	Cs ppm	Cu ppm	Fe %	Ga ppm	Ge ppm	Hf ppm	Hg ppm	In ppm	K %	La ppm	Li ppm	Mg ppm	Mn ppm	Mo ppm	Na ppm	Nb ppm	Ni ppm
814205	SP002	518995	1143689	40	50	0.03	1.38	9.3	177	<0.2	<10	40	0.83	0.17	0.02	<0.01	86.2	11.1	106	2.18	74.1	7.31	10	0.18	0.45	0.01	0.04	0.06	22	2.9	0.07	488	0.86	<0.01	0.28	27.2
814206	SP002	518995	1143689	50	60	0.03	1.37	9.2	28	<0.2	<10	30	0.83	0.15	0.02	0.01	63.7	10.5	122	2.34	76	7.52	9.8	0.2	0.47	0.01	0.042	0.06	23.9	3.1	0.07	419	0.76	<0.01	0.3	27.9
814207	SP002	518995	1143689	60	70	0.03	1.29	9.3	10	<0.2	<10	30	0.93	0.14	0.02	0.01	59.9	11.5	146	2.26	81.7	7.68	9.54	0.22	0.47	0.01	0.039	0.06	23.9	2.9	0.08	395	0.7	<0.01	0.28	30.2
814208	SP002	518995	1143689	70	80	0.03	1.36	10.1	7	<0.2	<10	40	0.98	0.14	0.02	0.01	61.4	12	150	2.34	88.7	8.42	9.58	0.24	0.47	0.01	0.042	0.06	26.6	2.8	0.08	409	0.66	<0.01	0.26	30.7
814210	SP002	518995	1143689	80	90	0.03	1.1	8.8	7	<0.2	<10	30	0.83	0.13	0.01	0.01	53.6	12.4	112	2.45	76.8	7	7.96	0.2	0.46	0.01	0.033	0.07	23.4	2.4	0.09	350	0.54	<0.01	0.23	30
814211	SP002	518995	1143689	90	100	0.02	0.98	7.7	21	<0.2	<10	30	0.83	0.13	0.01	0.01	39.6	9.9	118	2.33	69.5	6.34	7.47	0.19	0.48	<0.01	0.028	0.08	22.7	2.4	0.09	259	0.41	<0.01	0.23	30.6
814212	SP002	518995	1143689	100	110	0.02	0.83	6.6	5	<0.2	<10	30	0.75	0.13	0.01	0.01	33.2	8.6	94	2.53	65	5.49	6.27	0.17	0.49	<0.01	0.024	0.1	21.1	2.2	0.1	194	0.39	<0.01	0.2	28.4
814213	SP002	518995	1143689	110	120	<0.01	0.75	6.6	5	<0.2	<10	30	0.79	0.15	0.01	0.01	34.6	7.4	95	2.06	59.3	5	6.1	0.09	0.49	<0.01	0.019	0.08	19.8	2.1	0.1	143	0.42	<0.01	0.19	30.3
814214	SP002	518995	1143689	120	130	<0.01	0.77	7.2	<5	<0.2	<10	30	0.77	0.13	0.01	0.01	31	7.9	94	2.57	64	4.84	6.42	0.1	0.45	<0.01	0.021	0.11	21.3	2.4	0.12	157	0.34	<0.01	0.17	32.8
814215	SP002	518995	1143689	130	140	<0.01	0.81	7.6	<5	<0.2	<10	30	0.77	0.13	0.01	0.01	30.4	7.9	95	2.54	64.7	4.97	6.55	0.1	0.48	<0.01	0.022	0.11	21.3	2.4	0.12	160	0.38	<0.01	0.17	33.7
814216	SP002	518995	1143689	140	150	<0.01	0.8	6.4	<5	<0.2	<10	30	0.71	0.13	0.01	0.01	26.9	7.6	96	2.79	61.9	4.73	6.51	0.1	0.47	<0.01	0.023	0.14	21.6	2.8	0.14	157	0.35	<0.01	0.18	31.4
814217	SP002	518995	1143689	150	160	0.01	0.88	7.1	8	<0.2	<10	40	0.77	0.12	0.01	0.01	27.2	8.4	102	2.87	66.2	4.89	6.77	0.11	0.45	<0.01	0.027	0.15	22.4	3.1	0.16	163	0.38	<0.01	0.15	31
814218	SP002	518995	1143689	160	170	<0.01	0.91	8.7	<5	<0.2	<10	30	0.83	0.11	0.01	0.01	29.3	8.6	102	2.5	68.5	5.18	7.32	0.09	0.46	<0.01	0.03	0.1	25	2.8	0.14	177	0.51	<0.01	0.17	34.6
814219	SP002	518995	1143689	170	180	<0.01	0.64	8.1	8	<0.2	<10	30	0.69	0.11	0.01	0.01	22	7.1	76	2.44	55.3	3.87	5.12	0.09	0.37	<0.01	0.019	0.12	17	2.3	0.12	126	0.33	<0.01	0.15	30
814220	SP003	518738	1143498	**0**	**10**	0.02	1.43	6.7	111	<0.2	<10	80	0.58	0.09	0.15	0.02	42.7	9.4	93	0.67	18	4.79	7.27	<0.05	0.05	0.02	0.034	0.05	12.8	2.9	0.07	449	1.02	<0.01	0.85	12.2
814221	SP003	518738	1143498	10	20	0.02	1.51	7.6	45	<0.2	<10	60	0.6	0.1	0.08	0.01	39.3	8	108	0.71	18.5	5.25	7.86	<0.05	0.04	0.02	0.039	0.05	12.7	3	0.06	260	1.21	<0.01	0.87	13.1
814222	SP003	518738	1143498	20	30	0.03	1.94	12	148	<0.2	<10	40	0.67	0.1	0.04	0.01	39.9	9.9	122	0.68	25.2	8.32	9.4	0.05	0.07	0.02	0.049	0.04	12.2	3	0.05	196	1.8	<0.01	1.02	13.9
814223	SP003	518738	1143498	30	40	0.02	2.1	23	49	<0.2	<10	30	0.71	0.15	0.03	<0.01	66.2	12.6	121	0.48	33.7	12.4	10	0.05	0.23	0.01	0.056	0.02	9.7	1.7	0.02	231	2.29	<0.01	0.82	12.7
814224	SP003	518738	1143498	40	50	0.02	1.61	22.5	24	<0.2	<10	20	0.54	0.09	0.04	0.01	61.4	5.9	78	0.33	30.7	9.36	9.09	<0.05	0.36	0.01	0.053	0.01	9.7	0.9	0.01	153	1.7	<0.01	0.4	9.4
814225	SP003	518738	1143498	50	60	0.01	1.65	25.4	177	<0.2	<10	20	0.58	0.07	0.05	0.01	54.4	5.1	79	0.29	38.4	9.76	9.94	<0.05	0.34	0.01	0.063	0.01	9	0.8	0.01	109	1.89	<0.01	0.41	9.7
814226	SP003	518738	1143498	60	70	0.01	1.7	31.7	515	<0.2	<10	20	0.66	0.13	0.05	0.01	47	6.6	74	0.32	39.3	10.55	10.85	<0.05	0.32	0.02	0.064	0.01	9.2	1	0.02	132	2.31	<0.01	0.47	10.6
814227	SP003	518738	1143498	70	80	0.01	1.63	22.7	234	<0.2	<10	30	0.39	0.17	0.05	0.01	83.2	5.5	61	0.32	27.8	7.83	9.96	<0.05	0.36	0.02	0.053	0.01	11	0.9	0.02	107	1.75	<0.01	0.38	8.8
814228	SP003	518738	1143498	80	90	0.01	1.41	20.4	571	<0.2	<10	20	0.38	0.09	0.05	<0.01	96.1	4.7	57	0.23	25.5	7.25	9.61	<0.05	0.36	0.02	0.058	0.01	10.8	0.6	0.01	94	1.59	<0.01	0.32	7.5
814229	SP003	518738	1143498	90	100	0.01	1.27	18.4	139	<0.2	<10	30	0.35	0.07	0.06	0.01	133	3.9	58	0.17	21	6.1	7.28	<0.05	0.33	0.01	0.039	0.01	10.1	0.4	0.01	95	1.17	<0.01	0.17	6.5
814230	SP003	518738	1143498	100	110	0.02	1.7	22.3	122	<0.2	<10	30	0.43	0.1	0.06	<0.01	110.5	4.4	65	0.31	29.1	7.83	12.05	<0.05	0.46	0.01	0.063	0.01	12.8	0.9	0.02	120	2.05	<0.01	0.37	10.3
814231	SP003	518738	1143498	110	120	0.02	1.39	34.7	260	<0.2	<10	30	0.47	0.06	0.06	0.01	148	4.7	52	0.21	21.1	7.71	7.21	<0.05	0.31	0.01	0.039	0.01	13.3	0.7	0.02	132	1.72	<0.01	0.22	8.5
814232	SP003	518738	1143498	120	130	0.01	1.31	35.2	711	<0.2	<10	30	0.5	0.05	0.05	0.01	116	5.2	53	0.17	24.2	7.93	8.15	<0.05	0.29	0.01	0.042	<0.01	10.6	0.5	0.01	110	1.81	<0.01	0.23	8.9
814233	SP003	518738	1143498	130	140	0.01	1.45	12.9	208	<0.2	<10	20	0.4	1.05	0.05	<0.01	73	4	74	0.25	28	6.87	10.5	<0.05	0.39	0.01	0.054	0.01	10.7	0.6	0.02	93	1.47	<0.01	0.3	8.1
814234	SP003	518738	1143498	140	150	0.01	1.33	7.2	244	<0.2	<10	20	0.25	0.12	0.06	<0.01	134.5	3	66	0.23	17	4.65	7.76	<0.05	0.46	0.01	0.037	0.01	13.2	0.6	0.02	87	0.89	<0.01	0.17	6.4
814235	SP003	518738	1143498	150	160	0.01	1.4	7.3	923	<0.2	<10	30	0.27	0.13	0.06	<0.01	138	3.1	66	0.25	17.3	4.76	8.02	<0.05	0.47	0.01	0.039	0.01	13.6	0.6	0.02	91	0.88	<0.01	0.16	6.3
814236	SP003	518738	1143498	160	170	0.02	1.46	8.6	11	<0.2	<10	20	0.36	0.06	0.05	<0.01	72.1	2.8	64	0.25	24.3	5.95	10.45	<0.05	0.46	0.01	0.048	0.01	12.6	0.6	0.02	90	1.21	<0.01	0.25	5.6
814237	SP003	518738	1143498	170	180	0.01	1.61	15.9	24	<0.2	<10	20	0.48	0.08	0.05	<0.01	57.2	4.5	95	0.27	38.5	9.28	13.15	0.05	0.44	0.01	0.07	0.01	11.4	0.6	0.02	140	1.83	<0.01	0.3	8.7
814238	SP003	518738	1143498	180	190	0.01	1.56	12.8	59	<0.2	<10	20	0.5	0.09	0.05	0.01	57.4	4.3	80	0.28	31.4	7.83	11.35	0.05	0.5	0.01	0.06	0.01	11.5	0.7	0.02	109	1.43	<0.01	0.22	8.8
814239	SP003	518738	1143498	190	200	0.02	1.42	11.3	105	<0.2	<10	20	0.39	0.07	0.05	<0.01	73.2	3.8	74	0.26	27.9	7.25	10.65	<0.05	0.49	<0.01	0.054	0.01	11.3	0.6	0.02	101	1.26	<0.01	0.2	8.1
814240	SP003	518738	1143498	200	210	0.03	1.55	11.2	12	<0.2	<10	20	0.44	0.08	0.06	0.01	87.9	4.7	90	0.27	27.7	7.21	10.1	0.05	0.47	0.01	0.047	0.01	12.7	0.8	0.02	125	1.23	<0.01	0.17	8.9
814241	SP003	518738	1143498	210	220	0.02	1.54	15.7	71	<0.2	<10	20	0.4	0.11	0.06	<0.01	63.8	4.1	61	0.29	29.3	6.5	9.67	0.05	0.47	0.01	0.046	0.01	11.2	0.7	0.02	117	1.46	<0.01	0.2	8.4
814256	SP004	518642	1143498	**0**	**10**	0.3	1.35	17.1	11	2.2	<10	190	0.7	0.11	0.32	0.03	45.6	39.5	115	0.48	30.8	8.07	8.31	<0.05	0.08	0.02	0.045	0.06	9.9	2.1	0.08	1200	2.71	<0.01	0.97	15.7
814257	SP004	518642	1143498	10	20	0.06	1.67	16.8	44	<0.2	<10	130	0.74	0.12	0.13	0.02	56.3	50.4	114	0.5	32.7	9.63	9.3	0.06	0.08	0.01	0.046	0.05	8.5	2	0.05	1410	3.56	<0.01	1.02	14.3
814258	SP004	518642	1143498	20	30	0.17	1.38	30.6	8	<0.2	<10	370	0.87	0.11	0.07	0.03	59.5	54.7	119	0.39	44	11.65	10.1	0.14	0.1	0.05	0.052	0.03	7.2	1.7	0.03	2220	3.84	0.01	0.8	21
814259*	SP004	518642	1143498			NSS	NSS	NSS	657	NSS	NSS	NSS	NSS	NSS	NSS	NSS	NSS	NSS	NSS	NSS	NSS	NSS	NSS	NSS	NSS	NSS	NSS	NSS	NSS	NSS	NSS	NSS	NSS	NSS	NSS	NSS
814260	SP004	518642	1143498	30	40	0.13	1.18	22.5	8	<0.2	<10	220	0.89	0.11	0.04	0.02	36.6	25.5	101	0.34	45	9.6	9.8	0.13	0.21	0.03	0.047	0.02	5.2	1.2	0.02	1340	3.48	0.01	0.37	15.7
814261	SP004	518642	1143498	40	50	0.05	1.09	17.1	14	<0.2	<10	80	0.67	0.09	0.04	0.02	29.8	15.8	97	0.31	34.8	8.46	9.06	0.12	0.28	0.02	0.046	0.02	4.5	0.9	0.02	591	3.06	<0.01	0.28	14.5
814262	SP004	518642	1143498	50	60	0.15	1.21	30.8	60	<0.2	<10	400	0.94	0.12	0.06	0.03	58.3	42.3	103	0.37	42.1	10.6	9.43	0.13	0.1	0.04	0.047	0.02	6.9	1.4	0.03	2220	3.36	0.01	0.59	21
814263	SP004	518642	1143498	60	70	0.04	1.32	21.6	48	<0.2	<10	40	0.73	0.12	0.06	0.01	33.3	13	136	0.39	39	9.5	11.9	0.14	0.38	0.02	0.062	0.02	5.7	1	0.02	335	3.7	<0.01	0.3	16.4
814264	SP004	518642	1143498	70	80	0.03	1.29	26.6	11	<0.2	<10	30	0.86	0.11	0.06	0.02	30.7	13.2	131	0.39	42.7	9.38	12.25	0.13	0.37	0.02	0.058	0.01	6	0.9	0.02	253	3.54	0.01	0.22	17.4
814265	SP004	518642	1143498	80	90	0.03	1.38	34.5	49	<0.2	<10	50	0.95	0.12	0.06	0.01	29.2	19	210	0.38	48.5	11.3	12.2	0.13	0.37	0.02	0.063	0.01	5.8	1	0.02	330	3.51	<0.01	0.2	22.3
814266	SP004	518642	1143498	90	100	0.04	1.45	36.8	11	<0.2	<10	50	1.04	0.12	0.05	0.02	39.2	20.9	250	0.33	51.9	12.5	12.55	0.15	0.34	0.02	0.067	0.01	5.3	0.9	0.02	379	4.48	<0.01	0.25	23.6
814267	SP004	518642	1143498	100	110	0.03	1.44	35.9	14	<0.2	<10	40	1.01	0.11	0.05	0.01	36	18.8	231	0.32	49.4	12	12	0.16	0.38	0.02	0.062	0.01	6.1	0.9	0.02	324	4.13	<0.01	0.23	22.7
814268	SP004	518642	1143498	110	120	0.02	1.36	29.2	14	<0.2	<10	40	0.77	0.1	0.07	0.01	27.8	12.1	131	0.39	38.1	8.59	11.05	0.14	0.44	0.02	0.054	0.01	6	1.1	0.02	239	3.02	<0.01	0.18	16.1
814269	SP004	518642	1143498	120	130	0.03	1.46	34.9	11	<0.2	<10	70	0.96	0.12	0.07	0.02	30.5	16.5	133	0.39	43.8	9.71	11.45	0.14	0.4	0.03	0.058	0.01	5.5	1.2	0.02	395	3.34	0.01	0.16	16.9
814270	SP004	518642	1143498	130	140	0.04	1.48	39.3	9	<0.2	<10	70	1.06	0.11	0.07	0.02	32.4	15.6	134	0.42	48.6	10.35	12.7	0.14	0.37	0.02	0.06	0.01	6.7	1.2	0.02	394	3.45	0.01	0.17	18.6
814271	SP004	518642	1143498	140	150	0.06	1.53	40.8	12	<0.2	<10	120	0.94	0.12	0.06	0.02	48.7	17.4	137	0.42	50.4	10.65	12.5	0.16	0.4	0.02	0.058	0.01	7.3	1.3	0.02	647	3.7	<0.01	0.19	17.9
814272	SP004	518642	1143498	150	160	0.05	1.55	35.9	17	<0.2	<10	50	0.98	0.12	0.07	0.01	41.6	16.6	166	0.46	45	10.15	12.3	0.13	0.39	0.02	0.055	0.01	8.2	1.4	0.03	319	3.29	0.01	0.18	19.5
814273	SP004	518642	1143498	160	170	0.06	1.61	42.8	16	<0.2	<10	140	1.15	0.12	0.08	0.02	43.6	18.3	138	0.5	50.6	10.25	13.25	0.13	0.44	0.02	0.061	0.02	7.3	1.5	0.03	749	3.81	0.01	0.17	19.3
814274	SP004	518642	1143498	170	180	0.1	1.56	40.6	12	<0.2	<10	270	1.1	0.13	0.08	0.02	38.6	23.8	134	0.46	51.2	10.5	12.25	0.12	0.34	0.02	0.059	0.02	6.9	1.4	0.03	1340	3.71	0.01	0.16	18.7
814275	SP004	518642	1143498	180	190	0.09	1.52	42.9	12	<0.2	<10	230	1.15	0.14	0.06	0.02	35.1	23.9	205	0.38	57.3	12.05	12.4	0.14	0.29	0.02	0.064	0.01	6.3	1.4	0.03	1240	4.29	0.01	0.18	24.5
814276	SP004	518642	1143498	190	200	0.09	1.38	46.8	17	<0.2	<10	200	1.36	0.12	0.07	0.01	25.8	23.3	157	0.4	58.4	11.65	11.5	0.14	0.29	0.01	0.061	0.01	5.3	1.5	0.03	1090	4.31	0.01	0.16	22.5
814277	SP004	518642	1143498	200	210	0.1	1.51	47.9	15	<0.2	<10	240	1.23	0.13	0.07	0.02	32.2	25.8	132	0.45	52.9	10.55	12.5	0.13	0.34	0.02	0.061	0.02	7.7	1.6	0.03	1200	4.22	0.01	0.18	19.7
814278	SP004	518642	1143498	210	220	0.11	1.49	44.6	7	<0.2	<10	250	1.22	0.14	0.06	0.02	31	28.6	187	0.41	55.3	11.7	12.75	0.12	0.28	0.02	0.067	0.01	7.2	1.5	0.03	1210	4.27	0.01	0.16	22.9
814279	SP004	518642	1143498	220	230	0.16	1.11	44.4	7	<0.2	<10	690	1.26	0.13	0.06	0.01	29.8	37.7	84	0.34	43.1	8.51	10.75	0.13	0.33	0.02	0.046	0.02	5.2	1.3	0.03	2850	3.64	0.01	0.16	17.1
814280	SP004	518642	1143498	230	240	0.15	1.29	67.8	<5	<0.2	<10	900	1.43	0.22	0.05	0.02	35.8	41.8	90	0.43	58.5	11	11.6	0.14	0.34	0.03	0.052	0.02	7.9	1.3	0.02	3710	4.56	0.01	0.21	21.4
814281	SP004	518642	1143498	240	250	0.05	0.84	42.3	<5	<0.2	<10	250	1.01	0.12	0.04	0.01	17.8	10.7	65	0.26	40.7	6.91	10.1	0.11	0.32	0.01	0.042	0.02	4.9	0.7	0.02	1080	2.23	<0.01	0.18	16.9
814282	SP004	518642	1143498	250	260	0.02	0.75	34.6	<5	<0.2	<10	110	0.98	0.11	0.04	0.01	14.75	5.5	59	0.25	37	6.74	9.11	0.13	0.3	0.01	0.032	0.02	4.1	0.6	0.02	450	1.85	0.01	0.18	18
814283	SP004	518642	1143498	260	270	0.01	0.57	25	<5	<0.2	<10	40	0.79	0.1	0.03	0.01	10.65	2.6	74	0.2	29.2	5.16	7.4	0.11	0.27	0.01	0.028	0.02	3.5	0.6	0.02	155	1.38	<0.01	0.15	16.1
814284	SP004	518642	1143498	270	280	0.01	0.52	22.9	<5	<0.2	<10	50	0.73	0.09	0.03	0.01	12.05	2.4	42	0.18	28	4.82	6.88	0.1	0.24	0.01	0.024	0.02	3.5	0.4	0.02	207	1.24	<0.01	0.13	17.1
814285	SP004	518642	1143498	280	290	0.01	0.51	25	<5	<0.2	<10	40	0.8	0.08	0.03	0.01	12.5	2.1	58	0.17	30	4.92	7.44	0.1	0.25	0.01	0.03	0.02	3.6	0.3	0.02	176	1.28	<0.01	0.14	21.1
814288	KP017	527800	1143498	**0**	**10**	0.04	1.18	13.9	50	<0.2	<10	110	0.52	0.07	0.21	0.02	33.6	23.7	100	0.4	28.7	3.61	5.8	0.14	0.07	0.02	0.017	0.06	16.6	3.5	0.26	668	0.49	<0.01	0.14	49.1
814289	KP017	527800	1148600	10	20	0.05	1.48	25.1	<5	<0.2	<10	140	0.75	0.09	0.13	0.02	57.5	38.7	149	0.53	43.3	5.29	7.7	0.15	0.07	0.01	0.023	0.04	19.2	4.8	0.24	965	0.79	<0.01	0.1	72.6
814290	KP017	527800	1148600	20	30	0.06	1.61	24.9	6	<0.2	<10	130	0.77	0.09	0.1	0.02	68.3	40.7	141	0.58	46.4	5.4	8.39	0.15	0.06	0.01	0.024	0.05	20.4	5.8	0.24	960	0.98	0.01	0.08	80.7
814291	KP017	527800	1148600	30	40	0.07	1.64	22.2	<5	<0.2	<10	180	0.77	0.09	0.11	0.03	76.2	49.6	140	0.57	55.3	5.19	8.35	0.14	0.07	0.01	0.023	0.05	21.1	5.7	0.31	1340	0.81	0.01	0.05	92.7
814292	KP017	527800	1148600	40	50	0.07	1.56	17.6	<5	<0.2	<10	120	0.68	0.08	0.13	0.02	77.3	34.9	143	0.47	46.4	4.59	7.33	0.16	0.07	0.01	0.02	0.04	22.6	6	0.44	986	0.59	0.01	<0.05	83.5
814293	KP017	527800	1148600	50	60	0.03	1.65	13.6	<5	<0.2	<10	60	0.64	0.08	0.16	0.01	41.8	24	130	0.48	50	4.41	7.22	0.15	0.07	0.01	0.018	0.04	24.3	5.8	0.61	526	0.28	<0.01	<0.05	81.8
814294	KP017	527800	1148600	60	70	0.02	1.61	10.7	<5	<0.2	<10	30	0.53	0.07	0.17	0.01	23.2	15.8	124	0.5	56.6	4.21	6.82	0.16	0.07	0.01	0.018	0.04	28.7	6	0.76	238	0.16	0.01	<0.05	82.8

Appendix C:Pits, Au and other elements in the regolith of the Lawra area analysed by ICP and FA-AAS Techniques

Sample ID	Pit ID	UTM-E	UTM-N	From (m)	To (m)	Ag ppm	Al ppm	As ppm	Au ppb	Au ppm	B ppm	Ba ppm	Be ppm	Bi ppm	Ca %	Cd ppm	Ce ppm	Co ppm	Cr ppm	Cs ppm	Cu ppm	Fe %	Ga ppm	Ge ppm	Hf ppm	Hg ppm	In ppm	K %	La ppm	Li ppm	Mg ppm	Mn ppm	Mo ppm	Na ppm	Nb ppm	Ni ppm
814308	KP018	527900	1148600	**0**	**10**	0.02	0.49	12.4	<5	<0.2	<10	50	0.24	0.05	0.07	0.02	21.6	6.7	43	0.33	13.6	1.76	3.63	0.12	0.04	0.01	0.01	0.02	13.1	1.1	0.04	186	0.25	<0.01	0.16	12.4
814309	KP018	527900	1148600	10	20	0.02	0.58	14	<5	<0.2	<10	40	0.26	0.05	0.04	0.01	24.9	6.1	46	0.4	17	1.94	4.16	0.12	0.03	0.01	0.012	0.02	14.6	1.3	0.03	142	0.27	<0.01	0.14	12.6
814310	KP018	527900	1148600	20	30	0.03	0.7	19.7	7	<0.2	<10	60	0.35	0.08	0.03	<0.01	33.3	8.3	51	0.59	24.8	2.41	5.11	0.05	0.05	0.02	0.015	0.02	17.4	1.6	0.02	188	0.34	<0.01	0.14	16.1
814311	KP018	527900	1148600	30	40	0.03	0.77	20.2	9	<0.2	<10	60	0.32	0.08	0.03	<0.01	36.2	10.4	54	0.57	27.4	2.84	5.16	0.05	0.07	0.02	0.016	0.03	16.9	1.7	0.02	240	0.32	0.01	0.12	16.2
814312	KP018	527900	1148600	40	50	0.02	0.67	22.6	<5	<0.2	<10	40	0.31	0.08	0.03	<0.01	34.3	13	53	0.5	30.4	3.13	5.28	0.05	0.12	0.01	0.017	0.02	15.5	1.4	0.02	203	0.3	0.01	0.12	17.2
814313	KP018	527900	1148600	50	60	0.02	0.64	23.6	6	<0.2	<10	50	0.34	0.08	0.04	<0.01	35.7	12.6	56	0.44	30.1	3.2	4.93	0.06	0.14	0.02	0.015	0.02	18.1	1.2	0.02	212	0.25	0.01	0.09	18
814314	KP018	527900	1148600	60	70	0.02	0.57	26.1	<5	<0.2	<10	40	0.32	0.08	0.04	0.01	32.8	10.8	63	0.37	33.6	3.53	4.63	0.06	0.17	0.01	0.015	0.02	17.3	1	0.02	193	0.24	<0.01	0.1	19.8
814325	KP019	528000	1148600	**0**	**10**	0.02	0.67	16.9	17	<0.2	<10	80	0.35	0.1	0.18	0.03	30.7	9.5	100	0.25	31.4	3.79	4.7	<0.05	0.05	0.02	0.016	0.04	7.9	1.1	0.06	276	0.69	0.01	0.2	27.5
814326	KP019	528000	1148600	10	20	0.03	0.86	18.2	<5	<0.2	<10	60	0.44	0.12	0.1	0.02	37.1	9.9	106	0.39	36.5	4.03	6.16	0.05	0.05	0.02	0.019	0.04	9.7	1.3	0.05	172	0.51	<0.01	0.2	30.8
814327	KP019	528000	1148600	20	30	0.03	0.72	17.2	23	<0.2	<10	40	0.37	0.12	0.05	0.01	39.3	8.6	99	0.34	31.8	3.74	5.05	<0.05	0.03	0.01	0.016	0.03	8	1.1	0.03	123	0.62	0.01	0.16	26.3
814328	KP019	528000	1148600	30	40	0.02	0.82	19.2	64	<0.2	<10	40	0.35	0.11	0.04	0.01	33.9	9.1	102	0.36	36.6	4.15	5.74	<0.05	0.04	0.01	0.018	0.03	9.2	1.1	0.03	90	0.41	<0.01	0.14	28.3
814329	KP019	528000	1148600	40	50	0.03	0.93	22.1	5	<0.2	<10	30	0.38	0.13	0.03	0.01	40.6	9.7	109	0.4	45.4	4.92	7.16	0.05	0.07	0.02	0.022	0.03	10.9	1.2	0.03	86	0.46	0.01	0.16	31.5
814330	KP019	528000	1148600	50	60	0.02	0.79	24	8	<0.2	<10	20	0.39	0.12	0.02	0.01	35	8.7	104	0.3	48.7	5	7.04	0.05	0.12	0.02	0.019	0.02	9.4	1	0.02	69	0.41	<0.01	0.12	30.3
814331	KP019	528000	1148600	60	70	0.02	0.68	26.1	6	<0.2	<10	20	0.43	0.1	0.01	0.01	31.7	8.7	102	0.22	48.1	5.6	6.25	<0.05	0.2	0.02	0.019	0.02	8.7	0.6	0.02	67	0.35	<0.01	0.08	30
814332	KP019	528000	1148600	70	80	0.01	0.53	25.2	<5	<0.2	<10	10	0.37	0.1	0.01	0.01	31.7	8.2	99	0.18	43.2	5.19	5.7	<0.05	0.23	0.01	0.016	0.01	7.6	0.5	0.01	60	0.32	<0.01	0.06	28.8
814342	KP020	528100	1148600	**0**	**10**	0.03	0.71	16.2	<5	<0.2	<10	50	0.3	0.09	0.12	0.02	34.1	8.2	32	0.38	24.5	2.23	4	0.05	0.06	0.01	0.011	0.05	11.7	1.7	0.09	151	0.49	<0.01	0.17	17.6
814343	KP020	528100	1148600	10	20	0.03	0.84	17.6	147	<0.2	<10	40	0.32	0.1	0.08	0.01	33.8	10.7	36	0.44	26.7	2.51	4.59	0.05	0.04	0.01	0.01	0.04	12.9	2	0.07	107	0.56	0.01	0.15	19.4
814344	KP020	528100	1148600	20	30	0.02	1.07	19	10	<0.2	<10	40	0.36	0.11	0.04	0.01	40.8	9.8	38	0.58	33.8	2.88	5.78	0.05	0.05	0.01	0.013	0.04	15.2	2.7	0.06	61	0.52	0.01	0.15	22.9
814345	KP020	528100	1148600	30	40	0.02	1.11	21.8	5	<0.2	<10	30	0.36	0.11	0.02	0.01	41.4	11.5	38	0.61	41.2	3.04	6.45	<0.05	0.07	0.01	0.014	0.03	13	2.9	0.05	69	0.55	0.01	0.13	25.9
814346	KP020	528100	1148600	40	50	0.02	0.96	20.6	5	<0.2	<10	20	0.29	0.1	0.02	<0.01	33.2	8.1	33	0.57	38	2.83	5.56	<0.05	0.07	0.01	0.011	0.03	11.7	2.4	0.04	46	0.48	<0.01	0.1	22.6
814347	KP020	528100	1148600	50	60	0.06	0.84	22.1	8	<0.2	<10	20	0.34	0.11	0.02	<0.01	34.9	7.3	30	0.56	37.7	2.69	5.12	<0.05	0.1	0.01	0.01	0.03	13.1	2.3	0.05	43	0.44	<0.01	0.08	22.6
814348	KP020	528100	1148600	60	70	0.05	0.82	29.2	68	<0.2	<10	20	0.36	0.12	0.02	0.01	32.6	8.1	34	0.54	41.6	3.08	5.02	0.05	0.1	0.01	0.01	0.02	14.3	2.1	0.08	58	0.5	0.01	0.05	25.9
814350	KP020	528100	1148600	70	80	0.1	1.28	13	254	<0.2	<10	140	0.65	0.13	0.15	0.02	50	17.6	151	0.47	27.5	8.29	8.1	0.05	0.02	0.03	0.049	0.05	12.6	1.9	0.06	657	1.65	0.01	0.73	14.7
814352	KP020	528100	1148600	80	90	0.08	0.82	28.3	<5	<0.2	<10	20	0.4	0.11	0.04	0.01	34.8	10.4	36	0.51	45.4	3.2	4.8	0.06	0.08	0.01	0.009	0.02	16.2	2.1	0.14	84	0.51	0.01	<0.05	28.4
814353	KP020	528100	1148600	90	100	0.26	0.89	46.1	6	<0.2	<10	20	0.54	0.12	0.04	0.02	42.8	18.7	37	0.58	56.7	3.68	5.15	0.08	0.08	0.01	0.009	0.02	20.4	2.5	0.19	161	0.9	<0.01	<0.05	41.6
814361	KP021	528200	1148600	**0**	**10**	0.1	0.48	9.5	5	<0.2	<10	50	0.22	0.08	0.09	0.02	20	5.6	31	0.34	11.3	1.51	3.02	0.05	0.06	0.01	0.009	0.04	13.3	1.1	0.05	263	0.28	0.01	0.19	10.1
814362	KP021	528200	1148600	10	20	0.08	0.55	11.1	<5	<0.2	<10	50	0.22	0.08	0.07	0.02	24	6.4	32	0.38	13.7	1.72	3.69	0.05	0.09	0.01	0.011	0.03	15.3	1.2	0.05	255	0.32	0.02	0.19	11.3
814363	KP021	528200	1148600	20	30	0.11	0.68	12	7	<0.2	<10	50	0.28	0.09	0.06	0.01	30.3	7.2	34	0.43	16	2.03	4.31	0.06	0.1	0.01	0.011	0.04	17.8	1.2	0.04	278	0.33	0.03	0.18	12.1
814364	KP021	528200	1148600	30	40	0.11	0.73	12.6	8	<0.2	<10	60	0.27	0.1	0.07	0.01	32.7	9	34	0.42	18	2.47	4.52	0.05	0.13	0.01	0.014	0.04	17.5	1.1	0.04	338	0.32	0.04	0.16	12.4
814365	KP021	528200	1148600	40	50	0.12	0.6	10.6	13	<0.2	<10	40	0.24	0.11	0.07	0.01	28.6	7	30	0.34	16.6	2.51	3.96	0.05	0.15	0.01	0.011	0.03	15.5	0.9	0.04	242	0.24	0.04	0.14	10.9
814366	KP021	528200	1148600	50	60	0.09	0.43	7.6	<5	<0.2	<10	30	0.22	0.1	0.07	0.01	25.1	6.4	24	0.27	15	2.36	3.25	0.05	0.18	0.01	0.009	0.02	14.5	0.7	0.03	208	0.17	0.03	0.1	8.3

Appendix C:Pits, Au and other elements in the regolith of the Lawra area analysed by ICP and FA-AAS Techniques

Sample ID	Pit ID	UTM-E	UTM-N	From (m	To (m)	P %	Pb ppm	Rb ppm	Re ppm	S %	Sb ppm	Sc ppm	Se ppm	Sn ppm	Sr ppm	Ta ppm	Te ppm	Th ppm	Ti ppm	Tl ppm	U ppm	V ppm	W ppm	Y ppm	Zn ppm	Zr ppm
813351	KP001	526650	1149550	**0**	**10**	80	7.4	26.3	<0.001	0.01	0.34	7.4	0.5	0.4	47.4	0.01	0.03	2.4	0.023	0.21	0.41	57	0.21	22.9	67	4
813352	KP001	526650	1149550	10	20	60	6.6	30.4	<0.001	0.01	0.29	6.9	0.4	0.4	38.5	<0.01	0.04	2.3	0.029	0.24	0.39	60	0.17	16.35	63	3.8
813353	KP001	526650	1149550	20	30	50	5.7	31.6	<0.001	0.01	0.26	7.5	0.4	0.4	35.2	<0.01	0.03	2.3	0.029	0.22	0.39	61	0.18	18.95	64	3.8
813354	KP001	526650	1149550	30	40	40	5.9	32.5	<0.001	0.01	0.24	7	0.4	0.4	36.3	<0.01	0.03	2.6	0.029	0.22	0.39	61	0.15	17.65	69	3.4
813355	KP001	526650	1149550	40	50	40	6.5	32.2	<0.001	0.01	0.24	6.4	0.4	0.4	39	<0.01	0.03	2.2	0.026	0.22	0.35	59	0.13	18.1	69	3
813356	KP001	526650	1149550	50	60	30	5.2	34.3	<0.001	0.01	0.18	6.2	0.3	0.3	42.9	<0.01	0.02	2.2	0.026	0.22	0.37	51	0.13	18.35	74	3
813357	KP001	526650	1149550	60	70	30	5.6	36.7	<0.001	0.01	0.22	6.1	0.4	0.3	42.7	<0.01	0.03	2.3	0.026	0.24	0.37	53	0.12	19.15	73	3.1
813358	KP001	526650	1149550	70	80	40	5.4	32.3	<0.001	<0.01	0.24	5.2	0.7	0.3	36.7	<0.01	0.04	1.9	0.025	0.22	0.32	52	<0.05	22.8	72	2.7
813359	KP001	526650	1149550	80	90	40	6.3	34.6	<0.001	<0.01	0.22	5.3	0.7	0.3	42.9	<0.01	0.02	2.1	0.023	0.24	0.36	47	<0.05	26.2	71	2.7
813360	KP001	526650	1149550	90	100	50	6.5	31.8	0.001	<0.01	0.25	5.4	1.1	0.3	43.8	<0.01	0.03	2.1	0.023	0.23	0.37	49	<0.05	31.1	73	2.6
813361	KP001	526650	1149550	100	110	140	6.9	25.1	<0.001	<0.01	0.31	6.9	0.7	0.4	67.3	<0.01	0.05	2.3	0.023	0.19	0.36	58	0.06	21.9	60	4.2
813386	KP003	527050	1149550	**0**	**10**	100	2.5	5.5	<0.001	<0.01	0.18	2.5	<0.2	0.3	16.9	<0.01	0.02	1.5	0.007	0.03	0.35	18	<0.05	5.3	15	1.5
813387	KP003	527050	1149550	10	20	90	2.8	5.1	<0.001	0.01	0.18	2.8	0.4	0.3	12.2	<0.01	0.01	1.5	0.006	0.03	0.38	20	<0.05	5.91	16	1
813388	KP003	527050	1149550	20	30	120	4.8	7.9	0.001	<0.01	0.29	4	0.3	0.4	13	<0.01	0.04	2	0.006	0.06	0.53	32	<0.05	6.76	19	1.3
813389	KP003	527050	1149550	30	40	110	4	7.7	<0.001	<0.01	0.24	4	<0.2	0.4	13.1	<0.01	0.04	2	0.005	0.05	0.51	29	<0.05	7.36	19	1.2
813391	KP003	527050	1149550	40	50	160	8.8	9.1	<0.001	<0.01	0.52	5.1	0.4	0.5	12	<0.01	0.08	2.4	0.006	0.11	0.72	55	0.05	6.2	30	1.6
813392	KP003	527050	1149550	50	60	160	11.3	10.1	0.001	<0.01	0.55	5.8	0.3	0.6	12.9	<0.01	0.07	2.9	0.008	0.17	0.8	63	0.05	5.77	36	2.7
813393	KP003	527050	1149550	60	70	140	10.8	9.5	<0.001	<0.01	0.5	5.6	0.2	0.6	11.9	<0.01	0.08	3	0.008	0.15	0.78	62	0.06	5.68	36	3.3
813394	KP003	527050	1149550	70	80	110	8.5	8.9	<0.001	<0.01	0.41	4.9	<0.2	0.5	11.2	<0.01	0.06	2.9	0.008	0.11	0.62	55	0.05	5.1	34	3.8
813395	KP003	527050	1149550	80	90	90	7.4	8.6	<0.001	<0.01	0.34	4.7	<0.2	0.5	10.3	<0.01	0.06	3.1	0.008	0.1	0.62	48	<0.05	5.37	34	4.7
813396	KP003	527050	1149550	90	100	70	7.1	8.6	0.001	<0.01	0.35	5.1	0.4	0.6	11.2	<0.01	0.05	3.4	0.007	0.1	0.66	47	<0.05	5.86	33	4.6
813397	KP003	527050	1149550	100	110	50	4.5	8.3	<0.001	<0.01	0.31	5.2	<0.2	0.5	11.5	<0.01	0.04	3.3	0.007	0.06	0.61	41	<0.05	6.13	30	5.4
813398	KP003	527050	1149550	110	120	70	6.8	8.6	<0.001	<0.01	0.36	5.7	0.2	0.6	12.4	<0.01	0.05	3.2	0.008	0.09	0.64	46	<0.05	7.12	38	5
813399	KP003	527050	1149550	120	130	60	6.9	8.1	<0.001	<0.01	0.38	5.4	0.2	0.5	12	<0.01	0.05	3.2	0.008	0.07	0.62	49	<0.05	6.37	39	5.3
813401	KP003	527050	1149550	130	140	70	7.1	7.3	0.001	<0.01	0.36	5.1	<0.2	0.5	10.9	<0.01	0.04	3.2	0.007	0.08	0.61	47	<0.05	7.6	43	4.3
813402	KP003	527050	1149550	140	150	70	5	7.4	<0.001	<0.01	0.36	5.9	0.3	0.5	11.7	<0.01	0.06	3.2	0.007	0.06	0.63	48	<0.05	8.9	45	4.6
813403	KP003	527050	1149550	150	160	140	3.9	5.3	<0.001	<0.01	0.27	5.3	<0.2	0.4	11.3	<0.01	0.06	2.6	0.006	0.04	0.53	49	<0.05	10	56	3.3
813404	KP003	527050	1149550	160	170	80	4.3	6.3	<0.001	<0.01	0.34	5.8	0.2	0.5	10.6	<0.01	0.04	3	0.008	0.06	0.58	51	<0.05	8.26	52	4.7
813405	KP003	527050	1149550	170	180	80	3.4	5.9	0.001	<0.01	0.32	5.7	0.3	0.5	11.1	<0.01	0.05	2.8	0.006	0.05	0.58	47	<0.05	9.66	53	3.8
813406	KP003	527050	1149550	180	190	150	4.5	5.3	<0.001	<0.01	0.37	5.8	0.3	0.4	11.4	<0.01	0.05	2.6	0.006	0.04	0.57	51	<0.05	9.8	61	3.4
813407	KP003	527050	1149550	190	200	200	3.9	4	<0.001	<0.01	0.25	5.3	0.2	0.3	12.5	<0.01	0.05	2	<0.005	0.03	0.43	46	<0.05	10.85	73	2.5
813408	KP004	527250	1149550	**0**	**10**	100	2.8	4.8	<0.001	<0.01	0.19	2.4	<0.2	0.3	19.5	<0.01	0.03	1.4	0.006	0.02	0.32	18	<0.05	5.95	18	1.3
813410	KP004	527250	1149550	10	20	120	4.6	6.9	<0.001	<0.01	0.27	3.6	0.3	0.4	21.3	<0.01	0.02	1.9	0.006	0.04	0.46	27	<0.05	7.82	22	1.3
813411	KP004	527250	1149550	20	30	140	6.4	8.4	<0.001	<0.01	0.33	4.6	<0.2	0.5	20.5	<0.01	0.03	2.5	0.006	0.07	0.61	36	<0.05	7.27	27	1.6
813412	KP004	527250	1149550	30	40	120	8.3	8.4	<0.001	<0.01	0.32	4.7	<0.2	0.5	17.4	<0.01	0.02	2.8	0.007	0.09	0.59	39	<0.05	6.88	34	2.2
813413	KP004	527250	1149550	40	50	100	8.1	7.1	<0.001	<0.01	0.29	4.2	<0.2	0.4	15.9	<0.01	0.03	2.6	0.006	0.11	0.54	39	<0.05	7.17	40	2.3
813414	KP004	527250	1149550	50	60	80	7.1	6.6	0.001	<0.01	0.31	4.2	<0.2	0.4	12.9	<0.01	0.03	2.7	0.007	0.09	0.55	39	<0.05	7.68	41	2.9
813415	KP004	527250	1149550	60	70	70	8.1	7.1	<0.001	<0.01	0.34	5	0.5	0.4	13.3	<0.01	0.02	2.9	0.008	0.08	0.58	41	<0.05	10.8	46	3.4
813416	KP004	527250	1149550	70	80	60	7.3	6.8	<0.001	<0.01	0.32	4.9	0.5	0.4	11.3	<0.01	0.02	2.6	0.009	0.06	0.53	37	<0.05	9.99	42	4.2
813417	KP004	527250	1149550	80	90	40	5.6	6.7	<0.001	<0.01	0.26	5	0.4	0.5	11.9	<0.01	0.02	2.9	0.008	0.06	0.49	38	<0.05	9.25	41	4.5
813418	KP004	527250	1149550	90	100	50	4.7	6.6	<0.001	<0.01	0.26	5.9	0.5	0.5	12.3	<0.01	0.03	3.1	0.007	0.06	0.51	37	<0.05	12.2	45	4.1
813419	KP004	527250	1149550	100	110	50	3.6	5.9	<0.001	<0.01	0.27	6.1	0.7	0.5	13.1	<0.01	0.03	2.9	0.007	0.04	0.46	38	<0.05	12.95	52	4.1
813420	KP004	527250	1149550	110	120	70	4.5	5.6	<0.001	<0.01	0.35	7.1	0.8	0.5	14.6	<0.01	0.03	3	0.007	0.05	0.47	43	<0.05	14.8	74	3.9
813421	KP004	527250	1149550	120	130	90	4.5	5.2	<0.001	<0.01	0.31	6.9	0.6	0.5	15.1	<0.01	0.03	3.1	0.008	0.04	0.47	48	<0.05	16.9	96	3.9
813422	KP004	527250	1149550	130	140	130	6.3	3.9	<0.001	<0.01	0.43	7.7	0.8	0.5	16.1	<0.01	0.02	2.9	0.009	0.04	0.42	50	<0.05	20.4	113	3.9
813423	KP004	527250	1149550	140	150	160	5.9	3.3	<0.001	<0.01	0.37	7.3	0.6	0.5	14.7	<0.01	0.03	3.2	0.008	0.03	0.43	51	<0.05	19.6	114	3.3
813429	KP005	527450	1149550	**0**	**10**	150	4.6	4.9	<0.001	0.01	0.25	2.1	0.3	0.2	38.6	<0.01	0.03	1.4	0.005	0.02	0.34	23	0.05	4.5	25	2.1
813430	KP005	527450	1149550	10	20	120	4.9	5	<0.001	<0.01	0.29	2.6	0.3	0.3	37.8	<0.01	0.03	1.4	0.005	0.03	0.37	27	0.06	5.42	26	2.2
813432	KP005	527450	1149550	20	30	120	5.3	5.9	<0.001	<0.01	0.33	3.1	0.4	0.3	34.3	<0.01	0.04	1.6	0.005	0.04	0.41	31	0.06	5.55	26	2.1
813433	KP005	527450	1149550	30	40	130	6.2	6.9	<0.001	<0.01	0.39	3.7	0.4	0.3	35.5	<0.01	0.04	1.8	<0.005	0.05	0.48	39	0.05	6.06	27	2.4
813434	KP005	527450	1149550	40	50	120	9.5	6.9	0.001	0.01	0.68	3.8	0.2	0.3	28	<0.01	0.08	1.7	<0.005	0.06	0.73	47	0.08	4.18	25	2.3
813435	KP005	527450	1149550	50	60	80	8	6.8	<0.001	<0.01	0.69	4	0.3	0.3	22.7	<0.01	0.06	1.9	<0.005	0.06	0.62	39	0.06	5.49	28	3.4
813436	KP005	527450	1149550	60	70	60	5.9	5.1	0.001	<0.01	0.83	3.7	0.4	0.2	23.5	<0.01	0.07	1.6	0.005	0.03	0.55	44	0.07	5.59	35	4.1
813437	KP005	527450	1149550	70	80	60	5.4	4.8	<0.001	<0.01	0.77	3.9	0.5	0.2	25.2	<0.01	0.09	1.6	0.005	0.03	0.55	47	0.06	7.16	43	4.2
813438	KP005	527450	1149550	80	90	50	5.7	3.1	<0.001	<0.01	0.6	3.3	0.3	<0.2	23.5	<0.01	0.07	1.3	<0.005	0.02	0.39	46	0.23	7.78	61	4.2
813440	KP005	527450	1149550	90	100	40	5.3	3.4	<0.001	<0.01	0.68	3.1	0.4	0.2	26.5	<0.01	0.08	1.3	<0.005	0.02	0.34	42	0.06	8	60	4.6
813441	KP005	527450	1149550	100	110	40	5.6	2.2	<0.001	<0.01	0.57	2.4	0.3	0.2	30	<0.01	0.08	1.1	<0.005	<0.02	0.24	38	0.05	7.21	74	5.2
813442	KP005	527450	1149550	110	120	60	5.4	2.3	<0.001	<0.01	0.92	3	0.4	<0.2	29.9	<0.01	0.1	1	<0.005	0.02	0.25	42	0.07	6.28	72	4.4
813443	KP005	527450	1149550	120	130	40	4.7	1.4	<0.001	<0.01	0.55	2.3	0.2	<0.2	31.4	<0.01	0.06	0.9	<0.005	<0.02	0.19	40	0.06	5.28	84	4.7
813444	KP006	527650	1149550	**0**	**10**	240	6.5	5.2	<0.001	0.01	0.7	2.2	0.4	0.2	34.6	<0.01	0.08	1.9	0.005	0.03	0.37	27	0.14	3.52	38	2.5
813445	KP006	527650	1149550	10	20	200	7.7	5	<0.001	<0.01	1.01	2.4	0.6	0.2	28.3	<0.01	0.12	1.9	<0.005	0.05	0.43	30	0.17	3.31	35	2.3
813446	KP006	527650	1149550	20	30	180	8.3	5.3	<0.001	<0.01	1.28	2.9	0.4	0.2	20.2	<0.01	0.13	1.7	<0.005	0.05	0.44	40	0.21	3.4	41	2.6
813447	KP006	527650	1149550	30	40	160	8.4	4.9	<0.001	<0.01	1.08	3	0.4	0.2	16.3	<0.01	0.15	1.8	<0.005	0.04	0.4	43	0.26	3.52	49	3
813448	KP006	527650	1149550	40	50	120	7.8	3.4	<0.001	<0.01	0.92	3	0.4	0.2	16.8	<0.01	0.11	1.7	<0.005	0.03	0.31	38	0.25	3.53	59	3.3
813451	KP006	527650	1149550	50	60	90	5.5	2.4	<0.001	<0.01	0.82	2.3	0.5	<0.2	15.6	<0.01	0.1	1.5	<0.005	0.02	0.24	28	0.31	3.25	58	3.1
813452	KP006	527650	1149550	60	70	80	5.7	2	<0.001	<0.01	0.63	2.4	0.2	<0.2	17.7	<0.01	0.09	1.7	<0.005	0.02	0.24	28	0.29	3.62	60	3.2
813453	KP006	527650	1149550	70	80	60	4.1	1.5	<0.001	<0.01	0.54	1.8	0.3	<0.2	16.9	<0.01	0.07	1.4	<0.005	<0.02	0.16	20	0.21	3.27	51	2.5
813454	KP006	527650	1149550	80	90	60	5.8	1.7	<0.001	0.01	0.6	2.3	0.4	<0.2	19.2	<0.01	0.1	1.7	<0.005	<0.02	0.19	23	0.21	3.86	54	2.7
813455	KP006	527650	1149550	90	100	60	5.9	1.7	<0.001	0.01	0.63	2.7	0.2	<0.2	21.4	<0.01	0.09	2.1	<0.005	0.02	0.23	29	0.1	4.41	61	2.8
813456	KP006	527650	1149550	100	110	60	4.6	1.4	<0.001	0.01	0.51	2.8	0.2	<0.2	26.8	<0.01	0.07	1.8	<0.005	<0.02	0.19	26	0.08	4.93	72	2.7
813457	KP006	527650	1149550	110	120	50	5.2	1.2	0.001	0.01	0.49	2.8	0.3	<0.2	28.5	<0.01	0.05	1.7	<0.005	<0.02	0.17	25	0.07	4.93	77	2.2
813458	KP006	527650	1149550	120	130	60	5.7	1.4	<0.001	<0.01	0.76	2.8	0.4	<0.2	26.7	<0.01	0.08	1.8	<0.005	<0.02	0.23	26	0.08	4.97	71	2.8
813459	KP006	527650	1149550	130	140	50	4.9	1.3	<0.001	0.01	0.68	2.4	0.3	<0.2	26.4	<0.01	0.06	1.8	<0.005	<0.02	0.22	24	0.07	4.22	75	2.6

Appendix C:Pits, Au and other elements in the regolith of the Lawra area analysed by ICP and FA-AAS Techniques

Sample ID	Pit ID	UTM-E	UTM-N	From (m	To (m)	P %	Pb ppm	Rb ppm	Re ppm	S %	Sb ppm	Sc ppm	Se ppm	Sn ppm	Sr ppm	Ta ppm	Te ppm	Th ppm	Ti ppm	Tl ppm	U ppm	V ppm	W ppm	Y ppm	Zn ppm	Zr ppm
813460	KP006	527650	1149550	140	150	50	4.8	1	<0.001	0.01	0.48	2.2	<0.2	<0.2	24.5	<0.01	0.06	1.5	<0.005	<0.02	0.16	22	0.07	3.73	77	2.1
813461	KP007	527850	1149550	**0**	**10**	160	3.7	4.6	<0.001	0.01	0.15	2.4	0.2	0.2	25.9	<0.01	0.02	1.5	0.005	0.03	0.3	22	0.05	4.11	28	2.1
813462	KP007	527850	1149550	10	20	150	4.9	5	<0.001	0.01	0.15	3.2	0.2	0.2	18.2	<0.01	0.03	1.6	0.005	0.03	0.33	28	0.07	5.14	28	1.9
813463	KP007	527850	1149550	20	30	140	6.5	6	<0.001	0.01	0.17	3.9	0.3	0.3	17.3	<0.01	0.03	1.9	0.005	0.05	0.39	35	0.07	6.42	31	2
813464	KP007	527850	1149550	30	40	130	8.8	7	<0.001	0.01	0.17	4.4	0.3	0.3	17.3	<0.01	0.04	2.2	0.005	0.06	0.45	41	0.06	7.11	35	2
813465	KP007	527850	1149550	40	50	110	8.4	7.3	<0.001	0.01	0.18	4.8	0.3	0.3	17.2	<0.01	0.04	2.4	0.005	0.06	0.46	37	0.06	7.95	32	2.3
813466	KP007	527850	1149550	50	60	80	7.6	7.2	<0.001	<0.01	0.14	4.2	0.4	0.3	18.3	<0.01	0.04	2.5	0.005	0.05	0.37	37	0.05	8.69	39	2.7
813467	KP007	527850	1149550	60	70	60	8	7.2	<0.001	<0.01	0.18	4.1	0.3	0.3	18.5	<0.01	0.05	2.7	0.005	0.05	0.41	43	0.05	8.34	43	3.5
813468	KP007	527850	1149550	70	80	70	8.8	7.5	<0.001	<0.01	0.21	4.2	0.3	0.3	14.5	<0.01	0.05	2.9	0.006	0.05	0.56	45	0.1	7.19	36	3.5
813469	KP007	527850	1149550	80	90	70	10.1	6.4	<0.001	0.02	0.4	4.3	0.2	0.4	15.4	<0.01	0.05	2.8	0.007	0.08	0.63	53	0.09	7.1	39	5.1
813470	KP007	527850	1149550	90	100	60	9.9	6.4	<0.001	0.01	0.34	4.4	0.4	0.4	17.3	<0.01	0.06	2.7	0.007	0.07	0.55	50	0.07	7.38	41	5
813472	KP007	527850	1149550	100	110	70	10.6	6	<0.001	0.01	0.33	4.4	0.3	0.4	13.9	<0.01	0.07	2.7	0.008	0.07	0.67	52	0.08	6.84	42	4.9
813473	KP007	527850	1149550	110	120	60	11.9	6.6	<0.001	0.02	0.36	4.7	<0.2	0.6	13.7	0.01	0.07	2.9	0.008	0.08	0.72	57	0.07	6.21	45	6.5
813474	KP007	527850	1149550	120	130	50	13.6	5.8	0.001	0.01	0.33	4.6	<0.2	0.4	13.8	<0.01	0.06	2.7	0.008	0.06	0.63	55	0.07	5.53	51	6.5
813475	KP007	527850	1149550	130	140	40	5.8	2.4	<0.001	0.01	0.18	3.4	<0.2	0.2	14.4	<0.01	0.05	1.2	<0.005	0.02	0.2	37	<0.05	4.54	73	2.8
813476	KP007	527850	1149550	140	150	40	5.4	2	<0.001	0.01	0.2	3.4	<0.2	0.2	14.7	<0.01	0.06	1.1	<0.005	<0.02	0.19	39	<0.05	4.6	74	3
813477	KP007	527850	1149550	150	160	60	4.9	1.3	<0.001	0.01	0.18	3.2	<0.2	<0.2	15.7	<0.01	0.06	0.8	<0.005	<0.02	0.13	38	<0.05	4.42	82	2.2
813478	KP007	527850	1149550	160	170	50	4.7	1.6	<0.001	0.01	0.19	3.2	<0.2	<0.2	13.2	<0.01	0.06	1	<0.005	<0.02	0.14	38	<0.05	4.19	78	2.4
813479	KP007	527850	1149550	170	180	40	4.8	1.9	<0.001	<0.01	0.19	3	<0.2	0.2	11.4	<0.01	0.07	1	<0.005	<0.02	0.14	36	<0.05	3.7	70	2.5
813480	KP008	526900	1148600	**0**	**10**	200	5	10.7	<0.001	0.01	0.25	2.9	0.2	0.4	31.6	<0.01	0.03	1.7	0.009	0.05	0.54	27	0.07	6.84	23	1.9
813481	KP008	526900	1148600	10	20	150	5.5	9.1	<0.001	<0.01	0.24	3.2	<0.2	0.4	14.9	<0.01	0.03	1.6	0.007	0.06	0.53	29	0.07	6.56	18	1.1
813482	KP008	526900	1148600	20	30	140	4.8	9.2	<0.001	<0.01	0.23	3.5	0.4	0.4	12.1	<0.01	0.03	1.8	0.006	0.06	0.6	31	0.06	6.33	17	1
813483	KP008	526900	1148600	30	40	130	5	9.4	<0.001	<0.01	0.26	3.9	0.2	0.5	9.6	<0.01	0.05	1.9	0.006	0.08	0.64	35	0.07	6.78	14	1
813484	KP008	526900	1148600	40	50	110	5	9.6	<0.001	<0.01	0.34	4.2	0.3	0.6	8.6	<0.01	0.05	2.2	0.007	0.08	0.64	41	0.06	6.69	13	1.4
813485	KP008	526900	1148600	50	60	110	6.3	8.7	<0.001	0.01	0.48	4.3	0.2	0.5	10.2	<0.01	0.06	2.2	0.007	0.06	0.64	49	0.07	6.15	18	1.8
813486	KP008	526900	1148600	60	70	80	5.4	9.9	<0.001	<0.01	0.33	4.6	<0.2	0.6	8.3	<0.01	0.05	2.5	0.006	0.09	0.62	42	0.06	5.91	16	2.2
813487	KP008	526900	1148600	70	80	70	5.4	10.8	<0.001	0.01	0.22	5.1	0.4	0.4	8	<0.01	0.03	2.9	0.006	0.11	0.58	38	<0.05	6.33	23	2.1
813488	KP008	526900	1148600	80	90	60	4.1	10.8	<0.001	0.01	0.24	5.8	0.5	0.5	8.5	<0.01	0.04	3	0.005	0.11	0.57	38	<0.05	6.76	29	2.4
813490	KP008	526900	1148600	90	100	60	5.4	10	<0.001	0.01	0.25	6	0.4	0.5	9.6	<0.01	0.05	3.2	0.005	0.1	0.6	43	<0.05	7.39	38	2.5
813491	KP008	526900	1148600	100	110	60	3.9	8.8	<0.001	0.01	0.22	5.8	0.4	0.4	11.7	<0.01	0.04	2.8	<0.005	0.08	0.53	39	<0.05	9.32	49	2.2
813492	KP008	526900	1148600	110	120	50	3.9	9.6	<0.001	<0.01	0.26	5.8	0.4	0.4	11.4	<0.01	0.05	2.9	<0.005	0.09	0.52	37	<0.05	9.39	50	2.1
813493	KP008	526900	1148600	120	130	50	3.8	8.1	<0.001	0.01	0.24	5.4	0.5	0.3	14.4	<0.01	0.04	2.9	<0.005	0.07	0.54	38	<0.05	11.45	67	2
813495	KP008	526900	1148600	130	140	60	6.4	7.2	<0.001	0.01	0.32	5.2	0.4	0.3	13.6	<0.01	0.05	2.7	<0.005	0.07	0.5	41	<0.05	9.9	62	2
813496	KP008	526900	1148600	140	150	70	5.8	6.5	<0.001	0.01	0.33	5.4	0.5	0.3	19.1	<0.01	0.05	2.6	<0.005	0.06	0.48	43	<0.05	10.95	75	2.1
813497	KP008	526900	1148600	150	160	70	5.5	6.1	<0.001	0.01	0.37	4.7	0.4	0.3	17	<0.01	0.05	2.5	0.005	0.06	0.46	40	<0.05	10.35	73	1.8
813498	KP008	526900	1148600	160	170	60	7.2	6.6	<0.001	0.01	0.51	5.3	0.5	0.3	19.4	<0.01	0.07	2.7	<0.005	0.07	0.46	45	<0.05	9.61	72	1.7
813499	KP008	526900	1148600	170	180	60	6.5	7.1	<0.001	0.01	0.49	5.2	0.5	0.3	16.1	<0.01	0.08	2.6	<0.005	0.07	0.44	44	<0.05	8.49	61	2.3
813500	KP008	526900	1148600	180	190	90	5.8	5.9	<0.001	0.01	0.45	4.2	0.4	0.3	16.5	<0.01	0.06	2.3	0.005	0.05	0.42	40	<0.05	9.09	70	1.7
813551	KP008	526900	1148600	190	200	140	4.8	13.6	<0.001	0.01	0.4	5.5	0.4	0.4	9.5	<0.01	0.06	3.9	0.01	0.12	0.61	51	<0.05	8.61	65	3.6
813552	KP008	526900	1148600	200	210	130	6.2	12.9	<0.001	0.01	0.4	5.3	0.4	0.4	12.9	<0.01	0.06	3.2	0.007	0.11	0.55	49	<0.05	8.58	65	2.8
813553	KP009	527000	1148600	**0**	**10**	420	7	14.8	<0.001	0.02	0.33	4.5	0.6	0.4	184	<0.01	0.06	2.3	0.01	0.08	0.62	33	0.14	10.05	51	3
813554	KP009	527000	1148600	10	20	210	5.7	11.5	<0.001	0.02	0.29	4.3	0.6	0.4	35.6	<0.01	0.05	2.1	0.008	0.09	0.67	35	0.12	8.28	30	1.4
813556	KP009	527000	1148600	20	30	200	6.2	11.4	<0.001	0.01	0.31	4.4	0.6	0.4	24.5	<0.01	0.05	2.2	0.008	0.1	0.69	37	0.1	8.09	30	1.2
813557	KP009	527000	1148600	30	40	170	9.7	11.3	<0.001	0.01	0.48	6	0.6	0.5	13.7	<0.01	0.08	3.4	0.01	0.13	0.92	62	0.16	6.44	36	2.5
813558	KP009	527000	1148600	40	50	160	9	11.4	<0.001	0.01	0.51	6.7	0.7	0.5	12.9	<0.01	0.08	3.6	0.011	0.14	0.93	71	0.16	7.57	38	3.8
813559	KP009	527000	1148600	50	60	160	11.4	11.1	<0.001	0.01	0.54	6.8	0.7	0.6	12.9	<0.01	0.08	3.6	0.011	0.15	0.94	75	0.12	8.03	44	3.9
813560	KP009	527000	1148600	60	70	180	11.9	11.4	<0.001	0.01	0.57	7.8	0.7	0.6	16.2	<0.01	0.08	3.7	0.012	0.14	1.01	76	0.11	9.07	51	3.8
813562	KP009	527000	1148600	70	80	170	8.9	9.2	<0.001	0.01	0.49	7.7	0.6	0.6	12.8	<0.01	0.06	3.2	0.015	0.1	0.76	74	0.1	8.96	54	5.6
813563	KP009	527000	1148600	80	90	170	7.1	7.6	<0.001	0.01	0.47	7.8	0.6	0.6	10.9	<0.01	0.06	3.2	0.015	0.09	0.79	76	0.07	8.47	52	5.9
813564	KP009	527000	1148600	90	100	160	7.3	6.5	<0.001	0.01	0.45	7.6	0.5	0.6	11.8	<0.01	0.05	3.2	0.017	0.08	0.82	74	0.07	8.76	54	7.1
813565	KP009	527000	1148600	100	110	130	6.8	5.7	<0.001	0.01	0.41	6.9	0.5	0.6	11.5	<0.01	0.05	2.9	0.016	0.07	0.68	69	0.08	7.93	47	7.3
813566	KP009	527000	1148600	110	120	120	4.6	4.3	<0.001	0.01	0.32	6.7	0.5	0.5	9.8	<0.01	0.05	2.8	0.016	0.05	0.58	64	0.05	6.93	46	7.7
813567	KP009	527000	1148600	120	130	120	4	4.1	<0.001	0.01	0.3	7	0.5	0.5	7.8	<0.01	0.05	2.8	0.014	0.05	0.54	63	<0.05	7.94	48	8.2
813568	KP009	527000	1148600	130	140	170	2	1.7	<0.001	0.01	0.28	6	0.4	0.4	8.2	<0.01	0.04	2.2	0.02	0.02	0.43	57	<0.05	7.78	59	10.2
813570	KP009	527000	1148600	140	150	150	2.2	2.1	<0.001	0.01	0.27	5.8	0.4	0.3	7	<0.01	0.03	2.1	0.017	0.03	0.4	57	<0.05	7.53	55	9
813571	KP009	527000	1148600	150	160	140	3.6	2.2	<0.001	0.01	0.31	5.7	0.4	0.4	6.2	<0.01	0.04	2.4	0.015	0.04	0.42	61	<0.05	7.04	47	7.4
813572	KP009	527000	1148600	160	170	170	3.1	1.8	<0.001	0.01	0.37	6.5	0.5	0.5	6.8	<0.01	0.05	2.5	0.021	0.02	0.49	65	<0.05	7.1	55	9
813573	KP009	527000	1148600	170	180	140	2.9	2.5	<0.001	0.01	0.34	6.8	0.4	0.5	5.2	<0.01	0.04	2.7	0.018	0.03	0.47	67	<0.05	8.5	44	8.4
813574	KP009	527000	1148600	180	190	140	1.2	1.2	<0.001	<0.01	0.36	5.2	0.2	0.4	4	<0.01	0.02	1.6	0.015	0.02	0.36	47	0.24	6.49	36	6.6
813579	KP010	527100	1148600	**0**	**10**	120	3.1	4	<0.001	0.01	1.04	5.8	1.3	0.4	6.6	<0.01	0.33	1.9	0.006	0.03	0.58	49	0.86	6.77	16	1.8
813580	KP010	527100	1148600	10	20	100	2.5	3	<0.001	0.01	1.07	5.4	1.1	0.4	6.7	<0.01	0.34	1.9	0.005	0.02	0.5	50	0.71	6.86	20	3.2
813581	KP010	527100	1148600	20	30	160	4.3	6	<0.001	0.01	0.96	5.5	0.9	0.5	8	<0.01	0.26	1.6	0.006	0.05	0.7	47	0.43	9.03	20	0.9
813583	KP010	527100	1148600	30	40	200	5.6	10	<0.001	0.01	0.77	6.2	1	0.7	8.7	<0.01	0.22	1.6	0.007	0.09	0.87	53	0.41	9.09	14	0.9
813584	KP010	527100	1148600	40	50	190	5.9	9.8	<0.001	0.01	0.78	6.4	0.8	0.6	7.8	<0.01	0.21	1.8	0.007	0.09	0.91	58	0.49	9.08	16	1
813585	KP010	527100	1148600	50	60	160	6.1	10.3	<0.001	0.01	0.95	9	1	0.7	7.8	<0.01	0.27	2.6	0.007	0.09	1.03	63	0.45	11.6	16	2.8
813586	KP010	527100	1148600	60	70	140	5.6	7.9	<0.001	0.01	1.26	9.5	1.4	0.6	7.2	<0.01	0.45	2.7	0.007	0.07	0.98	62	0.47	11.95	15	3.6
813587	KP010	527100	1148600	70	80	110	4.9	4.9	<0.001	0.01	1.3	8.1	1.7	0.5	7.6	<0.01	0.44	2.5	0.006	0.05	0.84	82	0.2	7.83	12	4.5
813588	KP010	527100	1148600	80	90	30	3.5	2.2	<0.001	<0.01	2.81	4.8	0.9	0.4	5.4	<0.01	2.86	2.7	<0.005	0.02	0.36	21	0.66	5.94	5	4.5
813589	KP010	527100	1148600	90	100	70	4.4	2	<0.001	<0.01	2.17	5.7	0.9	0.4	17.2	<0.01	0.81	1.8	0.006	0.02	0.45	74	0.14	6.08	7	4.4
813590	KP010	527100	1148600	100	110	50	3.9	1.3	<0.001	<0.01	3.06	5.8	1.2	0.3	15.6	<0.01	2.21	2	<0.005	<0.02	0.45	55	0.33	7.19	9	4.4
813591	KP010	527100	1148600	110	120	110	3	1.3	<0.001	<0.01	1.65	8.1	0.9	0.4	12.9	<0.01	0.15	1.7	0.01	<0.02	0.54	123	0.06	6.35	14	5.2
813592	KP010	527100	1148600	120	130	90	3.5	1.4	<0.001	<0.01	2.8	7.3	0.9	0.4	13.5	<0.01	1.49	1.9	0.007	<0.02	0.55	95	0.26	7.43	13	4.8
813593	KP010	527100	1148600	130	140	90	3.4	1.4	<0.001	<0.01	2.68	7.2	1.1	0.4	11.5	<0.01	1.5	2	0.007	<0.02	0.51	82	0.29	8.09	14	4.6

Appendix C:Pits, Au and other elements in the regolith of the Lawra area analysed by ICP and FA-AAS Techniques

Sample ID	Pit ID	UTM-E	UTM-N	From (m	To (m)	P %	Pb ppm	Rb ppm	Re ppm	S %	Sb ppm	Sc ppm	Se ppm	Sn ppm	Sr ppm	Ta ppm	Te ppm	Th ppm	Ti ppm	Tl ppm	U ppm	V ppm	W ppm	Y ppm	Zn ppm	Zr ppm
813594	KP010	527100	1148600	140	150	90	3.5	1.1	<0.001	<0.01	1.65	6.8	0.6	0.4	16	<0.01	0.68	1.6	0.008	<0.02	0.4	86	0.06	7.5	16	4.9
813595	KP011	527200	1148600	**0**	**10**	230	4.7	8.4	<0.001	0.01	0.55	4.1	0.5	0.4	15.2	<0.01	0.02	2	0.011	0.08	0.55	37	0.14	9.08	34	2.2
813596	KP011	527200	1148600	10	20	160	6.5	7.2	<0.001	<0.01	0.58	4.2	0.4	0.4	5	<0.01	0.03	2.2	0.009	0.09	0.57	36	0.12	8.09	30	3
813597	KP011	527200	1148600	20	30	160	6	8.4	<0.001	<0.01	0.63	5	0.5	0.5	4.8	<0.01	0.03	2.4	0.009	0.1	0.66	45	0.13	9.04	34	3.4
813598	KP011	527200	1148600	30	40	160	6.2	8.8	<0.001	<0.01	0.72	5.7	0.7	0.6	4.8	<0.01	0.03	2.7	0.009	0.13	0.72	49	0.14	10.1	40	4
813599	KP011	527200	1148600	40	50	180	5	7.1	<0.001	<0.01	0.73	5.7	0.7	0.5	3.6	<0.01	0.05	2.6	0.01	0.1	0.64	54	0.14	9.57	65	4.9
813600	KP011	527200	1148600	50	60	190	4.2	5.5	<0.001	<0.01	0.75	4.9	0.4	0.4	2.9	<0.01	0.05	2.5	0.01	0.09	0.56	50	0.14	8.54	84	5.4
813601	KP011	527200	1148600	60	70	200	13.9	3.3	<0.001	<0.01	0.75	4.1	0.6	0.3	2.2	<0.01	0.04	1.9	0.01	0.05	0.41	44	0.1	7.92	103	5.7
813603	KP011	527200	1148600	70	80	180	3	3	<0.001	<0.01	0.87	3.7	0.5	0.3	2.2	<0.01	0.04	1.7	0.01	0.04	0.34	38	0.09	7.68	97	5.7
813610	KP012	527300	1148600	**0**	**10**	150	5.8	5.8	<0.001	0.01	0.35	2.6	0.5	0.4	15.1	<0.01	0.01	1.5	0.009	0.04	0.45	23	0.05	11.1	18	1.3
813611	KP012	527300	1148600	10	20	90	5.2	4	<0.001	<0.01	0.43	2.8	0.5	0.4	2.9	<0.01	0.01	1.7	0.008	0.05	0.51	26	<0.05	9.54	19	2.1
813612	KP012	527300	1148600	20	30	80	5.8	4	<0.001	<0.01	0.48	3	0.3	0.5	2.4	<0.01	0.01	2	0.009	0.04	0.55	30	<0.05	9.08	19	3.1
813613	KP012	527300	1148600	30	40	80	6.3	4.2	<0.001	<0.01	0.48	3.2	0.5	0.5	2.7	<0.01	0.01	1.9	0.009	0.05	0.54	28	0.05	10.25	19	3
813614	KP012	527300	1148600	40	50	80	6.2	4.7	<0.001	<0.01	0.53	3.6	0.8	0.6	4.3	<0.01	0.01	2	0.009	0.04	0.58	29	0.05	11.8	19	3.4
813615	KP012	527300	1148600	50	60	70	7.6	4.1	<0.001	<0.01	0.59	3.3	0.5	0.6	5.2	<0.01	0.02	2.3	0.009	0.05	0.59	29	<0.05	10.5	21	4.2
813616	KP012	527300	1148600	60	70	50	6.7	3.2	<0.001	<0.01	0.57	2.7	0.5	0.5	4.9	0.01	0.03	2	0.008	0.03	0.38	21	0.06	7.34	13	4.7
813617	KP012	527300	1148600	70	80	40	5.4	2.7	<0.001	0.01	0.59	2.3	0.5	0.5	4.1	<0.01	0.03	1.8	0.007	0.03	0.33	18	0.09	6.32	11	4.6
813618	KP012	527300	1148600	80	90	40	4.4	1.6	<0.001	<0.01	0.45	1.6	0.3	0.3	2.8	<0.01	0.02	1.3	0.008	0.02	0.25	17	0.06	4.17	13	3.4
813626	KP013	527400	1148600	**0**	**10**	230	5.2	5.8	<0.001	0.01	0.58	3.6	0.7	0.4	19.6	<0.01	0.07	1.4	0.008	0.04	0.39	38	0.06	12.65	32	1.9
813627	KP013	527400	1148600	10	20	240	4.6	4.3	<0.001	0.01	0.56	3.6	0.7	0.4	5.1	<0.01	0.06	1.3	0.008	0.04	0.37	41	0.05	11.2	35	2.2
813628	KP013	527400	1148600	20	30	260	4.3	4.2	<0.001	<0.01	0.58	4	0.7	0.4	3.9	<0.01	0.06	1.3	0.009	0.04	0.35	42	0.05	11.1	37	3.1
813629	KP013	527400	1148600	30	40	390	4.4	2.5	<0.001	<0.01	0.66	3.7	0.6	0.4	2.6	<0.01	0.1	1	0.011	0.02	0.29	46	0.05	9.68	57	3.5
813630	KP013	527400	1148600	40	50	370	4.2	2.6	<0.001	<0.01	0.57	3.7	0.6	0.4	2.3	<0.01	0.08	1.1	0.01	0.02	0.29	44	<0.05	10.4	55	3.7
813631	KP013	527400	1148600	50	60	360	4.5	2.7	<0.001	<0.01	0.6	3.6	0.6	0.5	2.2	<0.01	0.08	1.3	0.01	0.03	0.29	44	<0.05	10.9	56	4.1
813647	KP014	527500	1148600	**0**	**10**	170	7.9	5.8	<0.001	0.01	0.35	3.5	0.8	0.3	13.2	<0.01	0.08	1.6	0.007	0.05	0.47	38	<0.05	13.6	56	2.2
813648	KP014	527500	1148600	10	20	150	6.4	5.4	<0.001	<0.01	0.36	4.1	0.8	0.4	9	<0.01	0.08	1.6	0.006	0.06	0.49	43	<0.05	14.85	63	2.2
813649	KP014	527500	1148600	20	30	130	4.8	5.1	<0.001	0.01	0.31	4.4	0.8	0.5	8.1	<0.01	0.07	1.8	0.006	0.05	0.47	45	<0.05	15.2	81	2.8
813651	KP014	527500	1148600	30	40	100	3.9	4.4	<0.001	<0.01	0.26	4.4	0.7	0.4	8.4	0.01	0.06	1.6	0.006	0.04	0.41	39	<0.05	15.55	92	2.9
813652	KP014	527500	1148600	40	50	90	3.4	4	<0.001	<0.01	0.22	4.4	0.6	0.4	9.5	<0.01	0.05	1.5	0.005	0.03	0.36	36	<0.05	17	103	2.8
813668	KP015	527600	1148600	**0**	**10**	360	4.4	6.4	<0.001	0.02	0.26	3.6	0.7	0.3	21	<0.01	0.06	1.4	0.009	0.04	0.48	40	0.05	9.99	40	1.8
813670	KP015	527600	1148600	10	20	310	3.9	5.2	<0.001	0.01	0.24	3.9	0.6	0.3	4.3	<0.01	0.07	1.5	0.008	0.06	0.48	44	<0.05	9.83	45	2.7
813671	KP015	527600	1148600	20	30	300	3.2	4	<0.001	<0.01	0.19	3.6	0.5	0.3	3.6	<0.01	0.07	1.3	0.008	0.04	0.4	44	<0.05	7.9	58	3.6
813672	KP015	527600	1148600	30	40	370	3	1.1	<0.001	<0.01	0.15	3	0.3	0.3	6	<0.01	0.14	0.8	0.011	<0.02	0.28	38	<0.05	5.34	87	5.2
813673	KP015	527600	1148600	40	50	340	2.7	1.2	<0.001	<0.01	0.14	3	0.4	0.3	3.6	<0.01	0.09	0.8	0.012	<0.02	0.27	37	<0.05	5.61	91	5.1
813674	KP015	527600	1148600	50	60	350	2.8	1	<0.001	<0.01	0.12	2.9	0.3	0.3	4.7	<0.01	0.08	0.7	0.012	<0.02	0.25	36	<0.05	5.64	90	5.5
813687	KP016	527700	1148600	**0**	**10**	190	5.4	6.2	<0.001	0.01	0.22	3	0.7	0.3	19.2	0.01	0.06	1.1	0.008	0.04	0.35	28	<0.05	14.65	35	1.1
813688	KP016	527700	1148600	10	20	170	5.6	6.4	<0.001	0.01	0.21	3	0.6	0.3	16.4	<0.01	0.06	1.1	0.007	0.04	0.35	29	<0.05	15.05	34	1.2
813690	KP016	527700	1148600	20	30	140	6	6.9	<0.001	0.01	0.27	3.7	0.7	0.4	10.7	0.01	0.08	1.3	0.007	0.06	0.4	35	<0.05	17.85	38	2.3
813691	KP016	527700	1148600	30	40	140	5.6	6.3	<0.001	<0.01	0.26	3.7	0.7	0.4	8	0.01	0.07	1.3	0.009	0.05	0.38	38	<0.05	16.6	40	3
813692	KP016	527700	1148600	40	50	120	5.5	5.7	<0.001	<0.01	0.25	3.5	0.6	0.4	6.7	0.01	0.07	1.3	0.008	0.05	0.34	38	<0.05	15.4	39	3.4
813693	KP016	527700	1148600	50	60	100	4.3	4.6	<0.001	<0.01	0.19	3	0.6	0.3	5.6	0.01	0.07	1.1	0.009	0.04	0.27	34	<0.05	15	36	3.3
813694	KP016	527700	1148600	60	70	80	3.3	3.3	<0.001	<0.01	0.17	2.5	0.6	0.3	3.2	0.01	0.05	0.9	0.009	0.02	0.22	31	<0.05	14.65	36	3.3
813695	KP016	527700	1148600	70	80	70	3.5	2.9	<0.001	<0.01	0.15	2.5	0.6	0.3	2.5	0.01	0.05	0.9	0.01	0.02	0.22	32	<0.05	14.9	37	3.2
813696	KP016	527700	1148600	80	90	160	6	2.6	<0.001	<0.01	0.38	2.7	0.5	0.3	2.8	0.01	0.05	1.4	0.016	0.03	0.32	34	<0.05	12.8	41	5.7
813697	KP016	527700	1148600	90	100	190	5.5	2	<0.001	0.01	0.6	2.2	0.6	0.3	4.1	<0.01	0.05	1.2	0.019	0.03	0.26	32	<0.05	13.1	39	6.7
813698	KP016	527700	1148600	100	110	110	3	1.9	<0.001	0.01	0.37	2.3	0.3	0.3	1.6	<0.01	0.04	1.1	0.015	0.02	0.22	32	<0.05	12.85	39	4.9
813699	KP016	527700	1148600	110	120	130	3.2	1.8	<0.001	0.01	0.46	2.2	0.4	0.3	2.1	<0.01	0.06	0.9	0.015	0.02	0.23	31	<0.05	14.1	39	4.3
813706	SP001	519090	1143591	**0**	**10**	620	10	9.2	<0.001	0.03	0.42	8.5	1	0.8	69.1	<0.01	0.03	3.3	0.035	0.08	1.8	178	0.09	15.4	24	5.4
813707	SP001	519090	1143591	10	20	730	14.8	5.1	<0.001	0.02	0.55	13	0.6	0.8	27.6	<0.01	0.07	5.1	0.046	0.06	2.8	321	0.1	11.9	24	9.5
813708	SP001	519090	1143591	20	30	660	17.9	4.3	<0.001	0.02	0.55	12.3	0.4	0.8	26.4	<0.01	0.07	4.8	0.042	0.06	2.61	299	0.09	10.15	23	9.6
813709	SP001	519090	1143591	30	40	700	20	4.8	<0.001	0.02	0.55	13.5	0.7	0.9	28.2	<0.01	0.08	5.1	0.045	0.07	2.74	314	0.08	9.91	24	10.6
813710	SP001	519090	1143591	40	50	680	13.8	6.3	<0.001	0.02	0.49	11.6	0.6	0.8	47	<0.01	0.07	4.1	0.04	0.07	2.37	256	0.09	11.95	25	7.4
813711	SP001	519090	1143591	50	60	700	15.8	10.1	0.001	0.03	0.36	8.8	0.7	0.8	90.5	<0.01	0.04	3.5	0.036	0.1	2	197	0.08	15.3	28	6.4
813712	SP001	519090	1143591	60	70	740	22.2	5.7	<0.001	0.02	0.54	14.2	0.6	0.9	52.2	<0.01	0.08	4.5	0.041	0.08	2.64	289	0.1	12.5	27	7.5
813713	SP001	519090	1143591	70	80	640	17.2	4	<0.001	0.01	0.49	13.3	0.4	1	29.9	<0.01	0.06	4.9	0.041	0.06	2.42	269	0.07	10.3	23	9.3
813714	SP001	519090	1143591	80	90	690	17.9	2.1	<0.001	0.01	0.5	15.8	0.5	0.9	15.7	<0.01	0.06	5.3	0.043	0.06	2.8	292	0.07	8.82	24	14.6
813715	SP001	519090	1143591	90	100	760	16	1.9	<0.001	0.01	0.43	14.6	0.4	0.9	13.1	<0.01	0.06	5.3	0.041	0.05	2.87	298	0.07	8.41	22	14.9
813716	SP001	519090	1143591	100	110	740	15.7	1.9	<0.001	0.01	0.44	16.6	0.7	0.9	12.9	<0.01	0.06	5.3	0.04	0.05	2.96	290	0.06	9.36	23	14.8
813717	SP001	519090	1143591	110	120	870	22.4	1.7	<0.001	0.01	0.49	16.2	0.6	0.9	10.9	<0.01	0.08	5.2	0.044	0.06	3.32	344	0.08	9.81	27	16.2
813718	SP001	519090	1143591	120	130	740	24.7	1.7	<0.001	0.01	0.5	16.2	0.5	0.9	10.1	<0.01	0.08	5.1	0.041	0.08	2.78	306	0.07	9.68	23	13.7
813720	SP001	519090	1143591	130	140	830	17.5	1.5	<0.001	0.01	0.46	16	0.5	0.8	9	<0.01	0.07	4.8	0.041	0.08	3.17	330	0.07	10.2	30	12.7
813721	SP001	519090	1143591	140	150	720	21.6	1.6	<0.001	<0.01	0.43	10.8	0.5	0.8	10.8	0.01	0.09	6.5	0.037	0.09	3.37	294	0.09	9.92	25	12.4
813722	SP001	519090	1143591	150	160	790	23	1.2	<0.001	<0.01	0.4	12	0.5	0.8	10.2	0.01	0.08	6.1	0.037	0.09	3.85	297	0.09	11.85	26	12
813723	SP001	519090	1143591	160	170	670	21.9	1.5	<0.001	<0.01	0.39	11.1	0.6	0.8	11.6	0.01	0.07	5.5	0.035	0.08	2.84	268	0.08	12.1	30	11.1
813724	SP001	519090	1143591	170	180	660	16.7	1.6	<0.001	<0.01	0.38	11.3	0.6	0.9	12.1	0.01	0.06	5.8	0.036	0.08	2.59	249	0.08	12.15	20	13.4
813725	SP001	519090	1143591	180	190	610	15.2	1.7	<0.001	<0.01	0.36	10.6	0.6	0.9	11.1	0.01	0.06	5.9	0.037	0.07	2.52	237	0.08	12.55	18	13.3
813726	SP001	519090	1143591	190	200	670	22.8	1.5	<0.001	<0.01	0.4	11.6	0.6	0.8	10.1	0.01	0.08	7.2	0.038	0.07	3.11	255	0.08	11.3	17	13.3
813727	SP001	519090	1143591	200	210	650	18.2	1.4	<0.001	<0.01	0.44	12.6	0.6	0.8	8.4	0.01	0.09	6.7	0.037	0.05	2.95	269	0.08	12.7	19	12.6
813728	SP001	519090	1143591	210	220	550	12.2	1.8	0.001	<0.01	0.47	15.5	0.8	0.8	7.5	<0.01	0.09	5.1	0.035	0.05	2.44	251	0.06	13.6	20	10.6
813729	SP001	519090	1143591	220	230	550	12	1.6	0.001	<0.01	0.44	16.9	0.7	0.8	7.4	<0.01	0.08	7.2	0.032	0.05	2.52	247	0.05	13.65	19	11
813730	SP001	519090	1143591	230	240	640	17.8	1.4	0.001	<0.01	0.43	16.9	0.8	0.9	5.8	0.01	0.1	5.3	0.033	0.05	3.01	249	0.06	14.05	24	11.4
813731	SP001	519090	1143591	240	250	430	11.5	1.7	0.002	<0.01	0.35	13.7	0.5	0.9	3.7	<0.01	0.06	5.1	0.026	0.05	2.06	179	<0.05	15.65	16	12.1
813732	SP001	519090	1143591	250	260	480	12.6	1.8	0.001	<0.01	0.33	13.1	0.6	0.8	3.6	<0.01	0.07	5	0.028	0.06	2.28	192	<0.05	13.85	18	10.6

Appendix C:Pits, Au and other elements in the regolith of the Lawra area analysed by ICP and FA-AAS Techniques

Sample ID	Pit ID	UTM-E	UTM-N	From (m	To (m)	P %	Pb ppm	Rb ppm	Re ppm	S %	Sb ppm	Sc ppm	Se ppm	Sn ppm	Sr ppm	Ta ppm	Te ppm	Th ppm	Ti ppm	Tl ppm	U ppm	V ppm	W ppm	Y ppm	Zn ppm	Zr ppm
813733	SP001	519090	1143591	260	270	450	18.4	1.7	0.001	<0.01	0.32	13.2	0.5	0.7	3.3	<0.01	0.06	4.7	0.025	0.08	2.15	181	<0.05	13.7	17	9.8
813734	SP001	519090	1143591	270	280	420	17.2	1.7	<0.001	<0.01	0.27	11	0.3	0.7	3.4	0.01	0.05	4.6	0.024	0.07	1.98	166	<0.05	14.7	19	10.1
813735	SP001	519090	1143591	280	290	410	17.3	1.7	<0.001	<0.01	0.31	9.4	0.3	0.6	2.8	0.01	0.05	4.2	0.025	0.07	1.77	166	0.06	11.45	15	9.8
813736	SP001	519090	1143591	290	300	370	15.4	2.1	<0.001	<0.01	0.25	9.6	0.3	0.7	3.9	0.01	0.05	4.7	0.023	0.09	1.77	152	<0.05	15.65	16	10.4
813737	SP001	519090	1143591	300	310	350	17.4	1.7	<0.001	<0.01	0.26	8.5	0.3	0.6	3	<0.01	0.04	3.8	0.022	0.09	1.53	149	0.05	12.5	15	9.5
813738	SP001	519090	1143591	310	320	410	14.5	1.8	<0.001	<0.01	0.26	9.7	0.3	0.7	3.7	0.01	0.05	4.4	0.024	0.08	1.79	165	<0.05	13.85	16	10
813739	SP001	519090	1143591	320	330	420	16.9	1.8	<0.001	<0.01	0.32	10.2	0.3	0.7	3.6	0.01	0.06	4.7	0.024	0.08	1.77	172	0.05	14.8	18	10.3
813740	SP002	518995	1143689	**0**	**10**	320	8.4	10.4	<0.001	0.01	0.24	5.2	0.3	0.4	17.9	0.01	0.05	3.2	0.034	0.06	1.01	114	0.09	9.09	20	3.7
813741	SP002	518995	1143689	10	20	300	9.8	9.4	<0.001	0.01	0.28	6	0.3	0.6	8.6	<0.01	0.06	3.3	0.032	0.09	1.25	130	0.09	7.91	17	2.4
813742	SP002	518995	1143689	20	30	280	8.9	11.7	<0.001	0.01	0.26	6.4	0.4	0.6	7.8	<0.01	0.06	3.3	0.033	0.09	1.28	128	0.09	7.72	16	2.2
813743	SP002	518995	1143689	30	40	240	9.7	12.3	<0.001	0.01	0.25	6.5	0.4	0.7	7.1	<0.01	0.05	4	0.034	0.1	1.37	125	0.08	6.79	16	2.9
813744	SP002	518995	1143689	40	50	210	13.7	14	<0.001	<0.01	0.28	7.8	0.3	1	8.7	<0.01	0.06	5.5	0.042	0.13	1.47	157	0.07	6.11	18	8.8
813745	SP002	518995	1143689	50	60	200	13.3	15.6	<0.001	<0.01	0.27	9.2	0.4	1.2	9.8	<0.01	0.06	6.4	0.044	0.13	1.56	176	0.06	8.12	21	14
813746	SP002	518995	1143689	60	70	210	14.2	15.2	<0.001	<0.01	0.28	9.7	0.3	1.3	9.6	<0.01	0.05	6.6	0.046	0.15	1.6	186	0.05	10.05	22	15.2
813747	SP002	518995	1143689	70	80	210	13.9	14.7	<0.001	<0.01	0.27	10	0.3	1.1	8.6	0.01	0.06	6.6	0.046	0.15	1.66	189	0.06	11	23	15.8
813748	SP002	518995	1143689	80	90	190	15.1	14.1	<0.001	<0.01	0.28	9.9	0.3	1.2	8.7	0.01	0.07	6.6	0.047	0.17	1.67	191	0.06	11.8	23	15.6
813749	SP002	518995	1143689	90	100	170	13.3	14.9	<0.001	<0.01	0.26	9.4	0.3	1.2	8	0.01	0.06	6.6	0.049	0.16	1.56	174	0.05	11.8	23	14.9
814079	SP005	518570	1143443	**0**	**10**	440	16.8	7.6	<0.001	<0.01	0.36	8.1	0.5	0.9	8.7	0.01	0.06	4.8	0.033	0.11	1.95	188	0.08	6.06	17	3.3
814080	SP005	518570	1143443	10	20	320	14.9	5.7	<0.001	<0.01	0.35	8.9	0.3	1.2	9.7	0.01	0.06	7.1	0.04	0.09	2	207	0.06	3.66	15	12.2
814081	SP005	518570	1143443	20	30	280	15.8	5.6	<0.001	<0.01	0.37	10.6	0.3	1.2	12.2	0.01	0.06	7.3	0.038	0.08	1.87	212	0.06	3.94	14	15.7
814082	SP005	518570	1143443	30	40	390	22	3.8	<0.001	<0.01	0.36	12.5	0.2	1.3	14.5	0.01	0.07	7.8	0.04	0.22	2.26	238	0.06	4.72	20	18.6
814083	SP005	518570	1143443	40	50	160	12.4	14	<0.001	<0.01	0.25	8.5	0.3	1.1	7.5	<0.01	0.05	6	0.045	0.16	1.39	158	<0.05	10.75	21	13.9
814084	SP005	518570	1143443	50	60	320	24.8	3.4	0.001	0.01	0.32	13.2	0.5	1.2	13.2	0.01	0.05	7.4	0.036	0.44	1.93	224	0.08	4.84	20	19.2
814085	SP005	518570	1143443	60	70	250	14.3	5.2	<0.001	0.01	0.36	12.7	0.5	1.3	14	0.01	0.06	8.4	0.041	0.14	1.91	213	0.08	5.19	15	23.1
814086	SP005	518570	1143443	70	80	240	9.7	4.3	<0.001	0.01	0.35	13.4	0.5	1.3	14.7	0.01	0.06	8.3	0.041	0.08	1.84	207	0.08	5.44	16	24.2
814087	SP005	518570	1143443	80	90	300	12.6	3.5	<0.001	0.01	0.45	15.8	0.5	1.2	14	0.01	0.08	8.1	0.042	0.1	2.12	261	0.09	5.75	20	21.6
814088	SP005	518570	1143443	90	100	250	14.8	5.3	<0.001	0.01	0.46	14.9	0.5	1.3	14.1	0.01	0.09	8.7	0.043	0.12	2.03	251	0.09	6.4	19	23.1
814089	SP005	518570	1143443	100	110	250	14.8	5	0.001	0.01	0.45	15	0.5	1.2	14	0.01	0.09	8.2	0.043	0.12	1.93	255	0.1	6.4	19	23.1
814090	SP005	518570	1143443	110	120	210	14.1	5.8	<0.001	0.01	0.34	13	0.5	1.4	15.4	0.01	0.06	8.8	0.041	0.09	1.85	202	0.07	6.06	15	23.3
814091	SP005	518570	1143443	120	130	180	16.3	6	<0.001	0.01	0.35	13.9	0.5	1.5	16.4	0.01	0.06	9.6	0.045	0.11	1.9	208	0.07	6.37	12	26.6
814092	SP005	518443	1143443	**0**	**10**	200	15.2	3.2	<0.001	0.01	0.35	14.2	0.5	1.3	14.6	0.01	0.06	8	0.038	0.11	1.72	206	0.06	5.61	15	22
814110	SP006	518443	1143096	10	20	480	13	7.9	<0.001	0.02	0.48	12.5	0.8	0.8	14.4	0.01	0.12	5.9	0.04	0.06	1.97	243	0.12	5.97	21	7.5
814111	SP006	518443	1143096	20	30	370	11.1	7.2	<0.001	0.02	0.41	11	0.9	0.9	5.9	0.01	0.11	6.4	0.041	0.06	1.99	212	0.1	5.53	17	10
814112	SP006	518443	1143096	30	40	320	11.6	7.6	0.001	0.02	0.37	11.4	1	1	4.7	0.01	0.12	6.9	0.039	0.07	2.11	198	0.09	5.64	14	11
814113	SP006	518443	1143096	40	50	230	11	4	<0.001	0.01	0.33	11.6	0.7	0.9	3.6	<0.01	0.11	6.9	0.037	0.05	1.97	209	0.07	4.08	12	14.9
814114	SP006	518443	1143096	50	60	250	11.8	4.1	<0.001	0.01	0.39	14.2	0.8	1.1	3.4	0.01	0.13	8.2	0.041	0.05	2.41	253	0.07	4.9	13	19.7
814115	SP006	518443	1143096	60	70	190	9.5	3	<0.001	0.01	0.45	12.1	0.7	0.9	2.9	0.01	0.12	7.5	0.035	0.04	1.89	221	0.06	4.42	12	18.3
814116	SP006	518443	1143096	70	80	190	8.2	2.4	<0.001	0.01	0.33	10.8	0.6	0.9	2.7	0.01	0.09	6.5	0.032	0.03	1.6	194	0.07	4.61	12	16.5
814117	SP006	518443	1143096	80	90	200	10.1	2.3	<0.001	0.01	0.35	11.7	0.6	0.8	2.8	<0.01	0.11	6.2	0.03	0.04	1.6	200	0.05	4.69	15	15.9
814118	SP006	518443	1143096	90	100	210	9.5	2.8	<0.001	0.01	0.33	13.2	0.6	0.9	3	0.01	0.11	6.4	0.033	0.04	1.8	224	0.05	5.32	15	16.8
814120	SP006	518443	1143096	100	110	230	11.1	2.4	<0.001	0.01	0.33	13.3	0.6	0.9	2.3	0.01	0.1	6.7	0.033	0.04	1.84	248	0.05	5.45	13	15.7
814121	SP006	518443	1143096	110	120	260	12.9	1.9	<0.001	0.01	0.41	14.3	0.6	0.9	2.3	0.01	0.1	6.5	0.032	0.04	1.89	249	0.06	5.41	18	16.1
814122	SP006	518443	1143096	120	130	220	12.1	2.1	<0.001	0.01	0.31	12.9	0.6	0.9	2.4	0.01	0.1	6.5	0.031	0.04	1.83	221	0.05	5.68	18	15.4
814123	SP006	518443	1143096	130	140	210	11.7	2.4	<0.001	0.01	0.33	12.7	0.6	0.9	2.9	0.01	0.09	6.5	0.034	0.04	1.82	226	0.05	5.11	14	16.3
814124	SP006	518443	1143096	140	150	210	10.4	3.5	<0.001	0.01	0.31	12.4	0.6	0.9	2.9	<0.01	0.09	6.7	0.033	0.04	1.82	226	0.05	5.18	13	16.2
814125	SP006	518443	1143096	150	160	220	8.2	2.1	<0.001	0.01	0.31	11.8	0.5	0.7	2	0.01	0.09	5.3	0.031	0.03	1.75	209	0.05	4.76	15	14.4
814143	SP007	518235	1143093	**0**	**10**	230	7.1	8.2	<0.001	0.01	0.33	6.2	0.5	0.5	10.6	<0.01	0.07	3.6	0.029	0.06	0.98	108	0.08	7.37	17	2.7
814144	SP007	518235	1143093	10	20	210	7.1	10	<0.001	0.01	0.27	7.4	0.6	0.5	7.9	<0.01	0.08	4.3	0.03	0.08	1.12	110	0.07	7.7	19	3.3
814145	SP007	518235	1143093	20	30	180	6.9	11.6	<0.001	0.01	0.27	8.1	0.6	0.6	7.4	<0.01	0.08	4.9	0.029	0.09	1.11	112	0.07	7.53	18	5.4
814146	SP007	518235	1143093	30	40	180	7.9	13.7	<0.001	0.01	0.26	9.2	0.6	0.7	7.8	<0.01	0.09	5.6	0.027	0.12	1.22	115	0.07	8.59	20	7.3
814147	SP007	518235	1143093	40	50	170	9.6	16	<0.001	0.01	0.27	10.4	0.6	0.9	8.1	<0.01	0.09	6.3	0.027	0.15	1.34	134	0.06	9.32	21	10.8
814148	SP007	518235	1143093	50	60	170	10.5	15.7	<0.001	0.01	0.31	10.4	0.6	0.9	7.9	0.01	0.08	6.4	0.027	0.16	1.33	146	0.06	9.91	21	12.6
814149	SP007	518235	1143093	60	70	160	10.6	16.3	<0.001	0.01	0.28	10.7	0.6	0.9	8.2	0.01	0.08	6.9	0.027	0.17	1.43	146	0.06	11.25	21	13.7
814150	SP007	518235	1143093	70	80	160	10.9	16	<0.001	0.01	0.27	10.6	0.5	0.9	8.3	0.01	0.09	6.8	0.027	0.17	1.4	145	0.05	11.45	21	13.9
814151	SP007	518235	1143093	80	90	530	5.4	34.2	<0.001	0.01	0.3	9.2	0.4	0.4	54.5	<0.01	0.05	2.6	0.078	0.2	0.4	86	0.27	8.78	71	7.9
814152	SP007	518235	1143093	90	100	180	11.4	16	<0.001	0.01	0.32	11.6	0.6	1	9.3	0.01	0.1	7.1	0.03	0.17	1.47	166	0.07	13.7	21	17.1
814153	SP007	518235	1143093	100	110	150	10.4	14.6	<0.001	<0.01	0.28	10.4	0.6	1	8.6	<0.01	0.04	5.8	0.028	0.16	1.31	151	0.05	15.05	22	15.6
814154	SP007	518235	1143093	110	120	140	10.7	14.4	<0.001	<0.01	0.28	10.1	0.9	1	8.6	<0.01	0.04	5.9	0.028	0.16	1.27	143	0.05	15.25	21	15.2
814155	SP007	518235	1143093	120	130	130	11.3	15.6	<0.001	<0.01	0.27	10.4	0.8	1.1	9.6	<0.01	0.05	6.2	0.029	0.16	1.31	145	0.05	17.5	21	17.1
814156	SP007	518235	1143093	130	140	140	11.6	14.2	<0.001	<0.01	0.28	10.3	0.8	1	9.2	<0.01	0.04	6.1	0.029	0.18	1.32	149	0.05	18.2	21	15.9
814157	SP007	518235	1143093	140	150	120	10.5	13.5	<0.001	<0.01	0.24	9.8	0.6	1	8.6	<0.01	0.04	5.7	0.029	0.15	1.28	144	<0.05	17.65	21	14.5
814171	SP008	518539	1143097	**0**	**10**	320	8.4	7	<0.001	0.01	0.25	6.2	0.5	0.8	12.5	<0.01	0.05	4.7	0.029	0.05	1.12	137	0.07	5.7	12	4.6
814172	SP008	518539	1143097	10	20	310	8.7	5.8	<0.001	<0.01	0.3	7.6	0.5	0.9	4	<0.01	0.04	5.8	0.031	0.06	1.34	165	0.08	6.08	13	6.8
814173	SP008	518539	1143097	20	30	290	8.7	8.7	<0.001	<0.01	0.2	9.1	0.5	1.3	3.5	<0.01	0.02	6.9	0.031	0.09	1.38	139	0.07	8.72	13	8.7
814174	SP008	518539	1143097	30	40	290	9.2	8.1	<0.001	<0.01	0.29	8.8	0.7	1.2	3.2	<0.01	0.04	7.4	0.033	0.07	1.57	165	0.07	7.87	12	9.5
814175	SP008	518539	1143097	40	50	250	9.7	7.7	<0.001	<0.01	0.27	8.9	0.8	1.2	3.3	<0.01	0.05	7.3	0.036	0.07	1.7	169	0.07	6.81	11	10.8
814176	SP008	518539	1143097	50	60	220	11.8	5.1	<0.001	<0.01	0.38	10.2	1.1	1.1	3.7	<0.01	0.07	8.4	0.047	0.06	2.39	245	0.08	5.82	11	21
814177	SP008	518539	1143097	60	70	180	11	4	<0.001	<0.01	0.4	10.6	0.7	1.3	5.1	0.01	0.07	8.6	0.049	0.05	2.09	254	0.07	5.74	10	25.2
814178	SP008	518539	1143097	70	80	160	9.5	3.1	<0.001	<0.01	0.3	8.8	0.6	1.2	5.6	0.01	0.07	8	0.047	0.05	1.58	222	0.05	5.36	10	21
814201	SP002	518995	1143689	**0**	**10**	160	12.3	14.2	<0.001	<0.01	0.26	10.9	0.9	1.1	7.1	<0.01	0.06	6.4	0.049	0.17	1.74	191	0.06	13.5	26	16.9
814202	SP002	518995	1143689	10	20	150	12.2	13	<0.001	<0.01	0.27	11.3	0.7	1.1	6.6	<0.01	0.08	6.2	0.05	0.16	1.79	192	0.05	14.65	26	17.2
814203	SP002	518995	1143689	20	30	110	13.7	14.9	<0.001	<0.01	0.24	11.3	0.7	1.1	6.3	<0.01	0.07	6.5	0.051	0.2	1.63	171	0.06	14.7	29	17.1
814204	SP002	518995	1143689	30	40	110	16	11.7	0.001	0.01	0.28	10.9	0.7	0.9	5.6	0.01	0.07	6.2	0.05	0.2	1.51	162	0.08	14.55	31	16.4

Appendix C:Pits, Au and other elements in the regolith of the Lawra area analysed by ICP and FA-AAS Techniques

Sample ID	Pit ID	UTM-E	UTM-N	From (m	To (m)	P %	Pb ppm	Rb ppm	Re ppm	S %	Sb ppm	Sc ppm	Se ppm	Sn ppm	Sr ppm	Ta ppm	Te ppm	Th ppm	Ti ppm	Tl ppm	U ppm	V ppm	W ppm	Y ppm	Zn ppm	Zr ppm
814205	SP002	518995	1143689	40	50	90	12.4	10.2	0.001	<0.01	0.23	10.5	0.7	0.8	4.6	0.01	0.08	5.5	0.05	0.18	1.62	148	0.06	15.5	34	14.1
814206	SP002	518995	1143689	50	60	80	9.7	10.6	<0.001	<0.01	0.23	11.1	0.8	0.8	4.9	0.01	0.07	5.5	0.052	0.17	1.73	148	0.06	17.65	37	14.7
814207	SP002	518995	1143689	60	70	80	10.8	9.8	<0.001	<0.01	0.22	11.3	0.9	0.7	4.4	0.02	0.08	5.2	0.052	0.15	1.6	146	0.06	17.65	39	13.8
814208	SP002	518995	1143689	70	80	80	10.2	9.6	<0.001	<0.01	0.23	11.9	0.9	0.7	4.6	0.01	0.08	5.3	0.049	0.17	1.71	159	0.06	19.05	45	13.2
814210	SP002	518995	1143689	80	90	80	9.3	10.2	0.001	<0.01	0.21	9.5	0.8	0.5	3.8	0.01	0.08	4.6	0.049	0.15	1.05	127	0.06	17.7	40	12.8
814211	SP002	518995	1143689	90	100	90	7.8	10.3	<0.001	<0.01	0.17	8.5	0.8	0.4	3.5	0.02	0.07	4.4	0.051	0.13	0.83	115	0.06	18	38	13.5
814212	SP002	518995	1143689	100	110	90	6.5	12.1	<0.001	<0.01	0.15	7	0.8	0.4	3.2	0.01	0.08	3.9	0.053	0.14	0.68	97	0.05	17.4	35	13.6
814213	SP002	518995	1143689	110	120	100	5.8	8.5	<0.001	<0.01	0.18	6.5	0.8	0.4	2.4	0.01	0.09	3.4	0.051	0.1	0.61	87	<0.05	17.45	34	14.9
814214	SP002	518995	1143689	120	130	90	5.6	11.7	<0.001	<0.01	0.17	7	0.6	0.4	2.5	0.01	0.09	3.2	0.054	0.11	0.58	87	<0.05	17.8	36	14.3
814215	SP002	518995	1143689	130	140	90	5.7	11.8	<0.001	<0.01	0.17	7.2	0.9	0.4	2.6	0.01	0.08	3.3	0.055	0.12	0.6	88	0.05	18.25	37	14.8
814216	SP002	518995	1143689	140	150	80	5.5	14.3	<0.001	<0.01	0.19	7.3	0.9	0.4	2.5	0.01	0.09	3.2	0.057	0.14	0.54	86	<0.05	17.75	36	14.2
814217	SP002	518995	1143689	150	160	70	5.6	15.3	<0.001	<0.01	0.18	7.9	0.6	0.4	2.7	<0.01	0.08	3.2	0.055	0.15	0.55	89	<0.05	18.85	39	12.9
814218	SP002	518995	1143689	160	170	90	5.6	10.5	<0.001	<0.01	0.2	8.7	0.5	0.4	2.8	0.01	0.06	3.4	0.054	0.13	0.59	95	0.05	20.2	44	14
814219	SP002	518995	1143689	170	180	90	4.6	11.4	<0.001	<0.01	0.15	5.6	0.6	0.4	2.1	0.01	0.08	2.6	0.047	0.11	0.49	68	<0.05	15.45	33	10.8
814220	SP003	518738	1143498	**0**	**10**	420	8.6	11.2	<0.001	<0.01	0.25	7	0.6	0.8	17.1	<0.01	0.03	3.1	0.029	0.07	1.31	117	0.08	8.25	17	2.1
814221	SP003	518738	1143498	10	20	390	8.6	11.3	<0.001	<0.01	0.28	7.5	0.7	0.8	10.5	<0.01	0.03	3.4	0.032	0.06	1.34	130	0.08	7.62	17	2.1
814222	SP003	518738	1143498	20	30	380	10.4	9.8	<0.001	<0.01	0.38	9.8	1	0.9	6.5	<0.01	0.04	4.4	0.035	0.08	1.88	185	0.08	7.75	17	4.1
814223	SP003	518738	1143498	30	40	350	11.5	5	<0.001	<0.01	0.46	14.1	0.7	0.8	5.8	<0.01	0.05	4.9	0.04	0.06	2.83	255	0.08	5.22	18	11.4
814224	SP003	518738	1143498	40	50	260	7.9	2.6	<0.001	<0.01	0.41	15.4	0.4	0.8	7.3	<0.01	0.06	4.4	0.032	0.04	2.33	204	0.06	4.06	15	14.6
814225	SP003	518738	1143498	50	60	360	7.4	2.3	<0.001	<0.01	0.35	15.8	0.2	0.8	7.3	<0.01	0.05	5.6	0.032	0.04	2.51	189	0.06	3.84	17	14
814226	SP003	518738	1143498	60	70	400	7.1	3	0.001	<0.01	0.35	17.3	0.3	0.9	7.8	<0.01	0.06	6.4	0.033	0.04	2.91	194	0.07	3.77	20	14.5
814227	SP003	518738	1143498	70	80	260	7.5	2.5	<0.001	<0.01	0.33	14.9	0.3	0.9	9.1	<0.01	0.06	5.8	0.028	0.04	2.4	153	0.05	3.9	16	14.5
814228	SP003	518738	1143498	80	90	230	7.3	1.4	<0.001	<0.01	0.32	14.9	0.2	0.9	9.1	<0.01	0.05	6	0.026	0.04	2.27	145	0.05	3.81	15	15.5
814229	SP003	518738	1143498	90	100	250	7.2	0.8	<0.001	<0.01	0.26	13	<0.2	0.7	9.1	<0.01	0.03	4.9	0.023	0.03	2.07	119	<0.05	3.52	15	11.1
814230	SP003	518738	1143498	100	110	260	10.5	2.1	<0.001	<0.01	0.35	16.1	0.3	1.2	11	<0.01	0.04	7	0.031	0.05	2.21	170	0.06	4.5	15	18.9
814231	SP003	518738	1143498	110	120	510	10	1	<0.001	<0.01	0.29	15.4	<0.2	0.8	9.8	<0.01	0.04	4.3	0.025	0.03	2.53	121	<0.05	4.19	19	10.8
814232	SP003	518738	1143498	120	130	500	8.2	0.8	<0.001	<0.01	0.31	14.7	<0.2	0.9	8.4	<0.01	0.04	4.9	0.023	0.02	3.13	116	0.09	3.78	19	10
814233	SP003	518738	1143498	130	140	280	7.1	1.5	<0.001	<0.01	0.41	13.3	0.2	1	8.5	<0.01	0.04	6.3	0.027	0.03	1.97	154	0.08	3.78	14	16.2
814234	SP003	518738	1143498	140	150	190	8.1	1.1	<0.001	<0.01	0.28	10.9	<0.2	1	10.4	<0.01	0.03	5.5	0.022	0.03	1.58	121	<0.05	3.93	13	15.3
814235	SP003	518738	1143498	150	160	190	7.8	1.2	<0.001	<0.01	0.29	11.3	0.3	1	10.7	<0.01	0.03	5.5	0.022	0.03	1.62	125	<0.05	4.01	12	15.6
814236	SP003	518738	1143498	160	170	250	7.3	1.2	0.001	<0.01	0.29	12.1	<0.2	1	9.2	<0.01	0.06	6.5	0.028	0.03	1.72	148	0.06	3.74	11	17
814237	SP003	518738	1143498	170	180	380	7.8	1.3	<0.001	<0.01	0.44	19.2	<0.2	1.1	10.1	<0.01	0.08	7.2	0.034	0.03	2.72	223	0.07	4.4	20	17.7
814238	SP003	518738	1143498	180	190	310	6.3	1.3	0.001	<0.01	0.54	16.5	<0.2	1.2	9.6	<0.01	0.08	6.6	0.03	0.03	2.41	181	0.05	4.21	19	17.6
814239	SP003	518738	1143498	190	200	310	6.3	1.2	<0.001	<0.01	0.37	15.6	0.4	1.2	9.9	<0.01	0.05	6	0.028	0.02	2.09	171	0.05	4.07	17	18.3
814240	SP003	518738	1143498	200	210	310	8.4	1.2	<0.001	<0.01	0.38	15.9	0.2	1.2	10.8	<0.01	0.06	5.9	0.028	0.03	2.13	180	<0.05	4.52	19	16.6
814241	SP003	518738	1143498	210	220	290	8.1	1.5	<0.001	<0.01	0.77	14.8	0.2	1.1	10.8	<0.01	0.06	5.8	0.028	0.04	1.9	153	<0.05	4.2	16	16.2
814256	SP004	518642	1143498	**0**	**10**	800	14.6	10.6	<0.001	0.02	0.45	8.9	0.5	0.8	42.6	<0.01	0.06	2.9	0.031	0.13	1.87	206	0.11	6.4	23	3.3
814257	SP004	518642	1143498	10	20	490	16.8	7.6	<0.001	0.01	0.47	9.7	0.8	0.9	17.8	<0.01	0.08	3.7	0.038	0.18	2.18	242	0.1	5.06	19	3.9
814258	SP004	518642	1143498	20	30	580	14.5	5.2	<0.001	0.01	0.54	12.8	0.8	0.8	11.6	0.01	0.1	3.8	0.039	0.32	2.51	270	0.1	4.93	35	5.4
814259*	SP004	518642	1143498			NSS	NSS	NSS	NSS	<0.01	NSS	NSS	NSS	NSS	NSS	NSS	NSS	NSS	NSS	NSS	NSS	NSS	NSS	NSS	NSS	NSS
814260	SP004	518642	1143498	30	40	530	11.2	3.2	<0.001	<0.01	0.46	12.7	0.7	0.8	6.9	<0.01	0.09	3.9	0.034	0.23	1.49	231	0.07	3.74	32	10.5
814261	SP004	518642	1143498	40	50	390	10	2.7	<0.001	<0.01	0.47	11	0.2	0.7	6.7	<0.01	0.09	3.4	0.03	0.11	1.19	207	0.06	3.13	35	11.6
814262	SP004	518642	1143498	50	60	590	13.3	4.7	<0.001	<0.01	0.47	11.7	0.7	0.8	9.3	<0.01	0.1	3.7	0.036	0.35	2.1	223	0.08	4.96	37	5.2
814263	SP004	518642	1143498	60	70	400	7.9	3.1	<0.001	<0.01	0.59	15.2	0.3	1	9.9	<0.01	0.13	4.3	0.036	0.06	1.45	259	0.07	3.78	35	17.1
814264	SP004	518642	1143498	70	80	500	6.3	2.4	<0.001	<0.01	0.61	16.2	0.5	1	10.7	<0.01	0.11	4.2	0.034	0.05	1.57	266	0.07	4.27	33	15.3
814265	SP004	518642	1143498	80	90	680	6.9	2.1	<0.001	<0.01	0.76	19	0.3	1	11.7	<0.01	0.16	4	0.036	0.05	1.89	328	0.1	5	44	13.6
814266	SP004	518642	1143498	90	100	730	8.5	2.1	<0.001	<0.01	0.82	19.4	0.7	1	10.4	<0.01	0.15	4.2	0.04	0.06	2.3	370	0.12	5.01	46	13.2
814267	SP004	518642	1143498	100	110	720	7	2	<0.001	<0.01	0.74	18.5	0.5	0.9	9.7	<0.01	0.12	3.9	0.038	0.04	2.09	350	0.11	4.61	45	13.8
814268	SP004	518642	1143498	110	120	560	5.9	2.4	<0.001	<0.01	0.52	13.9	0.4	1.1	13.5	<0.01	0.11	3.8	0.034	0.04	1.53	264	0.07	3.97	28	16.2
814269	SP004	518642	1143498	120	130	690	7.3	2.4	<0.001	<0.01	0.57	15.2	0.5	1.1	14.7	<0.01	0.09	3.9	0.036	0.06	1.65	300	0.07	4.71	32	14.8
814270	SP004	518642	1143498	130	140	690	7.9	2.8	<0.001	<0.01	0.64	17.1	0.4	1.1	15.3	<0.01	0.12	4.1	0.036	0.07	1.71	302	0.06	5.18	35	14.6
814271	SP004	518642	1143498	140	150	660	11.4	2.9	<0.001	<0.01	0.6	16.5	0.7	1.1	13.8	<0.01	0.12	4.4	0.038	0.1	1.84	316	0.08	5.1	35	16.3
814272	SP004	518642	1143498	150	160	660	8.9	2.9	<0.001	<0.01	0.7	17.9	0.4	1.2	15.7	<0.01	0.15	4.2	0.038	0.06	1.74	311	0.07	4.92	34	15.4
814273	SP004	518642	1143498	160	170	650	10.6	3.1	<0.001	<0.01	0.6	18.6	0.6	1.3	17.2	<0.01	0.14	4.8	0.038	0.11	2.16	306	0.06	5.33	32	17.1
814274	SP004	518642	1143498	170	180	720	11.9	3	0.001	<0.01	0.6	16.9	0.5	1.2	18	<0.01	0.12	4.5	0.036	0.16	2.13	307	0.07	5.48	34	14
814275	SP004	518642	1143498	180	190	760	11.4	2.3	<0.001	<0.01	0.7	18.5	0.6	1	14.6	<0.01	0.13	4.3	0.039	0.14	2.24	347	0.08	5.53	41	11.3
814276	SP004	518642	1143498	190	200	960	9.9	2.2	<0.001	<0.01	0.68	17.4	0.5	1.1	15.4	<0.01	0.1	4	0.037	0.12	2.11	322	0.08	6.36	43	10.5
814277	SP004	518642	1143498	200	210	880	13.3	2.8	<0.001	<0.01	0.68	17	0.6	1.2	16.5	<0.01	0.11	4.8	0.039	0.15	2.04	329	0.08	5.61	33	13.7
814278	SP004	518642	1143498	210	220	880	15.2	2.6	<0.001	<0.01	0.74	17.7	0.5	1.1	15.5	<0.01	0.14	4.4	0.04	0.15	1.93	358	0.08	5.6	37	11.4
814279	SP004	518642	1143498	220	230	800	12.6	2.2	<0.001	<0.01	0.47	12.1	0.6	0.9	13.5	<0.01	0.1	4.3	0.039	0.27	1.64	255	0.08	5.14	25	12.9
814280	SP004	518642	1143498	230	240	1020	13.3	2.4	<0.001	<0.01	0.51	16.3	0.5	0.9	10.9	<0.01	0.12	4.9	0.046	0.32	1.92	338	0.09	6.82	35	10.1
814281	SP004	518642	1143498	240	250	540	5	1.7	<0.001	<0.01	0.28	12.1	0.2	0.8	7.1	0.01	0.08	3.6	0.038	0.09	1.71	163	<0.05	5.36	17	9.8
814282	SP004	518642	1143498	250	260	530	3.3	2	<0.001	<0.01	0.23	10.6	0.4	0.6	5.9	0.01	0.06	3	0.032	0.05	1.57	124	<0.05	5.28	15	8.2
814283	SP004	518642	1143498	260	270	450	1.7	1.5	<0.001	<0.01	0.17	8.5	0.3	0.5	4.8	0.01	0.05	2.5	0.026	0.02	1.11	84	<0.05	4.71	11	6.7
814284	SP004	518642	1143498	270	280	440	1.9	1.3	<0.001	<0.01	0.15	8.5	0.4	0.6	4.9	0.01	0.04	2.5	0.027	0.02	0.96	80	<0.05	4.75	12	5.8
814285	SP004	518642	1143498	280	290	480	1.9	1.3	<0.001		0.19	9.4	<0.2	0.6	4.5	0.01	0.04	2.4	0.025	0.02	0.99	83	<0.05	4.72	13	6.6
814288	KP017	527800	1143498	**0**	**10**	170	5.8	5.8	<0.001	0.01	0.29	5	0.6	0.4	26.9	<0.01	0.04	2	0.006	0.03	0.48	39	<0.05	11.95	49	2.4
814289	KP017	527800	1148600	10	20	150	9.2	5.2	<0.001	<0.01	0.46	6.8	0.8	0.4	17.2	<0.01	0.05	2.2	0.005	0.07	0.61	56	<0.05	14.5	52	2.6
814290	KP017	527800	1148600	20	30	140	8.5	5.5	<0.001	<0.01	0.43	7.1	0.6	0.4	14.4	<0.01	0.05	2.3	0.005	0.08	0.69	59	<0.05	15.8	54	2.4
814291	KP017	527800	1148600	30	40	100	10.4	5.1	<0.001	<0.01	0.4	6.9	0.6	0.4	14.5	<0.01	0.05	2.4	0.006	0.08	0.64	53	<0.05	14.15	65	2.6
814292	KP017	527800	1148600	40	50	70	8	4	<0.001	<0.01	0.36	5.9	0.7	0.4	17.3	<0.01	0.04	2.3	<0.005	0.07	0.59	46	<0.05	13.05	67	2.4
814293	KP017	527800	1148600	50	60	60	5.5	3.9	<0.001	<0.01	0.31	5.9	0.7	0.3	15.4	<0.01	0.03	2.6	<0.005	0.04	0.52	41	<0.05	14	79	2.2
814294	KP017	527800	1148600	60	70	50	3.1	3.6	<0.001	<0.01	0.27	5.7	0.7	0.3	14.9	<0.01	0.04	2.6	<0.005	0.03	0.51	34	<0.05	16.75	87	2.1

Appendix C:Pits, Au and other elements in the regolith of the Lawra area analysed by ICP and FA-AAS Techniques

Sample ID	Pit ID	UTM-E	UTM-N	From (m	To (m)	P %	Pb ppm	Rb ppm	Re ppm	S %	Sb ppm	Sc ppm	Se ppm	Sn ppm	Sr ppm	Ta ppm	Te ppm	Th ppm	Ti ppm	Tl ppm	U ppm	V ppm	W ppm	Y ppm	Zn ppm	Zr ppm
814308	KP018	527900	1148600	**0**	**10**	100	2.9	4.6	<0.001	<0.01	0.16	2.4	0.2	0.3	14.4	<0.01	0.02	1.2	0.007	0.02	0.24	20	<0.05	8.08	15	2
814309	KP018	527900	1148600	10	20	90	3	4.2	<0.001	<0.01	0.15	2.6	0.5	0.3	8.8	<0.01	0.02	1.3	0.006	0.03	0.27	22	<0.05	9.16	14	1.5
814310	KP018	527900	1148600	20	30	80	4	5	<0.001	<0.01	0.19	3.4	0.3	0.4	8.5	<0.01	0.02	1.5	0.006	0.04	0.3	27	<0.05	11.35	16	2.3
814311	KP018	527900	1148600	30	40	70	4.6	4.8	<0.001	<0.01	0.19	3.6	0.2	0.5	8	<0.01	0.03	1.7	0.006	0.04	0.33	30	<0.05	10.45	19	2.8
814312	KP018	527900	1148600	40	50	50	5	4.3	<0.001	<0.01	0.2	3.7	0.3	0.4	7.4	<0.01	0.04	1.7	0.006	0.04	0.29	31	<0.05	8.95	19	4.6
814313	KP018	527900	1148600	50	60	40	5	3.9	<0.001	<0.01	0.19	3.5	0.3	0.4	8.5	<0.01	0.03	1.8	0.006	0.03	0.25	31	<0.05	10.8	20	4.7
814314	KP018	527900	1148600	60	70	40	4.3	3.4	<0.001	<0.01	0.22	3.4	0.3	0.4	8.5	<0.01	0.03	1.6	0.008	0.03	0.2	32	<0.05	10.8	23	5.5
814325	KP019	528000	1148600	**0**	**10**	210	6	4.3	<0.001	0.01	0.29	2.4	<0.2	0.2	30	<0.01	0.04	1.3	0.008	0.03	0.36	39	<0.05	3.74	22	2.5
814326	KP019	528000	1148600	10	20	180	6.1	5	<0.001	0.01	0.32	3.1	0.3	0.2	20.3	<0.01	0.06	1.4	0.006	0.04	0.39	42	<0.05	4.68	21	2.1
814327	KP019	528000	1148600	20	30	130	6.8	3.9	<0.001	<0.01	0.36	2.6	0.2	0.2	11.5	<0.01	0.07	1.2	0.006	0.03	0.34	39	0.05	3.73	18	1.7
814328	KP019	528000	1148600	30	40	110	6.2	4	<0.001	<0.01	0.33	3	0.2	0.2	10	<0.01	0.05	1.4	0.006	0.04	0.38	42	0.05	4.25	19	2.1
814329	KP019	528000	1148600	40	50	110	6.9	4	<0.001	<0.01	0.38	3.5	0.4	0.2	9.3	<0.01	0.06	1.7	0.006	0.04	0.43	49	0.05	4.98	22	3.7
814330	KP019	528000	1148600	50	60	80	6.3	3	<0.001	<0.01	0.4	3.4	0.4	0.2	7.2	<0.01	0.07	1.7	0.006	0.03	0.38	50	0.05	4.52	21	6.1
814331	KP019	528000	1148600	60	70	80	6	2	<0.001	<0.01	0.44	3	<0.2	<0.2	5.7	<0.01	0.05	1.9	0.006	0.02	0.36	48	0.05	3.76	22	9
814332	KP019	528000	1148600	70	80	70	6.2	1.5	<0.001	<0.01	0.39	2.7	0.2	<0.2	5.6	<0.01	0.07	1.9	0.005	0.02	0.33	48	<0.05	3.43	22	9
814342	KP020	528100	1148600	**0**	**10**	150	4.1	4.4	<0.001	<0.01	0.14	1.9	<0.2	0.2	22.8	<0.01	0.03	1.2	0.005	0.03	0.33	19	<0.05	3.66	27	2.4
814343	KP020	528100	1148600	10	20	120	4.1	4.1	<0.001	<0.01	0.15	2.2	<0.2	0.2	16.4	<0.01	0.04	1.3	0.005	0.04	0.38	21	<0.05	3.92	24	1.8
814344	KP020	528100	1148600	20	30	100	4.1	4	<0.001	<0.01	0.16	2.7	0.3	0.2	10.6	<0.01	0.04	1.4	0.005	0.04	0.42	24	<0.05	4.52	28	2.4
814345	KP020	528100	1148600	30	40	90	4	3.8	<0.001	<0.01	0.16	2.9	0.3	0.2	9.3	<0.01	0.06	1.4	<0.005	0.05	0.4	25	<0.05	3.97	31	3.3
814346	KP020	528100	1148600	40	50	70	3.2	3.1	<0.001	<0.01	0.15	2.4	0.2	<0.2	8.1	<0.01	0.04	1.2	<0.005	0.03	0.33	21	<0.05	3.02	28	3.6
814347	KP020	528100	1148600	50	60	60	37.6	2.6	<0.001	<0.01	0.18	2.3	<0.2	<0.2	8.6	<0.01	0.05	1.2	<0.005	0.03	0.33	19	<0.05	3.16	31	4.1
814348	KP020	528100	1148600	60	70	60	51	2.2	<0.001	<0.01	0.23	2	0.3	<0.2	8.9	<0.01	0.07	1.1	<0.005	0.02	0.34	20	<0.05	2.96	37	4.2
814350	KP020	528100	1148600	70	80	760	54.7	10.7	<0.001	0.01	0.43	8.4	0.5	0.7	21.4	<0.01	0.07	2.5	0.033	0.07	1.43	191	0.1	8.52	24	0.9
814352	KP020	528100	1148600	80	90	60	48.2	2	<0.001	<0.01	0.24	2	0.2	<0.2	12.3	<0.01	0.06	1.1	<0.005	0.02	0.34	21	<0.05	3.41	49	3.4
814353	KP020	528100	1148600	90	100	90	77.9	2.1	<0.001	<0.01	0.44	2.2	0.2	<0.2	14.9	<0.01	0.06	1.1	<0.005	0.03	0.46	23	<0.05	4.62	62	3.4
814361	KP021	528200	1148600	**0**	**10**	100	42.8	3.9	<0.001	<0.01	0.08	1.6	<0.2	0.2	17.7	<0.01	0.03	1.2	0.006	0.02	0.25	14	<0.05	5.62	11	2.4
814362	KP021	528200	1148600	10	20	100	29.5	3.8	<0.001	<0.01	0.1	1.8	0.3	0.2	14.9	<0.01	0.03	1.3	0.005	0.03	0.28	16	<0.05	6.76	10	3.1
814363	KP021	528200	1148600	20	30	70	29.9	4.4	<0.001	<0.01	0.09	2.1	<0.2	0.2	13.2	<0.01	0.03	1.4	0.006	0.03	0.35	18	<0.05	7.33	11	4.2
814364	KP021	528200	1148600	30	40	70	39.9	4.3	<0.001	<0.01	0.1	2.2	0.2	0.2	15	<0.01	0.03	1.6	0.006	0.03	0.41	19	<0.05	7.59	11	4.8
814365	KP021	528200	1148600	40	50	50	46.6	3.8	<0.001	<0.01	0.09	1.8	<0.2	0.2	13.7	<0.01	0.02	1.5	0.006	0.03	0.36	16	<0.05	6.58	10	5.1
814366	KP021	528200	1148600	50	60	30	56	2.9	<0.001	<0.01	0.06	1.3	0.2	0.2	12.3	<0.01	0.03	1.3	0.005	0.02	0.25	12	<0.05	6.02	8	5.7